RETINAL IMMUNOBIOLOGY AND RETINOPATHY

EDITED BY: Andrew W. Taylor, Darren James Lee and Heping Xu
PUBLISHED IN: Frontiers in Immunology

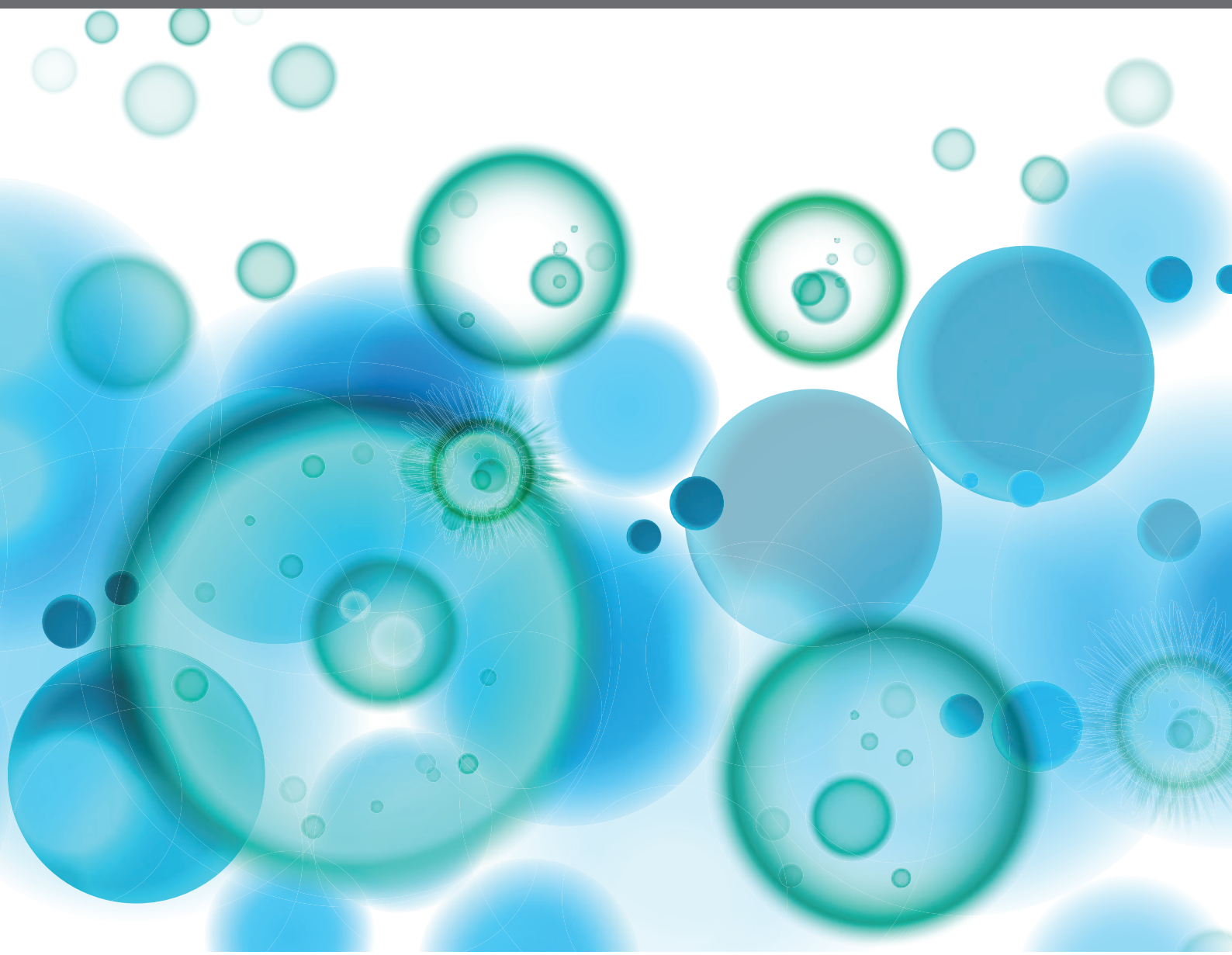

frontiers Research Topics

frontiers

ISSN 1664-8714
ISBN 978-2-88971-515-2
DOI 10.3389/978-2-88971-515-2

About Frontiers

Frontiers is more than just an open-access publisher of scholarly articles: it is a pioneering approach to the world of academia, radically improving the way scholarly research is managed. The grand vision of Frontiers is a world where all people have an equal opportunity to seek, share and generate knowledge. Frontiers provides immediate and permanent online open access to all its publications, but this alone is not enough to realize our grand goals.

Frontiers Journal Series

The Frontiers Journal Series is a multi-tier and interdisciplinary set of open-access, online journals, promising a paradigm shift from the current review, selection and dissemination processes in academic publishing. All Frontiers journals are driven by researchers for researchers; therefore, they constitute a service to the scholarly community. At the same time, the Frontiers Journal Series operates on a revolutionary invention, the tiered publishing system, initially addressing specific communities of scholars, and gradually climbing up to broader public understanding, thus serving the interests of the lay society, too.

Dedication to Quality

Each Frontiers article is a landmark of the highest quality, thanks to genuinely collaborative interactions between authors and review editors, who include some of the world's best academicians. Research must be certified by peers before entering a stream of knowledge that may eventually reach the public - and shape society; therefore, Frontiers only applies the most rigorous and unbiased reviews.
Frontiers revolutionizes research publishing by freely delivering the most outstanding research, evaluated with no bias from both the academic and social point of view. By applying the most advanced information technologies, Frontiers is catapulting scholarly publishing into a new generation.

What are Frontiers Research Topics?

Frontiers Research Topics are very popular trademarks of the Frontiers Journals Series: they are collections of at least ten articles, all centered on a particular subject. With their unique mix of varied contributions from Original Research to Review Articles, Frontiers Research Topics unify the most influential researchers, the latest key findings and historical advances in a hot research area! Find out more on how to host your own Frontiers Research Topic or contribute to one as an author by contacting the Frontiers Editorial Office: frontiersin.org/about/contact

RETINAL IMMUNOBIOLOGY AND RETINOPATHY

Topic Editors:
Andrew W. Taylor, Boston University, United States
Darren James Lee, University of Oklahoma Health Sciences Center, United States
Heping Xu, Queen's University Belfast, United Kingdom

Topic Editor Andrew Taylor has a sponsored research agreement and is a consultant with Palatin Technologies Inc. in Cranbury, New Jersey. All other Topic Editors declare no competing interests with regards to the Research Topic subject.

Citation: Taylor, A. W., Lee, D. J., Xu, H., eds. (2021). Retinal Immunobiology and Retinopathy. Lausanne: Frontiers Media SA. doi: 10.3389/978-2-88971-515-2

Table of Contents

frontiers in Immunology

EDITORIAL
published: 01 September 2021
doi: 10.3389/fimmu.2021.758375

Editorial: Retinal Immunobiology and Retinopathy

Darren J. Lee[1,2], *Heping Xu*[3] *and Andrew W. Taylor*[4*]

[1] Department of Microbiology and Immunology, University of Oklahoma Health Sciences Center, Oklahoma City, OK, United States, [2] Department of Ophthalmology/Dean McGee Eye Institute, University of Oklahoma Health Sciences Center, Oklahoma City, OK, United States, [3] The Wellcome-Wolfson Institute for Experimental Medicine, Queen's University Belfast, Belfast, United Kingdom, [4] Department of Ophthalmology, Boston University School of Medicine, Boston, MA, United States

Keywords: ocular immune privilege, age-related macular degeneration, diabetic retinopathy, glaucoma, uveitis, immune tolerance, retinal pigment epithelial cells, microglial cells

Editorial on the Research Topic

Retinal Immunobiology and Retinopathy

The term "Ocular Immune Privilege" (OIP) was used by Sir Peter Medawar in 1948 to describe the observation that a foreign tissue graft placed in the anterior chamber of the eye did not undergo rejection (1). In the last 72 years advances in the understanding of the mechanisms that contribute to the maintenance of OIP have been made (2). These mechanisms include: 1) sequestration, a lack of lymphatics, and tight junctions that create an efficient blood-barrier surrounding retinal vessels lining the inner retina, and tight junctions between retinal epithelial cells separating the outer retina from the highly vascular choroid; 2) expression of inhibitory soluble and membrane bound factors, such as transforming growth factor-beta, alpha-melanocyte stimulating hormone, FasL, and thrombospondin; and 3) inhibition of systemic immune responses, such as the induction of regulatory T cells and suppressive antigen presenting cells. While the benefit of OIP is the protection of delicate intraocular tissues from inflammation-mediated damage, it leaves the eye vulnerable to infection. Furthermore, while the mechanisms of OIP are considerable, diseases such as autoimmune uveitis, diabetic retinopathy, age-related macular degeneration, and optic neuropathy can break through the mechanisms of OIP. We are pleased to present a compendium of original research and review articles on the Research Topic "Retinal Immunobiology and Retinopathy" that discuss the mechanisms of OIP and the diseases of interest.

A thorough discussion of OIP mechanisms and the treatments available for retinal disease is reviewed by Takeda et al. This review provides a detailed discussion of immunological mechanisms that contribute to non-infectious or autoimmune uveitis, diabetic retinopathy, retinopathy of prematurity, retinitis pigmentosa, and vitreoretinal lymphoma.

Microglia cells are important in maintaining OIP and are present throughout the retina as reviewed by Rashid et al. In this timely and broadly relevant review, the origin and maintenance of retinal microglia, the role of microglia in the healthy and diseased retina, and therapies for retinal diseases that target microglia are discussed. Since microglia are present throughout the retina, they can further modulate the immune response by augmenting or inhibiting ocular inflammation. Therefore, a greater understanding of the role that microglial cells have in ocular inflammation could come from knowing the transcriptional signature of microglia during inflammation. As such, Bell et al. have characterized the transcriptome of microglia during the "early" activation, peak, and two weeks after endotoxin induced uveitis (EIU) and found that the acute transcriptional changes that occur to microglia during EIU return to their original state. The EIU model shows that the activation of endogenous inflammatory pathways

OPEN ACCESS

Edited and reviewed by:
Herman Waldmann,
University of Oxford, United Kingdom

***Correspondence:**
Andrew W. Taylor
awtaylor@bu.edu

Specialty section:
This article was submitted to Immunological Tolerance and Regulation, a section of the journal Frontiers in Immunology

Received: *13 August 2021*
Accepted: *17 August 2021*
Published: *01 September 2021*

Citation:
Lee DJ, Xu H and Taylor AW (2021) Editorial: Retinal Immunobiology and Retinopathy. Front. Immunol. 12:758375. doi: 10.3389/fimmu.2021.758375

can override the mechanisms of OIP. Mursalin et al. describe the resulting rapid and disastrous inflammation that can happen following Toll-like receptor (TLR)-2 and TLR-4 stimulation within the eye.

Age-related macular degeneration (AMD) is the largest cause of blindness resulting from photoreceptor degeneration. Myeloid derived suppressor cells (MDSCs) are suppressive immune cells from the myeloid lineage initially identified by their association with tumor cells for their potent immunosuppressive capacity. The role of MDSCs in the maintenance of OIP to prevent AMD is reviewed by Kauppinen et al. In fact, CX3CR1$^{-/-}$ mice exhibit an increased number of mononuclear phagocytes in the subretinal space and is associated with photoreceptor degeneration. Lavalette et al. show that CD36, a member of the class B scavenger receptor family involved in TLR-signaling on mononuclear phagocytes can promote sterile inflammation, and is necessary for photoreceptor degeneration in two different CX3CR1$^{-/-}$ AMD models. An important component of OIP is maintenance of the blood ocular barrier. An elegant study by Matsubara et al. describes how AMD results from loss of barrier function through secretion of granzyme B.

Diabetic retinopathy is the most common microvascular complication of diabetes, and is the largest cause of blindness among those of working-age. Inflammation and angiogenesis are hallmarks of diabetic retinopathy. The proangiogenic and proinflammatory cytokine macrophage migration inhibitory factor (MIF1) is an upstream activator of innate immunity. El-Asrar et al. show that MIF1 is significantly elevated in proliferative diabetic retinopathy (PDR), illustrating how diabetes diminishes OIP. Another component of inflammation is the complement system. Apart from C1q for the purpose of synaptic pruning, complement activation does not normally occur inside the eye, but has been observed in the diabetic retina. Shahulhameed et al. report a significant elevation of C3 deposition in the capillary wall and the co-localization of Complement Factor H in activated CD11b^{+} microglia in retina samples from diabetic donors. This suggests a feedback mechanism for arresting excessive complement activation in the diabetic retina by activated microglia.

Uveitis is inflammation of the eye and the third leading cause of blindness in countries with healthcare access. The majority of chronic uveitis cases are idiopathic or can be associated with a systemic autoimmune disease. As such, targeting inhibition of inflammatory pathways can be an effective treatment for uveitis. Efforts are underway to identify normally expressed signaling molecules that suppress the immune response, such as kallistatin, a serine proteinase inhibitor with anti-inflammatory properties. A report by Muhammad et al. demonstrates the suppression of experimental autoimmune uveitis (EAU) with kallistatin, and further shows that kallistatin induces regulatory T cells. T cell function is modulated through epigenetic modification, and two inhibitors that block DNA methylation have been approved for human disease. Zou et al. demonstrate that the DNA methylation inhibitor, zebularine, is effective in suppressing inflammatory T cells, promoting regulatory T cells, and suppresses EAU.

Glaucoma is the most prevalent neurodegenerative disease marked by progressive damage to the optic nerve and death of retinal ganglion cells. Therapies for glaucoma are based on lowering the intraocular pressure (IOP), but because elevated IOP is not necessary or sufficient to cause glaucoma-related neuropathy, there are likely additional mechanisms involved. In the mini-review by Jiang et al., they discuss the evidence that the neuropathy occurs due to a loss of OIP resulting in T cell-related low-grade intraocular inflammation.

The 12 featured articles in this Research Topic: Retinal Immunobiology and Retinopathy provide a broad discussion of the mechanisms of OIP, demonstrate that in different retinal diseases inflammatory pathways can break through the mechanisms of OIP, and show that therapies that have modes-of-action like the mechanisms of OIP are effective at treating retinal disease. While many therapies to treat retinal inflammatory diseases have been developed, additional mechanisms remain to be elucidated to develop better and more effective therapies for retinal inflammatory diseases.

AUTHOR CONTRIBUTIONS

The writing of this editorial was a collaborative effort between DL, HX, and AT. DL wrote the first draft which was then revised by HX and AT. All authors contributed to the article and approved the submitted version.

FUNDING

Grant funding: EY024951 (DL) and EY025961 (AT).

REFERENCES

1. Medawar PB. Immunity to Homologous Grafted Skin; the Fate of Skin Homografts Transplanted to the Brain, to Subcutaneous Tissue, and to the Anterior Chamber of the Eye. *Br J Exp Pathol* (1948) 29:58–69.
2. Taylor AW, Ng TF. Negative Regulators That Mediate Ocular Immune Privilege. *J Leukoc Biol* (2018) 103:1179–87.doi: 10.1002/JLB.3MIR0817-337R

Conflict of Interest: AT has a sponsored research agreement and is a consultant with Palatin Technologies Inc. (Cranbury, New Jersey). HX has a sponsored research agreement with Boehringer Ingelheim and a consultant agreement with F. Hoffmann-La Roche Ltd.

The remaining author declares that the research was conducted in the absence of any commercial or financial relationships that could be construed as a potential conflict of interest.

frontiers in Immunology

ORIGINAL RESEARCH
published: 16 August 2019
doi: 10.3389/fimmu.2019.01950

The DNA Methylation Inhibitor Zebularine Controls CD4$^+$ T Cell Mediated Intraocular Inflammation

Yanli Zou[1†], Xiao Hu[1†], Lauren P. Schewitz-Bowers[2,3†], Madeleine Stimpson[2,3], Li Miao[1], Xiaofei Ge[1], Liu Yang[1], Yan Li[1], Paul W. Bible[1], Xiaofeng Wen[1], Jing Jing Li[1], Yizhi Liu[1], Richard W. J. Lee[2,3] and Lai Wei[1*]*

[1] State Key Laboratory of Ophthalmology, Zhongshan Ophthalmic Center, Sun Yat-sen University, Guangzhou, China, [2] Translational Health Sciences, University of Bristol, Bristol, United Kingdom, [3] National Institute for Health Research Biomedical Research Centre at Moorfields Eye Hospital NHS Foundation Trust and UCL Institute of Ophthalmology, London, United Kingdom

OPEN ACCESS

Edited by:
Kutty Selva Nandakumar, Southern Medical University, China

Reviewed by:
Georges Verjans, Erasmus Medical Center, Netherlands
Rupesh Agrawal, Tan Tock Seng Hospital, Singapore

***Correspondence:**
Richard W. J. Lee
richard.lee@bristol.ac.uk
Lai Wei
weil9@mail.sysu.edu.cn

[†]These authors have contributed equally to this work

Specialty section:
This article was submitted to Autoimmune and Autoinflammatory Disorders, a section of the journal Frontiers in Immunology

Received: *09 May 2019*
Accepted: *01 August 2019*
Published: *16 August 2019*

Citation:
Zou Y, Hu X, Schewitz-Bowers LP, Stimpson M, Miao L, Ge X, Yang L, Li Y, Bible PW, Wen X, Li JJ, Liu Y, Lee RWJ and Wei L (2019) The DNA Methylation Inhibitor Zebularine Controls CD4$^+$ T Cell Mediated Intraocular Inflammation. Front. Immunol. 10:1950. doi: 10.3389/fimmu.2019.01950

CD4$^+$ T cell mediated uveitis is conventionally treated with systemic immunosuppressive agents, including corticosteroids and biologics targeting key inflammatory cytokines. However, their long-term utility is limited due to various side effects. Here, we investigated whether DNA methylation inhibitor zebularine can target CD4$^+$ T cells and control intraocular inflammation. Our results showed that zebularine restrained the expression of inflammatory cytokines IFN-γ and IL-17 in both human and murine CD4$^+$ T cells *in vitro*. Importantly, it also significantly alleviated intraocular inflammation and retinal tissue damage in the murine experimental autoimmune uveitis (EAU) model *in vivo*, suggesting that the DNA methylation inhibitor zebularine is a candidate new therapeutic agent for uveitis.

Keywords: uveitis, zebularine, DNA methylation inhibitor, CD4$^+$ T cell, intraocular inflammation

INTRODUCTION

Autoimmune uveitis is a heterogeneous collection of diseases characterized by intraocular inflammation (1). Affected patients are at risk of visual impairment or blindness (2), in particular those who are resistant or intolerant to conventional immunosuppressive therapies (3–5). Consequently there is a need to develop improved approaches to achieve control of intraocular inflammation.

Abnormal activation of the T helper (Th) cells and imbalance between inflammatory Th1/Th17 and regulatory T (Treg) cells play a key role in the pathogenesis of autoimmune uveitis (6–8). Modulating Th cell differentiation and function has been proposed as a therapeutic strategy for uveitis (9). The expression of signature cytokines and master transcription factors, as well as Th functions, are under tight control of coordinated epigenetic alterations (10, 11). And many genome-wide and locus-specific epigenetic changes have been found in patients with immune-mediated diseases such as systemic lupus erythematosus and rheumatoid arthritis (12). Therefore, modulating the epigenetic program that controls Th1, Th17, and Treg functions may serve as a new way to control the intraocular inflammation in uveitis.

Two key epigenetic mechanisms—DNA methylation and histone modifications—regulate chromatin accessibility, and have been the targets of a series of compounds developed in recent years for the treatment of cancers and immune-mediated diseases (12). Among these small-molecule inhibitors, two DNA methyltransferase (DNMT) inhibitor pro-drugs, 5-azacytidine

and 2′-deoxy-5-azacytidine have been approved for the treatment of myelodysplastic syndrome and acute myeloid leukemia (13). In addition, an anti-inflammatory effect of these two drugs has also been observed in murine models of asthma (14) and experimental autoimmune encephalomyelitis (15). We therefore hypothesize that another DNA methylation inhibitor, zebularine, which has relatively low cellular toxicity and a longer half-life (16), has the potential to suppress uveitis.

Here, to elucidate whether zebularine is able to control the intraocular inflammation through regulating the expression of inflammatory cytokines in $CD4^+$ T cells, we explored the changes of IFN-γ, IL-17, and Foxp3 (17) in response to zebularine treatment in Th1, Th17, and Treg cells. In addition, the immunosuppressive effects of zebularine *in vivo* were also evaluated using the murine experimental autoimmune uveitis model.

MATERIALS AND METHODS

Human Peripheral Blood $CD4^+$ T Cell Isolation

$CD4^+$ T cells were obtained by negative selection from peripheral blood of healthy controls (HCs) ($N = 4$; 3 female and 1 male; average age of 42) following informed consent in accordance with National Health Service Research Ethic Committee approved protocols at the University Hospitals Bristol Foundation Trust, United Kingdom (04/Q2002/84). Written, informed consent was obtained from all study participants. $CD4^+$ T cells were obtained by incubating up to 80 ml uncoagulated peripheral blood with RosetteSep™ Human $CD4^+$ T cell Enrichment Cocktail (Stemcell Technologies, Canada) according to the manufacturer's instructions. Blood was then layered on Ficoll-Paque PLUS (GE Healthcare, USA) and centrifuged for 1,200 × g for 20 min. Enriched $CD4^+$ T cells were removed from the density gradient and washed in RPMI-1640 (Thermofisher) supplemented with 10% fetal calf serum (FCS). The purity of human $CD4^+$ T cells was >95%.

Mice

Female C57BL/6 2-Hb mice (8–10 weeks) were purchased from Guangdong Medical Laboratory Animal Center (China) and maintained in a SPF facility in Zhongshan Ophthalmic Center of Sun Yat-sen University. All animal experiments were approved by the Institutional Animal Care and Use Committee of Zhongshan Ophthalmic Center. All animal work was performed in compliance with the ARVO Statement for the Use of Animals in Ophthalmic and Vision Research.

Antibodies and Reagents

Zebularine was purchased from Tocris Bioscience (UK). The recombinant mouse interleukin-6 (rmIL-6), rmIL-12, recombinant human transforming growth factor beta 1 (rhTGF-β1) were purchased from R&D Systems (USA). Functional antibodies anti-CD3 (145-2C11) and anti-CD28 (37.51), FACS antibodies anti-IL-17A (eBio17B7), anti-IFN-γ (XMG1.2) and anti-Foxp3 (FJK-16s) were from eBioscience (USA). CD4 (L3T4) and naïve $CD4^+$ T cell Magnetic-activated cell sorting (MACS) isolation kits were purchased from Miltenyi (Germany). The complete Freund's adjuvant and pertussis toxin were purchased from Sigma-Aldrich (USA).

Cell Culture

Human peripheral $CD4^+CCR6^-$ and $CD4^+CCR6^+$ cells ($N = 4$; 3 female and 1 male; average age of 42) were FACS-sorted from isolated $CD4^+$ T cells, resuspended to 2×10^6 cells/mL in RPMI-1640 supplemented with 10% FCS, L-glutamine, and penicillin/streptomycin (all Thermofisher, stimulated with plate-bound anti-CD3 (5 μg/mL; clone UCHT1) and anti-CD28 (5 μg/mL;clone CD28.2) antibodies (eBioscience) ($CCR6^-$ cells) or with plate-bound antibodies and a polarizing cytokine mixture of 20 ng/mL IL-6, 10 ng/mL IL-23, 10 ng/mL IL-1β (all from R&D Systems), 100 ng/mL anti-IFN-γ, 100 ng/mL anti-IL-4 (eBioscience) ($CCR6^+$ cells) for 5 days. Zebularine was also added at the indicated concentrations at the beginning of cultures. For murine $CD4^+$ T cells, spleen and lymph node cells were filtered through a 40-μm cell strainer, followed by the red blood cell lysis using ammonium-chloride-potassium (ACK) buffer. Total $CD4^+$ T cells were then isolated with the CD4 (L3T4) T cell isolation kit using the autoMACS Pro Separator (Miltenyi, Germany) and stimulated by plate-bound of anti-CD3 (5 μg/mL) and anti-CD28 (2 μg/mL) antibodies, as well as mIL-12 10 ng/mL, mIL-2 10 ng/mL, anti-IL-4 10 μg/mL (Th1); mIL-6 20 ng/mL, rhTGF-β1 1 ng/mL, anti-IL-4 10 μg/mL, anti-IFN-γ 10 μg/mL (Th17); and mIL-2 50 ng/mL, rhTGF-β1 2 ng/mL (Treg) for 3 days. When zebularine was used, the indicated doses of drug were added at the beginning of the culture.

RNA-seq Analysis

Total RNA from Th1, Th17, and Treg cells was extracted with the MasterPure Complete DNA and RNA Purification Kit (Epicentre, UK) according to the manufacture's instruction. A total of 100 ng RNA was sonicated into fragments of 300–400 base pairs using Bioruptor (Diagenode, Belgium). mRNA library was prepared using VAHTS mRNA-seq V3 Library Prep Kit for Illumina (Vazyme, Nanjing, China) following the manufacture's protocol and sequenced on the Illumina HiSeq2500 sequencer with HiSeq SR Cluster Kit V4 and HiSeq SBS Kit V4 50 cycle kit (Illumina). The initial processing was performed by CASAVA (v1.8.2). Sequencing reads were then subjected to quality control processed by FastQC (v0.11.5) and trimmed by Cutadapt (v1.9.1). Quality controlled reads were then analyzed using DEseq2.

Quantitative Real-Time PCR (qPCR)

Total RNA from T cells was extracted with the MasterPure Complete DNA and RNA Purification Kit (Epicentre, UK), and cDNA was synthesized with the PrimeScript™ cDNA Synthesis Kit (Takara, Japan). qRT-PCR was performed using SYBR Green PCR Master Mix (KAPA Biosystems, USA) on the Light Cycler 480 instrument (Roche, Switzerland). The samples were run in duplicate and the relative expression was determined by normalizing the expression of each gene to glyceraldehyde 3-phosphate dehydrogenase (GAPDH) using the $2^{-\Delta\Delta Ct}$ method. The primers used are shown in the **Supplementary Table 1**.

Drug Treatment in Mice

Zebularine was reconstituted with 0.9% saline to make a 1 μg/μL stock and stored at −80°C. Zebularine was administered to the mice at 10 μg/g body weight by intraperitoneal injection. The injection was started on day 7 post-immunization and performed daily for 7 consecutive days. The control group was injected with 0.9% saline only. Body weights of both groups were monitored after drug treatment.

EAU Induction and Scoring

C57BL/6 mice were immunized subcutaneously, at the base of tail (100 μL) and in both thighs (50 μL), with total 50 μg human interphotoreceptor retinoid binding (IRBP) $_{651-670}$ emulsified with complete Freund's adjuvant supplemented with 3.5 mg *Mycobacterium tuberculosis*. Each mouse also received 1 μg pertussis toxin (Tocris Bioscience, UK) intraperitoneally. To assess the clinical score of EAU, we performed dilated-pupil

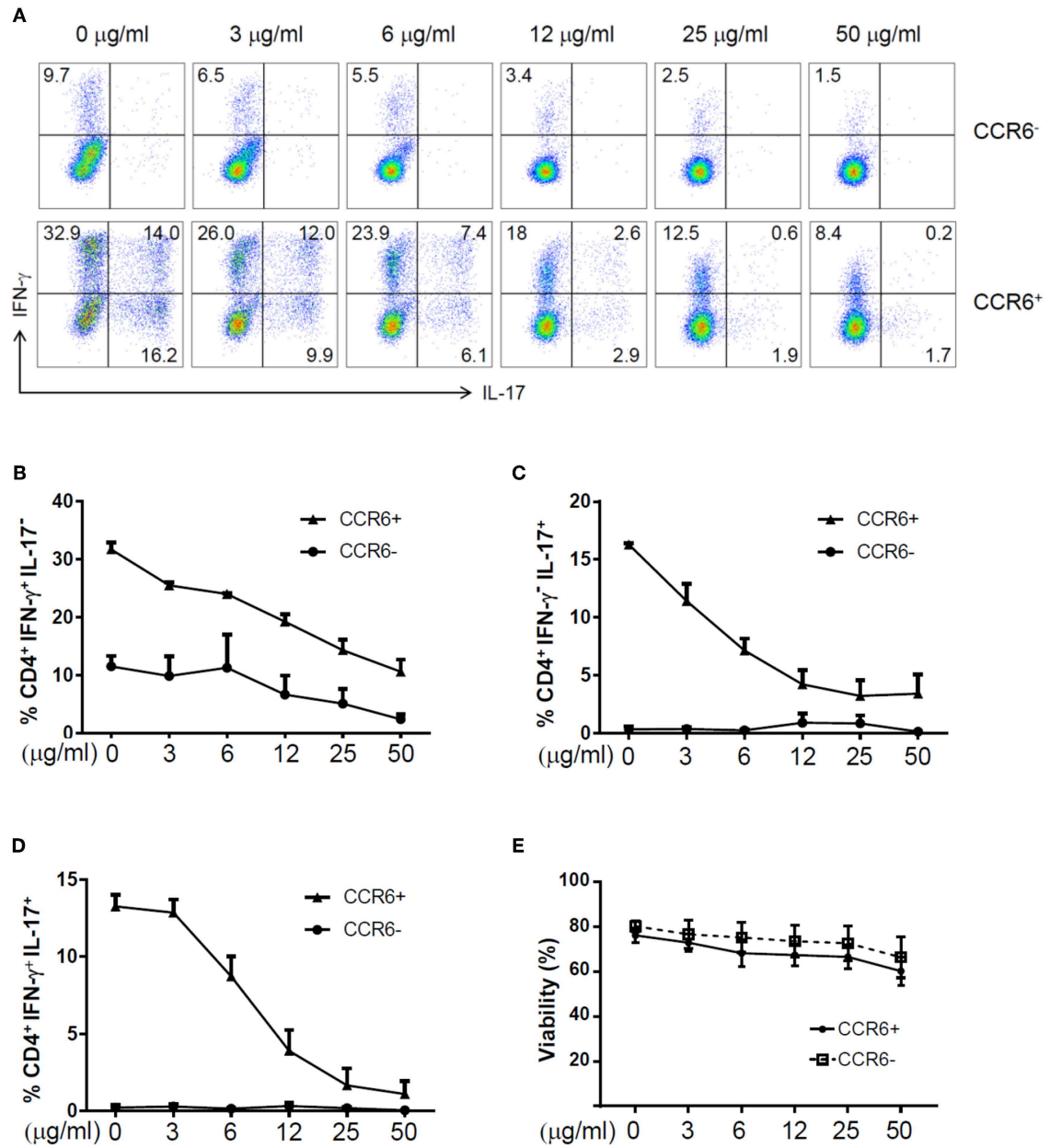

FIGURE 1 | The expression of IFN-γ and IL-17A in zebularine-treated human CD4$^+$ T cells *in vitro*. **(A)** Representative dot plots ($N = 4$; 3 female and 1 male; average age of 42) for stimulated human CD4$^+$CCR6$^-$ and CD4$^+$CCR6$^+$ cells on Day 5, stained with IFN-γ and IL-17A. The frequency of CD4$^+$IFN-γ$^+$IL-17$^-$ **(B)**, CD4$^+$IFN-γ$^-$IL-17$^+$ **(C)**, and CD4$^+$IFN-γ$^+$IL-17$^+$ **(D)** Cells in zebularine-treated human CD4$^+$CCR6$^+$ and CD4$^+$CCR6$^-$ cells. **(E)** Viability of CD4$^+$CCR6$^-$ and CD4$^+$CCR6$^+$ cells treated with different doses of zebularine. Means ± SD are shown.

fundus examination with a Micron III murine fundus camera (Phoenix Research Labs, USA) and histological assessment of FFPE sections of the retinal tissues from EAU mice (18). The clinical scores were given by two independent experienced observers in a blindfold manner based on the criteria for EAU scoring as described previously (19).

Flow Cytometry and FACS Sorting

For FACS-sorted human cells, pre-enriched $CD4^+$ T cells were incubated with a combination of primary antibodies against cell surface markers at 4°C for 30 min and then washed using PBS (v/v 10% FCS and 1mM EDTA). Antibodies used for human CCR6 T cell FACS sorts were anti-CD4 AF700 (BD Biosciences), anti-CD3 BV510 (BD Biosciences) and CCR6 PE (BD Biosciences). 7-AAD (Biolegend, USA) was used to discriminate living cells. Cells were sorted into $CD4^+CCR6^-$ and $CD4^+CCR6^+$ subsets using a BD Influx (BD Biosciences) and routinely >95% purity was achieved. Both human and murine cultured or single cell suspensions collected from human CCR6 5-day cultures and retina, spleen, or lymph nodes from mice were stimulated with 20 ng/ml phorbol myristate acetate (PMA), 1 μM ionomycin (Sigma-Aldrich, USA) and 1 μl/ml GolgiStop (BD Biosciences) for 4 h at 37°C. After 4 h, cells were washed with PBS (v/v 10% FCS and 1mM EDTA), stained with Infrared Live/Dead fixable dye (ThermoFisher) fixed and permeabilized (Cytofix/perm solution; BD Biosciences) and stained with anti-IL-17A, anti-IFN-γ, and anti-Foxp3 antibodies. Samples were acquired using a BD LSRFortessa™ X-20 (BD Biosciences). Results were analyzed using Flowjo v10 (Treestar).

Bisulfite Sequencing

Total DNA isolated from mouse polarized Treg cells was extracted with the MasterPure Complete DNA and RNA Purification Kit (Epicentre, UK). Sodium bisulfite treatment of total DNA was performed using the EZ DNA Methylation-Gold Kit (Zymo Research, USA) according to the manufacturer's instruction. PCR amplification was performed on the T100 Thermal Cycler (Bio-Rad, USA) in a final volume of 50 μL. PCR products were purified with the Zymoclean Gel DNA Recovery Kit (Zymo Research, USA). The sequencing results were analyzed by BiQ Analyzer (Max Planck Institut Informatik, Germany). The following primers pairs were used: Foxp3 enhancer CpG

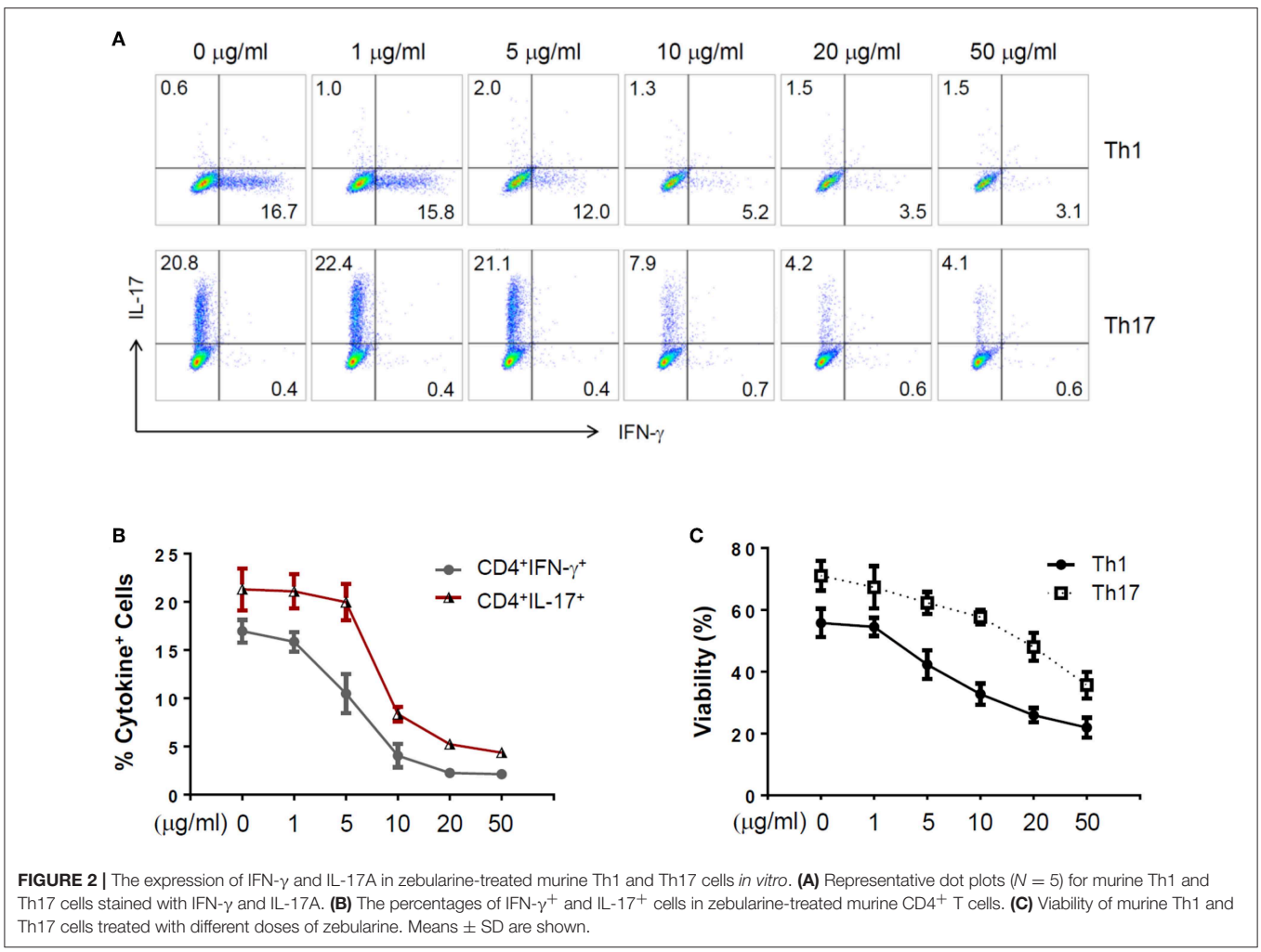

FIGURE 2 | The expression of IFN-γ and IL-17A in zebularine-treated murine Th1 and Th17 cells *in vitro*. **(A)** Representative dot plots ($N = 5$) for murine Th1 and Th17 cells stained with IFN-γ and IL-17A. **(B)** The percentages of $IFN\text{-}\gamma^+$ and $IL\text{-}17^+$ cells in zebularine-treated murine $CD4^+$ T cells. **(C)** Viability of murine Th1 and Th17 cells treated with different doses of zebularine. Means ± SD are shown.

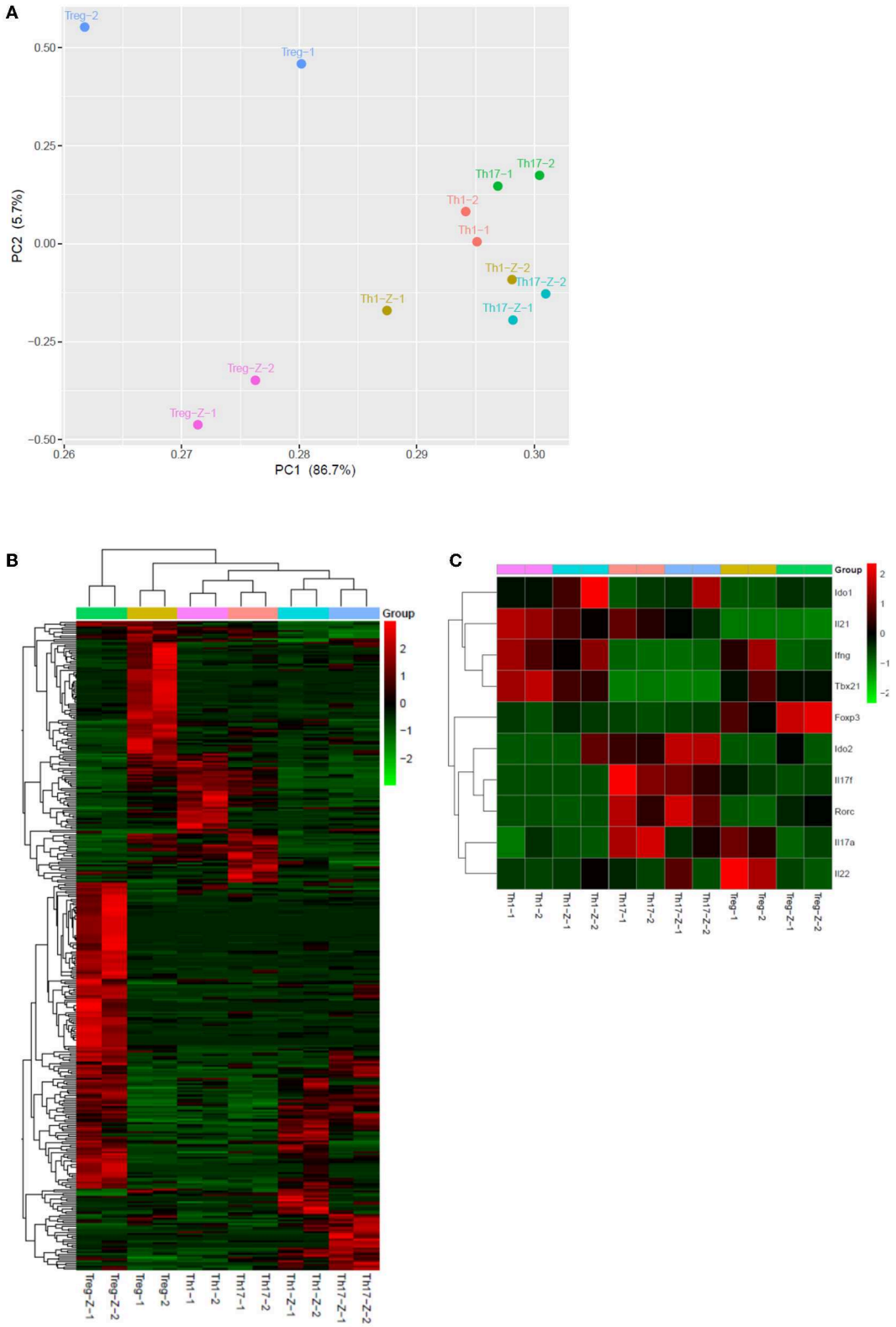

FIGURE 3 | Genome-wide expression profiles of Th1, Th17, and Treg cells in response to zebularine stimulation. **(A)** Principle component analysis of genes with at least two-fold changes between any two conditions and $P < 0.05$ (one-way ANOVA). -Z represents the conditions with zebularine stimulation. **(B)** Hierarchical clustering analysis of Th1, Th17, and Treg cells with (-Z) or without zebularine stimulation. **(C)** Hierarchical clustering of genes of interest in Th1, Th17, and Treg cells.

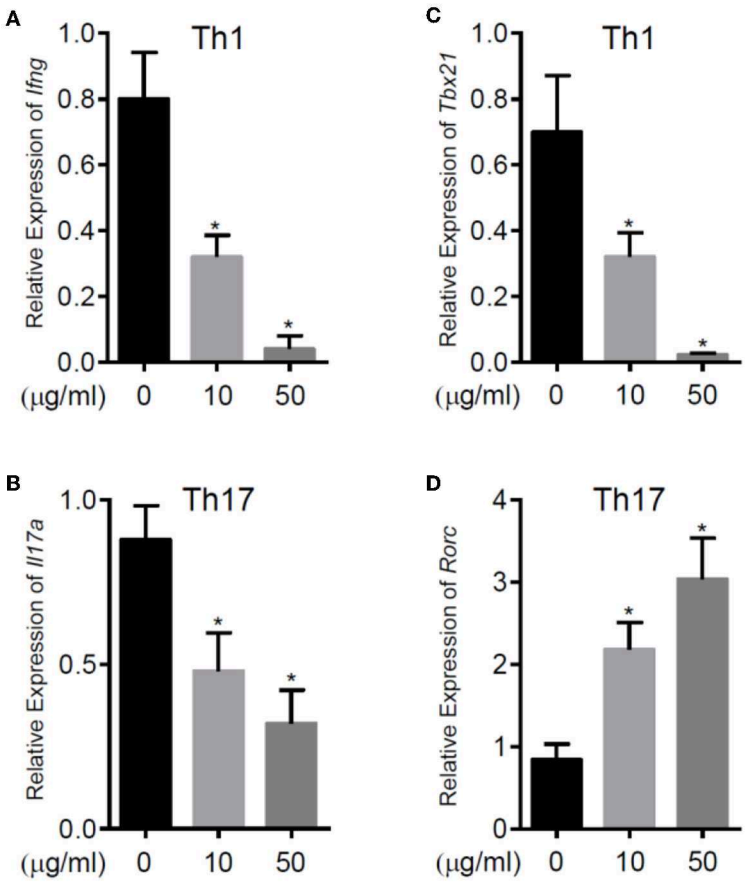

FIGURE 4 | The relative RNA expression of *Ifng* **(A)** and *Tbx21* **(C)** in murine Th1 cells, *Il17a* **(B)** and *Rorc* **(D)** in murine Th17 cells. RNA was extracted from murine $CD4^+$ T cell subsets polarized for 3 days with or without zebularine and evaluated by qRT-PCR. $N = 5$, $^*P < 0.05$.

island (−5782 to −5558): (F: AATG TGGG TATT AGGT AAAA TTTT T; R: AAAC CCTA AAAC TACC TCTA AC), Foxp3 promoter CpG island (−5252 to −5030): (F: TAGG TGAT TGAT AAGT AGGA GAAG TTAG TA; R: TACC CCCA TTAC TTAT AACC ATTTC).

Statistical Analysis

Statistical analysis was performed with Prism Graphpad 7.0 (GraphPad Software, USA). Mann-Whitney *U* test or one-way ANOVA test was used accordingly.

RESULTS

Zebularine Restrains the Expression of IFN-γ and IL-17A in $CD4^+$ T Cells *in vitro*

To assess the effects of zebularine on the expression of proinflammatory cytokines, we first examined the human peripheral $CD4^+$ T cells. FACS-sorted $CD4^+CCR6^-$ and $CD4^+CCR6^+$ cells were stimulated with anti-CD3/anti-CD28 antibodies or under the Th17 polarizing condition, respectively. As shown in **Figure 1**, the frequency of IFN-γ^+IL-17^- cells was significantly reduced in both $CCR6^+$ and $CCR6^-$ cells in response to zebularine treatment (**Figures 1A,B**), while IL-17 expression was restrained by zebularine in a dose dependent manner (**Figures 1A,C,D**). The viability of $CD4^+$ T cells was not significantly affected by zebularine treatment (**Figure 1E**). These data suggest that zebularine is able to control the inflammatory cytokine expression in human $CD4^+$ T cells.

To further explore the immunomodulatory effect of zebularine in murine cells, we differentiated murine peripheral $CD4^+$ T cells into inflammatory Th1 and Th17 conditions. Similar to the findings in human $CD4^+$ T cells, zebularine was found to significantly suppress the protein expression of IFN-γ and IL-17A (**Figures 2A,B**) in murine Th1 and Th17 cells, respectively. However, the cell viability was significantly compromised in response to those high dose zebularine treatments (**Figure 2C**). To confirm the global changes zebularine stimulation may lead to on $CD4^+$ T cells, we performed genome-wide expression analysis of murine Th1 and Th17 cells in response to zebularine stimulation using the mRNA-seq technology. The principal component analysis (**Figure 3A**) and hierarchical clustering analysis (**Figure 3B**) of all of the differentially expressed genes (defined as a two-fold change between any two conditions, with a one-way ANOVA

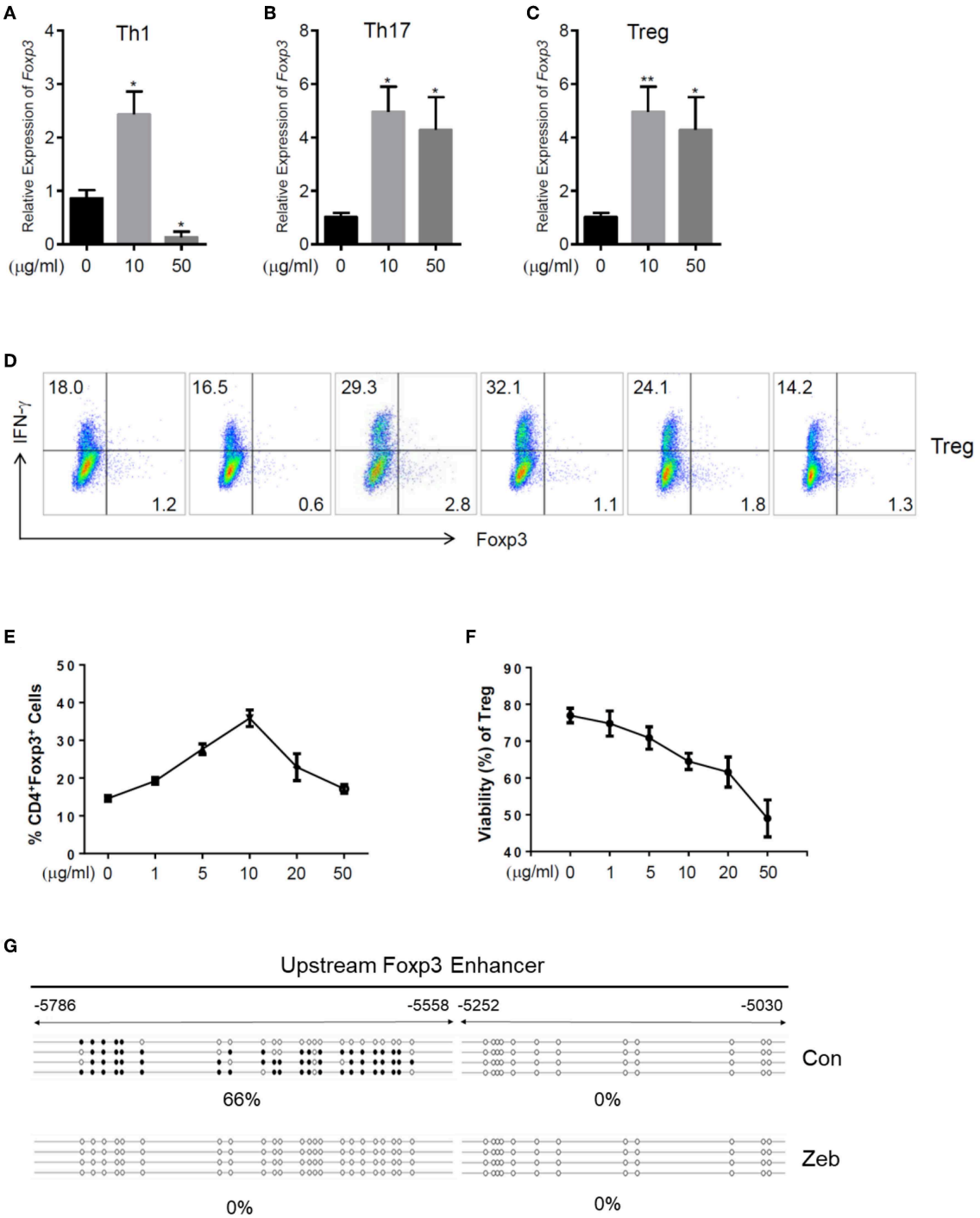

FIGURE 5 | Zebularine promotes the expression of Foxp3 in murine CD4$^+$ T cells *in vitro*. **(A–C)** The relative RNA expression of *Foxp3* in zebularine-treated murine Th1, Th17 and Treg cells $^*P < 0.05$; $^{**}P < 0.01$. **(D)** Representative dot plots ($N = 5$) for murine Treg cells stained with IFN-γ and Foxp3. **(E)** The percentages of Foxp3$^+$ cells in zebularine-treated murine CD4$^+$ T cells. Means ± SD are shown. **(F)** Viability of murine Treg cells treated with different doses of zebularine. Means ± SD are shown. **(G)** Methylation status of the CpG islands located in *Foxp3* enhancer in murine Treg cells treated with zebularine or vehicle. •, methylated CpG; ○, unmethylated CpG.

$P < 0.05$) revealed that zebularine significantly changed global gene expression profiles of Th1 and Th17 cells, in addition to the significant modulation of *Il17a* expression in Th17 cells (**Figure 3C**). We next performed quantitative PCR analysis to confirm the changes of mRNA expression of the inflammatory cytokines and key transcription factor *Tbx21*, which encodes

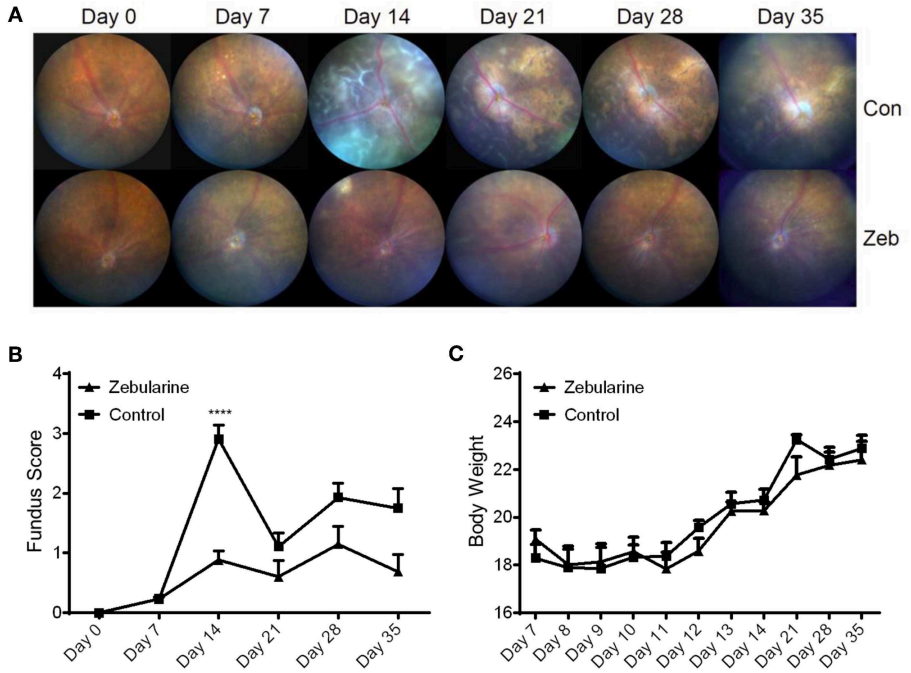

FIGURE 6 | The intraocular inflammation of EAU mice was attenuated by zebularine treatment *in vivo*. The representative fundus images **(A)** and fundus scores **(B)** (means ± SD) of EAU mice treated with zebularine ($N = 10$) or vehicle ($N = 10$) were shown ****$P < 0.0001$. **(C)** Body weights of EAU mice (means ± SD) treated with zebularine ($N = 10$) or vehicle ($N = 10$) were monitored every day during treatment and every week after treatment.

the Th1 master regulator Tbet found by RNA-seq analysis. The expression of *Ifng* (**Figure 4A**), *Tbx21* (**Figure 4C**), and *Il17a* (**Figure 4B**) was significantly decreased by zebularine in Th1 and Th17 cells, respectively, while the relative RNA expression of *Rorc* was increased in Th17 cells in response to zebularine treatment (**Figure 4D**). Taken together, our data demonstrated the immunomodulatory function of zebularine on both human and murine $CD4^+$ T cells *in vitro*.

Zebularine Promotes the Expression of Foxp3 in Murine $CD4^+$ T Cells *in vitro*

In addition to the effects on cytokine expression, we also investigated whether zebularine modulated the expression of Foxp3, the key transcription factor controlling the development and function of Treg (20). The genome-wide expression analysis demonstrated a significant response of Treg cells to the zebularine stimulation (**Figures 3A,B**). As shown in **Figures 3C**, **5A,B**, the RNA expression of *Foxp3* was activated and significantly increased in response to the treatment of zebularine in Th1 and Th17 cells. Under inducible Treg polarizing condition, high dose of zebularine was not able to further elevate the expression of Foxp3 (**Figures 5C–E**). It is noteworthy that zebularine treatment at 10 μg/mL significantly decreased the viability of Th1 cells (**Figure 2C**), while the Treg cells were still highly viable (**Figure 5F**). These data suggest that zebularine promotes the expression of Foxp3 in $CD4^+$ T cells.

The epigenetic regulation of Foxp3 expression by DNA methylation alterations was well documented by previous studies (21). Therefore, we next assessed whether the methylation status of the CpG islands located in *Foxp3* enhancer was changed by zebularine in Treg cells, using the bisulfite sequencing technique. As shown in **Figure 5G**, the *Foxp3* upstream enhancer (−5786 to −5558) was hypermethylated in the vehicle-treated control cells (66% methylated), while all 23 CpG islands were demethylated in cells treated with zebularine (10 μg/mL). These data further demonstrate that zebularine promotes the expression of Foxp3 in $CD4^+$ T cells through demethylating its enhancer region.

Zebularine Controls Intraocular Inflammation *in vivo*

To investigate the anti-inflammatory effect of zebularine *in vivo*, we treated EAU mice intraperitoneally with zebularine and investigated the changes of intraocular inflammation. Fundus examination was performed every 7 days to evaluate the severity of intraocular inflammation in EAU mice. As shown in **Figures 6A,B**, the retinal tissue damage started on Day 7 and peaked at Day 14 post immunization. However, zebularine treatment significantly reduced the severity of intraocular inflammation and retinal tissue damage, evidenced by the fundus clinical score reduction from 2.91 ± 0.24 (vehicle treated group) to 0.88 ± 0.16 (zebularine treated group) on Day 14. Importantly, during the 5 weeks when mice received zebularine treatment, we did not observe any body weight changes (**Figure 6C**). Consistent with the fundus examination result, histological analyses of the retinal tissues from EAU mice on the disease peak Day 14 post immunization revealed that zebularine treatment

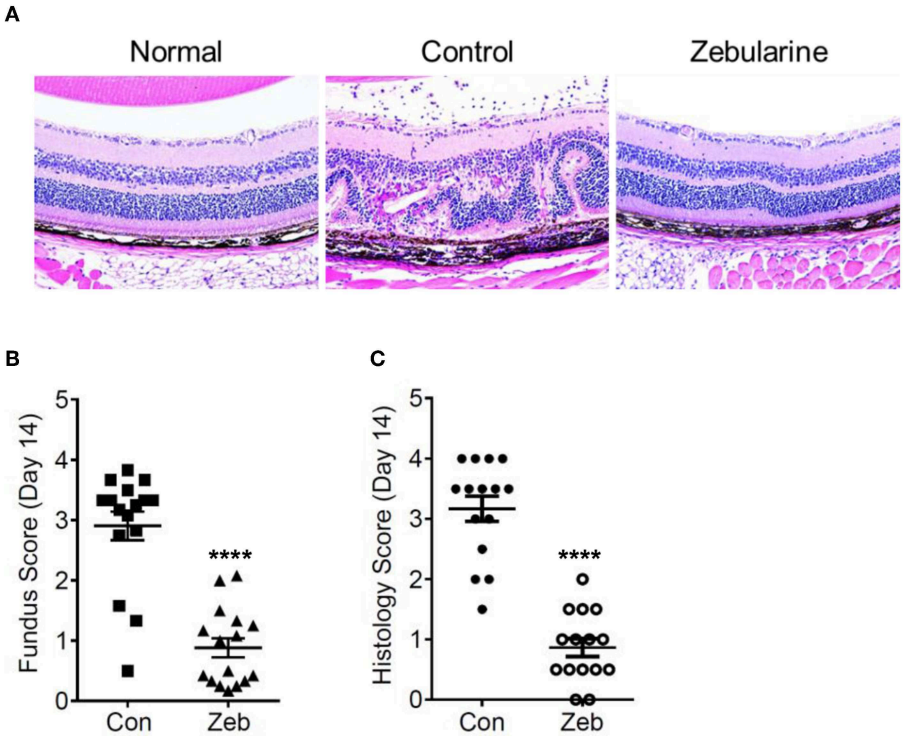

FIGURE 7 | Histological analyses of the retinal tissues from EAU mice treated with zebularine or vehicle on Day 14 post immunization. **(A)** Representative HE histological sections of EAU mice treated with zebularine or vehicle. The fundus scores and histology scores of EAU mice treated with zebularine ($N = 16$) or vehicle ($N = 15$) on Day 14 are shown in **(B,C)**. Means ± SD are shown $^{****}P < 0.0001$.

significantly alleviated intraocular inflammation and retinal tissue damage (**Figures 7A–C**). Taken together, our data suggest that zebularine significantly reduces intraocular inflammation and retinal damage *in vivo*.

Since zebularine restrained inflammatory cytokine expression in $CD4^+$ T cells *in vitro*, we next prepared single cell suspensions from the eyes, cervical lymph nodes (CLN), peripheral lymph nodes (PLN) and spleen of EAU mice treated with or without zebularine on Day 14 post-immunization and analyzed the changes of IFN-γ, IL-17, and Foxp3 expression. As shown in **Figures 8A–E**, the frequency of both intraocular $CD4^+$IFN-γ^+ and $CD4^+$IL-17^+ cells was reduced by zebularine, while the frequency of $CD4^+Foxp3^+$ cells was elevated (**Figures 8B,F**). In contrast, the expression of IFN-γ, IL-17, and Foxp3 was not significantly changed in CLN, PLN, and spleen (**Figures 8A–F**). Therefore, these data further demonstrate that zebularine controls ocular specific inflammation without significantly altering the systemic $CD4^+$ T cell populations.

DISCUSSION

$CD4^+$ T cells mediate systemic and local inflammation in uveitis (22). Our current study suggests that the DNA methylation inhibitor zebularine suppresses the expression of inflammatory cytokines IFN-γ and IL-17 in $CD4^+$ T cells *in vitro* and *in vivo*, promotes Foxp3 expression, and alleviates the severity of intraocular inflammation and retinal tissue damage in EAU mice. To our knowledge, this is the first report showing that zebularine is a potential therapeutic agent for uveitis.

Previous studies have demonstrated the clinical utility of DNA methylation inhibitors in oncology, especially in the treatment of myelodysplastic syndrome and acute myeloid leukemia (12). However, it is only recently that these drugs have been evaluated in the context of experimental models of inflammatory disease (14, 15, 23–27). This showed that systemic administration of the two DNA methylation inhibitors azacytidine and decitabine for treating immune-mediated diseases was limited due to their significant cytotoxicity and side-effects (28). In contrast, our data revealed limited cytotoxicity of zebularine on human $CD4^+$ T cells *in vitro* and limited systemic toxicity of zebularine in mice *in vivo*, suggesting that zebularine may be a better immunosuppressive agent in comparison to the other DNA methylation inhibitors. Importantly, several reports have identified indoleamine 2,3-dioxygenase (IDO) as the targets of zebularine through which zebularine carried out immunomodulatory functions on cancer and autoimmunity treatments (29–31). Our data on $CD4^+$ T cells provided another possible mechanism by which zebularine carried out its immunosuppressive function.

Tbet, RORγt, and Foxp3 are the canonical transcription factors promoting Th1, Th17, and Treg polarization (11). We

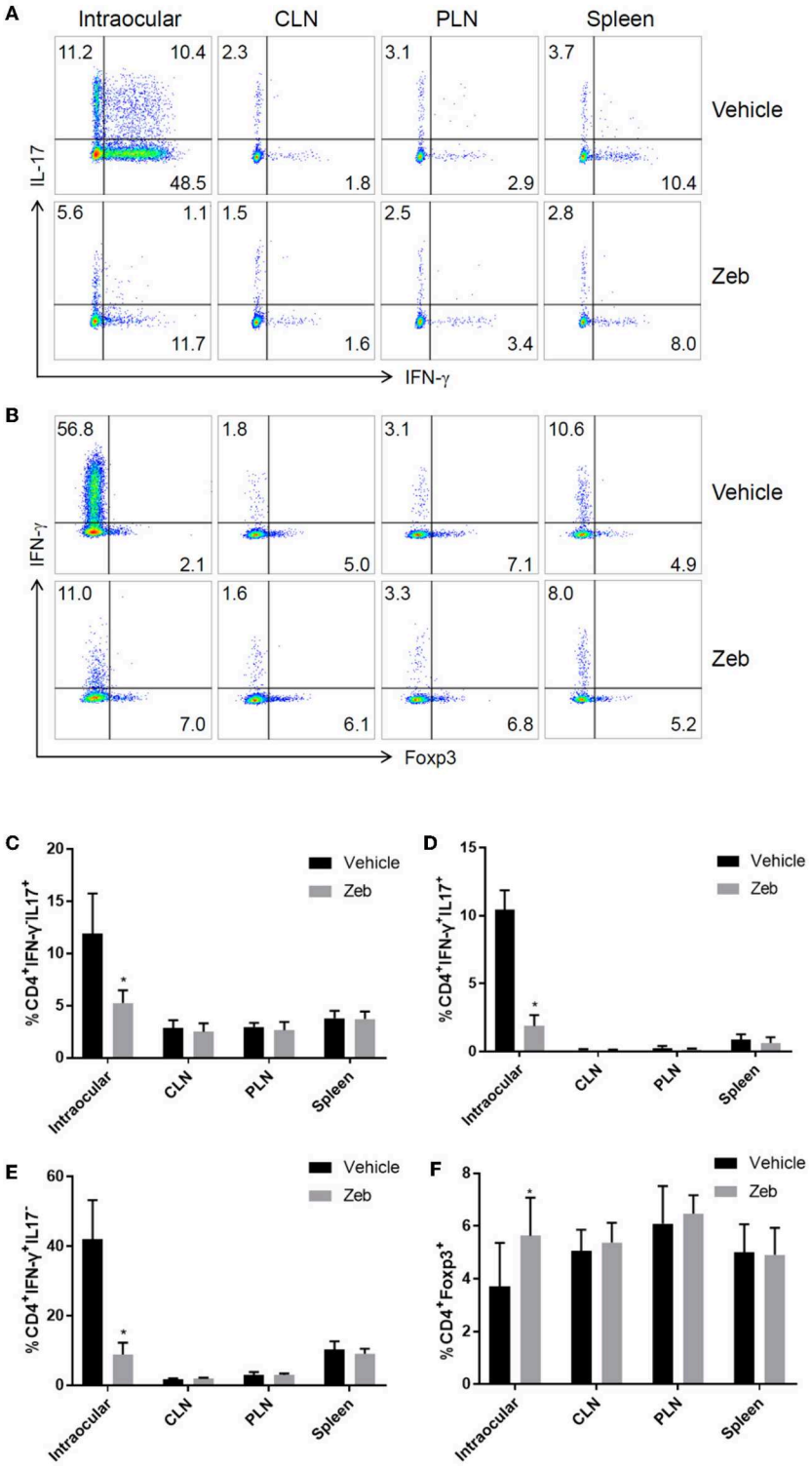

FIGURE 8 | Analysis of $CD4^+$ T cells in inflamed eyes, as well as lymph nodes. **(A,B)** The representative FACS analysis of the frequency of IFN-γ^+, IL-17^+, and $Foxp3^+$ cells in single cell suspensions (pooled from 5 mice) prepared from the eyes, cervical lymph nodes (CLN), peripheral lymph nodes (PLN), and spleens of EAU mice treated with ($N = 5$) or without zebularine ($N = 5$) on Day 14 post-immunization. **(C–F)** Summary of two analysis (total of 10 EAU mice treated with zebularine and 10 without zebularine) of the frequency of IFN-γ^+, IL-17^+, and $Foxp3^+$ cells in eyes and lymph nodes (each analysis represented the pooled cell population from 5 mice per group). *$P < 0.05$, paired T test (student T).

found that zebularine suppressed the expression of *Tbx21* (encoding Tbet), but promoted the expression of *Foxp3* and *Rorc* (encoding RORγt). Suppression of Tbet in Th1 cells correlated well with the significant reduction of IFN-γ in response to zebularine treatment. Promotion of Foxp3 expression, which is consistent with previous reports that other DNA methylation inhibitors also activate Foxp3 expression in murine models of asthma, EAE and diabetes (14, 24, 32, 33), explained the significant alleviation of intraocular inflammation found in EAU mice. However, upregulation of *Rorc* expression seemed contradictory to the reduction of IL-17 expression by zebularine found both *in vitro* and *in vivo*. Although RORγt is the critical transcription factor promoting IL-17 expression and Th17 differentiation, other transcription factors such as STAT3, IRF4, and BATF are also responsible for the coordinated regulation of IL-17 expression (34). Therefore, the suppression of IL-17 expression by zebularine may depend on a RORγt independent pathway.

Our study demonstrates that zebularine restrains IFN-γ and IL-17 expression and promotes Foxp3 expression in $CD4^+$ T cells and may serve as a candidate therapeutic agent for autoimmune uveitis. Further study is warranted to elucidate the molecular mechanisms by which zebularine epigenetically regulates the expression of these key cytokines and transcription factors in T cells.

DATA AVAILABILITY

The datasets generated for this study are available on request to the corresponding author.

ETHICS STATEMENT

$CD4^+$ T cells were obtained from peripheral blood from healthy controls (HCs) following informed consent in accordance with National Health Service Research Ethic Committee approved protocols at the University Hospitals Bristol Foundation Trust, United Kingdom (04/Q2002/84). Written informed consent was obtained from all study participants. All animal experiments were approved by the Institutional Animal Care and Use Committee of Zhongshan Ophthalmic Center. All animal work was performed in compliance with the ARVO Statement for the Use of Animals in Ophthalmic and Vision Research.

AUTHOR CONTRIBUTIONS

LW conceived and designed the experiments. YiL, RL, and LW supervised and coordinated the work. YZ, XH, and LS-B performed most experiments and analyzed data. MS, LM, XG, LY, YaL, PB, XW, and JL provided technical assistance and performed experiments. LW drafted and finalized the manuscript.

FUNDING

National Basic Research Program of China 2015CB964601, Li Foundation Heritage and National Natural Science Foundation of China 81570828 (LW); and the National Institute for Health Research Biomedical Research Centre based at Moorfields Eye Hospital (National Health Service) Foundation Trust and University College London Institute of Ophthalmology (RL).

ACKNOWLEDGMENTS

We thank Dr. Andrew Herman for cell sorting and the University of Bristol Faculty of Biomedical Sciences Flow Cytometry Facility.

SUPPLEMENTARY MATERIAL

The Supplementary Material for this article can be found online at: https://www.frontiersin.org/articles/10.3389/fimmu.2019.01950/full#supplementary-material

REFERENCES

1. Jabs DA, Nussenblatt RB, Rosenbaum JT. Standardization of uveitis nomenclature for reporting clinical data. Results of the First International Workshop. *Am J Ophthalmol*. (2005) 140:509–16. doi: 10.1016/j.ajo.2005.03.057
2. Forrester JV, Klaska IP, Yu T, Kuffova L. Uveitis in mouse and man. *Int Rev Immunol*. (2013) 32:76–96. doi: 10.3109/08830185.2012.747524
3. Lin P, Suhler EB, Rosenbaum JT. The future of uveitis treatment. *Ophthalmology*. (2014) 121:365–76. doi: 10.1016/j.ophtha.2013.08.029
4. Papotto PH, Marengo EB, Sardinha LR, Goldberg AC, Rizzo LV. Immunotherapeutic strategies in autoimmune uveitis. *Autoimmun Rev*. (2014) 13:909–16. doi: 10.1016/j.autrev.2014.05.003
5. Fan H, Morand EF. Targeting the side effects of steroid therapy in autoimmune diseases: the role of GILZ. *Discov Med*. (2012) 13:123–33.
6. Noack M, Miossec P. Th17 and regulatory T cell balance in autoimmune and inflammatory diseases. *Autoimmun Rev*. (2014) 13:668–77. doi: 10.1016/j.autrev.2013.12.004
7. Eisenstein EM, Williams CB. The T(reg)/Th17 cell balance: a new paradigm for autoimmunity. *Pediatr Res*. (2009) 65(5 Pt 2):26R–31R. doi: 10.1203/PDR.0b013e31819e76c7
8. Lee RW, Nicholson LB, Sen HN, Chan CC, Wei L, Nussenblatt RB, et al. Autoimmune and autoinflammatory mechanisms in uveitis. *Semin Immunopathol*. (2014) 36:581–94. doi: 10.1007/s00281-014-0433-9
9. Perez VL, Caspi RR. Immune mechanisms in inflammatory and degenerative eye disease. *Trends Immunol*. (2015) 36:354–63. doi: 10.1016/j.it.2015.04.003
10. Wei G, Wei L, Zhu J, Zang C, Hu-Li J, Yao Z, et al. Global mapping of H3K4me3 and H3K27me3 reveals specificity and plasticity in lineage fate determination of differentiating CD4+ T cells. *Immunity*. (2009) 30:155–67. doi: 10.1016/j.immuni.2008.12.009
11. O'Shea JJ, Paul WE. Mechanisms underlying lineage commitment and plasticity of helper CD4+ T cells. *Science*. (2010) 327:1098–102. doi: 10.1126/science.1178334
12. Tough DF, Tak PP, Tarakhovsky A, Prinjha RK. Epigenetic drug discovery: breaking through the immune barrier. *Nat Rev Drug Discov*. (2016) 15:835–53. doi: 10.1038/nrd.2016.185
13. Christman JK. 5-Azacytidine and 5-aza-2′-deoxycytidine as inhibitors of DNA methylation: mechanistic studies and their implications for cancer therapy. *Oncogene*. (2002) 21:5483–95. doi: 10.1038/sj.onc.1205699
14. Wu CJ, Yang CY, Chen YH, Chen CM, Chen LC, Kuo ML. The DNA methylation inhibitor 5-azacytidine increases regulatory T cells and alleviates airway inflammation in ovalbumin-sensitized mice. *Int Arch Allergy Immunol*. (2013) 160:356–64. doi: 10.1159/000343030
15. Chan MW, Chang CB, Tung CH, Sun J, Suen JL, Wu SF. Low-dose 5-aza-2′-deoxycytidine pretreatment inhibits experimental autoimmune encephalomyelitis by induction of regulatory T cells. *Mol Med*. (2014) 20:248–56. doi: 10.2119/molmed.2013.00159

16. Billam M, Sobolewski MD, Davidson NE. Effects of a novel DNA methyltransferase inhibitor zebularine on human breast cancer cells. *Breast Cancer Res Treat*. (2010) 120:581–92. doi: 10.1007/s10549-009-0420-3
17. Zhu J, Paul WE. Heterogeneity and plasticity of T helper cells. *Cell Res*. (2010) 20:4–12. doi: 10.1038/cr.2009.138
18. Zhang W, Li Y, Lin J, Wan S, Gao H, Zhang L, et al. Comparison of hematoxylin-eosin staining and methyl violet staining for displaying ghost cells. *Eye Sci*. (2013) 28:140–3.
19. Agarwal RK, Silver PB, Caspi RR. Rodent models of experimental autoimmune uveitis. *Methods Mol Biol*. (2012) 900:443–69. doi: 10.1007/978-1-60761-720-4_22
20. Huehn J, Polansky JK, Hamann A. Epigenetic control of FOXP3 expression: the key to a stable regulatory T-cell lineage? *Nat Rev Immunol*. (2009) 9:83–9. doi: 10.1038/nri2474
21. Morikawa H, Sakaguchi S. Genetic and epigenetic basis of Treg cell development and function: from a FoxP3-centered view to an epigenome-defined view of natural Treg cells. *Immunol Rev*. (2014) 259:192–205. doi: 10.1111/imr.12174
22. Luger D, Caspi RR. New perspectives on effector mechanisms in uveitis. *Semin Immunopathol*. (2008) 30:135–43. doi: 10.1007/s00281-008-0108-5
23. Mangano K, Fagone P, Bendtzen K, Meroni PL, Quattrocchi C, Mammana S, et al. Hypomethylating agent 5-aza-2′-deoxycytidine (DAC) ameliorates multiple sclerosis in mouse models. *J Cell Physiol*. (2014) 229:1918–25. doi: 10.1002/jcp.24641
24. Zheng Q, Xu Y, Liu Y, Zhang B, Li X, Guo F, et al. Induction of Foxp3 demethylation increases regulatory CD4+CD25+ T cells and prevents the occurrence of diabetes in mice. *J Mol Med*. (2009) 87:1191–205. doi: 10.1007/s00109-009-0530-8
25. Dunn J, Qiu H, Kim S, Jjingo D, Hoffman R, Kim CW, et al. Flow-dependent epigenetic DNA methylation regulates endothelial gene expression and atherosclerosis. *J Clin Invest*. (2014) 124:3187–99. doi: 10.1172/JCI74792
26. Cao Q, Wang X, Jia L, Mondal AK, Diallo A, Hawkins GA, et al. Inhibiting DNA Methylation by 5-Aza-2′-deoxycytidine ameliorates atherosclerosis through suppressing macrophage inflammation. *Endocrinology*. (2014) 155:4925–38. doi: 10.1210/en.2014-1595
27. Guo H, Wang W, Zhao N, He X, Zhu L, Jiang X. Inhibiting cardiac allograft rejection with interleukin-35 therapy combined with decitabine treatment in mice. *Transpl Immunol*. (2013) 29:99–104. doi: 10.1016/j.trim.2013.10.001
28. Issa JP, Garcia-Manero G, Giles FJ, Mannari R, Thomas D, Faderl S, et al. Phase 1 study of low-dose prolonged exposure schedules of the hypomethylating agent 5-aza-2′-deoxycytidine (decitabine) in hematopoietic malignancies. *Blood*. (2004) 103:1635–40. doi: 10.1182/blood-2003-03-0687
29. Liu H, Xue ZT, Sjögren HO, Salford LG, Widegren B. Low dose Zebularine treatment enhances immunogenicity of tumor cells. *Cancer Lett*. (2007) 257:107–15. doi: 10.1016/j.canlet.2007.07.013
30. Nittby H, Ericsson P, Förnvik K, Strömblad S, Jansson L, Xue Z, et al. Zebularine induces long-term survival of pancreatic islet allotransplants in streptozotocin treated diabetic rats. *PLoS ONE* 8:e71981. doi: 10.1371/journal.pone.0071981
31. Xue ZT, Sjögren HO, Salford LG, Widegren B. An epigenetic mechanism for high, synergistic expression of indoleamine 2,3-dioxygenase 1 (IDO1) by combined treatment with zebularine and IFN-gamma: potential therapeutic use in autoimmune diseases. *Mol Immunol*. (2012) 51:101–11. doi: 10.1016/j.molimm.2012.01.006
32. Kennedy A, Schmidt EM, Cribbs AP, Penn H, Amjadi P, Syed K, et al. A novel upstream enhancer of FOXP3, sensitive to methylation-induced silencing, exhibits dysregulated methylation in rheumatoid arthritis Treg cells. *Eur J Immunol*. (2014) 44:2968–78. doi: 10.1002/eji.201444453
33. Someya K, Nakatsukasa H, Ito M, Kondo T, Tateda KI, Akanuma T, et al. Improvement of Foxp3 stability through CNS2 demethylation by TET enzyme induction and activation. *Int Immunol*. (2017) 29:365–75. doi: 10.1093/intimm/dxx049
34. Ciofani M, Madar A, Galan C, Sellars M, Mace K, Pauli F, et al. A validated regulatory network for Th17 cell specification. *Cell*. (2012) 151:289–303. doi: 10.1016/j.cell.2012.09.016

Conflict of Interest Statement: The authors declare that the research was conducted in the absence of any commercial or financial relationships that could be construed as a potential conflict of interest.

frontiers in Immunology

REVIEW
published: 20 August 2019
doi: 10.3389/fimmu.2019.01975

Microglia in Retinal Degeneration

Khalid Rashid[1], *Isha Akhtar-Schaefer*[1] *and Thomas Langmann*[1,2]*

[1] *Laboratory for Experimental Immunology of the Eye, Department of Ophthalmology, Faculty of Medicine and University Hospital Cologne, University of Cologne, Cologne, Germany,* [2] *Center for Molecular Medicine Cologne, Cologne, Germany*

The retina is a complex tissue with multiple cell layers that are highly ordered. Its sophisticated structure makes it especially sensitive to external or internal perturbations that exceed the homeostatic range. This necessitates the continuous surveillance of the retina for the detection of noxious stimuli. This task is mainly performed by microglia cells, the resident tissue macrophages which confer neuroprotection against transient pathophysiological insults. However, under sustained pathological stimuli, microglial inflammatory responses become dysregulated, often worsening disease pathology. In this review, we provide an overview of recent studies that depict microglial responses in diverse retinal pathologies that have degeneration and chronic immune reactions as key pathophysiological components. We also discuss innovative immunomodulatory therapy strategies that dampen the detrimental immunological responses to improve disease outcome.

Keywords: retina, microglia, neuroprotection, chronic inflammation, immunomodulation

OPEN ACCESS

Edited by:
Heping Xu,
Queen's University Belfast,
United Kingdom

Reviewed by:
Wai T. Wong,
National Eye Institute (NEI),
United States
Przemyslaw Sapieha,
Université de Montréal, Canada

***Correspondence:**
Thomas Langmann
thomas.langmann@uk-koeln.de

Specialty section:
This article was submitted to Immunological Tolerance and Regulation, a section of the journal Frontiers in Immunology

Received: *27 May 2019*
Accepted: *05 August 2019*
Published: *20 August 2019*

Citation:
Rashid K, Akhtar-Schaefer I and Langmann T (2019) Microglia in Retinal Degeneration. Front. Immunol. 10:1975. doi: 10.3389/fimmu.2019.01975

INTRODUCTION

The retina is part of the central nervous system with more than 60 distinct retinal cell types, high level organization, and a evolutionarily conserved structure (1, 2). The mammalian retina contains three distinct glia cells types; Müller cells, astrocytes, and microglia (3, 4). Müller cells are specialized radial cells that span all retinal layers and account for about 90% of the retinal glia population (3, 5). They support functioning and metabolism of retinal neurons by releasing trophic factors, recycling neurotransmitter glutamate, and controlling extracellular ion homeostasis (6). Retinal astrocytes perform similar functions to Müller cells, ranging from neurotrophic, metabolic and mechanical support of neurons, and maintenance of the blood retinal barrier (3, 7). Retinal astrocytes are however almost entirely restricted to the nerve fiber layer, and to a lesser extent to the ganglion cell layer (7, 8). Microglia, the third glial cell type, represent the resident tissue macrophages and play important roles in retinal homeostasis, recovery from injury and progression of disease (9, 10).

As early as 1897, Spanish neuroscientist Ramón y Cajal began to appreciate that there were more cell types in the brain than just neurons and astrocytes (11, 12). In pursuit of this hypothesis, he developed the gold chloride sublimate staining approach that labeled astrocytes and other cells that he named the "third element" (12, 13). Del Río-Hortega, another Spanish neuroscientist later separated the cells in the "third element," becoming the first scientist to describe microglia as distinct cellular entity (12, 14). He described their ramified morphology in the normal brain using elegant drawings and provided evidence of their morphological transformations during tissue brain pathology (12, 14). These tremendous findings have withstood the test of time and remain highly relevant today.

In the normal retina, microglia cells are located in the plexiform layers where they exhibit elaborate ramified processes responsible for immune surveillance of the retina (4). Noxious insults

in the retina such as oxidative stress, hypoxia or inherited mutations trigger microglia reactivity manifested by amoeboid morphology, increased proliferation and migration to the sites of injury (10, 15). While this initial "constructive" inflammatory response can rapidly enhance tissue repair and return to homeostasis, sustained microglial inflammatory responses can instigate severe alterations in retinal integrity, and aggravate neuronal demise (16). This review therefore offers a comprehensive overview on the dual role of microglia in the retina, examining their contribution in various retinal neurodegenerative disorders and in aging and parainflammation. In addition, we discuss recent strategies that have been shown to suppress microglial inflammatory responses in the retina and prevent neuronal cell death.

ORIGIN AND MAINTENANCE OF MICROGLIA IN THE RETINA

Earlier attempts to find answers to the uncertainties existing around the origin and maintenance of retinal microglia were made by transplanting bone marrow (BM) derived cells from eGFP-transgenic mice into irradiated normal adult mice (17). Retinal flat mounts of the recipient mice were found to contain BM derived eGFP$^+$ cells as early as 8-weeks post transplantation, and by the 6th month, all retinal myeloid cells were eGFP$^+$ (17). Using *CX3CR1-GFP/+* mice as BM donors, where GFP expression is restricted to monocyte lineage cells, a separate study observed recruitment of monocyte-derived cells into the retinal tissue 4 weeks post-transplantation (18). Of note, both studies observed that under steady state conditions, retinal microglia exhibited very low proliferation rates (17, 18). However, in a separate study where mice were irradiated and injected with eGFP+ BM cells prior to induction of retinal injury, only a minute number of donor cells were observed in the uninjured normal retina up to 12 months following BM transplantation (19). In contrast, a massive recruitment of BM derived cells into the retina was observed following injury (19). The authors partially attributed the low recruitment of donor cells to the uninjured eye to shielding eyes and heads of mice prior to irradiation (19). They argued that in the previous experiments, irradiation could have unintentionally damaged photoreceptors and enhanced migration of BM-derived cells to the injured retina (19). Indeed, additional factors not mentioned by the authors, such as large amounts of circulating cytokines, CNS vascular changes, and temporary disruptions of the blood-brain barrier alterations may confound interpretation of results following irradiation (20, 21).

Therefore, to further analyse the contribution of circulating BM derived progenitors on the turnover of resident microglia in the CNS, a separate study employed parabiosis experiments (22). Parabiosis, the surgical joining of two organisms, allowed for the sharing of the blood circulation between wild type and GFP transgenic mice without affecting their blood-brain nor the blood-retinal barrier (21–23). The obtained results revealed that under steady-state conditions, CNS microglia were a closed system with the capacity to self-renew and were not replenished by BM derived cells (22). Indeed, it was later established that microglia were derived from primitive myeloid progenitors originating from the yolk sac and that postnatal hematopoietic progenitors did not significantly contribute to microglia homeostasis (24).

A subsequent study (25) demonstrated that the brain harbored latent nestin$^+$ microglial progenitors throughout the CNS (25). Pharmacological depletion of microglia using selective CSF1R inhibitor PLX3397 triggered rapid proliferation of nestin$^+$ cells throughout the CNS, which later differentiated into microglia and repopulated the entire brain within 1 week of inhibitor cessation (25). Interestingly, this regeneration mirrored some aspects of normal development, as embryonic stem cells require a nestin$^+$ stage on their way to becoming microglia (25, 26). However, subsequent microglia ablation studies have strongly disputed the presence of nestin$^+$ microglia progenitor cells and instead provide evidence that microglia repopulation following pharmacological or genetic depletion occurs solely from residual non-depleted internal pools which exert massive proliferation and transiently express nestin (27–29). Similarly, retinas depleted of microglia using selective CSF1R inhibitor PLX5622 were not repopulated from nestin$^+$ precursors (30, 31). Rather, repopulated retinal microglia exhibited dual extra retinal origins; first from residual microglia in the optic nerve and secondly from ciliary body/iris macrophages (30). Residual optic nerve microglia repopulated the retina along the center-to-periphery axis, while macrophages in the ciliary body/iris repopulated the retina along the periphery and accounted for around 15% of the repopulated microglia (30). Of note, these findings uncovered for the first time radial migratory routes of retinal microglia and demonstrated the presence of peripheral macrophage-derived microglia which were significantly less ramified than their central counterparts (30). In a parallel study, it was shown that microglia repopulation in the retina was regulated via neuronal-microglial crosstalk in the form of CX3CL1-CX3CR1 signaling which potentiated microglia proliferation and morphological maturation (31). Most importantly, the latter study demonstrated that that the repopulated cells fully restored microglia functions in the retina including immunosurveillance and synaptic maintenance (31).

MICROGLIA IN THE HEALTHY RETINA

Microglial cells play active roles in maintaining the normal structure and functioning of the retina. During retinal development, microglia cells are largely confined to the ganglion cell layer and inner plexiform layer, where they phagocytose cellular corpses of excessively produced retinal ganglion cells (RGCs) early in development (32). Moreover, in the early postnatal stages when there is a robust synaptic remodeling, microglia are involved in pruning of weak presynaptic terminals of RGCs (33). This process occurs in a complement C3-CR3-dependent mechanism, where activated C3 (iC3b/C3b) selectively labels the weak RGCs terminals triggering a C3-receptor dependent phagocytosis pathway in microglia (4, 33). Importantly, microglial dependent apoptosis

of RGCs and the elimination of costly neural connections deemed unfit for proper functioning plays a crucial role in the normal postnatal development of the retina and cortical visual areas (32, 33).

Following the development phase, microglia cells move to occupy the inner and outer plexiform layers where they adopt a quiescent phenotype characterized by very small somata and extensively ramified filopodia-like processes (4). They form a mosaic network of evenly distributed non-overlapping cells that provide immunological surveillance to the entire retina by the continuous movement of their processes (4, 34). It is also possible that the dynamic activity of the filopodial structures serves a housekeeping function, enabling microglia eliminate accumulated waste metabolic products and cellular debris in the retinal microenvironment (35). In addition, the extensive processes facilitate close relationships with other retinal cells such as the neurons, promoting the maintenance of their synaptic structures and neurotransmission (3, 36). Indeed, sustained microglia depletion in the retina has been shown to result in the degeneration of photoreceptor synapses with subsequent progressive decline in the magnitude of electroretinographic responses to light stimuli (36).

Cross-talk between microglia and other retinal cells is enabled by the assortment of cell surface molecules on the microglial cell membrane (4, 37). These surface proteins are key regulators of tissue homeostasis that limit unnecessary microglia activation in the healthy retina (9). CD200-CD200R interaction is an important example that induces a negative inhibitory signal to restrain microglia from tissue damaging activation (38, 39). CD200 (previously known as OX2) is a broadly expressed membrane glycoprotein in ganglion cells, photoreceptors, vascular endothelium and the retinal pigment epithelium (RPE), while its receptor, CD200R, is predominantly expressed in retinal microglia (4, 9, 40). Studies on mice lacking CD200 have reported heightened pro-inflammatory responses in experimental animal models of uveoretinitis and exudative form of age related macular degeneration (38–40). Conversely, enhancement of CD200R signaling ameliorates pathological outcome in optic nerve injury and experimental autoimmune uveoretinitis animal models, suggesting that CD200-CD200R interaction could be an exploitable avenue for therapeutic intervention (39, 41).

Sialic acids, covalently linked to cellular membrane proteins and lipids, also contribute to the inhibition of the innate immune system in the CNS including the retina (42, 43). The interaction between polysialic acid chains (PSA) present on the glycocalyx of healthy neurons and Sialic acid binding immunoglobulin-like lectin 11 (Siglec11) receptor of microglia restricts unwanted microglial activation in the brain and retina (42, 44). The inhibitory signals are propagated via immunoreceptor tyrosine-based inhibitory motifs (ITIM) contained in the cytosolic domain of Siglec-11 in microglia (43). Therefore, given its immunomodulatory capacity, several studies have reported Siglec-11-ITIM mediated neuroprotective effects which will be discussed further later in this review (42, 44, 45).

A further neuroimmune regulator is CX3CL1 (fractalkine), a constitutively expressed neuron derived chemokine which binds to its sole receptor CX3CR1 present in microglia and maintains them in a quiescent mode (46). Indeed, numerous studies have demonstrated the immunomodulatory and neuroprotective effects of CX3CL1-CX3CR1 interaction in the brain and retina (46, 47). For instance, transplantation of mesenchymal stem cells engineered to secrete CX3CR1 in the subretinal space inhibited microglial activation and expression of pro-inflammatory factors in light-induced retinal degeneration in rats (48). In contrast, deletion of CX3CR1 in an rd10 retinal degeneration mouse model augmented microglial activation and infiltration into the photoreceptor layers with concomitant increase in photoreceptor demise (49). Remarkably, delivery of exogenous CX3CL1 to the rd10 mouse eye significantly slowed down the tempo of photoreceptor demise, underscoring CX3CL1-CX3CR1 signaling axis as an influential regulator of microglial activity (49).

Microglia also exchange functionally significant signals with Müller cells both in health and disease states, and this bidirectional communication can act as mediator of neuron-microglia crosstalk [**Figure 1**; (50, 51)]. Indeed, previous studies had demonstrated that certain microglia-derived neurotrophic factors such as BDNF and CNTF were neuroprotective for photoreceptor cells despite these cells not expressing their receptors (52–55). Subsequent studies later established that microglia derived neurotrophic factors interact with Müller cells and induce or inhibit the release of secondary factors including basic fibroblast growth factor (bFGF), leukemia inhibitory factor (LIF) and glial cell line-derived neurotrophic factor (GDNF) that could act directly on photoreceptors and mediate survival or apoptosis during stress conditions in the retina (56–60). Recent investigations have also revealed additional microglia-Müller cell cross-talk via translocator protein (TSPO; 18 kDa) signaling axis, where Müller cells release TSPO's endogenous ligand, diazepam binding inhibitor (DBI) protein, which binds microglial TSPO and suppresses microglial activation during retinal pathology (61).

As a result of the heterocellular signaling and crosstalk in the retina, microglia cells are rendered extremely sensitive to slight changes in their environment, demanding efficient inhibitory mechanisms to maintain them in a quiescent neuroprotective state (4). RPE cells prominently support the maintenance of an immunosuppressive intraocular environment by secreting inhibitory factors into the subretinal space between the neural retina-RPE interface (62). This blocks the undesirable infiltration of microglia cells and other mononuclear phagocytes into the photoreceptor layers and subretinal space, rendering these regions devoid of immune cells in the healthy retina (10, 63). Conversely, in both wet and dry forms of age related macular degeneration, there is an accumulation of mononuclear phagocytes in the subretinal space where they may contribute to disease pathogenesis (63). Some of the inhibitory factors released by RPE cells into the subretinal space include transforming growth factor-β (TGF-β), thrombospondin-1 (TSP-1) and somatostatin (SOM) (64–66).

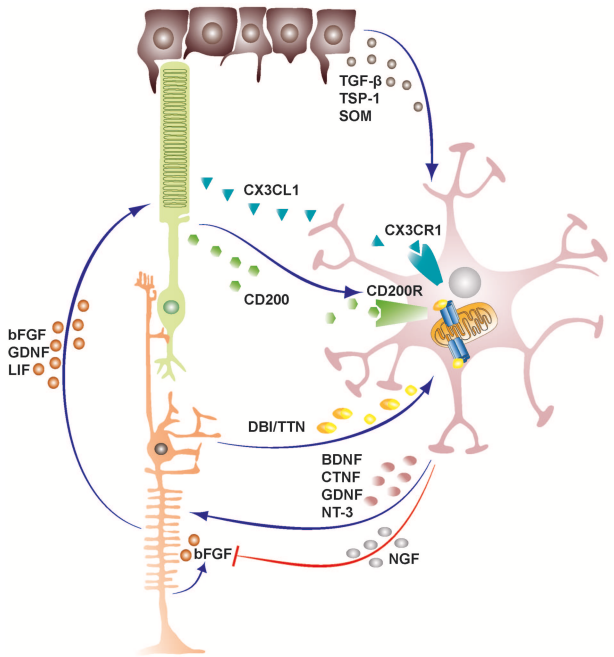

FIGURE 1 | Schematic representation depicting cellular cross-talk between retinal cells and microglia. Retinal cells constantly communicate with microglia via various soluble factors and receptors to restrain microglia from tissue damaging activation and maintain them in a quiescent protective state. The bidirectional communicational between microglia and Müller cells can act as a mediator of neuron-microglia crosstalk. Microglia derived factors may either induce or inhibit release of secondary factors from Müller cells. TGF-β, transforming growth factor beta; TSP-1, thrombospondin-1; SOM, somatostatin; DBI, diazepine binding inhibitor; TTN, triakontatetraneuropeptide; BDNF, brain derived neurotrophic factor; CTNF, ciliary neurotrophic factor; GDNF, glial cell line-derived neurotrophic factor; NT-3, neurotrophin-3; NGF, nerve growth factor; bFGF, basic fibroblast growth factor; LIF, leukemia inhibitory factor.

MICROGLIA IN THE DISEASED RETINA

A sustained chronic pro-inflammatory environment is an important common denominator of retinal degenerative diseases and neurological disorders that affect vision (10). Neuroinflammatory responses in the retina are orchestrated by microglial cells which constitute the resident immune cell population (67). Under acute conditions, microglia-mediated neuroinflammation promotes neuroprotection and regenerative processes and facilitates a rapid return to tissue homeostasis (68, 69). However, under chronic conditions where the insult persists over time, such as in retinal degenerative disorders, microglia become pathologically activated and release exaggerated amounts of inflammatory mediators that promote tissue damage and disease exacerbation (16, 68, 70). Consequently, modulation of microglial reactivity has emerged over the years as a promising therapeutic approach to attenuate neuronal demise and potentially slow down the onset and progression of retinal degenerative diseases. Therefore, the next sections will discuss the role microglia-related mechanisms in major retinal degenerative diseases like age-related macular degeneration, hereditary retinopathies, glaucoma, diabetic retinopathy as well as in aging. In addition, promising regimens that have shown potent immunomodulatory effects in animal models of retinal diseases and/or in human tissue culture as well as patient studies will be discussed.

Microglia in Age Related Macular Degeneration

AMD, with a global prevalence of ∼170 million people, refers to a progressive deterioration of the macula (71). It is a neurodegenerative disease with a multifactorial etiology and is currently considered the leading cause of debilitating vision loss among the elderly (72). Early clinical features of the disease includes fundoscopic manifestation of drusen between the RPE and Bruch's Membrane and fundus autofluorescence that derives primarily from accumulation of lipofuscin granules in the RPE (73, 74). Unfortunately, 15% of patients presenting with early AMD symptoms will advance to the late stages of the disease which progresses in two main forms; (I) Neovascular or "wet" AMD characterized by the ingrowth of immature leaky choroidal blood vessel through the RPE and into the avascular outer retina and (II) Geographic atrophy or "dry" AMD characterized by deterioration of the RPE and associated support functions around the macula with concomitant loss of the overlying photoreceptors (75, 76). While effective treatments involving the inhibition of vascular endothelial growth factor (VEGF) exist for wet AMD, no truly effective form of treatment is available for dry AMD form which affects the majority of patients (77).

There is substantial evidence to indicate the involvement of inflammation and dysregulated innate immunity in the pathogenesis of AMD (73, 75, 78). Dysregulated innate immunity in AMD is associated with complement factors, inflammasome activation, and reactive microglia (71). Wet AMD patients for instance show elevated levels of complement fragments C3a and Ba as well as a wide range of cytokines in their aqueous humor (73, 79). Similarly, soft drusen from AMD donors contain bioactive fragments of complement components C3a and C5a which can induce VEGF expression and predispose patients to choroidal neovascularization (CNV) (80). Drusen from AMD donors can induce inflammasome activation in myeloid and mononuclear cells, suggesting that macular drusen in AMD is a potent pro-inflammatory stimulus (81). Indeed, the widespread accumulation of drusen components as seen in AMD is a prominent chemoattractant stimulus for microglia cells which results in their translocation to the subretinal space (82–84).

Consistently, enlarged amoeboid microglia have been found in the vicinity of RPE cells overlying drusen in retinal sections from dry AMD patients (70). In the outer retina, reactive microglia or microglia-derived factors can induce NLRP3 inflammasome activation in RPE cells with concomitant secretion of the proinflammatory cytokine IL-1β (85–87). NLRP3 inflammasome activation can subsequently induce RPE degeneration via caspase-1-mediated pyroptosis, contributing to AMD pathology (88). Notably, human ocular tissue sections from geographic atrophy or neovascular AMD donors exhibit NLRP3 inflammasome activation (88). Eventually, RPE degeneration

causes secondary photoreceptor cell death, resulting in loss of visual function (75). Moreover, the pro-inflammatory environment fostered by accumulating subretinal microglia can directly induce death of nearby photoreceptors (89). We have indeed demonstrated on several instances that conditioned medium from reactive human and murine microglial cells triggers caspase-mediated photoreceptor cell death (85, 90). These findings therefore strongly suggest that microglia reactivity is a driving force in photoreceptor degeneration and progression of retinal degenerative disorders.

Indeed, the role of microglial reactivity in severity of disease has been clearly demonstrated in several mouse models of AMD. However, it is important to note that conclusions drawn from these studies are limited in nature since rodents lack an anatomical macula. Nonetheless, these models effectively mimic distinct features of human pathology including accumulation of immune cells such as macrophages or microglia in the subretinal space, photoreceptor degeneration, choroidal neovascularization, funduscopically visible drusen-like lesions, and RPE degeneration (91). We will therefore discuss a few of these models here to highlight the crucial role played by microglia in AMD pathogenesis. However, for a more detailed discussion on the animal models of AMD, the reader is directed to other articles (91–93).

Bright white light for example can be used to mimic the photoreceptor cell death and retinal degeneration witnessed in human AMD patients (94). Intense light causes bleaching of rhodopsin and excessive phototransduction signaling, resulting in photoreceptor apoptosis in an AP-1 dependent manner (94, 95). This is followed by a robust migration of microglia to the outer retina, making the light-damage model useful for studying physiological as well as pathological consequences of reactive microglia accumulation in the subretinal space as seen in human AMD patients (70). Of note is that microglial activation states and morphological changes are early events that precede recruitment to the outer retina following light induced damage (96). This recruitment of microglia to the outer retina following light damage is mediated in-part by chemokines (C-C motif) ligand 2 (Ccl2) (97) and (C-X3-C motif) ligand 1 (Cx3cl1/fractalkine) (98) and by the complement anaphylatoxin receptor C5aR (99). Once in the subretinal space, microglia and other mononuclear phagocytes enhance their phagocytic capacity and produce high levels of pro-inflammatory factors including IL-1β, TNF-α, IL-6, CCL2, and iNOS (100). An overt consequence of this massive recruitment of amoeboid microglia in the subretinal space is a severe thinning of the outer nuclear layer as a result of photoreceptor degeneration via pro-inflammatory and phagocytosis mechanisms (16, 61, 89).

Another useful model for dry AMD is generated by immunizing mice with carboxyethylpyrrole (CEP)-adducted proteins (101). CEP is an oxidation product of docosahexaenoic acid (DHA) and is present in the eyes of AMD patients and in their serum at higher levels than in age-matched non-AMD controls (91, 101). This model mimics many aspects of the dry AMD pathology observed in human patients, including presence of sub-RPE drusen like deposits, RPE degeneration and infiltration of phagcoytes around hypertrophied photoreceptors and degenerating RPE (102). However in this model, RPE atrophy is more pronounced in regions devoid of immune cells in their vicinity, suggesting that subretinal mononuclear phagocytes are not involved in initiating RPE pathology, but may rather exert beneficial effects by removing debris released from apoptotic corpses of RPE cells (102). Indeed, some of the infiltrating macrophages found in the subretinal space contained melanin pigment, confirming RPE engulfment (102). This model could therefore be useful in understanding what processes or factors tips the scales toward neurotoxic damaging phagocytes in subretinal microglia.

To study microglial immune responses in wet AMD, a laser induced bruch's membrane photocoagulation model is used (71). Briefly, laser photocoagulation results in the rupture of Bruch's membrane, leading to the ingrowth of immature leaky blood vessels into the outer avascular retina (103). A local inflammatory reaction is triggered at the laser burn site and is accompanied by a rapid recruitment and accumulation of amoeboid microglia and other mononuclear phagocytes (104–106). The recruited mononuclear phagocytes produce high levels of pro-inflammatory cytokines and the pro-angiogenic factor VEGF, worsening disease progression and severity (104, 105). Indeed, blocking the VEGF receptor signaling significantly inhibits microglia accumulation in the laser spots with concomitant reduction in CNV (107). Conversely, blocking ifnar1/IFN-β or CX3CR1 signaling drastically enhances microglia reactivity and recruitment to the laser lesion site, exacerbating the development of CNV lesions in mice (104, 105).

Microglia in Hereditary Retinopathies

Hereditary degenerations of the human retina are a diverse group of clinically and genetically heterogeneous blinding diseases with more than 260 causal genes identified to date (108). Inherited retinopathies are mostly monogenic, with the causal mutations predominantly occurring in genes expressed in photoreceptors and RPE (4, 109). The most prevalent and severe form of inherited retinopathies is retinitis pigmentosa (RP), where vision loss is brought about by primary degeneration of rods, followed by the degeneration of cones (110). Microglia in human RP patients become reactive in response to signals from degenerating rods and migrate to the photoreceptor layers (70). These bloated microglia in the outer retina of RP patients engage in the phagocytosis of rod debris, as evidenced by their rhodopsin intracellular inclusions (70). In addition to phagocytosis of degenerate cells (70), proposed these reactive microglia in the outer retina exacerbate photoreceptor cell death including adjacent healthy cones by secreting pro-inflammatory neurotoxic factors. Using animal models that recapitulate aspects of human disease, scientists have proven this hypothesis and demonstrated accumulation of reactive microglia in the degenerating retinas that produce high levels pro-inflammatory cytokines and chemokines aggravating photoreceptor demise.

The rodless mouse, discovered approximately 93 years ago by the medical geneticist Keeler, was the first ever reported murine model of retinal degeneration (111). This natural mouse line carries a nonsense mutation in the *Pde6b* gene that codes for the β-subunit of cGMP phosphodiesterase (PDE), and mimics

to a great extent the RP in human patients bearing mutations in the human homolog of the gene (112). Rd1 mice display an early onset and a rapid rate of photoreceptor degeneration, such that by 4 weeks of age, only a single layer of photoreceptors consisting predominantly of cone photoreceptors is left in the outer nuclear layer (113). Microglia cells are present in the outer nuclear layer of the photoreceptors by post-natal day 10 where they exhibit a highly proliferative capacity (114). Of note is that their distribution coincides with the spatiotemporal pattern of photoreceptor cell death, implying that microglial cells are intimately engaged with the degenerative process and are not mere bystanders of disease (114). During their migration to the outer nuclear layer of the photoreceptors, microglia lose their filopodial-like processes, and by the time they emerge in the subretinal space, they are fully transformed into amoeboid phagocytes whose pseudopodia can often be seen (114). These bloated infiltrating microglia have been shown to secrete high levels of TNF-α, chemokines CCL2 (alias MCP-1) and (CCL5, alias RANTES) accentuating the ongoing photoreceptor demise (115).

In the retinal degeneration 10 (*rd10*) mouse which harbors a missense mutation in the Pde6b gene but displays a much slower onset of retinal degeneration, a similar infiltration of microglia into the outer nuclear layer is observed at around P21 as the number of apoptotic rods increase (16). Interestingly, microglia activation in *rd10* mice, indicated by the upregulation of microglia specific genes Cx3cr1, Aif1, Irf8, C1qc is already apparent at P12 before the onset of neurodegeneration (116). Upon activation, microglia migrate toward the degenerating photoreceptors and transition into amoeboid cells containing multiple phagosomes where they produce large amounts of the pro-inflammatory cytokine IL-1β and potentiate photoreceptor apoptosis (16). In addition, the reactive outer retina microglia engage in indiscriminate phagocytosis of stressed but living photoreceptors, aggravating neuronal demise, and disease severity (16). Of note is that the number of infiltrating microglia is significantly reduced in *ccr2*$^{-/-}$ *rd10* mice, indicating that the *ccr2/ccl2* signaling pathway plays a crucial role in mobilizing mononuclear phagocytes into the degenerating photoreceptor layer (117). Moreover, the reduced microglial infiltration was also associated with an increase in retinal thickness and function, strongly affirming microglia's involvement in inducing degenerative changes during retinal pathology (117).

In addition to the commonly used *rd1* and *rd10* mutants, *rd7* and *rd8* mutant mouse strains also display widespread microglia activation (118). In the *rd7* mice where retinal degeneration occurs as a result of a spontaneous mutation in the Nr2e3 gene (119), reactive microglia are found under abnormal foldings (retinal rosettes) that develop in the outer nuclear layer and inner segments of photoreceptors (118). These reactive microglia phagocytose large amounts of debris between photoreceptor and RPE layers, resulting in the accumulation of lysosomes containing autofluorescent material (118). Activated-lysosome-laden microglia, which appear as autofluorescent dots in fundus images, secrete high amounts of pro-inflammatory cytokines IL-1β, IL-6, and TNF-α thereby accelerating retinal degeneration (118). Similarly, in the *rd8* mice bearing a mutation in the Crb1 gene, increased amounts of microglia/macrophages positive for pro-inflammatory markers CD16, MHC-II, and iNOS accumulate in the subretinal space when compared to age matched wild type controls (120). This enhanced accumulation of reactive microglia overexpressing complement (C3 and CFB) and pro-inflammatory (TNF-α and NFκB) genes, is a specific response to degenerative changes that occur in the *rd8* retina including development of retinal dystrophic lesions (120, 121).

Microglia in Diabetic Retinopathies

Diabetic retinopathy (DR) is a severe ocular complication of diabetes mellitus and is also the leading cause of blindness among the working age populations of industrialized regions (122). DR can be clinically divided into two forms; (i) an early non-proliferative form (NPDR) characterized by increased vascular permeability, retinal microvasculature degeneration, basement membrane thickening, and loss of pericytes in the retinal capillaries (ii) an advanced proliferative form (PDR) involving pathological neovascularization, vitreous hemorrhage, and retinal scars and detachment (123). Based on vascular abnormalities such as acellular capillaries, microscopic capillary loss, and microaneurysms, DR has traditionally been regarded as a classical microvascular disease (122). However, in recent years, numerous studies have highlighted the crucial role played by inflammation in the pathogenesis of DR (124–126).

Early indications of inflammation involvement in the pathogenesis of DR came from a study reporting a low incidence and high regression rate of DR when diabetic patients were treated with salicylates for rheumatoid arthritis complications (127). Since then, ample evidence exists to show that DR is a low grade chronic inflammatory condition characterized by leukostasis, RPE, and endothelial cell damage and associated blood retinal barrier (BRB) alteration. Subsequently, these events compromise the immune suppressive environment in the retina resulting in increased expression of pro-inflammatory factors (124, 128, 129). Indeed, several clinical studies have shown that the levels of many pro-inflammatory cytokines including TNF-α, IL-1β, IL-6, and IL-8 are elevated in the vitreous of DR patients (124, 128). In addition, persistent hyperglycaemia results in increased polyol and hexosamine pathways flux, inducing cellular oxidative stress and the generation of advanced glycation or lipoxidation end products (AGEs or ALEs) (122, 130). High levels of pro-inflammatory cytokines and the accumulation of AGEs and ALEs compromise cellular physiology and induce microglia activation (131, 132). Furthermore, oxidative stress induced by the noxious hyperglycaemic environment can trigger NFκB-mediated inflammatory responses in retinal microglia (133).

In human DR, hypertrophic and amoeboid microglia are present at different stages of the disease (134). In the NPDR form, there is a moderate increase in the number of reactive microglia which are mostly clustered around perivascular vessels and fresh hemorrhages in microaneurysms (135). In the intermediate pre-proliferative form, there is a dramatic increase in reactive microglia which cluster around cotton-wool spots and dilated vessels (135). Lastly in the PDR form, a marked increase in reactive microglia number is seen in the ganglion cell layer and

around new immature blood vessels in the nerve fiber layer and the optic nerve head where the proliferative process is most prominent (135). Strikingly, reactive microglia in human DR are closely associated with perivascular compartments where they are postulated to exacerbate vascular permeability by propagating inflammatory responses (135, 136).

Similarly in murine models, changes to retinal microglia are a prominent feature of diabetic retinopathy (137, 138). In the $Ins2^{Akita}$ mouse model which harbors a spontaneous missense mutation in the insulin 2 gene, discrete pockets containing bloated microglia with shorter less branched processes can be observed in the diseased retina (138). Moreover, the normal laminar arrangement of the retinal microglia is markedly disrupted in these mice from 10 weeks of age (137). These DR induced microglia morphological alterations might result partly from disruptions in microglial Cx3cr1 signaling, as the detrimental morphological abnormalities are exacerbated in the absence of Cx3cr1 signaling (137).

In the Goto-Kakizaki (GK) inbred rat model of type II diabetes, numerous $Iba1^{+}$ amoeboid microglia/macrophages overexpressing inducible form of nitric oxide synthase (iNOS) can be found all over the retina and in the subretinal space following 12 months of hyperglycaemia (139). The enhanced trafficking of microglia/macrophages to the subretinal space at week 12 is correlated with a reduction in the number of "tunnel-like" invaginations which mediate a physiological transcellular pathway in RPE cells (139). Alteration of this transcellular pathway and subsequent subretinal accumulation of activated microglia/macrophages induces morphological abnormalities in the outer retina including disorganization of photoreceptor outer segments (139). Notably, intraocular injection of a protein kinase C zeta (PKCζ) inhibitor suppresses iNOS expression in microglia/macrophages and impairs their recruitment to the subretinal space (139).

Microglia reaction is also elicited in pharmacologically induced diabetes where toxic glucose analogs alloxan and streptozotocin (STZ) are used to preferentially destroy pancreatic beta cells and induce a state of insulin-dependent diabetes (134, 140, 141). Starting at 4 months of age, an upsurge of microglia is observed in the different retinal layers and especially the outer plexiform and ganglion cell layer in STZ treated rats (134). There is also a significant shift in microglia phenotype toward activated amoeboid cells with hypertrophied cell bodies (134, 142). As the disease progresses, microglia in the outer plexiform layer extend their processes into the outer nuclear layer, with some CD11b positive microglia occasionally being found in the photoreceptor layers and subretinal space (134). Interestingly in alloxan treated mice, microglia morphological changes including shortened processes and hypertrophied cellular somas precede neuronal apoptosis and BRB breakdown in this model, implying that microglia cells play an important role in the onset and development of DR (141).

Microglia in Glaucoma

Glaucoma refers to a distinctive group of optic neuropathies characterized by the progressive demise of retinal ganglion cells (RGCs) and their axons, thinning of the retinal nerve fiber layer and cupping of the optic disc (143). Glaucoma, estimated to affect ∼79.6 million people by 2020, is the most frequent cause of irreversible blindness worldwide (144, 145). Major risk factors for the development and progression of glaucoma include old age, race, ocular and systemic hypertension, diabetes, and high myopia (146–148). To date, the only proven therapeutic approach to prevent development and slow down disease progression is the lowering of intraocular pressure (IOP) via drug treatment, laser therapy or surgery (51, 143). However, despite effectiveness of the intraocular pressure-lowering approach which eliminates the primary source of injury, evidence exists of a secondary degeneration that persists, affecting neighboring neurons and continuing the pathological process (149–151). An important mechanism that has been proposed to provoke such secondary degeneration of the RGCs in optic nerve disorders is the dysregulation of innate immunity and the associated neurodegenerative inflammatory responses (152).

Consistent with this hypothesis, aqueous humor from glaucoma patients have been shown in several studies to contain higher levels of pro-inflammatory cytokines and chemokines, suggesting that neuroinflammatory processes play a key role in glaucomatous neurodegeneration (153–156). Microglia, the resident tissue macrophages, are the principal sources of pro-inflammatory mediators in the retina and have been shown in both human and experimentally induced glaucoma in rodents to be central players in perpetuating the neuroinflammatory process in glaucoma (4, 157–159). In human glaucoma eyes, clusters of large amoeboid, reactive microglia gather around the compressed lamina cribrosa and its surrounding blood vessels, forming concentric circles (159). Enlarged reactive microglia, occurring either singly or in clusters, are also found in the parapapillary chorioretinal region (where the RPE and the bruch's membrane terminate) of glaucomatous optic nerve heads (ONH) (159). Proteomic and subsequent immunohistochemical analysis detected abundant expression of toll like receptor 2 (TLR2), TLR4, and TLR7 in microglia of diseased patients, implicating TLR signaling as a pathomechanism in glaucomatous neurodegeneration (160). Moreover, these reactive microglia were shown to express abundant levels of matrix metalloproteinases (MMP) 1, MMP-2, MMP-3, and MMP-14, pro-inflammatory factors TNF-α and NOS-2 and the anti-inflammatory cytokine TGF-β (158). The high expression of TGF-β suggests that microglia attempt to downregulate the degenerative reactions in the glaucomatous ONH, but as the disease progresses, their contribution turns detrimental leading to neurodegeneration and degradation of the extracellular matrix (158).

Murine models of glaucoma where increased ocular hypertension occurs naturally or is experimentally induced using genetic manipulation or surgical procedures have been instrumental in understanding microglia's role in disease pathogenesis (161). Using DBA/2J (D2) mice, an established model of chronic inherited glaucoma carrying spontaneous mutations in TYRP1 (tyrosinase-related protein 1) and GPNMB (glycosylated protein nmb), microglia activation and proliferation was shown to occur at stages prior to overt RGCs neurodegeneration (162, 163). These findings provide evidence

supporting an active involvement of microglial activation in the onset and progression of RGCs neurodegeneration in the glaucomatous retina (162, 163). Microglia mediate the neurodegeneration of RGCs, at least in-part, by secreting high amounts of TNF-α (164). Consistently, mice deficient for TNF-R1 are significantly protected against RGCs loss following optic nerve crush when compared to control animals with a functional TNF death receptor signaling (164). Moreover, both TNF-α and its receptor TNF-R1 are upregulated in glaucomatous retinas in the RGCs and retinal glial cells, respectively, suggesting a direct contribution of the TNF-α signaling cascade in optic nerve degeneration in glaucoma (165, 166). Notably, blocking TNF-α activity with Etanercept, a clinically approved agent, inhibits microglial inflammation with concomitant attenuation of axonal degeneration in the optic nerve and RGC demise (167).

Nitric oxide (NO) synthesized by microglia also plays a role in the pathophysiology of glaucoma (168, 169). Increased levels of iNOS and NO have been shown to occur in the ONH of glaucomatous patients and experimental animal models of glaucoma (168–171). Importantly, pharmacological inhibition of NO synthesis using timolol and aminoguanidine in rats with elevated IOP drastically suppresses the degeneration of RGCs, showing that NO-mediated mechanisms contribute to neuronal cell death during glaucoma (169, 172).

Increased IL-6 expression has also been reported as a key component of the retinal microglia response in glaucoma, although the available evidence is contradictory (173–175). Early *in-vitro* experiments conducted on primary glia cultures isolated from rat retina demonstrated that microglia, and not astrocytes were the primary sources of IL-6 following elevated pressure conditions (175). Interestingly, microglial secreted IL-6 was shown to significantly abate apoptotic cell death in RGCs injured by elevated pressure, suggesting a beneficial effect of this cytokine in countering proapoptotic signals in the glaucomatous retina (174). In contrast, other investigations have reported that while an IL6 deficiency promotes an anti-inflammatory, pro-survival retinal environment, it also induces an exaggerated TNF-α response in the presence of glaucomatous stressors such as ocular hypertension (176). Moreover, $IL6^{-/-}$ mice are protected from IOP induced structural degeneration of the optic nerve and subsequent decrease in vision acuity, suggesting that IL-6 may play a specific role in the progression of RGC axonopathy and vision loss (173). Further studies are therefore needed to delineate ambiguities and lack of clarity in reported outcomes prior to the development of IL-6 as a therapeutic target.

TARGETING MICROGLIA FOR THE TREATMENT OF RETINAL DEGENERATIVE DISEASES

Microglia participates in both physiological and pathophysiological functions in the retina (4). Therefore, despite the fact that neuroinflammatory responses from overly reactive microglia play a critical role in the onset and progression of retinal degenerative disorders, complete blocking of retinal microglial functions would result to undesirable effects (36). Hence, valid immunotherapeutic approaches for the treatment of retinal degeneration should be those that inhibit dysregulated microglial-mediated pro-inflammatory responses and/or simultaneously enhance their beneficial neuroprotective functions. In the remainder of this review, we discuss promising therapeutic strategies that have been used to modulate microgliosis and improve disease outcome during retinal pathologies.

Polysialic Acid Receptors

In the vertebrate nervous system, healthy neuronal cells carry a polysialic acid (PolySia) cap on their glycocalyx made up of α2-8-glycosidically linked N-acetylneuraminic acid residues and which are attached by means of Hildebrandt et al. (177) and Schnaar et al. (178). The glycosylation state of healthy neurons is vigilantly monitored by cell surface carbohydrate binding receptors on microglia referred to sialic acid-binding immunoglobulin-like lectins (Siglecs) (43). Neural cell-adhesion molecule (NCAM), involved in cell–cell interactions and cell–extracellular-matrix adhesion, is the most prominent neuronal protein modified by PolySia (179). Polysialylated neuronal cell adhesion molecule (PolySia-NCAM) binds a CD33-related, primate lineage-specific Siglec-11 receptor on microglia, and this interaction serves to limit microglia immune responses and maintaining them in a quiescent neuroprotective state [**Figure 2**; (43)]. The inhibitory signaling of Siglecs is mediated through conserved ITIM-domains contained in their cytosolic tails (180). Upon ligand binding, ITIM is phosphorylated by Src-kinases, leading to a subsequent recruitment of protein-tyrosine phosphatases Src-homology region 2 domain-containing phosphatase 1 (SHP1) and SHP2 (180). Once recruited, SHPs dephosphorylate activated tyrosine residues on immunoreceptor tyrosine-based activation motif (ITAM), inhibiting Syk kinase mediated inflammatory signaling, ROS production and phagocytosis (180–183). Indeed, the interaction of ectopically expressed human Siglec-11 in mouse microglia with PolySia residues on neurons potently downregulates LPS-induced pro-inflammatory gene transcription and phagocytic capacity in microglia, confirming that ITIM-signaling impedes the inflammatory, and phagocytosis-associated ITAM-Syk cascade (181).

Under pathological conditions such as elevated inflammation and oxidative stress, degradation of sialic acid caps occurs leaving neurons and other cells with a damaged glycocalyx (184–186). During such pathological conditions, soluble sialic acid residues actually accumulate in serum signifying the removal of sialic acid caps from glycoproteins (184, 185). Desialylated neuronal glycocalyx are then opsonized by complement component C1q, leading to their subsequent phagocytosis and clearance by the activating-signaling receptor complement receptor 3 (CR3) in microglia/macrophages (43). Consistently, blockage of CD11b as part of the complement receptor 3 (CR3) attenuates desialylated neurite phagocytosis by macrophages (187). However, excessive C1q mediated microglial phagocytosis of desialylated neurons would exacerbate ongoing neuronal loss in retinal degenerative disorders (188). This phenomenon is clearly observed in glaucoma mouse models where C1q localizes with neuronal synapses early on in the disease, and

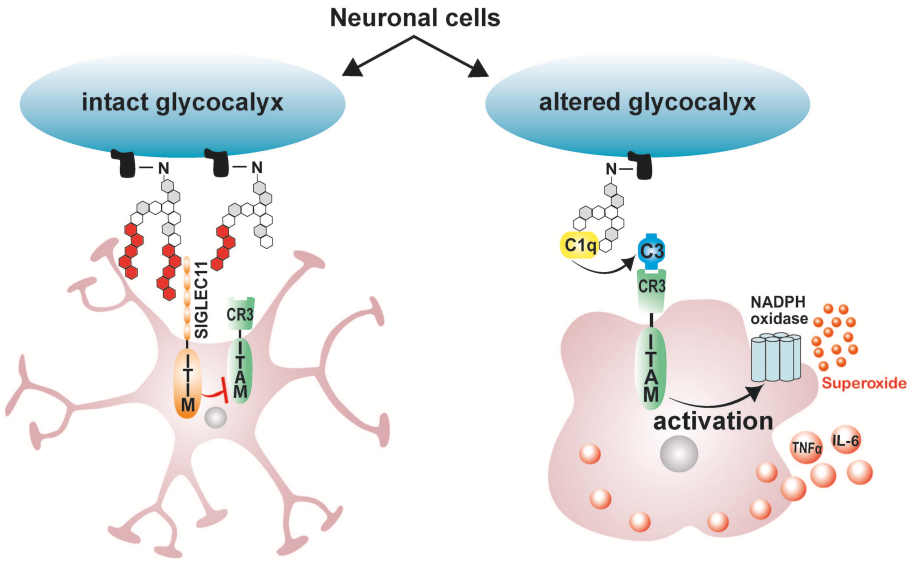

FIGURE 2 | Schematic model depicting the immunomodulatory effects of neuronal polysialic acids on microglia. Healthy neuronal cells have an intact glycocalyx displaying a polysialic acid (PolySia) cap. The PolySia cap is recognized and bound by Siglec-11, an inhibitory ITIM-signaling receptor. This interaction between neuronal PolySia and Siglec-11 inhibits microglia activation and maintains retinal homeostasis. However, during pathological conditions, neuronal glycocalyx is altered, leading to degradation of sialic acid caps. The exposed neuronal glycocalyx is then opsonized by complement component C1q, leading to subsequent recognition by ITAM-containing complement receptor 3 (CR3) in microglia and activation of inflammatory signaling and ROS production. ITIM, immunoreceptor tyrosine-based inhibition motif; ITAM, immunoreceptor tyrosine-based activation motif.

blocking neuronal opsonization by depleting C1q protects mice from glaucoma induced neurodegeneration (188). These findings therefore suggest that treatment with exogenous polysialic acids may be neuroprotective by limiting disease induced microglial inflammatory responses and phagocytic capacity.

Indeed, treatment of human macrophages challenged with LPS or amyloid-β_{1-42} with nanomolar concentrations of low molecular weight polySia with an average degree of polymerization 20 (polySia avDP20) significantly reduces pro-inflammatory gene transcription, inflammation-induced phagocytosis, and oxidative burst (44). Similarly in the retina, treatment with polySia avDP20 was shown to significantly reduce microglial activation, vascular leakage and production of deleterious ROS in humanized transgenic mice expressing SIGLEC-11 following laser-induced choroidal neovascularization (42). Interestingly, higher doses of polySia avDP20 were shown to block alternative complement activation and membrane attack complex formation in the diseased retina but in a SIGLEC-11 independent manner (42).

Translocator Protein Ligands

Translocator protein (18 kDa; TSPO), formerly referred to as the peripheral benzodiazepine receptor (PBR), is a highly conserved 5α-helical transmembrane protein located on the outer mitochondrial membrane (OMM) (189). TSPO exhibits a high constitutive expression in steroidogenic tissues such as adrenal glands, gonads and the placenta, but is very weakly expressed in the normal healthy brain (190, 191). However, during neuropathology, there is a strong increase in TSPO protein expression in the brain which colocalizes predominantly with activated microglia (190, 192, 193). This strong upregulation of TSPO in the brain from a very low baseline led to the development of numerous TSPO positron-emission tomography (PET) ligands for the non-invasive imaging of neuroinflammation (194, 195). Similarly, during retinal inflammation and disease, there is a strong upregulation of TSPO in reactive migratory microglia, and this induction accurately marks the extent and duration of retinal inflammation (190, 193). Interestingly, as activated microglia upregulate TSPO expression during retinal inflammation and disease, astrocytes, and Müller cells upregulate the production and secretion of Diazepam binding inhibitor (DBI), a 9 kDa endogenous TSPO protein ligand (61). DBI is then taken up by microglia cells, and the binding of DBI to microglial TSPO serves to limit the magnitude of microglial inflammatory responses [**Figure 3**; (61)]. Secreted DBI can also be cleaved extracellularly by acidic endopeptidases into its biologically active cleavage product triakontatetraneuropeptide (TTN) (196). TTN interaction with retinal microglial TSPO similarly suppresses inflammatory responses and facilitates a return of activated microglia to baseline quiescence (61, 196). Exploiting this endogenous immunomodulatory pathway, we tested the ability of a synthetic and highly specific TSPO ligand, XBD173 (AC-5216, emapunil), to influence microglial reactivity in the acute white light-induced retinal degeneration mouse model (193). White light exposure is an environmental risk factor that contributes to the faster onset and progression of human retinal degeneration disorders such as AMD and Retinitis Pigmentosa (197–200). Consistently, rodents exposed to bright white light experience a synchronized burst of photoreceptor

cell death and thinning of the outer nuclear layer (94, 95, 193). Photoreceptor demise is brought about by rhodopsin bleaching and excessive phototransduction signaling, which creates an intracellular death signal that translocates transcription factor AP-1 to the nucleus to mediate photoreceptor apoptosis (59, 94, 95). Using this model, we demonstrated that the TSPO ligand XBD173 markedly inhibited accumulation of amoeboid microglia in the outer retina with concomitant preservation of the outer nuclear layer (193). Moreover, XBD173 efficiently suppressed pro-inflammatory induced gene expression and morphological transition in microglia with concomitant reduction in microglial neurotoxicity on cultured photoreceptors (190). However, the precise mechanisms involved in the TSPO ligands neuroprotective effects remain largely unknown, but likely involves, at least in part, enhanced steroidogenesis.

Indeed, the most studied physiological function of TSPO involves the translocation of cholesterol from the outer to the inner mitochondrial membrane as a rate limiting step for steroidogenesis (189, 201). TSPO's implication in steroidogenesis has been based upon its localization to the OMM, presence of a high affinity cholesterol recognition amino acid consensus (CRAC) motif, high expression in steroidogenic cells and the ability of TSPO ligands to stimulate steroid synthesis (202–204). In our own *in-vitro* experiments in the lab, we have demonstrated that treatment of microglia cells with XBD173 induces pregnenolone synthesis, and that inhibition of this process with aminoglutethimide partially abolishes XBD173 therapeutic effects (190). Similarly, the endogenous ligand TTN induces synthesis of pregnenolone derived Dehydroepiandrosterone (DHEA), inhibiting microglia-mediated proinflammatory responses (61). Outside the retina, DBI and synthetic TSPO binding ligands stimulates cholesterol translocation to the inner mitochondrial membrane increasing pregnenolone formation by isolated adrenocortical, Leydig and glia cell mitochondria (205, 206). In addition, gene silencing to inhibit DBI expression in Leydig cells was shown to significantly suppress hormone-induced steroidogenesis but not adenylate cyclase nor cholesterol side chain cleavage (P450SCC) enzyme activities (207). Of note is that the absence of TSPO in mutant rats causes increased neutral lipid accumulation in the adrenal glands and testis, reduced circulating testosterone and undetectable levels of the neurosteroid allopregnanolone (208). Together, these findings strongly suggest that TSPO and its ligands regulate steroid and neurosteroid levels.

Steroid hormones have subsequently been shown to attenuate neuroinflammatory reactions via autocrine and paracrine signaling mechanisms (209). Binding of steroids to their cytoplasmic and nuclear bound receptors results in the rapid inhibition of pro-inflammatory gene transcription via both genomic and non-genomic mechanisms (210). In the retina, a synthetic progesterone, norgestrel, exerts potent neuroprotective effects in the rd10 mouse model of human RP by reducing the extent of neuronal apoptosis with concurrent preservation of the photoreceptor layer (211). Norgestrel mediated rescue of stressed photoreceptors was shown to be mediated by the pleiotropic cytokine LIF, the pro-survival growth factor bFGF and the fractalkine-CX3CR1 signaling cascade (211–213). In addition, norgestrel directly targets reactive microglia in the rd10 mouse, attenuating their pro-inflammatory gene expression and NO production and significantly lessening microglial neurotoxicity on photoreceptor like cells *in vitro* (214). Moreover, the steroid hormone 17β-estradiol (βE2), which can be synthesized in the brain from testosterone, has been shown to protect rats against light-induced retinal degeneration by upregulating the NRF2-antioxidant pathway and reducing ROS production (215). In summary, TSPO ligands, working in part via inducing neurosteroidogenesis, present as attractive therapeutic regimens to dampen inflammatory responses from overly reactive microglia during retinal degenerative diseases.

Interferon-β

Interferon-β (IFN-β) belongs to the type I IFN family which are best known for their ability to induce a cellular antimicrobial state during a viral or bacterial infection (216, 217). IFN-β also possesses strong immunomodulatory properties, making it a first-line immunotherapy against relapsing remitting Multiple Sclerosis (MS) (217). IFN-β mediates neuroprotection against MS, an inflammatory and demyelinating CNS disorder characterized by multifocal brain lesions, by recruiting microglia to the lesion sites, enhancing their phagocytic capacity and accelerating clearance of accumulated myelin debris (218–220). Conversely, experimental autoimmune encephalomyelitic (EAE) mice which mimic the disease process of MS develop an exacerbated disease course accompanied by microglial hyperactivation and increased lethality in the absence of myeloid IFN-β signaling (221). Therefore, based on the immunomodulatory properties of IFN-β in MS neuropathology, we hypothesized that IFN-β may confer neuroprotection against chronic inflammation observed in neovascular age related macular degeneration (AMD) and thereby improve disease outcome.

We used the laser-induced choroidal neovascularization (CNV) mouse model that mimics features of exudative AMD to test this hypothesis (103). Briefly, laser photocoagulation results in the rupture of the Bruch's membrane, leading to the ingrowth of immature leaky blood vessels from the choroid to the subretinal space (103). Of note is that Bruch's membrane rupture is accompanied by rapid recruitment of myeloid cells to the lesion sites with concomitant elevation of proinflammatory and angiogenic factors, triggering the formation and growth of new blood vessels from the choroid (75, 222). Using this model, we demonstrated that IFN-β strongly inhibits microglia/macrophage activation and recruitment and induces a transition of microglia morphology toward a neuroprotective ramified with more cellular processes (104). Moreover, IFN-β treated animals showed considerable improvement in disease outcome signified by a reduction in vascular leakage and neoangiogenesis (104). These results corroborated those of a previous study which showed that local administration of IFN-β exacerbated wound healing of retinal lesions produced by laser photocoagulation in rabbits (223). Conversely, global or microglia specific conditional deletion of IFN-β/IFNAR1 signaling in mice resulted in an exacerbated disease marked by

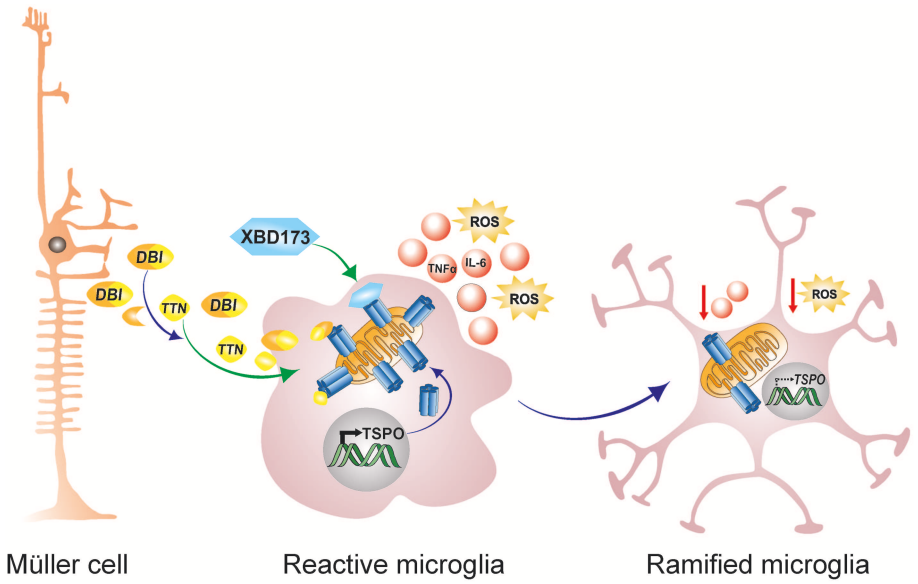

FIGURE 3 | Endogenous and exogenous TSPO ligands dampen microglial activation. During retinal pathophysiology, microglia upregulate TSPO expression while Müller cells simultaneously upregulate the production and secretion of the endogenous TSPO ligand DBI. Secreted DBI can subsequently be cleaved extracellularly into the biologically active product TTN. Extracellular DBI and TTN are taken up by microglia, and their binding to the TSPO receptor serves to limit the magnitude of microglial inflammatory responses. DBI, diazepine binding inhibitor; TTN, triakontatetraneuropeptide; TSPO, translocator protein 18 kDa.

reactive microgliosis and enhanced vascular leakage (104). These findings strongly suggest that Ifnar1/IFN-β signaling, particularly in microglia, prevents chronic inflammation and pathological neovascularization in the retina and could be therapeutically targeted in wet AMD and other retinal inflammatory disorders. Remarkably, IFN-β treatment was reported to completely reverse subfoveal neovascularization and choroiditis in an MS patient, underscoring the importance of IFN-β in the management of ocular inflammation and neovascularization (224).

Several mechanisms have been proposed for IFN-β immunomodulatory and anti-angiogenic effects. One such mechanism involves the IFN-β induced expression of suppressor of cytokine signaling 1 (SOCS1) and SOCS3 (225, 226). IFN-β and other type I IFNs activate the transcription of SOCS1 and SOCS3 as part of a negative feedback loop to curb prolonged signaling by pro-inflammatory cytokines via the JAK-STAT pathway (227). Once produced, SOCS1 and SOCS3 are recruited to cytokine receptors where they inhibit the catalytic activity of JAK tyrosine kinases and negatively regulate inflammatory responses (228, 229). This phenomenon has been clearly demonstrated in the retinas of experimental autoimmune uveoretinitis (EAU) mice lacking SOCS3 in myeloid cells (230). These retinas showed elevated levels of pro-angiogenic factor VEGF-A and pro-inflammatory cytokines IL-1β, TNF-α, and IFN-γ (230). Consequently, myeloid-specific SOCS3 deficient mice displayed exaggerated retinal degeneration and accelerated retinal angiogenesis compared to their wildtype counterparts (230). In contrast, overexpression of SOCS1 was shown to protect retinal cells against staurosporine and H_2O_2-induced apoptosis (231). Notably, the overexpression SOCS1 in EAU mice significantly lessens disease severity by suppressing inflammatory chemokine expression and inhibiting recruitment of inflammatory cells into the retina (231).

IFN-β is also known to mediate its immunomodulatory effects via the noncanonical activation of the PI3K–AKT–mTOR pathway (232, 233). A recent study indeed revealed a central role of IFN-β signaling in the regulation of the PI3K–AKT pathway, by demonstrating that neurons from *Ifnb*$^{-/-}$ mice exhibited striking reductions in Pi3K and Akt mRNA and protein levels (234). Moreover, phosphorylated Pi3k and Akt, which signify active signaling, were even more pronouncedly reduced in the IFN-β incompetent neurons (234). Following activation, PI3K–AKT–mTOR pathway has been shown to exert anti-inflammatory and neuroprotective effects (215, 235). Activation of mTORC1, downstream of PI3K–AKT induces the phosphorylation of STAT3 at Ser^{727}, thereby enhancing expression of the counter regulator of inflammatory signaling, SOCS3 (236). Of note, the pharmacological blockade of Pi3k-Akt pathway abolishes the antioxidative and neuroprotective effects conferred by the steroid hormone βE2 following light induced retinal degeneration in rats (215). Similarly, in LPS activated primary rat microglia, pharmacological blockade of the Pi3k-Akt-mTOR pathway significantly enhances inflammatory cyclooxygenase-2 (COX-2) activity and elevates production of associated downstream prostanoids PGE_2 and PGD_2 (237, 238).

Furthermore, IFN-β mediated activation of the PI3-AKT pathway negatively regulates the activity of the pro-inflammatory enzyme glycogen synthase kinase-3 (GSK-3) (239). GSK-3 is a critical mediator of inflammatory responses in the CNS and has been shown to downregulate production of anti-inflammatory

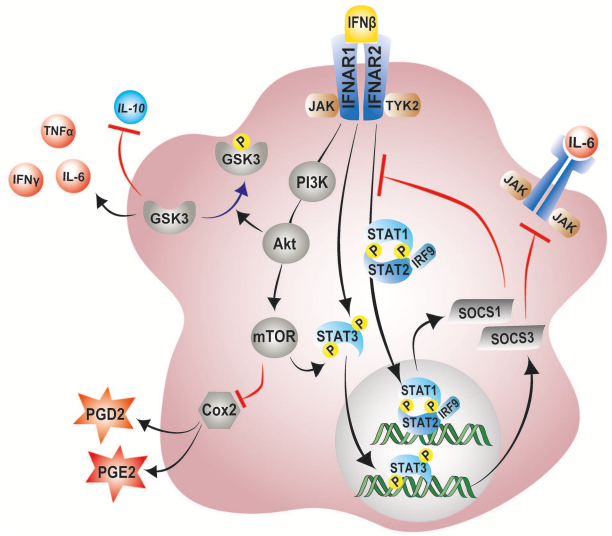

FIGURE 4 | Modulation of microglial inflammatory responses by IFN-β signaling. IFN-β ligation to its receptor complex, IFNAR, triggers activation of the associated tyrosine kinases JAK1 and TYK2 and the subsequent phosphorylation of STAT1, STAT2, and STAT3 transcription factors. Phosphorylated STAT1 and STAT2 can recruit IRF-9 to the form the trimolecular complex STAT1–STAT2–IRF9 (ISGF3). Phosphorylated STAT3, and ISGF3 translocate to the nucleus and induce the transcription of various interferon-stimulated genes including SOCS1 and SOCS3 as part of a negative feedback loop. SOCS1 and SOCS3 inhibit excessive signaling by pro-inflammatory cytokines via the JAK-STAT pathway. IFN-β can also non-canonically activate the PI3K–AKT–mTOR pathway and suppress microglial inflammatory responses. mTORC1, downstream of PI3K–AKT can phosphorylate and activate STAT3, thereby enhancing expression of SOCS3. Activation of AKT downstream of IFN-β-PI3 inhibits GSK-3 activity through phosphorylation, negatively regulating GSK-3 mediated inflammatory responses, and promoting IL-10 expression. JAK1, Janus kinase 1; TYK2, tyrosine kinase 2; STAT, signal transducer and activator of transcription; IRF9, interferon regulatory factor 9; PI3K, phosphoinositide 3-kinase; AKT, protein Kinase B; mTOR, mammalian target of rapamycin; GSK-3, glycogen synthase kinase 3.

cytokine IL-10 and promote that of pro-inflammatory cytokines TNF-α, IFN-γ, and IL-6 in microglia and macrophages (239, 240). Activation of AKT downstream of IFN-β-PI3 causes inhibition of GSK-3 by serine phosphorylation, negatively regulating inflammatory responses in the CNS [**Figure 4**; (239)]. Notably, treatment of *rd10* mice with a small molecule inhibitor of GSK-3 suppresses pro-inflammatory responses in the retina with concomitant reduction in photoreceptor demise and preservation of visual function (241). However, further research in this area is necessary to delineate the contributions of this pathway to the immunomodulatory effects of IFN-β on microglia during retinal inflammation and disease.

Minocycline

Minocycline is a highly lipophilic, semi-synthetic tetracycline derivative which is mainly used in the treatment of acne vulgaris and rheumatoid arthritis (242). However, due to its ability to readily penetrate the CNS and its profound anti-inflammatory properties, minocycline has recently emerged as a powerful immunomodulatory drug that is well-suited for CNS disorders (242, 243). Minocycline blocks microglial activation in response to a variety of inflammatory stimuli by inhibiting Toll-like receptor 2 (TLR2) and TLR4 signaling as well as several MAP kinases including p38, c-Jun-N-terminal activated protein kinase (JNK) 1/2, and extracellular signal regulated kinase (ERK) 1/2 (244, 245). In addition, minocycline inhibits NFκB transcriptional activity by suppressing the degradation of inhibitor of kappa B-alpha (IκBα) (244, 246).

Consistent with its anti-inflammatory properties, minocycline benefits during retinal pathophysiology have been confirmed in several experimental models. In a light-induced retinal degeneration mouse model, minocycline treatment was shown to significantly inhibit photoreceptor apoptosis and preserve retinal structure (89). Moreover, minocycline potently inhibited microgliosis and the accumulation of reactive amoeboid microglia in the subretinal space following light induced retinal damage (89). In an *rd10* mouse model of human RP, treatment with minocycline significantly reduced microglia-mediated photoreceptor apoptosis, improving retinal structure and function (247). In a rat model of diabetic retinopathy, minocycline treatment represses the release of pro-inflammatory cytokines IL-1β, and TNF-α with concomitant reduction in caspase-3 mediated apoptosis in the retina (248). Similarly, in a streptozotocin-induced rat model of DR, minocycline treatment inhibited the abnormal expression of poly (ADP-ribose) polymerase 1 (PARP1), a chromatin-associated enzyme that promotes proinflammatory responses in glial cells, with concurrent reduction in the number of apoptotic cells in the diabetic retina (249). In the DBA/2J chronic mouse model of glaucoma, minocycline inhibited microglial activation, and increased the fraction of microglia in a ramified neuroprotective state (250). Of note, minocycline improved RGC axonal transport and integrity in the glaucomatous retina (250).

Minocycline protective effects have also been examined in the human retina (251). Retinitis pigmentosa mediated decline in visual field was shown to be reversed upon long term minocycline treatment (251). In a NIH proof of concept clinical study involving patients with diabetic macula edema (NTC01120899), a vision threatening form of DR, treatment with oral minocycline reduced abnormal vascular permeability and leakage with concomitant improvement in vision acuity (252). Taken together, these findings demonstrate the broad range immunomodulatory and neuroprotective effects of minocycline and underscore the importance of further testing to establish this antibiotic as an immunotherapy against retinal pathologies.

CONCLUSION

Studies using rodent models in the past decade have been instrumental in understanding the role of microglial responses in retinal pathologies. Ample evidence generated from these studies shows unequivocally that microglia reactivity and chronic inflammation is a common hallmark of various retinal pathologies, and that pharmacological targeting of overly reactive microglia ameliorates disease pathogenesis. However,

why and how immunologic checkpoints become overwhelmed resulting in dysregulation of microglial inflammatory responses remains poorly understood. Therefore, prior to development of microglial-based therapeutic approaches, further studies are needed to understand the etiological factors and molecular mechanisms that propagate microglial responses during retinal degeneration. In addition, owing to the numerous overlapping insults that predispose retinal pathologies, it will be prudent to develop microglia based therapeutic approaches that will complement, or even synergize, other retinal therapeutic approaches.

AUTHOR CONTRIBUTIONS

All authors listed have made a substantial, direct and intellectual contribution to the work, and approved it for publication.

FUNDING

This study was funded by the Velux Foundation, the German Academic Exchange Service (DAAD), and the Deutsche Forschungsgemeinschaft (FOR2240 project 6).

REFERENCES

1. Gollisch T, Meister M. Eye smarter than scientists believed: neural computations in circuits of the retina. *Neuron.* (2010) 65:150–64. doi: 10.1016/j.neuron.2009.12.009
2. Matsuda T, Cepko CL. Electroporation and RNA interference in the rodent retina *in vivo* and *in vitro*. *Proc Natl Acad Sci USA*. (2004) 101:16–22. doi: 10.1073/pnas.2235688100
3. Vecino E, Rodriguez FD, Ruzafa N, Pereiro X, Sharma SC. Glia–neuron interactions in the mammalian retina. *Prog Retin Eye Res.* (2016) 51:1–40. doi: 10.1016/j.preteyeres.2015.06.003
4. Karlstetter M, Scholz R, Rutar M, Wong WT, Provis JM, Langmann T. Retinal microglia: just bystander or target for therapy? *Prog Retin Eye Res.* (2015) 45:30–57. doi: 10.1016/j.preteyeres.2014.11.004
5. Goldman D. Müller glial cell reprogramming and retina regeneration. *Nat Rev Neurosci.* (2014) 15:431–42. doi: 10.1038/nrn3723
6. Reichenbach A, Bringmann A. New functions of Müller cells. *Glia.* (2013) 61:651–78. doi: 10.1002/glia.22477
7. Ramírez JM, Triviño A, Ramírez AI, Salazar JJ. Organization and function of astrocytes in human retina. In: Castellano B, González B, Nieto-Sampedro M, editors. *Understanding Glial Cells.* Boston, MA: Springer US. p. 47–62. doi: 10.1007/978-1-4615-5737-1_3
8. Fernández-Sánchez L, Lax P, Campello L, Pinilla I, Cuenca N. Astrocytes and Müller cell alterations during retinal degeneration in a transgenic rat model of retinitis pigmentosa. *Front Cell Neurosci.* (2015) 9:484. doi: 10.3389/fncel.2015.00484
9. Langmann T. Microglia activation in retinal degeneration. *J Leukoc Biol.* (2007) 81:1345–51. doi: 10.1189/jlb.0207114
10. Chen M, Xu H. Parainflammation, chronic inflammation, and age-related macular degeneration. *J Leukoc Biol.* (2015) 98:713–25. doi: 10.1189/jlb.3RI0615-239R
11. Ramon y Cajal. Algo sobre la significacion fisiologica de la neuroglia. *Rev Trimest Microgr.* (1897) 2:33–47.
12. Sierra A, de Castro F, del Río-Hortega J, Rafael Iglesias-Rozas J, Garrosa M, Kettenmann H. The "Big-Bang" for modern glial biology: translation and comments on Pío del Río-Hortega 1919 series of papers on microglia. *Glia.* (2016) 64:1801–40. doi: 10.1002/glia.23046
13. Ramon y Cajal. Contribucion al conocimiento de la neuroglia del cerebro humano. *Trab Lab Invest Biol Univer Madrid.* (1913) 11:215–315.
14. Río-Hortega. "Tercer elemento" de Los Centros Nerviosos. II. Intervencion de la microglia en los procesos patologicos (Cellulas en bastocito y cuerpos granulo-adiposos). *Bol Soc Esp Biol.* (1919) 9:91–103.
15. Masuda T, Shimazawa M, Hara H. Retinal diseases associated with oxidative stress and the effects of a free radical scavenger (Edaravone). *Oxid Med Cell Longev.* (2017) 2017:9208489. doi: 10.1155/2017/9208489
16. Zhao L, Zabel MK, Wang X, Ma W, Shah P, Fariss RN, et al. Microglial phagocytosis of living photoreceptors contributes to inherited retinal degeneration. *EMBO Mol Med.* (2015) 7:1179–97. doi: 10.15252/emmm.201505298
17. Xu H, Chen M, Mayer EJ, Forrester JV, Dick AD. Turnover of resident retinal microglia in the normal adult mouse. *Glia.* (2007) 55:1189–98. doi: 10.1002/glia.20535
18. Kezic J, McMenamin PG. Differential turnover rates of monocyte-derived cells in varied ocular tissue microenvironments. *J Leukoc Biol.* (2008) 84:721–9. doi: 10.1189/jlb.0308166
19. Kaneko H, Nishiguchi KM, Nakamura M, Kachi S, Terasaki H. Characteristics of bone marrow–derived microglia in the normal and injured retina. *Investig Opthalmol Vis Sci.* (2008) 49:4162. doi: 10.1167/iovs.08-1738
20. Diserbo M, Agin A, Lamproglou I, Mauris J, Staali F, Multon E, Amourette C. Blood-brain barrier permeability after gamma whole-body irradiation: an *in vivo* microdialysis study. *Can J Physiol Pharmacol.* (2002) 80:670–8. doi: 10.1139/y02-070
21. Ransohoff RM. Microgliosis: the questions shape the answers. *Nat Neurosci.* (2007) 10:1507–9. doi: 10.1038/nn1207-1507
22. Ajami B, Bennett JL, Krieger C, Tetzlaff W, Rossi FMV. Local self-renewal can sustain CNS microglia maintenance and function throughout adult life. *Nat Neurosci.* (2007) 10:1538–43. doi: 10.1038/nn2014
23. Kamran P, Sereti K-I, Zhao P, Ali SR, Weissman IL, Ardehali R. Parabiosis in mice: a detailed protocol. *J Vis Exp.* (2013) e50556. doi: 10.3791/50556
24. Ginhoux F, Greter M, Leboeuf M, Nandi S, See P, Gokhan S, et al. Fate mapping analysis reveals that adult microglia derive from primitive macrophages. *Science.* (2010) 330:841–5. doi: 10.1126/science.1194637
25. Elmore MRP, Najafi AR, Koike MA, Dagher NN, Spangenberg EE, Rice RA, et al. Colony-stimulating factor 1 receptor signaling is necessary for microglia viability, unmasking a microglia progenitor cell in the adult brain. *Neuron.* (2014) 82:380–97. doi: 10.1016/j.neuron.2014.02.040
26. Hughes EG, Bergles DE. Hidden progenitors replace microglia in the adult brain. *Neuron.* (2014) 82:253–5. doi: 10.1016/j.neuron.2014.04.010
27. Zhan L, Krabbe G, Du F, Jones I, Reichert MC, Telpoukhovskaia M, et al. Proximal recolonization by self-renewing microglia re-establishes microglial homeostasis in the adult mouse brain. *PLoS Biol.* (2019) 17:e3000134. doi: 10.1371/journal.pbio.3000134
28. Bruttger J, Karram K, Wörtge S, Regen T, Marini F, Hoppmann N, et al. Genetic cell ablation reveals clusters of local self-renewing microglia in the mammalian central nervous system. *Immunity.* (2015) 43:92–106. doi: 10.1016/j.immuni.2015.06.012
29. Huang Y, Xu Z, Xiong S, Sun F, Qin G, Hu G, et al. Repopulated microglia are solely derived from the proliferation of residual microglia after acute depletion. *Nat Neurosci.* (2018) 21:530–40. doi: 10.1038/s41593-018-0090-8
30. Huang Y, Xu Z, Xiong S, Qin G, Sun F, Yang J, et al. Dual extra-retinal origins of microglia in the model of retinal microglia repopulation. *Cell Discov.* (2018) 4:9. doi: 10.1038/s41421-018-0011-8
31. Zhang Y, Zhao L, Wang X, Ma W, Lazere A, Qian H-H, et al. Repopulating retinal microglia restore endogenous organization and function under CX3CL1-CX3CR1 regulation. *Sci Adv.* (2018) 4:eaap8492. doi: 10.1126/sciadv.aap8492
32. Bodeutsch N, Thanos S. Migration of phagocytotic cells and development of the murine intraretinal microglial network: an *in vivo* study using fluorescent dyes. *Glia.* (2000) 32:91–101. doi: 10.1002/1098-1136(200010)32:1<91::AID-GLIA90>3.0.CO;2-X
33. Schafer DP, Lehrman EK, Kautzman AG, Koyama R, Mardinly AR, Yamasaki R, et al. Microglia sculpt postnatal neural circuits in an activity and complement-dependent manner. *Neuron.* (2012) 74:691–705. doi: 10.1016/j.neuron.2012.03.026

34. Damani MR, Zhao L, Fontainhas AM, Amaral J, Fariss RN, Wong WT. Age-related alterations in the dynamic behavior of microglia. *Aging Cell.* (2011) 10:263–76. doi: 10.1111/j.1474-9726.2010.00660.x
35. Nimmerjahn A, Kirchhoff F, Helmchen F. Resting microglial cells are highly dynamic surveillants of brain parenchyma *in vivo*. *Science.* (2005) 308:1314–8. doi: 10.1126/science.1110647
36. Wang X, Zhao L, Zhang J, Fariss RN, Ma W, Kretschmer F, et al. Requirement for microglia for the maintenance of synaptic function and integrity in the mature retina. *J Neurosci.* (2016) 36:2827–42. doi: 10.1523/JNEUROSCI.3575-15.2016
37. Kierdorf K, Prinz M. Factors regulating microglia activation. *Front Cell Neurosci.* (2013) 7:44. doi: 10.3389/fncel.2013.00044
38. Broderick C, Hoek RM, Forrester JV, Liversidge J, Sedgwick JD, Dick AD. Constitutive retinal CD200 expression regulates resident microglia and activation state of inflammatory cells during experimental autoimmune uveoretinitis. *Am J Pathol.* (2002) 161:1669–77. doi: 10.1016/S0002-9440(10)64444-6
39. Copland DA, Calder CJ, Raveney BJE, Nicholson LB, Phillips J, Cherwinski H, et al. Monoclonal antibody-mediated CD200 receptor signaling suppresses macrophage activation and tissue damage in experimental autoimmune uveoretinitis. *Am J Pathol.* (2007) 171:580–8. doi: 10.2353/ajpath.2007.070272
40. Horie S, Robbie SJ, Liu J, Wu W-K, Ali RR, Bainbridge JW, et al. CD200R signaling inhibits pro-angiogenic gene expression by macrophages and suppresses choroidal neovascularization. *Sci Rep.* (2013) 3:3072. doi: 10.1038/srep03072
41. Huang R, Lan Q, Chen L, Zhong H, Cui L, Jiang L, et al. CD200Fc attenuates retinal glial responses and RGCs apoptosis after optic nerve crush by modulating CD200/CD200R1 interaction. *J Mol Neurosci.* (2018) 64:200–10. doi: 10.1007/s12031-017-1020-z
42. Karlstetter M, Kopatz J, Aslanidis A, Shahraz A, Caramoy A, Linnartz-Gerlach B, et al. Polysialic acid blocks mononuclear phagocyte reactivity, inhibits complement activation, and protects from vascular damage in the retina. *EMBO Mol Med.* (2017) 9:154–66. doi: 10.15252/emmm.201606627
43. Linnartz-Gerlach B, Mathews M, Neumann H. Sensing the neuronal glycocalyx by glial sialic acid binding immunoglobulin-like lectins. *Neuroscience.* (2014) 275:113–24. doi: 10.1016/j.neuroscience.2014.05.061
44. Shahraz A, Kopatz J, Mathy R, Kappler J, Winter D, Kapoor S, et al. Anti-inflammatory activity of low molecular weight polysialic acid on human macrophages. *Sci Rep.* (2015) 5:16800. doi: 10.1038/srep16800
45. Wielgat P, Braszko JJ. The participation of sialic acids in microglia–neuron interactions. *Cell Immunol.* (2012) 273:17–22. doi: 10.1016/j.cellimm.2011.12.002
46. Wolf Y, Yona S, Kim K-W, Jung S. Microglia, seen from the CX3CR1 angle. *Front Cell Neurosci.* (2013) 7:26. doi: 10.3389/fncel.2013.00026
47. Zieger M, Ahnelt PK, Uhrin P. CX3CL1 (Fractalkine) protein expression in normal and degenerating mouse retina: *in vivo* studies. *PLoS ONE.* (2014) 9:e106562. doi: 10.1371/journal.pone.0106562
48. Huang L, Xu W, Xu G. Transplantation of CX3CL1-expressing mesenchymal stem cells provides neuroprotective and immunomodulatory effects in a rat model of retinal degeneration. *Ocul Immunol Inflamm.* (2013) 21:276–85. doi: 10.3109/09273948.2013.791925
49. Zabel MK, Zhao L, Zhang Y, Gonzalez SR, Ma W, Wang X, et al. Microglial phagocytosis and activation underlying photoreceptor degeneration is regulated by CX3CL1-CX3CR1 signaling in a mouse model of retinitis pigmentosa. *Glia.* (2016) 64:1479–91. doi: 10.1002/glia.23016
50. Wang M, Wong WT. Microglia-Müller cell interactions in the retina. In: Ash J, Grimm C, Hollyfield J, Anderson R, LaVail M, Bowes Rickman C, editors. *Recent Advances in Retinal Degeneration. Advances in Experimental Medicine and Biology*, Vol. 801. New York, NY: Springer (2014). p. 333–8. doi: 10.1007/978-1-4614-3209-8_42
51. Madeira MH, Boia R, Santos PF, Ambrósio AF, Santiago AR. Contribution of microglia-mediated neuroinflammation to retinal degenerative diseases. *Mediat Inflamm.* (2015) 2015:673090. doi: 10.1155/2015/673090
52. Ugolini G, Cremisi F, Maffei L. TrkA, TrkB and p75 mRNA expression is developmentally regulated in the rat retina. *Brain Res.* (1995) 704:121–4. doi: 10.1016/0006-8993(95)01191-9
53. Kirsch M, Lee M-Y, Meyer V, Wiese A, Hofmann H-D. Evidence for multiple, local functions of ciliary neurotrophic factor (CNTF) in retinal development: expression of CNTF and its receptor and *in vitro* effects on target cells. *J Neurochem.* (2002) 68:979–90. doi: 10.1046/j.1471-4159.1997.68030979.x
54. Wilson RB, Kunchithapautham K, Rohrer B. Paradoxical role of BDNF: BDNF ± retinas are protected against light damage-mediated stress. *Invest Ophthalmol Vis Sci.* (2007) 48:2877–86. doi: 10.1167/iovs.06-1079
55. Wen R, Song Y, Liu Y, Li Y, Zhao L, Laties AM. CNTF negatively regulates the phototransduction machinery in rod photoreceptors: implication for light-induced photostasis plasticity. In: Anderson RE, LaVail MM, Hollyfield JG, editors. *Recent Advances in Retinal Degeneration Advances in Experimental Medicine and Biology*, Vol. 613. New York, NY: Springer. (2008). p. 407–13. doi: 10.1007/978-0-387-74904-4_48
56. Harada T, Harada C, Nakayama N, Okuyama S, Yoshida K, Kohsaka S, et al. Modification of glial-neuronal cell interactions prevents photoreceptor apoptosis during light-induced retinal degeneration. *Neuron.* (2000) 26:533–41. doi: 10.1016/S0896-6273(00)81185-X
57. Harada T, Harada C, Kohsaka S, Wada E, Yoshida K, Ohno S, et al. Microglia-Müller glia cell interactions control neurotrophic factor production during light-induced retinal degeneration. *J Neurosci.* (2002) 22:9228–36. doi: 10.1523/JNEUROSCI.22-21-09228.2002
58. Wang M, Ma W, Zhao L, Fariss RN, Wong WT. Adaptive Müller cell responses to microglial activation mediate neuroprotection and coordinate inflammation in the retina. *J Neuroinflammation.* (2011) 8:173. doi: 10.1186/1742-2094-8-173
59. Wenzel A, Grimm C, Samardzija M, Reme CE. Molecular mechanisms of light-induced photoreceptor apoptosis and neuroprotection for retinal degeneration. *Prog Retin Eye Res.* (2005) 24:275–306. doi: 10.1016/j.preteyeres.2004.08.002
60. Shen W, Zhu L, Lee S-R, Chung SH, Gillies MC. Involvement of NT3 and P75NTR in photoreceptor degeneration following selective Müller cell ablation. *J Neuroinflammation.* (2013) 10:137. doi: 10.1186/1742-2094-10-137
61. Wang M, Wang X, Zhao L, Ma W, Rodriguez IR, Fariss RN, et al. Macroglia-microglia interactions via TSPO signaling regulates microglial activation in the mouse retina. *J Neurosci.* (2014) 34:3793–806. doi: 10.1523/JNEUROSCI.3153-13.2014
62. Zamiri P, Sugita S, Streilein JW. Immunosuppressive properties of the pigmented epithelial cells and the subretinal space. In: Niederkorn JY, Kaplan HJ, editors. *Immune Response and the Eye.* Basel: KARGER. p. 86–93. doi: 10.1159/000099259
63. Sennlaub F, Auvynet C, Calippe B, Lavalette S, Poupel L, Hu SJ, et al. CCR2(+) monocytes infiltrate atrophic lesions in age-related macular disease and mediate photoreceptor degeneration in experimental subretinal inflammation in Cx3cr1 deficient mice. *EMBO Mol Med.* (2013) 5:1775–93. doi: 10.1002/emmm.201302692
64. Pfeffer BA, Flanders KC, Guérin CJ, Danielpour D, Anderson DH. Transforming growth factor beta 2 is the predominant isoform in the neural retina, retinal pigment epithelium-choroid and vitreous of the monkey eye. *Exp Eye Res.* (1994) 59:323–33. doi: 10.1006/exer.1994.1114
65. Miyajima-Uchida H, Hayashi H, Beppu R, Kuroki M, Fukami M, Arakawa F, et al. Production and accumulation of thrombospondin-1 in human retinal pigment epithelial cells. *Invest Ophthalmol Vis Sci.* (2000) 41:561–7. Available online at: https://iovs.arvojournals.org/article.aspx?articleid=2199849
66. Zamiri P, Masli S, Streilein JW, Taylor AW. Pigment epithelial growth factor suppresses inflammation by modulating macrophage activation. *Investig Opthalmology Vis Sci.* (2006) 47:3912–8. doi: 10.1167/iovs.05-1267
67. Karlstetter M, Ebert S, Langmann T. Microglia in the healthy and degenerating retina : insights from novel mouse models. *Immunobiology.* (2010) 215:685–91. doi: 10.1016/j.imbio.2010.05.010
68. Gupta N, Shyamasundar S, Patnala R, Karthikeyan A, Arumugam TV, Ling E-A, et al. Recent progress in therapeutic strategies for microglia-mediated neuroinflammation in neuropathologies. *Expert Opin Ther Targets.* (2018) 22:765–81. doi: 10.1080/14728222.2018.1515917
69. Bellver-Landete V, Bretheau F, Mailhot B, Vallières N, Lessard M, Janelle M-E, et al. Microglia are an essential component of the neuroprotective scar that forms after spinal cord injury. *Nat Commun.* (2019) 10:518. doi: 10.1038/s41467-019-08446-0

70. Gupta N, Brown KE, Milam AH. Activated microglia in human retinitis pigmentosa, late-onset retinal degeneration, and age-related macular degeneration. *Exp Eye Res.* (2003) 76:463–71. doi: 10.1016/S0014-4835(02)00332-9
71. Ambati J, Atkinson JP, Gelfand BD. Immunology of age-related macular degeneration. *Nat Rev Immunol.* (2013) 13:438–51. doi: 10.1038/nri3459
72. Pennington KL, DeAngelis MM. Epidemiology of age-related macular degeneration (AMD): associations with cardiovascular disease phenotypes and lipid factors. *Eye Vis.* (2016) 3:34. doi: 10.1186/s40662-016-0063-5
73. Fritsche LG, Fariss RN, Stambolian D, Abecasis GR, Curcio CA, Swaroop A. Age-related macular degeneration: genetics and biology coming together. *Annu Rev Genomics Hum Genet.* (2014) 15:151–71. doi: 10.1146/annurev-genom-090413-025610
74. Tong Y, Ben Ami T, Hong S, Heintzmann R, Gerig G, Ablonczy Z, et al. Hyperspectral autofluorescence imaging of drusen and retinal pigment epithelium in donor eyes with age-related macular degeneration. *Retina.* (2016) 36 (Suppl. 1):S127–36. doi: 10.1097/IAE.0000000000001325
75. Ambati J, Fowler BJ. Mechanisms of age-related macular degeneration. *Neuron.* (2012) 75:26–39. doi: 10.1016/j.neuron.2012.06.018
76. Chichagova V, Hallam D, Collin J, Zerti D, Dorgau B, Felemban M, et al. Cellular regeneration strategies for macular degeneration: past, present and future. *Eye.* (2018) 32:946–71. doi: 10.1038/s41433-018-0061-z
77. Taskintuna I, Elsayed MEAA, Schatz P. Update on clinical trials in dry age-related macular degeneration. *Middle East Afr J Ophthalmol.* (2016) 23:13–26. doi: 10.4103/0974-9233.173134
78. Schick T, Steinhauer M, Aslanidis A, Altay L, Karlstetter M, Langmann T, et al. Local complement activation in aqueous humor in patients with age-related macular degeneration. *Eye.* (2017) 31:810–3. doi: 10.1038/eye.2016.328
79. Jonas JB, Tao Y, Neumaier M, Findeisen P. Cytokine concentration in aqueous humour of eyes with exudative age-related macular degeneration. *Acta Ophthalmol.* (2012) 90:e381–8. doi: 10.1111/j.1755-3768.2012.02414.x
80. Nozaki M, Raisler BJ, Sakurai E, Sarma JV, Barnum SR, Lambris JD, et al. Drusen complement components C3a and C5a promote choroidal neovascularization. *Proc Natl Acad Sci USA*. (2006) 103:2328–33. doi: 10.1073/pnas.0408835103
81. Doyle SL, Campbell M, Ozaki E, Salomon RG, Mori A, Kenna PF, et al. NLRP3 has a protective role in age-related macular degeneration through the induction of IL-18 by drusen components. *Nat Med.* (2012) 18:791–8. doi: 10.1038/nm.2717
82. Indaram M, Ma W, Zhao L, Fariss RN, Rodriguez IR, Wong WT. 7-Ketocholesterol increases retinal microglial migration, activation and angiogenicity: a potential pathogenic mechanism underlying age-related macular degeneration. *Sci Rep.* (2015) 5:9144. doi: 10.1038/srep09144
83. Rodriguez IR, Clark ME, Lee JW, Curcio CA. 7-ketocholesterol accumulates in ocular tissues as a consequence of aging and is present in high levels in drusen. *Exp Eye Res.* (2014) 128:151–5. doi: 10.1016/j.exer.2014.09.009
84. Penfold PL, Madigan MC, Gillies MC, Provis JM. Immunological and aetiological aspects of macular degeneration. *Prog Retin Eye Res.* (2001) 20:385–414. doi: 10.1016/S1350-9462(00)00025-2
85. Madeira MH, Rashid K, Ambrósio AF, Santiago AR, Langmann T. Blockade of microglial adenosine A2A receptor impacts inflammatory mechanisms, reduces ARPE-19 cell dysfunction and prevents photoreceptor loss *in vitro*. *Sci Rep.* (2018) 8:2272. doi: 10.1038/s41598-018-20733-2
86. Nebel C, Aslanidis A, Rashid K, Langmann T. Activated microglia trigger inflammasome activation and lysosomal destabilization in human RPE cells. *Biochem Biophys Res Commun.* (2017) 484:681–6. doi: 10.1016/j.bbrc.2017.01.176
87. Ma W, Zhao L, Fontainhas AM, Fariss RN, Wong WT. Microglia in the mouse retina alter the structure and function of retinal pigmented epithelial cells: a potential cellular interaction relevant to AMD. *PLoS ONE.* (2009) 4:e7945. doi: 10.1371/journal.pone.0007945
88. Tseng WA, Thein T, Kinnunen K, Lashkari K, Gregory MS, D'Amore PA, et al. NLRP3 inflammasome activation in retinal pigment epithelial cells by lysosomal destabilization: implications for age-related macular degeneration. *Investig Opthalmol Vis Sci.* (2013) 54:110–20. doi: 10.1167/iovs.12-10655
89. Scholz R, Sobotka M, Caramoy A, Stempfl T, Moehle C, Langmann T. Minocycline counter-regulates pro-inflammatory microglia responses in the retina and protects from degeneration. *J Neuroinflammation.* (2015) 12:209. doi: 10.1186/s12974-015-0431-4
90. Wiedemann J, Rashid K, Langmann T. Resveratrol induces dynamic changes to the microglia transcriptome, inhibiting inflammatory pathways and protecting against microglia-mediated photoreceptor apoptosis. *Biochem Biophys Res Commun.* (2018) 501:239–45. doi: 10.1016/j.bbrc.2018.04.223
91. Pennesi ME, Neuringer M, Courtney RJ. Animal models of age related macular degeneration. *Mol Aspects Med.* (2012) 33:487–509. doi: 10.1016/j.mam.2012.06.003
92. Zeiss CJ. Review paper: animals as models of age-related macular degeneration. *Vet Pathol.* (2010) 47:396–413. doi: 10.1177/0300985809359598
93. Fletcher EL, Jobling AI, Greferath U, Mills SA, Waugh M, Ho T, et al. Studying age-related macular degeneration using animal models. *Optom Vis Sci.* (2014) 91:878–86. doi: 10.1097/OPX.0000000000000322
94. Grimm C, Remé CE. Light damage as a model of retinal degeneration. In: Weber B, Langmann T, editors. *Methods in Molecular Biology.* Clifton, NJ; Totowa, NJ: Humana Press. p. 87–97. doi: 10.1007/978-1-62703-080-9_6
95. Wenzel A, Grimm C, Marti A, Kueng-Hitz N, Hafezi F, Niemeyer G, et al. c-fos controls the "private pathway" of light-induced apoptosis of retinal photoreceptors. *J Neurosci.* (2000) 20:81–8. doi: 10.1523/JNEUROSCI.20-01-00081.2000
96. Santos AM, MartÃ-n-Oliva D, Ferrer-MartÃ-n RM, Tassi M, Calvente R, Sierra A, et al. Microglial response to light-induced photoreceptor degeneration in the mouse retina. *J Comp Neurol.* (2010) 518:477–92. doi: 10.1002/cne.22227
97. Rutar M, Natoli R, Provis JM. Small interfering RNA-mediated suppression of Ccl2 in Müller cells attenuates microglial recruitment and photoreceptor death following retinal degeneration. *J Neuroinflammation.* (2012) 9:761. doi: 10.1186/1742-2094-9-221
98. Zhang M, Xu G, Liu W, Ni Y, Zhou W. Role of fractalkine/CX3CR1 interaction in light-induced photoreceptor degeneration through regulating retinal microglial activation and migration. *PLoS ONE.* (2012) 7:e35446. doi: 10.1371/journal.pone.0035446
99. Song D, Sulewski ME, Wang C, Song J, Bhuyan R, Sterling J, et al. Complement C5a receptor knockout has diminished light-induced microglia/macrophage retinal migration. *Mol Vis.* (2017) 23:210–18.
100. Guillonneau X, Eandi CM, Paques M, Sahel J-A, Sapieha P, Sennlaub F. On phagocytes and macular degeneration. *Prog Retin Eye Res.* (2017) 61:98–128. doi: 10.1016/j.preteyeres.2017.06.002
101. Hollyfield JG. Age-related macular degeneration: the molecular link between oxidative damage, tissue-specific inflammation and outer retinal disease: the Proctor lecture. *Invest Ophthalmol Vis Sci.* (2010) 51:1275–81. doi: 10.1167/iovs.09-4478
102. Hollyfield JG, Perez VL, Salomon RG. A hapten generated from an oxidation fragment of docosahexaenoic acid is sufficient to initiate age-related macular degeneration. *Mol Neurobiol.* (2010) 41:290–8. doi: 10.1007/s12035-010-8110-z
103. Lambert V, Lecomte J, Hansen S, Blacher S, Gonzalez M-LA, Struman I, et al. Laser-induced choroidal neovascularization model to study age-related macular degeneration in mice. *Nat Protoc.* (2013) 8:2197–211. doi: 10.1038/nprot.2013.135
104. Lückoff A, Caramoy A, Scholz R, Prinz M, Kalinke U, Langmann T. Interferon-beta signaling in retinal mononuclear phagocytes attenuates pathological neovascularization. *EMBO Mol Med.* (2016) 8:670–8. doi: 10.15252/emmm.201505994
105. Combadière C, Feumi C, Raoul W, Keller N, Rodéro M, Pézard A, et al. CX3CR1-dependent subretinal microglia cell accumulation is associated with cardinal features of age-related macular degeneration. *J Clin Invest.* (2007) 117:2920–8. doi: 10.1172/JCI31692
106. Lückoff A, Scholz R, Sennlaub F, Xu H, Langmann T. Comprehensive analysis of mouse retinal mononuclear phagocytes. *Nat Protoc.* (2017) 12:1136–50. doi: 10.1038/nprot.2017.032
107. Huang H, Parlier R, Shen J, Lutty GA, Vinores SA. VEGF receptor blockade markedly reduces retinal microglia/macrophage infiltration into laser-induced CNV. *PLoS ONE.* (2013) 8:e71808. doi: 10.1371/journal.pone.0071808

108. *RetNet^{TM}—Retinal Information Network*. Available online at: https://sph.uth.edu/retnet/ (accessed April 12, 2019).
109. Colella P, Auricchio A. Gene therapy of inherited retinopathies: a long and successful road from viral vectors to patients. *Hum Gene Ther.* (2012) 23:796–807. doi: 10.1089/hum.2012.123
110. Hartong DT, Berson EL, Dryja TP. Retinitis pigmentosa. *Lancet.* (2006) 368:1795–809. doi: 10.1016/S0140-6736(06)69740-7
111. Keeler CE. The inheritance of a retinal abnormality in white mice. *Proc Natl Acad Sci USA.* (1924) 10:329–33. doi: 10.1073/pnas.10.7.329
112. Chang B, Hawes NL, Hurd RE, Davisson MT, Nusinowitz S, Heckenlively JR. Retinal degeneration mutants in the mouse. *Vision Res.* (2002) 42:517–25. doi: 10.1016/S0042-6989(01)00146-8
113. Farber DB, Flannery JG, Bowes-Rickman C. The rd mouse story: seventy years of research on an animal model of inherited retinal degeneration. *Prog Retin Eye Res.* (1994) 13:31–64. doi: 10.1016/1350-9462(94)90004-3
114. Zeiss CJ, Johnson EA. Proliferation of microglia, but not photoreceptors, in the outer nuclear layer of the *rd-1* mouse. *Investig Opthalmol Vis Sci.* (2004) 45:971–6. doi: 10.1167/iovs.03-0301
115. Zeng H, Zhu X, Zhang C, Yang L-P, Wu L, Tso MOM. Identification of sequential events and factors associated with microglial activation, migration, and cytotoxicity in retinal degeneration in rd Mice. *Investig Opthalmol Vis Sci.* (2005) 46:2992–9. doi: 10.1167/iovs.05-0118
116. Blank T, Goldmann T, Koch M, Amann L, Schön C, Bonin M, et al. Early microglia activation precedes photoreceptor degeneration in a mouse model of CNGB1-linked retinitis pigmentosa. *Front Immunol.* (2018) 8:1930. doi: 10.3389/fimmu.2017.01930
117. Guo C, Otani A, Oishi A, Kojima H, Makiyama Y, Nakagawa S, et al. Knockout of ccr2 alleviates photoreceptor cell death in a model of retinitis pigmentosa. *Exp Eye Res.* (2012) 104:39–47. doi: 10.1016/j.exer.2012.08.013
118. Wang N-K, Lai C-C, Liu C-H, Yeh L-K, Chou CL, Kong J, et al. Origin of fundus hyperautofluorescent spots and their role in retinal degeneration in a mouse model of Goldmann-Favre syndrome. *Dis Model Mech.* (2013) 6:1113–22. doi: 10.1242/dmm.012112
119. Akhmedov NB, Piriev NI, Chang B, Rapoport AL, Hawes NL, Nishina PM, et al. A deletion in a photoreceptor-specific nuclear receptor mRNA causes retinal degeneration in the rd7 mouse. *Proc Natl Acad Sci USA.* (2000) 97:5551–6. doi: 10.1073/pnas.97.10.5551
120. Aredo B, Zhang K, Chen X, Wang CX-Z, Li T, Ufret-Vincenty RL. Differences in the distribution, phenotype and gene expression of subretinal microglia/macrophages in C57BL/6N (Crb1 rd8/rd8) versus C57BL6/J (Crb1 wt/wt) mice. *J Neuroinflammation.* (2015) 12:6. doi: 10.1186/s12974-014-0221-4
121. Chen X, Kezic J, Bemard C, Mcmenamin PG, Med D. Rd8 mutation in the CrbJ gene of COl Jc-eYFP transgenic reporter mice resuits in abnormal numbers of CDJ J c-positive ceils in the retina. *J Neuropathol Exp Neurol.* (2013) 72:782–90. doi: 10.1097/NEN.0b013e31829e8375
122. Altmann C, Schmidt MHH. The role of microglia in diabetic retinopathy: inflammation, microvasculature defects and neurodegeneration. *Int J Mol Sci.* (2018) 19:E110. doi: 10.3390/ijms19010110
123. Lechner J, O'Leary OE, Stitt AW. The pathology associated with diabetic retinopathy. *Vis Res.* (2017) 139:7–14. doi: 10.1016/j.visres.2017.04.003
124. Demircan N, Safran BG, Soylu M, Ozcan AA, Sizmaz S. Determination of vitreous interleukin-1 (IL-1) and tumour necrosis factor (TNF) levels in proliferative diabetic retinopathy. *Eye.* (2006) 20:1366–9. doi: 10.1038/sj.eye.6702138
125. Koskela UE, Kuusisto SM, Nissinen AE, Savolainen MJ, Liinamaa MJ. High vitreous concentration of IL-6 and IL-8, but not of adhesion molecules in relation to plasma concentrations in proliferative diabetic retinopathy. *Ophthalmic Res.* (2013) 49:108–14. doi: 10.1159/000342977
126. Muramatsu D, Wakabayashi Y, Usui Y, Okunuki Y, Kezuka T, Goto H. Correlation of complement fragment C5a with inflammatory cytokines in the vitreous of patients with proliferative diabetic retinopathy. *Graefe's Arch Clin Exp Ophthalmol.* (2013) 251:15–17. doi: 10.1007/s00417-012-2024-6
127. Powell EU, Field R. Diabetic retinopathy and rheumatoid arthritis. *Lancet.* (1964) 284:17–8. doi: 10.1016/S0140-6736(64)90008-X
128. Boss JD, Singh PK, Pandya HK, Tosi J, Kim C, Tewari A, et al. Assessment of neurotrophins and inflammatory mediators in vitreous of patients with diabetic retinopathy. *Investig Opthalmol Vis Sci.* (2017) 58:5594–603. doi: 10.1167/iovs.17-21973
129. Abu El Asrar AM, Maimone D, Morse PH, Gregory S, Reder AT. Cytokines in the vitreous of patients with proliferative diabetic retinopathy. *Am J Ophthalmol.* (1992) 114:731–6. doi: 10.1016/S0002-9394(14)74052-8
130. Tomlinson DR, Gardiner NJ. Glucose neurotoxicity. *Nat Rev Neurosci.* (2008) 9:36–45. doi: 10.1038/nrn2294
131. Zong H, Ward M, Stitt AW. AGEs, RAGE, and diabetic retinopathy. *Curr Diab Rep.* (2011) 11:244–52. doi: 10.1007/s11892-011-0198-7
132. Milne R, Brownstein S. Advanced glycation end products and diabetic retinopathy. *Amino Acids.* (2013) 44:1397–407. doi: 10.1007/s00726-011-1071-3
133. Du Y, Smith MA, Miller CM, Kern TS. Diabetes-induced nitrative stress in the retina, and correction by aminoguanidine. *J Neurochem.* (2002) 80:771–9. doi: 10.1046/j.0022-3042.2001.00737.x
134. Zeng XX, Ng YK, Ling EA. Neuronal and microglial response in the retina of streptozotocin-induced diabetic rats. *Vis Neurosci.* (2000) 17:463–71. doi: 10.1017/S0952523800173122
135. Zeng H, Green WR, Tso MOM. Microglial activation in human diabetic retinopathy. *Arch Ophthalmol.* (2008) 126:227–32. doi: 10.1001/archophthalmol.2007.65
136. Grigsby JG, Cardona SM, Pouw CE, Muniz A, Mendiola AS, Tsin ATC, et al. The role of microglia in diabetic retinopathy. *J Ophthalmol.* (2014) 2014:705783. doi: 10.1155/2014/705783
137. Kezic JM, Chen X, Rakoczy EP, McMenamin PG. The effects of age and Cx$_3$ cr1 deficiency on retinal microglia in the *Ins2 ^{Akita}* diabetic mouse. *Investig Opthalmol Vis Sci.* (2013) 54:854–63. doi: 10.1167/iovs.12-10876
138. Barber AJ, Antonetti DA, Kern TS, Reiter CEN, Soans RS, Krady JK, et al. The Ins2 ^{Akita} mouse as a model of early retinal complications in diabetes. *Investig Opthalmol Vis Sci.* (2005) 46:2210. doi: 10.1167/iovs.04-1340
139. Omri S, Behar-Cohen F, de Kozak Y, Sennlaub F, Verissimo LM, Jonet L, et al. Microglia/macrophages migrate through retinal epithelium barrier by a transcellular route in diabetic retinopathy: role of PKCζ in the Goto Kakizaki rat model. *Am J Pathol.* (2011) 179:942–53. doi: 10.1016/j.ajpath.2011.04.018
140. Lenzen S. The mechanisms of alloxan- and streptozotocin-induced diabetes. *Diabetologia.* (2008) 51:216–26. doi: 10.1007/s00125-007-0886-7
141. Gaucher D, Chiappore J-A, Pâques M, Simonutti M, Boitard C, Sahel JA, et al. Microglial changes occur without neural cell death in diabetic retinopathy. *Vision Res.* (2007) 47:612–23. doi: 10.1016/j.visres.2006.11.017
142. Chen X, Zhou H, Gong Y, Wei S, Zhang M. Early spatiotemporal characterization of microglial activation in the retinas of rats with streptozotocin-induced diabetes. *Graefe's Arch Clin Exp Ophthalmol.* (2015) 253:519–25. doi: 10.1007/s00417-014-2727-y
143. Jonas JB, Aung T, Bourne RR, Bron AM, Ritch R, Panda-Jonas S. Glaucoma. *Lancet.* (2017) 390:2183–93. doi: 10.1016/S0140-6736(17)31469-1
144. Quigley HA, Broman AT. The number of people with glaucoma worldwide in 2010 and 2020. *Br J Ophthalmol.* (2006) 90:262–7. doi: 10.1136/bjo.2005.081224
145. Stevens GA, White RA, Flaxman SR, Price H, Jonas JB, Keeffe J, et al. Global prevalence of vision impairment and blindness: magnitude and temporal trends, 1990–2010. *Ophthalmology.* (2013) 120:2377–84. doi: 10.1016/j.ophtha.2013.05.025
146. Kass MA, Heuer DK, Higginbotham EJ, Johnson CA, Keltner JL, Miller JP, et al. The ocular hypertension treatment study: a randomized trial determines that topical ocular hypotensive medication delays or prevents the onset of primary open-angle glaucoma. *Arch Ophthalmol.* (2002) 120:701–13; discussion 829-30. doi: 10.1001/archopht.120.6.701
147. Rudnicka AR, Mt-Isa S, Owen CG, Cook DG, Ashby D. Variations in primary open-angle glaucoma prevalence by age, gender, and race: a bayesian meta-analysis. *Investig Opthalmology Vis Sci.* (2006) 47:4254–61. doi: 10.1167/iovs.06-0299
148. Leske MC, Wu SY, Honkanen R, Nemesure B, Schachat A, Hyman L, et al. Nine-year incidence of open-angle glaucoma in the barbados eye studies. *Ophthalmology.* (2007) 114:1058–64. doi: 10.1016/j.ophtha.2006.08.051
149. Bessero A-C, Clarke PG. Neuroprotection for optic nerve disorders. *Curr Opin Neurol.* (2010) 23:10–15. doi: 10.1097/WCO.0b013e3283344461

150. Baltmr A, Duggan J, Nizari S, Salt TE, Cordeiro MF. Neuroprotection in glaucoma—is there a future role? *Exp Eye Res.* (2010) 91:554–66. doi: 10.1016/j.exer.2010.08.009
151. Cordeiro MF, Levin LA. Clinical evidence for neuroprotection in glaucoma. *Am J Ophthalmol.* (2011) 152:715–6. doi: 10.1016/j.ajo.2011.06.015
152. Tezel G. Immune regulation toward immunomodulation for neuroprotection in glaucoma. *Curr Opin Pharmacol.* (2013) 13:23–31. doi: 10.1016/j.coph.2012.09.013
153. Yan X, Tezel G, Wax MB, Edward DP. Matrix metalloproteinases and tumor necrosis factor α in glaucomatous optic nerve head. *Arch Ophthalmol.* (2000) 118:666–73. doi: 10.1001/archopht.118.5.666
154. Kuchtey J, Rezaei KA, Jaru-Ampornpan P, Sternberg P, Kuchtey RW, Kuchtey RW. Multiplex cytokine analysis reveals elevated concentration of interleukin-8 in glaucomatous aqueous humor. *Invest Ophthalmol Vis Sci.* (2010) 51:6441–7. doi: 10.1167/iovs.10-5216
155. Sawada H, Fukuchi T, Tanaka T, Abe H. Tumor necrosis factor-α concentrations in the aqueous humor of patients with Glaucoma. *Investig Opthalmology Vis Sci.* (2010) 51:903–6. doi: 10.1167/iovs.09-4247
156. Chua J, Vania M, Cheung CMG, Ang M, Chee SP, Yang H, et al. Expression profile of inflammatory cytokines in aqueous from glaucomatous eyes. *Mol Vis.* (2012) 18:431–8.
157. Zeng H-L, Shi J-M. The role of microglia in the progression of glaucomatous neurodegeneration- a review. *Int J Ophthalmol.* (2018) 11:143–9. doi: 10.18240/ijo.2018.01.22
158. Yuan L, Neufeld AH. Activated microglia in the human glaucomatous optic nerve head. *J Neurosci Res.* (2001) 64:523–32. doi: 10.1002/jnr.1104
159. Neufeld AH. Microglia in the optic nerve head and the region of parapapillary chorioretinal atrophy in Glaucoma. *Arch Ophthalmol.* (1999) 117:1050–6. doi: 10.1001/archopht.117.8.1050
160. Luo C, Yang X, Kain AD, Powell DW, Kuehn MH, Tezel G. Glaucomatous tissue stress and the regulation of immune response through glial toll-like receptor signaling. *Investig Opthalmology Vis Sci.* (2010) 51:5697–707. doi: 10.1167/iovs.10-5407
161. Ishikawa M, Yoshitomi T, Zorumski CF, Izumi Y. Experimentally induced mammalian models of Glaucoma. *Biomed Res Int.* (2015) 2015:281214. doi: 10.1155/2015/281214
162. Bosco A, Steele MR, Vetter ML. Early microglia activation in a mouse model of chronic glaucoma. *J Comp Neurol.* (2011) 519:599–620. doi: 10.1002/cne.22516
163. Inman DM, Horner PJ. Reactive nonproliferative gliosis predominates in a chronic mouse model of glaucoma. *Glia.* (2007) 55:942–53. doi: 10.1002/glia.20516
164. Tezel G, Yang X, Yang J, Wax MB. Role of tumor necrosis factor receptor-1 in the death of retinal ganglion cells following optic nerve crush injury in mice. *Brain Res.* (2004) 996:202–12. doi: 10.1016/j.brainres.2003.10.029
165. Yuan L, Neufeld AH. Tumor necrosis factor-alpha: a potentially neurodestructive cytokine produced by glia in the human glaucomatous optic nerve head. *Glia.* (2000) 32:42–50. doi: 10.1002/1098-1136(200010)32:1<42::AID-GLIA40>3.3.CO;2-V
166. Tezel G, Li LY, Patil RV, Wax MB. TNF-α and TNF-α receptor-1 in the retina of normal and glaucomatous eyes. *Invest Ophthalmol Vis Sci.* (2001) 42:1787–94. Available online at: https://iovs.arvojournals.org/article.aspx?articleid=2200019
167. Roh M, Zhang Y, Murakami Y, Thanos A, Lee SC, Vavvas DG, et al. Etanercept, a widely used inhibitor of tumor necrosis factor-α (TNF- α), prevents retinal ganglion cell loss in a rat model of glaucoma. *PLoS ONE.* (2012) 7:e40065. doi: 10.1371/journal.pone.0040065
168. Neufeld AH, Hernandez MR, Gonzalez M. Nitric oxide synthase in the human glaucomatous optic nerve head. *Arch Ophthalmol.* (1997) 115:497–503. doi: 10.1001/archopht.1997.01100150499009
169. Vidal L, Díaz F, Villena A, Moreno M, Campos JG, Vargas IP de. Nitric oxide synthase in retina and optic nerve head of rat with increased intraocular pressure and effect of timolol. *Brain Res Bull.* (2006) 70:406–13. doi: 10.1016/j.brainresbull.2006.07.009
170. Cho KJ, Kim JH, Park H-YL, Park CK. Glial cell response and iNOS expression in the optic nerve head and retina of the rat following acute high IOP ischemia–reperfusion. *Brain Res.* (2011) 1403:67–77. doi: 10.1016/j.brainres.2011.06.005
171. Shibata M, Sugiyama T, Hoshiga M, Hotchi J, Okuno T, Oku H, et al. Changes in optic nerve head blood flow, visual function, and retinal histology in hypercholesterolemic rabbits. *Exp Eye Res.* (2011) 93:818–24. doi: 10.1016/j.exer.2011.09.014
172. Neufeld AH, Sawada A, Becker B. Inhibition of nitric-oxide synthase 2 by aminoguanidine provides neuroprotection of retinal ganglion cells in a rat model of chronic glaucoma. *Proc Natl Acad Sci USA.* (1999) 96:9944–8. doi: 10.1073/pnas.96.17.9944
173. Echevarria FD, Formichella CR, Sappington RM. Interleukin-6 deficiency attenuates retinal ganglion cell axonopathy and glaucoma-related vision loss. *Front Neurosci.* (2017) 11:318. doi: 10.3389/fnins.2017.00318
174. Sappington RM, Chan M, Calkins DJ. Interleukin-6 protects retinal ganglion cells from pressure-induced death. *Investig Opthalmol Vis Sci.* (2006) 47:2932–42. doi: 10.1167/iovs.05-1407
175. Sappington RM, Calkins DJ. Pressure-induced regulation of IL-6 in retinal glial cells: involvement of the ubiquitin/proteasome pathway and NFκB. *Investig Opthalmology Vis Sci.* (2006) 47:3860–9. doi: 10.1167/iovs.05-1408
176. Echevarria FD, Rickman AE, Sappington RM. Interleukin-6: a constitutive modulator of glycoprotein 130, neuroinflammatory and cell survival signaling in retina. *J Clin Cell Immunol.* (2016) 7:439. doi: 10.4172/2155-9899.1000439
177. Hildebrandt H, Dityatev A. Polysialic acid in brain development and synaptic plasticity. *Top Curr Chem.* (2015) 366:55–96. doi: 10.1007/128_2013_446
178. Schnaar RL, Gerardy-Schahn R, Hildebrandt H. Sialic acids in the brain: gangliosides and polysialic acid in nervous system development, stability, disease, and regeneration. *Physiol Rev.* (2014) 94:461–518. doi: 10.1152/physrev.00033.2013
179. Rutishauser U. Polysialic acid in the plasticity of the developing and adult vertebrate nervous system. *Nat Rev Neurosci.* (2008) 9:26–35. doi: 10.1038/nrn2285
180. Angata T, Kerr SC, Greaves DR, Varki NM, Crocker PR, Varki A. Cloning and Characterization of Human Siglec-11. *J Biol Chem.* (2002) 277:24466–74. doi: 10.1074/jbc.M202833200
181. Wang Y, Neumann H. Alleviation of neurotoxicity by microglial human siglec-11. *J Neurosci.* (2010) 30:3482–8. doi: 10.1523/JNEUROSCI.3940-09.2010
182. Ulanova M, Asfaha S, Stenton G, Lint A, Gilbertson D, Schreiber A, et al. Involvement of Syk protein tyrosine kinase in LPS-induced responses in macrophages. *J Endotoxin Res.* (2007) 13:117–25. doi: 10.1177/0968051907079125
183. Gurung P, Fan G, Lukens JR, Vogel P, Tonks NK, Kanneganti T-D. Tyrosine kinase SYK licenses MyD88 adaptor protein to instigate IL-1α-mediated inflammatory disease. *Immunity.* (2017) 46:635–48. doi: 10.1016/j.immuni.2017.03.014
184. Linnartz B, Neumann H. Microglial activatory (immunoreceptor tyrosine-based activation motif)- and inhibitory (immunoreceptor tyrosine-based inhibition motif)-signaling receptors for recognition of the neuronal glycocalyx. *Glia.* (2013) 61:37–46. doi: 10.1002/glia.22359
185. Goswami K, Nandakumar DN, Koner BC, Bobby Z, Sen SK. Oxidative changes and desialylation of serum proteins in hyperthyroidism. *Clin Chim Acta.* (2003) 337:163–8. doi: 10.1016/j.cccn.2003.08.009
186. Moseley R, Waddington R, Embery G. Degradation of glycosaminoglycans by reactive oxygen species derived from stimulated polymorphonuclear leukocytes. *Biochim Biophys Acta Mol Basis Dis.* (1997) 1362:221–31. doi: 10.1016/S0925-4439(97)00083-5
187. Linnartz-Gerlach B, Schuy C, Shahraz A, Tenner AJ, Neumann H. Sialylation of neurites inhibits complement-mediated macrophage removal in a human macrophage-neuron Co-Culture System. *Glia.* (2016) 64:35–47. doi: 10.1002/glia.22901
188. Howell GR, Macalinao DG, Sousa GL, Walden M, Soto I, Kneeland SC, et al. Molecular clustering identifies complement and endothelin induction as early events in a mouse model of glaucoma. *J Clin Invest.* (2011) 121:1429–44. doi: 10.1172/JCI44646

189. Rupprecht R, Papadopoulos V, Rammes G, Baghai TC, Fan J, Akula N, et al. Translocator protein (18 kDa) (TSPO) as a therapeutic target for neurological and psychiatric disorders. *Nat Rev Drug Discov.* (2010) 9:971–88. doi: 10.1038/nrd3295
190. Karlstetter M, Nothdurfter C, Aslanidis A, Moeller K, Horn F, Scholz R, et al. Translocator protein (18kDa) (TSPO) is expressed in reactive retinal microglia and modulates microglial inflammation and phagocytosis. *J Neuroinflammation.* (2014) 11:3. doi: 10.1186/1742-2094-11-3
191. Selvaraj V, Stocco DM. The changing landscape in translocator protein (TSPO) function. *Trends Endocrinol Metab.* (2015) 26:341–8. doi: 10.1016/j.tem.2015.02.007
192. Daugherty DJ, Selvaraj V, Chechneva OV, Liu X-B, Pleasure DE, Deng W. A TSPO ligand is protective in a mouse model of multiple sclerosis. *EMBO Mol Med.* (2013) 5:891–903. doi: 10.1002/emmm.201202124
193. Scholz R, Caramoy A, Bhuckory M, Rashid K, Chen M, Xu H, et al. Targeting translocator protein (18kDa) (TSPO) dampens pro-inflammatory microglia reactivity in the retina and protects from degeneration. *J Neuroinflammation.* (2015) 12:201. doi: 10.1186/s12974-015-0422-5
194. Banati RB, Middleton RJ, Chan R, Hatty CR, Wai-Ying Kam W, Quin C, et al. Positron emission tomography and functional characterization of a complete PBR/TSPO knockout. *Nat Commun.* (2014) 5:5452. doi: 10.1038/ncomms6452
195. Liu G-J, Middleton RJ, Hatty CR, Kam WW-Y, Chan R, Pham T, et al. The 18 kDa translocator protein, microglia and neuroinflammation. *Brain Pathol.* (2014) 24:631–53. doi: 10.1111/bpa.12196
196. Costa E, Guidotti A. Diazepam binding inhibitor (DBI): a peptide with multiple biological actions. *Life Sci.* (1991) 49:325–44. doi: 10.1016/0024-3205(91)90440-M
197. Heckenlively JR, Rodriguez JA, Daiger SP. Autosomal dominant sectoral retinitis pigmentosa. *Arch Ophthalmol.* (1991) 109:84–91. doi: 10.1001/archopht.1991.01080010086038
198. Cruickshanks KJ, Klein R, Klein BEK. Sunlight and age-related macular degeneration. *Arch Ophthalmol.* (1993) 111:514–8. doi: 10.1001/archopht.1993.01090040106042
199. Cruickshanks KJ, Klein R, Klein BE, Nondahl DM. Sunlight and the 5-year incidence of early age-related maculopathy: the beaver dam eye study. *Arch Ophthalmol.* (2001) 119:246–50. doi: 10.1001/archopht.119.9.1354
200. Fletcher AE, Bentham GC, Agnew M, Young IS, Augood C, Chakravarthy U, et al. Sunlight exposure, antioxidants, and age-related macular degeneration. *Arch Ophthalmol.* (2008) 126:1396–403. doi: 10.1001/archopht.126.10.1396
201. Papadopoulos V, Aghazadeh Y, Fan J, Campioli E, Zirkin B, Midzak A. Translocator protein-mediated pharmacology of cholesterol transport and steroidogenesis. *Mol Cell Endocrinol.* (2015) 408:90–8. doi: 10.1016/j.mce.2015.03.014
202. Jamin N, Neumann J-M, Ostuni MA, Vu TKN, Yao Z-X, Murail S, et al. Characterization of the cholesterol recognition amino acid consensus sequence of the peripheral-type benzodiazepine receptor. *Mol Endocrinol.* (2005) 19:588–94. doi: 10.1210/me.2004-0308
203. Batarseh A, Barlow KD, Martinez-Arguelles DB, Papadopoulos V. Functional characterization of the human translocator protein (18kDa) gene promoter in human breast cancer cell lines. *Biochim Biophys Acta.* (2012) 1819:38–56. doi: 10.1016/j.bbagrm.2011.09.001
204. Tu LN, Zhao AH, Stocco DM, Selvaraj V. PK11195 effect on steroidogenesis is not mediated through the translocator protein (TSPO). *Endocrinology.* (2015) 156:1033–9. doi: 10.1210/en.2014-1707
205. Papadopoulos V, Berkovich A, Krueger KE, Costa E, Guidotti A. Diazepam binding inhibitor and its processing products stimulate mitochondrial steroid biosynthesis via an interaction with mitochondrial benzodiazepine receptors *. *Endocrinology.* (1991) 129:1481–8. doi: 10.1210/endo-129-3-1481
206. Romeo E, Cavallaro S, Korneyev A, Kozikowski AP, Ma D, Polo A, et al. Stimulation of brain steroidogenesis by 2-aryl-indole-3-acetamide derivatives acting at the mitochondrial diazepam-binding inhibitor receptor complex. *J Pharmacol Exp Ther.* (1993) 267:462–71.
207. Boujrad N, Hudson JR, Papadopoulos V. Inhibition of hormone-stimulated steroidogenesis in cultured Leydig tumor cells by a cholesterol-linked phosphorothioate oligodeoxynucleotide antisense to diazepam-binding inhibitor. *Proc Natl Acad Sci USA.* (1993) 90:5728–31. doi: 10.1073/pnas.90.12.5728
208. Owen DR, Fan J, Campioli E, Venugopal S, Midzak A, Daly E, et al. TSPOmutations in rats and a human polymorphism impair the rate of steroid synthesis. *Biochem J.* (2017) 474:3985–99. doi: 10.1042/BCJ20170648
209. Vasconcelos AR, Cabral-Costa JV, Mazucanti CH, Scavone C, Kawamoto EM. The role of steroid hormones in the modulation of neuroinflammation by dietary interventions. *Front Endocrinol.* (2016) 7:9. doi: 10.3389/fendo.2016.00009
210. Barnes PJ. How corticosteroids control inflammation: quintiles prize lecture 2005. *Br J Pharmacol.* (2006) 148:245–54. doi: 10.1038/sj.bjp.0706736
211. Byrne AM, Roche SL, Ruiz-Lopez AM, Jackson ACW, Cotter TG. The synthetic progestin norgestrel acts to increase LIF levels in the rd10 mouse model of retinitis pigmentosa. *Mol Vis.* (2016) 22:264–74. doi: 10.1016/j.redox.2016.10.002
212. Doonan F, O'Driscoll C, Kenna P, Cotter TG. Enhancing survival of photoreceptor cells *in vivo* using the synthetic progestin Norgestrel. *J Neurochem.* (2011) 118:915–27. doi: 10.1111/j.1471-4159.2011.07354.x
213. Roche SL, Wyse-Jackson AC, Ruiz-Lopez AM, Byrne AM, Cotter TG. Fractalkine-CX3CR1 signaling is critical for progesterone-mediated neuroprotection in the retina. *Sci Rep.* (2017) 7:43067. doi: 10.1038/srep43067
214. Roche SL, Wyse-Jackson AC, Gómez-Vicente V, Lax P, Ruiz-Lopez AM, Byrne AM, et al. Progesterone attenuates microglial-driven retinal degeneration and stimulates protective fractalkine-CX3CR1 signaling. *PLoS ONE.* (2016) 11:e0165197. doi: 10.1371/journal.pone.0165197
215. Zhu C, Wang S, Wang B, Du F, Hu C, Li H, et al. 17β-Estradiol up-regulates Nrf2 via PI3K/AKT and estrogen receptor signaling pathways to suppress light-induced degeneration in rat retina. *Neuroscience.* (2015) 304:328–39. doi: 10.1016/j.neuroscience.2015.07.057
216. McNab F, Mayer-Barber K, Sher A, Wack A, O'Garra A. Type I interferons in infectious disease. *Nat Rev Immunol.* (2015) 15:87–103. doi: 10.1038/nri3787
217. González-Navajas JM, Lee J, David M, Raz E. Immunomodulatory functions of type I interferons. *Nat Rev Immunol.* (2012) 12:125–35. doi: 10.1038/nri3133
218. Kocur M, Schneider R, Pulm A-K, Bauer J, Kropp S, Gliem M, et al. IFNβ secreted by microglia mediates clearance of myelin debris in CNS autoimmunity. *Acta Neuropathol Commun.* (2015) 3:20. doi: 10.1186/s40478-015-0192-4
219. Stetson DB, Medzhitov R. Review type I interferons in host defense. *Immunity.* (2006) 25:373–81. doi: 10.1016/j.immuni.2006.08.007
220. Dendrou CA, Fugger L, Friese MA. Immunopathology of multiple sclerosis. *Nat Rev Immunol.* (2015) 15:545–58. doi: 10.1038/nri3871
221. Prinz M, Schmidt H, Mildner A, Knobeloch K-P, Hanisch U-K, Raasch J, et al. Distinct and nonredundant *in vivo* functions of IFNAR on myeloid cells limit autoimmunity in the central nervous system. *Immunity.* (2008) 28:675–86. doi: 10.1016/j.immuni.2008.03.011
222. Liu J, Copland DA, Horie S, Wu W-K, Chen M, Xu Y, et al. Myeloid cells expressing VEGF and Arginase-1 following uptake of damaged retinal pigment epithelium suggests potential mechanism that drives the onset of choroidal angiogenesis in mice. *PLoS ONE.* (2013) 8:e72935. doi: 10.1371/journal.pone.0072935
223. Kimoto T, Takahashi K, Tobe T, Fujimoto K, Uyama M, Sone S. Effects of local administration of interferon-beta on proliferation of retinal pigment epithelium in rabbit after laser photocoagulation. *Jpn J Ophthalmol.* (2002) 46:160–9.
224. Cirino AC, Mathura JR, Jampol LM. of chronic recurrent OF Resolution of activity (choroiditis and choroidal neovascularization) of chronic recurrent punctate inner choroidopathy after treatment with interferon B-1A. *Retina.* (2006) 26:1091–2. doi: 10.1097/01.iae.0000254891.48272.13
225. Schreiber G. The molecular basis for differential type I interferon signaling. *J Biol Chem.* (2017) 292:7285–94. doi: 10.1074/jbc.R116.774562
226. Akhtar LN, Qin H, Muldowney MT, Yanagisawa LL, Kutsch O, Clements JE, et al. Suppressor of cytokine signaling 3 inhibits antiviral IFN-beta signaling to enhance HIV-1 replication in macrophages. *J Immunol.* (2010) 185:2393–404. doi: 10.4049/jimmunol.0903563

227. Ivashkiv LB, Donlin LT. Regulation of type I interferon responses. *Nat Rev Immunol.* (2014) 14:36–49. doi: 10.1038/nri3581
228. Yoshimura A, Naka T, Kubo M. SOCS proteins, cytokine signalling and immune regulation. *Nat Rev Immunol.* (2007) 7:454–65. doi: 10.1038/nri2093
229. Krebs DL, Hilton DJ. SOCS Proteins: negative regulators of cytokine signaling. *Stem Cells.* (2001) 19:378–87. doi: 10.1634/stemcells.19-5-378
230. Chen M, Zhao J, Ali IHA, Marry S, Augustine J, Bhuckory M, et al. Cytokine signaling protein 3 deficiency in myeloid cells promotes retinal degeneration and angiogenesis through arginase-1 up-regulation in experimental autoimmune uveoretinitis. *Am J Pathol.* (2018) 188:1007–20. doi: 10.1016/j.ajpath.2017.12.021
231. Yu C-R, Mahdi RR, Oh H-M, Amadi-Obi A, Levy-Clarke G, Burton J, et al. Suppressor of cytokine signaling-1 (SOCS1) inhibits lymphocyte recruitment into the retina and protects SOCS1 transgenic rats and mice from ocular inflammation. *Invest Ophthalmol Vis Sci.* (2011) 52:6978–86. doi: 10.1167/iovs.11-7688
232. Burke JD, Platanias LC, Fish EN. Beta interferon regulation of glucose metabolism is PI3K/Akt dependent and important for antiviral activity against coxsackievirus B3. *J Virol.* (2014) 88:3485–95. doi: 10.1128/JVI.02649-13
233. Platanias LC. Mechanisms of type-I- and type-II-interferon-mediated signalling. *Nat Rev Immunol.* (2005) 5:375–86. doi: 10.1038/nri1604
234. Liu Y, Marin A, Ejlerskov P, Rasmussen LM, Prinz M, Issazadeh-Navikas S. Neuronal IFN-beta–induced PI3K/Akt-FoxA1 signalling is essential for generation of FoxA1 þ T reg cells. *Nat Commun.* (2017) 8:14709. doi: 10.1038/ncomms14709
235. Dong H, Zhang X, Dai X, Lu S, Gui B, Jin W, et al. Lithium ameliorates lipopolysaccharide-induced microglial activation via inhibition of toll-like receptor 4 expression by activating the PI3K/Akt/FoxO1 pathway. *J Neuroinflammation.* (2014) 11:140. doi: 10.1186/s12974-014-0140-4
236. Zhu YP, Brown JR, Sag D, Zhang L, Suttles J. Adenosine 5'-monophosphate-activated protein kinase regulates IL-10-mediated anti-inflammatory signaling pathways in macrophages. *J Immunol.* (2015) 194:584–94. doi: 10.4049/jimmunol.1401024
237. de Oliveira ACP, Candelario-Jalil E, Bhatia HS, Lieb K, Hüll M, Fiebich BL. Regulation of prostaglandin E2 synthase expression in activated primary rat microglia: evidence for uncoupled regulation of mPGES-1 and COX-2. *Glia.* (2008) 56:844–55. doi: 10.1002/glia.20658
238. de Oliveira AC, Candelario-Jalil E, Langbein J, Wendeburg L, Bhatia HS, Schlachetzki JC, et al. Pharmacological inhibition of Akt and downstream pathways modulates the expression of COX-2 and mPGES-1 in activated microglia. *J Neuroinflammation.* (2012) 9:2. doi: 10.1186/1742-2094-9-2
239. Jope RS, Cheng Y, Lowell JA, Worthen RJ, Sitbon YH, Beurel E. Stressed and Inflamed, Can GSK3 Be Blamed? *Trends Biochem Sci.* (2017) 42:180–92. doi: 10.1016/j.tibs.2016.10.009
240. Huang W-C, Lin Y-S, Wang C-Y, Tsai C-C, Tseng H-C, Chen C-L, et al. Glycogen synthase kinase-3 negatively regulates anti-inflammatory interleukin-10 for lipopolysaccharide-induced iNOS/NO biosynthesis and RANTES production in microglial cells. *Immunology.* (2009) 128:e275–86. doi: 10.1111/j.1365-2567.2008.02959.x
241. Sánchez-Cruz A, Villarejo-Zori B, Marchena M, Zaldivar-Díez J, Palomo V, Gil C, et al. Modulation of GSK-3 provides cellular and functional neuroprotection in the rd10 mouse model of retinitis pigmentosa. *Mol Neurodegener.* (2018) 13:19. doi: 10.1186/s13024-018-0251-y
242. Garrido-Mesa N, Zarzuelo A, Gálvez J. Minocycline: far beyond an antibiotic. *Br J Pharmacol.* (2013) 169:337–52. doi: 10.1111/bph.12139
243. Domercq M, Matute C. Neuroprotection by tetracyclines. *Trends Pharmacol Sci.* (2004) 25:609–12. doi: 10.1016/j.tips.2004.10.001
244. Nikodemova M, Duncan ID, Watters JJ. Minocycline exerts inhibitory effects on multiple mitogen-activated protein kinases and IκBα degradation in a stimulus-specific manner in microglia. *J Neurochem.* (2006) 96:314–23. doi: 10.1111/j.1471-4159.2005.03520.x
245. Halder SK, Matsunaga H, Ishii KJ, Akira S, Miyake K, Ueda H. Retinal cell type-specific prevention of ischemia-induced damages by LPS-TLR4 signaling through microglia. *J Neurochem.* (2013) 126:243–60. doi: 10.1111/jnc.12262
246. Kobayashi K, Imagama S, Ohgomori T, Hirano K, Uchimura K, Sakamoto K, et al. Minocycline selectively inhibits M1 polarization of microglia. *Cell Death Dis.* (2013) 4:e525. doi: 10.1038/cddis.2013.54
247. Peng B, Xiao J, Wang K, So K-F, Tipoe GL, Lin B. Suppression of microglial activation is neuroprotective in a mouse model of human retinitis pigmentosa. *J Neurosci.* (2014) 34:8139–50. doi: 10.1523/JNEUROSCI.5200-13.2014
248. Krady JK, Basu A, Allen CM, Xu Y, LaNoue KF, Gardner TW, et al. Minocycline reduces proinflammatory cytokine expression, microglial activation, and caspase-3 activation in a rodent model of diabetic retinopathy. *Diabetes.* (2005) 54:1559–65. doi: 10.2337/diabetes.54.5.1559
249. Wu Y, Chen Y, Wu Q, Jia L, Du X. Minocycline inhibits PARP-1 expression and decreases apoptosis in diabetic retinopathy. *Mol Med Rep.* (2015) 12:4887–94. doi: 10.3892/mmr.2015.4064
250. Bosco A, Inman DM, Steele MR, Wu G, Soto I, Marsh-Armstrong N, et al. Reduced retina microglial activation and improved optic nerve integrity with minocycline treatment in the DBA/2J mouse model of glaucoma. *Investig Opthalmol Vis Sci.* (2008) 49:1437–46. doi: 10.1167/iovs.07-1337
251. Baumgartner WA, Baumgartner AM. Rationale for an experimental treatment of retinitis pigmentosa: 140-Month test of hypothesis with one patient. *Med Hypotheses.* (2013) 81:720–8. doi: 10.1016/j.mehy.2013.07.036
252. Cukras CA, Petrou P, Chew EY, Meyerle CB, Wong WT. Oral minocycline for the treatment of diabetic macular edema (DME): results of a phase I/II clinical study. *Investig Opthalmol Vis Sci.* (2012) 53:3865. doi: 10.1167/iovs.11-9413

Conflict of Interest Statement: The authors declare that the research was conducted in the absence of any commercial or financial relationships that could be construed as a potential conflict of interest.

frontiers in Immunology

ORIGINAL RESEARCH
published: 04 December 2019
doi: 10.3389/fimmu.2019.02752

The Proinflammatory and Proangiogenic Macrophage Migration Inhibitory Factor Is a Potential Regulator in Proliferative Diabetic Retinopathy

Ahmed M. Abu El-Asrar[1,2], Ajmal Ahmad[1], Mohammad Mairaj Siddiquei[1], Alexandra De Zutter[3], Eef Allegaert[4], Priscilla W. Gikandi[1], Gert De Hertogh[4], Jo Van Damme[3], Ghislain Opdenakker[3] and Sofie Struyf[3]*

[1] Department of Ophthalmology, College of Medicine, King Saud University, Riyadh, Saudi Arabia, [2] Dr. Nasser Al-Rashid Research Chair in Ophthalmology, College of Medicine, King Saud University, Riyadh, Saudi Arabia, [3] Department of Microbiology and Immunology, Rega Institute for Medical Research, KU Leuven, Leuven, Belgium, [4] Laboratory of Histochemistry and Cytochemistry, KU Leuven, Leuven, Belgium

OPEN ACCESS

Edited by:
Heping Xu,
Queen's University Belfast, United Kingdom

Reviewed by:
Yun Le,
University of Oklahoma Health Sciences Center, United States
Yousif Subhi,
University of Copenhagen, Denmark

***Correspondence:**
Ahmed M. Abu El-Asrar
abuelasrar@yahoo.com

Specialty section:
This article was submitted to Immunological Tolerance and Regulation, a section of the journal Frontiers in Immunology

Received: *24 September 2019*
Accepted: *11 November 2019*
Published: *04 December 2019*

Citation:
Abu El-Asrar AM, Ahmad A, Siddiquei MM, De Zutter A, Allegaert E, Gikandi PW, De Hertogh G, Van Damme J, Opdenakker G and Struyf S (2019) The Proinflammatory and Proangiogenic Macrophage Migration Inhibitory Factor Is a Potential Regulator in Proliferative Diabetic Retinopathy. Front. Immunol. 10:2752. doi: 10.3389/fimmu.2019.02752

The macrophage migration inhibitory factor (MIF)/CD74 signaling pathway is strongly implicated in inflammation and angiogenesis. We investigated the expression of MIF and its receptor CD74 in proliferative diabetic retinopathy (PDR) to reveal a possible role of this pathway in the pathogenesis of PDR. Levels of MIF, soluble (s)CD74, soluble intercellular adhesion molecule-1 (sICAM-1) and vascular endothelial growth factor (VEGF) were significantly increased in the vitreous from patients with PDR compared to nondiabetic control samples. We detected significant positive correlations between the levels of MIF and the levels of sICAM-1 ($r = 0.43$; $p = 0.001$) and VEGF ($r = 0.7$; $p < 0.001$). Through immunohistochemical analysis of PDR epiretinal membranes, significant positive correlations were also found between microvessel density (CD31 expression) and the numbers of blood vessels expressing MIF ($r = 0.56$; $p = 0.045$) and stromal cells expressing MIF ($r = 0.79$; $p = 0.001$) and CD74 ($r = 0.59$; $p = 0.045$). Similar to VEGF, MIF was induced in Müller cells cultured under hypoxic conditions and MIF induced phosphorylation of ERK1/2 and VEGF production in Müller cells. Intravitreal administration of MIF in normal rats induced increased retinal vascular permeability and significant upregulation of phospho-ERK1/2, NF-κB, ICAM-1 and vascular cell adhesion molecule-1 expression in the retina. MIF induced migration and proliferation of human retinal microvascular endothelial cells. These results suggest that MIF/CD74 signaling is involved in PDR angiogenesis.

Keywords: proliferative diabetic retinopathy, migration inhibitory factor, CD74, angiogenesis, Müller cells

INTRODUCTION

Ischemia-induced retinal angiogenesis and excessive deposition of extracellular matrix lead to the formation of fibrovascular membranes at the vitreoretinal interface in proliferative diabetic retinopathy (PDR). This outgrowth of fibrovascular tissue, composed of new blood vessels, leukocytes and α-smooth muscle actin (α-SMA)-expressing myofibroblasts (1–4), often causes serious vision loss due to recurrent vitreous hemorrhage and/or traction retinal detachment.

Several studies support the paradigm that inflammation, neovascularization and fibrosis are critical mechanisms for PDR initiation and progression as the authors showed overexpression of inflammatory, angiogenic and fibrogenic factors inducing those processes (1–5).

In PDR, hypoxia seems to drive neovascularization through upregulation of angiogenic factors (6, 7). In particular vascular endothelial growth factor (VEGF), upregulated in retinal cells in response to oxygen deprivation (8, 9), plays a pivotal role in promoting retinal neovascularization and vascular leakage (10, 11). In addition to angiogenesis, recruitment of leukocytes occurs in the ocular microenvironment of patients with PDR (1–5). Recent data support a causal relationship between persistent inflammation and angiogenesis (12, 13) and this interplay might also be critical for PDR development and progression. Accordingly, some of the signaling molecules of the inflammatory response, such as cytokines, chemokines and their receptors might play an essential role in PDR angiogenesis and progression. Therefore, a new challenge in PDR research is the identification of the molecular links between inflammation and angiogenesis.

Macrophage migration inhibitory factor (MIF) is a widely expressed proinflammatory cytokine originally discovered as a product isolated from the culture medium of activated T lymphocytes that inhibited the random migration of cultured macrophages *in vitro* (14). Today a wide spectrum of biological properties has been attributed to MIF. MIF is closely involved in autoimmune and inflammatory diseases (15–17). The biological effects of MIF are mediated through its primary receptor CD74, which is the major histocompatibility class II-associated invariant chain (18). The binding of MIF to its receptor CD74 leads to the activation of extracellular signal regulated kinase (ERK) 1 and 2 and the proinflammatory transcription factor nuclear factor-κB (NF-κB) (15). Recently, it was demonstrated that the MIF/CD74 signaling pathway promotes macrophage-mediated inflammation in type 1 diabetes (19). In addition, the chemokine receptors CXCR2 and CXCR4 were identified as functional receptors for MIF. By activating CXCR2 and CXCR4, MIF displays chemokine-like functions and stimulates leukocyte chemotaxis (20).

Besides its role in inflammation, MIF has potent proangiogenic properties and in conjunction with its cell surface receptor CD74 emerges as an important regulator of pathological angiogenesis associated with several types of malignant tumors (21–23). Exogenous MIF stimulated *in vitro* endothelial cell migration, proliferation and tube formation, key steps in the angiogenesis cascade (24–26). Furthermore, MIF induced angiogenesis in multiple *in vivo* models (25). Several studies reported overexpression of MIF and CD74 in multiple cancers (21–23, 27) and that the MIF/CD74 signaling pathway promotes tumor progression and angiogenesis (21–24, 27–33). Furthermore, anti-MIF antibodies suppressed angiogenesis in animal models of cancer (33). Recently, it was demonstrated that small molecule inhibitors of MIF, inhibit cancer development in animal models (29, 34), reduce the severity of experimental autoimmune encephalomyelitis (17) and lower blood glucose in an animal model of non-insulin-dependent diabetes mellitus (35). MIF was proposed as the link that connects the inflammatory response to tumor-associated angiogenesis (24, 28–31). The angiogenic activity in tumors was attributed to the fact that MIF acts as a potent inducer of the angiogenic factors VEGF, CXCL5, and CXCL8 in tumor cells (21, 28, 30).

Given the key roles of the MIF/CD74 signaling pathway in angiogenesis and inflammation, we hypothesized that this pathway may be involved in the pathogenesis of PDR. To test this hypothesis, we investigated the expression of MIF and CD74 in the ocular microenvironment of patients with PDR and correlated their levels with the angiogenic activity in epiretinal fibrovascular membranes and the vitreous levels of VEGF and the inflammatory biomarker soluble intercellular adhesion molecule 1 (sICAM-1). We examined the effect of intravitreal administration of MIF on the retinas from normal rats. We analyzed *in vitro* the expression of MIF in human retinal Müller glial cells following exposure to hydrogen peroxide (H_2O_2)-induced oxidative stress and the hypoxia mimetic agent cobalt chloride ($CoCl_2$) and monitored expression of VEGF in Müller cells following exposure to MIF. Finally, we investigated the response of human retinal microvascular endothelial cells (HRMECs) to treatment with MIF.

MATERIALS AND METHODS

Patient Samples

Undiluted vitreous fluid samples were obtained from 36 patients with PDR during pars plana vitrectomy for the treatment of tractional retinal detachment, and/or nonclearing vitreous hemorrhage and processed as described previously (1–5). The diabetic patients were 23 males and 13 females whose ages ranged from 27 to 74 years with a median [IQR] of 54 [44-59]. The PDR group consisted of 20 patients who had insulin-dependent diabetes mellitus and 16 patients who had non-insulin-dependent diabetes mellitus. Vitreous fluid samples obtained from 20 patients who had undergone vitrectomy for the treatment of rhegmatogenous retinal detachment with no proliferative vitreoretinopathy (PVR) were used as the control samples. Clinical check-up confirmed that control subjects were free from diabetes or other systemic disease. The controls were 14 males and 6 females whose ages ranged from 26 to 73 years with a median [IQR] of 55 [38-66]. The ages ($p = 0.526$; Mann-Whitney test) and male/female ratios ($p = 0.547$; Chi-Square test) did not differ significantly between nondiabetic control patients and PDR patients.

Fourteen patients with PDR undergoing pars plana vitrectomy for the repair of tractional retinal detachment donated epiretinal fibrovascular membranes. At the time of the procedure, using previously published criteria, retinal neovascular activity was clinically graded (36). We made a distinction between active neovascularization (visible perfused new vessels on the retina or optic disc present within epiretinal membranes) and inactive involuted disease (nonvascularized, white fibrotic epiretinal membranes). For comparison, epiretinal fibrocellular membranes were obtained from ten patients without diabetes undergoing vitreoretinal surgery for the treatment of retinal

detachment complicated by PVR. The epiretinal membranes were processed as previously described (1–4).

The study was conducted according to the tenets of the Declaration of Helsinki. Before undergoing vitrectomy, all patients signed a preoperative informed written consent and approved the use of the excised epiretinal membranes and aspirated vitreous fluid for further analysis and clinical research. The Research Center and Institutional Review Board of the College of Medicine, King Saud University approved the study design and protocol.

Immunohistochemical Staining of Human Epiretinal Membranes and Quantitations

For CD31, α-SMA and MIF detection, antigen retrieval was performed by boiling the sections in citrate based buffer [pH 5.9–6.1] [BOND Epitope Retrieval Solution 1; Leica, Diegem, Belgium] for 10 min. For CD45 and CD74 detection, antigen retrieval was performed by boiling the sections in Tris/EDTA buffer [pH 9] [BOND Epitope Retrieval Solution 2; Leica] for 20 min. Subsequently, the sections were incubated for 1 h with mouse monoclonal anti-CD31 (ready-to-use; clone JC70A; Dako, Glostrup, Denmark), mouse monoclonal anti-CD45 (ready-to-use; clones 2B11+PD7/26; Dako), mouse monoclonal antibody against α-SMA (ready-to-use; clone 1A4; Dako), mouse monoclonal anti-CD74 antibody (1:50; ab9514, Abcam, Cambridge, UK) and rabbit polyclonal anti-MIF antibody (1:200; ab65869, Abcam). Optimal working conditions for the antibodies were determined in pilot experiments on kidney, tonsil and liver sections. The sections were then incubated for 20 min with an alkaline phosphatase-conjugated IgG. Immune interactions were visualized with the Fast Red chromogen (Leica; 15 min incubation). Finally, a faint counterstain with Mayer's hematoxylin was performed.

To identify the phenotype of cells expressing MIF and CD74, sequential double immunohistochemistry was performed. The sections were first incubated with anti-CD45, followed by treatment with peroxidase-conjugated secondary antibody and 3, 3′-diaminobenzidine tetrahydrochloride substrate. Next, the second primary antibodies (anti-MIF or anti-CD74) were added and detected by alkaline phosphatase-conjugated secondary antibody and Fast Red reactions. No counterstain was applied. In negative controls, the incubation step with primary antibody was omitted from the protocol and only the ready-to-use antibody diluent (Cat No 52022; Dako) was applied.

Immunoreactive blood vessels and cells were counted in five representative fields, using an eyepiece calibrated grid in combination with the 40x objective as previously described (1–4). The level of vascularization in epiretinal membranes was determined by immunodetection of the vascular endothelium marker CD31.

Enzyme-Linked Immunosorbent Assays

Enzyme-linked Immunosorbent Assay (ELISA) kits for human MIF (Cat No DMF00B), human VEGF (Cat No SVE00) and human sICAM-1 (Cat No SCD540) were purchased from R&D Systems (Minneapolis, MN, USA). Levels of human MIF, VEGF and sICAM-1 in vitreous fluid and MIF and VEGF in culture medium were determined using those ELISA kits according to the manufacturer's instructions. The minimum detection limits for MIF, VEGF and sICAM-1 ELISA kits were 0.016 ng/ml, 9 pg/ml and 0.096 ng/ml, respectively.

Human Retinal Müller Glial Cell and Retinal Microvascular Endothelial Culture

Human retinal Müller glial cells (MIO-M1) (a generous gift from Prof. A. Limb, Institute of Ophthalmology, University College London, UK) were cultured with DMEM containing 1 g/L glucose with 10% (v/v) fetal bovine serum and 1% penicillin/streptomycin. Confluent cells were starved overnight in serum-free DMEM to minimize the effects of serum and subsequently either left untreated or stimulated for 24 h. The following stimuli were used: recombinant human MIF (2, 20 or 100 ng/ml) (Cat No: 289-MF, R&D Systems), 100 μM H_2O_2 (Cat No: H101351000, Scharlau, Sentmenat, Spain) or 300 μM $CoCl_2$ (AVONCHEM Limited, Nacclesfield, Cheshire, UK). Human retinal microvascular endothelial cells (HRMECs; Cell Systems, Kirkland, WA, USA) were cultured in Endothelial Cell Basal Medium-2 (EBM-2) supplemented with the EGM-2 MV SingleQuots kit (both from Lonza, Verviers, Belgium).

Intravitreal Injection of MIF

Intravitreal injection into the eyes of Sprague Dawley rats (220–250 g) was performed as previously described (37). While the animals were kept under deep anesthesia, 5 μl of sterilized solution containing 5 ng recombinant MIF or sterile phosphate buffer saline (PBS) was injected into the right or left eye, respectively. Four days after intravitreal administration the rats were sacrificed, retinas were carefully dissected, snap frozen in liquid nitrogen, and stored at −80°C.

Measurement of Blood-Retinal Barrier Breakdown

Blood-retinal barrier (BRB) breakdown in excised retinas was evaluated 4 days after intravitreal injection as previously described (37). Briefly, deeply anesthetized rats were intravenously injected with 50 mg/kg fluorescein isothiocyanate (FITC)-conjugated dextran (3–5 kDa, Sigma-Aldrich Corp., St. Louis, MO, USA). After 30 min, a blood sample was collected, and each rat was then perfused with PBS. The retinas were carefully excised, weighed and homogenized to extract the FITC-conjugated dextran. Fluorescence was measured using a spectra Max Gemini-XPS microplate reader (Molecular Devices, Sunnyvale, CA, USA) with excitation and emission wavelengths of 485 and 538 nm, respectively, with PBS as a blank. A correction for autofluorescence was made by subtracting the autofluorescence of retinal tissue from non-treated rats. The concentration of FITC-conjugated dextran in each retina was calculated from a standard curve of FITC-conjugated dextran in water. For normalization, the retinal FITC-conjugated dextran amount was divided by the retinal weight and by the concentration of FITC-conjugated dextran in the plasma. BRB breakdown was calculated using the following equation, with the

results being expressed in μl/(g*h).

$$\frac{Retinal\ FITC-dextran\ (\mu g)/retinal\ weight\ (g)}{Plasma\ FITC-dextran\ concentration\ (\mu g/\mu l)\ *circulation\ time\ (h)}$$

Western Blot Analysis of Human Vitreous Fluid, Müller Cell Lysates and Rat Retinas

Retina and cell lysates were homogenized in western blot lysis buffer [30 mM Tris-HCl; pH 7.5, 5 mM EDTA, 1% Triton X-100, 250 mM sucrose, 1 mM Sodium vanadate, and a complete protease inhibitor cocktail from Roche (Mannheim, Germany)]. After centrifugation of the homogenates (14,000 × g; 15 min, 4°C), protein concentrations were measured in the supernatants (DC protein assay kit; Bio-Rad Laboratories, Hercules, CA). Equal amounts (50 μg) of the protein extracts were subjected to SDS–PAGE and transferred onto nitrocellulose membranes. To determine the presence of soluble (s) CD74 in the vitreous samples, equal volumes (15 μl) of vitreous samples were boiled in Laemmli's sample buffer (1:1, v/v) under reducing conditions for 10 min and analyzed as described (2–4).

Immunodetection was performed with the use of mouse monoclonal anti-CD74 antibody (1:1,000; ab-9514, Abcam), rabbit monoclonal anti-phospho-ERK1/2 antibody (1:1,500; MAB1018; R&D Systems), mouse monoclonal anti-p65 subunit of NF-κB antibody (1:500, sc-136548, Santa Cruz Biotechnology Inc, Santa Cruz, CA, USA), mouse monoclonal anti-ICAM-1 antibody (1:500, sc-8439, Santa Cruz Biotechnology Inc), mouse monoclonal anti-vascular cell adhesion molecule-1antibody (VCAM-1) (1:500, sc-13160, Santa Cruz Biotechnology Inc) and mouse monoclonal anti-VEGF antibody (1:750, MAB293, R&D Systems). Nonspecific binding sites were blocked (1.5 h, room temperature) with 5% non-fat milk made in Tris-buffered saline containing 0.1% Tween-20 (TBS-T). Three TBS-T washings (5 min each) were performed before the secondary antibody treatment at room temperature for 1 h. Immune reactive bands were visualized with luminol reagent (sc-2048; Santa Cruz Biotechnology Inc.). To verify equal loading, membranes were stripped and reprobed with β-actin-specific antibody (1:2,000; sc-47778; Santa Cruz Biotechnology Inc.). Band intensities were quantified using GeneTools software (Syngene by Synoptic Ltd., Cambridge, UK).

Chemotaxis Assay

Chemotaxis of HRMECs was evaluated with an xCELLigence system (ACEA Biosciences, San Diego, CA) as described before (38). Migration was evaluated in response to different concentrations of recombinant human MIF (Cat No 289-MF, R&D Systems), 10 ng/ml of VEGF (Cat No 583702, Biolegend, San Diego, CA) or dilution medium. First, 160 μl of stimulus diluted in MCDB131 medium (Gibco/ThermoFisher Scientific, Waltham, MA, USA) supplemented with 0.4% (v/v) fetal calf serum were added to the wells of the lower chamber of a Cell Invasion/Migration (CIM)-Plate (ACEA Biosciences). After assembly of the lower and upper chamber, 50 μl of serum-free MCDB131 medium was added in the upper wells. After equilibration of the plate (1 h at 37°C), HRMECs were added in the upper chamber at 4×10^4 cells in 100 μl/well. After an additional incubation period (30 min at room temperature) to allow settling of the cells, migration was monitored every minute for 15 h in the xCELLigence apparatus. Cell migration from the upper to the lower compartment was recorded as changes in electrical impedance. These changes were converted into cell indices, as a measure of cell migration.

Proliferation Assay

To assess the proliferative effect of MIF, HRMECs were seeded at 5×10^3 cells in 100 μl/well of a 96-well plate in culture medium (*vide supra*). The next day, cells were washed with serum-free MCDB131 medium and stimulated in proliferation medium [MCDB131 medium supplemented with 2mM GlutaMAX™ (Gibco), 30 μg/ml Gentamicin and 3% fetal calf serum]. Either different concentrations of MIF, 10 ng/ml VEGF or proliferation medium were added to the wells. After 48 h, cell proliferation was assessed using the ATPlite Luminescence Assay kit (PerkinElmer, Waltham, MA) according to the manufacturer's instructions.

Statistical Analysis

Statistical analyses of the data were performed using SPSS version 21.0. Normal distribution of the data was verified using the Shapiro-Wilk (S-W) test and normal Q-Q plots. Normally distributed data were presented as mean ± SD and an independent *t*-test was used to compare the groups. For normally distributed data, Pearson correlation coefficients were calculated. Non-parametric tests (Kruskal-Wallis test, Mann-Whitney test and Spearman's correlation coefficients) were performed for not normally distributed data, which were presented as median and interquartile range [IQR; Q1–Q3]. Proportions were compared using the Chi-Square test. The level of statistical significance was set at 0.05.

RESULTS

Analysis of Angiogenic and Inflammatory Activities and the Expression of the Myofibroblast Marker α-SMA in Epiretinal Fibrovascular Membranes From Patients With PDR

As a negative control, the experimental staining procedure was performed with omission of the primary antibody and no staining was observed (**Figure 1A**). Subsequently, we used staining for the vascular endothelial cell marker CD31, the leukocyte common antigen CD45 and α-SMA to evaluate ongoing angiogenesis, inflammation, and fibrosis, respectively. All membranes showed neovessels positive for CD31 (**Figures 1B,C**). Representative examples of CD31 staining in membranes with active (**Figure 1B**) and involuted (**Figure 1C**) disease are shown. Furthermore, leukocytes expressing CD45 (**Figure 1D**), as well as spindle-shaped cells expressing α-SMA (**Figure 1E**) were detected in all membranes.

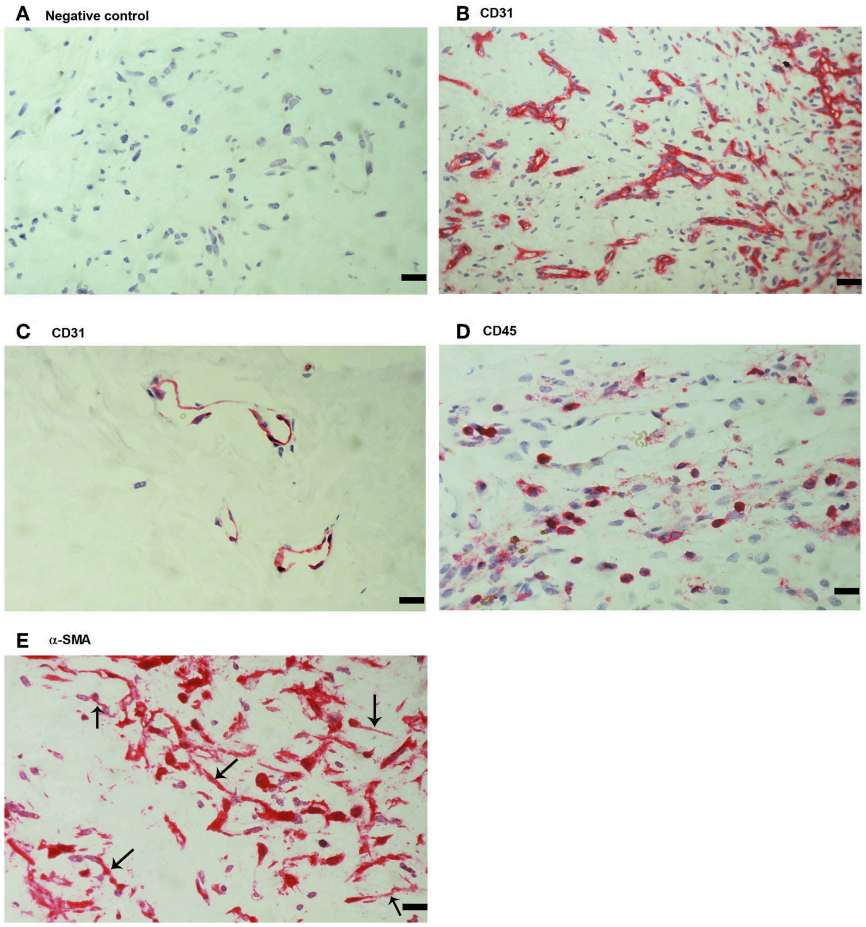

FIGURE 1 | Detection of endothelial cells, leukocytes and myofibroblasts in proliferative diabetic retinopathy (PDR) epiretinal fibrovascular membranes. No staining was observed in the negative control slide following the full staining procedure with omission of the primary antibody from the staining protocol **(A)**. Immunohistochemical staining for CD31 showing pathologic new blood vessels expressing this endothelial cell marker in a membrane from a patient with active neovascularization **(B)** and in a membrane from a patient with involuted PDR **(C)**. Note that the membrane from the patient with involuted PDR is composed mostly of fibrous tissue. Immunohistochemical staining for the leukocyte common antigen CD45 showing numerous leukocytes in the stroma **(D)**. Immunohistochemical staining for α-smooth muscle actin (α-SMA) showing immunoreactivity in myofibroblasts (arrows) **(E)**. (Scale bar, 10 μm).

Expression of MIF and Its Receptor CD74 in Epiretinal Fibrovascular Membranes From Patients With PDR

Next, immunohistochemical analysis was used to reveal whether MIF, an inflammatory and angiogenic molecule associated with tumor pathology, is also expressed in the context of PDR. MIF immunoreactivity was observed in all membranes. **Figure 2** shows representative images of membranes derived from patients with active (**Figure 2A**) or involuted (**Figure 2B**) disease. Immunoreactivity for MIF was noted in both endothelial cells lining blood vessels (**Figures 2A,B**) and stromal cells (**Figure 2C**). In the stroma, MIF expression was detected in spindle-shaped cells, as well as in CD45-expressing leukocytes. In serial sections, the distribution and morphology of spindle-shaped cells expressing MIF (**Figure 2C**) were similar to those of myofibroblasts expressing α-SMA (**Figure 1E**). Double immunostaining confirmed co-expression of CD45 and MIF in stromal and intravascular cells (**Figures 2D,E**).

Since MIF activity requires binding to CD74 (15, 17), we also evaluated CD74 expression in epiretinal PDR membranes. CD74 immunoreactivity was detected in vascular endothelial cells (**Figure 3A**) and stromal cells (**Figure 3B**). CD74-expressing stromal cells were spindle-shaped cells (**Figure 3B**) resembling those being α-SMA positive in **Figure 1E** and leukocytes co-expressing CD45 (**Figures 3C,D**).

Correlations Between Microvessel Density and the Expression of MIF and CD74 in Epiretinal Fibrovascular Membranes From Patients With PDR

Quantification of CD31-positive vessels in tumors is a standard method of measuring intra-tumoral microvessel

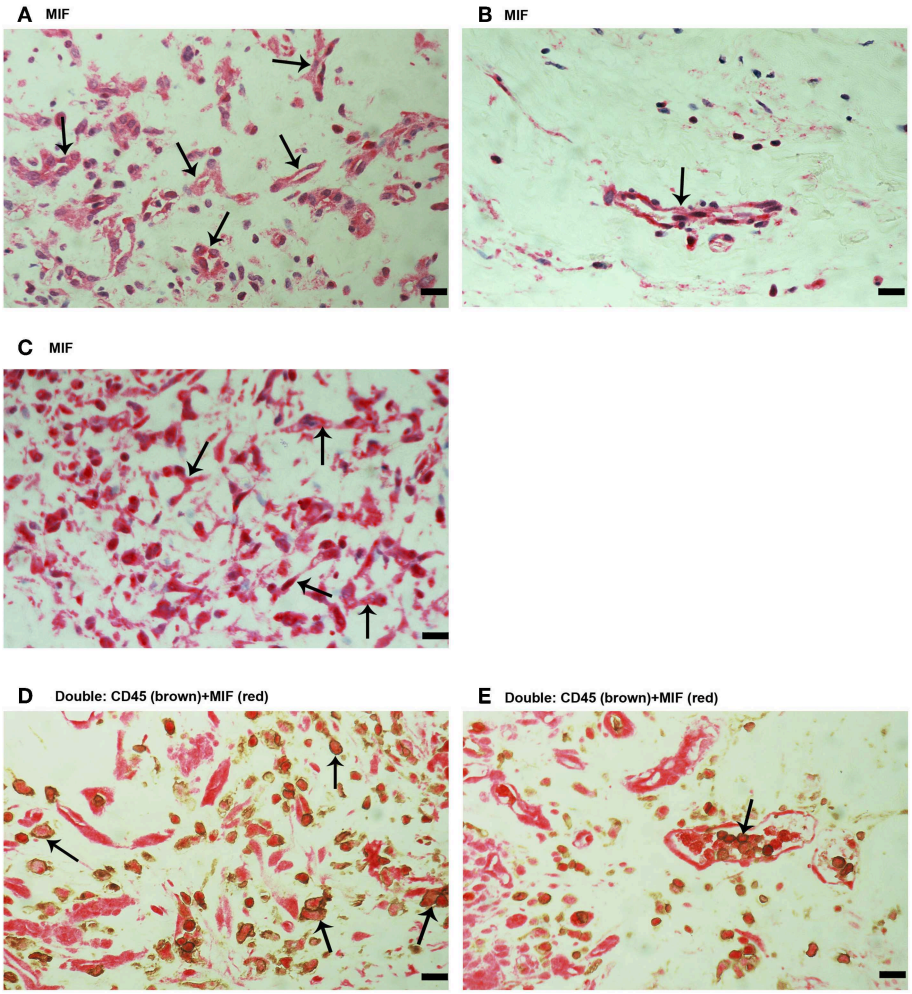

FIGURE 2 | Characterization of macrophage migration inhibitory factor (MIF) expressing cells in proliferative diabetic retinopathy (PDR) epiretinal fibrovascular membranes. Immunohistochemical staining for MIF showing immunoreactivity in vascular endothelial cells (arrows) in a membrane from a patient with active angiogenesis **(A)** and in a membrane from a patient with involuted PDR **(B)**. Immunoreactivity for MIF was also detected in stromal spindle- shaped cells (arrows) **(C)**. Double immunohistochemistry for CD45 (brown) and MIF (red) demonstrated expression of MIF in stromal leukocytes (arrows) **(D)** and intravascular leukocytes (arrow) **(E)**. No counterstain to visualize the cell nuclei was applied **(D,E)**. (Scale bar, 10 μm).

density (MVD). Several studies reported that the level of MVD reflects the angiogenesis process in tumor tissues (22–24, 30, 31).

The mean number of blood vessels expressing CD31 was significantly higher in membranes from patients with active PDR than in membranes from patients with involuted PDR (**Table 1**) (**Figures 1B,C**). The numbers of blood vessels expressing MIF and stromal cells expressing MIF and CD74 were significantly higher in membranes from patients with active PDR than in membranes from patients with inactive PDR (**Table 1**) (**Figures 2A,B**).

Significant positive correlations (Pearson correlation coefficients) were detected between the numbers of blood vessels expressing CD31 and the numbers of blood vessels expressing MIF ($r = 0.56$; $p = 0.045$) and stromal cells expressing MIF ($r = 0.79$; $p = 0.001$) and CD74 ($r = 0.59$; $p = 0.045$) (**Table 2**).

Immunohistochemical Analysis of PVR Epiretinal Fibrocellular Membranes

No immunoreactivity was detected in negative control slides (**Figure 4A**). All PVR membranes contained spindle-shaped α-SMA$^+$ myofibroblasts (**Figure 4B**) and CD45$^+$ leukocytes (**Figure 4C**). Immunostainings for MIF (**Figure 5A**) and CD74 (**Figure 5B**) revealed spindle-shaped cells expressing cytoplasmic immunoreactivity, which were in distribution and morphology similar to the α-SMA$^+$ myofibroblasts (**Figure 4B**) in serial sections. In addition, double-labeling experiments showed that cells expressing MIF (**Figure 5C**) and CD74 (**Figure 5D**) co-expressed CD45.

Levels of MIF, VEGF, and sICAM-1 in Vitreous Samples

In addition, we used ELISA to compare MIF levels in vitreous samples from 36 patients with PDR to those of 20 nondiabetic

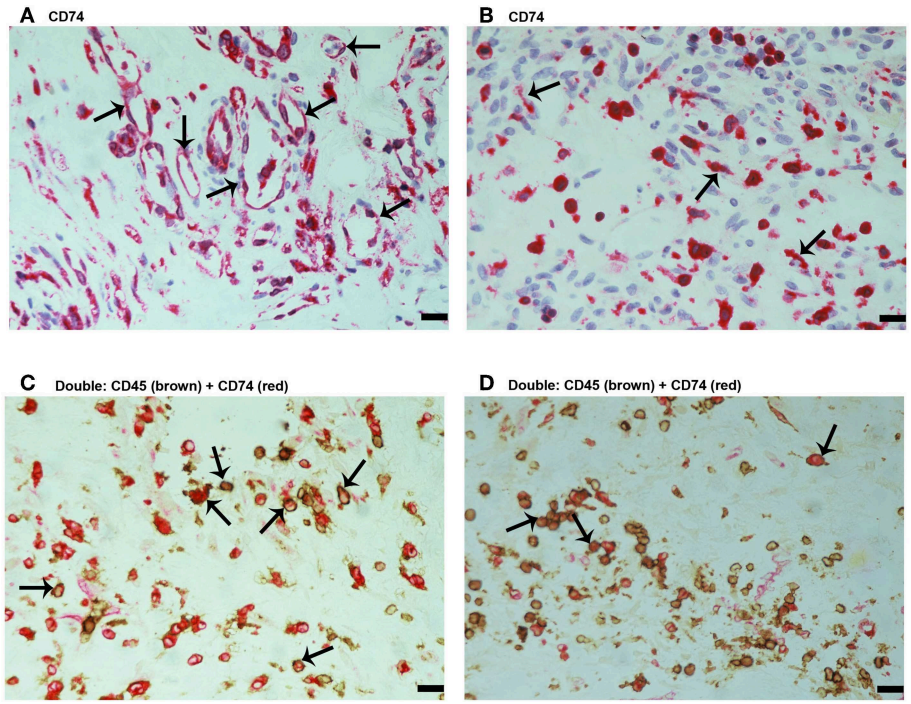

FIGURE 3 | Characterization of CD74 expressing cells in proliferative diabetic retinopathy epiretinal fibrovascular membranes. CD74 Immunoreactivity was detected in vascular endothelial cells (arrows) **(A)** and in stromal spindle-shaped cells (arrows) **(B)**. Double immunohistochemistry for CD45 (brown) and CD74 (red) showed co-expression in stromal cells (arrows). No counterstain to visualize the cell nuclei was applied **(C,D)**. (Scale bar, 10 μm).

TABLE 1 | Mean number of immunoreactive blood vessels and stromal cells in epiretinal fibrovascular membranes in relation to the angiogenic activity of proliferative diabetic retinopathy (PDR).

Variable	Active PDR ($n = 9$) Mean ± SD (Range)	Involuted PDR ($n = 5$) Mean ± SD (Range)	p-value (Independent t-test)
Blood vessels expressing CD31	110.8 ± 40.4 (75–175)	23.3 ± 10.4 (15-35)	<0.001*
Blood vessels expressing MIF	69.2 ± 10.2 (65–90)	42.9 ± 26.8 (15-84)	0.043*
Stromal cells expressing MIF	93.3 ± 31.3 (65–150)	39.0 ± 30.3 (6-80)	0.009*
Blood vessels expressing CD74	32.2 ± 19.5 (5-55)	21.8 ± 10.0 (11-35)	0.228
Stromal cells expressing CD74	150.6 ± 48.2 (80–215)	79.0 ± 51.3 (25-160)	0.023*

*Statistically significant at 5% level of significance.
MIF, migration inhibitory factor.

TABLE 2 | Correlations (Pearson correlation coefficients) between microvessel density (MVD) and the numbers of immunoreactive blood vessels and stromal cells in proliferative diabetic retinopathy (PDR) epiretinal fibrovascular membranes.

	Variable	r	p-value
MVD	Blood vessels expressing MIF	0.56	0.045*
	Stromal cells expressing MIF	0.79	0.001*
	Blood vessels expressing CD74	0.2	0.52
	Stromal cells expressing CD74	0.59	0.045*

*Statistically significant at 5% level of significance.
MIF, migration inhibitory factor.

controls. MIF was detected in 17 of 20 (85%) vitreous samples from nondiabetic controls, and in all vitreous samples from patients with PDR. In nondiabetic controls, we found a median [IQR] level of 3.2 [1.7–4.6] ng/ml. In contrast, the median [IQR] concentration in patients with PDR reached 15.4 [10.0–20.0] ng/ml, a concentration approximately 5-fold higher than that recorded in nondiabetic controls ($p < 0.001$; Mann-Whitney test) (**Table 3**).

The angiogenic biomarker VEGF was detected in 9 of 20 (45%) vitreous samples from nondiabetic controls and in 33 of 36 (91.6%) vitreous samples from PDR patients. The proinflammatory biomarker sICAM-1 was detected in 18 of 20 (90%) vitreous samples from nondiabetic controls and in all vitreous samples from patients with PDR. The levels of VEGF and sICAM-1 were significantly higher in PDR ($p < 0.001$ for both comparisons; Mann-Whitney test) (**Table 3**).

Significant positive correlations (Spearman's correlation coefficient) were found between vitreous fluid levels of MIF and levels of VEGF ($r = 0.70$; $p < 0.001$) and sICAM-1 ($r = 0.43$; $p = 0.001$). In addition, a significant positive correlation was observed between vitreous fluid levels of VEGF and the levels of sICAM-1 ($r = 0.32$; $p = 0.023$). Although

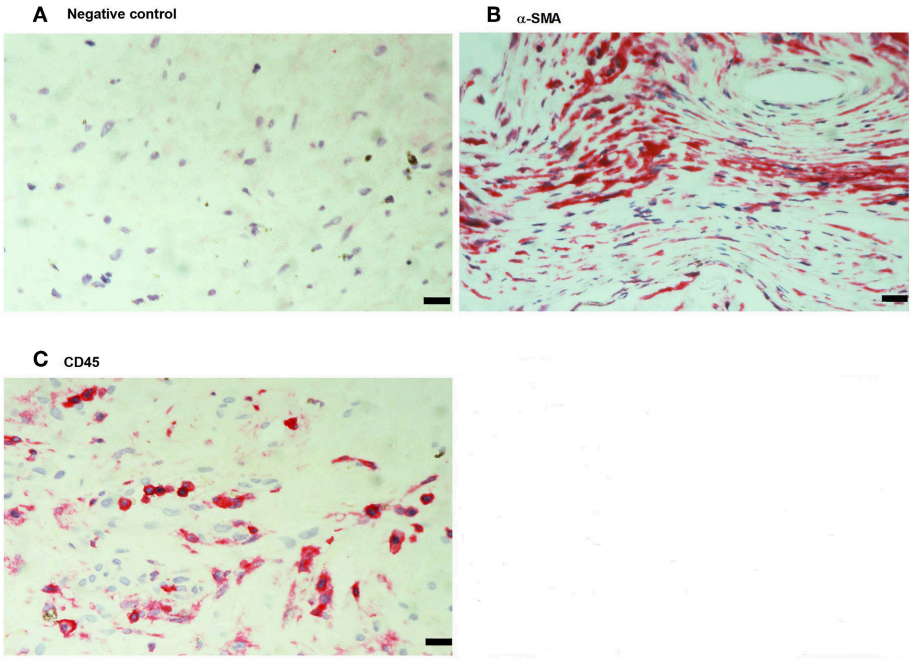

FIGURE 4 | Detection of myofibroblasts and leukocytes in proliferative vitreoretinopathy (PVR) epiretinal fibrocellular membranes. Negative control slide showing no labeling **(A)**. Immunohistochemical staining for α-smooth muscle actin (α-SMA) showing immunoreactivity in spindle-shaped myofibroblasts **(B)**. Immunohistochemical staining for CD45 showing numerous leukocytes in the stroma **(C)**. (Scale bar, 10 μm).

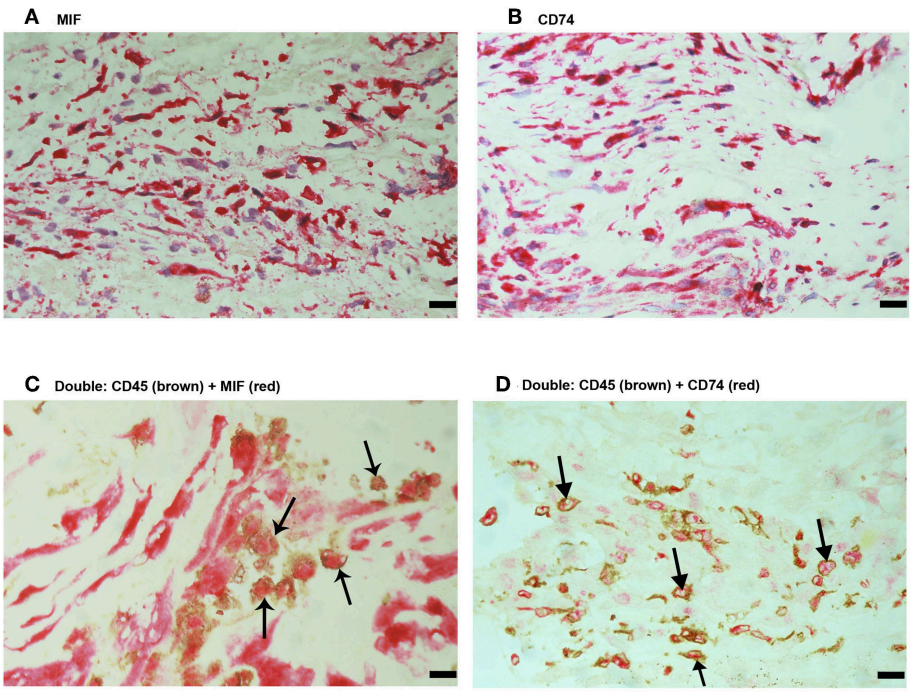

FIGURE 5 | Characterization of macrophage migration inhibitory factor-(MIF-) and CD74-expressing cells in proliferative vitreoretinopathy (PVR) epiretinal fibrocellular membranes. Immunohistochemical staining for MIF **(A)** and CD74 **(B)** showing immunoreactivity in spindle-shaped myofibroblasts. Double Immunohistochemistry for CD45 (brown) and MIF (red) **(C)** or CD74 (red) **(D)** demonstrated co-expression in leukocytes. No counterstain to visualize the cell nuclei was applied (arrows) **(C,D)**. (Scale bar, 10 μm).

TABLE 3 | Comparisons of migration inhibitory factor (MIF), vascular endothelial growth factor (VEGF) and soluble intercellular adhesion molecule-1 (sICAM-1) in vitreous samples from patients with proliferative diabetic retinopathy (PDR) and nondiabetic patients with rhegmatogenous retinal detachment (RD).

	PDR ($n = 36$) Median (IQR)	RD ($n = 20$) Median (IQR)	*p*-value (Mann-Whitney test)
MIF (ng/ml)	15.4 (10.0–20.1)	3.2 (1.7–4.6)	<0.001*
VEGF (pg/ml)	356.0 (151.0–712.3)	1.5 (0.0–18.3)	<0.001*
sICAM-1 (ng/ml)	17.2 (6.2–24.0)	4.1 (1.0–9.2)	<0.001*

*Statistically significant at 5% level of significance.
IQR, interquartile range (Q1–Q3).

the correlations between MIF and sICAM-1 and between VEGF and sICAM-1 were weak, yet they were statistically significant (**Figure 6**).

Relationship Between ELISA Levels of MIF in Vitreous Samples and Angiogenic Activity of PDR

Comparisons of MIF levels among PDR patients with active neovascularization ($n = 20$), PDR patients with involuted (quiescent) neovascularization ($n = 16$), and nondiabetic controls ($n = 20$) was conducted with the Kruskal-Wallis test. The levels differed significantly between the 3 groups ($p < 0.001$). Pairwise comparisons (Mann-Whitney test) demonstrated that the median [IQR] MIF level was significantly higher in active PDR (19.6 [15.4–24.5] ng/ml) than in involuted PDR (9.6 [8.3–14.7] ng/ml) ($p < 0.001$) and controls (3.2 [1.7–4.6] ng/ml) ($p < 0.001$). Furthermore, the median MIF level in involuted PDR was significantly higher than in controls ($p < 0.001$).

Detection of sCD74 in Vitreous Samples

Using Western blot analysis, we demonstrated the presence of sCD74 in vitreous samples from patients with PDR. In agreement with previous studies (39, 40), sCD74 protein was detected as two protein bands with molecular weights of around 30 and 40 kDa. Densitometric analysis of the bands demonstrated a significant increase in both the 30 kDa band ($p = 0.002$; Mann-Whitney test) and the 40 kDa band ($p = 0.006$; Mann-Whitney test) intensities in samples from PDR patients ($n = 8$) compared to samples from nondiabetic control patients ($n = 8$) (**Figure 7**).

MIF Induces Upregulation of VEGF and Phospho-ERK1/2 in Retinal Müller Cells

As we observed a positive correlation between the vitreous fluid levels of MIF and VEGF, we performed short-term induction experiments on Müller cells with MIF as an inducer of VEGF production. At 100 ng/ml, MIF significantly enhanced the levels of VEGF in the culture medium (**Figure 8**). However, 2 and 20 ng/ml MIF did not affect the expression of VEGF as compared to untreated control (**Figure 8**). Western blot analysis demonstrated that treatment of Müller cells with MIF (100 ng/ml) induced significant upregulation of the protein levels of phospho-ERK1/2 (**Figure 9A**). In contrast, expression of the p65 subunit of NF-κB was not significantly altered ($p = 0.057$; Mann-Whitney test) (**Figure 9B**).

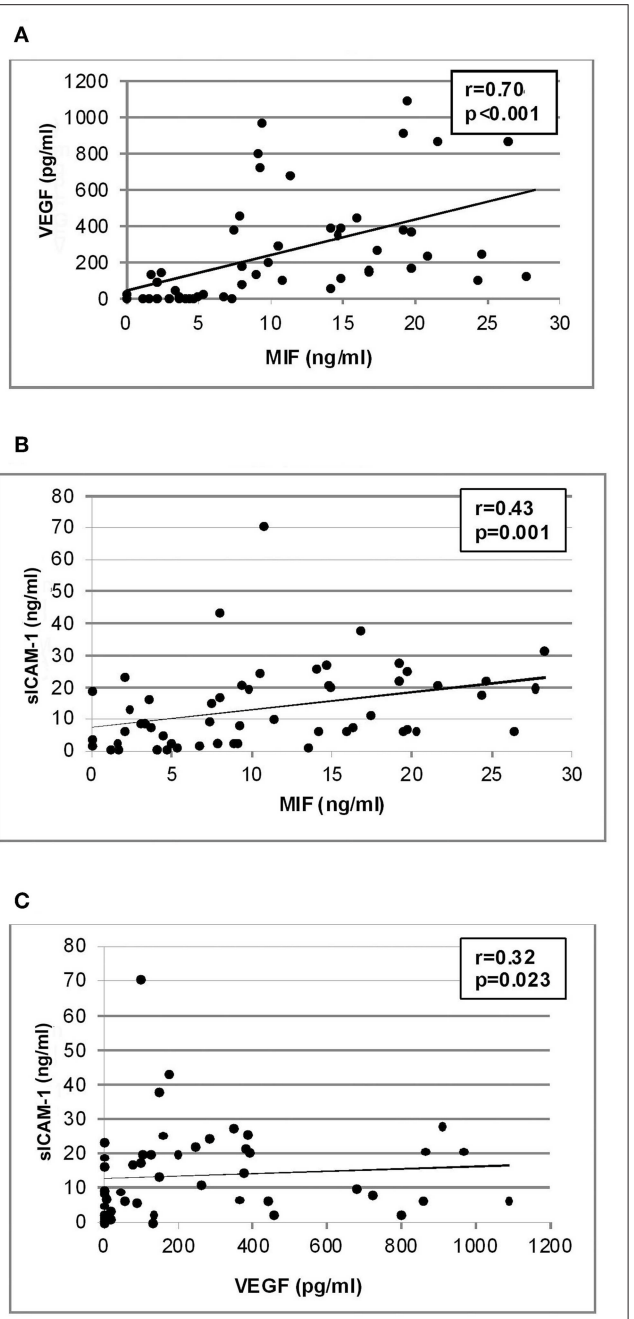

FIGURE 6 | Correlation analyses to reveal interactions between vitreous fluid levels of migration inhibitory factor (MIF), vascular endothelial growth factor (VEGF) and soluble intercellular adhesion molecule-1 (sICAM-1). Significant positive correlations between vitreous fluid levels of MIF and levels of VEGF **(A)** and sICAM-1 **(B)** and between vitreous fluid levels of VEGF and levels of sICAM-1 **(C)** were found.

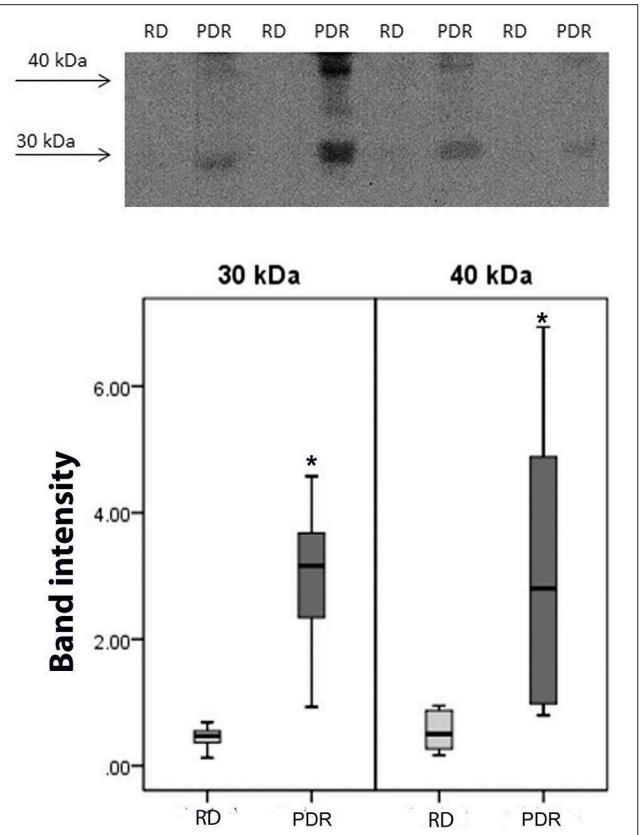

FIGURE 7 | Detection of soluble (s) CD74 in vitreous fluid. The expression of sCD74 in vitreous samples from patients with proliferative diabetic retinopathy (PDR; $n = 8$) and from nondiabetic patients with rhegmatogenous retinal detachment (RD; $n = 8$) was determined by Western blot analysis. A representative set of samples is shown. Densitometric analysis of the bands demonstrated a significant increase in both the sCD74 isoforms with molecular weights of around 30 and 40 kDa in samples from PDR patients compared to samples from nondiabetic control patients. Results are expressed as median (interquartile range) (*$p < 0.05$).

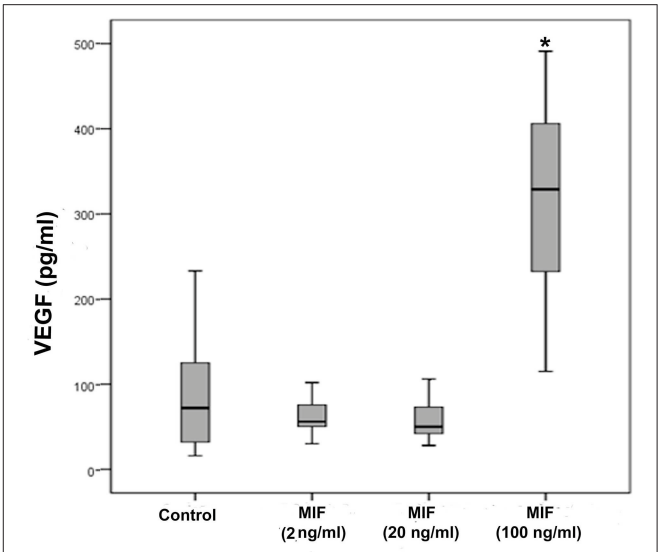

FIGURE 8 | Macrophage migration inhibitory factor (MIF) induces vascular endothelial growth factor (VEGF) expression in Müller cells. Müller cells were left untreated or treated with MIF (2, 20 or 100 ng/ml) for 24 h. Levels of VEGF were quantified in the culture media by ELISA. Results are expressed as median (interquartile range) from three different experiments. In each experiment, every experimental condition was included 8 times. (*$p < 0.05$ compared to the values obtained from untreated cells).

The Hypoxia Mimetic Agent $CoCl_2$ Induces Upregulation of MIF and VEGF in Retinal Müller Cells

Retinal Müller cells are not only a major source of VEGF (41), these cells also produced enhanced amounts of MIF in addition to VEGF after treatment with 300 μM of $CoCl_2$ (**Figure 10**). However, oxidative stress, mimicked by addition of 100 μM of H_2O_2 to the Müller cell cultures did not affect the expression of MIF as compared to untreated control (**Figure 10**).

MIF Induces Migration and Proliferation of Human Retinal Microvascular Endothelial Cells

As MIF has been described to be involved in pathological neovascularization of tumors, we tested in the following experiments whether HRMECs are also responsive to MIF. When added to the lower compartment of a chemotaxis chamber, MIF rather potently induced migration of the HRMECs. Indeed, the minimal effective dose required to trigger a significant chemotactic response was only 0.1 ng/ml. VEGF, however, was a more efficient chemoattractant (**Figure 11A**). Furthermore, MIF also induced proliferation of HRMECs. When 0.01 ng/ml or higher concentrations of MIF were added to the endothelial cell cultures, proliferation increased on average to 60% above background (**Figure 11B**).

In vivo Effect of Intravitreal Administration of MIF

Finally, 5 ng of MIF was injected in the eyes of normal rats. Fluorescein isothiocyanate-conjugated dextran was used to determine the subsequent change in vascular permeability. **Figure 12A** shows that intravitreal administration of MIF ($n = 12$) significantly increased retinal vascular permeability by about two-fold compared with vehicle (PBS)-injected eyes ($n = 11$). Furthermore, MIF induced significant upregulation of the protein levels of phospho-ERK1/2 (**Figure 12B**), the p65 subunit of NF-κB (**Figure 12C**), ICAM-1 (**Figure 12D**), VCAM-1 (**Figure 12E**), and VEGF (**Figure 12F**) in the retinas, compared to the values obtained from the contralateral eyes that received PBS alone.

DISCUSSION

In the current study, we detected for the first time co-expression of MIF and its receptor CD74 in endothelial cells, leukocytes and myofibroblasts in epiretinal fibrovascular membranes from patients with PDR. In addition, there were

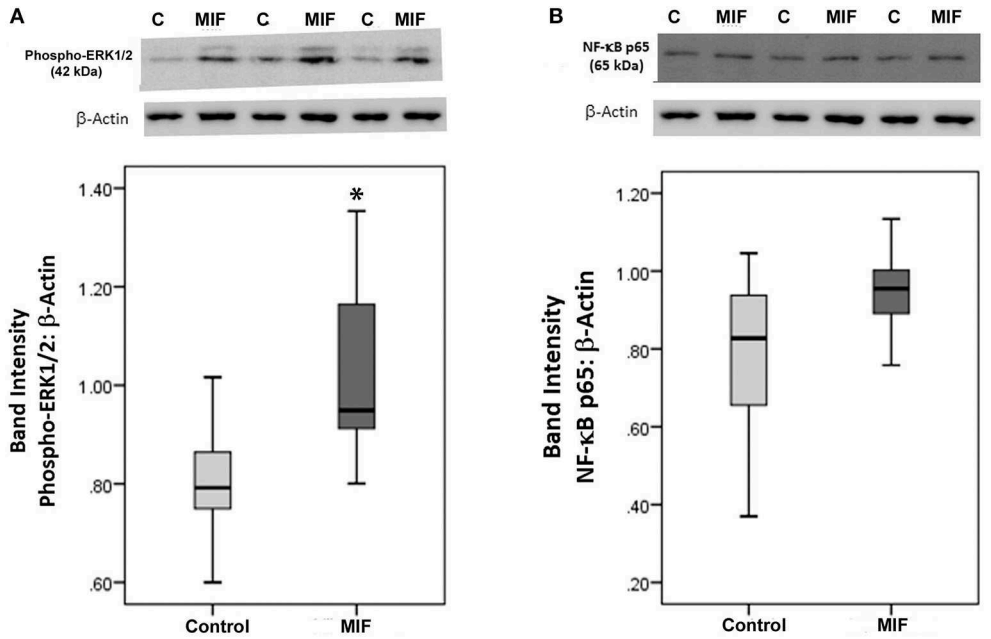

FIGURE 9 | Macrophage migration inhibitory factor (MIF) activates the ERK1/2 pathway in Müller cells. Müller cells were left untreated or treated with MIF (100 ng/ml) for 24 h. Protein expression of phospho-ERK1/2 **(A)** and p65 subunit of NF-κB **(B)** in the cell lysates was determined by Western blot analysis. After transfer of the proteins to the nitrocellulose membrane, the membrane was cut horizontally and the lower and upper part were stained with anti-phospo-ERK1/2 and anti-NFκB, respectively. Afterwards, the lower part of the membrane was stripped and reprobed with anti-β-actin. Therefore, phospho-ERK1/2 **(A)** and p65 subunit of NF-κB **(B)** expression were normalized to the same loading control. Results are expressed as median (interquartile range) from three different experiments. In each experiment, every experimental condition was tested in quadruplicate (*$p < 0.05$ compared with the values obtained from untreated cells).

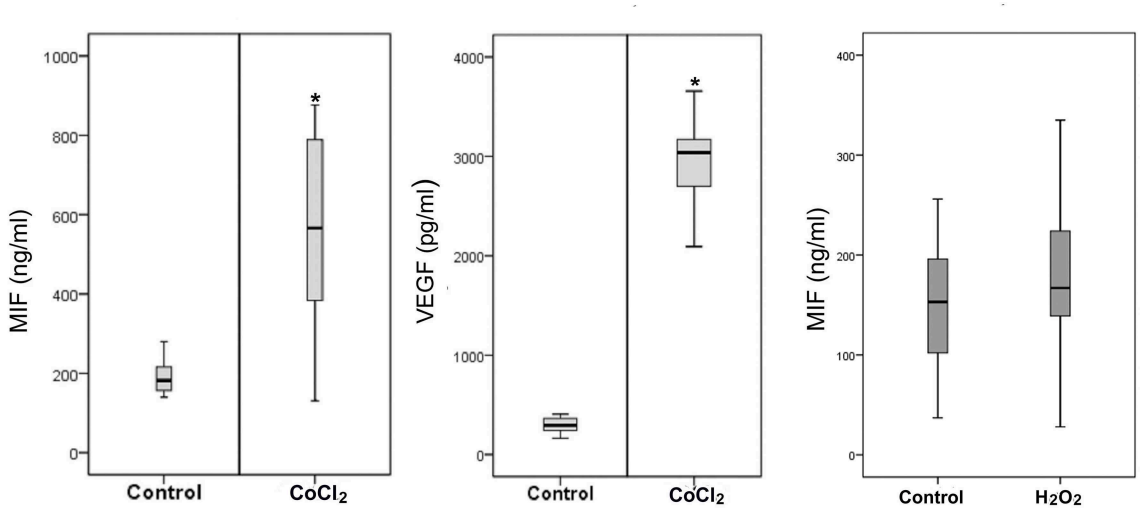

FIGURE 10 | Hypoxia induces production of macrophage migration inhibitory factor (MIF) and vascular endothelial growth factor (VEGF) by Müller cells. Müller cells were left untreated or treated with cobalt chloride ($CoCl_2$) (300 μM) or hydrogen peroxide (H_2O_2) (100 μM) for 24 h. Levels of MIF and VEGF were quantified in the culture media by ELISA. Results are expressed as median (interquartile range) from three different experiments. In each experiment, every experimental condition was included 8 times (*$p < 0.05$ compared to the values obtained from untreated cells).

significant positive correlations between the levels of MIF and CD74 expression and the angiogenic activity in PDR epiretinal fibrovascular membranes. Our immunohistochemical data are in line with those of previous studies that demonstrated MIF and CD74 expression by tumor-associated fibroblasts, leukocytes and endothelial cells (27). Several studies proposed that the MIF/CD74 signaling pathway is an important regulator in pathological tumor-associated angiogenesis (21–23, 27) and

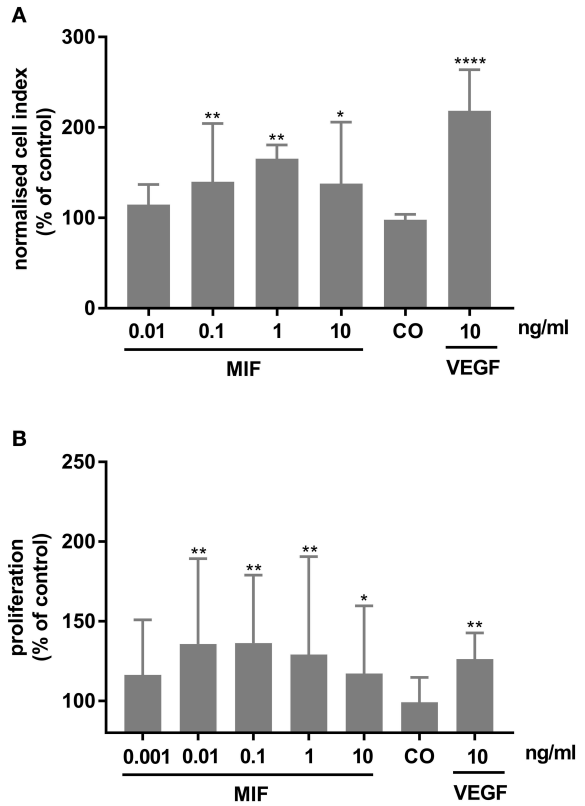

FIGURE 11 | Macrophage migration inhibitory factor (MIF) stimulates migration and proliferation of human retinal microvascular endothelial cells (HRMECs). **(A)** HRMECs were stimulated with dilution medium alone (CO), MIF (0.01, 0.1, 1, 10 ng/ml) or VEGF (10 ng/ml). Electrical impedance was measured every minute for 15 h using the xCELLigence RTCA-DP system and automatically converted to cell indices by the xCELLigence software. The results shown are derived from the time point where the maximal cell index was reached (about 12 h after initiation). The median (interquartile range) percentage of migration compared to control is shown ($n \geq 3$). **(B)** The number of HRMECs was quantified 48 h after addition of dilution medium, VEGF (10 ng/ml) or MIF (0.001 to 10 ng/ml). Results are expressed relative to control (untreated cells). The relative proliferation is shown as median (interquartile range) ($n = 4$ in triplicate). (****$p < 0.0001$; **$p < 0.01$; *$p < 0.05$ compared to unstimulated cells).

showed that MIF expression levels correlated with tumor angiogenesis (30, 31). In animal models of cancer, it was demonstrated that MIF had the potential to promote tumor growth and tumor-associated angiogenesis and that anti-MIF antibodies suppressed angiogenesis in these models (33). Several reports demonstrated that MIF directly and potently induces angiogenesis in multiple *in vitro* and *in vivo* models (24–26). In the present study, we demonstrated that MIF induced HRMEC migration and proliferation, early key steps during angiogenesis. These findings implied that MIF and CD74 might play roles as a ligand-receptor complex in PDR angiogenesis. Previously, it has been shown that MIF expression was also upregulated in an animal model of corneal neovascularization and that MIF-deficient mice had less neovascularization (42). In a mouse model of oxygen-induced ischemic retinal neovascularization, MIF deficiency reduced pathological preretinal angiogenesis and the expression of proinflammatory and proangiogenic factors (43).

In this study, we also demonstrated that MIF and sCD74 were significantly upregulated in the vitreous fluid from patients with PDR, and that vitreous MIF levels were significantly higher in PDR eyes with active neovascularization compared with eyes with quiescent disease. Our findings are in agreement with a previous study that demonstrated upregulated expression of MIF in the vitreous fluid from patients with PDR (44). Our analysis showed significant positive correlations between the vitreous fluid levels of MIF and those of the inflammatory biomarker sICAM-1 and the angiogenic biomarker VEGF. In addition, we demonstrated that intravitreal injection of MIF in normal rats induced significant upregulation of ICAM-1 and VCAM-1 in the retina. Our findings are consistent with previous reports documenting the role of MIF in upregulating ICAM-1 and VCAM-1 in different types of cells (45, 46). In an animal model of retinal detachment, MIF was identified by a proteomics screen to be the most important cytokine upregulated in retinal detachment. Administration of a MIF inhibitor blocked pathological damage responses by protecting photoreceptors and reducing gliosis (47).

Among the proangiogenic factors, VEGF is considered as the most potent one with a pivotal role in PDR (10, 11). To corroborate the findings at the cellular level, stimulation with MIF caused upregulation of VEGF in Müller cells. Müller cells are considered to contribute to pathological retinal neovascularization by being the principle VEGF-producing cell type (41). In addition, Matsuda et al. demonstrated expression of MIF in rat Müller cells (48). To our knowledge, the present study is the first to report the capability of MIF to target Müller cells and to induce upregulation of phospho-ERK1/2 and the synthesis and secretion of VEGF. Additionally, intravitreal injection of MIF induced a significant upregulation of VEGF, phospho-ERK1/2 and the p65 subunit of NF-κB in the retina of rats. This is in line with previous studies documenting the capacity of MIF to induce VEGF and phosphorylation of ERK1/2 in tumor cells (23, 28–30). These findings suggest that one possible mechanism of MIF-induced angiogenesis in PDR is related to the upregulation of VEGF. In addition, upregulation of VEGF is a major contributor to BRB breakdown in diabetes (49–51). Our findings also suggest that MIF-induced BRB breakdown might be related to upregulation of VEGF. Furthermore, we showed that stimulation with the hypoxia mimetic agent $CoC1_2$ promoted VEGF and MIF expressions in Müller cells. Similarly, previous studies demonstrated that MIF was induced by hypoxia in cancer cells (30, 52, 53).

In addition to its well characterized role in inflammation and angiogenesis, MIF is upregulated in fibrotic disorders, such as idiopathic pulmonary fibrosis (54, 55) and systemic sclerosis (56). Additionally, MIF expression increased during the wound healing of rat skin injured by excision and anti-MIF antibodies induced a delay in wound healing (57). In the present study, immunohistochemical analysis

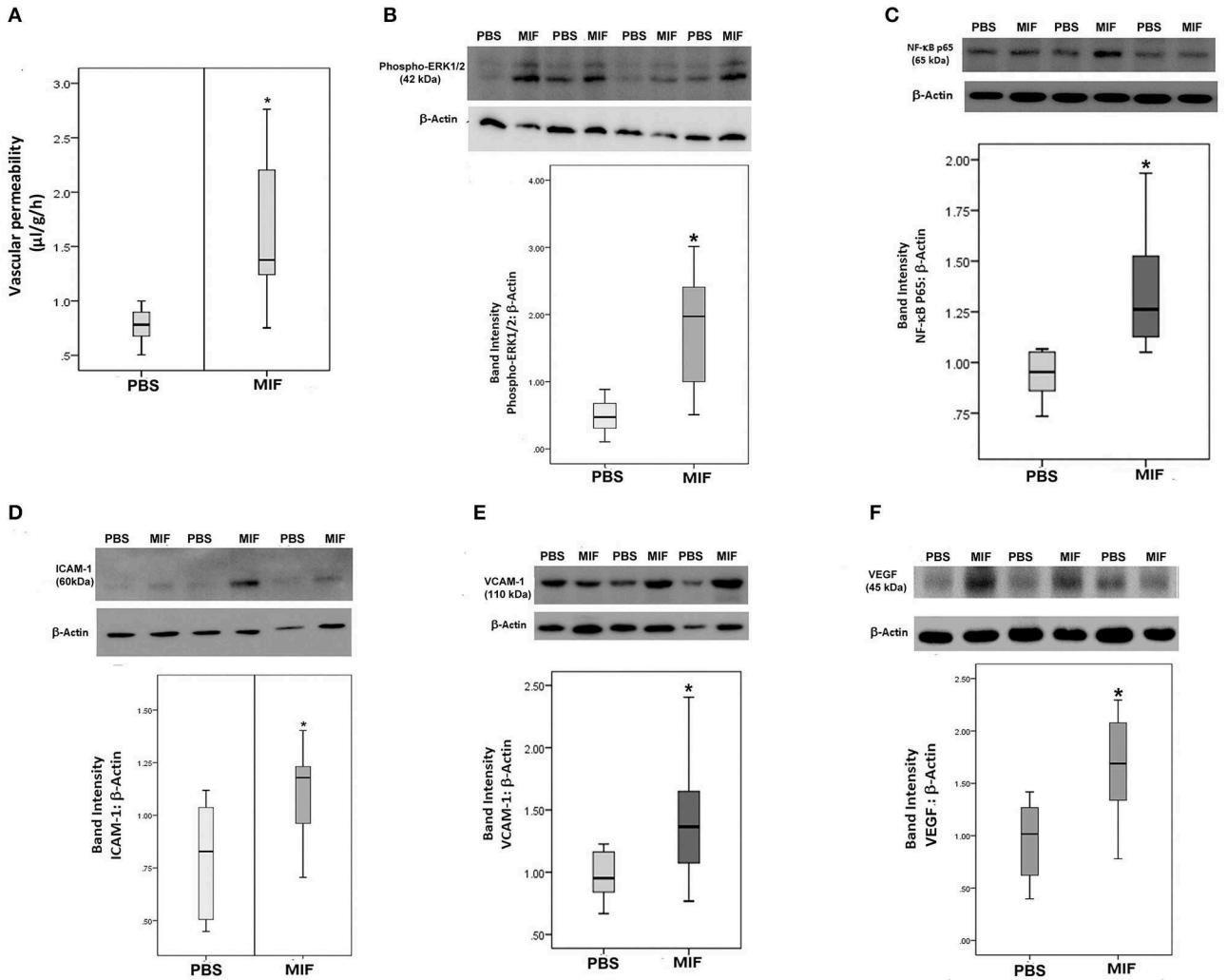

FIGURE 12 | Macrophage migration inhibitory factor (MIF) induces blood-retinal barrier (BRB) breakdown and *in vivo* activation of inflammatory pathway. MIF ($n = 12$) was injected intravitreally at the dose of 5 ng in 5 µl in one eye and the same volume of phosphate buffer saline (PBS; $n = 11$) was injected in the contralateral eye of normal rats. BRB breakdown was quantified with the FITC-conjugated dextran technique **(A)**. As demonstrated by Western blot analysis of rat retinas, intravitreal administration of MIF induced a significant upregulation of the expression of phospho-ERK1/2 **(B)**, p65 subunit of NF-κB **(C)**, intercellular adhesion molecule-1 (ICAM-1) **(D)**, vascular cell adhesion molecule-1 (VCAM-1) **(E)** and vascular endothelial growth factor (VEGF) **(F)** compared with intravitreal administration of PBS. Results are expressed as median (interquartile range) (*$p < 0.05$ compared to the values obtained from PBS-injected eyes).

demonstrated MIF and CD74 localization in myofibroblasts, the key cellular mediator of fibrosis (58), in epiretinal membranes from patients with PDR and PVR. Similarly, dermal fibroblasts from skin wound lesions (57) and systemic sclerosis (56) produced higher amounts of MIF than normal dermal fibroblasts. It was demonstrated i*n vitro* that transient exposure of fibroblasts to MIF induced fibroblast activation and promoted fibroblast proliferation, migration and replenishment of cell monolayers after scratching (59). In a recent study, an interesting genetic association of MIF with epiretinal membrane formation was found, suggesting a potential contribution of MIF to formation of the membranes (60).

In conclusion, the proinflammatory and proangiogenic cytokine MIF and its receptor CD74 are upregulated in the intraocular microenvironment of patients with PDR, particularly in patients with active angiogenesis. Additionally, intravitreal administration of MIF significantly increased retinal vascular permeability in rats. MIF stimulation of Müller cells induced increased secretion of VEGF and $CoC1_2$ induced the production of MIF from Müller cells *in vitro*. Stimulation of endothelial cells isolated from human retinas with MIF induced migration and proliferation, confirming its reported angiogenic effects. Therefore, the MIF/CD74 signaling pathway might play an important role in PDR angiogenesis and progression and could become a primary

therapeutic target for improving the vascular function in patients with PDR.

DATA AVAILABILITY STATEMENT

The datasets generated for this study are available on request to the corresponding author.

ETHICS STATEMENT

The study was conducted according to the tenets of the Declaration of Helsinki. Before undergoing vitrectomy, all patients signed a preoperative informed written consent and approved the use of the excised epiretinal membranes and aspirated vitreous fluid for further analysis and clinical research. The Research Centre and Institutional Review Board of the College of Medicine, King Saud University approved the study design and protocol.

AUTHOR CONTRIBUTIONS

AMA designed the manuscript, supplied funding, interpreted the data, and wrote the manuscript. AA, MS, EA, and AD performed experiments and interpreted the data. PG analyzed the data. GD designed, supervised, and interpreted IHC stainings. JV designed experiments. GO provided funding and designed experiments. SS provided funding, designed experiments, interpreted the data, and wrote the manuscript. All authors read and approved the final manuscript.

FUNDING

This work was supported by King Saud University through Vice Deanship of Research Chair, Dr. Nasser Al-Rashid Research Chair in Ophthalmology (AA) and by the Research Foundation of Flanders (FWO-Vlaanderen; grants No G0D2517N and GOA5716N) and C1 funding (2017–2023) of the KU Leuven (SS and GO). AD holds a Ph.D. fellowship from the Research Foundation of Flanders.

ACKNOWLEDGMENTS

The authors thank Ms. Connie B. Unisa-Marfil for secretarial assistance; Mr. Wilfried Versin and Ms. Kathleen Van Den Eynde for excellent technical assistance.

REFERENCES

1. Abu El-Asrar AM, Nawaz MI, De Hertogh G, Alam K, Siddiquei MM, Van den Eynde K, et al. S100A4 is upregulated in proliferative diabetic retinopathy and correlates with markers of angiogenesis and fibrogenesis. *Mol Vis*. (2014) 20:1209–24.
2. Abu El-Asrar AM, Mohammad G, Nawaz MI, Siddique MM, Van den Eynde K, Mousa A, et al. Relationship between vitreous levels of matrix metalloproteinases and vascular endothelial growth factor in proliferative diabetic retinopathy. *PLoS ONE*. (2013) 8:e85857. doi: 10.1371/journal.pone.0085857
3. Abu El-Asrar AM, Alam K, Nawaz MI, Mohammad G, Van den Eynde K, Siddique MM, et al. Upregulated expression of heparanase in the vitreous of patients with proliferative diabetic retinopathy originates from activated endothelial cells and leukocytes. *Invest Ophthalmol Vis Sci*. (2015) 56:8239–47. doi: 10.1167/iovs.15-18025
4. Abu El-Asrar AM, Struyf S, Mohammad G, Gouwy M, Ruytinx P, Siddiquei MM, et al. Osteoprotegerin is a new regulator of inflammation and angiogenesis in proliferative diabetic retinopathy. *Invest Ophthalmol Vis Sci*. (2017) 58:3189–201. doi: 10.1167/iovs.16-20993
5. Nawaz MI, Van Raemdonck K, Mohammad G, Kangave D, Van Damme J, Abu El-Asrar AM, et al. Autocrine CCL2, CXCL4, CXCL9 and CXCL10 signal in retinal endothelial cells and are enhanced in diabetic retinopathy. *Exp Eye Res*. (2013) 109:67–76. doi: 10.1016/j.exer.2013.01.008
6. Hanahan D, Folkman J. Patterns and emerging mechanisms of the angiogenic switch during tumorigenesis. *Cell*. (1996) 86:353–64. doi: 10.1016/S0092-8674(00)80108-7
7. Carmeliet P. Angiogenesis in health and disease. *Nat Med*. (2003) 9:653–60. doi: 10.1038/nm0603-653
8. Shima DT, Adamis AP, Ferrara N, Yeo KT, Yeo TK, Allende R, et al. Hypoxic induction of endothelial cell growth factors in retinal cells: identification and characterization of vascular endothelial growth factor (VEGF) as the mitogen. *Mol Med*. (1995) 1:182–93. doi: 10.1007/BF03401566
9. Stone J, Itin A, Alon T, Pe'er J, Gnessin H, Chan-Ling T, et al. Development of retinal vasculature is mediated by hypoxia-induced vascular endothelial growth factor (VEGF) expression by neuroglia. *J Neurosci*. (1995) 15(7 Pt 1):4738–47. doi: 10.1523/JNEUROSCI.15-07-04738.1995
10. Miller JW, Le Couter J, Strauss EC, Ferrara N. Vascular endothelial growth factor A in intraocular vascular disease. *Ophthalmology*. (2013) 120:106–14. doi: 10.1016/j.ophtha.2012.07.038
11. Spranger J and Pfeiffer AF. New concepts in pathogenesis and treatment of diabetic retinopathy. *Exp Clin Endocrinol Diab*. (2001) 109(Suppl. 2):S438–50. doi: 10.1055/s-2001-18601
12. Kim YW, West XZ, Byzova TV. Inflammation and oxidative stress in angiogenesis and vascular disease. *J Mol Med (Berl)*. (2013) 91: 323–8. doi: 10.1007/s00109-013-1007-3
13. Ono M. Molecular links between tumor angiogenesis and inflammation: inflammatory stimuli of macrophages and cancer cells as targets for therapeutic strategy. *Cancer Sci*. (2008) 99:1501–6. doi: 10.1111/j.1349-7006.2008.00853.x
14. Bloom BR, Bennett B. Mechanism of a reaction *in vitro* associated with delayed-type hypersensitivity. *Science*. (1966) 153:80–2. doi: 10.1126/science.153.3731.80
15. Su H, Na N, Zhang X, Zhao Y. The biological function and significance of CD74 in immune diseases. *Inflamm Res*. (2017) 66:209–16. doi: 10.1007/s00011-016-0995-1
16. Sánchez-Zamora YI, Rodriguez-Sosa M. The role of MIF in type 1 and type 2 diabetes mellitus. *J Diabetes Res*. (2014) 2014:804519. doi: 10.1155/2014/804519
17. Kithcart AP, Cox GM, Sielecki T, Short A, Pruitt J, Papenfuss T, et al. A small-molecule inhibitor of macrophage migration inhibitory factor for the treatment of inflammatory disease. *FASEB J*. (2010) 24:4459–66. doi: 10.1096/fj.10-162347
18. Leng L, Metz CN, Fang Y, Xu J, Donnelly S, Baugh J, et al. MIF signal transduction initiated by binding to CD74. *J Exp Med*. (2003) 197:1467–76. doi: 10.1084/jem.20030286
19. Korf H, Breser L, Van Hoeck J, Godoy J, Cook DP, Stijlemans B, et al. MIF inhibition interferes with the inflammatory and T cell-stimulatory capacity of NOD macrophages and delays autoimmune diabetes onset. *PLoS ONE*. (2017) 12:e0187455. doi: 10.1371/journal.pone.0187455
20. Bernhagen J, Krohn R, Lue H, Gregory JL, Zernecke A, Koenen RR, et al. MIF is a noncognate ligand of CXC chemokine receptors in

inflammatory and atherogenic cell recruitment. *Nat Med*. (2007) 13:587–96. doi: 10.1038/nm1567
21. McClelland M, Zhao L, Carskadon S, Arenberg D. Expression of CD74, the receptor for macrophage migration inhibitory factor, in non-small cell lung cancer. *Am J Pathol*. (2009) 174:638–46. doi: 10.2353/ajpath.2009.080463
22. Gai JW, Wahafu W, Song L, Ping H, Wang M, Yang F, et al. Expression of CD74 in bladder cancer and its suppression in association with cancer proliferation, invasion and angiogenesis in HT-1376 cells. *Oncol Lett*. (2018) 15:7631–8. doi: 10.3892/ol.2018.8309
23. Cheng RJ, Deng WG, Niu CB, Li YY, Fu Y. Expression of macrophage migration inhibitory factor and CD74 in cervical squamous cell carcinoma. *Int J Gynecol Cancer*. (2011) 21:1004–12. doi: 10.1097/IGC.0b013e31821c45b7
24. Hira E, Ono T, Dhar DK, El-Assal ON, Hishikawa Y, Yamanoi A, et al. Overexpression of macrophage migration inhibitory factor induces angiogenesis and deteriorates prognosis after radical resection for hepatocellular carcinoma. *Cancer*. (2005) 103:588–98. doi: 10.1002/cncr.20818
25. Amin MA, Volpert OV, Woods JM, Kumar P, Harlow LA, Koch AE. Migration inhibitory factor mediates angiogenesis via mitogen-activated protein kinase and phosphatidylinositol kinase. *Circ Res*. (2003) 93:321–9. doi: 10.1161/01.RES.0000087641.56024.DA
26. Yang Y, Degranpré P, Kharfi A, Akoum A. Identification of macrophage migration inhibitory factor as a potent endothelial cell growth-promoting agent released by ectopic human endometrial cells. *J Clin Endocrinol Metab*. (2000) 85:4721–7. doi: 10.1210/jc.85.12.4721
27. Richard V, Kindt N, Decaestecker C, Gabius HJ, Laurent G, Noël JC, et al. Involvement of macrophage migration inhibitory factor and its receptor (CD74) in human breast cancer. *Oncol Rep*. (2014) 32:523–9. doi: 10.3892/or.2014.3272
28. Veillat V, Carli C, Metz CN, Al-Abed Y, Naccache PH, Akoum A. Macrophage migration inhibitory factor elicits an angiogenic phenotype in human ectopic endometrial cells and triggers the production of major angiogenic factors via CD44, CD74, and MAPK signaling pathways. *J Clin Endocrinol Metab*. (2010) 95:E403–12. doi: 10.1210/jc.2010-0417
29. Choudhary S, Hegde P, Pruitt JR, Sielecki TM, Choudhary D, Scarpato K, et al. Macrophage migratory inhibitory factor promotes bladder cancer progression via increasing proliferation and angiogenesis. *Carcinogenesis*. (2013) 34:2891–9. doi: 10.1093/carcin/bgt239
30. Xu X, Wang B, Ye C, Yao C, Lin Y, Huang X, et al. Overexpression of macrophage migration inhibitory factor induces angiogenesis in human breast cancer. *Cancer Lett*. (2008) 261:147–57. doi: 10.1016/j.canlet.2007.11.028
31. Shun CT, Lin JT, Huang SP, Lin MT, Wu MS. Expression of macrophage migration inhibitory factor is associated with enhanced angiogenesis and advanced stage in gastric carcinomas. *World J Gastroenterol*. (2005) 11:3767–71. doi: 10.3748/wjg.v11.i24.3767
32. Hagemann T, Robinson SC, Thompson RG, Charles K, Kulbe H, Balkwill FR. Ovarian cancer cell-derived migration inhibitory factor enhances tumor growth, progression, and angiogenesis. *Mol Cancer Ther*. (2007) 6:1993–2002. doi: 10.1158/1535-7163.MCT-07-0118
33. Nishihira J, Ishibashi T, Fukushima T, Sun B, Sato Y, Todo S. Macrophage migration inhibitory factor (MIF): its potential role in tumor growth and tumor-associated angiogenesis. *Ann N Y Acad Sci*. (2003) 995:171–82. doi: 10.1111/j.1749-6632.2003.tb03220.x
34. Nagarajan P, Tober KL, Riggenbach JA, Kusewitt DF, Lehman AM, Sielecki T, et al. MIF antagonist (CPSI-1306) protects against UVB-induced squamous cell carcinoma. *Mol Cancer Res*. (2014) 12:1292–302. doi: 10.1158/1541-7786.MCR-14-0255-T
35. Sanchez-Zamora Y, Terrazas LI, Vilches-Flores A, Leal E, Juárez I, Whitacre C, et al. Macrophage migration inhibitory factor is a therapeutic target in treatment of non-insulin-dependent diabetes mellitus. *FASEB J*. (2010) 24:2583–90. doi: 10.1096/fj.09-147066
36. Aiello LP, Avery RL, Arrigg PG, Keyt BA, Jampel HD, Shah ST, et al. Vascular endothelial growth factor in ocular fluid of patients with diabetic retinopathy and other retinal disorders. *N Engl J Med*. (1994) 331:1480–7. doi: 10.1056/NEJM199412013312203
37. Mohammad G, Siddiquei MM, Othman A, Al-Shabrawey M, Abu El-Asrar AM. High-mobility group box-1 protein activates inflammatory signaling pathway components and disrupts retinal vascular-barrier in the diabetic retina. *Exp Eye Res*. (2013) 107:101–9. doi: 10.1016/j.exer.2012.12.009
38. Ruytinx P, Janssens R, Berghmans N, Gouwy M, Ronsse I, Liekens S, et al. Relative distribution and biological characterization of CXCL4L1 isoforms in platelets from healthy donors. *Biochem Pharmacol*. (2017) 145:123–31. doi: 10.1016/j.bcp.2017.08.020
39. Rebmann V, Dornmair K, Grosse-Wilde H. Biochemical analysis of plasma-soluble invariant chains and their complex formation with soluble HLA-DR. *Tissue Antigens*. (1997) 49:438–42. doi: 10.1111/j.1399-0039.1997.tb02776.x
40. Wu G, Sun Y, Wang K, Chen Z, Wang X, Chang F, et al. Relationship between elevated soluble CD74 and severity of experimental and clinical ALI/ARDS. *Sci Rep*. (2016) 6:30067. doi: 10.1038/srep30067
41. Bringmann A, Pannicke T, Grosche J, Francke M, Wiedemann P, Skatchkov SN, et al. Müller cells in the healthy and diseased retina. *Prog Retin Eye Res*. (2006) 25:397–424. doi: 10.1016/j.preteyeres.2006.05.003
42. Usui T, Yamagami S, Kishimoto S, Seiich Y, Nakayama T, Amano S. Role of macrophage migration inhibitory factor in corneal neovascularization. *Invest Ophthalmol Vis Sci*. (2007) 48:3545–50. doi: 10.1167/iovs.06-0695
43. Wang J, Lin J, Kaiser U, Wohlfart P, Hammes HP. Absence of macrophage migration inhibitory factor reduces proliferative retinopathy in a mouse model. *Acta Diabetol*. (2017) 54:383–92. doi: 10.1007/s00592-016-0956-8
44. Mitamura Y, Takeuchi S, Matsuda A, Tagawa Y, Mizue Y, Nishihira J. Macrophage migration inhibitory factor levels in the vitreous of patients with proliferative diabetic retinopathy. *Br J Ophthalmol*. (2000) 84:636–9. doi: 10.1136/bjo.84.6.636
45. Shyu LY, Yeh TM, Chang HH, Lin DP, Teng YH, Chen LC, et al. Macrophage migration inhibitory factor induces ICAM-1and thrombomobulin expression *in vitro*. *Thromb Res*. (2012) 129:43–9. doi: 10.1016/j.thromres.2011.08.011
46. Amin MA, Haas CS, Zhu K, Mansfield PJ, Kim MJ, Lackowski NP, et al. Migration inhibitory factor up-regulates vascular cell adhesion molecule-1 and intercellular adhesion molecule-1 via Src, PI3 kinase, and NFkappaB. *Blood*. (2006) 107:2252–61. doi: 10.1182/blood-2005-05-2011
47. Kim B, Kusibati R, Heisler-Taylor T, Mantopoulos D, Ding J, Abdel-Rahman MH, et al. MIF Inhibitor ISO-1 protects photoreceptors and reduces gliosis in experimental retinal detachment. *Sci Rep*. (2017) 7:14336. doi: 10.1038/s41598-017-14298-9
48. Matsuda A, Tagawa Y, Yoshida K, Matsuda H, Nishihira J. Expression of macrophage migration inhibitory factor in rat retina and its immunohistochemical localization. *J Neuroimmunol*. (1997) 77:85–90. doi: 10.1016/S0165-5728(97)00061-1
49. Kusari J, Zhou SX, Padillo E, Clarke KG, Gil DW. Inhibition of vitreoretinal VEGF elevation and blood-retinal barrier breakdown in streptozotocin-induced diabetic rats by brimonidine. *Invest Ophthalmol Vis Sci*. (2010) 51:1044–51. doi: 10.1167/iovs.08-3293
50. Ishida S, Usui T, Yamashiro K, Kaji Y, Ahmed E, Carrasquillo KG, et al. VEGF164 is proinflammatory in the diabetic retina. *Invest Ophthalmol Vis Sci*. (2003) 44:2155–62. doi: 10.1167/iovs.02-0807
51. Qaum T, Xu Q, Joussen AM, Clemens MW, Qin W, Miyamoto K, et al. VEGF-initiated blood-retinal barrier breakdown in early diabetes. *Invest Ophthalmol Vis Sci*. (2001) 42:2408–13.
52. Larsen M, Tazzyman S, Lund EL, Junker N, Lewis CE, Kristjansen PE, et al. Hypoxia-induced secretion of macrophage migration-inhibitory factor from MCF-7 breast cancer cells is regulated in a hypoxia-inducible factor-independent manner. *Cancer Lett*. (2008) 265:239–49. doi: 10.1016/j.canlet.2008.02.012
53. Bacher M, Schrader J, Thompson N, Kuschela K, Gemsa D, Waeber G, et al. Up-regulation of macrophage migration inhibitory factor gene and protein expression in glial tumor cells during hypoxic and hypoglycemic stress indicates a critical role for angiogenesis in glioblastoma multiforme. *Am J Pathol*. (2003) 162:11–7. doi: 10.1016/S0002-9440(10)63793-5
54. Bargagli E, Olivieri C, Nikiforakis N, Cintorino M, Magi B, Perari MG, et al. Analysis of macrophage migration inhibitory factor (MIF) in patients with idiopathic pulmonary fibrosis. *Respir Physiol Neurobiol*. (2009) 167:261–7. doi: 10.1016/j.resp.2009.05.004

55. Günther S, Bordenave J, Hua-Huy T, Nicco C, Cumont A, Thuillet R, et al. Macrophage migration inhibitory factor (MIF) inhibition in a murine model of bleomycin-induced pulmonary fibrosis. *Int J Mol Sci*. (2018) 19:E4105. doi: 10.3390/ijms19124105
56. Kim JY, Kwok SK, Hur KH, Kim HJ, Kim NS, Yoo SA, et al. Up-regulated macrophage migration inhibitory factor protects apoptosis of dermal fibroblasts in patients with systemic sclerosis. *Clin Exp Immunol*. (2008) 152:328–35. doi: 10.1111/j.1365-2249.2008.03637.x
57. Abe R, Shimizu T, Ohkawara A, Nishihira J. Enhancement of macrophage migration inhibitory factor (MIF) expression in injured epidermis and cultured fibroblasts. *Biochim Biophys Acta*. (2000) 1500:1–9. doi: 10.1016/S0925-4439(99)00080-0
58. Wynn TA. Cellular and molecular mechanisms of fibrosis. *J Pathol*. (2008) 214:199–210. doi: 10.1002/path.2277
59. Dewor M, Steffens G, Krohn R, Weber C, Baron J, Bernhagen J. Macrophage migration inhibitory factor (MIF) promotes fibroblast migration in scratch-wounded monolayers *in vitro*. *FEBS Lett*. (2007) 581:4734–42. doi: 10.1016/j.febslet.2007.08.071
60. Cebulla CM, Stevenson W, Van Law H, Heisler-Taylor T, Hamadmad S, Shah MH, et al. MIF promoter polymorphisms are associated with epiretinal membrane but not retinal detachment with PVR in an American population. *Exp Eye Res*. (2019) 185:107667. doi: 10.1016/j.exer.2019.05.007

Conflict of Interest: The authors declare that the research was conducted in the absence of any commercial or financial relationships that could be construed as a potential conflict of interest.

frontiers in Immunology

ORIGINAL RESEARCH
published: 08 January 2020
doi: 10.3389/fimmu.2019.03032

CD36 Deficiency Inhibits Retinal Inflammation and Retinal Degeneration in *Cx3cr1* Knockout Mice

Sophie Lavalette[1], *Jean-Baptiste Conart*[1], *Sara Touhami*[1], *Christophe Roubeix*[1], *Marianne Houssier*[1], *Sébastien Augustin*[1], *William Raoul*[1,2], *Christophe Combadière*[3], *Maria Febbraio*[4], *Huy Ong*[5], *Sylvain Chemtob*[6], *José-Alain Sahel*[1], *Cécile Delarasse*[1], *Xavier Guillonneau*[1]* *and Florian Sennlaub*[1]*

[1] Institut de la Vision, Sorbonne Université, INSERM, CNRS, Paris, France, [2] Université de Tours, Inserm, N2C UMR 1069, Faculté de Médecine, Tours, France, [3] Sorbonne Université, Inserm, CNRS, Centre d'Immunologie et des Maladies Infectieuses, Cimi-Paris, Paris, France, [4] Department of Dentistry, University of Alberta, Edmonton, AB, Canada, [5] Faculty of Pharmacy, Université de Montréal, Montreal, QC, Canada, [6] Departments of Pediatrics, Ophthalmology and Pharmacology, Université de Montréal, Montreal, QC, Canada

Background: CD36, a member of the class B scavenger receptor family, participates in Toll-like receptor signaling on mononuclear phagocytes (MP) and can promote sterile pathogenic inflammation. We here analyzed the effect of CD36 deficiency on retinal inflammation and photoreceptor degeneration, the hallmarks of age-related macular degeneration (AMD), that characterize *Cx3cr1*$^{-/-}$mice.

Methods: We analyzed subretinal MP accumulation, and cone- and rod-degeneration in light-challenged and aged, CD36 competent or deficient, hyper-inflammatory *Cx3cr1*$^{-/-}$ mice, using histology and immune-stained retinal flatmounts. Monocytes (Mo) were subretinally adoptively transferred to evaluate their elimination rate from the subretinal space and Interleukin 6 (IL-6) secretion from cultured Mo-derived cells (MdCs) of the different mouse strains were analyzed.

Results: CD36 deficient *Cx3cr1*$^{-/-}$ mice were protected against age- and light-induced subretinal inflammation and associated cone and rod degeneration. CD36 deficiency in *Cx3cr1*$^{-/-}$ MPs inhibited their prolonged survival in the immune-suppressive subretinal space and reduced the exaggerated IL-6 secretion observed in *Cx3cr1*$^{-/-}$ MPs that we previously showed leads to increased subretinal MP survival.

Conclusion: *Cd36* deficiency significantly protected hyperinflammatory *Cx3cr1*$^{-/-}$ mice against subretinal MP accumulation and associated photoreceptor degeneration. The observed CD36-dependent induction of pro-inflammatory IL-6 might be at least partially responsible for the prolonged MP survival in the immune-suppressive environment and its pathological consequences on photoreceptor homeostasis.

Keywords: age related macular degeneration, mononuclear phagocyte, CX3CR1, CD36, IL-6, photoreceptor

OPEN ACCESS

Edited by:
Heping Xu,
Queen's University Belfast,
United Kingdom

Reviewed by:
Erica Lucy Fletcher,
The University of Melbourne, Australia
Bernahrd Ryffel,
Centre National de la Recherche Scientifique (CNRS), France

***Correspondence:**
Xavier Guillonneau
xavier.guillonneau@inserm.fr
Florian Sennlaub
florian.sennlaub@inserm.fr

Specialty section:
This article was submitted to Immunological Tolerance and Regulation, a section of the journal Frontiers in Immunology

Received: *24 October 2019*
Accepted: *10 December 2019*
Published: *08 January 2020*

Citation:
Lavalette S, Conart J-B, Touhami S, Roubeix C, Houssier M, Augustin S, Raoul W, Combadière C, Febbraio M, Ong H, Chemtob S, Sahel J-A, Delarasse C, Guillonneau X and Sennlaub F (2020) CD36 Deficiency Inhibits Retinal Inflammation and Retinal Degeneration in Cx3cr1 Knockout Mice. Front. Immunol. 10:3032. doi: 10.3389/fimmu.2019.03032

INTRODUCTION

Age-related Macular Degeneration (AMD) is a common (1), highly heritable, neuroinflammatory disorder characterized by central, sizeable deposits under the retinal pigment epithelium (drusen) in its early form and choroidal neovascularisation (CNV, wet AMD) or an extending lesion of the outer central retina (geographic atrophy) in its late form (2).

We (3–6) and others (7, 8) showed that both advanced forms [wet AMD (5) and Geographic Atrophy, GA (3, 4, 6)] are associated with non-resolving accumulation of mononuclear phagocytes (MP) in the subretinal space. MPs are a family of cells that include monocyte (Mo), resident macrophages (rMϕ) such as microglial cells (MC), and monocyte-derived inflammatory macrophages/dendritic cells (MdC) that arise during inflammation (9). Physiologically, the subretinal space does not contain blood- and lymphatic-vessels, and is additionally devoid of immune cells, including resident MCs (4, 5, 7, 8, 10). Among others this particularity is due to the potent immunosuppressive, pro-apoptotic factors produced by the RPE that eliminate infiltrating leukocytes (4, 11). While MP accumulation observed around large drusen in early AMD (4, 6) might control debris accumulation, we showed that MdCs invariably participate in the infiltrate in and around GA lesions (6), where they are closely associated with rod and cone degeneration (3). Indeed, MPs, and in particular MdCs, an important source of inflammatory cytokines that play a critical role in animal models of pathological choroidal neovascularisation (CNV) (12, 13) and photoreceptor degeneration (5, 6, 14–18). In particular we showed that the inflammatory cytokines CCL2, IL-6, and IL-1 lead to the excessive MdC accumulation, diminish the subretinal immunosuppressivity and induce photoreceptor degeneration and CNV, respectively (3, 4, 6, 18, 19).

In the eye, CX3CL1 is constitutively expressed as a transmembrane protein in inner retinal neurons (20, 21) and provides a tonic inhibitory signal to CX3CR1 bearing retinal MCs that keeps these cells in a quiescent surveillance mode under physiological conditions (5, 22). *Cx3cr1* deficiency in mice leads to a strong increase of subretinal MP accumulation with age, after light-challenge and laser-injury (5, 23, 24), in diabetes (25), and in a paraquat-induced retinopathy model (26).

We showed that *Cx3cr1*-deficient MPs express high levels of Apolipoprotein E, also observed in humanized transgenic mice expressing the AMD-risk APOE2 isoform (TRE2-mice) and subretinal MPs of AMD patients (4, 6, 27). The excessive expression of APOE in turn can activate the CD14/TLR2/TLR4-dependent innate immunity receptor complex (IIRC) on MPs (4, 27), likely by modifying the cholesterol content of the lipid raft, in which the complex is located (28). Its activation in subretinal MPs induces CCL2 (27), which increases Mo recruitment (6), but also IL-6, which we show reduces RPE FasL expression and MP elimination (4). The age-dependent accumulation of subretinal *Cx3cr1*-deficient MPs is associated with a significant degeneration of rods and cones (5, 29, 30), but not with RPE atrophy. They therefore quite accurately model the transitional zone of GA and a subtype of GA called incomplete outer retinal atrophy [iORA; (31)].

CD36, a member of the class B scavenger receptor family, is expressed in a variety of cell types and binds a diverse array of ligands (32). It is expressed on Mϕ, MC, RPE cells, and microvascular endothelial cells (32), all cell types potentially involved in AMD. On vascular endothelial cells CD36 has been shown to mediate the antiproliferative effect of the thrombospondins (33, 34). Its expression on RPE cells has been shown to influence the phagocytosis of rod outer segments (ROS) (35, 36), in particular oxydized ROS (37, 38), but also oxydized lipoproteins (39), whose CD36-mediated uptake activates the NLRP3 inflammasome in the RPE (40). Finally, it is expressed on MC and Mϕ where it is a co-receptor of the toll-like receptor 2 (TLR2) and activates a proinflammatory signaling cascade and the release of inflammatory cytokines (41, 42). On the other hand, internalization of apoptotic bodies via CD36 can inhibit proinflammatory pathways (43, 44).

We have previously shown that CD36 expression regulates COX-2 and VEGF expression in RPE cells. Its deficiency leads to a slow, age-related choroidal involution and mild retinal degeneration (45). On the other hand deficiency of CD36 protected against subretinal inflammation and photoreceptor degeneration in an acute model of light toxicity, as it inhibited the release of neurotoxic IL-1beta from subretinal MPs (42).

Here we investigated the influence of CD36 on inflammation and photoreceptor degeneration in *Cx3cr1*-deficient mice that we previously showed develop pathogenic subretinal MP accumulation with age and after a non-toxic light-challenge.

RESULTS

CD36 Deficiency Prevents Age-Related, Chronic, Pathogenic Subretinal Inflammation in Cx3cr1-Knockout Mice

We first sought to determine whether *Cd36* deficiency would alter disease onset and progression in $Cx3cr1^{-/-}$ mice. Quantification of subretinal IBA-1^{+} MPs on retinal and RPE/choroidal flatmounts of 2–3 month and 12 month old animals showed that the age-related increase in subretinal MPs observed in $Cx3cr1^{-/-}$ mice was significantly inhibited in the absence of CD36 (**Figures 1A,B**). Next, we evaluated whether *Cd36* deficiency influenced the rod and cone degeneration that is associated with MP accumulation in $Cx3cr1^{-/-}$ mice (5, 6, 29). Micrographs revealed that $Cx3cr1^{-/-}Cd36^{-/-}$ mice were protected against the thinning of the outer nuclear layer that hosts the photoreceptor nuclei, which is observed in aged *Cx3cr1*-deficient mice (6) (**Figure 2A**). Photoreceptor nuclei row counts (**Figure 2B**) and calculation of the area under the curve showed *CD36* deficiency protected against the photoreceptor cell loss observed in $Cx3cr1^{-/-}$ mice (**Figure 2C**), while only a slight decrease was observed in $CD36^{-/-}$ compared to control-mice. Similarly, *CD36* deficiency completely protected against cone loss observed on peanut agglutinin stained retinal flatmounts of 12 month-old $Cx3cr1^{-/-}$ mice (**Figures 2D–F**). Thus, we show that CD36 contributes importantly to the

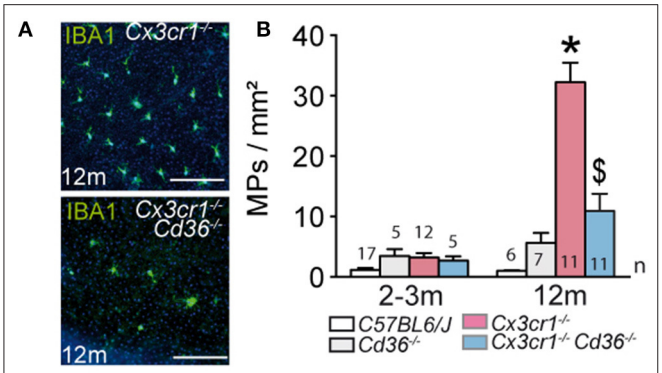

FIGURE 1 | CD36 deficiency prevents age-related chronic subretinal inflammation in Cx3cr1-knockout mice. **(A)** Representative images of 12 month old IBA-1 (green) stained RPE flatmounts of 12 months old *Cx3cr1*$^{-/-}$ and *Cx3cr1*$^{-/-}$*Cd36*$^{-/-}$ mice. **(B)** Quantification of subretinal IBA-1+MPs in 2-3 months (left) and 12 months (right) old mice of the indicated strains (*Mann & Whitney test at 12 months of *Cx3cr1*$^{-/-}$ vs. 3 months old *Cx3cr1*$^{-/-}$ mice $p = 0.0002$; $^{\$}$Mann & Whitney test at 12 months of *Cx3cr1*$^{-/-}$ vs. 12 months old *Cx3cr1*$^{-/-}$*Cd36*$^{-/-}$ mice $p < 0.0001$). n = number of replicates indicated in the graphs; replicates represent quantification of eyes from different mice of at least three different cages. Scale bar **(A)** = 50 m.

chronic, age-related subretinal MP accumulation and associated photoreceptor degeneration observed in *Cx3cr1*$^{-/-}$ mice.

CD36 Deficiency Prevents Pathogenic Subretinal Inflammation in Acute, Light-Induced Cx3cr1-Knockout Mice

Next, we evaluated its impact on acute light-induced stress. The intensity of the light-challenge model used herein was calibrated to induce substantial subretinal MP infiltration in AMD-prone *Cx3cr1*$^{-/-}$-mice but not in *C57BL6/J* controls (6). Quantification of subretinal IBA-1^{+} MPs on retinal and RPE/choroidal flatmounts of 2–3 month old animals that were exposed to 4500 lux of green light with fully dilated pupils for 96 h, followed by 10 days of housing in the normal animal quarters, revealed an increase in subretinal MPs in *Cx3cr1*$^{-/-}$ mice, which was significantly inhibited in the absence of CD36 (**Figures 3A,B**). To quantify photoreceptor apoptosis in light-challenged mice we prepared TUNEL stained retinal flatmounts as previously described (5, 18). Flatmounts from *Cx3cr1*$^{-/-}$mice displayed TUNEL positive cells in the outer nuclear layer, where the photoreceptor nuclei are located, to a much greater extent than *C57BL6/J* controls as previously reported (6). Importantly, *Cx3cr1*$^{-/-}$*Cd36*$^{-/-}$ mice were protected against the photoreceptor apoptosis observed in Cx3cr1$^{-/-}$mice (**Figure 3C**).

Taken together, CD36-deficiency very significantly inhibited the acute subretinal inflammation and associated photoreceptor apoptosis induced in the light-challenged *Cx3cr1*$^{-/-}$mice, similar to our observations in chronic age-related inflammation.

CD36 Deficiency Normalizes the Resistance to Subretinal Elimination of Cx3cr1-Deficient Monocytes and Reduces Their IL-6 Production *in vitro*

We have previously shown that subretinal MPs in aged- and light-challenges *Cx3cr1*$^{-/-}$ mice are in part derived from infiltrating Mo (6). We showed that subretinally injected WT Mos, MCs or Mφs quickly undergo apoptosis and are eliminated (4), and that such clearance was significantly delayed when MPs lacked CX3CR1 (4). We demonstrated that this resistance was at least in part due to the fact that Cx3cr1-deficient MPs overexpress interleukin 6 (IL-6), which downregulates FasL expression the RPE that normally induces subretinal MP elimination (4).

To evaluate whether CD36 expression on MPs influences their susceptibility to be eliminated by the RPE, we adoptively transferred CFSE-labeled Mos from the different mouse strains into the subretinal space of wildtype mice. The surviving CFSE^{+} Mos were then enumerated 24 h after injection (**Figure 4A**). As previously shown, *Cx3cr1*-deficient Mo were significantly more numerous than subretinally injected wildtype Mos. Importantly, the deletion of *Cd36* in *Cx3cr1*-deficient Mo completely reversed this effect (**Figure 4B**).

Cx3cr1-deficient MPs express increased levels of APOE, which we showed activates the TLR2-CD14-dependent innate immunity receptor cluster and induces IL-6 (4). CD36 is a co-receptor of the toll-like receptor 2 (TLR2) and involved in the proinflammatory signaling cascade and the release of inflammatory cytokines (41, 42). Indeed, IL-6 transcription measured by RT-PCR (**Figure 4C**) and IL-6 secretion evaluated by ELISA (**Figure 4D**) was significantly increased in bone marrow derived Mo from *Cx3cr1*-deficient mice compared to control, but the deletion of *Cd36* in *Cx3cr1*-deficient Mo prevented this increase of expression.

Taken together this data demonstrates that *Cd36* deletion in *Cx3cr1*-deficient Mos inhibits the over-expression of IL-6 in *Cx3cr1*-deficient Mos and reverses their ability to withstand the immunosuppressive environment of the subretinal space.

DISCUSSION

We previously showed that the deletion of *Cx3cr1*, a gene that is exclusively expressed on MPs in the adult eye, is sufficient to trigger an age-related or light-induced pathogenic non-resolving subretinal inflammation. We here demonstrate that the deletion of CD36 in *Cx3cr1*-deficient mice prevented the age- and light-challenge-dependent accumulation of subretinal MPs and protected against the associated photoreceptor cell death. Our data demonstrates that CD36 expression on Mo is necessary for the over-expression of IL-6 that we observe in *Cx3cr1*-deficient MdCs. We previously showed that IL-6 expression in *Cx3cr1*-deficient MPs is necessary for the accumulation of subretinal MPs in *Cx3cr1*-deficient mice, as it induces the downregulation of FasL expression the RPE that induces subretinal MP elimination in wildtype animals (4). Indeed, when we subretinally adoptively transferred *Cx3cr1*$^{-/-}$- and *Cd36*$^{-/-}$*Cx3cr1*$^{-/-}$-Mo to wildtype recipients, the deletion

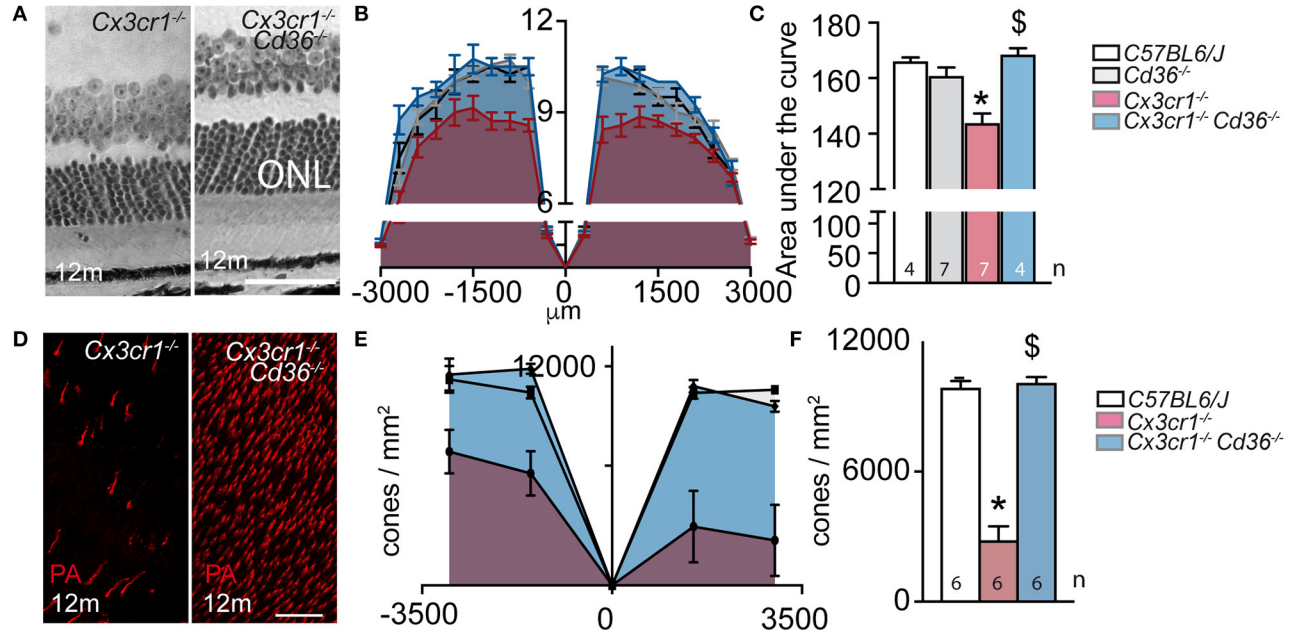

FIGURE 2 | CD36 deficiency prevents age-related rod and cone degeneration in Cx3cr1-knockout mice. **(A)** Micrographs, taken 1,000 µm from the optic nerve, of 12 month-old *Cx3cr1*$^{-/-}$ and *Cx3cr1*$^{-/-}$*Cd36*$^{-/-}$ mice. **(B)** Photoreceptor nuclei rows at increasing distances (−3,000 µm: inferior pole, +3,000 µm: superior pole) from the optic nerve (0 µm) in 12 month-old mice. **(C)** Quantification of the area under the curve of photoreceptor nuclei row counts of 12 month-old mice of the indicated transgenic mouse strains (Mann Whitney wildtype vs. *Cx3cr1*$^{-/-}$ mice $^{*}p = 0.0024$; Mann Whitney *Cx3cr1*$^{-/-}$ vs. *Cx3cr1*$^{-/-}$*Cd36*$^{-/-}$ mice $^{\$}p = 0.0024$). **(D)** Micrographs, taken in the superior periphery of peanut agglutinin (staining cone segments, red) stained 12 month-old *Cx3cr1*$^{-/-}$ and *Cx3cr1*$^{-/-}$*Cd36*$^{-/-}$ mice. **(E)** Cone density quantification on retinal flatmounts in peripheral and central, inferior and superior retina (−3,000 µm: inferior pole, +3,000 µm: superior pole, optic nerve: 0 µm) and their average **(F)** in 12 month-old mice of the indicated mouse strains (Mann Whitney wildtype vs. *Cx3cr1*$^{-/-}$ mice $^{*}p = 0.0022$; Mann Whitney *Cx3cr1*$^{-/-}$ vs. *Cx3cr1*$^{-/-}$*Cd36*$^{-/-}$ mice $^{\$}p = 0.0022$). ONL, outer nuclear layer; PNA, peanut agglutinin Scale bar **(A,D)** = 50 µm. *n* = number of replicates indicated in the graphs; replicates represent quantification of eyes from different mice of at least three different cages.

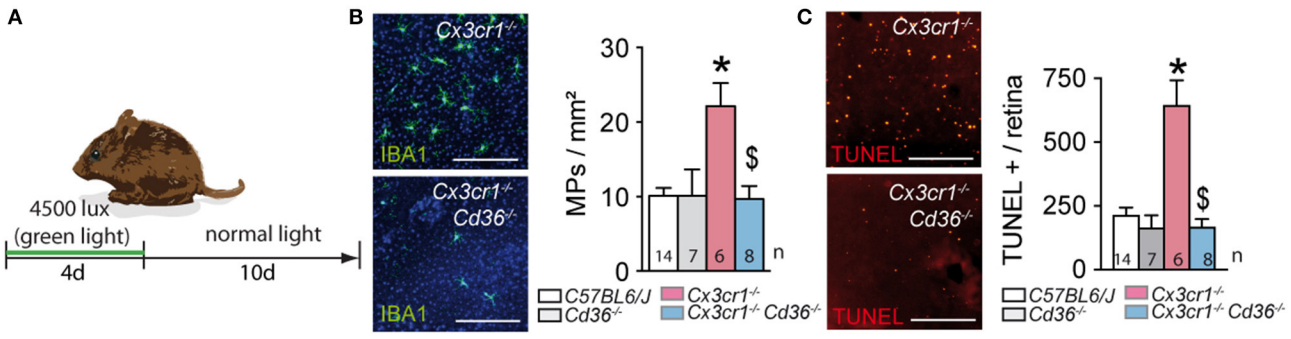

FIGURE 3 | CD36 deficiency prevents pathogenic subretinal inflammation in acute, light-induced Cx3cr1-knockout mice. **(A)** Schematic representation of the light-challenge model. **(B)** Representative images and quantification of IBA-1 (green) stained RPE flatmounts of 2 month-old mice of the indicated strains after 10 days after the light-challenge (*Mann & Whitney test C57BL/6J control mice vs. *Cx3cr1*$^{-/-}$ mice $p = 0.0014$; $^{\$}$Mann & Whitney test *Cx3cr1*$^{-/-}$ vs. *Cx3cr1*$^{-/-}$*Cd36*$^{-/-}$ mice $p = 0.02$). **(C)** Representative images and quantification of TUNEL+ cells in the outer nuclear layer of TUNEL-stained retinal flatmounts of d14 light-challenged mice of the indicated strains (*Mann & Whitney test C57BL/6J control mice vs. *Cx3cr1*$^{-/-}$ mice $p = 0.0005$; $^{\$}$Mann & Whitney test *Cx3cr1*$^{-/-}$ vs. *Cx3cr1*$^{-/-}$*Cd36*$^{-/-}$ mice $p = 0.0012$). *n,* indicated for each bar; Scale bar **(A)** = 50 µm.

of *Cd36* on *Cx3cr1*$^{-/-}$-monocytes restored the susceptible to subretinal elimination to the level observed in wildtype monocytes. Taken together our data demonstrates that Cd36 deficiency inhibits retinal inflammation and retinal degeneration in Cx3cr1 knockout mice.

We previously showed that *Cx3cr1*-deficient MPs are characterized by an over-expression of APOE that triggers NFκB activation and cytokine secretion. *ApoE*-deletion in *Cx3cr1*-deficient mice significantly prevents the accumulation of pathogenic subretinal MPs (4, 6, 27), similar to *Cd36* deficiency.

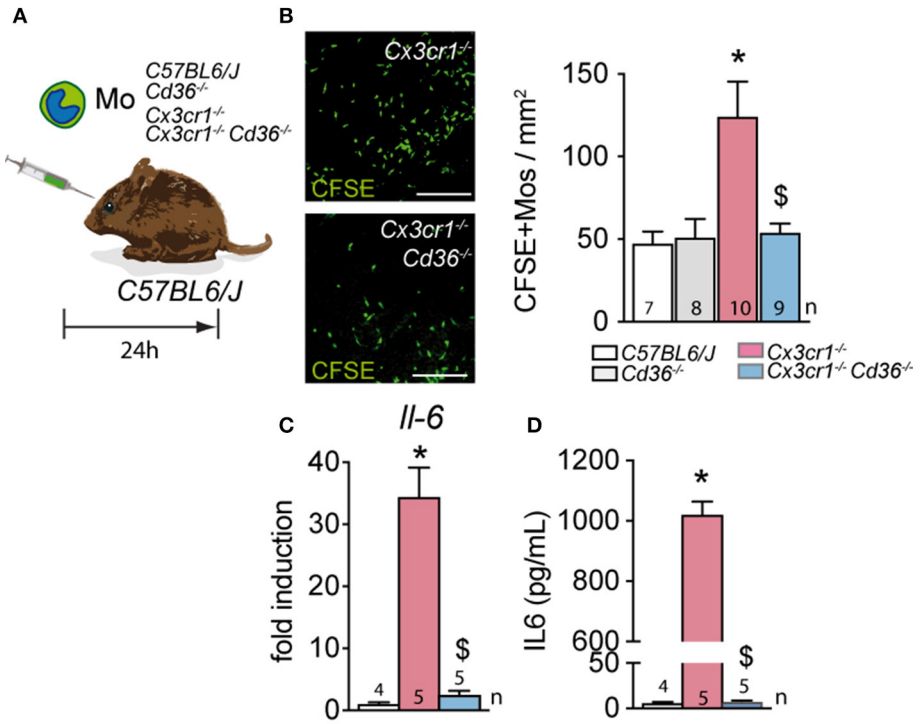

FIGURE 4 | CD36 deficiency normalizes the resistance to subretinal elimination of Cx3cr1-deficient monocytes and reduces their IL-6 production *in vitro.* **(A)** Schematic representation of the subretinal adoptive transfer experiments. **(B)** Representative images and quantification of CSFE+ Mo of the indicated strains on RPE flatmounts 24 h after subretinal transfer to the subretinal space of wildtype mice (*Mann & Whitney test C57BL/6J Mo vs. *Cx3cr1*$^{-/-}$ Mo $p = 0.0019$; $^{\$}$Mann & Whitney test *Cx3cr1*$^{-/-}$ vs. *Cx3cr1*$^{-/-}$*Cd36*$^{-/-}$ Mos $p = 0.0079$). **(C)** Quantitative RT–PCR of IL-6 mRNA normalized with S26 mRNA of C57BL/6J, *Cx3cr1*$^{-/-}$, and *Cx3cr1*$^{-/-}$*Cd36*$^{-/-}$ monocytes cultured for 24 h (*Mann & Whitney test C57BL/6J Mo vs. *Cx3cr1*$^{-/-}$ Mo $p = 0.0159$; $^{\$}$Mann & Whitney test *Cx3cr1*$^{-/-}$ vs. *Cx3cr1*$^{-/-}$*Cd36*$^{-/-}$ Mos $p = 0.0159$). **(D)** IL-6 ELISA of the supernatants of C57BL/6J, *Cx3cr1*$^{-/-}$-, and *Cx3cr1*$^{-/-}$*Cd36*$^{-/-}$ monocytes cultured for 24 h (*Mann & Whitney test C57BL/6J Mo vs. *Cx3cr1*$^{-/-}$ Mo $p = 0.0159$; $^{\$}$Mann & Whitney test *Cx3cr1*$^{-/-}$ vs. *Cx3cr1*$^{-/-}$*Cd36*$^{-/-}$ Mos $p = 0.0079$). *n,* indicated for each bar; Scale bar **(A)** = 50 μm.

Mechanistically, we showed that the excess of APOE activates the CD14/TLR2-dependent innate immunity receptor complex (IIRC) on MPs (4, 27). This is likely due to APOE-induced cholesterol extraction from the lipid rafts of MPs, which lifts the physiological separation of CD14 (located in the lipid raft) from TLR2 (located in non-lipid raft membrane) and triggers NFκB activation and cytokine secretion in the absence of TLR ligands, as previously demonstrated for APOA-I (28, 46).

CD36 is also part of the innate immunity receptor complex (47, 48) and an obligate co-receptor of the toll-like receptor 2 (TLR2). Its inhibition blocks the TLR2-dependent NFκB activation and pro-inflammatory signaling cascade and the release of inflammatory cytokines such as IL-6 (41, 42). In *Cx3cr1*-deficient mice the deletion of *Cd36* therefore likely counters the APOE-induced activation of the IIRC, activation of NFκB and IL-6 secretion, which we show reduces RPE FasL expression and MP elimination (4). As a result, the CD36-deficient MPs are quickly eliminated from the subretinal space, preventing pathogenic subretinal inflammation. Interestingly, it has recently been demonstrated that *Cd36* deletion and pharmacological inhibition of CD36 also inhibits pathogenic inflammation in an acute model of light-induced degeneration in *Cx3cr1*-competent mice (42). The authors demonstrated that the protective effect is likely due to the inhibition of IL-1 that we showed also plays an important role in photoreceptor degeneration in *Cx3cr1*-deficient mice (3, 18).

In summary, the inhibition of CD36 on MPs in diseases that are characterized by pathogenic subretinal inflammation such as AMD, holds the promise to reduce MP accumulation and their production of pathogenic cytokines. On the other hand CD36 expressed by RPE cells has an important role in the maintenance of the choriocapillaries and the elimination of lipids from Bruchs membrane (39, 45). Ideally, future therapies for AMD might therefore want to specifically target CD36 on MPs.

MATERIALS AND METHODS

Animals

Cx3cr1$^{-/-}$*CD36*$^{-/-}$mouse strains on C57BL/6 background were generated from *Cx3cr1*$^{-/-}$mice and *CD36*$^{-/-}$mouse strains, which were generated as previously described (49, 50). All mice were negative for the *Crb1*^{rd8}, *Pde6b*^{rd1}, and *Gnat2*^{cpfl3} mutations. Mice were housed in the animal facility under specific pathogen-free condition, in a 12/12 h light/dark (100–500 lux) cycle with

water and normal diet food available *ad libitum*. All experimental protocols and procedures were approved by the local animal care ethics committee "Comité d'Éthique en Expérimentation Animale Charles Darwin" (N° p3/2008/54).

Light-Challenge Model

Two- to four-month-old mice were adapted to darkness for 6 h and pupils were fully dilated with 1% Atropine (Novartis). Animals were then exposed to green LED light (4500 Lux, JP Vezon équipements) for 4 days and subsequently kept in cyclic 12/12 h normal animal facility conditions. MP accumulation and retinal degeneration were assessed at 10 days after light exposure (6).

Immunohistochemistry and TUNEL Staining of Retinal Flatmounts

Eyes were enucleated, fixed in 4% paraformaldehyde for 20 min at room temperature and sectioned at the limbus; the cornea and lens were discarded. The retinas were peeled from the RPE/choroid/sclera and incubated overnight at 4°C in PBS-1% triton with the following primary antibodies: peanut agglutinin Alexa fluor® 594 (Thermo Fisher Scientific; 1/100), and goat polyclonal anti-IBA1 (1/100, Wako). After few washes, the retinas were incubated for 2 h at room temperature with appropriate Alexa Fluor® conjugated secondary antibodies (Thermo Fisher Scientific; 1:500) in PBS-1% triton and nuclei were counterstained with Hoechst (1:1,000, Sigma Aldrich). The retinas were flatmounted and viewed with a fluorescence microscope (DM5500, Leica). Images centered on the area with the lowest number of PNA+ cone arrestin+ cells were captured with a confocal laser-scanning microscope (FV1000, Olympus) using a 40X lens. Each cell population was manually counted in a masked fashion. IBA-1+ cells were quantified on flatmounts on the outer segment side of the detached retina while PNA+ cone arrestin+ cells were counted on confocal microscopy Z-stacks using ImageJ software.

For histology, eyes were fixed in 0.5% glutaraldehyde, 4% PFA for 2 h, dehydrated and mounted in Historesin (Leica). Five millimeters of oriented sections crossing inferior pole, optic nerve and superior pole were cut and stained with toluidin blue. Rows of nuclei in the ONL were counted at different distances from the optic nerve (6).

For Terminal deoxynucleotidyl transferase dUTP nick end labeling (TUNEL), 4% PFA fixed retinal flatmounts were pre-treated with frozen methanol for 30 min and then frozen methanol/acetic acid (2:1) for another 30 min. After washing with PBS, flatmounts were incubated overnight at 4°C with the reaction mixture as described by manufacturer's protocol (*In Situ* Cell Death Detection Kit, Roche Diagnostics) and then for 90 min at 37°C. After reaction was stopped by washing with PBS at RT, nuclei were counterstained with Hoechst (Sigma–Aldrich).

Cell Preparations and Cell Culture

Bone marrow-derived monocytes (in serum-free X-Vivo 15 medium) were performed as previously described (6). RT-PCRs using Sybr Green (Life Technologies) and ELISAs using mouse IL-6 DuoSet (R&D Systems) were performed as previously described (6).

Subretinal Mononuclear Phagocyte Cell Clearance

Bone marrow-derived monocytes (∼95% pure) were labeled in 10 μM CFSE (Life technologies). Cells were washed and resuspended in PBS. Twelve thousand cells (4 μl) were injected in the subretinal space of anesthetized 2 month-old mice using a microinjector and glass microcapillaries (Eppendorf). A hole was pierced with the glass capillary prior to the subretinal injection to avoid intra-ocular pressure increase and to allow retinal detachment with 4 μl of solution. The subretinal injection was verified by fundoscopy. Eyes were enucleated after 24 h, fixed in 4% PFA, and flatmounted. $CFSE^{+}$transplanted cells were counted on the subretinal aspect of the retinal flatmount and the RPE/choroid flatmount of each eye. Eyes with subretinal hemorrhages were discarded.

Statistical Analysis

Sample sizes for our experiments were determined according to our previous studies Graph Pad Prism 6 (GraphPad Software) was used for data analysis and graphic representation. All values are reported as mean ± SEM. Statistical analysis was performed by Mann–Whitney *U*-test (2-group comparisons). The *n* and *p*-values are indicated in the figure legends.

DATA AVAILABILITY STATEMENT

All datasets generated for this study are included in the article.

ETHICS STATEMENT

The animal study was reviewed and approved by Comité d'Ethique en Expérimentation Animale Charles Darwin.

AUTHOR CONTRIBUTIONS

SL, J-BC, ST, CR, MH, SA, and WR conducted the experiments. CC, MF, HO, SC, J-AS, CD, XG, and FS designed and analyzed the experiments.

FUNDING

This work was supported by grants from INSERM, ANR MACLEAR (ANR-15-CE14-0015-01), UNADEV- Aviesan 2018–2019 Les maladies de la vision: origines et traitements, LABEX LIFESENSES (ANR-10-LABX-65) supported by the ANR [Programme d'Investissements d'Avenir (ANR-11-IDEX-0004-02)], Carnot, and a generous donation by Doris and Michael Bunte.

REFERENCES

1. Wong WL, Su X, Li X, Cheung CM, Klein R, Cheng CY, et al. Global prevalence of age-related macular degeneration and disease burden projection for 2020 and 2040: a systematic review and meta-analysis. *Lancet Glob Health.* (2014) 2:e106–16. doi: 10.1016/S2214-109X(13)70145-1
2. Sarks SH. Ageing and degeneration in the macular region: a clinico-pathological study. *Br J Ophthalmol.* (1976) 60:324–41. doi: 10.1136/bjo.60.5.324
3. Eandi CM, Charles Messance H, Augustin S, Dominguez E, Lavalette S, Forster V, et al. Subretinal mononuclear phagocytes induce cone segment loss via IL-1beta. *eLife.* (2016). 5:9. doi: 10.7554/eLife.16490.009
4. Levy O, Calippe B, Lavalette S, Hu SJ, Raoul W, Dominguez E, et al. Apolipoprotein E promotes subretinal mononuclear phagocyte survival and chronic inflammation in age-related macular degeneration. *EMBO Mol Med.* (2015) 7:211–26. doi: 10.15252/emmm.201404524
5. Combadiere C, Feumi C, Raoul W, Keller N, Rodero M, Pezard A, et al. CX3CR1-dependent subretinal microglia cell accumulation is associated with cardinal features of age-related macular degeneration. *J Clin Invest.* (2007) 117:2920–8. doi: 10.1172/JCI31692
6. Sennlaub F, Auvynet C, Calippe B, Lavalette S, Poupel L, Hu SJ, et al. CCR2(+) monocytes infiltrate atrophic lesions in age-related macular disease and mediate photoreceptor degeneration in experimental subretinal inflammation in Cx3cr1 deficient mice. *EMBO Mol Med.* (2013) 5:1775–93. doi: 10.1002/emmm.201302692
7. Lad EM, Cousins SW, Van Arnam JS, Proia AD. Abundance of infiltrating CD163+ cells in the retina of postmortem eyes with dry and neovascular age-related macular degeneration. *Graefes Arch Clin Exp Ophthalmol.* (2015) 253:1941–5. doi: 10.1007/s00417-015-3094-z
8. Gupta N, Brown KE, Milam AH. Activated microglia in human retinitis pigmentosa, late-onset retinal degeneration, and age-related macular degeneration. *Exp Eye Res.* (2003) 76:463–71. doi: 10.1016/S0014-4835(02)00332-9
9. Nathan C, Ding A. Nonresolving inflammation. *Cell.* (2010) 140:871–82. doi: 10.1016/j.cell.2010.02.029
10. Penfold PL, Madigan MC, Gillies MC, Provis JM. Immunological and aetiological aspects of macular degeneration. *Prog Retin Eye Res.* (2001) 20:385–414. doi: 10.1016/S1350-9462(00)00025-2
11. Griffith TS, Brunner T, Fletcher SM, Green DR, Ferguson TA. Fas ligand-induced apoptosis as a mechanism of immune privilege. *Science.* (1995) 270:1189–92. doi: 10.1126/science.270.5239.1189
12. Tsutsumi C, Sonoda KH, Egashira K, Qiao H, Hisatomi T, Nakao S, et al. The critical role of ocular-infiltrating macrophages in the development of choroidal neovascularization. *J Leukoc Biol.* (2003) 74:25–32. doi: 10.1189/jlb.0902436
13. Sakurai E, Anand A, Ambati BK, van Rooijen N, Ambati J. Macrophage depletion inhibits experimental choroidal neovascularization. *Invest Ophthalmol Vis Sci.* (2003) 44:3578–85. doi: 10.1167/iovs.03-0097
14. Rutar M, Natoli R, Provis JM. Small interfering RNA-mediated suppression of Ccl2 in Muller cells attenuates microglial recruitment and photoreceptor death following retinal degeneration. *J Neuroinflammation.* (2012) 9:221. doi: 10.1186/1742-2094-9-221
15. Suzuki M, Tsujikawa M, Itabe H, Du ZJ, Xie P, Matsumura N, et al. Chronic photo-oxidative stress and subsequent MCP-1 activation as causative factors for age-related macular degeneration. *J Cell Sci.* (2012) 125:2407–15. doi: 10.1242/jcs.097683
16. Kohno H, Chen Y, Kevany BM, Pearlman E, Miyagi M, Maeda T, et al. Photoreceptor proteins initiate microglial activation via toll-like receptor 4 in retinal degeneration mediated by all-trans-retinal. *J Biol Chem.* (2013) 288:15326–41. doi: 10.1074/jbc.M112.448712
17. Cruz-Guilloty F, Saeed AM, Echegaray JJ, Duffort S, Ballmick A, Tan Y, et al. Infiltration of proinflammatory m1 macrophages into the outer retina precedes damage in a mouse model of age-related macular degeneration. *Int J Inflam.* (2013) 2013:503725. doi: 10.1155/2013/503725
18. Hu SJ, Calippe B, Lavalette S, Roubeix C, Montassar F, Housset M, et al. Upregulation of P2RX7 in Cx3cr1-deficient mononuclear phagocytes leads to increased interleukin-1β secretion and photoreceptor neurodegeneration. *J Neurosci.* (2015) 35:6987–96. doi: 10.1523/JNEUROSCI.3955-14.2015
19. Lavalette S, Raoul W, Houssier M, Camelo S, Levy O, Calippe B, et al. Interleukin-1beta inhibition prevents choroidal neovascularization and does not exacerbate photoreceptor degeneration. *Am J Pathol.* (2011) 178:2416–23. doi: 10.1016/j.ajpath.2011.01.013
20. Zieger M, Ahnelt PK, Uhrin P. CX3CL1 (Fractalkine) protein expression in normal and degenerating mouse retina: *in vivo* studies. *PLoS ONE.* (2014) 9:e106562. doi: 10.1371/journal.pone.0106562
21. Silverman MD, Zamora DO, Pan Y, Texeira PV, Baek SH, Planck SR, et al. Constitutive and inflammatory mediator-regulated fractalkine expression in human ocular tissues and cultured cells. *Invest Ophthalmol Vis Sci.* (2003) 44:1608–15. doi: 10.1167/iovs.02-0233
22. Ransohoff RM. Chemokines and chemokine receptors: standing at the crossroads of immunobiology and neurobiology. *Immunity.* (2009) 31:711–21. doi: 10.1016/j.immuni.2009.09.010
23. Raoul W, Keller N, Rodero M, Behar-Cohen F, Sennlaub F, Combadiere C. Role of the chemokine receptor CX3CR1 in the mobilization of phagocytic retinal microglial cells. *J Neuroimmunol.* (2008) 198:56–61. doi: 10.1016/j.jneuroim.2008.04.014
24. Ma W, Zhao L, Fontainhas AM, Fariss RN, Wong WT. Microglia in the mouse retina alter the structure and function of retinal pigmented epithelial cells: a potential cellular interaction relevant to AMD. *PLoS ONE.* (2009) 4:e7945. doi: 10.1371/journal.pone.0007945
25. Kezic JM, Chen X, Rakoczy EP, McMenamin PG. The effects of age and Cx3cr1 deficiency on retinal microglia in the Ins2Akita diabetic mouse. *Invest Ophthalmol Vis Sci.* (2013) 54:854–63. doi: 10.1167/iovs.12-10876
26. Chen M, Luo C, Penalva R, Xu H. Paraquat-induced retinal degeneration is exaggerated in CX3CR1-deficient mice and is associated with increased retinal inflammation. *Invest Ophthalmol Vis Sci.* (2013) 54:682–90. doi: 10.1167/iovs.12-10888
27. Levy O, Lavalette S, Hu SJ, Housset M, Raoul W, Eandi C, et al. APOE-isoforms control pathogenic subretinal inflammation in age related macular degeneration. *J Neurosci.* (2015) 35:13568–76. doi: 10.1523/JNEUROSCI.2468-15.2015
28. Guillonneau X, Eandi CM, Paques M, Sahel JA, Sapieha P, Sennlaub F. On phagocytes and macular degeneration. *Prog Retin Eye Res.* (2017) 61:98–128. doi: 10.1016/j.preteyeres.2017.06.002
29. Calippe B, Augustin S, Beguier F, Charles-Messance H, Poupel L, Conart JB, et al. Complement factor H inhibits CD47-mediated resolution of inflammation. *Immunity.* (2017) 46:261–72. doi: 10.1016/j.immuni.2017.01.006
30. Jobling AI, Waugh M, Vessey KA, Phipps JA, Trogrlic L, Greferath U, et al. The role of the microglial Cx3cr1 pathway in the postnatal maturation of retinal photoreceptors. *J Neurosci.* (2018) 38:4708–23. doi: 10.1523/JNEUROSCI.2368-17.2018
31. Sadda SR, Guymer R, Holz FG, Schmitz-Valckenberg S, Curcio CA, Bird AC, et al. Consensus definition for atrophy associated with age-related macular degeneration on OCT: classification of atrophy report 3. *Ophthalmology.* (2018) 125:537–48. doi: 10.1016/j.ophtha.2017.09.028
32. Febbraio M, Hajjar DP, Silverstein RL. CD36: a class B scavenger receptor involved in angiogenesis, atherosclerosis, inflammation, and lipid metabolism. *J Clin Invest.* (2001) 108:785–91. doi: 10.1172/JCI14006
33. Jimenez B, Volpert OV, Crawford SE, Febbraio M, Silverstein RL, Bouck N. Signals leading to apoptosis-dependent inhibition of neovascularization by thrombospondin-1. *Nat Med.* (2000) 6:41–8. doi: 10.1038/71517
34. Dawson DW, Pearce SF, Zhong R, Silverstein RL, Frazier WA, Bouck NP. CD36 mediates the *in vitro* inhibitory effects of thrombospondin-1 on endothelial cells. *J Cell Biol.* (1997) 138:707–17. doi: 10.1083/jcb.138.3.707
35. Finnemann SC, Silverstein RL. Differential roles of CD36 and alphavbeta5 integrin in photoreceptor phagocytosis by the retinal pigment epithelium. *J Exp Med.* (2001) 194:1289–98. doi: 10.1084/jem.194.9.1289
36. Ryeom SW, Sparrow JR, Silverstein RL. CD36 participates in the phagocytosis of rod outer segments by retinal pigment epithelium. *J Cell Sci.* (1996) 109:387–95.
37. Ryeom SW, Silverstein RL, Scotto A, Sparrow JR. Binding of anionic phospholipids to retinal pigment epithelium may be mediated by the scavenger receptor CD36. *J Biol Chem.* (1996) 271:20536–9. doi: 10.1074/jbc.271.34.20536

38. Sun M, Finnemann SC, Febbraio M, Shan L, Annangudi SP, Podrez EA, et al. Light-induced oxidation of photoreceptor outer segment phospholipids generates ligands for CD36-mediated phagocytosis by retinal pigment epithelium: a potential mechanism for modulating outer segment phagocytosis under oxidant stress conditions. *J Biol Chem.* (2006) 281:4222–30. doi: 10.1074/jbc.M509769200
39. Picard E, Houssier M, Bujold K, Sapieha P, Lubell W, Dorfman A, et al. CD36 plays an important role in the clearance of oxLDL and associated age-dependent sub-retinal deposits. *Aging.* (2010) 2:981–9. doi: 10.18632/aging.100218
40. Gnanaguru G, Choi AR, Amarnani D, D'Amore PA. Oxidized lipoprotein uptake through the CD36 receptor activates the NLRP3 inflammasome in human retinal pigment epithelial cells. *Invest Ophthalmol Vis Sci.* (2016) 57:4704–12. doi: 10.1167/iovs.15-18663
41. Hoebe K, Georgel P, Rutschmann S, Du X, Mudd S, Crozat K, et al. CD36 is a sensor of diacylglycerides. *Nature.* (2005) 433:523–7. doi: 10.1038/nature03253
42. Mellal K, Omri S, Mulumba M, Tahiri H, Fortin C, Dorion MF, et al. Immunometabolic modulation of retinal inflammation by CD36 ligand. *Sci. Rep.* (2019) 9:12903. doi: 10.1038/s41598-019-49472-8
43. Fadok VA, Bratton DL, Konowal A, Freed PW, Westcott JY, Henson PM. Macrophages that have ingested apoptotic cells *in vitro* inhibit proinflammatory cytokine production through autocrine/paracrine mechanisms involving TGF-beta, PGE2, and PAF. *J Clin Invest.* (1998) 101:890–8. doi: 10.1172/JCI1112
44. Voll RE, Herrmann M, Roth EA, Stach C, Kalden JR, Girkontaite I. Immunosuppressive effects of apoptotic cells. *Nature.* (1997) 390:350–1. doi: 10.1038/37022
45. Houssier M, Raoul W, Lavalette S, Keller N, Guillonneau X, Baragatti B, et al. CD36 deficiency leads to choroidal involution via COX2 down-regulation in rodents. *PLoS Med.* (2008) 5:e39. doi: 10.1371/journal.pmed.0050039
46. Smoak KA, Aloor JJ, Madenspacher J, Merrick BA, Collins JB, Zhu X, et al. Myeloid differentiation primary response protein 88 couples reverse cholesterol transport to inflammation. *Cell Metab.* (2010) 11:493–502. doi: 10.1016/j.cmet.2010.04.006
47. Pfeiffer A, Bottcher A, Orso E, Kapinsky M, Nagy P, Bodnar A, et al. Lipopolysaccharide and ceramide docking to CD14 provokes ligand-specific receptor clustering in rafts. *Eur J Immunol.* (2001) 31:3153–64. doi: 10.1002/1521-4141(200111)31:11<3153::aid-immu3153>3.0.co;2-0
48. Schmitz G, Orso E. CD14 signalling in lipid rafts: new ligands and co-receptors. *Curr Opin Lipidol.* (2002) 13:513–21. doi: 10.1097/00041433-200210000-00007
49. Combadiere C, Potteaux S, Gao JL, Esposito B, Casanova S, Lee EJ, et al. Decreased atherosclerotic lesion formation in CX3CR1/apolipoprotein E double knockout mice. *Circulation.* (2003) 107:1009–16. doi: 10.1161/01.CIR.0000057548.68243.42
50. Febbraio M, Abumrad NA, Hajjar DP, Sharma K, Cheng W, Pearce SF, et al. A null mutation in murine CD36 reveals an important role in fatty acid and lipoprotein metabolism. *J Biol Chem.* (1999) 274:19055–62. doi: 10.1074/jbc.274.27.19055

Conflict of Interest: The authors declare that the research was conducted in the absence of any commercial or financial relationships that could be construed as a potential conflict of interest.

frontiers in Immunology

ORIGINAL RESEARCH
published: 09 January 2020
doi: 10.3389/fimmu.2019.03033

Single Eye mRNA-Seq Reveals Normalisation of the Retinal Microglial Transcriptome Following Acute Inflammation

Oliver H. Bell[1], David A. Copland[1], Amy Ward[1], Lindsay B. Nicholson[1], Clemens A. K. Lange[2,3], Colin J. Chu[1] and Andrew D. Dick[1,4]*

[1] Academic Unit of Ophthalmology, Translational Health Sciences, University of Bristol, Bristol, United Kingdom, [2] Eye Clinic, Medical Centre, University of Freiburg, Freiburg, Germany, [3] Faculty of Medicine, University of Freiburg, Freiburg, Germany, [4] Institute of Ophthalmology and the National Institute for Health Research Biomedical Research Centre, Moorfields Eye Hospital and University College London, London, United Kingdom

Background: Whether retinal microglia can maintain or restore immune homeostasis during and after inflammation is unclear. We performed single-eye mRNA-sequencing on microglia at different timepoints following a single inflammatory stimulus to characterise their transcriptome during and after resolution of endotoxin-induced uveitis (EIU).

Experimental Approach: *Cx3cr1*^{CreER}*:R26-tdTomato* (C57BL/6) male heterozygotes were administered tamoxifen via different regimes at 4–5 weeks of age. Four weeks post-tamoxifen, mice were injected intravitreally with 10 ng lipopolysaccharide (endotoxin induced uveitis, EIU). Six-hundred retinal microglia were obtained by FACS from individual naïve retinas and at 4 h, 18 h, and 2 weeks following EIU induction. Samples were sequenced to a depth of up to 16.7 million reads using the SMART-Seq v4 Ultra Low Input RNA kit. The data was analysed using Partek software and Ingenuity Pathway Analysis. Genes were considered differentially-expressed (DEG) if the FDR step-up *p*-value was $\leq$0.05 and the fold-change was $\geq\pm$2.

Results: Flow cytometric analysis indicates that the *Cx3cr1*^{CreER}*:R26-tdTomato* strain is both sensitive (>95% tagging) and specific (>95% specificity) for microglia when tamoxifen is administered topically to the eye for 3 days. During "early" activation, 613 DEGs were identified. In contrast, 537 DEGs were observed during peak cellular infiltrate and none at 2 weeks, compared to baseline controls (1,069 total unique DEGs). Key marker changes were validated by qPCR, flow cytometry, and fluorescence microscopy. C5AR1 was identified and validated as a robust marker of differentiating microglial subsets during an LPS response.

Conclusion: Using EIU to provide a single defined inflammatory stimulus, mRNA-Seq identified acute transcriptional changes in retinal microglia which returned to their original transcriptome after 2 weeks. Yolk-sac derived microglia are capable of restoring their homeostatic state after acute inflammation.

Keywords: microglia, transcriptome, uveitis, retina, resolution, mRNA-Seq, lipopolysaccharide (LPS), heterogeneity

OPEN ACCESS

Edited by:
Andrew W. Taylor, Boston University School of Medicine, United States

Reviewed by:
Gianluca Matteoli, KU Leuven, Belgium
Thomas Langmann, University of Cologne, Germany

***Correspondence:**
David A. Copland
dave.copland@bristol.ac.uk

Specialty section:
This article was submitted to Immunological Tolerance and Regulation, a section of the journal Frontiers in Immunology

Received: *02 October 2019*
Accepted: *10 December 2019*
Published: *09 January 2020*

Citation:
Bell OH, Copland DA, Ward A, Nicholson LB, Lange CAK, Chu CJ and Dick AD (2020) Single Eye mRNA-Seq Reveals Normalisation of the Retinal Microglial Transcriptome Following Acute Inflammation. Front. Immunol. 10:3033. doi: 10.3389/fimmu.2019.03033

INTRODUCTION

It has been challenging to investigate microglia during inflammatory contexts primarily because distinguishing them from infiltrating monocytes and macrophages has been unreliable due to similar expression of cell-surface markers (1–6). Microglia contribute to an immunosuppressive environment, are derived from the yolk-sac, reside within two distinct niches in the retina, and show differential regulation because of inherent microglial heterogeneity (7, 8). Nonetheless conflicting data remains on how microglia regulate or promote inflammation depending on insult (9, 10). During inflammation microglia alter their homeostatic state (8, 11–13). In acute inflammation, markers including *C5ar1* show promise in delineating sub-populations of microglia mounting an LPS response (13). We wished to determine if the microglial transcriptome resets after an acute and resolving insult, or if homeostatic thresholds have been reset or altered permanently.

Recent advancements in transgenic mouse lines, but also in identification of markers that are "microglial-specific," for example *Cd44*, *P2ry12*, *Siglech*, and *Tmem119*, have contributed in various degrees toward microglial identification (12, 14–20). However, loss of these markers at the transcript level are observed when microglia are perturbed and some of these markers are lost at the protein level, highlighting the need for careful validation of these markers as microglial-specific given their expression is dependent upon the disease context (8, 11–13). The *Cx3cr1*^{CreER}*:R26-tdTomato* mouse strain permits binary discrimination of the microglia from other immune cells. The model utilises the high expression of *Cx3cr1* in microglia and the longevity (as low level self-replication) of microglia in comparison to other immune cells (14).

In this study, we validate the *Cx3cr1*^{CreER}*:R26-tdTomato* strain as sensitive and specific for tagging retinal microglia and perform mRNA-Sequencing on microglia obtained from individual retina during and after resolution of acute inflammation induced by intravitreal injection of LPS [the endotoxin-induced uveitis (EIU) model]. We show that the retinal microglia undergo acute transcriptional changes which resolve to their original homeostatic state by 2 weeks and support microglial heterogeneity in response to inflammatory signals.

MATERIALS AND METHODS

Mice

Cx3cr1^{CreER}*:R26-tdTomato* mice on a C57BL/6J background were provided by Clemens Lange (University of Freiburg, Germany). Breeding colonies of homozygotes were established, and offspring crossed with C57BL/6J mice to generate heterozygotes for experiments. Genotyping (via PCR) of breeding pairs was performed. Mice were confirmed as negative for the *Rd8* mutation (21).

All mice were housed at the University of Bristol Animal Services Unit under specific pathogen free conditions with food and water *ad libitum*. All procedures were conducted in concordance with the United Kingdom Home Office licence (PPL 30/3281) and were approved by the University of Bristol Ethical Review Group. The study also complied with the Association for Research in Vision and Ophthalmology (ARVO) Statement for the Use of Animals in Ophthalmic and Visual Research.

Tamoxifen Preparation and Administration

Tamoxifen (T5648; Sigma-Aldrich, Poole, UK) was dissolved in corn oil (C8267; Sigma-Aldrich) to a concentration of 20 or 5 mg/mL, for subcutaneous injection and topical administration, respectively. The solutions were freshly prepared by overnight incubation in an orbital shaker at 42°C and 300 rpm. Mice were injected with 200 μL subcutaneously [100 μL into both the lower (inguinal) left and right quadrants using a 25G needle] on days 1 and 3; alternatively, mice were administered 10 μL topically to the eye three times daily (minimum gap of 2 h between dosing) for up to 4 days.

Induction of EIU

Prior to anesthesia, pupils were dilated using topical tropicamide 1% w/v and phenylephrine 2.5% w/v (Minims; Chauvin Pharmaceuticals, Romford, UK). Mice were anaesthetised by intraperitoneal injection of 90 μL/10 g body weight of a solution containing 6 mg/mL ketamine (Ketavet; Zoetis Ireland Ltd., Dublin, Ireland) and 2 mg/mL Xylazine (Rompun; Bayer plc, Newbury, UK) mixed with sterile water.

Mice were selected for injection (or to be used as a control) in a constrained randomised order within blocks using Excel 2016 (Microsoft, Redmond, WA); blocks were dependent on cage allocations, which itself was dependent on the litter they were derived from. The allocations ensured that all experiments had littermate controls.

Intravitreal injections were performed as previously described (22). In brief, 2 μL volume of PBS containing 10 ng LPS from *E. coli* 055:B5 (Sigma-Aldrich) was delivered into the intravitreal space via the pars plana, using an operating microscope and a 33-gauge needle on a microsyringe (Hamilton Company, Reno, NV) under direct visualisation. Immediately following injection, 1% w/w chloramphenicol ointment (Martindale Pharma, Romford, UK) was applied topically, with the animals monitored and kept on a heat-pad during recovery.

EIU Clinical Assessment

At selected time-points (4 h, 18 h, and 2 weeks) post-injection, pupils were dilated and mice anaesthetised for clinical assessment. The Micron IV retinal imaging microscope (Phoenix Research Laboratories, Pleasanton, CA) was used to capture optical coherence tomography (OCT) scans, and brightfield and fluorescence fundal images.

Prior to imaging, the Micron IV CCD and OCT were calibrated in accordance with the manufacturer's protocol. The gain was set to +3 dB and the FPS to 15, or +12 dB and 2 for brightfield and tdTomato fluorescence imaging, respectively. For tdTomato imaging, a 550/25 nm bandpass excitation and 590 nm longpass emission filter were used (Edmund Optics, Barrington, NJ).

For OCT, the parameters were defined according to the manufacturers protocol, and scans were taken 30 times in rapid succession and averaged. Full-length B-scans were taken

horizontally and vertically with the optic disc centered. Images were stored in the TIFF file format.

Isolation and Flow Cytometric Phenotyping of Retinal Immune Cells

Eyes were dissected in 100 μL ice-cold PBS with aqueous, vitreous, and retina extracted by a limbal incision, lens removal and transfer into a 1.5 mL microcentrifuge tube. The tissue was mechanically disrupted by rapping the tube along an Eppendorf rack 12 times before transfer into a 96-well 60 μm nylon mesh filter plate (Merck Millipore, UK). The plate was centrifuged at 400 *xg* for 5 min and the supernatant aspirated. The remaining cell pellet was resuspended in FACS buffer (PBS supplemented with 3% v/v Foetal calf serum and 0.9 mg/mL sodium azide) and transferred to a 96-well V-bottom plate for FACS staining.

Single cell suspensions from spleen and brain were generated by mechanical dissociation through a 70 μm cell strainer with a syringe plunger. Cells were centrifuged at 400 *xg* for 3 min, erythrocytes lysed using ammonium-chloride-potassium (ACK) buffer, and cells resuspended in FACS buffer. Cells were incubated with purified rat anti-mouse CD16/32 Fc block [Clone 2.4G2; Becton Dickson (BD) Biosciences, Oxford, UK] and 7-aminoactinomycin D (7AAD; Thermo Fisher Scientific, Waltham, MA) diluted in FACS buffer for 20 min at 4°C. Cells were then incubated with an antibody cocktail containing fluorochrome-conjugated monoclonal antibodies (see **Supplementary Table 1**) against various mouse cell-surface markers for 20 min at 4°C. All mAbs were titrated and tested using control tissues.

Cell suspensions were acquired using a 4-laser Fortessa X-20 flow cytometer (BD Cytometry Systems, Oxford, UK). Compensation was performed using OneComp eBeads (Thermo Fisher Scientific), Anti-Rat Ig, κ/Negative Control Compensation Particles Set (BD Biosciences), or AbC total antibody compensation bead kit (Thermo Fisher Scientific). To compensate tdTomato, cell suspensions prepared from *Cx3cr1*^{CreER}*R26-tdTomato* homozygote brains were used. Fluorescence-minus-one (FMO) controls were used to assist in gating of the markers selected for validation. Following acquisition, analysis was performed using FlowJo software (Treestar, San Carlos, CA).

Fluorescence-Activated Cell Sorting

Retinal single cell suspensions were re-suspended in 200 μL FACS buffer containing DRAQ7 (DR77524; Biostatus, Shepshed, UK). Live microglial cells (tdTomato^{hi} DRAQ7^{-}) were immediately sorted using a BD Influx Cell Sorter. Retinal samples were prepared in small batches in order to maintain cell viability and ensure high quality RNA.

Cells were sorted into 0.2 mL endonuclease-free tubes containing 0.05 μL RNase inhibitor, 0.95 μL lysis buffer, and a variable amount of nuclease-free water depending on the number of cells collected: $9.5 - (\frac{x}{850} * 3)$ μL, where x is the number of cells isolated, using components of the SMART-Seq v4 Ultra Low Input RNA Kit for Sequencing (Takara Bio USA, Inc., Mountain View, CA). Samples were sorted in a constrained randomised order in blocks; blocks were made as small as possible and consisted of a balance of every experimental group to ensure that time- or order-dependent (batch) effects of sorting were mitigated.

mRNA-Sequencing

Sample and Library Preparation

Samples were prepared using the SMART-Seq v4 Ultra Low Input RNA Kit for Sequencing, according to the user manual, to convert the mRNA into cDNA and amplify by Long Distance (LD) PCR (16 cycles for 600 cells). cDNA was isolated using the Agencourt AMPure XP Kit (Beckman Coulter, Brea, CA) and quantified using the Agilent High Sensitivity DNA Kit on an Agilent 2100 Bioanalyser (Agilent Technologies, Santa Clara, CA). The library preparation was performed using the Nextera XT DNA Library Preparation Kit (Illumina Inc., San Diego, CA).

Sequencing and Analysis

Samples were sequenced to depths of up to 16.7 million single-end 75 nt length reads per sample using the Illumina NextSeq 500/550 High Output v2 kit (75 cycles) on an Illumina NextSeq 500 Sequencing System. Image analysis, base calling, and generation of sequence reads were produced using the NextSeq Control Software v2.0 (NCS) and Real-Time Analysis Software v2 (RTA). Data was converted to FASTQ files using the bcl2fastq2 v2.20 software (Illumina Inc.).

Sequencing data was initially quality-checked using FastQC[1], before alignment and initial analysis. The data was processed through an analysis pipeline using the Partek Flow (Build version 6.0.17.0614; Partek Inc., St. Louis, MO) software with the following task nodes (non-default parameters are specified in brackets): Trim adapters (inputting Nextera XT Index Kit v2 adapter sequences[2], Trim bases (From 3′ end, 1 base), Trim bases [from 3′ end with minimum quality score (Phred) of 30], Align reads using STAR (2.5.3a using mm10 as the reference index), Quantify to transcriptome (Partek E/M using mm10 – Ensembl Transcripts release 89 as the reference index) (**Supplementary Figures 1, 2**).

The Partek Flow data output was further analysed using Partek Genomics Suite (PGS) (Version 6.6, Build 6.16.0812). PGS normalises data using the reads per kilobase million (RPKM) approach and performs differential gene expression analysis using an ANOVA model; a gene is considered differentially-expressed (DEG) if it has an FDR step-up $p \leq 0.05$ and a fold-change $\geq \pm 2$. The data was subsequently analysed for enrichment of GO terms and the KEGG pathways; a pathway is considered significantly-enriched if the enrichment score is ≥ 3 (equivalent to a $p \leq 0.05$). The fold-change and p-values of all genes were then imported into Ingenuity Pathway Analysis (IPA) version 01-13 (Qiagen Bioinformatics, Aarhus, Denmark) and analysed according to the manual. Pathways were considered significantly

[1] Simon Andrews, Brian Howard, Phil Ewels. FastQC: a quality control tool for high throughput sequence data 2015. Available online at: http://www.bioinformatics.babraham.ac.uk/projects/fastqc/.

[2] Illumina. Illumina Adapter Sequences 2017. Available online at: https://support.illumina.com/content/dam/illumina-support/documents/documentation/chemistry_documentation/experiment-design/illumina-adapter-sequences-1000000002694-11.pdf).

altered if they had a $p \leq 0.05$ and a z-score (directionality score) $\geq \pm 2$. PGS and IPA were both used to generate figures.

Quantitative PCR

The remaining cDNA generated from the sorted cells was used for transcript-level validation. qPCR was performed using the TaqMan Universal Master Mix II, with UNG (4440038) and TaqMan gene expression probes (4331182) on a Quantstudio 3 Real-Time PCR system (A28137; all products from Thermo Fisher Scientific). Samples were run in technical duplicate, using 1 ng as the input amount, and analysed using the equation: $2^{\text{Cq(mean (control))}-\text{Cq(sample)}}$.

The probes used were: *Bst2* (mm1609165_g1), *C5ar1* (mm00500292_s1), *Cd44* (mm01277161_m1), *Fas* (mm01204974_m1), *Lair1* (mm00618113_m1), *Mertk* (mm00434920_m1), *Milr1* (mm01242703_m1), *P2ry12* (mm01950543_s1), *Siglech* (mm00618627_m1), *Slamf1* (mm00443317_m1).

Immunohistochemistry

Eyes from euthanised mice were enucleated and fixed in 4% v/v PFA for 1 h before dissection. The anterior portion of the eye (cornea, iris, ciliary body, and lens) was carefully removed and an eyecup prepared. The eyecup tissue was blocked in 5% v/v normal goat serum (Vector Laboratories, CA, USA), 1% v/v BSA, and 3% v/v Triton x-100 (both Sigma Aldrich) in PBS for 4 h at room temperature with gentle shaking. Eyecups were then incubated at 4°C overnight with a rabbit anti-mouse anti-RFP mAb (600-401-379; Rockland Immunochemicals Inc., Limerick, PA) and for target validation experiments a Super Bright 600-conjugated anti-mouse CD44 mAb (**Supplementary Table 1**) was used in combination. After thorough washing with PBS, samples were incubated overnight with the secondary antibody goat anti-rabbit Alexa-633 (A21070; Thermo Fisher Scientific). The eyecups were washed again, and the retina carefully removed and flatmounted in Vectashield hard-set antifade mounting media (H-1400; Vector Laboratories Ltd., Peterborough, UK) and imaged on a Leica SP5-AOBS confocal laser scanning microscope (Leica Microsystems Ltd., Wetzlar, Germany). Images were acquired with an xy pixel size $\leq$200 nm, and a z-step size of $\leq$400 nm.

Statistical Analysis and Image Processing

Data were analysed using GraphPad Prism 7 software (GraphPad Software Inc., San Diego, CA). The One-way ANOVA with Tukey's multiple comparisons test was used to compare multiple groups of data to a control group. A $p \leq 0.05$ was considered significant.

Huygens professional software (Scientific Volume Imaging B.V., Hilversum, The Netherlands) was used to deconvolve the Micron IV fluorescent images and fluorescence microscopy (**Supplementary Figure 3**). For the Micron images, the following parameters were used: lens immersion = 1.343 [refractive index of the 0.2% w/w carbomer eye gel (23)], embedding = 1.377 (24), peak emission = 581 nm, numerical aperture = 1.25, and xy pixel size of 130 nm; the background was estimated at 2 and a signal-to-noise ratio of 15 was used. Hot pixel correction (with a sensitivity of 4) was used prior to deconvolution. For fluorescence microscopy, the parameters were imported from the microscope and the default settings were used.

Microscopy images were processed using the Leica LAS X software (Leica Microsystems Ltd.) and FIJI [a distribution of ImageJ (25)]. Other images, and figures, were processed using Photoshop (Adobe Inc., San Jose, CA).

RESULTS

Subcutaneous and Topical Tamoxifen Administration Regimes Tag Retinal Microglia in the *Cx3cr1^{CreER}:R26-tdTomato* Mouse Line

Activation of the CreER system requires administration of tamoxifen or 4-hydroxytamoxifen, and various methods of administration are frequently employed such as subcutaneous injection and oral gavage (14, 26). Moreover, an efficacious 4-day topical regime for activating CreER systems within the eye was recently described (27). Therefore, we initially tested which tamoxifen administration regime tagged retinal microglia efficiently while minimising systemic immune cell labelling to preclude analysing cells subsequently recruited during inflammation.

Five regimes were tested, spanning from 1- to 4-day topical and subcutaneous administration. A no-tamoxifen control was included. At 4 weeks post-tamoxifen treatment, flow cytometric analysis of the retinas quantified the proportion of CD45^{int} CD11b^{+} microglia (in a naïve retina) that were tdTomato^{hi} as corroborated with fluorescent fundal imaging (**Figures 1A,B**). Microglia displayed a "resting" ramified morphology (**Figure 1C**). The 3- and 4-day topical, and the subcutaneous regime tagged $\geq$95% of microglia whereas the no-tamoxifen controls had 45% tagged constitutively (**Figure 1D**). All tdTomato^{hi} cells were microglia, indicating specificity in the normal adult mouse retina.

Cx3cr1^{CreER}:R26-tdTomato Mice Exhibit Typical Kinetics of the EIU Model

The stability of microglial tagging during inflammation is pivotal to the isolation of pure populations of microglia for downstream transcriptomic assessment before, during, and after inflammation. To determine this, we utilised endotoxin-induced uveitis (EIU), a self-resolving model of acute Toll-like receptor 4 (TLR4)-mediated ocular inflammation, that following a single inflammatory insult generates acute immune cell tissue infiltration (28, 29). We confirmed disease kinetics in the *Cx3cr1^{CreER}:R26-tdTomato* heterozygotes replicated our previous data in C57BL/6J mice (22). A time-course using OCT, deconvolved fluorescent fundal imaging, and confocal microscopy confirmed tdTomato expression throughout the expected time course of disease (**Figure 2**). Intravitreal administration of LPS results in peak cellular infiltrate at 18 h, which then resolves by 2 weeks (**Figure 2A**). Fluorescent fundal imaging demonstrates that the uniform distribution of microglia is altered in response

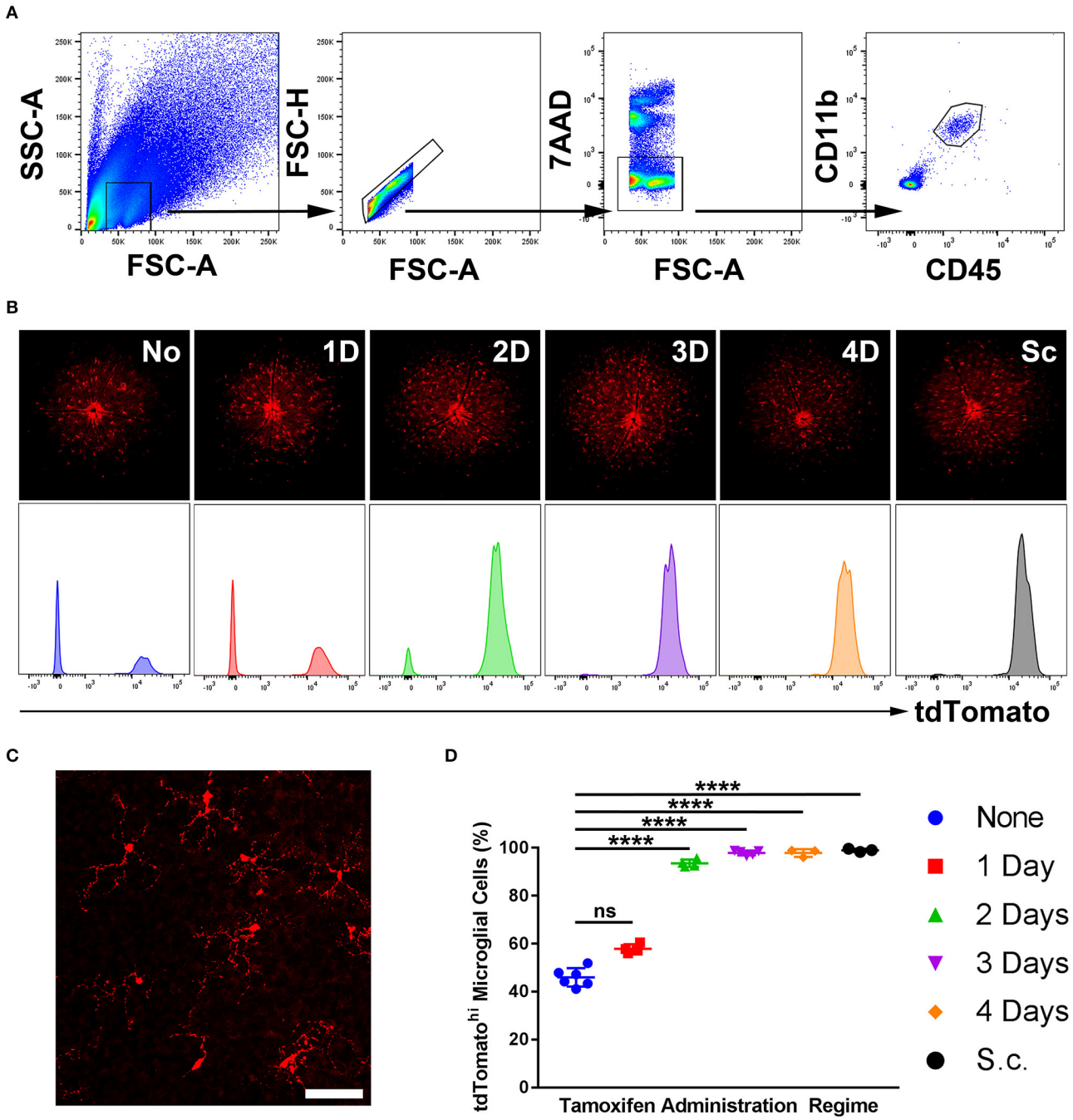

FIGURE 1 | Sensitivity of microglial recombination induced in *Cx3cr1*^{CreER}*:R26-tdTomato* mice using different tamoxifen administration regimes. **(A)** A representative flow cytometric gating strategy used to identify microglia in a naïve retina based on CD45 and CD11b expression. **(B)** Representative deconvolved tdTomato fluorescent fundal images of mice with representative tdTomato histograms (unit area scaling) on gated microglia from various tamoxifen administration regimes. **(C)** Confocal microscopy from a 3-day topical regime naïve retina shows microglia with a physiological ramified morphology, suggesting no gross perturbations in the microglia as a consequence of the transgenic model. **(D)** Aggregate data demonstrating the percentage of microglia that were tdTomato^{hi} (as quantified by flow cytometry) shows that a 3- and 4-day topical, in addition to subcutaneous, regimes result in full microglial tagging (n = 3–6). None, no tamoxifen administered; 1D, 1-day topical tamoxifen regime; 2D, 2-days topical tamoxifen regime; 3D, 3-days topical tamoxifen regime; 4D, 4-days topical tamoxifen regime; Sc, subcutaneous tamoxifen regime. ****$p \leq 0.0001$, ns, not significant. Scale bar = 30 μm.

to LPS, with defined areas of tdTomato^{+} cell accumulation observed at peak disease (**Figure 2B**). Confocal microscopy confirmed tdTomato^{+} cells in the naïve retina with a ramified morphology that became amoeboid at peak and recovered to a ramified appearance by 2 weeks post-EIU induction (**Figure 2C**).

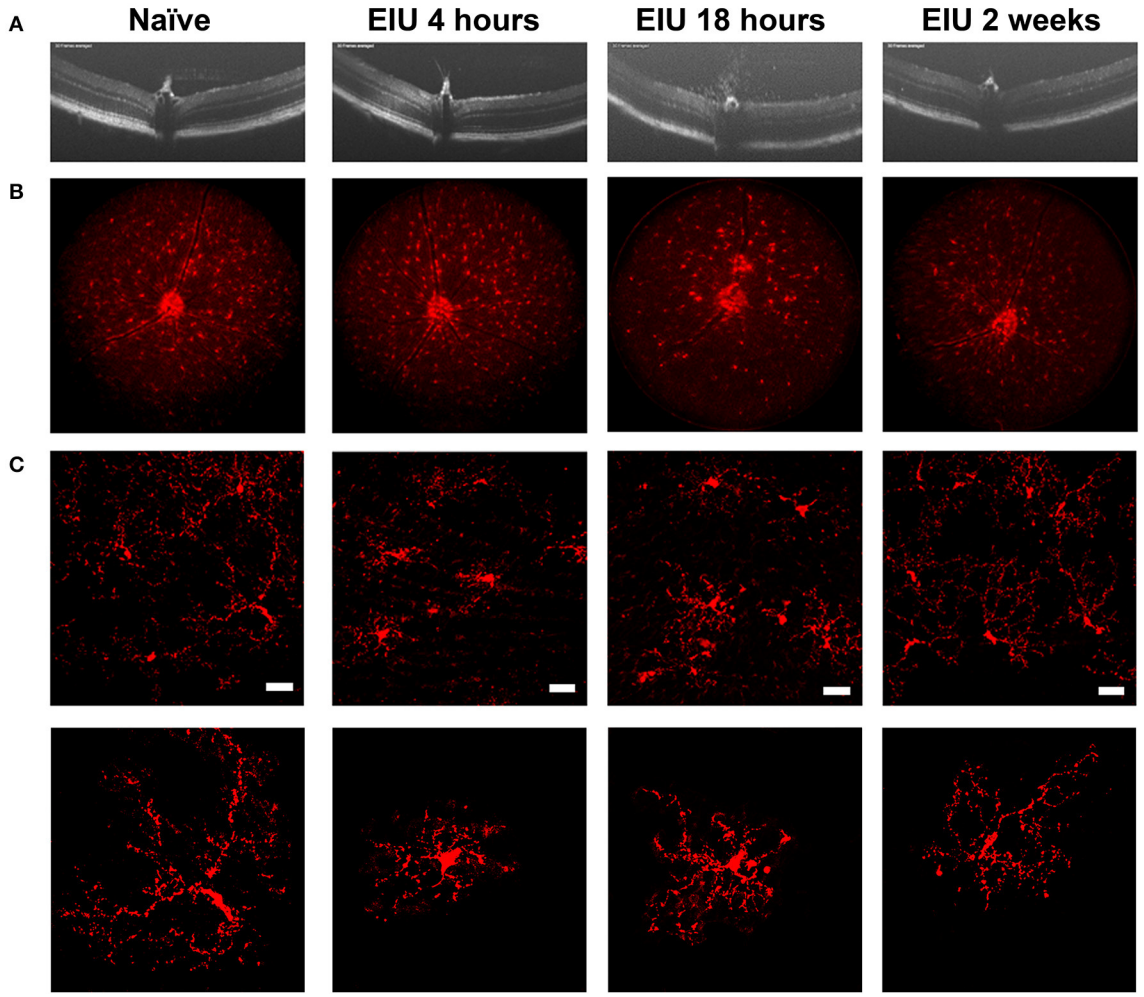

FIGURE 2 | The kinetics of endotoxin-induced uveitis (EIU) in the *Cx3cr1*^{CreER}*:R26-tdTomato* mouse strain. **(A)** OCT images showing disease-course in a single mouse (3-day topical regime), demonstrates the presence of infiltrating cells at 18 h post-injection with resolution by 2 weeks. **(B)** Deconvolved fluorescent fundal images acquired simultaneously show few changes in the distribution of tdTomato^{+} cells at 4 h post-injection, but changes at 18 h which resolve by 2 weeks. **(C)** Confocal microscopy of the tdTomato^{+} cells demonstrate a ramified toward amoeboid shift at 4- and 18 h post-injection that reverts to a ramified morphology by 2 weeks. Representative images of single cells are shown in the lower panel to highlight morphological changes. EIU, endotoxin-induced uveitis; OCT, optical coherence tomography. Scale bars = 30 μm.

Three-Day Topical Tamoxifen Induction Ensures Specificity of tdTomato Labelling in Microglia

With tdTomato expression confirmed as stable in the microglial population, we sought to determine whether this was exclusive to microglia in the context of immune cell infiltration, validating accurate isolation of the microglial transcriptome. To confirm the specificity for retinal microglial tagging during inflammation, we examined tamoxifen regimes which efficiently tagged microglia (3- and 4-day topical, and subcutaneous) in addition to a no-tamoxifen control. Flow cytometry was performed on peripheral tissues and a small portion of myeloid cells were observed as tdTomato^{hi}, primarily when tamoxifen was administered via the subcutaneous route (**Supplementary Figure 4**). However, to test the specificity within the retina, inflammation was required.

Retinas were retrieved at the peak cellular infiltrate stage of EIU (18 h) and flow cytometry was performed (**Supplementary Figure 5**). Single, live cells identified as tdTomato^{hi} were assessed by conventional microglia markers of CD45^{int} and CD11b^{+} (**Figures 3A,B**). A small proportion (5%) of all single live retinal cells express very low levels of tdTomato (**Figure 3A**, boxed), as described in the tdTomato reporter mice (in the absence of Cre/Cre^{ER})[3] due to a failure of a small proportion of ribosomes to terminate translation when reaching the stop codon that precedes *tdTomato* (30). Using this gating strategy, analysis from the 4-day topical and subcutaneous regimes demonstrates the presence of an additional population of non-microglial (CD45^{hi} CD11b^{-}) cells that were identified

[3]The Jackson Laboratory. 007914 - B6.Cg-Gt(ROSA)26Sor 2019. Available online at: https://www.jax.org/strain/007914.

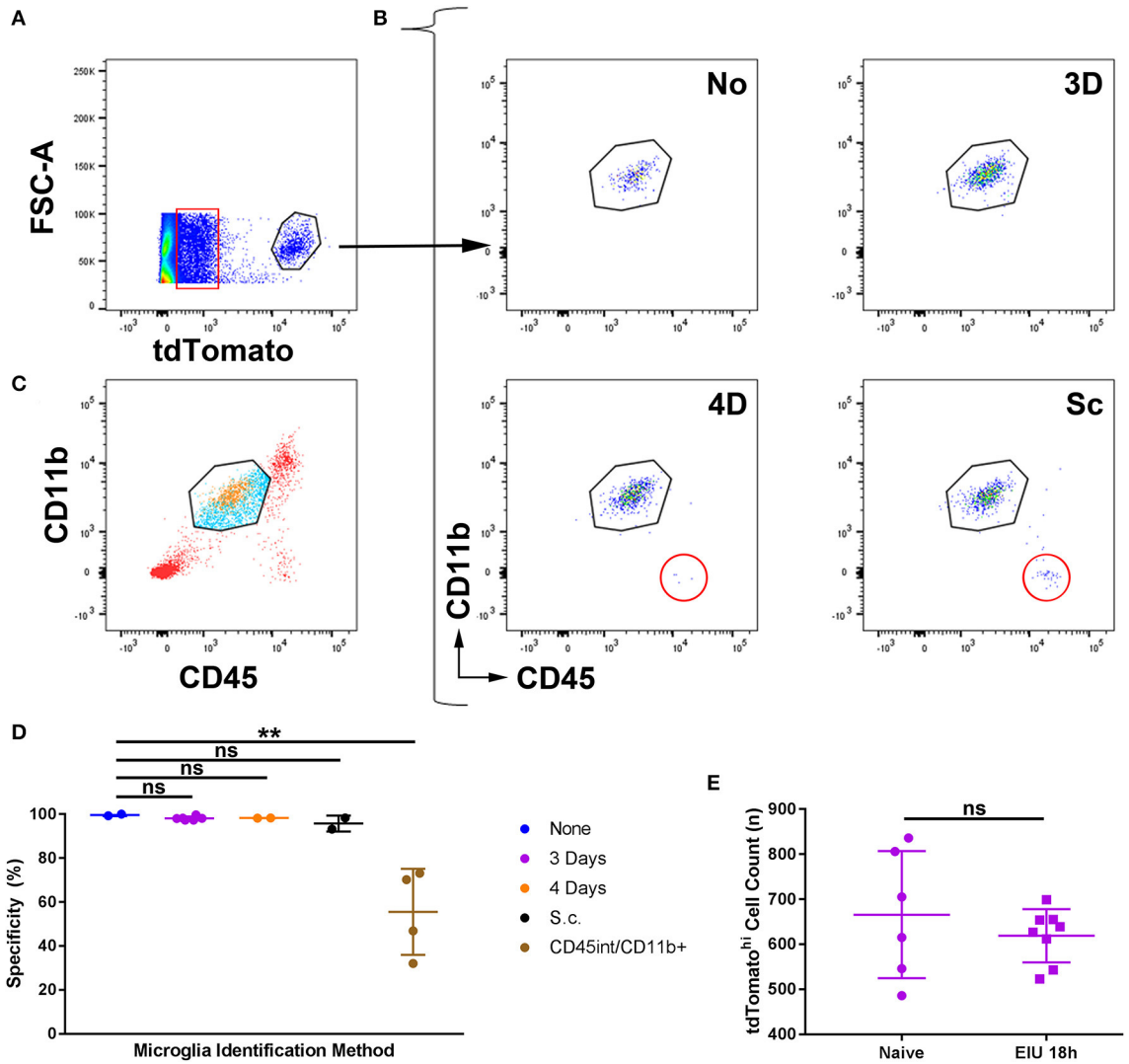

FIGURE 3 | The specificity of microglial tagging for different tamoxifen administration regimes in the *Cx3cr1*^{CreER}*:R26-tdTomato* mouse strain during active inflammation. **(A)** Peak EIU retinas following different tamoxifen administration regimes were prepared for flow cytometry. Live, cell singlets were gated based on tdTomato^{hi} expression. A small proportion (5%) of all live cells expressed low levels of tdTomato (boxed). **(B)** TdTomato^{hi} cells were gated based on CD45^{int} and CD11b^{+} expression, and in the 4-day and subcutaneous tamoxifen treated groups, non-microglial cells (CD45^{hi} CD11b^{-}) were present (circled). **(C)** Gating microglia based on CD45 and CD11b expression alone results in the inclusion of infiltrating immune cells (tdTomato^{-}, blue) in addition to retinal microglia (tdTomato^{hi}, orange) but exclusion of cells not fitting the microglial expression profile (CD45$^{hi/lo}$, red). **(D)** Aggregate data on the percentage specificity for microglia demonstrates that the 3-day topical route results in high specificity for microglia using tdTomato. The CD45^{int}/CD11b^{+} group uses the microglial gating strategy (from live cell singlets without using tdTomato) shown in panel B for a comparison of the mouse strain to conventional microglial identification strategies ($n = 2$–5). **(E)** Total counts from naïve and peak EIU retinas, following the 3-day topical tamoxifen regime, demonstrate equivalent numbers of tdTomato^{hi} cells ($n = 6$–8). None, no tamoxifen administered; 3D, 3-days topical tamoxifen regime; 4D, 4-days topical tamoxifen regime; Sc, subcutaneous tamoxifen regime. $^{**}p \leq 0.01$, ns, not significant.

in the tdTomato^{hi} subset (**Figure 3B**). Gating with CD45^{int} and CD11b^{+} but not tdTomato leads to the inclusion of non-microglial cells (**Figure 3C**) and greatly compromises specificity. The 3-day topical and no-tamoxifen control retained the specificity of tdTomato for microglia (**Figures 3B,D**), but as shown previously a no-tamoxifen control does not fully label the microglial population (**Figure 1**). As our approach for distinguishing microglia (CD45^{int} CD11b^{+} tdTomato^{hi}) from the tdTomato^{hi} group could include non-microglia that possess a similar transcriptional profile to retinal microglia, the total counts of the CD45^{int} CD11b^{+} tdTomato^{hi} group, from naïve and peak EIU retinas (3-day topical tamoxifen), were compared and no significant difference was observed confirming a pure microglial population (**Figure 3E**). All subsequent experiments performed used the 3-day topical tamoxifen regime.

Microglia Undergo Acute Transcriptional Changes During EIU That Fully Normalise to a Baseline State by 2 Weeks

The 3-day tamoxifen regime in the *Cx3cr1*^{CreER}*:R26-tdTomato* strain provides the sensitivity and specificity required for

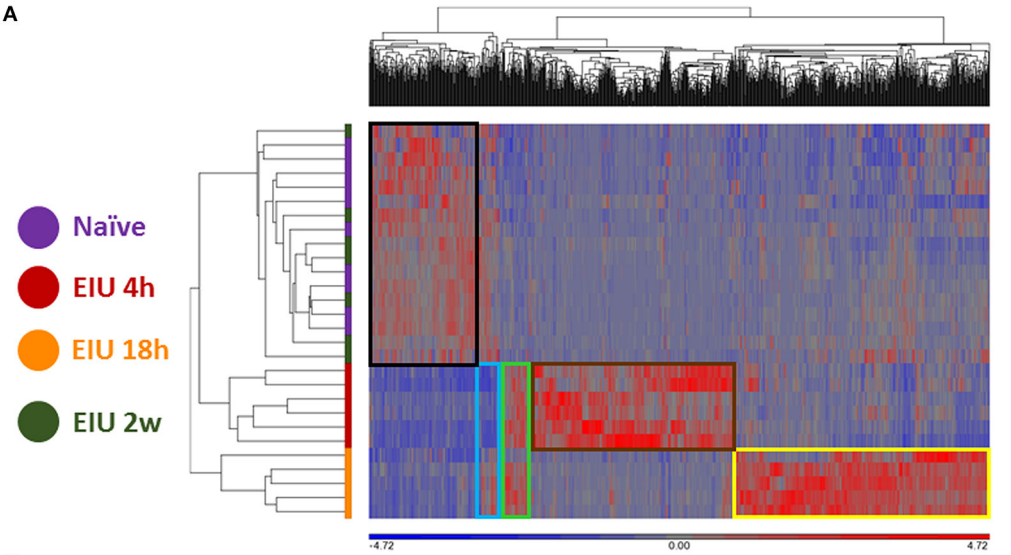

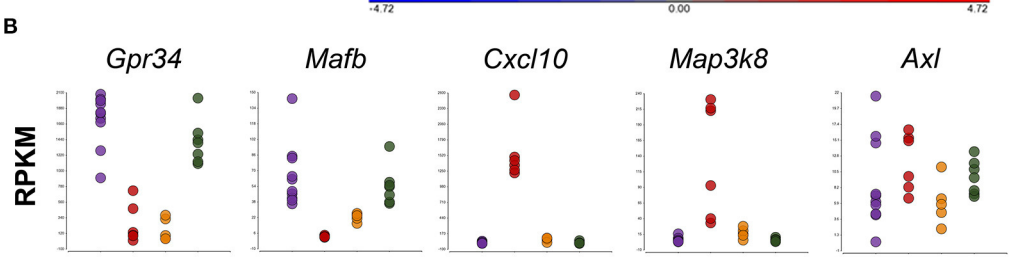

C

Up-Regulated

4h	18h	2w	IPA Canonical Pathway
****	*		Dendritic Cell Maturation
****			TREM1 Signaling
****	**		Neuroinflammation Signalling
****			iNOS Signalling
***			TNFR2 Signalling
***			Th17 Activation
***			Type I Diabetes Mellitus Signalling
***			Pattern Recognition Receptors
***			RIG1-like Receptors
**	*		SC Lung Cancer Signalling
**	**		Interferon Signalling
**	*		p38 MAPK Signalling
**	*		T Cell Exhaustion Signalling
**	*		Induction of Apoptosis by HIV1
**			IL-23 Signalling
**			IL-1 Signalling
**			MIF-mediated Glucocorticoid Regulation
**			IL-17F in Allergic Inflammatory Airway Diseases
*			FAT10 Cancer Signalling
**			MIF Regulation of Innate Immunity
	****		EIF2 Signalling
	*		Serine and Glycine Biosynthesis
*			Osteoarthritis
	*		VDR/RXR Activation
*			Hypoxia Signalling in the Cardiovascular System

Down-Regulated

4h	18h	2w	IPA Canonical Pathway
**			PPAR Signalling
**	*		Gαq Signalling
**	*		fMLP Signaling in Neutrophils
**	*		Cardiac Hypertrophy Signalling
*	*		Glioblastoma Multiforme Signalling
*	*		Wnt/Ca+ Pathway
	**		Aldosterone Signaling in Epithelial Cells
	*		Synaptic Long Term Potentiation

*** p value ≤ 0.05; ** p value ≤ $1*10^{-3}$;**
***** p value ≤ $1*10^{-6}$;**
****** p value ≤ $1*10^{-9}$**

FIGURE 4 | mRNA-Sequencing of microglia during and after EIU reveals transcriptional alterations that fully resolve. **(A)** Hierarchical clustering of differentially-expressed genes (DEGs) shows differences in the kinetics of the microglial transcriptome during EIU. Boxes highlight clusters of genes with different

(Continued)

FIGURE 4 | kinetics, and a restoration back to a homeostatic signal by 2 weeks (n = 5–10). **(B)** Scatterplots show changes in expression of previously described microglial genes to include a homeostatic gene (*Gpr34*), homeostatic transcription factor (*Mafb*), generic activation gene (*Cxcl10*), acute LPS-response gene (*Map3k8*), and "primed microglia" gene (*Axl*). **(C)** Heatmaps highlight canonical pathways, which were significantly different during at least one timepoint, change in direction (z-score) and p-value over time (n = 5–10); the pathways are in ascending order based on their overall (summary) p-value. The raw canonical pathway figures are presented in **Supplementary Figure 6**. EIU, endotoxin-induced uveitis. $^{*}p \leq 0.05$, $^{**}p \leq 1^{*}10^{-3}$, $^{***}p \leq 1^{*}10^{-6}$, $^{****}p \leq 1^{*}10^{-9}$.

reliable identification and isolation of distinct retinal microglia populations from other populations of infiltrating immune cells. To characterise changes in the microglial transcriptome during and after resolution of EIU, FACS (based on tdTomato) of 600 live microglia was performed from individual retinas collected at 4 h, 18 h, and 2 weeks post-injection in addition to naïve mice. The majority of these samples (28/30) yielded high-quality cDNA for sequencing using a validated pipeline (**Supplementary Figure 1**).

Our approach identified 1,069 unique differentially expressed genes (DEGs; 613 at 4 h, 537 at 18 h, and 0 at 2 weeks) visualised by hierarchical clustering, revealing a highly plastic transcriptome with most up-regulated genes being mutually exclusive at different timepoints. Boxes highlight clusters of genes that were normal at 4 h but up-regulated at 18 h (yellow), those which were up-regulated at 4 h but not 18 h (brown), those which were up-regulated at both time-points (green), those which were down-regulated at 4 h but recovered to pre-EIU levels by 18 h (light blue), and those which were down-regulated at both 4- and 18 h (black). Restoration back to a homeostatic signal was observed by 2 weeks because unsupervised clustering failed to distinguish naïve and 2-week post-injection samples (**Figure 4A**). A multitude of expected gene changes based on published literature were observed, including downregulation of microglial homeostatic genes (*Gpr34*, *Mafb*), expression of microglial activation and LPS-response genes (*Cxcl10*, *Map3k8*), in addition to no change in the "primed microglia" gene *Axl* (11, 12, 17, 31) (**Figure 4B**). A heatmap demonstrates the change in z-score over time of canonical pathways identified as significantly different (**Figure 4C**). The original canonical pathways (including bars showing exact p-values) are presented in **Supplementary Figure 6**.

Enriched GO terms (enrichment score) when naïve and 4 h EIU groups were compared included: immune system process (60.9), regulation of cytokine production (56.0), and response to stress (52.7). Similarly, the enriched KEGG pathways included: NF-Kappa B signaling pathway (34.1), toll-like receptor signaling pathway (31.7), and TNF signaling pathway (25.3). For the naïve and 18 h EIU comparison GO terms included: cytosolic part (89.7), extracellular organelle (70.67), translation (65.8), and immune system process (29.8); enriched KEGG pathways included: ribosome (58.8) and proteasome (42.9). LPS was found to be a "master regulator" by IPA, indicating agreement of our data with the curated lists and pathways.

Flow Cytometry and Fluorescence Microscopy Validate Key Transcriptional Alterations

Our next aim was for orthogonal validation of key and novel transcriptional changes, both at the RNA and protein level. Markers for validation were selected by systematic assessment based on magnitude of the relative change in expression, novelty, lack of prior validation at the protein level, whether they were a previously suggested microglial marker, were in contrast to or appeared crucial in light of other reports, and lastly the availability of testing reagents (**Supplementary Figure 7**). Ultimately, the final set of 10 markers selected represent a variety of expression patterns and kinetics to match the plastic landscape identified by hierarchical clustering. In line with published reports and an activated state, pro-inflammatory markers (*Slamf1*, *C5ar1*, *Fas*, and *Cd44*) were all upregulated at 4 h following LPS challenge. In addition, a novel microglial associated transcript, *Milr1* (a negative regulator of mast cell activation) and *Bst2* (a previously validated marker of late activation) were elevated by 18 h. In contrast, constitutively expressed microglial genes, including homeostatic genes (e.g., *P2ry12*, *Siglech*, *Mertk*, and *Lair1*) were down-regulated at the early time-point. In general, qPCR analysis validated the transcript-level changes observed at each time-point, confirming resolution and return to baseline levels by 2 weeks (**Figure 5**).

Flow cytometric analysis demonstrates increased expression in SLAMF1, MILR1, C5AR1, CD44, BST2, and LAIR1 at 18 h post-injection (**Figures 6A–D**). Furthermore, differences in the proportion of marker-positive cells were evident, with C5AR1, CD44, and BST2 upregulated in the majority of microglia (>50%), in contrast to the other makers which were elevated in a smaller fraction (<20%) of cells. The upregulation of CD44 was also confirmed in retinal flatmounts at 18 h using fluorescence microscopy (**Figure 6E**). Whilst P2RY12 was highly expressed in naïve microglia (>80%), no change in expression in response to LPS were observed. Similarly, low level SIGLECH, MERTK, and FAS expression in naïve populations remained unchanged and restricted to a small percentage of the microglia (<10%). We also compared expression of P2RY12 and SIGLECH on $CD45^{+}$ cells, as both are previously suggested markers that differentiate microglial populations from other immune cells (17, 20). Flow cytometric analysis clearly demonstrates that both markers are equally expressed on $CD45^{+}$ infiltrating cells, indicating these markers exhibit poor specificity for retinal microglia during the acute response (**Figure 6F**).

Stratifying Microglia Using C5AR1 Identifies Both Generalised and Restricted Microglial Responses

Recent reports show that *C5ar1* was one of several markers that was enriched in a subset of brain microglia (identified

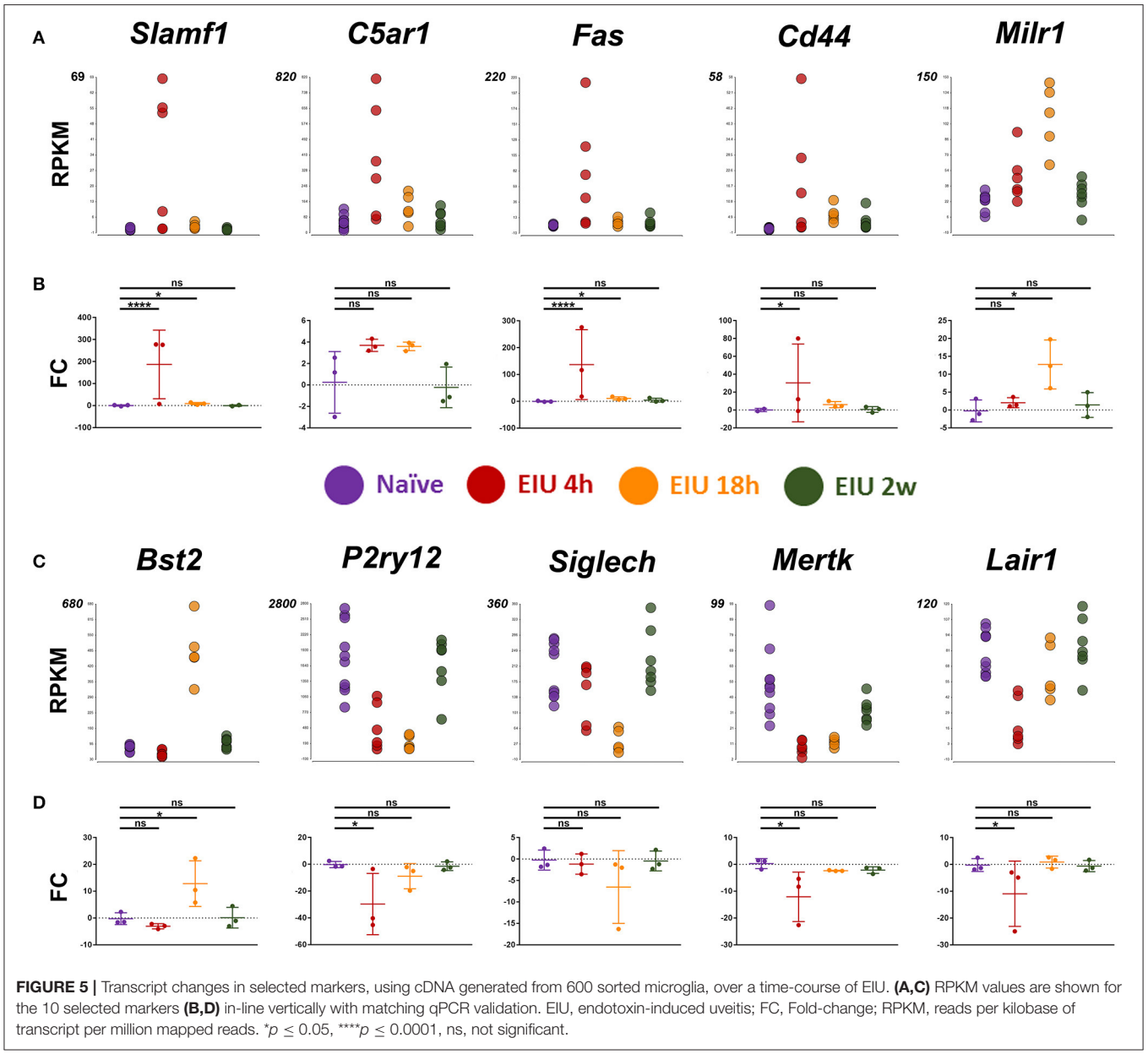

FIGURE 5 | Transcript changes in selected markers, using cDNA generated from 600 sorted microglia, over a time-course of EIU. **(A,C)** RPKM values are shown for the 10 selected markers **(B,D)** in-line vertically with matching qPCR validation. EIU, endotoxin-induced uveitis; FC, Fold-change; RPKM, reads per kilobase of transcript per million mapped reads. *$p \leq 0.05$, ****$p \leq 0.0001$, ns, not significant.

by sc-mRNA-Seq data) responding to systemic LPS challenge *in vivo* (13). Furthermore, mounting evidence from numerous reports identify heterogeneity in the microglial response during other pathological states (8, 32). We therefore examined whether stratifying microglia based on C5AR1 expression would delineate differences in the markers selected for validation, highlighting specificity to this subset of C5AR1-expressing cells, or generalised expression across the whole population of microglia.

Microglia were stratified into three main groups: C5AR1^{neg}, C5AR1^{lo}, and C5AR1^{hi}. The C5AR1-expressing microglia were sub-stratified based on whether the C5AR1 expression was equivalent to microglia observed within a naïve mouse (C5AR1^{lo}) or whether expression was elevated (C5AR1^{hi}; **Figure 7A**). C5AR1^{hi} expression correlated to the extent of immune cell (CD45^{+} TdTomato^{-}) infiltrate within the retinas and represents a potential microglial marker for disease scoring (**Figure 7B**). Flow cytometric analysis compared expression of the other surface markers in C5AR1^{neg} and C5AR1^{hi} subsets, as two distinctive populations, in naïve and peak EIU retinas. Delineating the two populations on this basis demonstrates elevation of several markers (SLAMF1, FAS, MILR1, and LAIR1) which are restricted to the C5AR1-expressing microglia (**Figure 7C**). In contrast CD44 and BST2 were enriched within the C5AR1-expressing population but also expressed by a large proportion of the C5AR1^{neg} microglia, thus representing more generalised markers of microglial perturbation (**Figure 7D**).

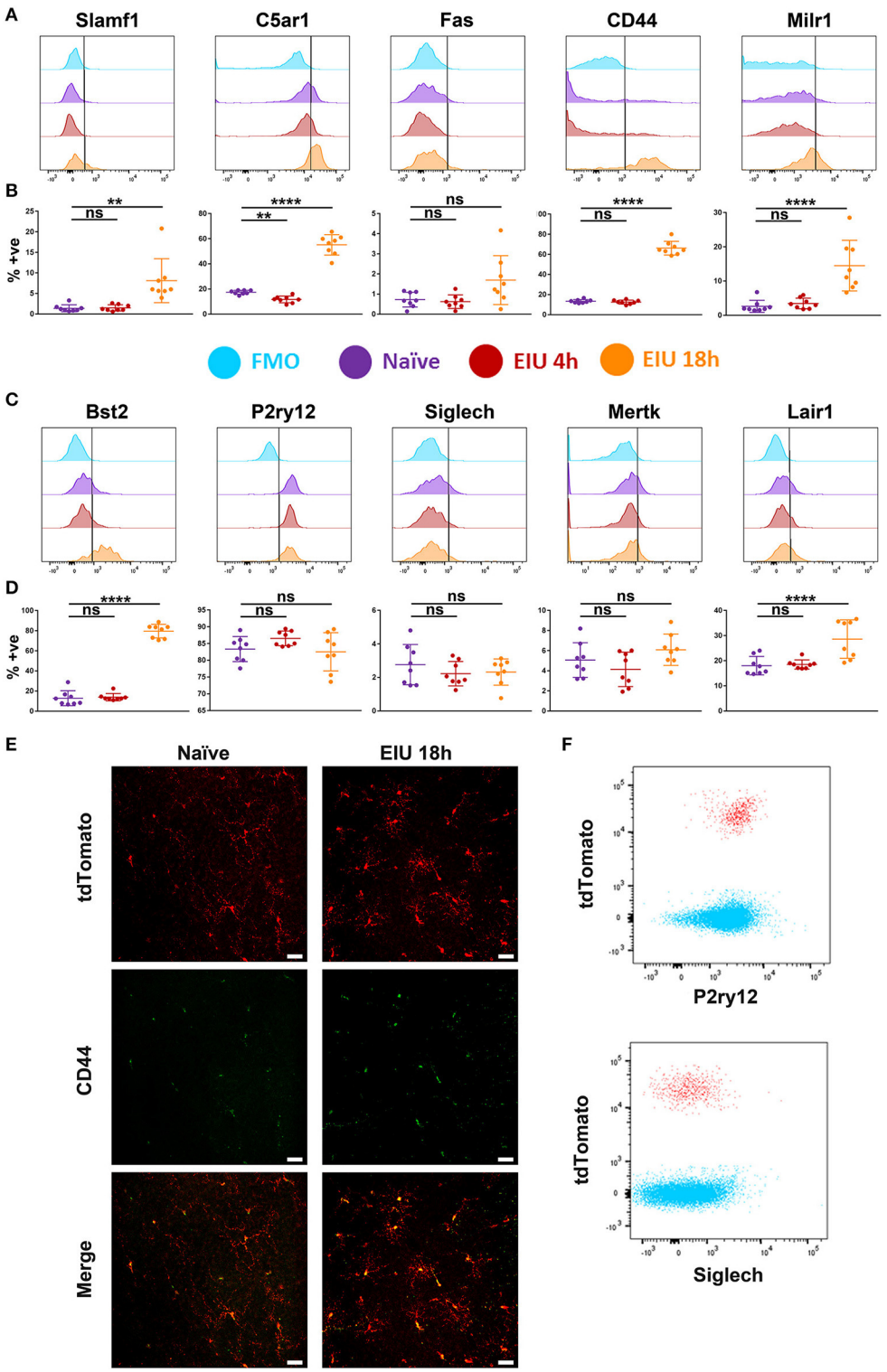

FIGURE 6 | Changes in protein expression of selected markers in microglia over a time-course of EIU. **(A,C)** A representative flow cytometric histogram is shown for the 10 selected markers **(B,D)** in-line vertically with matching scatterplots of the aggregate flow cytometry data summarising the percentage of microglia positive for each marker at each timepoint. Gates were drawn with the assistance of fluorescence-minus-one (FMO) controls (light blue). **(E)** Confocal microscopy also confirms the upregulation of CD44 in microglia during EIU. **(F)** Flow cytometric analysis demonstrates P2RY12 and SIGLECH expression on $CD45^+$ $tdTomato^-$ non-microglial immune cells (blue) and $CD45^+$ $tdTomato^+$ microglia (red) at 18 h EIU. % +ve, percentage positive; EIU, endotoxin-induced uveitis. $^{**}p \leq 0.01$, $^{****}p \leq 0.0001$, ns, not significant. Scale bars = 30 μm.

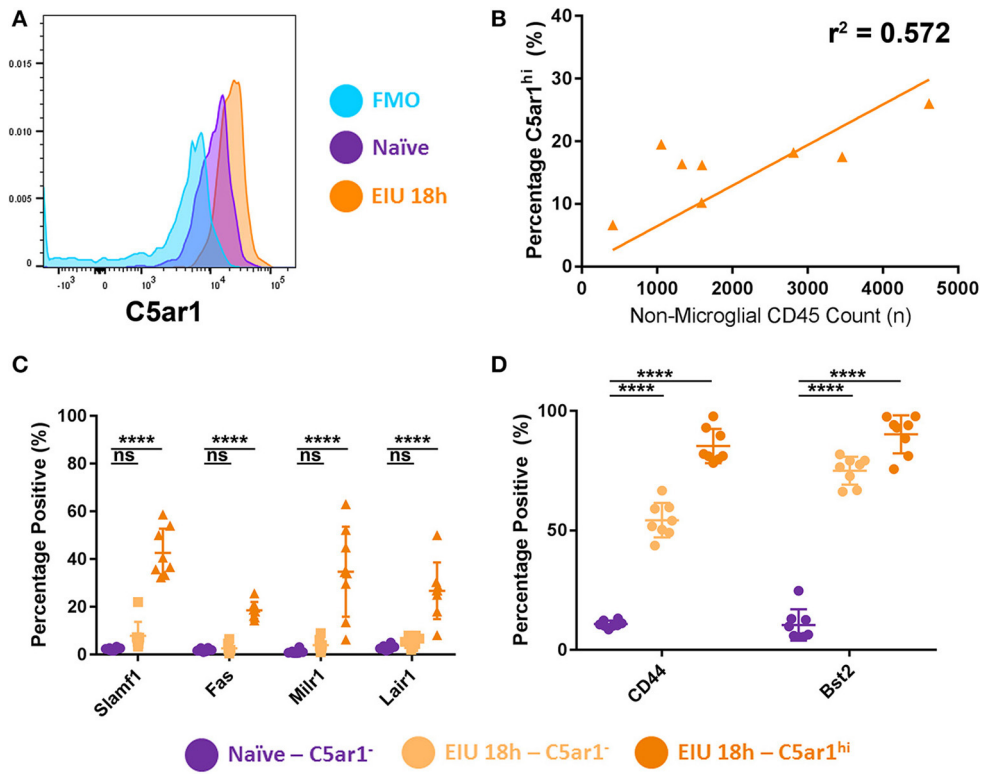

FIGURE 7 | Stratifying microglia using C5AR1 expression identifies both restricted and generalised responses. **(A)** A histogram shows microglial C5AR1 expression in a fluorescence-minus-one (FMO) control (blue), naïve retina (purple), and at 18 h EIU (orange). **(B)** Immune cell infiltrate correlates with C5AR1^{hi} expression in microglial populations ($p = 0.0298$). **(C)** Stratifying microglia into C5AR1^{-} and C5AR1^{hi} (elevated above the naïve level of expression) identifies changes in cell-surface protein expression that are restricted to C5AR1-expressing microglia, **(D)** but also changes in proteins which are generalised microglial responses (not exclusive to, but somewhat enriched in, the C5AR1-expressing microglia). ****$p \leq 0.0001$, ns, not significant.

DISCUSSION

Single eye mRNA-Seq revealed inflammation-responsive transcriptional changes in retinal microglia following LPS stimulation which resolve within 2 weeks, confirming the potential for these cells to reset their homeostatic state. In line with the literature, our data confirms recognised patterns of altered gene expression in homeostatic and activation pathways, an absence of changes in "primed microglia" genes, and identifies enriched pathways relating to immune function.

Hierarchical clustering of the 1,069 DEGs identified reveals a high level of plasticity in the microglial transcriptome, with the majority of up-regulated genes at early (4 h) and peak (18 h) being mutually exclusive across the time-points. At the transcript level at least, this highlights a consensus group of microglial LPS-response genes including (*Slamf1*, *C5ar1*, *Fas*, *Cd44*, *Milr1*, and *Bst2*). In contrast, we highlight a common cluster of down-regulated genes, including homeostatic regulators (*P2ry12*, *Siglech*, *Mertk*, *Lair1*).

Orthogonal validation by qPCR of the 10 markers selected representing key and novel transcripts, confirmed the RNA-Seq findings. However, altered expression of some of these membrane-associated makers did not translate to changes at the protein level, as determined by flow cytometry. In part, this may reflect the presence of intracellular protein that our flow cytometric approach did not detect, or represents genuine discrepancies between the transcriptome and proteome, as these are not always in direct proportion (33–35). Our results emphasise caution in reading out RNA-Seq alone as a true representation of the cell's activity and highlight the need for orthogonal validation. Nonetheless, the single eye mRNA-Seq approach identified key and novel transcriptional changes which informed subsequent testing on a smaller number of markers via low-throughput approaches.

We confirmed and validated some of the transcriptional changes by flow cytometry but found that the differences were enhanced, and an additional marker (FAS) was identified as significantly different, when microglia were first stratified based on their C5AR1 expression as suggested via a transcripts-led report (13). Furthermore, we identified markers which were exclusive to the C5AR1-expressing microglia (SLAMF1, FAS, MILR1, and LAIR1), but also generalised markers which were not (CD44 and BST2). This agrees with other reports which suggest that C5AR1 is needed for microglial polarisation to pro-inflammatory states, and that its knock-out improved outcomes in an Alzheimer's model (36). Furthermore, microglial heterogeneity has already been reported in Alzheimer's disease, light-damage models, and in response to LPS stimulation *in*

vivo (8, 13, 32). Understanding microglial heterogeneity, and identifying changes which are exclusive to subpopulations, is critical for developing targeted therapies.

Conflicting with previous reports investigating LPS-responses and experimental autoimmune encephalomyelitis (EAE), we did not find significant down-regulation of P2RY12 upon microglial activation (11, 13). In EAE, the microglia exhibit a chronic inflammatory state different to the acute LPS response, whilst the report investigating the LPS response used a systemic dose 400 times greater than our own local dose and had an endpoint 24 h post-injection which could explain the discrepancy. We suggest microglial loss of P2RY12 as context-dependent, for example when subject to a significant immune stimulus or persistent inflammation.

For this investigation, a clear marker to distinguish long-lived, yolk-sac derived microglia from infiltrating myeloid cells was critical, particularly during peak ocular inflammation at 18 h post-LPS injection. The *Cx3cr1*^{CreER}*:R26-tdTomato* line has been validated for this approach previously (14, 37), but as we demonstrate the systemic tamoxifen administration also labels peripheral leukocyte populations which are recruited to the eye during inflammation. Modifying a recently published protocol (27) demonstrates that the 3-day topical tamoxifen administration regime is robust in labelling retinal microglia in both a sensitive (**Figure 1**) and specific (**Figure 3**) manner, superior to the established subcutaneous route. Shortening of the originally-published topical protocol from 4 days to three is likely possible due to the very high expression of *Cx3cr1* in microglia and reduces confounders of animal handling and stress to the mice as a refinement[4] The high expression of *Cx3cr1* by microglia also explains why mice underwent tamoxifen-independent (or constitutive) recombination in 45% of the microglia as tamoxifen-independent recombination (constitutive receptor activation of the CreER) is a well-characterised phenomenon (38–40).

With other administration routes, we found that the specificity for microglia was reduced during ingress of immune cells with inflammation. This supports recent studies of microglia that highlight the need to confirm the specificity for microglia in their disease model and employ techniques with single-cell resolution to resolve the non-microglial cell populations (8, 41).

Taking all our data together, we show that three previously suggested markers (P2RY12, CD44, and SIGLECH) exhibit poor specificity for microglia. However, with the *Cx3cr1*^{CreER}*:R26-tdTomato* line it remains possible to validate potential markers, assuming the line retains specificity for microglia across disease contexts. Microglial subtypes can exhibit both differential and generalised responses to LPS.

In summary, we demonstrate that the homeostatic threshold of retinal microglia is reset following an acute inflammatory insult and identify potential markers for delineating the heterogeneity of microglia that may be used depending on context of retinal perturbation.

[4]National Centre for the Replacement R, Reduction of Animals in R. The 3Rs | NC3Rs 2018. Available online at: https://www.nc3rs.org.uk/the-3rs.

DATA AVAILABILITY STATEMENT

The datasets generated for this study can be found in the Gene Expression Omnibus (GEO) repository under the accession number GSE138247. Spreadsheets of gene expression values, in addition to the lists of DEGs (with *p*-values and fold-changes) are included as part of this upload.

ETHICS STATEMENT

All procedures were conducted in concordance with the United Kingdom Home Office licence (PPL 30/3281) and were approved by the University of Bristol Ethical Review Group. The study also complied with the Association for Research in Vision and Ophthalmology (ARVO) Statement for the Use of Animals in Ophthalmic and Visual Research.

AUTHOR CONTRIBUTIONS

OB, DC, AW, and CC performed the experiments. CL provided materials. OB, DC, CC, and AD planned and analysed the experiments. OB, DC, CC, LN, CL, and AD wrote the manuscript and planned the research project.

FUNDING

OB was funded as a National Eye Research Centre (NERC) Ph.D. studentship [R103433-101]. CL was supported by the SFB/TRR167. This work was supported by additional funding from the NERC and the Underwood Trust.

ACKNOWLEDGMENTS

The authors wish to thank Andrew Herman and Lorena Ballesteros (Flow Cytometry Facility, University of Bristol), Christy Waterfall and Jane Coghill (Genomics Facility, University of Bristol), Tom Batstone and Alex Paterson (Bioinformatics arm of the Genomics Facility), and Dominic Alibhai and Stephen Cross (Wolfson Bioimaging Facility, University of Bristol) for the technical assistance.

SUPPLEMENTARY MATERIAL

The Supplementary Material for this article can be found online at: https://www.frontiersin.org/articles/10.3389/fimmu.2019.03033/full#supplementary-material

REFERENCES

1. Dick AD, Ford AL, Forrester JV, Sedgwick JD. Flow cytometric identification of a minority population of MHC class II positive cells in the normal rat retina distinct from CD45lowCD11b/c+CD4low parenchymal microglia. *Br J Ophthalmol*. (1995) 79:834–40. doi: 10.1136/bjo.79.9.834
2. Cosenza-Nashat MA, Kim MO, Zhao ML, Suh HS, Lee SC. CD45 isoform expression in microglia and inflammatory cells in HIV-1 encephalitis. *Brain Pathol*. (2006) 16:256–65. doi: 10.1111/j.1750-3639.2006.00027.x
3. Sedgwick JD, Ford AL, Foulcher E, Airriess R. Central nervous system microglial cell activation and proliferation follows direct interaction with tissue-infiltrating T cell blasts. *J Immunol*. (1998) 160:5320–30.
4. Djukic M, Mildner A, Schmidt H, Czesnik D, Bruck W, Priller J, et al. Circulating monocytes engraft in the brain, differentiate into microglia and contribute to the pathology following meningitis in mice. *Brain*. (2006) 129(Pt 9):2394–403. doi: 10.1093/brain/awl206
5. De Martinis M, Modesti M, Ginaldi L. Phenotypic and functional changes of circulating monocytes and polymorphonuclear leucocytes from elderly persons. *Immunol Cell Biol*. (2004) 82:415–20. doi: 10.1111/j.0818-9641.2004.01242.x
6. Muller A, Brandenburg S, Turkowski K, Muller S, Vajkoczy P. Resident microglia, and not peripheral macrophages, are the main source of brain tumor mononuclear cells. *Int J Cancer*. (2015) 137:278–88. doi: 10.1002/ijc.29379
7. Lee YS, Amadi-Obi A, Yu CR, Egwuagu CE. Retinal cells suppress intraocular inflammation (uveitis) through production of interleukin-27 and interleukin-10. *Immunology*. (2011) 132:492–502. doi: 10.1111/j.1365-2567.2010.03379.x
8. O'Koren EG, Yu C, Klingeborn M, Wong AYW, Prigge CL, Mathew R, et al. Microglial function is distinct in different anatomical locations during retinal homeostasis and degeneration. *Immunity*. (2019) 50:723–37.e7. doi: 10.1016/j.immuni.2019.02.007
9. Okunuki Y, Mukai R, Nakao T, Tabor SJ, Butovsky O, Dana R, et al. Retinal microglia initiate neuroinflammation in ocular autoimmunity. *Proc Natl Acad Sci USA*. (2019) 116:9989–98. doi: 10.1073/pnas.1820387116
10. Calippe B, Augustin S, Beguier F, Charles-Messance H, Poupel L, Conart JB, et al. Complement factor H inhibits CD47-mediated resolution of inflammation. *Immunity*. (2017) 46:261–72. doi: 10.1016/j.immuni.2017.01.006
11. Zrzavy T, Hametner S, Wimmer I, Butovsky O, Weiner HL, Lassmann H. Loss of 'homeostatic' microglia and patterns of their activation in active multiple sclerosis. *Brain*. (2017) 140:1900–13. doi: 10.1093/brain/awx113
12. Holtman IR, Raj DD, Miller JA, Schaafsma W, Yin Z, Brouwer N, et al. Induction of a common microglia gene expression signature by aging and neurodegenerative conditions: a co-expression meta-analysis. *Acta Neuropathol Commun*. (2015) 3:31. doi: 10.1186/s40478-015-0203-5
13. Sousa C, Golebiewska A, Poovathingal SK, Kaoma T, Pires-Afonso Y, Martina S, et al. Single-cell transcriptomics reveals distinct inflammation-induced microglia signatures. *EMBO Rep*. (2018) 19:e46171. doi: 10.15252/embr.201846171
14. Goldmann T, Wieghofer P, Muller PF, Wolf Y, Varol D, Yona S, et al. A new type of microglia gene targeting shows TAK1 to be pivotal in CNS autoimmune inflammation. *Nat Neurosci*. (2013) 16:1618–26. doi: 10.1038/nn.3531
15. Lewis ND, Hill JD, Juchem KW, Stefanopoulos DE, Modis LK. RNA sequencing of microglia and monocyte-derived macrophages from mice with experimental autoimmune encephalomyelitis illustrates a changing phenotype with disease course. *J Neuroimmunol*. (2014) 277:26–38. doi: 10.1016/j.jneuroim.2014.09.014
16. Bennett ML, Bennett FC, Liddelow SA, Ajami B, Zamanian JL, Fernhoff NB, et al. New tools for studying microglia in the mouse and human CNS. *Proc Natl Acad Sci USA*. (2016) 113:E1738–46. doi: 10.1073/pnas.1525528113
17. Butovsky O, Jedrychowski MP, Moore CS, Cialic R, Lanser AJ, Gabriely G, et al. Identification of a unique TGF-β dependent molecular and functional signature in microglia. *Nat Neurosci*. (2014) 17:131–43. doi: 10.1038/nn.3599
18. Zhang Y, Chen K, Sloan SA, Bennett ML, Scholze AR, O'Keeffe S, et al. An RNA-sequencing transcriptome and splicing database of glia, neurons, and vascular cells of the cerebral cortex. *J Neurosci*. (2014) 34:11929-47. doi: 10.1523/JNEUROSCI.1860-14.2014
19. Beutner C, Linnartz-Gerlach B, Schmidt SV, Beyer M, Mallmann MR, Staratschek-Jox A, et al. Unique transcriptome signature of mouse microglia. *Glia*. (2013) 61:1429–42. doi: 10.1002/glia.22524
20. Chiu IM, Morimoto ET, Goodarzi H, Liao JT, O'Keeffe S, Phatnani HP, et al. A neurodegeneration-specific gene-expression signature of acutely isolated microglia from an amyotrophic lateral sclerosis mouse model. *Cell Rep*. (2013) 4:385–401. doi: 10.1016/j.celrep.2013.06.018
21. Mattapallil MJ, Wawrousek EF, Chan CC, Zhao H, Roychoudhury J, Ferguson TA, et al. The Rd8 mutation of the Crb1 gene is present in vendor lines of C57BL/6N mice and embryonic stem cells, and confounds ocular induced mutant phenotypes. *Invest Ophthalmol Vis Sci*. (2012) 53:2921–7. doi: 10.1167/iovs.12-9662
22. Chu CJ, Gardner PJ, Copland DA, Liyanage SE, Gonzalez-Cordero A, Kleine Holthaus SM, et al. Multimodal analysis of ocular inflammation using the endotoxin-induced uveitis mouse model. *Dis Models Mech*. (2016) 9:473–81. doi: 10.1242/dmm.022475
23. Rothstein EC, Nauman M, Chesnick S, Balaban RS. Multi-photon excitation microscopy in intact animals. *J Microsc*. (2006) 222(Pt 1):58–64. doi: 10.1111/j.1365-2818.2006.01570.x
24. Chen E. Refractive indices of the rat retinal layers. *Ophthalmic Res*. (1993) 25:65–8. doi: 10.1159/000267223
25. Schindelin J, Arganda-Carreras I, Frise E, Kaynig V, Longair M, Pietzsch T, et al. Fiji: an open-source platform for biological-image analysis. *Nat Methods*. (2012) 9:676–82. doi: 10.1038/nmeth.2019
26. Yona S, Kim KW, Wolf Y, Mildner A, Varol D, Breker M, et al. Fate mapping reveals origins and dynamics of monocytes and tissue macrophages under homeostasis. *Immunity*. (2013) 38:79–91. doi: 10.1016/j.immuni.2012.12.001
27. Boneva SK, Gross TR, Schlecht A, Schmitt SI, Sippl C, Jagle H, et al. Cre recombinase expression or topical tamoxifen treatment do not affect retinal structure and function, neuronal vulnerability or glial reactivity in the mouse eye. *Neuroscience*. (2016) 325:188–201. doi: 10.1016/j.neuroscience.2016.03.050
28. Rosenbaum JT, McDevitt HO, Guss RB, Egbert PR. Endotoxin-induced uveitis in rats as a model for human disease. *Nature*. (1980) 286:611–3. doi: 10.1038/286611a0
29. Smith JR, Hart PH, Williams KA. Basic pathogenic mechanisms operating in experimental models of acute anterior uveitis. *Immunol Cell Biol*. (1998) 76:497–512. doi: 10.1046/j.1440-1711.1998.00783.x
30. Arribere JA, Cenik ES, Jain N, Hess GT, Lee CH, Bassik MC, et al. Translation readthrough mitigation. *Nature*. (2016) 534:719–23. doi: 10.1038/nature18308
31. Dubbelaar ML, Kracht L, Eggen BJL, Boddeke E. The kaleidoscope of microglial phenotypes. *Front Immunol*. (2018) 9:1753. doi: 10.3389/fimmu.2018.01753
32. Keren-Shaul H, Spinrad A, Weiner A, Matcovitch-Natan O, Dvir-Szternfeld R, Ulland TK, et al. A unique microglia type associated with restricting development of Alzheimer's disease. *Cell*. (2017) 169:1276–90.e17. doi: 10.1016/j.cell.2017.05.018
33. Lemee JM, Clavreul A, Aubry M, Com E, de Tayrac M, Mosser J, et al. Integration of transcriptome and proteome profiles in glioblastoma: looking for the missing link. *BMC Mol Biol*. (2018) 19:13. doi: 10.1186/s12867-018-0115-6
34. Bai Y, Wang S, Zhong H, Yang Q, Zhang F, Zhuang Z, et al. Integrative analyses reveal transcriptome-proteome correlation in biological pathways and secondary metabolism clusters in *A. flavus* in response to temperature. *Sci Rep*. (2015) 5:14582. doi: 10.1038/srep14582
35. Wang D, Eraslan B, Wieland T, Hallstrom B, Hopf T, Zolg DP, et al. A deep proteome and transcriptome abundance atlas of 29 healthy human tissues. *Mol Syst Biol*. (2019) 15:e8503. doi: 10.15252/msb.20188503
36. Hernandez MX, Jiang S, Cole TA, Chu SH, Fonseca MI, Fang MJ, et al. Prevention of C5aR1 signaling delays microglial inflammatory polarization, favors clearance pathways and suppresses cognitive loss. *Mol Neurodegener*. (2017) 12:66. doi: 10.1186/s13024-017-0210-z
37. Luckoff A, Caramoy A, Scholz R, Prinz M, Kalinke U, Langmann T. Interferon-beta signaling in retinal mononuclear phagocytes attenuates pathological neovascularization. *EMBO Mol Med*. (2016) 8:670–8. doi: 10.15252/emmm.201505994
38. Kristianto J, Johnson MG, Zastrow RK, Radcliff AB, Blank RD. Spontaneous recombinase activity of Cre-ERT2 *in vivo*.

Transgenic Res. (2017) 26:411–7. doi: 10.1007/s11248-017-0018-1
39. Liu Y, Suckale J, Masjkur J, Magro MG, Steffen A, Anastassiadis K, et al. Tamoxifen-independent recombination in the RIP-CreER mouse. *PLoS ONE.* (2010) 5:e13533. doi: 10.1371/journal.pone.0013533
40. Ango F, Prezeau L, Muller T, Tu JC, Xiao B, Worley PF, et al. Agonist-independent activation of metabotropic glutamate receptors by the intracellular protein Homer. *Nature.* (2001) 411:962–5. doi: 10.1038/35082096
41. O'Koren EG, Mathew R, Saban DR. Fate mapping reveals that microglia and recruited monocyte-derived macrophages are definitively distinguishable by phenotype in the retina. *Sci Rep.* (2016) 6:20636. doi: 10.1038/srep20636

Conflict of Interest: The authors declare that the research was conducted in the absence of any commercial or financial relationships that could be construed as a potential conflict of interest.

frontiers in Immunology

ORIGINAL RESEARCH
published: 11 February 2020
doi: 10.3389/fimmu.2020.00154

A Systematic Investigation on Complement Pathway Activation in Diabetic Retinopathy

Shahna Shahulhameed[1†], Sushma Vishwakarma[1†], Jay Chhablani[2,3], Mudit Tyagi[2], Rajeev R. Pappuru[3], Saumya Jakati[4], Subhabrata Chakrabarti[1] and Inderjeet Kaur[1]*

[1] Prof Brien Holden Eye Research Centre, LV Prasad Eye Institute, Hyderabad, India, [2] Smt. Kanuri Santhamma Center for Vitreo Retinal Diseases, LV Prasad Eye Institute, Hyderabad, India, [3] Medical Retina and Vitreoretinal Surgery, University of Pittsburgh School of Medicine, Pittsburgh, PA, United States, [4] Ophthalmic Pathology Laboratory, LV Prasad Eye Institute, Hyderabad, India

OPEN ACCESS

Edited by:
Heping Xu,
Queen's University Belfast,
United Kingdom

Reviewed by:
Maria I. Bokarewa,
University of Gothenburg, Sweden
Alfred Hyoungju Kim,
Washington University School of Medicine in St. Louis, United States

***Correspondence:**
Inderjeet Kaur
inderjeet@lvpei.org

[†]These authors have contributed equally to this work

Specialty section:
This article was submitted to Autoimmune and Autoinflammatory Disorders, a section of the journal Frontiers in Immunology

Received: 30 October 2019
Accepted: 21 January 2020
Published: 11 February 2020

Citation:
Shahulhameed S, Vishwakarma S, Chhablani J, Tyagi M, Pappuru RR, Jakati S, Chakrabarti S and Kaur I (2020) A Systematic Investigation on Complement Pathway Activation in Diabetic Retinopathy. Front. Immunol. 11:154. doi: 10.3389/fimmu.2020.00154

The complement system plays a crucial role in retinal homeostasis. While the proteomic analysis of ocular tissues in diabetic retinopathy (DR) has shown the deposition of complement proteins, their exact role in the pathogenesis of DR is yet unclear. We performed a detailed investigation of the role of the complement system by evaluating the levels of major complement proteins including C3, C1q, C4b, Complement Factor B (CFB), and Complement Factor H (CFH) and their activated fragments from both the classical and alternative pathways in vitreous humor and serum samples from proliferative DR (PDR) patients and controls. Further, the expressions of complements and several other key pro- and anti-angiogenic genes in the serum and vitreous humor were analyzed in the blood samples of PDR and non-PDR (NPDR) patients along with controls without diabetes. We also assessed the pro-inflammatory cytokines and matrix metalloproteinases in the vitreous humor samples. There was a significant increase in C3 and its activated fragment C3bα' (110 kDa) along with a corresponding upregulation of CFH in the vitreous of PDR patients, which confirmed the increased activation of the alternative complement pathway in PDR. Likewise, a significant upregulation of angiogenic genes and downregulation of anti-angiogenic genes was seen in PDR and NPDR cases. Increased MMP9 activity and upregulation of inflammatory markers IL8 and sPECAM with a downregulation of anti-inflammatory marker IL-10 in PDR vitreous indicated the possible involvement of microglia in DR pathogenesis. Further, a significantly high C3 deposition in the capillary wall along with thickening of basement membranes and co-localization of CFH expression with $CD11b^{+ve}$ activated microglial cells in diabetic retina suggested microglia as a source of CFH in diabetic retina. The increased CFH levels could be a feedback mechanism for arresting excessive complement activation in DR eyes. A gradual increase of *CFH* and *CD11b* expression in retina with early to late changes in epiretinal membranes of DR patients indicated a major role for the alternative complement pathway in disease progression.

Keywords: retina, diabetic retinopathy, complement pathway, inflammation, microglia, angiogenesis, vitreous humor

INTRODUCTION

Diabetic retinopathy (DR), characterized by pathological ocular angiogenesis in retina, is a major cause of irreversible vision loss worldwide, with a global prevalence of 34.6% (1). DR has a complex pathophysiology that encompasses the entire retinal function, including compromised neuronal activity and alterations in retinal vasculature that further lead to gradual neurodegeneration, neuroinflammation, and visible vascular complications (2). The retina, being an immune-privileged organ, has its own unique immune regulatory mechanisms, including retinal neurons and RPE, and immune defense mechanisms comprising the microglial population and the complement system. The retinal immune defense mechanism is alerted by any kind of noxious signal and starts a cascade of inflammatory events as an adaptive response to restore the homeostatic balance (3). Low-level activation of the innate immune mechanisms, specifically the complement system, is required to preserve normal eye homeostasis and maintain retinal integrity while aging (4). However, this protective mechanism can have a detrimental impact if the insults persist for a longer duration and leads to irreversible functional loss, as is seen in neurodegenerative diseases such as Alzheimer's disease, Parkinson's disease, amyotrophic lateral sclerosis (ALS), and age-related macular degeneration (ARMD) (5). Increased complement activation-induced photoreceptor cell death has also been reported in retinal detachment, thereby further highlighting the impact of the complement system in various retinal pathologies (6, 7). The complement system, besides having a major role as an immune defense mechanism, is involved in several tissue-remodeling processes, such as liver regeneration and synaptic pruning during development, and also in retinal angiogenesis and neurodegenerative diseases (8–11). The role of the complement system in angiogenesis is of prime importance, since there are several eye diseases associated with abnormal ocular angiogenesis and neurodegeneration, such as retinopathy of prematurity (ROP), age-related macular degeneration (AMD), and proliferative diabetic retinopathy (PDR) (12–14).

The angiogenic and anti-angiogenic potential of complements in AMD and ROP is quite well-known based on experimental evidence derived from both animal and human studies. Bora et al. in 2005, reported C3 and MAC complex depositions in neovessels in mice model of laser-induced choroidal neovascularization (CNV), while the C3 knock out ($C3^{-/-}$) CNV mice showed an absence of neovascularization, with a reduced level of angiogenic factors, thereby suggesting complement component C3 as a pro-angiogenic factor (15). This was further supported by genetic association studies of complement proteins in AMD pathogenesis, where a strong association of CFB and CFH polymorphism was observed along with a strong deposition of complement components in the RPE-Bruch layer (16–18). Further, the deposition of C3 in the retinal microglia and macrophage population in the outer retinal layers was shown to induce retinal degeneration in a mouse model of AMD (19). A recent study on a retinal ischemic mouse model demonstrated the involvement of the alternative complement pathway, specifically C3 and Factor B, in promoting retinal cell apoptosis and vascular dysfunction (20). Conversely, the anti-angiogenic property of the complement system in a ROP mouse model was also documented, where it was shown that C3 and C5aR were required for inhibiting the polarization of macrophage toward its angiogenic potential (10). We have earlier demonstrated microglia-mediated excessive complement activation in the vitreous of ROP babies compared to age-matched controls, suggesting a possible role of the activation of the alternative complement pathway in ocular angiogenesis (21). This evidence points toward both the protective and the destructive roles of complements in different ocular pathologies that are incumbent on disease-specific changes in the retina while sharing some common clinical features.

Some of the recent clinical studies on DR reported an early neuronal loss in the retina prior to the onset of visible vascular changes (22, 23). Further, many basic research investigations have shown the activation of innate immune cells, mainly the microglial population, at different stages of disease progression in animal and human DR retinal tissues (24, 25). It is also quite evident that microglial activation ameliorates tissue damage with chronic inflammatory response under a prolonged duration of tissue insults (26). Several independent studies done on DR have shown an increased deposition of complement component mediators and effector molecules in the retina and vitreous. These included deposition of C3d and MAC complex in the choriocapillaries of DR eyes and reduced level of glycosylphosphatidyl inositol-anchored inhibitors of complements such as CD55 and CD59 in the walls of retinal vessels of DR eyes, suggesting the role of the complement pathway in DR (27, 28), although it is as yet unclear if this is a cause or an effect of prolonged diabetic insult. Though the vitreous proteome studies have detected several complement proteins such as C3, CFI, CFB, C4A, C4B, C2, C4BPA, CFD, and CFH in PDR subjects (29–32), their expression levels are highly variable among different studies and do not explain their exact involvement in DR pathology as observed earlier in ROP and AMD. Also, the complement genes do not show any genetic association with the risk of DR as observed in AMD and ROP. Lack of suitable tissues for such analysis and variable clinical phenotypes pose a major challenge. Further, since microglia and the complement system are involved in retinal defense mechanisms, it would be important to know whether they act independently or synergistically for contributing to DR pathology and whether these are implicated even in the early stages of DR. We hypothesized that a possible crosstalk between these defense mechanisms in uncontrolled diabetic conditions might ameliorate the development of DR and its progression by inducing neurodegeneration and neuroinflammation in the retina that eventually leads to abnormal angiogenesis, as seen in the later stages of DR. Thus, the present study aimed to understand the possible crosstalk between these defense mechanisms and its role in PDR pathogenesis.

We have initially performed a systematic investigation of the role of the complement pathway in PDR pathogenesis by analyzing classical and alternative pathway complement proteins and their activation in vitreous and serum samples of human DR

subjects. In addition, we have also correlated our findings with the expression of complement genes in retinal tissues obtained from diabetic cadaveric donors and blood samples of DR patients and controls. Microglial infiltration and its correlation with inflammation and neovascularization were further evaluated by analyzing angiogenic and inflammatory cytokines in the vitreous. Our study identified a localized elevation of C3, especially the 110 kDa activated fragment C3bα' and a concurrent upregulation of CFH along with activated microglial infiltration in the PDR vitreous. To the best of our knowledge, this is the first report on the upregulation of CFH levels in PDR vitreous as revealed through Western blotting and showed its co-localization with activated microglia, thereby suggesting its involvement in the pathogenesis of DR and possible crosstalk between these two defense systems in PDR progression. Further, a gradual increase in microglial-mediated activation of the alternative complement pathway based on *CFH* and *CD11b* gene expression in early to late changes in DR indicates the clinical relevance of the alternative complement pathway's role as a possible biomarker for disease progression.

MATERIALS AND METHODS

Enrollment of Study Participants and Sample Preparation

The study was performed according to the guidelines of the Declaration of Helsinki and approved by the Institutional Review Board. Vitreous samples (100 μl) were collected from normal controls ($n = 120$) and PDR subjects ($n = 120$) undergoing pars plana vitrectomy with prior written informed consent. Samples were collected in surgery rooms under aseptic conditions and then immediately transferred to the laboratory in cold condition. The samples were then centrifuged at 14,000 rpm for 10 min at 4°C to remove any cellular debris and then stored at −80 degrees for further use. Proteins were lysed in an equal volume of RIPA buffer and precipitated with ice-cold acetone overnight at −80°C. The precipitated proteins were collected by centrifugation at 14,000 rpm for 1 h at 4°C, and the protein pellets were dissolved in 1X PBS containing protease inhibitor. Blood samples were collected in vacutainers from PDR ($n = 38$), NPDR ($n = 38$), and control ($n = 38$) subjects, and the serum was separated within 1 h of sample collection by centrifugation at 1,500 rpm for 15 min. The samples were stored at −80°C and thawed prior to the experiments. The total protein concentration was calculated by bicinchoninic acid (BCA) assay. The demographic details of the subjects from whom the vitreous and serum samples were collected are provided in **Tables 1**, **2**.

TABLE 1 | Detailed demographic of study subjects used for vitreous protein analysis.

	Age	Gender	Duration of DM
Control vitreous	55.4 ± 1.02	F, $n = 60$, M, $n = 40$	Nil
PDR vitreous	56.17 ± 0.79	F, $n = 45$, M, $n = 55$	15.64 ± 0.83

Western Blotting

Western blotting was performed with the vitreous and serum samples to identify the role of the complement pathway in PDR pathogenesis. The levels of total C3 (Ms-C3, Catalog No. sc-28294, Santacruz) and of its activated proteolytic fragments in the vitreous humor were determined under non-reducing conditions in samples collected from PDR and no-DM subjects. Likewise, C3 and its activated fragments in serum samples were compared among PDR, NPDR, and no-DM subjects. The classical complement pathway was evaluated by analyzing proteins such as C1q (Ms C1q, Catalog No. ab71089, Abcam) in serum and C1q and C4b (Ms-C4b, Catalog No. sc-74524, Santacruz) in vitreous. The alternative complement pathway was evaluated by estimating the levels of factor Bb of CFB (Rb CFB, Catalog No. ab 72658, Abcam) and CFH (Ms-CFH, Catalog No. sc-166613, Santacruz). Western blotting for CD11b (Rb CD11b, Catalog No. ab133357, Abcam) was performed in the vitreous samples to evaluate the microglial infiltration under PDR pathogenesis and compared with no-DM control vitreous. SDS-PAGE-separated protein samples were transferred to a PVDF membrane (Catalog No. IPFL00010, Millipore) at a constant voltage of 25 V by wet transfer for a period of 1–2 h. After overnight incubation with primary antibodies at 4°C, IR dye conjugated specific secondary antibodies (Anti -Ms. 680RD, Catalog No. 926–68070, LICOR, Anti -Rb 800CW, Catalog No.926–32211, LI-COR) were added to the blots and incubated for 1 h at room temperature. The details of the antibodies used and their dilutions are given in **Supplementary Table S1**. The blots were developed, and bands were visualized under a LI-COR image scanner, and the band intensities were quantified and compared between test patients and controls using LI-COR image studio software.

Periodic Acid-Schiff (PAS) Staining

Cadaveric control ($n = 3$) and diabetic eyes from Type 2 DM with no retinopathy ($n = 3$) were collected in a sterile moist chamber within 24 h of death from Ramayamma International Eye Bank, LV Prasad Eye Institute, Hyderabad, India, according to the Tenets of the Declaration of Helsinki. The retina tissues were removed carefully from the eyes under a dissection microscope and fixed in 10% neutral buffered formalin, and paraffin sections were made. For PAS staining (Catalog No. 375810, Sigma), sections were deparaffinized at 60°C for 20–30 min and hydrated, followed by oxidization with 0.5% Periodic acid solution for 10 min. After washing with distilled water for 5 min, the sections were stained with Schiff's solution (Catalog No. 3952016, Sigma) for 15 min in the dark, followed by washing for 5 min and

TABLE 2 | Detailed demographics of study subjects used for serum protein analysis and mRNA expression analysis by qPCR.

	Age	Gender	Duration of DM
No-DM	65.8 ± 1.03	F, $n = 16$, M, $n = 22$	Nil
NPDR	59.83 ± 1.32	F, $n = 14$, M, $n = 24$	12.88 ± 1.4
PDR	53.86 ± 1.61	F, $n = 15$, M, $n = 23$	15.05 ± 0.9

then staining with Hematoxylin (Catalog No. H3136, Sigma) for 5 min. After washing, final dehydration and clearance was done using alcohol and Xylene (Catalog No. 40575, SD Fine-Chem Ltd) and mounted using DPX (Catalog No. POICHA-R-391780, SD Fine-Chem Ltd). The total number of blood vessels was counted manually in control and diabetic retina, and significance was calculated using a *t*-test.

Immunohistochemistry (IHC)

For IHC, antigen retrieval was carried out for the deparaffinized tissue sections using pH 6 Tris Citrate buffer. The sections were permeabilized using methanol for 30 min at −20°C, followed by washing thrice with 1X PBS. Blocking was done with 2% BSA, then sections were incubated with primary antibodies overnight at 4°C (Ms C3- Santacruz, 1:50, Catalog No. sc-28294, Ms CFH-Santacruz, 1:50, Catalog No. sc-166613, Rb CXCR4-Santacruz, 1:50, Catalog No. sc- 9036, Rb CD11b-CST, 1:200, Catalog No. 49420, Rb GFAP, 1:300, Dako, Catalog No. Z0334). After washing thrice with 1X PBS, the sections were incubated with appropriate fluorescent labeled secondary antibodies (Goat anti Rb594, Life Tech. Catalog No. A-11012, 1:300, Goat anti-Ms 594, Life Tech. Catalog No. A-11005, 1:300, Goat anti-Rb 488, Life Tech. Catalog No. A-11008, 1:300) for 1 h at room temperature. The sections were counterstained with DAPI, and the staining was examined under a fluorescent microscope (EVOS) using appropriate filters.

Gelatin Zymography

Gelatin zymography was done to analyze the activity of matrix metalloproteinases (MMP2 and MMP9) in the vitreous samples obtained from PDR and control subjects (33). Briefly, a 10 μg of vitreous proteins from PDR and no-DM controls were mixed with 4X lading dye with a final concentration of 1X and loaded into a gelatin-incorporated SDS-PAGE gel at a constant voltage of 125 V until the dye front reached the bottom of the gel. The gel was washed and kept for incubation with 1X renaturing solution (2.5% v/v Triton X- 100 in d. H_2O) for 30 min followed by overnight incubation with 1X developing buffer (0.05 M Tris HCl, pH 7.8, 0.2 M NaCl, 5 mM $CaCl_2$, 0.02% Brij 35) at 37°C. The gel was stained with Coomassie blue buffered (CBB) solution and de-stained until clear gelatinolytic bands were visible.

Enzyme-Linked Immunosorbent Assay (ELISA)

ELISA was carried out to evaluate the level of cytokines such as sPECAM, IL-8 and IL-10, sVEGFR1, and VEGF and VEGFR2 in the vitreous samples collected from PDR and control subjects. Vitreous humor samples were diluted with assay buffer at a dilution of 1:3. The standards were prepared by reconstituting them with 250 μL of deionized water. Twenty five micro liter of assay standards and quality controls were added into a 96-well plate, and then 25 μL of diluted test samples (vitreous humor) and 25 μL of targeted antibody-coated magnetic beads were added. The plate was kept for overnight incubation (16–20 h) at 4°C with constant shaking. The plate was then washed thrice with 1X wash buffer followed by incubation with 25 μL of detection antibodies for 1 h at room temperature under dark conditions. Following this, 25 μL of reporter tag comprised of streptavidin-phycoerythrin was added to each of the wells and incubated in the dark with gentle shaking for 30 min. The plates were washed thrice with wash buffer, and 150 μL of sheath fluid was added to each of the wells. The plate was scanned under a Luminex system with xPONENT® software. The generated results were exported in terms of median fluorescent intensity, and the concentrations of the analytes in the PDR and controls were calculated. The significance was calculated based on the *t*-test with a $p < 0.05$ using GraphPad Prism software.

RNA Isolation and Quantitative Real-Time PCR

Blood samples were collected in K3EDTA-coated 3-mL blood vacutainers from PDR, NPDR, and no-DM subjects, and total RNA was isolated using the TRIzol-chloroform method. RNA was isolated from diabetic ($n = 7$) and control ($n = 7$) retinal tissues and epiretinal membranes collected from PDR ($n = 4$) and control ($n = 4$) subjects while undergoing membrane peeling as a part of their surgical management after written informed consent had been obtained. Then, 1 μg of RNA was converted into cDNA using the iScript cDNA conversion kit (Catalog No. 1708891, Bio-Rad) as per the manufacturer's protocol for RNA obtained from blood and retinal tissues. For membranes, a high-capacity cDNA reverse transcription kit was used (Catalog No. 4368813, Applied Biosystems). Semi-quantitative PCR was performed on a 7900 HT platform using TaqMan assay chemistry for *C3* and *TGF*-β and SyBr green chemistry for the *VEGF, CFH,* and *CXCR4* genes. *C3, CFH,* and *CD11b* expression was also analyzed in retinal tissues and ERM samples from patients and controls using SyBr green chemistry. β-actin was used as the normalization control using standard thermal cycling conditions. The cycle threshold (Ct) values calculated for each test gene were obtained for each sample using SDS2.3 software, and fold change was calculated using $2^{-\Delta\Delta Ct}$. Data are represented as mean ± SEM, and significance was calculated. The primer sequences used for qRT are given in **Supplementary Table S2**.

RESULTS

Demographics of the Study Subjects

Vitreous samples were obtained from the study subjects while undergoing pars plana vitrectomy and blood samples were collected from subjects by venipuncture, with prior informed consent in all cases. None of the patients had received any intraocular anti-VEGF injections as a part of their ocular complications prior to sample collection. Further detailed demographic data for these subjects are provided in **Tables 1** and **2**.

Systematic Evaluation of Complement Pathway Activation by Analyzing the Central Complement Protein C3

Complement component C3 constitutes the central complement proteins that converge all the three pathways of the complement system. In order to understand the complement activation in

PDR vitreous, Western blotting for C3 was performed. The levels of total C3 molecules and of individual C3 activated fragments in PDR patients and controls were separated on PAGE and evaluated by quantifying the mean band intensity using Image Studio^{TM} Lite quantification software (LI-COR). These were then compared with no-DM controls based on equal protein loading based on Ponceau staining. There was a significant increase in total C3 in the PDR vitreous (1.9 ± 0.25, $^{**}p = 0.004$) compared to no-DM controls (0.98 ± 0.18) (**Figures 1A,B**). The total number of activated C3 fragments, including intact C3 (195 kDa), C3bα' (110 kDa), C3α (120 kDa), C3β (75 kDa), α-1 fragment of iC3b (65 kDa), and C3cα' fragment-2, (43 kDa) were analyzed in the PDR and no-DM controls. There was a significant increase in C3bα' (110 kDa) fragments ($^{*}p = 0.01$) in the vitreous of PDR subjects (6.9 ± 2.47) compared to controls (0.604 ± 0.15) (**Figure 1C**). Western blotting of the serum samples identified a slight but statistically insignificant increase in total C3 in PDR and NPDR compared to the no-DM samples (PDR vs. no-DM: 1.69 ± 0.58, $p = 0.7$, NPDR vs. no-DM: 1.38 ± 0.24, $p = 0.7$ and PDR vs. NPDR: 1.19 ± 0.23, $p = 0.9$). We did not identify any significant changes for any of the other C3 fragments in the serum samples (**Supplementary Figure 1**).

Contribution of the Classical and Alternative Pathway of Complement Activation in Diabetic Retinopathy

The classical pathway of complement activation was evaluated based on the levels of proteins such as C1q (vitreous and serum) and C4b (vitreous), while the alternative pathway of complement activation was evaluated based on the levels of activated Bb fragment of Factor B (vitreous). The Western blotting results identified no significant change in C1q and C4b in the vitreous of PDR compared to no-DM controls (C1q–PDR: 1.81 ± 0.44, controls: 1.32 ± 0.38 $p = 0.3$; C4b–PDR: 1.39 ± 0.4, control 1.08 ± 0.2, $p = 0.5$) (**Figures 2A,B,D**). Likewise, there was no significant change in C1q levels in the systemic circulation of PDR and NPDR compared to no-DM controls (PDR vs. no-DM: 1.12 ± 0.43, $p = 0.5$, PDR vs. NPDR: 0.75 ± 0.54, $p = 0.5$, NPDR vs. no DM: 1.43 ± 0.46, $p = 0.8$) (**Supplementary Figures 2A,B**). Thus, the classical pathway of complement activation was not involved in the complement activation of DR. However, Western blotting of Bb indicated a 61 kDa band in the vitreous samples (**Figure 2C**). The mean intensity of the 61 kDa band showed a significant downregulation of Bb in the vitreous of PDR samples compared to the controls (PDR: 0.97 ± 0.15, Controls: 1.89 ± 0.38, $^{*}p = 0.03$) (**Figure 2E**), suggesting that factor B in the PDR vitreous might be bound to form C3 convertase (C3bBb) for the activation of the alternative complement pathway.

Assessment of Regulation of the Alternative Complement Pathway by Complement Factor H (CFH)

CFH is a negative regulator of the alternative pathway of the complement. Western blotting of CFH identified a sharp 150 kDa band of CFH, and its levels were significantly higher in PDR compared to control vitreous (controls: 0.96 ± 0.172, PDR: 3.68 ± 0.66, $^{***}p = 0.0004$) (**Figures 3A,C**). In order to identify whether serum infiltration contributed to their increased level in PDR vitreous, CFH levels were independently compared between the serum samples of no-DM, NPDR, and PDR subjects (**Figure 3B**). CFH was found to be downregulated in the PDR serum as compared to NPDR and controls (PDR vs. no-DM: 0.78 ± 0.12, $p = 0.2$, PDR vs. NPDR: 0.66 ± 0.07, $p = 0.1$, NPDR vs. no-DM: 1.205 ± 0.2, $p = 0.9$) (**Figure 3D**). This indicated that the increased level of CFH in PDR vitreous was not due to the serum infiltration but was a localized phenomenon in the retina.

Validation of Complement Activation and CFH Upregulation by Immunohistochemistry Using Diabetic and Non-diabetic Cadaveric Retinal Tissues

Prior to the validation of complement activation in retinal tissues, H&E and PAS staining was performed to detect and confirm the early Vascular/DR changes in retina due to a prolonged history of diabetes (**Figures 4A,B**). The number of choriocapillaries was counted manually in each diabetic and control sections. Mean number of blood vessels was measured and the graph was plotted. A significantly increased number of choriocapillaries was found in diabetic retina compared to control retina (DM: 14.25 ± 3.7, control: 4.7 ± 1.85, $^{*}p = 0.01$) (**Figure 4C**). Further, retinal sections were stained using PAS stain. The thickness of vessel walls in five high power fields each in different diabetic retina and control retina were measured using an Aperio Image Scope (version: 12.4.3.5008) at Aperio AT2 Digital Scanner. Mean ± SE was calculated of the thickness in diabetic retina and control retina. A significant increase in vessel wall thickness was observed in diabetic retina compared to control retina (Control: 1.91 ± 0.46, Diabetic retina: 5.78 ± 1.48, $^{***}p = 0.0006$) (**Figure 4D**).

Immunohistochemistry (IHC) was performed to test for complement activation and Factor H upregulation in the retina from tissues of diabetic and non-diabetic donor eyes. The retinal tissues were also stained with markers of glial activation such as CD11b for activated microglia and glial fibrillary acidic protein (GFAP) for the macroglial population of the retina. The levels of CXCR4 were also evaluated in these retinal tissues for evaluating the presence of chemotactic cells. The IHC results clearly demonstrated intense staining of C3 in all the retinal layers compared to the control retinas (**Figures 5A–D**). GFAP was seen only in the inner retinal layers of both DM and control retinas, but the expression of GFAP in diabetic retina was found to be slightly higher than that of control retinas (**Figures 5A,B**), suggesting the onset of gliosis in DM retinas. Increased expressions of C3 and CD11b were observed in DM retina, whereas in the control retinas, the expressions of these markers were relatively low (**Figures 5C,D**). Further evaluation of the levels of CFH in retinas from control and diabetic donors (**Figures 5E,F**) indicated intense staining of CFH co-localizing with CD11b-positive cells in the retinal layers in DM retina, suggesting a possible

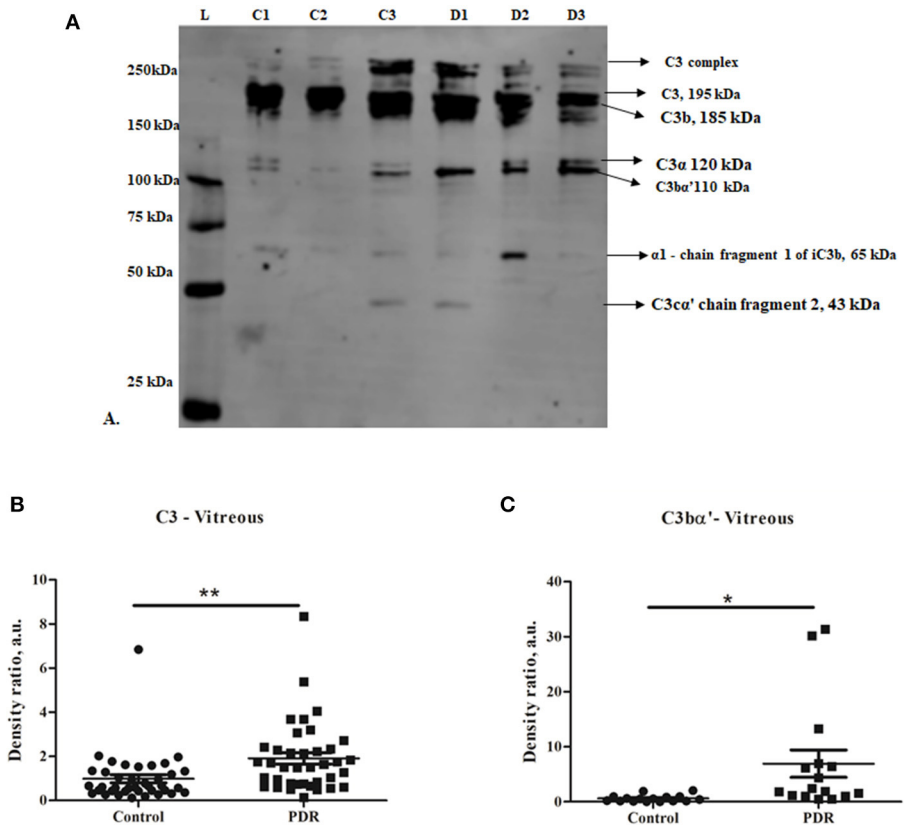

FIGURE 1 | (A) Representative Western blot of C3 in PDR and no-DM vitreous. **(B)** Quantification of total C3 in PDR and in no-DM control vitreous by densitometry (PDR, $n = 38$ and Control, $n = 38$). **(C)** Quantification of C3bα' (110 kDa) in PDR ($n = 16$) vitreous compared to control vitreous ($n = 16$). $^{**}p = 0.004$, $^{*}p = 0.03$, respectively; data represented as mean ± SEM, C, control vitreous; D, PDR vitreous; L, protein ladder.

feedback mechanism for excess complement activation by the microglial cells.

Assessment of Microglial Infiltration and Activation in Retina as Well as in PDR Vitreous

Further, the level of CXCR4, a chemokine receptor present in the microglial cells, was evaluated by IHC, which indicated a larger distribution of $CXCR4^{+ve}$cells in DM retina compared to the control retinas, wherein the CXCR4 staining was almost negligible, suggesting microglial activation, and enhanced chemotaxis in diabetes (**Figures 6A,B**). To evaluate whether this microglial population infiltrated into the vitreous cavity during the advanced stages of the disease, the levels of CD11b were also evaluated in the vitreous samples by Western blotting. The results indicated an intense band of activated microglial marker CD11b in the vitreous of PDR subjects that was absent in the controls (**Figure 6C**), providing additional evidence of microglial infiltration during PDR pathogenesis. In order to validate the contribution of microglial activation in disease progression, the activity of matrix metalloproteinases was evaluated in PDR vitreous samples. Microglia are the major source of gelatinolytic MMPs such as MMP9 and MMP2 in the retina. Both the levels and enzymatic activity of MMPs in the PDR vitreous were evaluated by gelatin zymography in the vitreous samples of patients and controls. The results indicated a clear gelatinolytic band of 82–85 kDa molecular weight in both PDR and control vitreous that corresponded to active MMP9. However, it was more pronounced in PDR vitreous, indicating increased gelatinolytic activity, and active MMP9 under the disease condition (**Figure 6D**). Since the upregulation of MMP9 activity is known to drive the growth of blood vessels, the levels of VEGF and VEGFR2 were compared in the vitreous samples of PDR and control subjects. A significant increase in the levels of sVEGFR1, VEGFR2 and VEGF was observed in the vitreous of PDR subjects compared to the controls (sVEGFR1, Control: 1227 ± 209, PDR: 3152 ± 327, $^{***}p = 0.0002$, VEGFR2, control: 2485 ± 348, PDR: 3929 ± 526, $^{*}p = 0.03$, VEGF, control: 105 ± 18.12, PDR: 356 ± 106, $^{*}p = 0.04$) (**Figure 6E**).

Quantitative Estimation of Inflammation in PDR and Control Samples Based on the Levels of Pro- and Anti-inflammatory Cytokines

The levels of inflammation in the vitreous samples were analyzed by the quantitative estimation of pro-inflammatory markers such

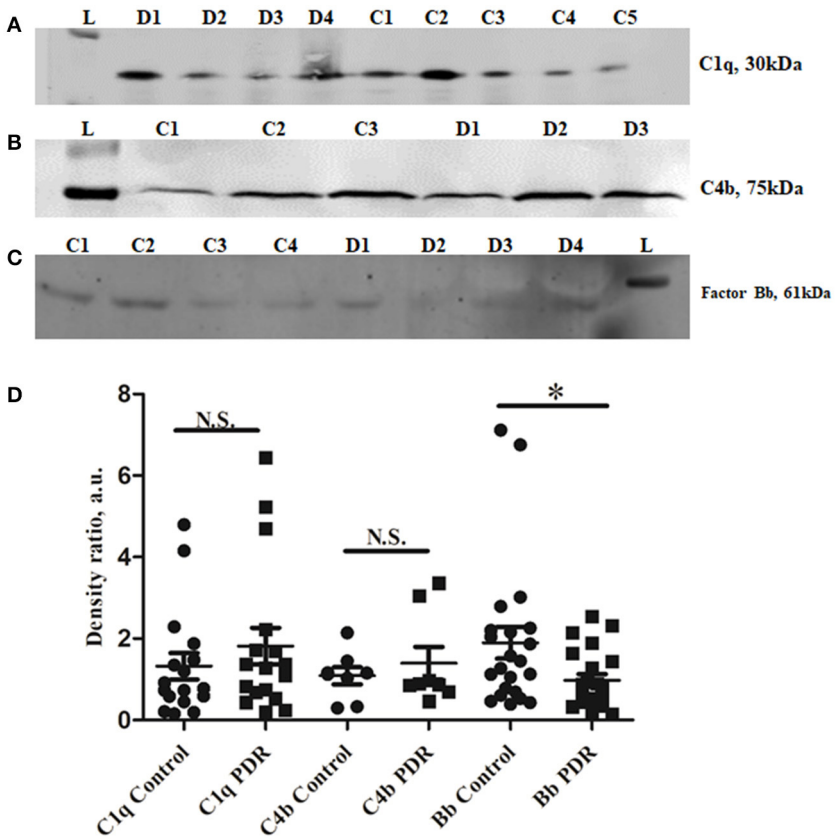

FIGURE 2 | Representative Western blots of **(A)** C1q, **(B)** C4b, and **(C)** Factor Bb in PDR and No-DM controls, **(D)**. Quantification of C1q in PDR ($n = 17$) and no-DM control ($n = 17$) vitreous, $p > 0.05$, C4b in PDR ($n = 8$) and no-DM control ($n = 8$) vitreous, $p > 0.05$ and Bb in PDR ($n = 22$) and no-DM control ($n = 22$) vitreous, $^{*}p = 0.03$. Data represented as mean ± SEM, D, PDR; C, controls; L, protein ladder; n.s., not significant.

as sPECAM and IL-8, along with an anti-inflammatory marker, IL-10. The levels of sPECAM and IL-8 were found to be higher in the vitreous of PDR compared to the controls (sPECAM: Control: 49.54 ± 4.76, PDR: 105.45 ± 16.69, $^{*}p = 0.01$, IL-8: Control: 12.79 ± 3.13, PDR: 29.47 ± 14.14, $p = 0.2$). In contrast, the level of anti-inflammatory cytokine IL-10 was found to be significantly downregulated in PDR vitreous as compared to the controls (Control: 2.24 ± 0.42, PDR: 0.57 ± 0.09, $^{**}p = 0.001$) (**Figures 7A,B**).

Gene Expression Profiling for Complement and Angiogenic Genes by Quantitative Real-Time PCR Among Different Disease Categories

Total RNA was isolated from PDR, NPDR, and control subjects, and quantitative real-time PCR was performed for the candidate genes such as *TGFβ1, THSB1, CXCR4, VEGF, C3,* and *CFH*. Significant changes in the gene expressions were observed for NPDR and PDR compared to controls for *THSB and CFH* (THSB1: NPDR vs. Control: 0.499 ± 0.15; $^{**}p = 0.008$, PDR vs. Control: 0.495 ± 0.09, $^{**}p = 0.004$) (CFH: NPDR vs. Control: 0.628 ± 0.12; $^{***}p = 0.0009$, PDR vs. Control: 0.45 ± 0.05, $^{***}p = 0.0001$), whereas genes such as *TGF β, VEGF,* and *C3* were found to be significantly changed only in PDR compared to controls (PDR vs. Control: *TGF β*: 0.734 ± 0.05, $^{**}p = 0.004$, *VEGF*: 1.538 ± 0.38, $^{*}p = 0.02$, *C3*: 1.457 ± 0.56, $^{*}p = 0.01$), and *CXCR4*- did not show any significant change (**Figure 7C**).

Activation of Microglia and CFH in Early vs. Advanced Stages of the Disease

Further, the differential expression profiling of genes involved in complement and microglial activation was performed in eyes with early- (retina from diabetic donor eyes) and late-stage DR (Epiretinal membranes [ERM]) to investigate their role in disease development and progression. Retinal tissues from diabetic donors with early DR changes showed a significant increase for the *C3* gene (13.082 ± 4.24, $^{**}p = 0.008$) compared to the control retina (without a history of diabetes and vascular changes), while it was insignificant for the *CD11b* (1.2 ± 0.32) and *CFH* (1.56 ± 0.49) genes (**Figure 7D**). On the contrary, eyes with late-stage DR exhibited significant changes in the expressions of complement genes (*C3:* 6.871 ± 1.85, $^{*}p = 0.05$ and *CFH: 2*3.35 ± 1.79, $^{**}p = 0.007$) and *CD11b* (17.88 ± 2.3, $^{*}p = 0.01$), which is a marker for microglial activation (**Figure 7E**). It may be noted that changes in the expression of the *CFH* and *CD11b* genes involved in microglial activation were much higher than in the *C3* gene in the ERM tissues of patients with late DR changes.

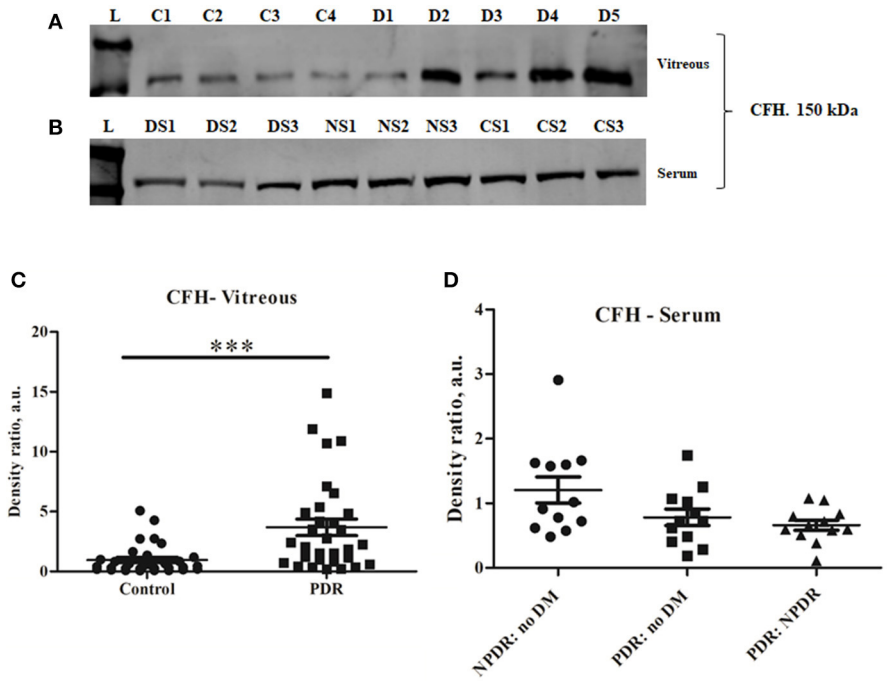

FIGURE 3 | Representative Western blot of **(A)** CFH (150 kDa) in PDR and No-DM controls and **(B)** CFH (150 kDa) in PDR, NPDR, and no-DM control serum. Quantitative estimates of **(C)** CFH band in PDR ($n = 31$) vs. no-DM control ($n = 31$) vitreous, ***$p < 0.0004$ and **(D)** CFH band in PDR ($n = 12$), NPDR ($n = 12$), and no-DM control ($n = 12$) serum, $p > 0.05$ (not significant). Data represented as mean ± SEM, D, PDR vitreous; C, control vitreous; L, protein ladder; DS, PDR serum; NS, NPDR; CS, Control serum; n.s., not significant.

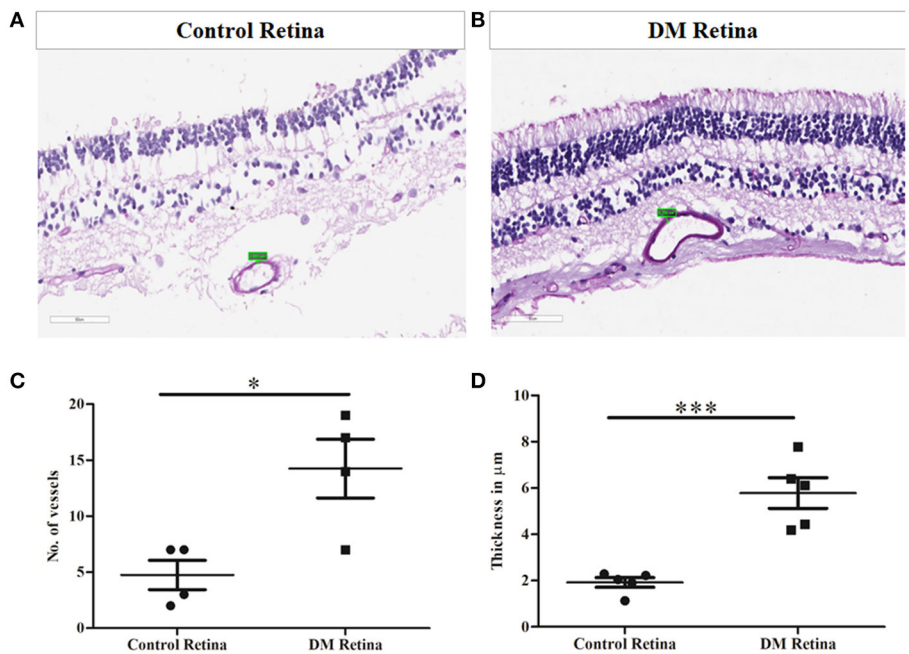

FIGURE 4 | Representative photomicrograph showing thickened and dilated blood vessels in diabetic retina **(B)** in comparison to control retina **(A)** (Periodic acid-Schiff, Magnification: 40X). **(C)** Quantification of number of capillaries in diabetic vs. control retinal tissues. **(D)** Quantification of capillary thickness in diabetic retina vs. control retina. *$p = 0.01$, ***$p = 0.0006$.

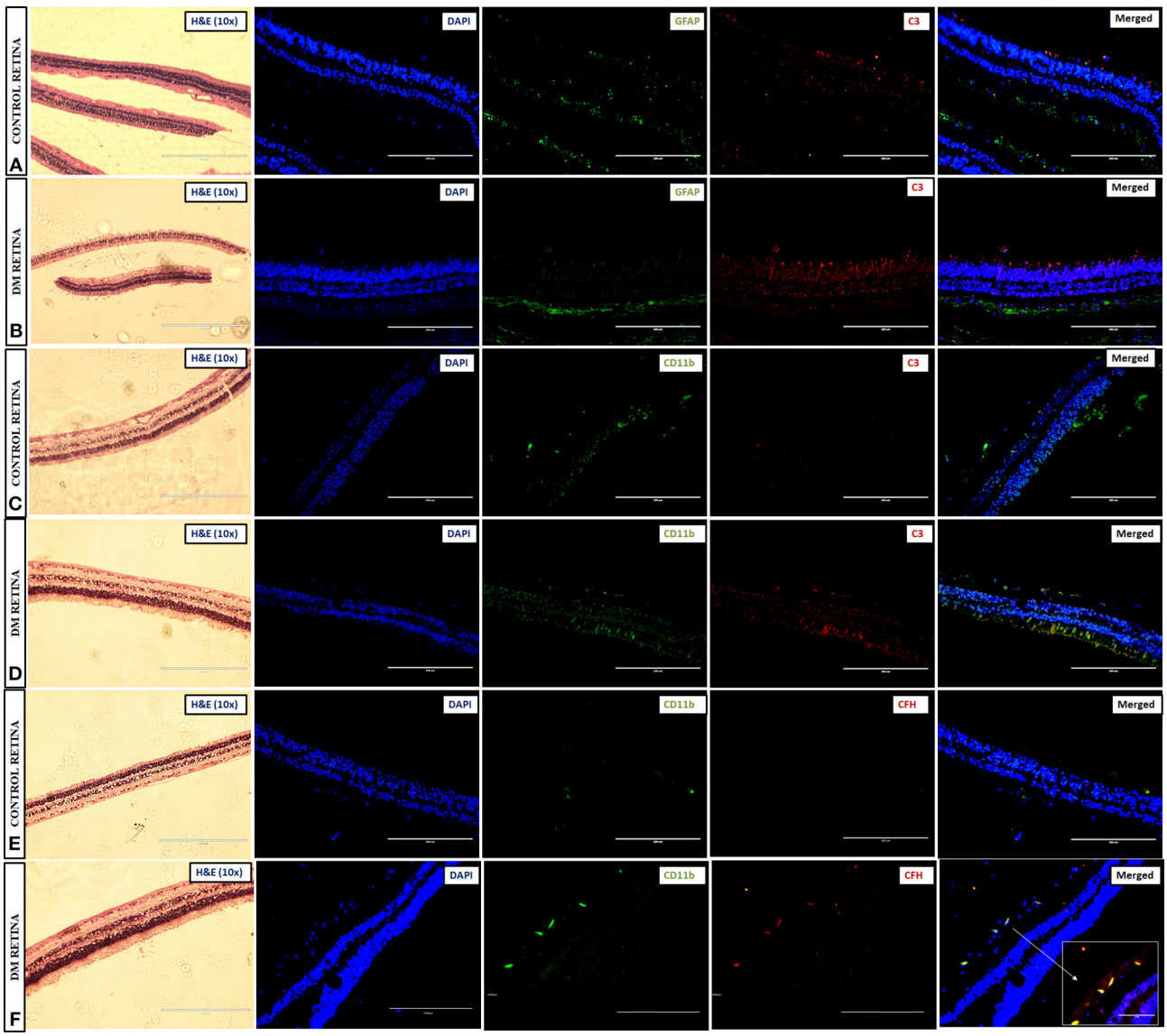

FIGURE 5 | Representative images of the 10X magnified H and E sections and post-immunofluorescence showing the localization of C3 and GFAP in retinal tissues collected from **(A)** control and **(B)** diabetic retina, C3, and CD11b in **(C)** control and **(D)** diabetic retina, and CFH and CD11b in **(E)** control and **(F)** diabetic retina, magnification 20X, scale bar 200 μm. Co-localized expression of CFH and CD11b is highlighted in 40X magnification in panel **(F)**.

DISCUSSION

Diabetic retinopathy is a serious neuro-vascular complication of the retina. The involvement of complement pathway genes in DR progression was proposed based on the identification of complement deposits in choriocapillaries of DR retina and reduced levels of complement pathway inhibitors in diabetic retina, though the mechanism and timing of their involvement were unclear (27, 28). The major aspect of this study was to check whether complement pathway proteins are involved in the early DR pathology or only in DR progression after being released into the vitreous cavity by blood-retina barrier breakdown in the advanced stages based on the analysis of retinal tissue specimens from diabetic and non-diabetic individuals.

C3 is the central complement protein, and the activation of complement pathways causes proteolytic fragmentation of C3. These fragments can bind to the nearby tissues and enhance the inflammatory process (34). Hitherto, a comprehensive study conducted by Garcia et al. identified a significant increase in 42 k Da fragment of C3 in PDR vitreous and found it to correlate with the mRNA expression in diabetic retina (29). In the present study, among the various fragments of C3 protein, a significant upregulation of only the C3bα' (110 kDa) fragment was noted in PDR vitreous. The reactive C3bα' is generated from the 120 kDa α-chain of C3 after the proteolytic removal of the 10 kDa C3a fragment and is part of active C3b (35). A significant increase in the level of C3bα' is indicative of enhanced complement pathway activation in PDR vitreous. However, no

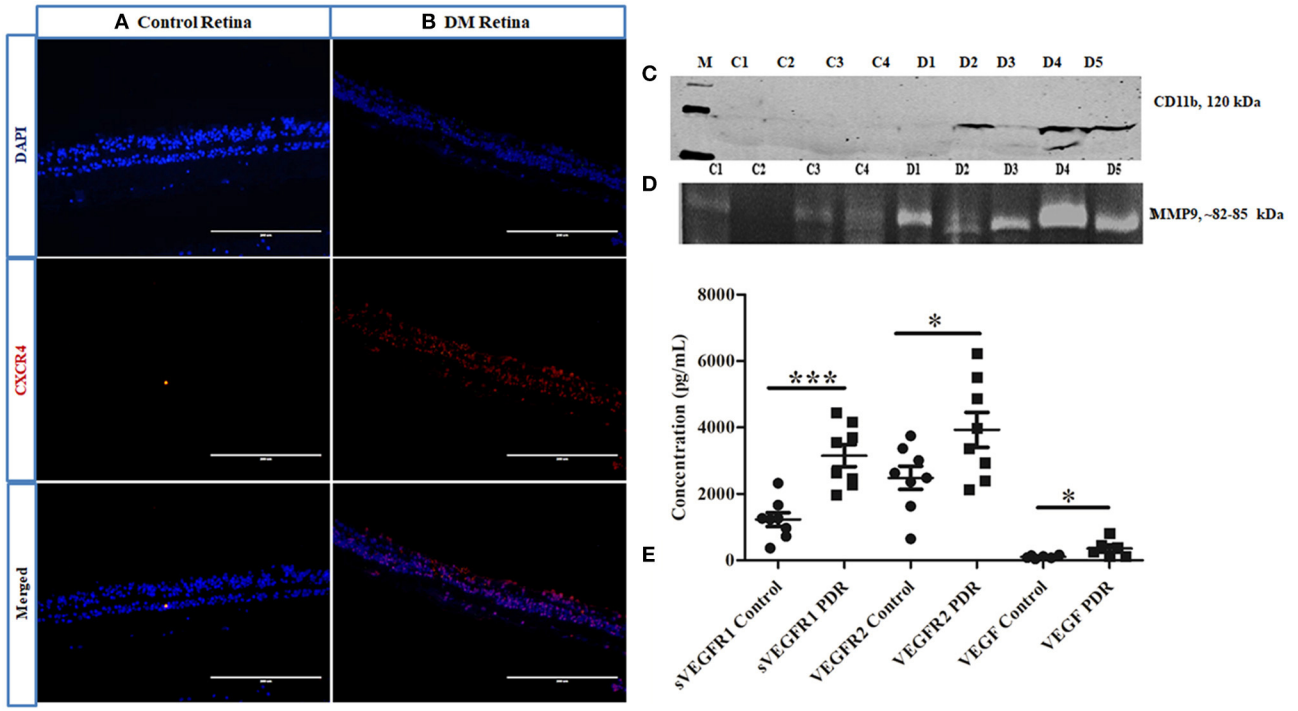

FIGURE 6 | Representative image of **(A,B)** immunofluorescence of CXCR4 in retinal tissues collected from control and diabetic retina, respectively, magnification 20X. **(C)** Representative Western blotting of CD11b in PDR vitreous ($n = 5$) compared to controls ($n = 4$); **(D)** Representative gelatin zymography of vitreous samples from PDR ($n = 10$) vs. controls ($n = 10$) (C, control; D, PDR). **(E)** Scatter plot with individual data points showing differential levels of soluble VEGF (***$p = 0.0002$) and VEGFR2 (*$p = 0.03$) (PDR, $n = 8$, Control, $n = 8$) and VEGF (*$p = 0.04$) (PDR, $n = 6$, Control, $n = 6$) by multiplex ELISA.

significant changes in the expression of the other complement proteins C1q and C4b in PDR and NPDR clearly ruled out any major involvement of the classical complement pathway in the disease pathogenesis.

A detailed analysis of the regulatory proteins involved in the alternative complement pathway such as CFB and CFH indeed confirmed a definitive role of the alternative pathway in DR pathogenesis. CFB, a specific protein, is required for the formation of C3 convertase (C3bBb) for activating the alternative complement pathway (36). The faintly visible but significant downregulation of fragment Bb of factor B seen in PDR vitreous (based on densitometry estimation) could be due to the formation of more C3bBb in PDR vitreous. CFH is a negative regulator/inhibitor of the alternative complement pathway, as it competes with FB for C3b binding and also acts as a co-factor for factor I to degrade C3b to C3bi (37). Typically, a low level of CFH is expected in PDR vitreous concurrent with the downregulation of free Bb in the PDR vitreous. However, an unexpected significant upregulation of CFH could be a feedback mechanism for maintaining the level of C3bα' in PDR vitreous. Several earlier studies have shown that the C3bα' region of C3b protein is involved in binding to CFH protein (38), and this possibly explains the significant upregulation of CFH. This feedback regulation of the alternative complement pathway by CFH was confirmed by a perfect correlation ($r = 0.78$, $^*p = 0.01$) in the increased levels for both CFH and C3bα' in randomly selected vitreous samples of PDR and no-DM controls (**Supplementary Figure 3**). On the other hand, the downregulation of serum CFH levels in PDR cases compared to NPDR and controls suggests that the upregulation of CFH seen in vitreous is contributed by the local/resident cells in the retina. It was previously reported that VEGF inhibition reduces CFH production in eye and kidney through reduced VEGFR2/PKC-α/CREB signaling (39). Therefore, the observed upregulation of CFH could possibly have been mediated by a simultaneously increased VEGF level in the PDR vitreous. Further, intense staining of complement proteins in the retinal tissues of diabetic donors with early vascular/DR changes as compared to control non-diabetic donor retina confirmed the role of CFH and C3 in diabetic retinopathy. Vascular basement membrane thickening is one of the earliest changes that occur in the retina due to diabetes (40). The thickening of basement membrane, as seen in PAS staining of the studied retinal tissues from the diabetic donor eyes, confirmed the early vascular stage of DR.

The retinal macrophages and microglia are known to synthesize C3 in aging retina (41). However, the present study identified a rather uniform distribution of complement deposition in all of the neural layers of diabetic retina, suggesting thereby that C3 and CFH could also be synthesized by other retinal cell types, including the $CD11b^{+ve}$ microglial population. The CFH in the neural retina was known to have an affinity toward the CR3 receptor in the microglial cells (42). This further

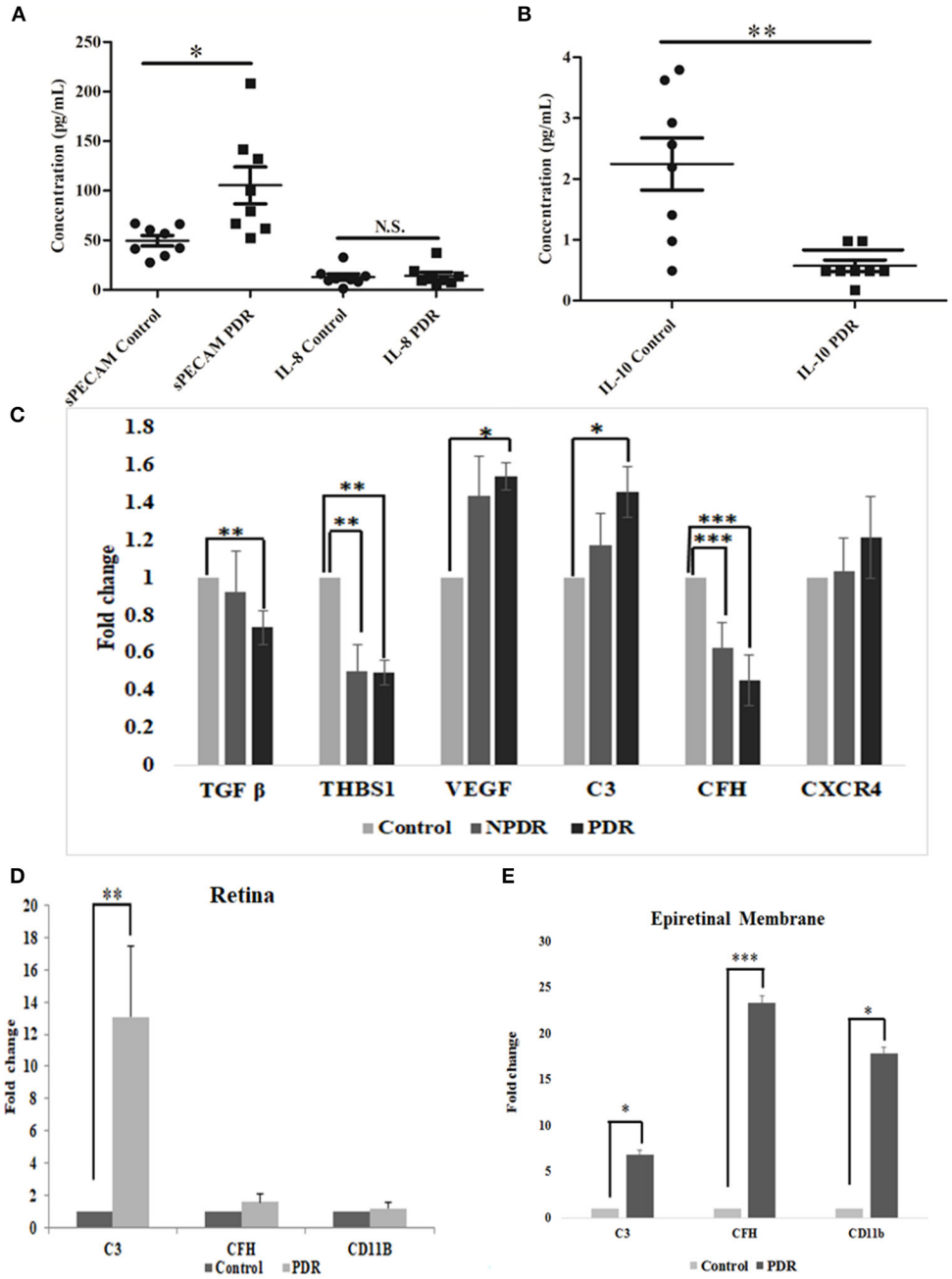

FIGURE 7 | Scatter plot with individual data points showing the quantitative estimation of inflammation in the vitreous samples based on Multiplex ELISA from PDR ($n = 8$) vs. controls ($n = 8$) (C, control; D, PDR) for **(A)** sPECAM and IL-8 and **(B)** IL-10 in PDR vs. control vitreous. Differential expression based on quantitative PCR for **(C)** complement and angiogenic genes from blood in PDR ($n = 20$) and NPDR ($n = 20$) vs. no-DM controls ($n = 20$), **(D)** early (diabetic retina) vs. late changes, and **(E)** ERM tissues in the proteins involved in the activation of the alternative complement pathway. Data represented as mean ± SEM. $^{*}p \leq 0.05$, $^{**}p \leq 0.01$, $^{***}p \leq 0.001$; ns, $p > 0.05$.

indicates that CFH upregulation in PDR could also be related to microglial activation. Surprisingly, increased CFH staining was found in the CD11b^{+ve} microglia in the inner nuclear layers in diabetic retina. This finding was consistent with our earlier report on retinopathy of prematurity (21). Significant gliosis was evidently seen in the diabetic retina tissues, as suggested by the upregulation of GFAP protein, while no expression of complement proteins was seen in the macroglial (Müller glia and astrocytes) cells, further emphasizing a major role of microglia in DR pathogenesis. Microglial cells, being the resident cells, become activated and move up from deep RGC layers toward photoreceptors. Microglial migration upon activation

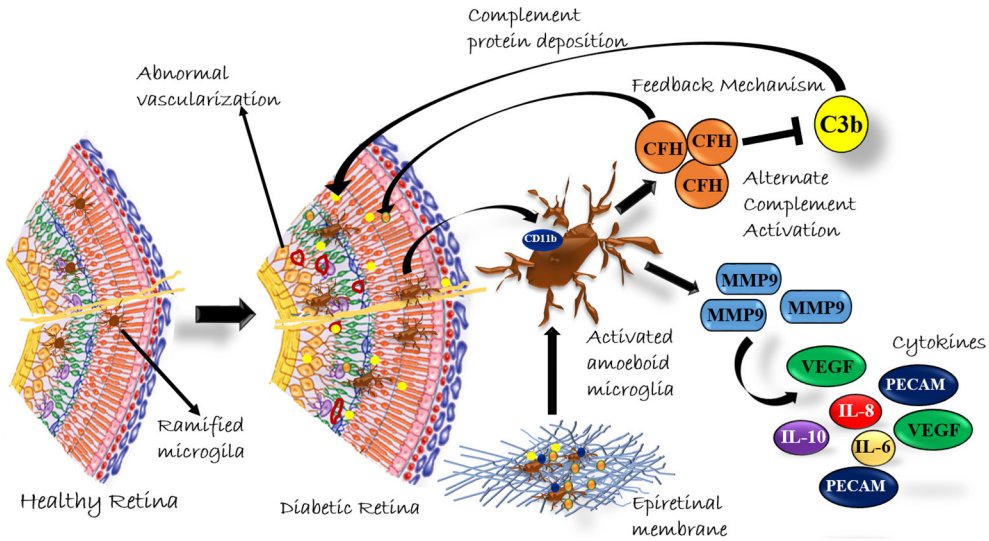

FIGURE 8 | A Schematic summary of the role of complement activation by microglial cells in diabetic retinopathy.

in the diabetic retina was confirmed based on the staining of CXCR4, a chemokine receptor known to be involved in both astroglial activation and microglial signaling (43) and increased levels of activated microglial protein CD11b in vitreous samples on Western blotting. Since an increased level of complement activation is known to cause damage to the retinal tissues (44), it could be speculated that the production of CFH by activated microglia prevents the damage of retinal neurons; this needs to be explored further.

IL-8, a pro-inflammatory cytokine, and IL-10, an anti-inflammatory cytokine, are secreted mainly by M1 and M2 microglia, respectively (45). The downregulation of IL-10 and upregulation of IL-8 further confirmed the activation of the proinflammatory M1 phenotype of microglia in PDR vitreous. Microglia, once activated, are known to secrete the matrix metalloproteinases (46). Together with an increase in pro-inflammatory markers such as IL-8 and MMP9, a significant upregulation of sPECAM and VEGF-VEGFR2 in the PDR vitreous confirmed excessive inflammation and angiogenesis in the PDR eyes. This further suggests that an inflammatory environment in the PDR retina could be a driving force for microglial activation and retinal damage in PDR.

In conclusion, our study provided a systematic analysis of classical and alternative complement pathway activation in PDR pathogenesis. The study, for the first time, showed a significant upregulation of 110 kDa C3bα' and concurrent increase of CFH in PDR vitreous, and this upregulation of complement cascade was localized to retina and not contributed by the blood-retina barrier breakdown that is a common sight in advanced PDR cases. The faintly visible detection of CFB in Western blotting could be due to a low concentration of detectable free CFB protein in the vitreous sample or a poor antibody. The correlation of genetic associations of variations in complement factor H and complement factor B with their expression in epiretinal membrane tissues and vitreous humor could firmly establish the role of the alternative complement pathway in DR pathogenesis. Lastly, our study suggested that the synergistic role of activated microglia and complement activation plays a major role in PDR pathogenesis (**Figure 8**). In the future, targeting microglial mediated complement activation could pave the way for effective therapeutic management of DR by reducing underlying neuro-inflammation and abnormal angiogenesis.

DATA AVAILABILITY STATEMENT

The raw data supporting the conclusions of this article will be made available by the authors, without undue reservation, to any qualified researcher.

ETHICS STATEMENT

The studies involving human participants were reviewed and approved by LV Prasad Eye Institute Ethics committee. The patients/participants provided their written informed consent to participate in this study.

AUTHOR CONTRIBUTIONS

IK conceived the idea and served as principal investigator. IK, JC, and SC wrote the protocol. SC, JC, MT, RP, SJ, and SC were co-investigators. SS performed most of the work and the protein analysis and IHC of retina and vitreous, SV performed gene expression analysis, IHC, and PAS staining for retina and retinal membranes, and SJ guided the IHC and PAS staining analysis. SS, SV, IK, and SC analyzed the data and wrote the manuscript, and all authors revised the paper and approved the submitted version.

FUNDING

In completing this work, IK was supported by DST-SERB, Ministry of Science and Technology, Government of India (EMR/2016/007068), the Department of Biotechnology, Government of India (BT/01/COE/06/02/10), Hyderabad Eye Research Foundation, and the Department of Biotechnology (BT/PR/16582/BID/667/2016), Government of India.

ACKNOWLEDGMENTS

The authors thank the study subjects for providing vitreous, serum, and retinal membrane samples for protein and RNA analysis, the family members of donors for kindly donating the cadaver eyes for performing immunostaining experiments, and the staff at the Ramayamma International Eye Bank, LV Prasad Eye Institute, Hyderabad, India for their help in the collection of the donor eyes. A major part of the present study was done as a part of the PhD thesis of SS, which has been submitted to the University of Hyderabad, where the online version is not yet archived.

SUPPLEMENTARY MATERIAL

The Supplementary Material for this article can be found online at: https://www.frontiersin.org/articles/10.3389/fimmu.2020.00154/full#supplementary-material

REFERENCES

1. Yau JW, Rogers SL, Kawasaki R, Lamoureux EL, Kowalski JW, Bek T, et al. Global prevalence and major risk factors of diabetic retinopathy. *Diabetes Care.* (2012) 35:556–64. doi: 10.2337/dc11-1909
2. Duh EJ, Sun JK, Stitt AW. Diabetic retinopathy: current understanding, mechanisms, and treatment strategies. *JCI Insight.* (2017) 2:e93751. doi: 10.1172/jci.insight.93751
3. Chen M, Xu H. Parainflammation, chronic inflammation, and age-related macular degeneration. *J Leukoc Biol.* (2015) 98:713–25. doi: 10.1189/jlb.3RI0615-239R
4. Mukai R, Okunuki Y, Husain D, Kim CB, Lambris JD, Connor KM. The complement system is critical in maintaining retinal integrity during aging. *Front Aging Neurosci.* (2018) 10:15. doi: 10.3389/fnagi.2018.00015
5. McGeer PL, McGeer EG. Inflammation and the degenerative diseases of aging. *Ann N Y Acad Sci.* (2004) 1035:104–16. doi: 10.1196/annals.1332.007
6. Yu J, Peng R, Chen H, Cui C, Ba J. Elucidation of the pathogenic mechanism of rhegmatogenous retinal detachment with proliferative vitreoretinopathy by proteomic analysis. *Invest Ophthalmol Vis Sci.* (2012) 53:8146–53. doi: 10.1167/iovs.12-10079
7. Sweigard JH, Matsumoto H, Smith KE, Kim LA, Paschalis EI, Okonuki Y, et al. Inhibition of the alternative complement pathway preserves photoreceptors after retinal injury. *Sci Transl Med.* (2015) 7:297ra116. doi: 10.1126/scitranslmed.aab1482
8. Strey CW, Markiewski M, Mastellos D, Tudoran R, Spruce LA, Greenbaum LE, et al. The proinflammatory mediators C3a and C5a are essential for liver regeneration. *J Exp Med.* (2003) 198:913–23. doi: 10.1084/jem.20030374
9. Stevens B, Allen NJ, Vazquez LE, Howell GR, Christopherson KS, Nouri N, et al. The classical complement cascade mediates CNS synapse elimination. *Cell.* (2007) 131:1164–78. doi: 10.1016/j.cell.2007.10.036
10. Langer HF, Chung KJ, Orlova VV, Choi EY, Kaul S, Kruhlak MJ, et al. Complement-mediated inhibition of neovascularization reveals a point of convergence between innate immunity and angiogenesis. *Blood.* (2010) 116:4395–403. doi: 10.1182/blood-2010-01-261503
11. Akhtar-Schafer I, Wang L, Krohne TU, Xu H, Langmann T. Modulation of three key innate immune pathways for the most common retinal degenerative diseases. *EMBO Mol Med.* (2018) 10:e8259. doi: 10.15252/emmm.201708259
12. Rajappa M, Saxena P, Kaur J. Ocular angiogenesis: mechanisms and recent advances in therapy. *Adv Clin Chem.* (2010) 50:103–21. doi: 10.1016/S0065-2423(10)50006-4
13. Balaiya S, Zhou Z, Chalam KV. Characterization of vitreous and aqueous proteome in humans with proliferative diabetic retinopathy and its clinical correlation. *Proteomics Insights.* (2017) 8:1178641816686078. doi: 10.1177/1178641816686078
14. Schori C, Trachsel C, Grossmann J, Zygoula I, Barthelmes D, Grimm C. The proteomic landscape in the vitreous of patients with age-related and diabetic retinal disease. *Invest Ophthalmol Vis Sci.* (2018) 59:AMD31–40. doi: 10.1167/iovs.18-24122
15. Bora PS, Sohn JH, Cruz JM, Jha P, Nishihori H, Wang Y, et al. Role of complement and complement membrane attack complex in laser-induced choroidal neovascularization. *J Immunol.* (2005) 174:491–7. doi: 10.4049/jimmunol.174.1.491
16. Edwards AO, Ritter R III, Abel KJ, Manning A, Panhuysen C, Farrer LA. Complement factor H polymorphism and age-related macular degeneration. *Science.* (2005) 308:421–4. doi: 10.1126/science.1110189
17. Mantel I, Ambresin A, Moetteli L, Droz I, Roduit R, Munier FL, et al. Complement factor B polymorphism and the phenotype of early age-related macular degeneration. *Ophthalmic Genet.* (2014) 35:12–7. doi: 10.3109/13816810.2013.766217
18. Cao S, Wang JC, Gao J, Wong M, To E, White VA, et al. CFH Y402H polymorphism and the complement activation product C5a: effects on NF-κB activation and inflammasome gene regulation. *Br J Ophthalmol.* (2016) 100:713–8. doi: 10.1136/bjophthalmol-2015-307213
19. Natoli R, Fernando N, Jiao H, Racic T, Madigan M, Barnett NL, et al. Retinal macrophages synthesize C3 and activate complement in AMD and in models of focal retinal degeneration. *Invest Ophthalmol Vis Sci.* (2017) 58:2977–90. doi: 10.1167/iovs.17-21672
20. Inafuku S, Klokman G, Connor KM. The alternative complement system mediates cell death in retinal ischemia reperfusion injury. *Front Mol Neurosci.* (2018) 11:278. doi: 10.3389/fnmol.2018.00278
21. Rathi S, Jalali S, Patnaik S, Shahulhameed S, Musada GR, Balakrishnan D, et al. Abnormal complement activation and inflammation in the pathogenesis of retinopathy of prematurity. *Front Immunol.* (2017) 8:1868. doi: 10.3389/fimmu.2017.01868
22. Chhablani J, Sharma A, Goud A, Peguda HK, Rao HL, Begum VU, et al. Neurodegeneration in type 2 diabetes: evidence from spectral-domain optical coherence tomography. *Invest Ophthalmol Vis Sci.* (2015) 56:6333–8. doi: 10.1167/iovs.15-17334
23. Kim K, Kim ES, Kim DG, Yu SY. Progressive retinal neurodegeneration and microvascular change in diabetic retinopathy: longitudinal study using OCT angiography. *Acta Diabetol.* (2019) 56:1275–82. doi: 10.1007/s00592-019-01395-6
24. Zeng XX, Ng YK, Ling EA. Neuronal and microglial response in the retina of streptozotocin-induced diabetic rats. *Vis Neurosci.* (2000) 17:463–71. doi: 10.1017/S0952523800173122
25. Zeng HY, Green WR, Tso MO. Microglial activation in human diabetic retinopathy. *Arch Ophthalmol.* (2008) 126:227–32. doi: 10.1001/archophthalmol.2007.65
26. Ramirez AI, de Hoz R, Salobrar-Garcia E, Salazar JJ, Rojas B, Ajoy D, et al. The role of microglia in retinal neurodegeneration: alzheimer's disease, parkinson, and glaucoma. *Front Aging Neurosci.* (2017) 9:214. doi: 10.3389/fnagi.2017.00214
27. Gerl VB, Bohl J, Pitz S, Stoffelns B, Pfeiffer N, Bhakdi S. Extensive deposits of complement C3d and C5b-9 in the choriocapillaris of eyes of patients with diabetic retinopathy. *Invest Ophthalmol Vis Sci.* (2002) 43:1104–8.

28. Zhang J, Gerhardinger C, Lorenzi M. Early complement activation and decreased levels of glycosylphosphatidylinositol-anchored complement inhibitors in human and experimental diabetic retinopathy. *Diabetes.* (2002) 51:3499–504. doi: 10.2337/diabetes.51.12.3499
29. Garcia-Ramirez M, Canals F, Hernandez C, Colome N, Ferrer C, Carrasco E, et al. Proteomic analysis of human vitreous fluid by fluorescence-based difference gel electrophoresis (DIGE): a new strategy for identifying potential candidates in the pathogenesis of proliferative diabetic retinopathy. *Diabetologia.* (2007) 50:1294–303. doi: 10.1007/s00125-007-0627-y
30. Gao BB, Chen X, Timothy N, Aiello LP, Feener EP. Characterization of the vitreous proteome in diabetes without diabetic retinopathy and diabetes with proliferative diabetic retinopathy. *J Proteome Res.* (2008) 7:2516–25. doi: 10.1021/pr800112g
31. Loukovaara S, Nurkkala H, Tamene F, Gucciardo E, Liu X, Repo P, et al. Quantitative Proteomics analysis of vitreous humor from diabetic retinopathy patients. *J Proteome Res.* (2015) 14:5131–43. doi: 10.1021/acs.jproteome.5b00900
32. Li J, Lu Q, Lu P. Quantitative proteomics analysis of vitreous body from type 2 diabetic patients with proliferative diabetic retinopathy. *BMC Ophthalmol.* (2018) 18:151. doi: 10.1186/s12886-018-0821-3
33. Toth M, Fridman R. Assessment of gelatinases (MMP-2 and MMP-9 by gelatin zymography. *Methods Mol Med.* (2001) 57:163–74. doi: 10.1385/1-59259-136-1:163
34. Nishida N, Walz T, Springer TA. Structural transitions of complement component C3 and its activation products. *Proc Natl Acad Sci USA.* (2006) 103:19737–42. doi: 10.1073/pnas.0609791104
35. Clay CD, Soni S, Gunn JS, Schlesinger LS. Evasion of complement-mediated lysis and complement C3 deposition are regulated by Francisella tularensis lipopolysaccharide O antigen. *J Immunol.* (2008) 181:5568–78. doi: 10.4049/jimmunol.181.8.5568
36. Noris M, Remuzzi G. Overview of complement activation and regulation. *Semin Nephrol.* (2013) 33:479–92. doi: 10.1016/j.semnephrol.2013.08.001
37. Schmidt CQ, Herbert AP, Hocking HG, Uhrin D, Barlow PN. Translational mini-review series on complement factor H: structural and functional correlations for factor H. *Clin Exp Immunol.* (2008) 151:14–24. doi: 10.1111/j.1365-2249.2007.03553.x
38. Jokiranta TS, Hellwage J, Koistinen V, Zipfel PF, Meri S. Each of the three binding sites on complement factor H interacts with a distinct site on C3b. *J Biol Chem.* (2000) 275:27657–62. doi: 10.1074/jbc.M002903200
39. Keir LS, Firth R, Aponik L, Feitelberg D, Sakimoto S, Aguilar E, et al. VEGF regulates local inhibitory complement proteins in the eye and kidney. *J Clin Invest.* (2017) 127:199–214. doi: 10.1172/JCI86418
40. Roy S, Ha J, Trudeau K, Beglova E. Vascular basement membrane thickening in diabetic retinopathy. *Curr Eye Res.* (2010) 35:1045–56. doi: 10.3109/02713683.2010.514659
41. Rutar M, Valter K, Natoli R, Provis JM. Synthesis and propagation of complement C3 by microglia/monocytes in the aging retina. *PLoS ONE.* (2014) 9:e93343. doi: 10.1371/journal.pone.0093343
42. Calippe B, Augustin S, Beguier F, Charles-Messance H, Poupel L, Conart JB, et al. Complement factor H inhibits CD47-mediated resolution of inflammation. *Immunity.* (2017) 46:261–72. doi: 10.1016/j.immuni.2017.01.006
43. Chuang HN, van Rossum D, Sieger D, Siam L, Klemm F, Bleckmann A, et al. Carcinoma cells misuse the host tissue damage response to invade the brain. *Glia.* (2013) 61:1331–46. doi: 10.1002/glia.22518
44. Xu H, Chen M. Targeting the complement system for the management of retinal inflammatory and degenerative diseases. *Eur J Pharmacol.* (2016) 787:94–104. doi: 10.1016/j.ejphar.2016.03.001
45. Martinez FO, Gordon S. The M1 and M2 paradigm of macrophage activation: time for reassessment. *F1000Prime Rep.* (2014) 6:13. doi: 10.12703/P6-13
46. del Zoppo GJ, Frankowski H, Gu YH, Osada T, Kanazawa M, Milner R, et al. Microglial cell activation is a source of metalloproteinase generation during hemorrhagic transformation. *J Cereb Blood Flow Metab.* (2012) 32:919–32. doi: 10.1038/jcbfm.2012.11

Conflict of Interest: The authors declare that the research was conducted in the absence of any commercial or financial relationships that could be construed as a potential conflict of interest.

frontiers in Immunology

ORIGINAL RESEARCH
published: 12 February 2020
doi: 10.3389/fimmu.2020.00215

Bacillus S-Layer-Mediated Innate Interactions During Endophthalmitis

Md Huzzatul Mursalin[1], *Phillip S. Coburn*[2,3], *Erin Livingston*[1], *Frederick C. Miller*[4], *Roger Astley*[2,3], *Ana L. Flores-Mireles*[5] *and Michelle C. Callegan*[1,2,3]*

[1] Department of Microbiology and Immunology, University of Oklahoma Health Sciences Center, Oklahoma City, OK, United States, [2] Department of Ophthalmology, University of Oklahoma Health Sciences Center, Oklahoma City, OK, United States, [3] Dean McGee Eye Institute, Oklahoma City, OK, United States, [4] Department of Cell Biology and Department of Family and Preventive Medicine, University of Oklahoma Health Sciences Center, Oklahoma City, OK, United States, [5] Department of Biological Sciences, University of Notre Dame, South Bend, IN, United States

Bacillus endophthalmitis is a severe intraocular infection. Hallmarks of *Bacillus* endophthalmitis include robust inflammation and rapid loss of vision. We reported that the absence of *Bacillus* surface layer protein (SLP) significantly blunted endophthalmitis severity. Here, we further investigated SLP in the context of *Bacillus*-retinal cell interactions and innate immune pathways to explore the mechanisms by which SLP contributes to intraocular inflammation. We compared phenotypes of Wild-type (WT) and SLP deficient (Δ*slpA*) *Bacillus thuringiensis* by analyzing bacterial adherence to and phagocytosis by human retinal Muller cells and phagocytosis by mouse neutrophils. Innate immune receptor activation by the *Bacillus* envelope and purified SLP was analyzed using TLR2/4 reporter cell lines. A synthetic TLR2/4 inhibitor was used as a control for this receptor activation. To induce endophthalmitis, mouse eyes were injected intravitreally with 100 CFU WT or Δ*slpA B. thuringiensis*. A group of WT infected mice was treated intravitreally with a TLR2/4 inhibitor at 4 h postinfection. At 10 h postinfection, infected eyes were analyzed for viable bacteria, inflammation, and retinal function. We observed that *B. thuringiensis* SLPs contributed to retinal Muller cell adherence, and protected this pathogen from Muller cell- and neutrophil-mediated phagocytosis. We found that *B. thuringiensis* envelope activated TLR2 and, surprisingly, TLR4, suggesting the presence of a surface-associated TLR4 agonist in *Bacillus*. Further investigation showed that purified SLP from *B. thuringiensis* activated TLR4, as well as TLR2 *in vitro*. Growth of WT *B. thuringiensis* was significantly higher and caused greater inflammation in untreated eyes than in eyes treated with the TLR2/4 inhibitor. Retinal function analysis also showed greater retention of A-wave and B-wave function in infected eyes treated with the TLR2/4 inhibitor. The TLR2/4 inhibitor was not antibacterial *in vitro*, and did not cause inflammation when injected into uninfected eyes. Taken together, these results suggest a potential role for *Bacillus* SLP in host-bacterial interactions, as well as in endophthalmitis pathogenesis via TLR2- and TLR4-mediated pathways.

Keywords: ocular infection, *Bacillus*, S-layer, immune response, inflammation, endophthalmitis, TLRs

OPEN ACCESS

Edited by:
Andrew W. Taylor,
Boston University, United States

Reviewed by:
Ashok Kumar,
Wayne State University, United States
Robert M. Shanks,
University of Pittsburgh, United States
Anthony St. Leger,
University of Pittsburgh, United States

***Correspondence:**
Michelle C. Callegan
michelle-callegan@ouhsc.edu

Specialty section:
This article was submitted to Immunological Tolerance and Regulation, a section of the journal Frontiers in Immunology

Received: *21 October 2019*
Accepted: *27 January 2020*
Published: *12 February 2020*

Citation:
Mursalin MH, Coburn PS, Livingston E, Miller FC, Astley R, Flores-Mireles AL and Callegan MC (2020) Bacillus S-Layer-Mediated Innate Interactions During Endophthalmitis. Front. Immunol. 11:215. doi: 10.3389/fimmu.2020.00215

INTRODUCTION

Endophthalmitis is a microbial infection of the posterior segment of the eye (1–6). Microbes can enter this part of the eye following a penetrating injury to the globe (post-traumatic), surgery or intraocular injection (post-operative), or following hematogenous spread from another infection site (endogenous) (7–15). Hallmarks of this disease include intraocular inflammation and retinal damage, resulting in some degree of vision loss. Unfortunately, blindness can occur and removal of the globe may be necessary, even when prompt and aggressive therapeutic measures are taken (5, 16–19). Endophthalmitis caused by *Bacillus* spp is more devastating compared to endophthalmitis caused by other bacterial pathogens associated with this disease (7, 20). Among members of the *Bacillus cereus sensu lato* group (comprised of *Bacillus anthracis, Bacillus cereus,* and *Bacillus thuringiensis*), only *B. cereus* and *B. thuringiensis* have been reported as the causative agents of intraocular infection (21–25). Significant vision loss has been reported to occur in the majority of *Bacillus* endophthalmitis cases, with half of those devastating cases resulting in removal of the globe (enucleation) (26–32). *Bacillus* endophthalmitis is indeed a medical emergency, and its rapid and severe course requires immediate therapeutic attention to prevent further deterioration of the eye (33–36). At present, there is no consistently effective therapeutic strategy which mitigates vision loss during severe cases of endophthalmitis, including those caused by *B. cereus* (16, 17, 37–41). The practice of adding anti-inflammatory agents to antibiotics has not proven effective in arresting inflammation and vision loss (42–45). It is clear that other therapeutic strategies are needed to prevent the sight-threatening consequences of this infection.

B. cereus spp are Gram-positive, motile, β-hemolytic, spore-forming rods, and are widely disseminated in nature (23, 24). We reported that the *Bacillus cereus* cell wall, and secreted toxins and proteases contributed to the pathogenicity of experimental endophthalmitis (5, 19, 46, 47). The PlcR quorum sensing system controls the synchronized synthesis of a majority of these extracellular virulence factors and is therefore important in *Bacillus* intraocular virulence (48–51). The absence of individual *B. cereus* toxins did not blunt intraocular virulence (19, 47). However, in the absence of PlcR, we observed delayed evolution, but not complete attenuation of *Bacillus* endophthalmitis, suggesting the contribution of the bacterial cell wall or other components to this disease (49).

We reported that metabolically inactive *B. cereus* triggered robust intraocular inflammation, suggesting that cell wall components contribute to the activation of pro-inflammatory pathways (5). *B. cereus* have an architecturally unique envelope. In addition to peptidoglycan, lipoteichoic acid, and lipoproteins, which are all common among Gram-positive ocular pathogens, the envelope of some *B. cereus* has flagella and a paracrystalline surface protein called the S-layer protein (SLP) (52–56). Structurally, SLPs are widely diverse among species and sequence similarities from different species are low.

Since SLPs are major surface antigens, the contributions of SLPs to microbial pathogenesis have been studied in some model organisms (56–63). As the outermost layer of the surface of some bacterial strains, SLPs promote adherence of bacteria to cell membranes and extracellular matrix components, and also contribute to biofilm formation (64–68). SLPs also act as barrier, protecting bacteria from complement-mediated phagocytosis and killing (69–72). A recent report from our laboratory demonstrated that the absence of *Bacillus* SlpA significantly reduced endophthalmitis disease severity in mice (73). We also demonstrated that *Bacillus* SLP preparations activated nuclear factor kappa-light-chain-enhancer of activated B cells (NF-κB) and induced the expression of inflammatory mediators from retinal cells (73). However, the underlying mechanisms by which SLPs impact endophthalmitis pathogenesis remains unclear.

The ocular environment is immune privileged, and its inner tissues contain different types of cells that not only maintain the structural integrity and homeostasis of this tissue, but also act as innate immune cells which express several innate receptors (74–81). During endophthalmitis, TLRs on retinal cells sense invading microbes and induce the production of inflammatory mediators, which leads to recruitment of polymorphonuclear neutrophils (PMN) into the eye (79, 82–84). Almost all TLRs signal through the myeloid differentiation primary response gene-88 (MyD88) dependent pathway. In addition to MyD88 pathway, TLR4 can mediate signaling through the Toll/interleukin-1 receptor (TIR) domain containing adaptor-inducing interferon-β (TRIF) pathway (85–88). We reported that the inflammatory response in *Bacillus* endophthalmitis is primarily facilitated through TLR2 and TLR4, but not through TLR5 (89–91). The absence of TLR2 or TLR4 resulted in less PMN infiltration, inflammatory mediator production, and pathological damage during *Bacillus* endophthalmitis (90, 91). Blocking TLRs in this disease may effectively blunt inflammation. Identifying *B. cereus* ligands that trigger these innate pathways may help us to more clearly understand the pathological events of this disease.

Bacillus endophthalmitis is at or near the top of the list of rapidly blinding ocular diseases, but the level of understanding of the host/pathogen relationship in this disease is fairly limited. The earliest host response in *Bacillus* endophthalmitis is the activation of TLRs that drive the intense intraocular inflammation. Since SLPs activated NF-κB and triggered the production of proinflammatory mediators in human retinal Muller cells, we hypothesized that *B. cereus* SLPs initiate early events in endophthalmitis pathogenesis through interactions with retinal cells and by activating innate pathways. Results from this study will broaden our understanding about the mechanisms of early and potentially damaging immune response and may aid in the development of potential therapeutics to prevent inflammation and vision loss during *Bacillus* endophthalmitis.

MATERIALS AND METHODS

Bacterial Strains

B. thuringiensis subsp. galleriae NRRL 4045 (WT) or its isogenic SLP deficient mutant (Δ*slpA*) (73, 92) were used to initiate experimental endophthalmitis in mice, as previously described (89–91, 93–98). *Staphylococcus aureus* strain 8325-4, *Enterococcus faecalis* strain E99, *Staphylococcus epidermidis* ATCC 12228, and *Streptococcus pneumoniae* strain TIGR4 were used for the preparation of bacterial cell envelopes.

Bacterial Adherence Assay

To quantify bacterial attachment to human retinal Muller cells (MIO-M1; a kind gift from Dr. Astrid Limb, UCL Institute of Ophthalmology, London), human retinal pigment epithelial cells (ARPE-19; American Type Culture Collection, Manassas, VA), and retinal photoreceptor-like 661W cells (99), we used an aerobic bacterial adherence assay. Immortalized human retinal pigmented epithelial (ARPE-19) and Muller cells were cultured in Dulbecco's Modified Eagle's Medium (DMEM)/F-12 (GIBCO, Grand Island, NY) supplemented with 10% fetal bovine serum (FBS, Sigma Aldrich, St. Louis MO) and 1% Pen Strep (GIBCO) Retinal photoreceptor-like 661W cells were cultured in DMEM containing GlutaMAX^{TM}-l (GIBCO), supplemented with 10% (v/v) FBS (100–103). All cells were maintained in a humidified 5% CO_2 incubator at 37°C.

Confluent monolayers of each of these cell types ($\sim 2 \times 10^6$ cells) were grown in 6-well plates, and transferred to antibiotic- and serum-free DMEM 6 h prior to performing the adherence assay. Overnight cultures of WT and Δ*slpA B. thuringiensis* were harvested by centrifugation and washed twice with DMEM to exclude the effects of secreted proteins, including any toxins. Antibiotic- and serum-free medium were removed from the cells, and bacteria were added to the wells at a multiplicity of infection (MOI) of 20 in a total volume of 2 ml DMEM. Equal numbers of WT and Δ*slpA B. thuringiensis* bacteria were added to cell free wells as controls. Cell-free controls were used to verify whether bacteria adhered to the plastic surface of the six- well plates. After a 40 min incubation in a humidified 5% CO_2 incubator at 37°C, retinal cells and adherent bacteria were washed twice with PBS. Adherent cells were then removed with a tissue cell scraper, vortexed, and serially diluted to quantify the adherent bacteria. The percent of adherent bacterial cells was calculated as the ratio of recovered bacteria to input bacteria multiplied by 100 (63, 66, 67, 104).

Isolation of Primary Neutrophils From Mice

Primary neutrophils were collected from mouse bone marrow by using a neutrophil isolation kit (MACS, Miltnyl Biotech, Gladbach, Germany) according to the manufacturer's instructions. Femurs were harvested from adult C57BL/6J mice. Bone marrow was collected in a 50 mL Falcon tube containing RPMI media (GIBCO) with 10% FBS (Sigma Aldrich) using a 10 ml syringe. The bone marrow was then centrifuged and washed with wash buffer (PBS, pH 7.2, 0.5% bovine serum albumin (BSA), and 2 mM EDTA). Cells were counted using a hemocytometer. For every 5×10^7 total cells, 200 μL of wash buffer and 50 μL neutrophil biotin-antibody cocktail were added. Cells were mixed and incubated for 10 min at 4°C. Cells were then washed and the pellet was resuspended in 400 μL of wash buffer and 100 μL of anti-biotin microbeads. Cells were mixed and incubated at 4°C. After 15 min, cells were washed and resuspended to 10^8 cells in 500 μL of buffer. For magnetic separation, an appropriate MACS column and separator were chosen according to the number of total cells and number of neutrophils. The LS column was used and placed inside a MACS separator. A 15 mL tube was placed under the column and the column was washed with 3 mL of wash buffer. When the wash buffer was completely removed, the 15 mL tube was replaced with a new one. The total sample (500 μL) was then loaded onto the column, and 3 mL of wash buffer was added 3 times onto the column and cells were collected. Cells were counted and centrifuged at 100 × *g* for 10 min, and resuspended in RPMI medium (96, 105, 106). One group of isolated cells was then immunolabeled with Ly6G and CD11 antibodies, washed, and fixed as previously described (107). Samples were analyzed using a MacsQuant flow cytometer and MacsQuantify software (Miltenyi Biotec). Neutrophil purity in each isolation was ∼85.6%.

Bacterial Phagocytosis Assay

Human retinal Muller cells (MIO-M1), neutrophil like HL-60 cells, and mouse primary neutrophils were used in a gentamicin exclusion assay to assess the impact of SLPs on phagocytosis. Undifferentiated HL-60 cells were differentiated into neutrophil like-cells by adding 1.3% DMSO for 6 days (108–110). After 6 days, cells had neutrophil-like morphology, as confirmed by microscopy (5). Approximately 1×10^5 of these cells were incubated at 20 MOI ($\sim 2 \times 10^6$) with WT or Δ*slpA B. thuringiensis* for 90 min. One group of cells was washed and treated with 200 μg/mL gentamicin for 60 min to kill all extracellular bacteria, and another group of cells was centrifuged, washed and lysed with 0.5% Triton X-100. This later group contained intra- and extracellular bacteria. After 60 min, the gentamicin-treated cells were centrifuged, washed to remove the residual antibiotic, and lysed with 0.5% Triton X-100. This group represented only the intracellular bacteria. Equal numbers of WT and Δ*slpA B. thuringiensis* ($\sim 2 \times 10^6$ in 2 mL) were incubated with 200 μg/mL gentamicin for 60 min and used as a control (96, 104, 111). CFU were enumerated by serial dilution and plating.

Preparation of Bacterial Cell Envelopes

B. thuringiensis subsp. galleriae NRRL 4045 (WT) and its isogenic SLP deficient mutant (Δ*slpA*), *S. aureus* 8325-4, *E. faecalis* E99, and *S. epidermidis* strain ATCC 12228 were each grown for 18 h at 37°C in brain heart infusion (BHI; VWR, Radnor PA) broth and 20 μl aliquots were removed, serially diluted, and plated to quantify bacteria. *S. pneumonia* was grown in Todd Hewitt Broth (THB; VWR) with 0.5% yeast extract and also grown for 18 h at 37°C. Cultures were harvested by centrifugation at 3,000 × *g* for 15 min at 4°C, and washed twice with PBS (pH 7.4) in endotoxin free water (HyPure cell culture grade water, GE Healthcare Life Science, Logan UT). Pellets were resuspended with equal volumes of PBS and heat inactivated at 65°C for 15 min. Sterility was tested by spread plating an aliquot of each culture onto a BHI agar plate. Cells were then centrifuged at 3,000 × *g* for 15 min, and pellets were washed twice with equal volumes of PBS. The bacterial pellets were then lyophilized, resuspended with equal volumes of PBS, and diluted to the required concentrations for use in the TLR2 and TLR4 reporter assays (5, 73, 112).

Purification of *Bacillus* SLP

WT and Δ*slpA B. thuringiensis* were grown for 18 h at 37°C in BHI, harvested by centrifugation at 3,000 × *g* for 15 min at

4°C, and washed twice with chilled HyPure cell culture grade water (GE Healthcare Life Science). As previously described, pellets were then resuspended in 1/10th of the initial volume of 3M guanidine hydrochloride (GHCL; pH 2.5; Sigma Aldrich) and incubated at 37°C for 1 h. The extracted SLP was separated from the pellets by centrifugation at 18,000 × *g* at 4°C for 15 min. Supernatants were dialyzed (Pur-A-Lyzer™ 50kDa dialysis kit, Sigma Aldrich) against 2L of tris/HCL (pH 8.0; Research Products International Corporation, Mt. Prospect, IL) at 4°C for 24 h with four exchanges of dialysis buffer to remove residual GHCL. Protein concentrations were quantified by bicinchoninic acid assay (Sigma Aldrich) according to the manufacturer's instructions. Endotoxin levels were quantified using the Pierce LAL chromogenic endotoxin kit (ThermoFisher Scientific, MA) according to the manufacturer's instructions. Purity was confirmed by PAGE and Coomassie staining, as previously described (73, 92).

TLR2/TLR4 Reporter Assay

HEK-Blue™ cells were purchased from Invivogen (San Diego, CA) and used as previously described (73). HEK-Blue™ hTLR2 and HEK-Blue™ hTLR4 were used for the recognition of TLR2 and TLR4 agonists, respectively. hTLR2 and hTLR4 cells were cultured (up to 20 passages) in DMEM containing GlutaMAX™-l (GIBCO), supplemented with 10% (v/v) FBS (Sigma Aldrich) and HEK-Blue Selection antibiotics (Invivogen) in a humidified 5% CO_2 incubator at 37°C. hTLR2 and hTLR4 reporter cell lines were treated with bacterial envelopes, or SLP fractions from WT or Δ*slpA B. thuringiensis* with or without the synthetic TLR2/4 inhibitor OxPAPC (Invivogen) to assess receptor activation/inhibition (73, 89).

B. thuringiensis, *S. aureus*, *S. epidermidis* at 10^6 envelopes/20 μl, and *E. faecalis* and *S. pneumoniae* at 10^8 envelopes/20 μl were used to assess TLR2/4 activation. The envelope inoculum number was determined based on the equivalent number of viable organisms present during early infection (5). To measure the TLR2/4 activation by purified SLP, 10 μg/ml SLP from WT *B. thuringiensis* was used. The SLP fraction from Δ*slpA B. thuringiensis* was used as an extract control. In both assays, Pam3Csk4 (0.25 ng/mL; Invivogen) was used as a positive control for the hTLR2, and a negative control for the hTLR4 reporter assays. LPS (100 ng/mL; Invivogen) was used as a positive control for the hTLR4, and a negative control for the hTLR2 reporter assays. Endotoxin free water (GE Healthcare Life Science) was used as a negative control for both hTLR2 and hTLR4 reporter assays. To inhibit TLR2/4 activation, an oxidized phospholipid OxPAPC (0.15μg/μL) was used with Pam3Csk4, LPS, and purified SLP (113). Samples, controls, and inhibitors (20 μL) were added to appropriate wells of 96-well plates. hTLR2 and hTLR4 reporter cells at 50 to 80% confluency were washed with pre-warmed PBS (pH 7.4; GIBCO). After detaching the cells with PBS, hTLR2 cells were resuspended to 5.0×10^4 and hTLR4 cells to 2.5×10^4 in 180 μl of HEK-Blue™ Detection medium (Invivogen). For the OxPAPC-treated groups, 5.0×10^4 /160 μl hTLR2 and 2.5×10^4/160 μl hTLR4 cell suspensions were prepared. Each cell suspension was immediately added into the appropriate wells of the 96-well plates, and incubated for 14 h at 37°C in 5% CO_2. Activation of TLR2 and TLR4 (production of SEAP) was measured using a spectrophotometer at 620-655nm. TLR2/4 activation was presented as percent of TLR2/4 activation relative to the positive controls Pam3Csk4 and LPS (73, 89, 114).

Mice and Intraocular Infection

All *in vivo* experiments were performed with C57BL/6J mice purchased from Jackson Labs (Bar Harbor ME, Stock No. 000664). Mice were housed on a 12 h on/12 h off light cycle in biohazard level 2 conditions and acclimated for at least 2 weeks to equilibrate their microbiota. Mice were 8–10 weeks of age at the time of the experiments. Mice were sedated using a combination of ketamine (85 mg/kg body weight; Ketathesia, Henry Schein Animal Health, Dublin, OH) and xylazine (14 mg/kg body weight; AnaSed, Akorn Inc., Decatur, IL). Four groups of C57BL/6J mice were used in this experiment. The first two groups of mice were infected with 100 CFU WT *B. thuringiensis*/0.5 μl BHI, and the third group was infected with 100 CFU Δ*slpA B. thuringiensis*/0.5 μl BHI into the right eye using a sterile glass capillary needle, as previously described (73, 89–91, 93, 95–98). The fourth group was not infected. At 4 h postinfection, the second group of infected mice and fourth group of uninfected mice were intravitreally treated with 30 ng/μL OxPAPC. At 10 h postinfection, electroretinography was performed prior to euthanasia by CO_2 inhalation, and then eyes were harvested for quantitation of viable intraocular bacteria, retinal function, and PMN infiltration, and analysis of ocular architecture by histology, as described below.

Intraocular Bacterial Quantitation

As previously described (73, 89–91, 93, 94, 96–98), eyes were harvested from euthanized mice at specific time points, homogenized in 400 μl PBS with sterile 1-mm glass beads (BioSpec Products, Inc., Bartlesville OK), serially diluted 10-fold in PBS, and plated onto BHI agar plates.

For *in vivo* bacterial growth analysis at different time points, experimental endophthalmitis was induced by intravitreally injecting approximately 100 CFU WT *B. thuringiensis* in 0.5 μl BHI into the right eyes of mice. At 4 h postinfection, one group of infected eyes was treated with OxPAPC, and another group served as the untreated control. At 2 h intervals thereafter, eyes were harvested for quantitation of intraocular bacterial growth (73, 89–91, 93, 94, 96–98).

In vitro Bacterial Quantitation

Potential antimicrobial activity of OxPAPC was assessed *in vitro*. WT *B. thuringiensis* was cultured for 18 h at 37°C with aeration in BHI medium. The culture was then diluted to 10^3 CFU/mL in fresh BHI containing 0.1, 1, or 10 μg/mL OxPAPC, and incubated for 18 h at 37°C. At 2 h intervals during this period, 20 μl aliquots were serially diluted 10-fold in PBS, and plated onto BHI agar plates (73, 93).

Retinal Function Analysis

Electroretinography (ERG) was used to quantify retinal function as previously described (5, 47, 51, 73, 91, 93, 94, 96, 97) in *Bacillus*-infected and OxPAPC-treated eyes. After infection/treatment, mice were dark adapted for 6 h. Mice were then anesthetized as described above, and pupils were dilated

with topical phenylephrine (Akorn, Inc., IL). Two gold wire electrodes were placed onto each cornea. Reference electrodes were attached to the tail and forehead. Eyes were then stimulated by five flashes of white light (1,200 cd s/m^2) and retinal responses were recorded as A-wave (retinal photoreceptor cell function) and B-wave (bipolar cell, Muller cell, and second order neuronal function) amplitudes for infected eyes and compared with the uninfected eyes of the same animal (Espion E2 software, Diagnosys LLC, Lowell MA) (5, 47, 51, 73, 91, 93, 94, 96, 97).

Histology

Infected/treated eyes were harvested from euthanized mice at 10 h postinfection. Harvested eyes were incubated in High Alcoholic Prefer fixative for 30 min, and then transferred to 70% ethanol. Paraffin-embedded eyes were sectioned and stained with hematoxylin and eosin (H&E) (73, 89, 90, 94, 96–98).

Inflammatory Cell Influx

Inflammatory cell infiltration was estimated by quantifying myeloperoxidase (MPO) using a sandwich ELISA (Hycult Biotech, Plymouth Meeting PA), as previously described. At 10 h postinfection, eyes were harvested, transferred into PBS supplemented with proteinase inhibitor cocktail (Roche Diagnostics, Indianapolis, IN) and homogenized using 1-mm sterile glass beads (BioSpec Products, Inc.). Uninfected eye homogenates were the negative controls. The lower limit of detection for this assay was 2 ng/ml (73, 89, 91, 96–98).

Statistics

GraphPad Prism 7 was used for the statistical analysis (GraphPad Software, Inc., La Jolla, CA). Mann-Whitney *U*-test was used for statistical comparisons unless otherwise specified. *P*-values of <0.05 were considered significant (93, 94, 96, 115). For all assays, *N*-values represented single biological replicates.

RESULTS

SlpA Contributes to the Adherence of *Bacillus* to Retinal Cells

As *Bacillus* migrate within the posterior segment of the eye, organisms physically interact with retinal cells (5, 73). The first step in this interaction is adherence, and we hypothesized that SLPs mediated that interaction. An experiment to evaluate the role of SlpA in bacterial attachment to retinal cells is depicted in **Figure 1**. In the absence of SlpA, significant reductions in percent Δ*slpA B. thuringiensis* adherence were seen with human retinal Muller MIO-M1 cells ($P < 0.0001$, **Figure 1A**), retinal pigment epithelial cells (ARPE-19) ($P = 0.0022$, **Figure 1B**), and retinal photoreceptor-like 661W cells ($P = 0.0022$, **Figure 1C**) compared to that of WT *B. thuringiensis*. No bacteria were recovered from cell-free controls, suggesting no adherence to the plastic surface of the wells. These findings demonstrated that SlpA contributed to bacterial adherence to retinal cells, suggesting that SLPs may play a role in bacterial adherence to retinal cells during the early stage of *Bacillus* endophthalmitis.

SlpA Protects *Bacillus* From Phagocytosis

Interactions between *Bacillus* and retinal and immune cells may be important in initiating the subsequent immune response. A gentamicin (Gen) exclusion phagocytosis assay was used to determine the role of SlpA in internalization by human retinal Muller cells (MIO-M1), neutrophil like HL-60 cells, and mouse primary neutrophils (**Figure 2**). Significant increases in internalization of Δ*slpA B. thuringiensis* were seen with human retinal Muller cells ($P = 0.0122$, **Figure 2A**), neutrophil like HL-60 cells ($P = 0.0049$, **Figure 2B**), and mouse primary neutrophils ($P = 0.0002$, **Figure 2C**) compared to that of WT *B. thuringiensis*. No bacteria were recovered after the incubation with gentamicin, indicating that WT and Δ*slpA B. thuringiensis* were susceptible to the antibiotic. Taken together, these results demonstrated that SlpA directly interfered with internalization by human retinal Muller cells and professional phagocytic cells, suggesting that SLP may protect the pathogen from phagocytosis during active infection.

Bacillus Envelope Contains an Unexpected TLR4 Agonist

Mice which lack functional TLR2 or TLR4 have a reduced intraocular inflammatory response upon intravitreal challenge with *Bacillus* (90, 91), suggesting that this organism interacts with those receptors. Here, we investigated whether the envelopes of common Gram-positive endophthalmitis pathogens (WT and Δ*slpA B. thuringiensis*, *S. aureus*, *S. epidermidis*, *E. faecalis*, and *S. pneumoniae*) activated TLR2 and TLR4 in hTLR2 or hTLR4 reporter cell line assays (**Figure 3**). Envelope preparations from all five species activated TLR2 (**Figure 3A**). Surprisingly, only WT *B. thuringiensis* envelopes significantly activated TLR4 ($P = 0.0286$), whereas other Gram-positive endophthalmitis pathogens did not (**Figure 3B**). Activation of TLR4 was significantly higher ($P = 0.0286$) in WT *B. thuringiensis* than Δ*slpA*. These results suggest that the *Bacillus* envelope possesses universal TLR2 agonists and one or more unexpected TLR4 agonists.

SLP of *Bacillus* Is Necessary for Activation of Both TLR2 and TLR4

SLP from WT *B. thuringiensis* induced inflammatory mediator expression from retinal Muller cells by activating the canonical NF-κB pathway (73). Since the envelope of *B. thuringiensis* activated TLR2/4, we next determined whether its SLP activated TLR2 and TLR4 in similar assays. Purified SLP from WT *B. thuringiensis* activated TLR2 to a significantly higher degree than the extract control from Δ*slpA B. thuringiensis* ($P = 0.0003$; **Figure 4A**). Purified SLP from *B. thuringiensis* also significantly activated TLR4 to a greater degree than did the extract control from Δ*slpA B. thuringiensis* ($P = 0.0003$; **Figure 4B**). To further evaluate the activation of TLR2 and TLR4 by SLP, we included an oxidized phospholipid (OxPAPC) in the reporter assay to inhibit the activation of both TLR2 and TLR4. OxPAPC significantly inhibited TLR2 activation by the TLR2 agonist Pam3Csk4 and by

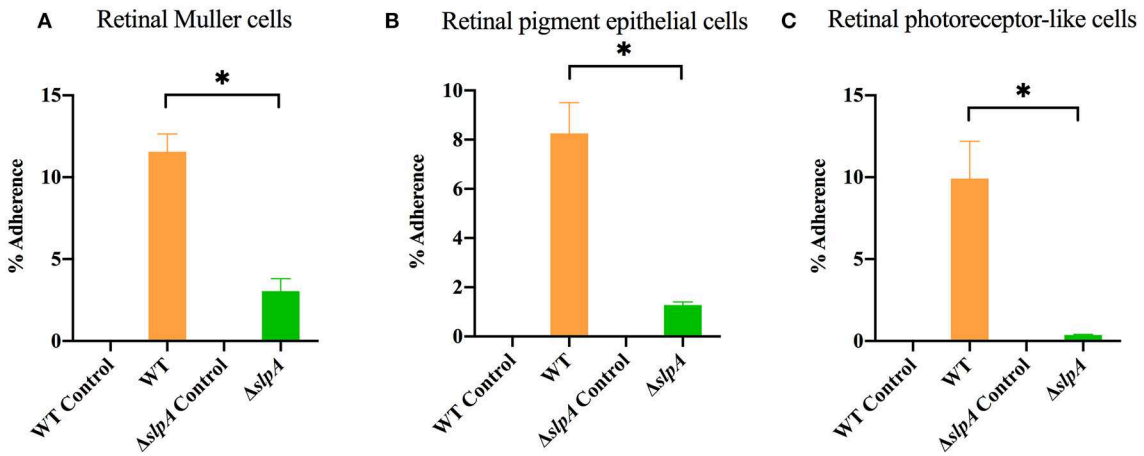

FIGURE 1 | *Bacillus* SLP contributes to adherence to retinal cells *in vitro*. Three different retinal cell types were incubated with WT *B. thuringiensis* or Δ*slpA B. thuringiensis* for 40 min to assess bacterial adherence. Compared to WT, Δ*slpA B. thuringiensis* demonstrated a significant reduction in adherence to **(A)** human retinal Muller MIO-M1 cells, **(B)** human retinal pigment epithelial (ARPE-19) cells, and **(C)** retinal photoreceptor-like 661W cells. WT and Δ*slpA B. thuringiensis* in cell-free wells served as controls. Values represent the mean ± SEM of $N \geq 5$ for at least two separate experiments; $^*P < 0.05$.

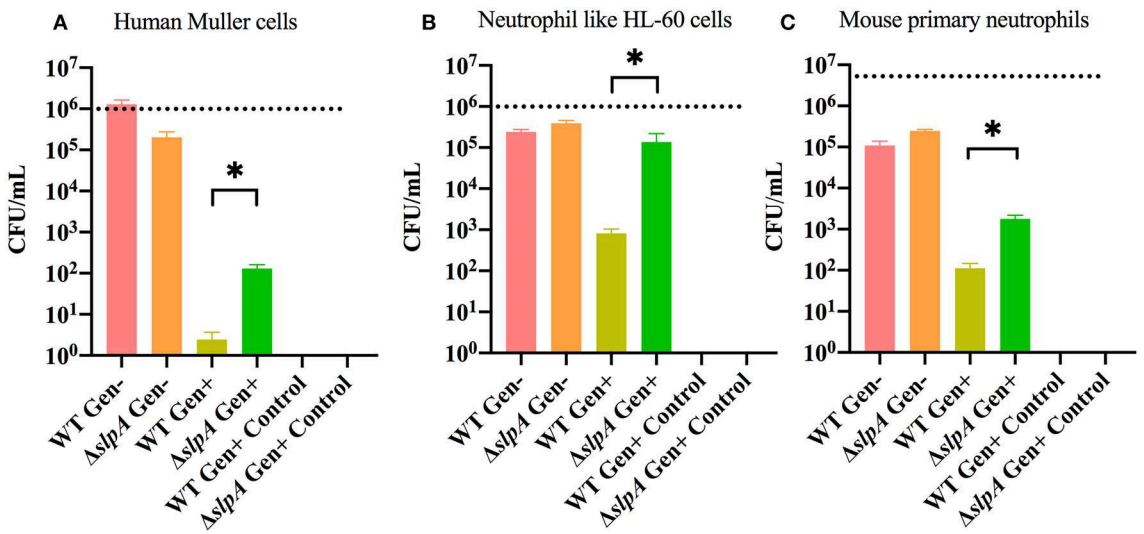

FIGURE 2 | *Bacillus* SLP provides protection from phagocytosis. Muller cells, neutrophil-like HL60 cells, and mouse primary neutrophils were incubated with WT or Δ*slpA B. thuringiensis* for 90 min. Cells were then treated with gentamicin for 60 min to kill external bacteria. Compared to WT *B. thuringiensis*, internalization of Δ*slpA B. thuringiensis* was significantly greater by **(A)** human retinal Muller cells, **(B)** neutrophil-like HL-60 cells, and **(C)** mouse primary neutrophils. Gen+, Gentamicin treated; Gen-, Gentamicin untreated. Values represent mean ± SEM of $N \geq 5$ for at least two separate experiments; $^*P < 0.05$. Dashed lines represent the initial bacterial inoculum.

purified SLP from WT *B. thuringiensis* ($P = 0.0022$; **Figure 4C**). OxPAPC also significantly reduced the activation of TLR4 by LPS and by purified SLP ($P = 0.0022$; **Figure 4D**) SLP-mediated TLR2 and TLR4 activation in OxPAPC treated groups were 74.7 and 70.7% lower than TLR2 or TLR4 activation in the untreated groups, respectively. Together these findings demonstrated that SLPs not only activated TLR2, but also TLR4. This suggests that SLP is a potent stimulator of both TLR2 and TLR4 innate pathways, and may contribute to the production of inflammatory mediators during experimental endophthalmitis.

Inhibition of TLR2/4 Activation Resulted in Reduced Bacterial Burden During Experimental *Bacillus* Endophthalmitis

There were no changes the intraocular bacterial burden in $TLR2^{-/-}$ or $TLR4^{-/-}$ mice infected with *B. cereus* (90, 91). Here, we investigated whether inhibition of both TLR2 and TLR4 activation affected bacterial growth during experimental endophthalmitis. **Figure 5A** depicts the experimental design. Inhibition of the TLR2/4 pathways by OxPAPC significantly reduced the bacterial load in WT infected mouse eyes relative

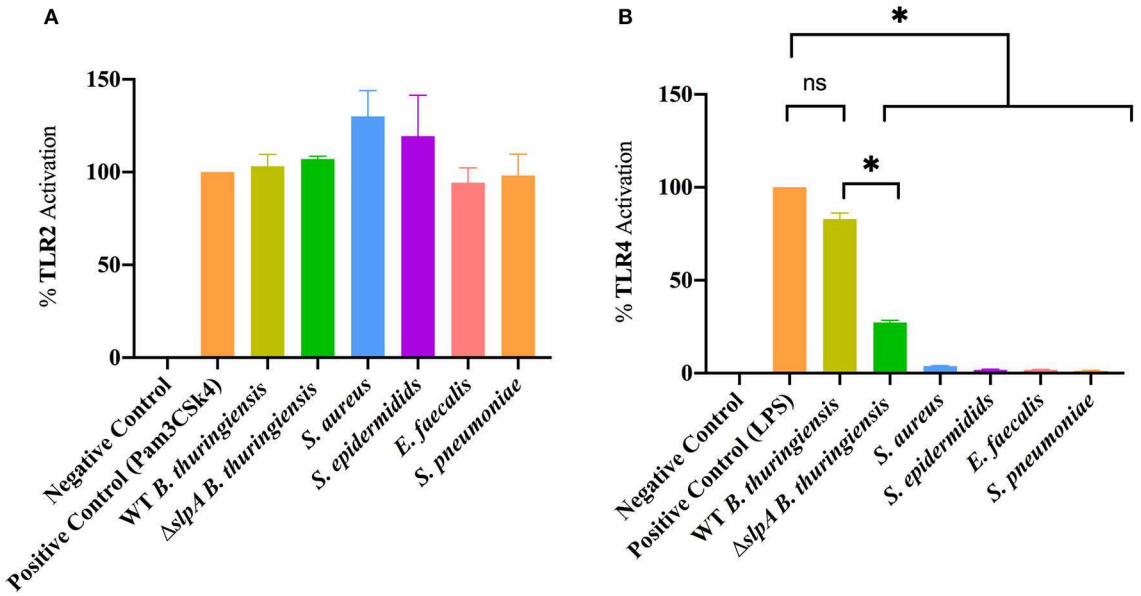

FIGURE 3 | *Bacillus* envelope possesses an unexpected TLR4 agonist. HEK-Blue^{TM} hTLR2 and hTLR4 reporter cells were incubated with envelope preparations of WT or Δ*slpA B. thuringiensis, S. aureus, S. epidermidis, E. faecalis*, or *S. pneumoniae* for 14 h at 37°C in 5% CO_2 **(A)** The envelopes of WT *and* Δ*slpA B. thuringiensis, S. aureus, S. epidermidis, E. faecalis*, and *S. pneumoniae* activated TLR2. **(B)** Among the five Gram-positive endophthalmitis pathogens, only the envelopes of WT *B. thuringiensis* activated TLR4. Values represent mean ± SEM of $N \geq 4$ for at least two separate experiments; *$P < 0.05$.

to that of untreated eyes ($P = 0.0007$; **Figure 5B**) at 10 h postinfection. There was no difference in bacterial load observed between WT and Δ*slpA* infected mouse eyes ($P = 0.3680$; **Figure 5B**). At this time, the growth rates of WT and Δ*slpA B. thuringiensis* infected eyes (2.2 and 1.9 h^{-1}) were faster than that in the WT-infected and OxPAPC treated eyes (0.76 h^{-1}). To determine whether OxPAPC possessed bactericidal activity, we analyzed WT *B. thuringiensis* growth in the presence of increasing concentrations (0.1, 1, and 10 μg/mL) of OxPAPC. As shown in **Figure 5C,** OxPAPC did not alter bacterial growth *in vitro* at any of the concentrations tested. To investigate whether this phenomenon of reduced bacterial load only occurred *in vivo*, we assessed bacterial growth at varying time points after infection after treatment with OxPAPC and observed that bacterial concentrations were significantly lower in OxPAPC treated groups at 8 h ($P = 0.0260$), 10 h ($P = 0.0043$) and 12 h ($P = 0.0152$) postinfection (**Figure 5D**). Taken together, these findings demonstrated that inhibition of TLR2/4 activation contributed to reduced bacterial burden during experimental *Bacillus* endophthalmitis.

Retinal Function Improved in the Absence of TLR2/4 Activation by SLP During Experimental *Bacillus* Endophthalmitis

Since the absence of individual TLRs (TLR2 or 4) and their adaptors (MyD88 and TRIF) resulted in retained retinal function in experimental *Bacillus* endophthalmitis (90, 91, 97), we investigated whether inhibition of both TLR2/4 by OxPAPC would have a similar outcome. Analysis of retinal function and the representative waveforms of eyes infected with WT, WT-infected and OxPAPC-treated, Δ*slpA B. thuringiensis*-infected, and OxPAPC-treated only is depicted in **Figure 6**. The A-wave amplitudes were significantly reduced in WT-infected eyes at 10 h postinfection ($P < 0.05$) to a retained response of ∼29%. Compared to WT-infected eyes, WT-infected/OxPAPC-treated, Δ*slpA*-infected, and OxPAPC-treated eyes showed significant retention of retinal function. At 10 h postinfection, the retained response of A-wave function in these groups was ∼100% (**Figure 6A**). The B-wave amplitudes were significantly reduced in the WT *B. thuringiensis*-infected eyes at 10 h postinfection ($P < 0.05$) to a retained response of ∼18% (**Figure 6B**). This response in eyes infected/treated with WT/OxPAPC, Δ*slpA B. thuringiensis*, and OxPAPC was retained to a significantly greater degree compared to that of WT-infected and untreated eyes. The retained responses of B-waves among these groups at 10 h postinfection was ∼79%. Representative waveforms demonstrating the differences in A- and B-wave amplitudes of eyes in these groups at 10 h postinfection are shown in **Figures 6C,D**. Together, these results demonstrated that WT-infected eyes treated with the TLR2/4 inhibitor OxPAPC retained greater retinal function compared to untreated WT *B. thuringiensis*-infected eyes. These results suggested that the activation of TLR2 and TLR4 innate pathways by SLP influenced the loss of retinal function during experimental endophthalmitis.

Inflammation Was Reduced and Ocular Architecture Was Preserved in the Absence of TLR2/4 Activation by SLP During Experimental *Bacillus* Endophthalmitis

PMN are the primary infiltrating cell type recruited to the site of infection during *Bacillus* endophthalmitis (6, 82, 98).

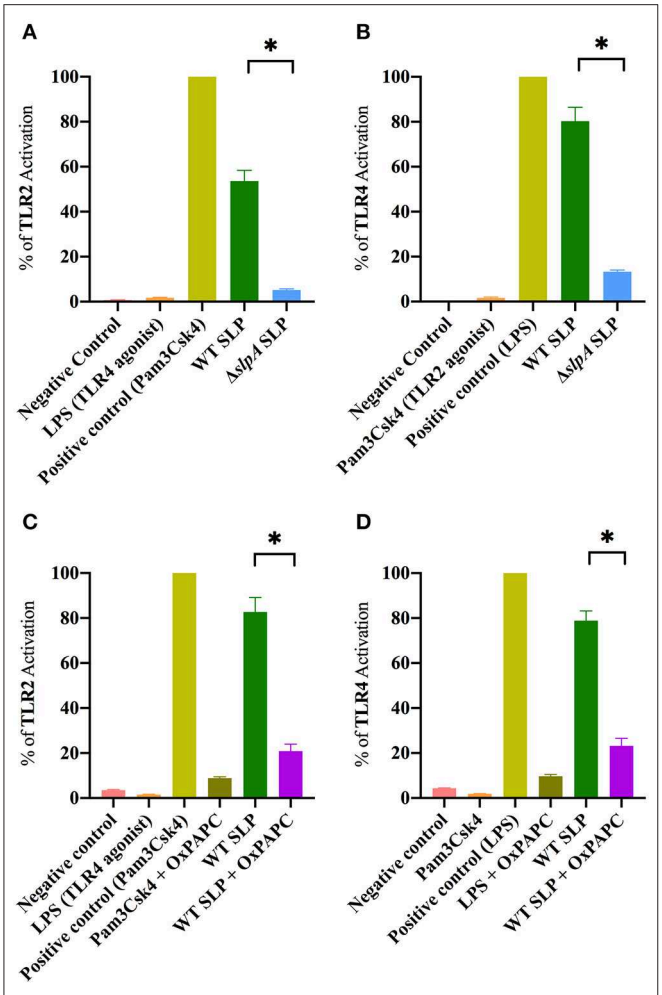

FIGURE 4 | *Bacillus* SLP is a potent activator of TLR2 and TLR4. **(A)** SLP from WT *B. thuringiensis* activated TLR2 to a significantly greater degree than did the extract control (Δ*slpA*). LPS, a TLR4 agonist, was used as a negative control. **(B)** WT SLP significantly activated TLR4 compared to the extract control (Δ*slpA*). Pam3Csk4, a TLR2 agonist, was used as a negative control. **(C)** Treatment with OxPAPC significantly inhibited TLR2 activation by the positive control Pam3Csk4 and WT SLP. **(D)** Treatment with OxPAPC significantly inhibited TLR4 activation by the positive control LPS and WT SLP. Values represent mean ± SEM of $N \geq 5$ for at least two separate experiments; $^*P < 0.05$.

Here, we examined the degree of inflammatory cell influx and retinal damage in WT-infected, WT-infected/OxPAPC-treated, Δ*slpA B. thuringiensis*-infected, and OxPAPC-treated eyes (**Figure 7**). PMN infiltration in the eye was estimated by quantifying myeloperoxidase (MPO) in eye homogenates. MPO concentrations were significantly greater at 10 h postinfection in WT-infected eyes compared to that of WT-infected/OxPAPC-treated ($P = 0.0016$), Δ*slpA*-infected ($P = 0.0022$), and OxPAPC-treated ($P = 0.0022$) eyes (**Figure 7A**). The levels of MPO in WT-infected/OXPAPC treated, Δ*slpA*-infected, and OXPAPC-treated eyes were 9-fold, 8-fold, and 38-fold lower compared to that of untreated WT-infected eyes. These results demonstrated that infection with Δ*slpA B. thuringiensis* and inhibition of the TLR2 and TLR4 pathways during experimental endophthalmitis each resulted in reduced MPO levels, indicating less PMN recruitment in these eyes.

A histological comparison of WT-infected, WT-infected/OxPAPC-treated, Δ*slpA*-infected, and OxPAPC-treated eyes is depicted in **Figure 7B**. At 10 h postinfection, the anterior and posterior segments of WT-infected/OxPAPC-treated, Δ*slpA*-infected, and OxPAPC-treated eyes were similar. The corneas and posterior segments of eyes in these groups had no inflammation and intact retinas. In contrast, untreated eyes infected with WT *B. thuringiensis* had substantial accumulation of infiltrating cells and fibrin in the posterior segment. Corneas in these eyes had significant edema, and retinal layers were detached and often indistinguishable. Together, these findings demonstrated that inhibition of the TLR2 and TLR4 pathways and infection with SlpA-deficient *B. thuringiensis* in experimental endophthalmitis had a similar outcome. In both cases, inflammation was reduced and ocular architecture was preserved. Taken together, these results suggest that SLP contributes to the pathogenesis of *Bacillus* endophthalmitis via TLR2 and TLR4.

DISCUSSION

The host-pathogen interaction is an early event that dictates the severity and outcome of an infectious disease (116). Although the ocular environment is an immune-privileged site, innate ocular immune defense mechanisms are capable of responding to invading pathogens (74, 75, 77, 78). Ocular defense mechanisms can be easily overwhelmed by infection with a pathogen that cannot be effectively cleared from the eye. *B. cereus* intraocular infection produces a more robust inflammatory response than other ocular bacterial pathogens such as *S. aureus*, *E. faecalis*, *S. epidermidis*, *S. pneumoniae*, *E. coli*, and *Klebsiella pneumoniae* (7, 73, 82, 117). In *Bacillus* endophthalmitis, within 4 h, PMNs move into the vitreous, and within 8 h into the retinal layers. PMNs not only can disrupt vision through bystander effects on cells in the retina, but their presence in the vitreous can also block the clarity of the visual axis (82, 98). Though *Bacillus* endophthalmitis is a rare intraocular infection, the potential to cause blindness is high, and better therapeutic strategies are needed to improve visual outcomes.

Compared to the envelopes of other Gram-positive intraocular pathogens, the envelope of *Bacillus* contains unique components such as flagella, pili, and a protein coat composed of SLPs (53–55, 60). Flagella aid in the rapid movement of *Bacillus* throughout all parts of the eye, from the initial site of infection into the anterior segment within 6–12 h (89). The absence of motility affected toxin production, and therefore, non-motile *B. cereus* caused less severe disease pathogenesis (19). We also reported that infection with pili-deficient *B. cereus* led to a reduced inflammatory response in the eye, suggesting the importance of pili in that aspect of this disease (93). In a recent report (73), we demonstrated that while the absence of SlpA did not change the growth, cytotoxicity, motility, hemolytic properties, or cell wall composition of

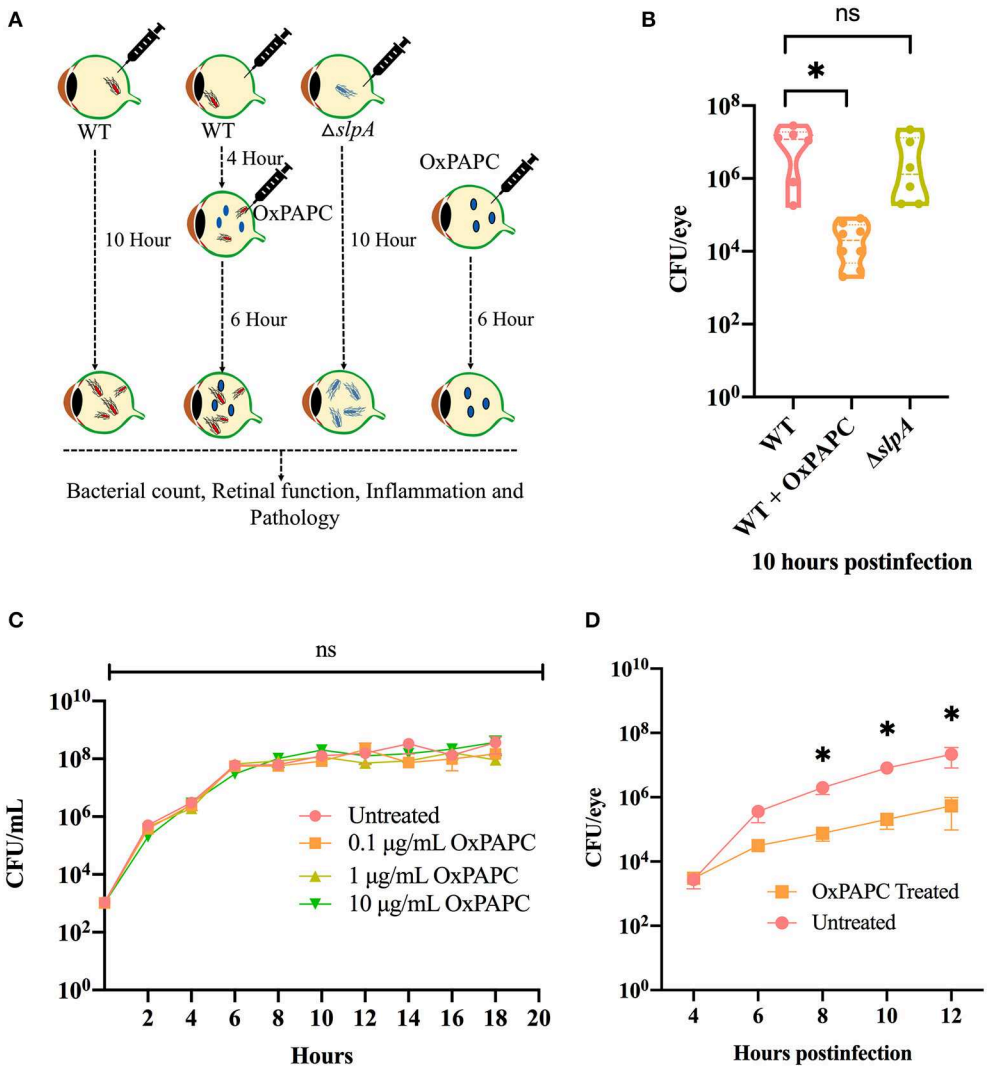

FIGURE 5 | OxPAPC treatment resulted in reduced intraocular bacterial load during *Bacillus* endophthalmitis. **(A)** Experimental design of *in vivo* inhibition of TLR2/4 activation. **(B)** C57BL/6J mouse eyes were infected with 100 CFU WT or Δ*slpA B. thuringiensis*. At 4 h postinfection WT infected eyes were treated with 30 ng/μL OxPAPC. At 10 h postinfection eyes were harvested, homogenized, and analyzed for bacterial growth. Compared to untreated WT-infected C57BL/6J mouse eyes, a significant reduction in bacterial burden was observed in the OxPAPC-treated group at 10 h postinfection. No difference in intraocular bacterial count was observed between WT and Δ*slpA* infected eyes at 10 h postinfection. Values represent mean ± SEM of log10 CFU/eye of $N \geq 5$ eyes for at least two separate experiments. **(C)** The *in vitro* growth of WT *B. thuringiensis* in BHI was not affected by the presence of 0.1, 1, or 10 μg/mL OxPAPC. Values represent the mean ± SEM of $N = 3$; multiple comparison, 2-way ANOVA **(D)** Treatment of eyes with OxPAPC 4 h after infection with 100 CFU of WT *B. thuringiensis* resulted in decreased bacterial growth. Data represent the mean ± SEM of log10 CFU/eye of $N \geq 5$ eyes per time point for at least two separate experiments; ns: $P > 0.05$, $^*P < 0.05$ at all time points.

B. thuringiensis, the absence of SlpA significantly reduced disease severity compared to severe disease caused by the WT parental strain experimental endophthalmitis. SLPs are a major contributor to the pathogenesis of *Bacillus* endophthalmitis (73), but the underlying mechanism by which SLPs contributes to pathogenesis were unknown.

SLPs form para-crystalline protein sheets that assemble on the bacterial surface (56). SLPs and their associated proteins facilitate numerous functions that are critical to cellular physiology and survival (57, 59). A primary function of SLPs are to promote colonization by contributing to the adherence to host tissue (68). It has been reported that SLP of *B. anthracis* helps the pathogen to adhere to HeLa cells, and infection with a SLP-deficient *B. anthracis* resulted in attenuated infection in guinea pigs (118). A recent report suggested that SLP of *Clostridium difficle* played an important role in the colonization to human intestinal epithelial cells by contributing to bacterial adherence (63). We have observed *B. cereus* and *B. thuringiensis* near the inner limiting membrane (ILM) of the retina during experimental endophthalmitis (5, 73). As physical contact between pathogen and the infected tissue is the initial event of any host-pathogen interaction, we compared whether SLPs influenced *Bacillus*

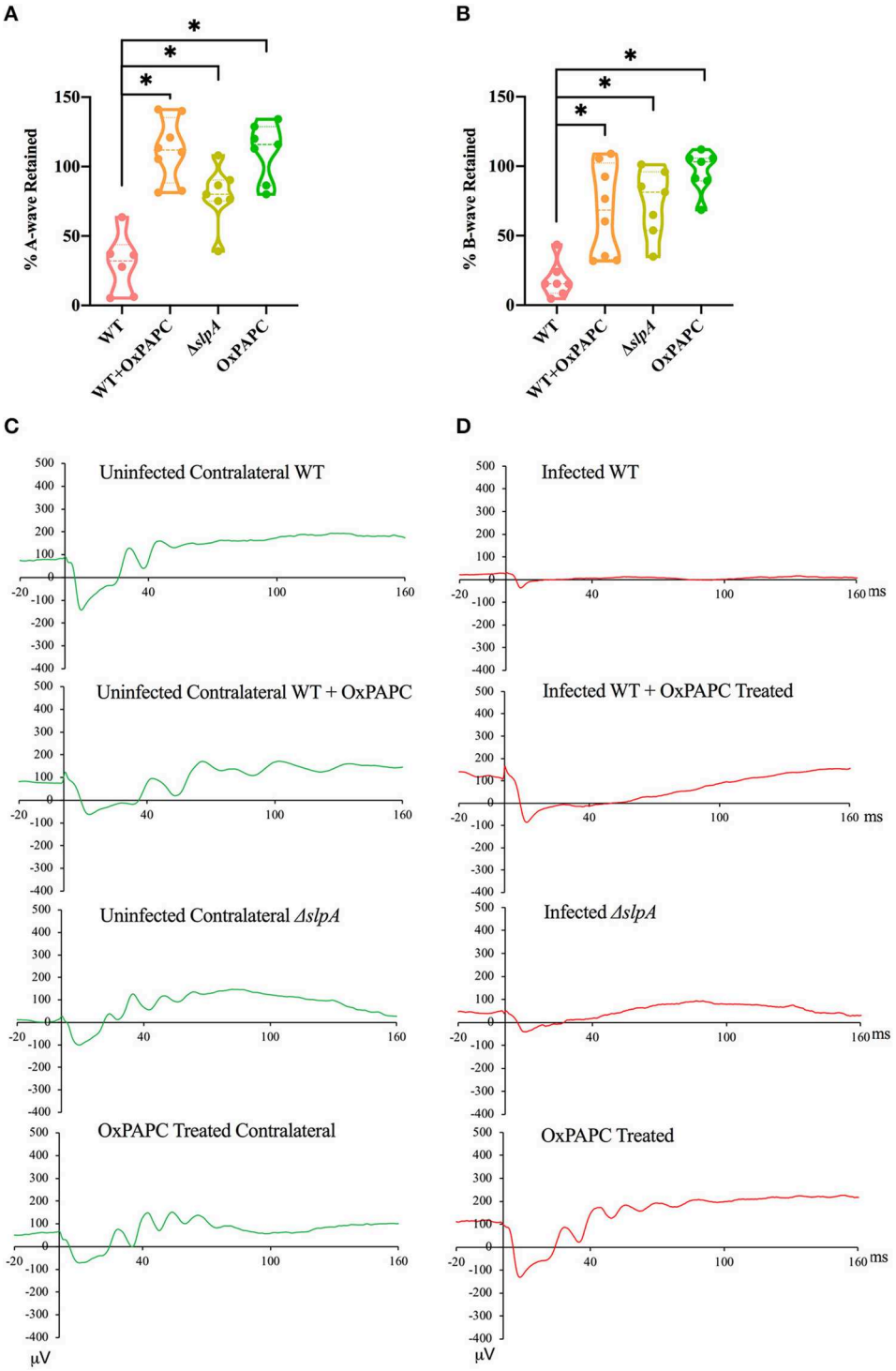

FIGURE 6 | Inhibition of SLP-mediated TLR2/4 activation resulted in significant retention of retinal function during *Bacillus* endophthalmitis. C57BL/6J mouse eyes were injected with 100 CFU WT or Δ*slpA B. thuringiensis*. WT infected and uninfected mouse eyes were treated with 30 ng/μL OxPAPC at 4 h postinfection, and retinal function was assessed by ERG. **(A)** A-wave retention was significantly higher in WT-infected /OxPAPC-treated, Δ*slpA*-infected, and OxPAPC-treated eyes, than WT-infected/untreated eyes. **(B)** B-wave retention was also significantly higher in WT-infected/OxPAPC-treated, Δ*slpA*-infected, and OxPAPC-treated eyes than the WT-infected/untreated eyes. **(C)** Shown are representative waveforms from the uninfected contralateral eyes from each group (green). **(D)** Representative waveforms from WT-infected, WT-infected/OxPAPC-treated, Δ*slpA*-infected, and OxPAPC-treated eyes at 10 h postinfection (red). Values represent the mean ± SEM of the % amplitude retained relative to the contralateral control eye for at least two separate experiments. Data are representative of $N \geq 6$ eyes; $^*P < 0.05$.

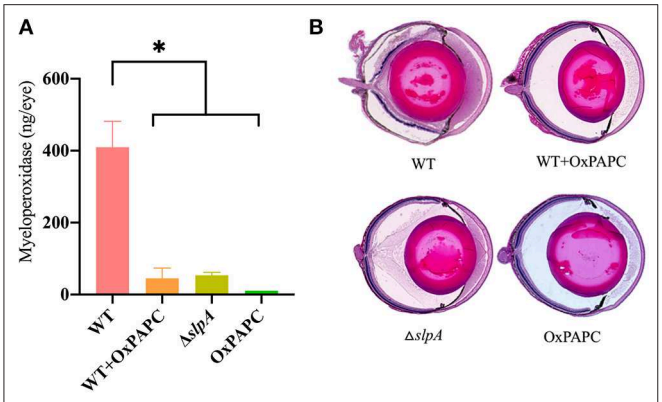

FIGURE 7 | Inhibition of SLP-mediated TLR2/4 activation resulted in reduced inflammatory cell influx and preserved ocular architecture during *Bacillus* endophthalmitis. C57BL/6J mouse eyes were infected with 100 CFU WT or Δ*slpA B. thuringiensis*. Uninfected eyes, or eyes injected with WT *B. thuringiensis* were treated with 30 ng/μL OxPAPC at 4 h postinfection. **(A)** Infiltration of PMN was assessed by quantifying MPO in whole eyes by sandwich ELISA. MPO levels were significantly greater in eyes infected with WT *B. thuringiensis* than in eyes infected with WT and treated with OxPAPC, eyes infected with only Δ*slpA B. thuringiensis*, and eyes treated with OxPAPC alone. Values represent the mean ± SEM of $N \geq 4$ eyes per group; $^*P < 0.05$. **(B)** Infected and treated eyes were harvested at 10 h postinfection and processed for hematoxylin and eosin staining. Magnification, 10×. Sections are representative of three eyes in each group.

adherence to different types of retinal cells. Muller cells are the major retinal cells that span from the outer limiting membrane (OLM) to the ILM, providing structural and hemostasis support (119–122). Since the end feet of retinal Muller cells are located in the ILM, these might be the first retinal cells to encounter pathogens in the posterior segment. RPE cells are important for phototransduction and represent the outer blood retinal barrier. Light-sensitive photoreceptor cells are located anterior to RPE cells (100–103). A recent report suggested that although 661W cells have been used as cone photoreceptor mimics, this cell line expresses markers specific to retinal ganglion cells, such as Rbpms, Brn3b (Pou4f2), Brn3c (Pou4f3), Thy1 and γ-synuclein (Sncg), and thus are retinal ganglion cell-like (99). Here, we demonstrated that SLP plays an important role in mediating *B. thuringiensis* adherence to these cell types *in vitro*, suggesting its role in bacterial attachment to retinal cells.

Evading host defense systems is a key event in successfully establishing an infection. Some organisms are evolutionarily equipped to conceal themselves from the unfriendly environment of the host (123–125). If present, SLPs can protect microorganisms from sudden shifts in pH, exposure to radiation, and changes in mechanical and osmotic stresses. SLPs can also shield bacteria from antimicrobial peptides, lytic enzymes, and bacteriophages (64). It has been reported that the SLP in *Eubacterium yurii* provides resistance to this pathogen against phagocytosis by PMN (72). In addition to providing structural and homeostasis support, Muller cells might also protect the retina by phagocytizing microbes (120, 126, 127). Here, we investigated the role of *B. cereus* SLPs in phagocytosis by human retinal Muller cells, neutrophil like HL-60 cells, and mouse primary neutrophils. We observed significantly less internalized WT *B. thuringiensis* than the Δ*slpA B. thuringiensis* mutant in all three phagocytic cell types. These findings support a role of SLP in promoting *Bacillus* adherence and evading phagocytosis.

Innate immune responses are the host's first line of defense against any invading pathogen, and TLRs are a key mediator in many inflammatory diseases (128, 129). TLRs are critical for initiating an ocular inflammatory response to microbes during keratitis, uveitis, and endophthalmitis (82, 89–91, 95, 130–132). We demonstrated that during *B. cereus* endophthalmitis, TLR2 and TLR4 each directly influenced the severity of intraocular inflammation (90, 91). We also reported the importance of MyD88 and TRIF adaptors in the pathogenesis of *B. cereus* endophthalmitis (97). Here, we demonstrated the activation of TLR2 by the envelope of Gram-positive ocular pathogens, and of these pathogens, only the envelope of *B. thuringiensis* activated TLR4. Since *Bacillus* is Gram-positive bacterium, it possesses several universal TLR2 agonists such as peptidoglycan, lipoteichoic acid, and lipoproteins. However, TLR4 agonists had yet to be identified.

As cell wall-associated proteins, SLPs have the potential to interact with retinal innate receptors. *C. difficile* SLPs have been shown to activate innate and adaptive immunity in a TLR4-dependent manner (133). SLP from *Lactobacillus helveticus* mediated a proinflammatory response through activation of both TLR2 and TLR4 in human macrophages (134). We reported that SLP activated the major transcription factor NF-κb, and induced proinflammatory cytokine production from retinal cells, suggesting that this protein might also activate retinal innate immune pathways (73). Here, by using TLR2 and TLR4 reporter cell lines, we showed for the first time that SLP not only activated TLR2, but also TLR4.

Assessing the role of TLRs and adaptor proteins in *Bacillus* endophthalmitis has been done using specific TLR- or adaptor protein-deficient mice (89–91, 97). Since SLP can signal through both TLR2 and TLR4, we used the oxidized phospholipid OxPAPC to inhibit both pathways (113). OxPAPC competes with CD14, lipid binding protein, and MD2, the accessory proteins that interact with bacterial lipids, and blocks the signaling of both TLR2 and TLR4 (135, 136). A recent report suggested that blocking both TLR2 and TLR4 might lay the foundation for the development of therapies that target inflammasomes during Gram-negative bacterial sepsis (137). OxPAPC has been reported to inhibit LPS (for TLR4) and Pam3Csk4 (for TLR2) ligand-mediated inflammatory responses in mice (138, 139). Anti-inflammatory effects of OxPAPC-directed attenuation of TLR signaling in response to pathogens and pathogen associated molecular patterns (PAMPs) are well recognized (140–142). Here, we showed that OxPAPC dramatically reduced TLR2 and TLR4 activation by their agonists and by *B. cereus* SLP *in vitro*. *In vivo*, we observed an unanticipated reduction in bacterial load in the WT infected-OxPAPC treated group. In contrast, OxPAPC did not alter bacterial growth *in vitro*. We previously reported that absence of TLR2, TLR4, or TLR5 or their adaptor MyD88 did not result in alterations

in bacterial burden during *Bacillus* endophthalmitis. But the absence of TRIF, which is a key adaptor for TLR4 signaling, resulted in a significantly reduced bacterial load during *Bacillus* endophthalmitis (89–91, 97). Here, OxPAPC treatment resulted in a reduced bacterial load in the eye from 6- to 12-h postinfection. A greater bacterial burden might be expected in tissue where an inflammatory response is insufficient; however, we did not observe this here. Deficiencies in cathelicidin-related antimicrobial peptide (CRAMP) which led to increased *S. aureus* and *Pseudomonas aeruginosa* burdens in mouse eyes with endophthalmitis and keratitis, respectively, have been reported (143, 144). Hence, it is reasonable to speculate that increased level of AMPs may lead to a lower bacterial burden. However, another report demonstrated that TRIF-deficient mice had low AMP expression levels in the gastrointestinal tract (145), so the physiological involvement of AMPs may be tissue- and infection-specific.

If the inflammation we observed here was ordained exclusively by bacterial burden, infections with WT or Δ*slpA B. thuringiensis* should have resulted in similar levels of inflammation, given that both strains grow similarly in the eye (73). However, the course of inflammation and retinal function loss in WT and Δ*slpA B. thuringiensis* eyes were significantly different, but the rates of bacterial growth in these groups were almost identical (2.2 and 1.99 h^{-1}). Since *B. thuringiensis* did not show any growth defects in the presence of increasing concentrations of OxPAPC, the possibility arises that blocking both TLR2 and TLR4 pathways might associated with the upregulation of AMPs in the vitreous. We did not detect expression of AMPs in the retinas of WT or TLR4$^{-/-}$ C57BL/6J mice infected with *Bacillus* at 4 h postinfection (95). Whether OxPAPC has effects other than inhibiting TLR2/4 activation or whether OxPAPC induces expression of AMPs in the retina is an open question.

The retina is a multilayered tissue containing nonregenerative light sensitive cells responsible for biochemical processes involved in proper vision (100). *Bacillus* endophthalmitis destroys these cells, resulting in retinal function loss. We reported that mice lacking individual TLRs (TLR2 or 4) and their adaptors, MyD88 and TRIF, have significant retention of retinal function during *Bacillus* endophthalmitis (89–91, 97). We also reported that infection with a Δ*slpA B. thuringiensis* resulted in better retention of retinal function compared to infection with a WT *B. thuringiensis* (73). Here, we observed that inhibition of both TLR2 and TLR4 signaling with OxPAPC resulted in significantly higher retained retinal function after infection with the WT strain, likely due to the preserved retinal architecture in these eyes. We reported that the absence of SlpA did not change the cytotoxic properties of *Bacillus* or altered its intraocular growth (73). Therefore, it is unlikely that the differences in retinal function loss between untreated WT-infected and WT infected-OxPAPC treated and Δ*slpA* infected eyes were due to variations in toxin production by WT and Δ*slpA B. thuringiensis*. However, the lower bacterial burden in WT infected-OxPAPC treated eyes might have resulted in a reduced cytotoxic effect on the retina which may have been reflected in the retained retinal function in OxPAPC-treated infected eyes.

Retinal detachment is a serious complication of endophthalmitis and has been reported to occur in 4–21% of cases (146). Retinal detachments, folds, and complete dissolution of retinal layers are common in severe cases of endophthalmitis (5, 17, 47). During *B. cereus* endophthalmitis, the absence of TLR2 and TLR4 in mice resulted in less infiltration of PMNs and fibrin accumulation, and preserved retinal architecture (90, 91). The lack of inflammation and intact retinal layers were similar to those reported in infected MyD88$^{-/-}$ and TRIF$^{-/-}$ eyes at 8 and 12 h postinfection (97). Here, we blocked the SLP-mediated TLR2 and TLR4 activation by OxPAPC and observed better preserved retinal architecture in the WT-infected/OxPAPC-treated and Δ*slpA*-infected groups relative to the untreated WT-infected group. We also observed elevated levels of MPO in the untreated group as compared to the treated and Δ*slpA*-infected groups. This suggests that TLR2/4 activation by SLP triggered the TLR2/4 pathways which resulted in the migration of PMNs to the eye and possibly bystander damage to the retina.

Our findings demonstrate for the first time that *Bacillus* SLP impacted endophthalmitis pathogenesis by activating both TLR2 and TLR4 pathways. In addition to identifying SLP as an unexpected TLR4 agonist, we revealed for the first time that inhibiting SLP-mediated TLR2/4 activation in experimental endophthalmitis could reduce disease severity. In *Bacillus* endophthalmitis, treatment failures are frequent despite prompt antibiotic, anti-inflammatory, and surgical intervention. Up to two-thirds of patients with *Bacillus* endophthalmitis lose significant vision, experiencing rapid inflammation and intraocular tissue damage that may also result in the need for enucleation (16, 17). As the number of cataract surgeries and intravitreal injections for degenerative retinal diseases continue to rise, the risk of endophthalmitis will also increase (147–150). Since TLRs and their adaptor proteins are major contributors to the initiation of potentially damaging inflammation in the eye, finding ligands that activate this pathway could be beneficial in formulating plausible strategies for therapeutic intervention to prevent vision loss in endophthalmitis caused by *Bacillus* and other bacterial pathogens.

DATA AVAILABILITY STATEMENT

The datasets generated for this study are available on request from the corresponding author.

ETHICS STATEMENT

The animal study was reviewed and approved by the Institutional Animal Care and Use Committee of the University of Oklahoma Health Sciences Center (protocol numbers 15-103 and 18-043). All animal experiments were performed in strict accordance with the recommendations in the Guide for the Care and Use of Laboratory Animals of the National Institute of Health and the Association for Research in Vision and Ophthalmology Statement for the Use of Animals in Ophthalmic and Vision Research.

AUTHOR CONTRIBUTIONS

MM and MC conceived and designed the experiments. FM, PC, and MC supervised and coordinated the work. AF-M provided the HL-60 cell line. MM performed most experiments and analyzed data. EL and RA provided technical assistance. MM drafted the manuscript. MM, FM, and MC reviewed, edited, and finalized the manuscript.

FUNDING

This work was supported by National Institutes of Health grants R01EY028810 and R01EY024140 (to MC). Our research is also supported in part by National Institutes of Health grants R01EY025947 and R21EY028066 (to MC), National Eye Institute Vision Core Grant P30EY021725 (to MC), a Presbyterian Health Foundation Research Support Grant Award (to MC), a Presbyterian Health Foundation Equipment Grant (to Robert E. Anderson, OUHSC), and an unrestricted grant to the Dean A. McGee Eye Institute from Research to Prevent Blindness.

ACKNOWLEDGMENTS

The authors thank Dr. Agnes Fouet (Institut Cochin, INSERM U1016, CNRS UMR8104, University Paris Descartes, Paris, France) for providing the bacterial strains and reviewing the manuscript, Dr. Felipe H. Santiago-Tirado (University of Notre Dame) for developing and providing the HL-60 cell line protocols, Dr. Feng Li and Mark Dittmar (OUHSC P30 Live Animal Imaging Core, Dean A. McGee Eye Institute, Oklahoma City, OK, USA), Dr. Grzegorz Gmyrek (OUHSC Department of Ophthalmology) for invaluable technical assistance, and the OUHSC P30 Cellular Imaging Core (Dean A. McGee Eye Institute, Oklahoma City, OK, USA) for histology expertise.

REFERENCES

1. Mahabadi N, Ngando IA, Czyz CN. *Bacterial Endophthalmitis*. StatPearls: Treasure Island, FL (2019).
2. Relhan N, Forster RK, Flynn HW Jr. Endophthalmitis: then and now. *Am J Ophthalmol*. (2018) 187:xx–xxvii. doi: 10.1016/j.ajo.2017.11.021
3. Ness T. Endophthalmitis. *Ophthalmologe*. (2018) 115:697–706. doi: 10.1007/s00347-018-0729-6
4. Teweldemedhin M, Gebreyesus H, Atsbaha AH, Asgedom SW, Saravanan M. Bacterial profile of ocular infections: a systematic review. *BMC Ophthalmol*. (2017) 17:212. doi: 10.1186/s12886-017-0612-2
5. Callegan MC, Booth MC, Jett BD, Gilmore MS. Pathogenesis of gram-positive bacterial endophthalmitis. *Infect Immun*. (1999) 67:3348–56. doi: 10.1128/IAI.67.7.3348-3356.1999
6. Astley RA, Coburn PS, Parkunan SM, Callegan MC. Modeling intraocular bacterial infections. *Prog Retin Eye Res*. (2016) 54:30–48. doi: 10.1016/j.preteyeres.2016.04.007
7. Parkunan SM. The pathogenesis of bacterial endophthalmitis. In: Durand ML, Miller JW, Young LHY, editors. *Endophthalmitis*. Springer International Publishing (2016). p. 17–47.
8. El Chehab H, Renard JP, Dot C. Post-traumatic endophthalmitis. *J Fr Ophtalmol*. (2016) 39:98–106. doi: 10.1016/j.jfo.2015.08.005
9. Essex RW, Yi Q, Charles PG, Allen PJ. Post-traumatic endophthalmitis. *Ophthalmology*. (2004) 111:2015–22. doi: 10.1016/j.ophtha.2003.09.041
10. Huber-Spitzy V, Grabner G, Haddad R, Haselberger C. Post-traumatic endophthalmitis caused by *Bacillus cereus*. *Klin Monbl Augenheilkd*. (1986) 188:52–4. doi: 10.1055/s-2008-1050574
11. Bhagat N, Li X, Zarbin MA. Post-traumatic Endophthalmitis. In: Durand ML, editor. *Endophthalmitis*. Springer (2016). p. 151–70. doi: 10.1007/978-3-319-29231-1_9
12. Rahmani S, Eliott D. Postoperative Endophthalmitis: a review of risk factors, prophylaxis, incidence, microbiology, treatment, and outcomes. *Semin Ophthalmol*. (2018) 33:95–101. doi: 10.1080/08820538.2017.1353826
13. Davidson SI. Post-operative bacterial endophthalmitis. *Trans Ophthalmol Soc UK*. (1985) 104(Pt 3):278–84.
14. Hanscom TA. Postoperative endophthalmitis. *Clin Infect Dis*. (2004) 38:542–6. doi: 10.1086/381262
15. Cunningham ET, Flynn HW, Relhan N, Zierhut M. Endogenous Endophthalmitis. *Ocul Immunol Inflamm*. (2018) 26:491–95. doi: 10.1080/09273948.2018.1466561
16. Callegan MC, Engelbert M, Parke DW II, Jett BD, Gilmore MS. Bacterial endophthalmitis: epidemiology, therapeutics, and bacterium-host interactions. *Clin Microbiol Rev*. (2002) 15:111–24. doi: 10.1128/CMR.15.1.111-124.2002
17. Callegan MC, Gilmore MS, Gregory M, Ramadan RT, Wiskur BJ, Moyer AL, et al. Bacterial endophthalmitis: therapeutic challenges and host-pathogen interactions. *Prog Retin Eye Res*. (2007) 26:189–203. doi: 10.1016/j.preteyeres.2006.12.001
18. Callegan MC, Kane ST, Cochran DC, Gilmore MS. Molecular mechanisms of *Bacillus* endophthalmitis pathogenesis. *DNA Cell Biol*. (2002) 21:367–73. doi: 10.1089/10445490260099647
19. Callegan MC, Kane ST, Cochran DC, Novosad B, Gilmore MS, Gominet M, et al. *Bacillus* endophthalmitis: roles of bacterial toxins and motility during infection. *Invest Ophthalmol Vis Sci*. (2005) 46:3233–8. doi: 10.1167/iovs.05-0410
20. Roy M, Chen JC, Miller M, Boyaner D, Kasner O, Edelstein E. Epidemic *Bacillus* endophthalmitis after cataract surgery I: acute presentation and outcome. *Ophthalmology*. (1997) 104:1768–72. doi: 10.1016/S0161-6420(97)30028-1
21. Le Saux N, Harding GK. *Bacillus cereus* endophthalmitis. *Can J Surg*. (1987) 30:28–9.
22. Rommel CT, Kaplan SJ. Post-traumatic *Bacillus cereus* endophthalmitis. *Trans Pa Acad Ophthalmol Otolaryngol*. (1986) 38:311–4.
23. Rasko DA, Altherr MR, Han CS, Ravel J. Genomics of the *Bacillus cereus* group of organisms. *FEMS Microbiol Rev*. (2005) 29:303–29. doi: 10.1016/j.femsre.2004.12.005
24. McDowell RH, Friedman H. *Bacillus Cereus*. StatPearls: Treasure Island, FL (2018).
25. Peker E, Cagan E, Dogan M, Kilic A, Caksen H, Yesilmen O. Periorbital cellulitis caused by *Bacillus thuringiensis*. *Eur J Ophthalmol*. (2010) 20:243–5. doi: 10.1177/112067211002000139
26. David DB, Kirkby GR, Noble BA. *Bacillus cereus* endophthalmitis. *Br J Ophthalmol*. (1994) 78:577–80. doi: 10.1136/bjo.78.7.577
27. Awan KJ. Bacillus endophthalmitis. *Ophthalmic Surg*. (1992) 23:368.
28. Kumar N, Garg N, Kumar N, Van Wagoner N. *Bacillus cereus* panophthalmitis associated with injection drug use. *Int J Infect Dis*. (2014) 26:165–6. doi: 10.1016/j.ijid.2014.01.019
29. Cowan CL Jr, Madden WM, Hatem GF, Merritt JC. Endogenous *Bacillus cereus* panophthalmitis. *Ann Ophthalmol*. (1987) 19:65–8.
30. Grossniklaus H, Bruner WE, Frank KE, Purnell EW. *Bacillus cereus* panophthalmitis appearing as acute glaucoma in a drug addict. *Am J Ophthalmol*. (1985) 100:334–5. doi: 10.1016/0002-9394(85)90809-8
31. Shamsuddin D, Tuazon CU, Levy C, Curtin J. *Bacillus cereus* panophthalmitis: source of the organism. *Rev Infect Dis*. (1982) 4:97–103. doi: 10.1093/clinids/4.1.97
32. Hatem G, Merritt JC, Cowan CL, Jr. *Bacillus cereus* panophthalmitis after intravenous heroin. *Ann Ophthalmol*. (1979) 11:431–40.

33. Slean GR, Shorstein NH, Liu L, Paschal JF, Winthrop KL, Herrinton LJ. Pathogens and antibiotic sensitivities in endophthalmitis. *Clin Exp Ophthalmol*. (2017) 45:481–88. doi: 10.1111/ceo.12910
34. Baker AS, Hemady R. *Bacillus*-induced endophthalmitis. *Br J Ophthalmol*. (1991) 75:255. doi: 10.1136/bjo.75.4.255
35. Lam KC. Endophthalmitis caused by *Bacillus cereus*: a devastating ophthalmological emergency. *Hong Kong Med J*. (2015) 21:475.e1–2. doi: 10.12809/hkmj154526
36. Miller JJ, Scott IU, Flynn HW Jr, Smiddy WE, Murray TG, Berrocal A, et al. Endophthalmitis caused by *Bacillus* species. *Am J Ophthalmol*. (2008) 145:883–8. doi: 10.1016/j.ajo.2007.12.026
37. Wang RC, Lou PL, Ryan EA, Kroll AJ. Antibiotic therapy in post-operative endophthalmitis. *Semin Ophthalmol*. (2002) 17:153–61. doi: 10.1076/soph.17.3.153.14787
38. Pan Q, Liu Y, Wang R, Chen T, Yang Z, Deng Y, et al. Treatment of *Bacillus cereus* endophthalmitis with endoscopy-assisted vitrectomy. *Medicine*. (2017) 96:e8701. doi: 10.1097/MD.0000000000008701
39. Sakalar YB, Ozekinci S, Celen MK. Treatment of experimental *Bacillus cereus* endophthalmitis using intravitreal moxifloxacin with or without dexamethasone. *J Ocul Pharmacol Ther*. (2011) 27:593–8. doi: 10.1089/jop.2011.0021
40. Khera M, Pathengay A, Jindal A, Jalali S, Mathai A, Pappuru RR, et al. Vancomycin-resistant Gram-positive bacterial endophthalmitis: epidemiology, treatment options, and outcomes. *J Ophthalmic Inflamm Infect*. (2013) 3:46. doi: 10.1186/1869-5760-3-46
41. Callegan MC, Cochran DC, Kane ST, Ramadan RT, Chodosh J, McLean C, et al. Virulence factor profiles and antimicrobial susceptibilities of ocular *Bacillus* isolates. *Curr Eye Res*. (2006) 31:693–702. doi: 10.1080/02713680600850963
42. Shivaramaiah HS, Relhan N, Pathengay A, Mohan N, Flynn HW Jr. Endophthalmitis caused by gram-positive bacteria resistant to vancomycin: clinical settings, causative organisms, antimicrobial susceptibilities, and treatment outcomes. *Am J Ophthalmol Case Rep*. (2018) 10:211–14. doi: 10.1016/j.ajoc.2018.02.030
43. Relhan N, Albini TA, Pathengay A, Kuriyan AE, Miller D, Flynn HW. Endophthalmitis caused by Gram-positive organisms with reduced vancomycin susceptibility: literature review and options for treatment. *Br J Ophthalmol*. (2016) 100:446–52. doi: 10.1136/bjophthalmol-2015-307722
44. Wiskur BJ, Robinson ML, Farrand AJ, Novosad BD, Callegan MC. Toward improving therapeutic regimens for *Bacillus* endophthalmitis. *Invest Ophthalmol Vis Sci*. (2008) 49:1480–7. doi: 10.1167/iovs.07-1303
45. Vahey JB, Flynn HW Jr. Results in the management of *Bacillus* endophthalmitis. *Ophthalmic Surg*. (1991) 22:681–6.
46. Callegan MC, Cochran DC, Kane ST, Gilmore MS, Gominet M, Lereclus D. Contribution of membrane-damaging toxins to *Bacillus* endophthalmitis pathogenesis. *Infect Immun*. (2002) 70:5381–9. doi: 10.1128/IAI.70.10.5381-5389.2002
47. Callegan MC, Jett BD, Hancock LE, Gilmore MS. Role of hemolysin BL in the pathogenesis of extraintestinal *Bacillus cereus* infection assessed in an endophthalmitis model. *Infect Immun*. (1999) 67:3357–66. doi: 10.1128/IAI.67.7.3357-3366.1999
48. Declerck N, Bouillaut L, Chaix D, Rugani N, Slamti L, Hoh F, et al. Structure of PlcR: Insights into virulence regulation and evolution of quorum sensing in Gram-positive bacteria. *Proc Natl Acad Sci U.S.A*. (2007) 104:18490–5. doi: 10.1073/pnas.0704501104
49. Callegan MC, Kane ST, Cochran DC, Gilmore MS, Gominet M, Lereclus D. Relationship of plcR-regulated factors to *Bacillus* endophthalmitis virulence. *Infect Immun*. (2003) 71:3116–24. doi: 10.1128/IAI.71.6.3116-3124.2003
50. Agaisse H, Gominet M, Okstad OA, Kolsto AB, Lereclus D. PlcR is a pleiotropic regulator of extracellular virulence factor gene expression in *Bacillus thuringiensis*. *Mol Microbiol*. (1999) 32:1043–53. doi: 10.1046/j.1365-2958.1999.01419.x
51. Gohar M, Faegri K, Perchat S, Ravnum S, Okstad OA, Gominet M, et al. The PlcR virulence regulon of *Bacillus cereus*. *PLoS ONE*. (2008) 3:e2793. doi: 10.1371/journal.pone.0002793
52. Fouet A, Mesnage S. *Bacillus anthracis* cell envelope components. *Curr Top Microbiol Immunol*. (2002) 271:87–113. doi: 10.1007/978-3-662-05767-4_5
53. Silhavy TJ, Kahne D, Walker S. The bacterial cell envelope. *Cold Spring Harb Perspect Biol*. (2010) 2:a000414. doi: 10.1101/cshperspect.a000414
54. Siegel SD, Liu J, Ton-That H. Biogenesis of the Gram-positive bacterial cell envelope. *Curr Opin Microbiol*. (2016) 34:31–37. doi: 10.1016/j.mib.2016.07.015
55. Dufresne K, Paradis-Bleau C. Biology and assembly of the bacterial envelope. *Adv Exp Med Biol*. (2015) 883:41–76. doi: 10.1007/978-3-319-23603-2_3
56. Sleytr UB, Messner P, Pum D, Sara M. Crystalline bacterial cell surface layers. *Mol Microbiol*. (1993) 10:911–6. doi: 10.1111/j.1365-2958.1993.tb00962.x
57. Fagan RP, Fairweather NF. Biogenesis and functions of bacterial S-layers. *Nat Rev Microbiol*. (2014) 12:211–22. doi: 10.1038/nrmicro3213
58. Mignot T, Denis B, Couture-Tosi E, Kolsto AB, Mock M, Fouet A. Distribution of S-layers on the surface of *Bacillus cereus* strains: phylogenetic origin and ecological pressure. *Environ Microbiol*. (2001) 3:493–501. doi: 10.1046/j.1462-2920.2001.00220.x
59. Gerbino E, Carasi P, Mobili P, Serradell MA, Gómez-Zavaglia A. Role of S-layer proteins in bacteria. *World J Microbiol Biotechnol*. (2015) 31:1877–87. doi: 10.1007/s11274-015-1952-9
60. Navarre WW, Schneewind O. Surface proteins of Gram-positive bacteria and mechanisms of their targeting to the cell wall envelope. *Microbiol Mol Biol Rev*. (1999) 63:174–229. doi: 10.1128/MMBR.63.1.174-229.1999
61. Hynonen U, Palva A. *Lactobacillus* surface layer proteins: structure, function and applications. *Appl Microbiol Biotechnol*. (2013) 97:5225–43. doi: 10.1007/s00253-013-4962-2
62. Bradshaw WJ, Roberts AK, Shone CC, Acharya KR. The structure of the S-layer of Clostridium difficile. *J Cell Commun Signal*. (2018) 12:319–31. doi: 10.1007/s12079-017-0429-z
63. Merrigan MM, Venugopal A, Roxas JL, Anwar F, Mallozzi MJ, Roxas BAP, et al. Surface-layer protein A (SlpA) is a major contributor to host-cell adherence of *Clostridium difficile*. *PLoS ONE*. (2013) 8:e78404. doi: 10.1371/journal.pone.0078404
64. Beveridge TJ, Pouwels PH, Sara M, Kotiranta A, Lounatmaa K, Kari K, et al. Functions of S-layers. *FEMS Microbiol Rev*. (1997) 20:99–149. doi: 10.1111/j.1574-6976.1997.tb00305.x
65. Ethapa T, Leuzzi R, Ng YK, Baban ST, Adamo R, Kuehne SA, et al. Multiple factors modulate biofilm formation by the anaerobic pathogen *Clostridium difficile*. *J Bacteriol*. (2013) 195:545–55. doi: 10.1128/JB.01980-12
66. Sakakibara J, Nagano K, Murakami Y, Higuchi N, Nakamura H, Shimozato K, et al. Loss of adherence ability to human gingival epithelial cells in S-layer protein-deficient mutants of *Tannerella forsythensis*. *Microbiology*. (2007) 153(Pt 3):866–76. doi: 10.1099/mic.0.29275-0
67. Zhang W, Wang H, Liu J, Zhao Y, Gao K, Zhang J. Adhesive ability means inhibition activities for *Lactobacillus* against pathogens and S-layer protein plays an important role in adhesion. *Anaerobe*. (2013) 22:97–103. doi: 10.1016/j.anaerobe.2013.06.005
68. Egelseer E, Schocher I, Sara M, Sleytr UB. The S-layer from *Bacillus stearothermophilus* DSM 2358 functions as an adhesion site for a high-molecular-weight amylase. *J Bacteriol*. (1995) 177:1444–51. doi: 10.1128/JB.177.6.1444-1451.1995
69. Shimotahira N, Oogai Y, Kawada-Matsuo M, Yamada S, Fukutsuji K, Nagano K, et al. The surface layer of *Tannerella forsythia* contributes to serum resistance and oral bacterial coaggregation. *Infect Immun*. (2013) 81:1198–206. doi: 10.1128/IAI.00983-12
70. Thompson SA. *Campylobacter* surface-layers (S-layers) and immune evasion. *Ann Periodontol*. (2002) 7:43–53. doi: 10.1902/annals.2002.7.1.43
71. Okuda K, Kigure T, Yamada S, Kaneko T, Ishihara K, Miura T, et al. Role for the S-layer of *Campylobacter rectus* ATCC33238 in complement mediated killing and phagocytic killing by leukocytes from guinea pig and human peripheral blood. *Oral Dis*. (1997) 3:113–20. doi: 10.1111/j.1601-0825.1997.tb00022.x
72. Kerosuo E, Haapasalo M, Lounatmaa K. *Eubacterium yurii* subspecies margaretiae is resistant to nonopsonic phagocytic ingestion. *Scand J Dent Res*. (1993) 101:304–10. doi: 10.1111/j.1600-0722.1993.tb01125.x
73. Mursalin MH, Coburn PS, Livingston E, Miller FC, Astley R, Fouet A, et al. S-layer impacts the virulence of *Bacillus* in Endophthalmitis. *Invest Ophthalmol Vis Sci*. (2019) 60:3727–39. doi: 10.1167/iovs.19-27453
74. Masli S, Vega JL. Ocular immune privilege sites. *Methods Mol Biol*. (2011) 677:449–58. doi: 10.1007/978-1-60761-869-0_28

75. Streilein JW, Ohta K, Mo JS, Taylor AW. Ocular immune privilege and the impact of intraocular inflammation. *DNA Cell Biol*. (2002) 21:453–9. doi: 10.1089/10445490260099746
76. Sugita S. Role of ocular pigment epithelial cells in immune privilege. *Arch Immunol Ther Exp*. (2009) 57:263–8. doi: 10.1007/s00005-009-0030-0
77. Perez VL, Saeed AM, Tan Y, Urbieta M, Cruz-Guilloty F. The eye: a window to the soul of the immune system. *J Autoimmun*. (2013) 45:7–14. doi: 10.1016/j.jaut.2013.06.011
78. Benhar I, London A, Schwartz M. The privileged immunity of immune privileged organs: the case of the eye. *Front Immunol*. (2012) 3:296. doi: 10.3389/fimmu.2012.00296
79. Stewart EA, Wei R, Branch MJ, Sidney LE, Amoaku WM. Expression of Toll-like receptors in human retinal and choroidal vascular endothelial cells. *Exp Eye Res*. (2015) 138:114–23. doi: 10.1016/j.exer.2015.06.012
80. Chang JH, McCluskey PJ, Wakefield D. Toll-like receptors in ocular immunity and the immunopathogenesis of inflammatory eye disease. *Br J Ophthalmol*. (2006) 90:103–8. doi: 10.1136/bjo.2005.072686
81. Kumar A, Yu FS. Toll-like receptors and corneal innate immunity. *Curr Mol Med*. (2006) 6:327–37. doi: 10.2174/156652406776894572
82. Miller FC, Coburn PS, Huzzatul MM, LaGrow AL, Livingston E, Callegan MC. Targets of immunomodulation in bacterial endophthalmitis. *Prog Retin Eye Res*. (2019) 73:100763. doi: 10.1016/j.preteyeres.2019.05.004
83. Lin X, Fang D, Zhou H, Su SB. The expression of Toll-like receptors in murine Muller cells, the glial cells in retina. *Neurol Sci*. (2013) 34:1339–46. doi: 10.1007/s10072-012-1236-1
84. Singh PK, Kumar A. Retinal photoreceptor expresses toll-like receptors (TLRs) and elicits innate responses following TLR ligand and bacterial challenge. *PLoS ONE*. (2015) 10:e0119541. doi: 10.1371/journal.pone.0119541
85. Tan RS, Ho B, Leung BP, Ding JL. TLR cross-talk confers specificity to innate immunity. *Int Rev Immunol*. (2014) 33:443–53. doi: 10.3109/08830185.2014.921164
86. Qureshi S, Medzhitov R. Toll-like receptors and their role in experimental models of microbial infection. *Genes Immun*. (2003) 4:87–94. doi: 10.1038/sj.gene.6363937
87. Delneste Y, Beauvillain C, Jeannin P. Innate immunity: structure and function of TLRs. *Med Sci*. (2007) 23:67–73. doi: 10.1051/medsci/200723167
88. Muzio M, Polentarutti N, Bosisio D, Manoj Kumar PP, Mantovani A. Toll-like receptor family and signalling pathway. *Biochem Soc Trans*. (2000) 28:563–6. doi: 10.1042/bst0280563
89. Parkunan SM, Astley R, Callegan MC. Role of TLR5 and flagella in *Bacillus* intraocular infection. *PLoS ONE*. (2014) 9:e100543. doi: 10.1371/journal.pone.0100543
90. Novosad BD, Astley RA, Callegan MC. Role of Toll-like receptor (TLR) 2 in experimental *Bacillus cereus* endophthalmitis. *PLoS ONE*. (2011) 6:e28619. doi: 10.1371/journal.pone.0028619
91. Parkunan SM, Randall CB, Coburn PS, Astley RA, Staats RL, Callegan MC. Unexpected roles for toll-like receptor 4 and TRIF in intraocular infection with Gram-positive bacteria. *Infect Immun*. (2015) 83:3926–36. doi: 10.1128/IAI.00502-15
92. Mesnage S, Haustant M, Fouet A. A general strategy for identification of S-layer genes in the *Bacillus cereus* group: molecular characterization of such a gene in *Bacillus thuringiensis* subsp. galleriae NRRL 4045. *Microbiology*. (2001) 147(Pt 5):1343–51. doi: 10.1099/00221287-147-5-1343
93. Callegan MC, Parkunan SM, Randall CB, Coburn PS, Miller FC, LaGrow AL, et al. The role of pili in *Bacillus cereus* intraocular infection. *Exp Eye Res*. (2017) 159:69–76. doi: 10.1016/j.exer.2017.03.007
94. Coburn PS, Miller FC, LaGrow AL, Land C, Mursalin H, Livingston E, et al. Disarming pore-forming toxins with biomimetic nanosponges in intraocular infections. *mSphere*. (2019) 4:e00262-19. doi: 10.1128/mSphere.00262-19
95. Coburn PS, Miller FC, LaGrow AL, Parkunan SM, Blake Randall C, Staats RL, et al. TLR4 modulates inflammatory gene targets in the retina during *Bacillus cereus* endophthalmitis. *BMC Ophthalmol*. (2018) 18:96. doi: 10.1186/s12886-018-0764-8
96. Parkunan SM, Randall CB, Astley RA, Furtado GC, Lira SA, Callegan MC. CXCL1, but not IL-6, significantly impacts intraocular inflammation during infection. *J Leukoc Biol*. (2016) 100:1125–34. doi: 10.1189/jlb.3A0416-173R
97. Parkunan SM, Roehrkasse AM, Staats RL, Callegan MC. Role of MyD88-dependent and MyD88-independent pathways in *Bacillus cereus* endophthalmitis. *Invest Ophthalmol Vis Sci*. (2014) 55:2872–72.
98. Ramadan RT, Ramirez R, Novosad BD, Callegan MC. Acute inflammation and loss of retinal architecture and function during experimental *Bacillus* endophthalmitis. *Curr Eye Res*. (2006) 31:955–65. doi: 10.1080/02713680600976925
99. Sayyad Z, Sirohi K, Radha V, Swarup G. 661W is a retinal ganglion precursor-like cell line in which glaucoma-associated optineurin mutants induce cell death selectively. *Sci Rep*. (2017) 7:16855. doi: 10.1038/s41598-017-17241-0
100. Masland RH. The neuronal organization of the retina. *Neuron*. (2012) 76:266–80. doi: 10.1016/j.neuron.2012.10.002
101. Hoon M, Okawa H, Della Santina L, Wong RO. Functional architecture of the retina: development and disease. *Prog Retin Eye Res*. (2014) 42:44–84. doi: 10.1016/j.preteyeres.2014.06.003
102. Wheway G, Nazlamova L, Turner D, Cross S. 661W photoreceptor cell line as a cell model for studying retinal ciliopathies. *Front Genet*. (2019) 10:308. doi: 10.3389/fgene.2019.00308
103. Thompson AF, Crowe ME, Lieven CJ, Levin LA. Induction of neuronal morphology in the 661W cone photoreceptor cell line with staurosporine. *PLoS ONE*. (2015) 10:e0145270. doi: 10.1371/journal.pone.0145270
104. Novakowski KE, Loukov D, Chawla V, Bowdish DM. Bacterial binding, phagocytosis, and killing: measurements using colony forming units. *Methods Mol Biol*. (2017) 1519:297–309. doi: 10.1007/978-1-4939-6581-6_20
105. Calzetti F, Tamassia N, Arruda-Silva F, Gasperini S, Cassatella MA. The importance of being "pure" neutrophils. *J Allergy Clin Immunol*. (2017) 139:352–55.e6. doi: 10.1016/j.jaci.2016.06.025
106. Sionov RV, Assi S, Gershkovitz M, Sagiv JY, Polyansky L, Mishalian I, et al. Isolation and characterization of neutrophils with anti-tumor properties. *J Vis Exp*. (2015):e52933. doi: 10.3791/52933
107. Royer DJ, Zheng M, Conrady CD, Carr DJJ. Granulocytes in ocular HSV-1 infection: opposing roles of mast cells and neutrophils. *Invest Ophthalmol Vis Sci*. (2015) 56:3763–75. doi: 10.1167/iovs.15-16900
108. Birnie GD. The HL60 cell line: a model system for studying human myeloid cell differentiation. *Br J Cancer Suppl*. (1988) 9:41–45.
109. Martin SJ, Bradley JG, Cotter TG. HL-60 cells induced to differentiate towards neutrophils subsequently die via apoptosis. *Clin Exp Immunol*. (1990) 79:448–53. doi: 10.1111/j.1365-2249.1990.tb08110.x
110. Zucker RM, Whittington K, Price BJ. Differentiation of HL-60 cells: cell volume and cell cycle changes. *Cytometry*. (1983) 3:414–8. doi: 10.1002/cyto.990030605
111. Czuprynski CJ, Henson PM, Campbell PA. Killing of *Listeria monocytogenes* by inflammatory neutrophils and mononuclear phagocytes from immune and nonimmune mice. *J Leukoc Biol*. (1984) 35:193–208. doi: 10.1002/jlb.35.2.193
112. Okugawa S, Moayeri M, Pomerantsev AP, Sastalla I, Crown D, Gupta PK, et al. Lipoprotein biosynthesis by prolipoprotein diacylglyceryl transferase is required for efficient spore germination and full virulence of *Bacillus anthracis*. *Mol Microbiol*. (2012) 83:96–109. doi: 10.1111/j.1365-2958.2011.07915.x
113. Walton KA, Cole AL, Yeh M, Subbanagounder G, Krutzik SR, Modlin RL, et al. Specific phospholipid oxidation products inhibit ligand activation of toll-like receptors 4 and 2. *Arterioscler Thromb Vasc Biol*. (2003) 23:1197–203. doi: 10.1161/01.ATV.0000079340.80744.B8
114. Haile LA, Polumuri SK, Rao R, Kelley-Baker L, Kryndushkin D, Rajaiah R, et al. Cell based assay identifies TLR2 and TLR4 stimulating impurities in Interferon beta. *Sci Rep*. (2017) 7:10490. doi: 10.1038/s41598-017-09981-w
115. LaGrow AL, Coburn PS, Miller FC, Land C, Parkunan SM, Luk BT, et al. A novel biomimetic nanosponge protects the retina from the *Enterococcus faecalis* cytolysin. *mSphere*. (2017) 2:e00335-17. doi: 10.1128/mSphere.00335-17
116. Motley ST, Morrow BJ, Liu X, Dodge IL, Vitiello A, Ward CK, et al. Simultaneous analysis of host and pathogen interactions during an *in vivo* infection reveals local induction of host acute phase response proteins, a novel bacterial stress response, and evidence of a host-imposed metal ion limited environment. *Cell Microbiol*. (2004) 6:849–65. doi: 10.1111/j.1462-5822.2004.00407.x

117. Astley R, Miller FC, Mursalin MH, Coburn PS, Callegan MC. An eye on *Staphylococcus aureus* toxins: roles in ocular damage and inflammation. *Toxins*. (2019) 11:E356. doi: 10.3390/toxins11060356
118. Kern J, Schneewind O. BslA, the S-layer adhesin of *B. anthracis*, is a virulence factor for anthrax pathogenesis. *Mol Microbiol*. (2010) 75:324–32. doi: 10.1111/j.1365-2958.2009.06958.x
119. Reichenbach A, Bringmann A. New functions of Muller cells. *Glia*. (2013) 61:651–78. doi: 10.1002/glia.22477
120. Newman E, Reichenbach A. The Muller cell: a functional element of the retina. *Trends Neurosci*. (1996) 19:307–12. doi: 10.1016/0166-2236(96)10040-0
121. Lindqvist N, Liu Q, Zajadacz J, Franze K, Reichenbach A. Retinal glial (Müller) cells: sensing and responding to tissue stretch. *Invest Ophthalmol Vis Sci*. (2010) 51:1683–90. doi: 10.1167/iovs.09-4159
122. Bringmann A, Wiedemann P. Müller glial cells in retinal disease. *Ophthalmologica*. (2012) 227:1–19. doi: 10.1159/000328979
123. Reddick LE, Alto NM. Bacteria fighting back: how pathogens target and subvert the host innate immune system. *Mol Cell*. (2014) 54:321–28. doi: 10.1016/j.molcel.2014.03.010
124. Barth K, Remick DG, Genco CA. Disruption of immune regulation by microbial pathogens and resulting chronic inflammation. *J Cell Physiol*. (2013) 228:1413–22. doi: 10.1002/jcp.24299
125. Finlay BB, McFadden G. Anti-immunology: evasion of the host immune system by bacterial and viral pathogens. *Cell*. (2006) 124:767–82. doi: 10.1016/j.cell.2006.01.034
126. Kumar A, Shamsuddin N. Retinal Muller glia initiate innate response to infectious stimuli via toll-like receptor signaling. *PLoS ONE*. (2012) 7:e29830. doi: 10.1371/journal.pone.0029830
127. Singh PK, Shiha MJ, Kumar A. Antibacterial responses of retinal Müller glia: production of antimicrobial peptides, oxidative burst and phagocytosis. *J Neuroinflamm*. (2014) 11:33. doi: 10.1186/1742-2094-11-33
128. Beutler BA. TLRs and innate immunity. *Blood*. (2009) 113:1399–407. doi: 10.1182/blood-2008-07-019307
129. Takeda K, Akira S. Toll-like receptors in innate immunity. *Int Immunol*. (2005) 17:1–14. doi: 10.1093/intimm/dxh186
130. Kaur A, Kumar V, Singh S, Singh J, Upadhyay N, Datta S, et al. Toll-like receptor-associated keratitis and strategies for its management. *3 Biotech*. (2015) 5:611–19. doi: 10.1007/s13205-015-0280-y
131. Yu F-SX, Hazlett LD. Toll-like receptors and the eye. *Invest Ophthalmol Vis Sci*. (2006) 47:1255–63. doi: 10.1167/iovs.05-0956
132. Chang JH, McCluskey PJ, Wakefield D. Recent advances in Toll-like receptors and anterior uveitis. *Clin Exp Ophthalmol*. (2012) 40:821–8. doi: 10.1111/j.1442-9071.2012.02797.x
133. Ryan A, Lynch M, Smith SM, Amu S, Nel HJ, McCoy CE, et al. A Role for TLR4 in *Clostridium difficile* infection and the recognition of surface layer proteins. *PLoS Pathog*. (2011) 7:e1002076. doi: 10.1371/journal.ppat.1002076
134. Taverniti V, Stuknyte M, Minuzzo M, Arioli S, De Noni I, Scabiosi C, et al. S-layer protein mediates the stimulatory effect of *Lactobacillus helveticus* MIMLh5 on innate immunity. *Appl Eviron Microbiol*. (2013) 79:1221–31. doi: 10.1128/AEM.03056-12
135. Oskolkova OV, Afonyushkin T, Preinerstorfer B, Bicker W, von Schlieffen E, Hainzl E, et al. Oxidized phospholipids are more potent antagonists of lipopolysaccharide than inducers of inflammation. *J Immunol*. (2010) 185:7706–12. doi: 10.4049/jimmunol.0903594
136. Bochkov VN, Oskolkova OV, Birukov KG, Levonen AL, Binder CJ, Stockl J. Generation and biological activities of oxidized phospholipids. *Antioxid Redox Signal*. (2010) 12:1009–59. doi: 10.1089/ars.2009.2597
137. Chu LH, Indramohan M, Ratsimandresey RA, Gangopadhyay A, Morris EP, Monack DM, et al. The oxidized phospholipid OxPAPC protects from septic shock by targeting the non-canonical inflammasome in macrophages. *Nat Commun*. (2018) 9:996. doi: 10.1038/s41467-018-03409-3
138. Bochkov VN, Kadl A, Huber J, Gruber F, Binder BR, Leitinger N. Protective role of phospholipid oxidation products in endotoxin-induced tissue damage. *Nature*. (2002) 419:77–81. doi: 10.1038/nature01023
139. Erridge C, Kennedy S, Spickett CM, Webb DJ. Oxidized phospholipid inhibition of toll-like receptor (TLR) signaling is restricted to TLR2 and TLR4: roles for CD14, LPS-binding protein, and MD2 as targets for specificity of inhibition. *J Biol Chem*. (2008) 283:24748–59. doi: 10.1074/jbc.M800352200
140. Ma Z, Li J, Yang L, Mu Y, Xie W, Pitt B, et al. Inhibition of LPS- and CpG DNA-induced TNF-alpha response by oxidized phospholipids. *Am J Physiol Lung Cell Mol Physiol*. (2004) 286:L808–16. doi: 10.1152/ajplung.00220.2003
141. Nonas S, Miller I, Kawkitinarong K, Chatchavalvanich S, Gorshkova I, Bochkov VN, et al. Oxidized phospholipids reduce vascular leak and inflammation in rat model of acute lung injury. *Am J Respir Crit Care Med*. (2006) 173:1130–8. doi: 10.1164/rccm.200511-1737OC
142. Meliton AY, Meng F, Tian Y, Sarich N, Mutlu GM, Birukova AA, et al. Oxidized phospholipids protect against lung injury and endothelial barrier dysfunction caused by heat-inactivated *Staphylococcus aureus*. *Am J Physiol Lung Cell Mol Physiol*. (2015) 308:L550–62. doi: 10.1152/ajplung.00248.2014
143. Talreja D, Singh PK, Kumar A. *In vivo* role of TLR2 and MyD88 signaling in eliciting innate immune responses in *Staphylococcal* Endophthalmitis. *Invest Ophthalmol Vis Sci*. (2015) 56:1719–32. doi: 10.1167/iovs.14-16087
144. Huang LC, Reins RY, Gallo RL, McDermott AM. Cathelicidin-deficient ($Cnlp^{-/-}$) mice show increased susceptibility to *Pseudomonas aeruginosa* Keratitis. *Invest Ophthalmol Vis Sci*. (2007) 48:4498–508. doi: 10.1167/iovs.07-0274
145. Kezic J, Taylor S, Gupta S, Planck SR, Rosenzweig HL, Rosenbaum JT. Endotoxin-induced uveitis is primarily dependent on radiation-resistant cells and on MyD88 but not TRIF. *J Leukoc Biol*. (2011) 90:305–11. doi: 10.1189/jlb.0111036
146. Doft BM, Kelsey SF, Wisniewski SR. Retinal detachment in the endophthalmitis vitrectomy study. *Arch Ophthalmol*. (2000) 118:1661–65. doi: 10.1001/archopht.118.12.1661
147. Hahn P, Yashkin AP, Sloan FA. Effect of prior anti-VEGF injections on the risk of retained lens fragments and endophthalmitis after cataract surgery in the elderly. *Ophthalmology*. (2016) 123:309–15. doi: 10.1016/j.ophtha.2015.06.040
148. Merani R, Hunyor AP. Endophthalmitis following intravitreal anti-vascular endothelial growth factor (VEGF) injection: a comprehensive review. *Int J Retina Vitreous*. (2015) 1:9. doi: 10.1186/s40942-015-0010-y
149. Gollogly HE, Hodge DO, St Sauver JL, Erie JC. Increasing incidence of cataract surgery: population-based study. *J Cataract Refr Sur*. (2013) 39:1383–89. doi: 10.1016/j.jcrs.2013.03.027
150. Dave VP, Pathengay A, Schwartz SG, Flynn HW Jr. Endophthalmitis following pars plana vitrectomy: a literature review of incidence, causative organisms, and treatment outcomes. *Clin Ophthalmol*. (2014) 8:2183–88. doi: 10.2147/OPTH.S71293

Conflict of Interest: The authors declare that the research was conducted in the absence of any commercial or financial relationships that could be construed as a potential conflict of interest.

frontiers in Immunology

MINI REVIEW
published: 13 February 2020
doi: 10.3389/fimmu.2020.00065

Adaptive Immunity: New Aspects of Pathogenesis Underlying Neurodegeneration in Glaucoma and Optic Neuropathy

Shuhong Jiang[1,2], *Marie Kametani*[1] *and Dong Feng Chen*[1]*

[1] Schepens Eye Research Institute of Massachusetts Eye and Ear, Department of Ophthalmology, Harvard Medical School, Boston, MA, United States, [2] State Key Laboratory of Ophthalmology, Zhongshan Ophthalmic Center, Sun Yat-sen University, Guangzhou, China

Glaucoma is a globally unmet medical challenge and the most prevalent neurodegenerative disease, which permanently damages the optic nerve and retinal ganglion cells (RGCs), leading to irreversible blindness. Present therapies target solely at lowering intraocular ocular pressure (IOP), a major risk factor of the disease; however, elevated IOP is neither necessary nor sufficient to cause glaucoma. Glaucomatous RGC and nerve fiber loss also occur in individuals with normal IOP. Recent studies have provided evidence indicating a link between elevated IOP and T cell-mediated autoimmune responses, particularly that are specific to heat shock proteins (HSPs), underlying the pathogenesis of neurodegeneration in glaucoma. Reactive glial responses and low-grade inflammation may initially represent an adaptive reaction of the retina to primary stress stimuli; whereas, sustained and excessive glial reactions lead to expanded immune responses, including adaptive immunity, that contribute to progressive neural damage in glaucoma. Emerging data suggest a similar mechanism in play in causing neurodegeneration of other forms of optic neuropathy, such as that resulted from acute ischemia and traumatic injuries. These studies may lead to the paradigm shift and offer a new basis for the development of novel mechanism-based diagnosis, therapy, and preventive interventions for glaucoma. As HSPs are induced under various conditions of neural stress and damage in the brain and spinal cord, these findings may have broader implications for our elucidating of the etiology of other neurodegenerative disorders in the central nervous system.

Keywords: glaucoma, optic neuropathy, heat shock proteins, T cells, glial response, neuroinflammation

OPEN ACCESS

Edited by:
Heping Xu,
Queen's University Belfast,
United Kingdom

Reviewed by:
Thomas Langmann,
Universität zu Köln, Germany
Stephanie C. Joachim,
Ruhr University Bochum, Germany

***Correspondence:**
Dong Feng Chen
Dongfeng_chen@meei.harvard.edu

Specialty section:
This article was submitted to Immunological Tolerance and Regulation, a section of the journal Frontiers in Immunology

Received: *02 November 2019*
Accepted: *10 January 2020*
Published: *13 February 2020*

Citation:
Jiang S, Kametani M and Chen DF (2020) Adaptive Immunity: New Aspects of Pathogenesis Underlying Neurodegeneration in Glaucoma and Optic Neuropathy. Front. Immunol. 11:65. doi: 10.3389/fimmu.2020.00065

INTRODUCTION

Glaucoma, which leads to progressive and irreversible vision loss, presents a critical medical challenge, partly due to the poorly studied mechanisms that damage the optic nerve and lead to the death of retinal ganglioncells (RGCs). While current therapy targets solely on lowering the intraocular pressure (IOP), studies have indicated that the pathogenesis of the disease is multifactorial (1). Factors such as genetics, age, and immunity are shown to be critical contributors. In addition, glaucoma can occur in patients with normal IOP, so called normal tension glaucoma

(NTG). The therapeutic approach that aims to lower the IOP is insufficient to halt, sometime limited slowing down of the progression of the disease (2). There is strong evidence supported by both experimental and clinical research that elevated IOP triggers secondary responses which are responsible for RGC degeneration in glaucoma. In this review, we examine the evidence regarding the involvement of innate and adaptive immunities, including the induction of T and B cell-mediated responses and microglial activation in the acquisition of pathogenicity in glaucoma. Furthermore, the involvement of heat-shock proteins (HSPs), such as HSP27 and HSP60, both as neuroprotective and degenerative roles in the disease progression is discussed.

THE EYE AS AN IMMUNE PRIVILEGED SITE AND THE CASE OF GLAUCOMA

The eye is recognized as an immune privileged site. Immune regulation in the eye is characterized by its active local immunosuppression, which is achieved, in part, through the blood-aqueous and blood-retina barriers, the unique feature of the pigment epithelial cells, and the local production of immunosuppressive cytokines and neuropeptides (3, 4). Immune cells that enter the eye in response to infection or injury usually are induced to undergo apoptosis via the activation of Fas-FasL signaling without causing inflammation or tissue damage (5). Antigenic material being introduced into the eye elicits immune deviation or suppression of T cell-mediated immunity that leads to peripheral immune tolerance to the antigens, a mechanism termed Anterior Chamber Associated Immune Deviation (6). Such immune privilege is thought to protect the retina, which has limited ability for regeneration and self-repair, from the damaging effects of an uncontrolled immune responses (7).

The eye's immune privileged status, however, is affected by diseased conditions, such as in the case of glaucoma, when the blood-retina barrier is compromised and cytokine productions are often altered (8). Activation of both innate and adaptive immune responses is evident in glaucoma. While systemic immune responses to the retina is strictly controlled, residential glial cells, including microglia, astrocytes, and Müller cells, play the roles of immune surveillance in the retina. They are found to become activated in the early stage of glaucoma (9). Recent evidence also reveals the critical involvement of systemic adaptive immune responses in the pathogenesis of glaucoma. Complex patterns of retinal proteins and autoantibodies against retinal specific antigens have been detected in the sera of patients with glaucoma (10, 11). Such patterns of serum protein and antibody profiles may be used for early diagnosis and detection of glaucoma and/or assessment of the progression of the disease (11–13). Further supporting a compromised blood-retinal barrier in glaucoma, autoantibodies were found to have access to the retina, and infiltration of inflammatory leukocytes and macrophages were noted preceding clinical symptoms of glaucoma (14, 15). Increased expression of matrix metalloproteinase in the astrocytes of the optic nerve head (ONH) is thought to associate with the loss of the retinal immune privilege, thus antibody penetration into the eye (16, 17). To date, elucidating the exact involvement of innate and adaptive immunity in pathogenesis of glaucoma remains the key to understanding of the disease etiology (18).

INNATE IMMUNE RESPONSES IN GLAUCOMA

The innate immunity is body's first line of defense against foreign organisms, and it offers a quick response that does not confer long-lasting protection against the same pathogen. In glaucoma, it is elevated IOP, not necessarily a foreign antigen, that triggers an innate immune response, which usually involves resident immune cells, such as microglia, as well as the infiltration of macrophages/monocytes (9). Neuroinflammatory responses generated by microglia are thought to play a leading role in glaucomatous pathophysiology. Studies show that glial activations occur at the early stage of the disease in glaucoma patients and animal models (19–21). Increased microglial activity, cell density, and their expression of complement C1q were noted in the retina and optic nerve in experimental model of glaucoma before RGC and axonal loss is observed (22, 23) and thought to be detrimental to retinal neurons. Support for this notion was the elevation of TNFα in the aqueous humor of glaucoma patients and rodent models of glaucoma, correlating with the worsening of RGC loss (24, 25). Suppression of microglial activation with minocycline or neutralization of TNFα protected RGCs from elevated IOP-induced cell death in rodents (26, 27).

Astrocytes and Müller glia, together called astroglia, also respond to the elevated IOP by developing reactive gliosis, which is characterized by the upregulation of glial fibrillary acidic protein and releasing of chemokines and cytokines, including TNFα. This response is also believed to be a pathological element that contributes to neural damage in glaucoma. More recently, studies revealed that reactive gliosis and TNFα production could be neuroprotective to RGCs. The timing of TNFα expression appears to be crucial as that the early induction of TNFα correlates with RGC survival, while longer-term expression causes RGC degeneration (28). In addition, reactive glial cells produce a variety of neuroprotective molecules, such as insulin-like growth factor-1 (IGF1), to protect RGCs from neural damage (29). Overall, the available evidence strongly suggests that reactive glia are involved in the pathology of glaucoma. To date, the key inflammatory signals that lead to glaucomatous neurodegeneration remain unknown.

INVOLVEMENT OF T CELLS IN GLAUCOMA

Activation of the innate immune system initiates and directs the adaptive immune responses, which involve T and B lymphocytes and are also featured in the glaucomatous pathogenesis. In contrast to the innate immune system, the adaptive immune system requires up to 7 days to be activated. Recent report on the involvement of heat shock protein (HSP)-specific T cells offers the key evidence support a role for autoimmunity

in glaucoma (30). However, analysis of T cells in patients and experimental models of glaucoma remains limited; there are only few studies focusing on the presence of specific T lymphocyte subsets in the sera of glaucoma patients. In part, this is because pathogenic antigens in the retina are long thought to induce T regulatory (Treg) cells through a mechanism of ACAID, therefore maintaining the ocular immune privilege. Recent studies of the peripheral blood of glaucoma patients revealed that the immunity activated in glaucoma may not be counterbalanced by an efficient immune suppression (30, 31). Patients with glaucoma exhibited a trend of decreased frequency of Treg and their CD4+ T cells presented a greater stimulation response characterized by increased proliferation and proinflammatory cytokine secretion. Elevated frequencies of $CD3^+CD8^+$ lymphocytes in both patients with NTG and primary open-angled glaucoma were noted, and $CD8^+$HLA-DR^+ lymphocytes were particularly prevalent in NTG. This was accompanied by the increased expre ssion of the soluble interleukin-2 (IL-2) receptor, a marker of T cell activation (32, 33).

The pathogenic role of T cells in glaucomatous neurodegeneration is supported by the evidence that adoptive transfer of T cells from glaucomatous mice results in a progressive loss of RGCs and their axons in recipient mice with a normal IOP (34). A link between elevated IOP and induction of anti-HSP autoimmunity has also been suggested (14, 35). HSP27 and HSP60 immunization in rats induced a pattern of RGC and axon degeneration similar to that was seen in patients with glaucoma (36). A transient infiltration of T cells in the retina was noted 2 weeks after the immunization. *In vitro* study further demonstrated T cell activation following HSP-immunization, which initiated the production of inflammatory cytokine and FasL, resulting in RGC apoptosis. Recently, using mice deficient in $CD4^+$ $\alpha\beta$ T cells, it was reported that $CD4^+$ T cells play a crucial role in propagating RGC degeneration, particularly during the prolonged period of progressive neural damage, in glaucoma (30). Uncovering the association between T cell-mediated autoimmunity and progressive neuron loss in glaucoma may allow the development of novel therapeutic interventions that eventually offer a cure for the disease.

HSPS AS PATHOGENIC AUTOANTIGENS IN T CELL-MEDIATED GLAUCOMATOUS NEURODEGENERATION

Adaptive immune responses are elicited by specific antigen stimulation, and HSPs have been identified as pathogenic autoantigens which evoke T cell responses in glaucoma (30). The stress response is a highly conserved mechanism of cellular responses to a wide variety of physiological challenges (37). The response is characterized by the induction of specific cellular proteins with protective functions, such as HSPs. Intracellular HSPs function as molecular chaperones to prevent protein aggregation and facilitate refolding of dysfunctional proteins, which is critical to the survival of all organisms (38). They are some most abundant intracellular proteins that protect cells from destruction and facilitate neural repair through astrocyte and microglial recruitment in the CNS. However, evidence reveals that their release into the extracellular environment is an indication of loss of cellular integrity, thus acts as "danger signals" and elicit both the innate and adaptive immune responses (39). Extracellular HSPs may activate microglia to secrete pro-inflammatory cytokines, such as IL-1β, IL-6, and TNF-α and trigger innate immune responses through toll like receptor 2 (TLR2) and TLR4 (40–42). They can also be processed and presented by antigen presenting cells to stimulate T cell responses. Continued and prolonged IOP elevation leads to HSP upregulation, autoantibody formation, and immune responses in glaucomatous eyes. Overexpression of HSP27 in neurons exacerbated RGC loss following IOP elevation without affecting RGC numbers under a normal IOP (30). These data suggest that elevated IOP not only upregulates HSPs, but also triggers their extracellular release and evoke immune responses.

Tezel et al. have demonstrated increased immunostaining of HSPs in the glaucomatous eyes (43). In a laser-induced rat and non-human primate models of glaucoma, elevated IOP induced expression of HSP27 and HSP70 (44–47). This elevation of HSPs following increased IOP is suggested to be neuroprotective, due in part to the study investigating the effects of geranylgeranylacetone, an HSP70 inducer developed as an anti-ulcer drug. Geranylgeranylacetone decreased elevated IOP-induced neuronal damage by reducing RGC apoptosis and axon loss (44). Subsequent studies by Wax et al. reported that immunization of rats with HSP27 or HSP60 induced significant RGC loss that was in conformity with the RGC- and nerve bundle-specific lesions observed in patients with NTG (36). Recent studies further demonstrate HSP-specific T cell responses in patients with glaucoma (30). Remarkably, mice raised in the absence of commensal microflora (germ-free mice) did not harbor HSP-specific T cells nor did they develop glaucomatous neurodegeneration after IOP elevation (30). These results are in line with the clinical observation that IOP is neither necessary nor sufficient for glaucomatous neuronal damage. It is the subsequent stress-induced events involving retinal inflammation and T cell-mediated responses that are keys to the pathogenesis of glaucoma. Taken together, family of HSPs are critical modulators of both the homeostatic and cytoprotective as well as pathogenic immune response and neurodegenerative arms of the retina and are thus integral to our understanding of neurodegeneration in glaucoma. Identification of key pathogenic autoantigens associated with glaucomatous T cell responses may also provide a foundation for future exploration of tolerance-based clinical intervention for preventing or treating the disease.

CONCLUDING REMARKS

Glaucoma is a globally unmet medical challenge due to its prevalence and debilitating consequences. The lack of cure for such a major disease reflects poor understanding of the disease's mechanisms. Numerous clinical and experimental data are now pointing to an unexpected interaction among

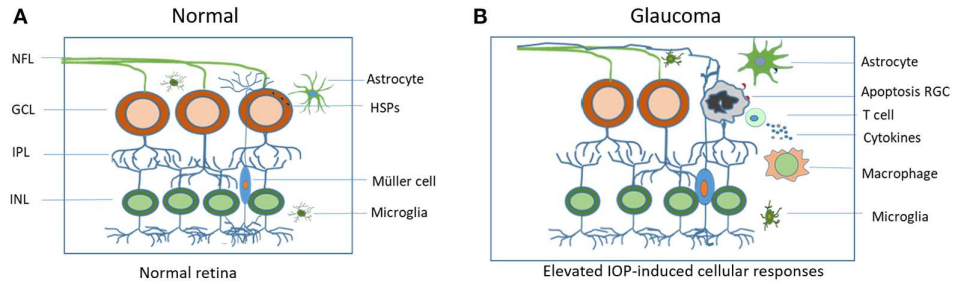

FIGURE 1 | Schematic illustration of elevated IOP-induced cellular responses in the retina. **(A)** Residential glial cells maintain cellular homeostasis in the normal retina. **(B)** In the glaucomatous retina, elevated IOP upregulates heat shock proteins (HSPs), initiates both the innate and adaptive immune responses that include microglial activation and T cell infiltration. Sustained and excessive immune responses lead to RGC apoptosis and vision loss. IOP, intraocular pressure; RGC, retinal ganglion cell; NFL, retinal nerve fiber layer.

elevated IOP, HSP-specific T cell responses and glaucomatous neurodegeneration and suggesting the crucial involvement of adaptive immunity in neurodegeneration associated with glaucoma. Although the primary response may be favorable in protecting the eye, the proceeding events that lead to long-lasting activation of glial cells and adaptive immune responses can be destructive. They disrupt the homeostasis of the retina and result in the dysfunction of the immune privilege status of the eye (**Figure 1**). The mechanisms of immune regulation in glaucoma demonstrate certain patterns which are similar to those seen in autoimmune diseases. The antigens and complex antibodies involved in the activation of immunity response are found in the sera of the patients. Although it remains unclear if the antibody production contributes to a cause or consequence of glaucoma, detection of these antibodies may serve as early diagnostic markers for the disease that may allow for proper and effective treatment prior to the late stage of the disease where progression has already occurred. Through careful examination of factors, including the activation of the glial cells, upregulation of HSPs, and the presence of different lymphocytes, development of new therapeutic treatment methods that aim to restore physiological mechanisms of self-tolerance, as well as an early detection of the disease may be possible. These studies may also have a broad impact on uncovering the pathogenesis of neurodegenerative disorders in the brain and spinal cord.

AUTHOR CONTRIBUTIONS

All authors listed have made a substantial, direct and intellectual contribution to the work, and approved it for publication.

FUNDING

This work was supported by NIH/NEI grants EY025913, EY025259, and P30EY003790 and Massachusetts Lions Foundation grant; National Natural Science Foundation of China 81760177 and Natural Science Foundation of Inner Mongolia A.R. 2011BS1107.

REFERENCES

1. Doucette LP, Rasnitsyn A, Seifi M, Walter MA. The interactions of genes, age, and environment in glaucoma pathogenesis. *Surv Ophthalmol.* (2015) 60:310–26. doi: 10.1016/j.survophthal.2015.01.004
2. Adams CM, Stacy R, Rangaswamy N, Bigelow C, Grosskreutz CL, Prasanna G. Glaucoma-next generation therapeutics: impossible to possible. *Pharm Res.* (2019) 36:25. doi: 10.1007/s11095-018-2557-4
3. Stein-Streilein J. Immune regulation and the eye. *Trends Immunol.* (2008) 29:548–54. doi: 10.1016/j.it.2008.08.002
4. Streilein JW, Wilbanks GA, Cousins SW. Immunoregulatory mechanisms of the eye. *J Neuroimmunol.* (1992) 39:185–200. doi: 10.1016/0165-5728(92)90253-H
5. Griffith TS, Brunner T, Fletcher SM, Green DR, Ferguson TA. Fas ligand-induced apoptosis as a mechanism of immune privilege. *Science.* (1995) 270:1189–92. doi: 10.1126/science.270.5239.1189
6. Wilbanks G, Streilein J. Characterization of suppressor cells in anterior chamber-associated immune deviation (ACAID) induced by soluble antigen. Evidence of two functionally and phenotypically distinct T-suppressor cell populations. *Immunology.* (1990) 71:383.
7. Moalem G, Leibowitz–Amit R, Yoles E, Mor F, Cohen IR, Schwartz M. Autoimmune T cells protect neurons from secondary degeneration after central nervous system axotomy. *Nat Med.* (1999) 5:49. doi: 10.1038/4734
8. Perez VL, Caspi RR. Immune mechanisms in inflammatory and degenerative eye disease. *Trends Immunol.* (2015) 36:354–63. doi: 10.1016/j.it.2015.04.003
9. Wei X, Cho KS, Thee EF, Jager MJ, Chen DF. Neuroinflammation and microglia in glaucoma: time for a paradigm shift. *J Neurosci Res.* (2019) 97:70–6. doi: 10.1002/jnr.24256
10. Tezel G, Seigel GM, Wax MB. Autoantibodies to small heat shock proteins in glaucoma. *Invest Ophthalmol Vis Sci.* (1998) 39:2277–87.
11. Beutgen VM, Perumal N, Pfeiffer N, Grus FH. Autoantibody biomarker discovery in primary open angle glaucoma using serological proteome analysis. *Front Immunol.* (2019) 10:381. doi: 10.3389/fimmu.2019.00381
12. Flammer J, Mozaffarieh M. What is the present pathogenetic concept of glaucomatous optic neuropathy? *Surv Ophthalmol.* (2007) 52:S162–73. doi: 10.1016/j.survophthal.2007.08.012
13. Thornton I, Luo C, Yang X, Soltau J, Tezel G. Immunoproteomic analysis of glaucomatous patient serum and aqueous humor antibodies: differential immunoreactivity against glaucomatous versus non-glaucomatous retinal proteins. *Invest Ophthalmol Vis Sci.* (2010) 51:2673. Available online at: https://iovs.arvojournals.org/article.aspx?articleid=2371330
14. Gramlich OW, Beck S, Hohenstein-Blaul NvT, Boehm N, Ziegler A, Vetter JM, et al. Enhanced insight into the autoimmune component of glaucoma: IgG autoantibody accumulation and pro-inflammatory conditions in human glaucomatous retina. *PLoS ONE.* (2013) 8:e57557. doi: 10.1371/journal.pone.0057557

15. Callahan MK, Ransohoff RM. Analysis of leukocyte extravasation across the blood-brain barrier: conceptual and technical aspects. *Curr Allergy Asthma Rep*. (2004) 4:65–73. doi: 10.1007/s11882-004-0046-9
16. Agapova OA, Ricard CS, Salvador-Silva M, Hernandez MR. Expression of matrix metalloproteinases and tissue inhibitors of metalloproteinases in human optic nerve head astrocytes. *Glia*. (2001) 33:205–16. doi: 10.1002/1098-1136(200103)33:3<205::AID-GLIA1019>3.0.CO;2-D
17. Yan X, Tezel G, Wax MB, Edward DP. Matrix metalloproteinases and tumor necrosis factor α in glaucomatous optic nerve head. *Arch Ophthalmol*. (2000) 118:666–73. doi: 10.1001/archopht.118.5.666
18. Vu TK, Jager MJ, Chen DF. The immunology of glaucoma. *Asia Pac J Ophthalmol*. (2012) 1:303–11. doi: 10.1097/APO.0b013e31826f57a3
19. Howell GR, MacNicoll KH, Braine CE, Soto I, Macalinao DG, Sousa GL, et al. Combinatorial targeting of early pathways profoundly inhibits neurodegeneration in a mouse model of glaucoma. *Neurobiol Dis*. (2014) 71:44–52. doi: 10.1016/j.nbd.2014.07.016
20. Bosco A, Romero CO, Breen KT, Chagovetz AA, Steele MR, Ambati BK, et al. Neurodegeneration severity can be predicted from early microglia alterations monitored *in vivo* in a mouse model of chronic glaucoma. *Dis Models Mech*. (2015) 8:443–55. doi: 10.1242/dmm.018788
21. Ramirez AI, de Hoz R, Salobrar-Garcia E, Salazar JJ, Rojas B, Ajoy D, et al. The role of microglia in retinal neurodegeneration: Alzheimer's disease, Parkinson, and glaucoma. *Front Aging Neurosci*. (2017) 9:214. doi: 10.3389/fnagi.2017.00214
22. Ebneter A, Casson RJ, Wood JP, Chidlow G. Microglial activation in the visual pathway in experimental glaucoma: spatiotemporal characterization and correlation with axonal injury. *Invest Ophthalmol Vis Sci*. (2010) 51:6448–60. doi: 10.1167/iovs.10-5284
23. Howell GR, Macalinao DG, Sousa GL, Walden M, Soto I, Kneeland SC, et al. Molecular clustering identifies complement and endothelin induction as early events in a mouse model of glaucoma. *J Clin Invest*. (2011) 121:1429–44. doi: 10.1172/JCI44646
24. Tezel Gln, Li LY, Patil RV, Wax MB. TNF-α and TNF-α receptor-1 in the retina of normal and glaucomatous eyes. *Invest Ophthalmol Vis Sci*. (2001) 42:1787–94.
25. Yuan L, Neufeld AH. Tumor necrosis factor-α: A potentially neurodestructive cytokine produced by glia in the human glaucomatous optic nerve head. *Glia*. (2000) 32:42–50. doi: 10.1002/1098-1136(200010)32:1<42::AID-GLIA40>3.0.CO;2-3
26. Bosco A, Steele M, Vetter M. Microglia cell activation and clustering herald the onset of glaucoma in DBA/2J retina. *Invest Ophthalmol Vis Sci*. (2008) 49:5492. doi: 10.1167/iovs.07-1337
27. Roh JH, Huang Y, Bero AW, Kasten T, Stewart FR, Bateman RJ, et al. Disruption of the sleep-wake cycle and diurnal fluctuation of β-amyloid in mice with Alzheimer's disease pathology. *Sci Transl Med*. (2012) 4:150ra22. doi: 10.1126/scitranslmed.3004291
28. Mac Nair CE, Nickells RW. Neuroinflammation in glaucoma and optic nerve damage. *Prog Mol Biol Transl Sci*. (2015) 134:343–63. doi: 10.1016/bs.pmbts.2015.06.010
29. Arroba AI, Campos-Caro A, Aguilar-Diosdado M, Valverde AM. IGF-1, inflammation and retinal degeneration: a close network. *Front Aging Neurosci*. (2018) 10:203. doi: 10.3389/fnagi.2018.00203
30. Chen H, Cho K-S, Vu TK, Shen C-H, Kaur M, Chen G, et al. Commensal microflora-induced T cell responses mediate progressive neurodegeneration in glaucoma. *Nat Commun*. (2018) 9:3209. doi: 10.1038/s41467-018-06428-2
31. Yang X, Zeng Q, Göktaş E, Gopal K, Al-Aswad L, Blumberg DM, et al. T-lymphocyte subset distribution and activity in patients with glaucoma. *Invest Ophthalmol Vis Sci*. (2019) 60:877–88. doi: 10.1167/iovs.18-26129
32. Mariotti S, Barbesino G, Caturegli P, Marino M, Manetti L, Fugazzola L, et al. Serum soluble interleukin 2 (IL-2) receptor (sIL-2R) in differentiated thyroid carcinoma. *J Endocrinol Invest*. (1994) 17:861–7. doi: 10.1007/BF03347792
33. Yang J, Patil RV, Yu H, Gordon M, Wax MB. T cell subsets and sIL-2R/IL-2 levels in patients with glaucoma. *Am J Ophthalmol*. (2001) 131:421–6. doi: 10.1016/S0002-9394(00)00862-X
34. Gramlich OW, Ding QJ, Zhu W, Cook A, Anderson MG, Kuehn MH. Adoptive transfer of immune cells from glaucomatous mice provokes retinal ganglion cell loss in recipients. *Acta Neuropathol Commun*. (2015) 3:56. doi: 10.1186/s40478-015-0234-y
35. Joachim SC, Grus FH, Kraft D, White-Farrar K, Barnes G, Barbeck M, et al. Complex antibody profile changes in an experimental autoimmune glaucoma animal model. *Invest Ophthalmol Vis Sci*. (2009) 50:4734–42. doi: 10.1167/iovs.08-3144
36. Wax MB, Tezel G, Yang J, Peng G, Patil RV, Agarwal N, et al. Induced autoimmunity to heat shock proteins elicits glaucomatous loss of retinal ganglion cell neurons via activated T-cell-derived fas-ligand. *J Neurosci*. (2008) 28:12085–96. doi: 10.1523/JNEUROSCI.3200-08.2008
37. Morimoto RI. Cells in stress: transcriptional activation of heat shock genes. *Science*. (1993) 259:1409. doi: 10.1126/science.8451637
38. Fink AL. Chaperone-mediated protein folding. *Physiol Rev*. (1999) 79:425–49. doi: 10.1152/physrev.1999.79.2.425
39. Van Eden W, Jansen MA, Ludwig I, van Kooten P, Van Der Zee R, Broere F. The enigma of heat shock proteins in immune tolerance. *Front Immunol*. (2017) 8:1599. doi: 10.3389/fimmu.2017.01599
40. Jin C, Cleveland JC, Ao L, Li J, Zeng Q, Fullerton DA, et al. Human myocardium releases heat shock protein 27 (HSP27) after global ischemia: the proinflammatory effect of extracellular HSP27 through toll-like receptor (TLR)-2 and TLR4. *Mol Med*. (2014) 20:280–9. doi: 10.2119/molmed.2014.00058
41. Rosenberger K, Dembny P, Derkow K, Engel O, Krüger C, Wolf SA, et al. Intrathecal heat shock protein 60 mediates neurodegeneration and demyelination in the CNS through a TLR4-and MyD88-dependent pathway. *Mol Neurodegener*. (2015) 10:5. doi: 10.1186/s13024-015-0003-1
42. Swaroop S, Sengupta N, Suryawanshi AR, Adlakha YK, Basu A. HSP60 plays a regulatory role in IL-1β-induced microglial inflammation via TLR4-p38 MAPK axis. *J Neuroinflammation*. (2016) 13:27. doi: 10.1186/s12974-016-0486-x
43. Tezel G, Hernandez MR, Wax MB. Immunostaining of heat shock proteins in the retina and optic nerve head of normal and glaucomatous eyes. *Arch Ophthalmol*. (2000) 118:511–8. doi: 10.1001/archopht.118.4.511
44. Ishii Y, Kwong JM, Caprioli J. Retinal ganglion cell protection with geranylgeranylacetone, a heat shock protein inducer, in a rat glaucoma model. *Invest Ophthalmol Vis Sci*. (2003) 44:1982–92. doi: 10.1167/iovs.02-0912
45. Qing G, Duan X, Jiang Y. Heat shock protein 72 protects retinal ganglion cells in rat model of acute glaucoma. *Yan ke Xue Bao*. (2005) 21:163–8.
46. Sakai M, Sakai H, Nakamura Y, Fukuchi T, Sawaguchi S. Immunolocalization of heat shock proteins in the retina of normal monkey eyes and monkey eyes with laser-induced glaucoma. *Jpn J Ophthalmol*. (2003) 47:42–52. doi: 10.1016/S0021-5155(02)00627-5
47. Park KH, Cozier F, Ong OC, Caprioli J. Induction of heat shock protein 72 protects retinal ganglion cells in a rat glaucoma model. *Invest Ophthalmol Vis Sci*. (2001) 42:1522–30.

Conflict of Interest: The authors declare that the research was conducted in the absence of any commercial or financial relationships that could be construed as a potential conflict of interest.

frontiers in Immunology

REVIEW
published: 20 March 2020
doi: 10.3389/fimmu.2020.00384

Potential Role of Myeloid-Derived Suppressor Cells (MDSCs) in Age-Related Macular Degeneration (AMD)

Anu Kauppinen[1]*, *Kai Kaarniranta*[2,3] *and Antero Salminen*[4]

[1] Faculty of Health Sciences, School of Pharmacy, University of Eastern Finland, Kuopio, Finland, [2] Department of Ophthalmology, Institute of Clinical Medicine, University of Eastern Finland, Kuopio, Finland, [3] Department of Ophthalmology, Kuopio University Hospital, Kuopio, Finland, [4] Department of Neurology, Institute of Clinical Medicine, University of Eastern Finland, Kuopio, Finland

Myeloid cells, such as granulocytes/neutrophils and macrophages, have responsibilities that include pathogen destruction, waste material degradation, or antigen presentation upon inflammation. During persistent stress, myeloid cells can remain partially differentiated and adopt immunosuppressive functions. Myeloid-derived suppressor cells (MDSCs) are primarily beneficial upon restoring homeostasis after inflammation. Because of their ability to suppress adaptive immunity, MDSCs can also ameliorate autoimmune diseases and semi-allogenic responses, e.g., in pregnancy or transplantation. However, immunosuppression is not always desirable. In certain conditions, such as cancer or chronically inflamed tissue, MDSCs prevent restorative immune responses and thereby aggravate disease progression. Age-related macular degeneration (AMD) is the most common disease in Western countries that severely threatens the central vision of aged people. The pathogenesis of this multifactorial disease is not fully elucidated, but inflammation is known to participate in both dry and wet AMD. In this paper, we provide an overview about the potential role of MDSCs in the pathogenesis of AMD.

Keywords: myeloid-derived suppressor cell, age-related macular degeneration, inflammation, innate immunity, adaptive immunity

OPEN ACCESS

Edited by:
Darren James Lee,
University of Oklahoma Health Sciences Center, United States

Reviewed by:
Alain Le Moine,
Université Libre de Bruxelles, Belgium
Kevin K. Fuller,
University of Oklahoma Health Sciences Center, United States

***Correspondence:**
Anu Kauppinen
anu.kauppinen@uef.fi

Specialty section:
This article was submitted to Immunological Tolerance and Regulation, a section of the journal Frontiers in Immunology

Received: *19 November 2019*
Accepted: *18 February 2020*
Published: *20 March 2020*

Citation:
Kauppinen A, Kaarniranta K and Salminen A (2020) Potential Role of Myeloid-Derived Suppressor Cells (MDSCs) in Age-Related Macular Degeneration (AMD). Front. Immunol. 11:384. doi: 10.3389/fimmu.2020.00384

INTRODUCTION

Hematopoietic stem cells (HSCs) produce lymphoid and myeloid blood cells. Lymphoid cells include T and B lymphocytes and natural killer (NK) cells, whereas myeloid cells include monocytes, macrophages, granulocytes, erythrocytes, megakaryocytes, and platelets (1). Despite their roles in the innate immune system, myeloid cells can also function as suppressors, although that task has more traditionally been associated with regulatory T cells. Myeloid-derived suppressor cells (MDSCs) remain immature and are a phenotypically and functionally heterogeneous cell population with immunosuppression as their common denominator. MDSCs are widely known for their capacity to suppress host T cell responses against tumor tissue, but they can also be generated upon other stressful conditions, from infections to autoimmunity and obesity, and suppress other cell types, including dendritic cells, NK cells, or macrophages (2–5). MDSCs are not uncommon in ocular diseases either, and they have been studied especially in experimental autoimmune uveitis, a murine model of posterior uveitis of autoimmune origin where retina-specific T cells promote

local inflammation, leading to the breakdown of the blood—retinal barrier (BRB), as well as retinal granulomas, folding, and detachment (6, 7). Monocytic MDSCs have also been shown to protect retinal ganglion cells from glutamate-induced damage (8). Despite the potential of MDSCs to enter the retina, their role in other retinal diseases, such as age-related macular degeneration (AMD), has remained elusive.

PATHOPHYSIOLOGY OF AMD

AMD is the leading cause of severe vision loss among the elderly in developed countries (9). Prolonged life expectancies further amplify its prevalence and cause a vast economic and national health burden. AMD disturbs central vision due to the loss of photoreceptors in the macula, a photoreceptor-dense retinal area responsible for the fine visual acuity (**Figure 1**) (10). There are two forms of the disease; advanced retinal atrophy is known as dry AMD, and it slowly disturbs the central vision (11). In wet (also known as exudative or neovascular) AMD, which comprises ca. 10–15% of the cases, fragile blood vessels sprout from the choroid into the retina (11). Those neovessels rupture easily and cause edema and acute vision loss (12). It is commonly believed that the disease begins as a slowly progressing dry form that later in some people converts into wet AMD but mechanisms have remained elusive. In a recent study, Krogh-Nielsen et al. suggested that difference between the two disease forms could be associated with age and AMD pathology-related changes in the structure and the functionality of the Bruch's membrane. They showed a positive correlation in dry AMD patients between age and the expression of tissue inhibitor of metalloproteinase (TIMP)-1, a regulator of matrix metalloproteinases (MMPs) with anti-angiogenic properties (13). Conversely, plasma levels of TIMP-3/MMP-2 ratios were significantly lower in patients with wet AMD (13).

As an age-related disease, changes resulting in clinical AMD accumulate over years, even decades. Normal aging contributes to retinal alterations, such as photoreceptor loss, Bruch's membrane thickening, choroid thinning, and formation of hard drusen in the retinal periphery; but in AMD, these become emphasized (11). In addition, AMD involves soft drusen formation at the macular area. Yellowish drusen are extracellular deposits of cellular debris, lipids, lipoproteins, amyloid deposits, and various proteins between the retinal pigment epithelium (RPE) and the Bruch's membrane (**Figure 1**) (11). They are typically among the first clinical signs upon diagnosis of AMD (14). Drusen-related proteins include various immune system-associated factors, such as complement components, and AMD-related soft drusen are also highly immunoreactive (11). Drusen material is known, for example, to activate inflammasome signaling in RPE cells and macrophage infiltration in the diseased retina (15–18).

The single-cell layer of retinal pigment epithelium (RPE) plays a significant role in the pathogenesis of AMD, and its degeneration is preceding the photoreceptor death in both dry and wet AMD (12, 19). In normal conditions, one major task of RPE cells is to phagocytize spent tips of photoreceptor outer segments (POS) and degrade them by autophagy (19). Efficient removal of waste material is critical, since ca. 10% of the photoreceptor layer volume becomes shed and degraded every day (20). However, aging deteriorates the functionality of intracellular degradation systems, which results in the accumulation of waste products in postmitotic and metabolically active RPE cells (19, 21). This results in increased oxidative stress and accumulation of non-degradable lipofuscin in lysosomes, which are responsible for waste removal by their enzymes (19). Lipofuscin inhibits autophagy, leading to the accumulation of aged mitochondria, which is one of the established characters of AMD (22, 23). In normal conditions, defective mitochondria become degraded by autophagy in a process called mitophagy; but upon autophagy blockade, they continue producing excessive amounts of reactive oxygen species (ROS). Dysfunctional autophagy promotes inflammation in RPE cells through inflammasome activation (24), and oxidative stress is the principal mechanism triggering the activation of NLRP3 receptor responsible for the inflammasome complex assembly (25). The vicious circle between dysfunctional autophagy, mitochondria, and inflammasome activation contributes to the development of pro-inflammatory retinal milieu that further promotes the deposition of lipofuscin and drusen material (19, 19). In addition to local pathology, systemic changes in the levels of certain factors, such as IL-6 or soluble TNF receptor II, have also been associated with AMD (26, 27).

ROLE OF MYELOID CELLS IN AMD PATHOLOGY

Inflammation is a physiological first-line response to any factor endangering cellular homeostasis (28). Cytokines and chemokines produced in response to pattern-recognition receptor (PRR) activation-induced signaling cascades alert the immune system to restore homeostasis. Chemokines are messengers specialized in attracting leukocytes to the inflamed tissue. In normal conditions, the eye has immune privilege maintained by the BRB, which restricts the infiltration of blood-derived leukocytes, but does not entirely prevent it, especially during aging (29). Microglia are resident inflammatory cells at the retina, which normally locate in the inner layers of the neural retina near to retinal blood vessels (10). Microglia cells play an important role in maintaining homeostasis at the retina where they migrate back and forth to the subretinal space between RPE cells and photoreceptors. In AMD, prolonged existence of stress factors contributes to the tendency of microglia to accumulate in the subretinal space, which aggravates retinal degeneration (10, 30). Relocation of microglia to the subretinal space induces extravasation of myeloid cells through retinal vessels to replace the lack of microglia in the inner retina (31). C-C chemokine receptor type 2-positive ($CCR2^{+}$) monocytes even differentiate into microglia-like cells after arrival (31).

AMD is associated with the rupture of BRB, allowing chemokines to recruit leukocytes also from the underlying choroid and systemic circulation to the retina (10). It has been shown both in dry AMD patients and the *Cryba1*

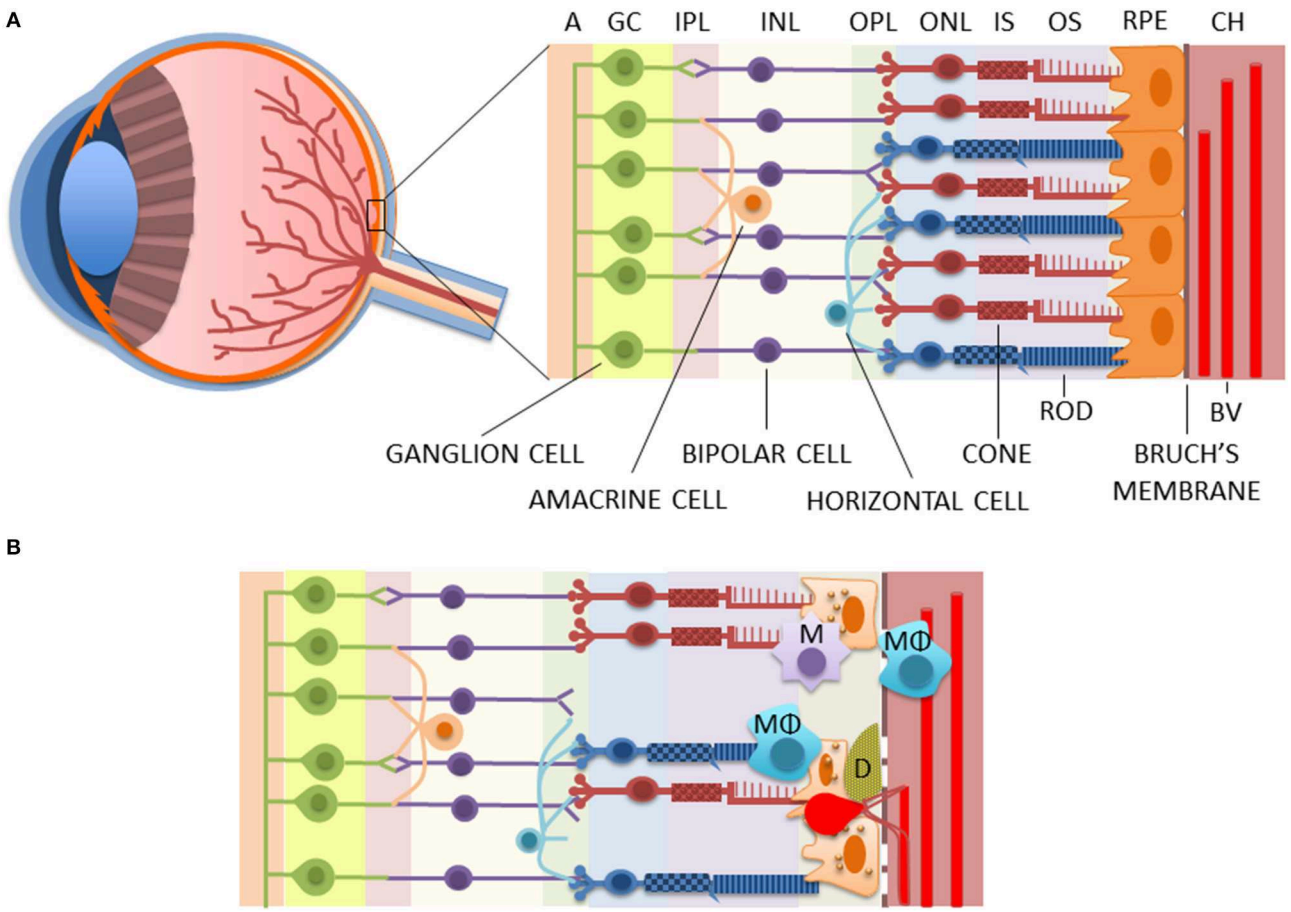

FIGURE 1 | The structure of healthy **(A)** and diseased **(B)** retinae. AMD is associated with the death of RPE and photoreceptors, rupturing of the Bruch's membrane, the accumulation of macrophages and microglia in the choroidea and/or subretinal area, and the deposition of drusen between the RPE and the Bruch's membrane, as well as the accumulation of lipofuscin inside the RPE cells. Moreover, in wet AMD, fragile blood vessels sprout from the choroidea in a process called choroidal neovascularization (CNV) to the retina where they leak causing edema and rapid vision loss. A, axons of optic nerves; BV, blood vessel; CH, the choroidea; D, drusen; GC, ganglion cells; INL, inner nuclear layer; IPL, inner plexiform layer; IS, inner segments of photoreceptors; M, microglia; MΦ, macrophage; ONL, outer nuclear layer; OPL, outer plexiform layer; OS, outer segments of photoreceptors; RPE, retinal pigment epithelium cells.

cKO mouse model with conditional knockout of the gene encoding βA3/A1-crystallin that early AMD is associated with infiltration of neutrophils to the choroid and the retina (32, 33). Infiltration of monocytes and their differentiation to macrophages upon retinal damage has been proven by various studies (34–37). Still, the fate of immune cells, especially microglia and monocyte/macrophages upon retinal damage is inadequately known (36). Despite observed leukocyte infiltration in the retina during the development of both AMD forms, it is possible that reduced oxygen consumption due to degeneration of photoreceptors alleviates the attraction of leukocytes in dry AMD. This view is supported by the fact that patients with advanced dry AMD lack significant macular edema or immune cell infiltration (38).

AMD-related leukocyte infiltration can be inflicted by impairment in receptors responding to chemokines that yield an increasing concentration gradient toward the inflamed tissue. C-X3-C Motif Receptor 1 (CX3CR1) and CCR2 are chemokine receptors implicated in drusen formation and the development of AMD (39). Interestingly, monocytes expressing both CX3CR1 and CCR2 receptors have been classified as inflammatory, whereas cells expressing only CX3CR1 have been termed anti-inflammatory (40). CX3CR1 and CCR2 ligands C-X3-C Motif Ligand 1 (CX3CL1 or fractalkine/human, neurotactin/mouse) and Monocyte Chemoattractant Protein 1 (MCP-1 or C-C Motif Chemokine Ligand 2, CCL2), respectively, recruit especially macrophages to inflamed tissue as well as microglia to and from the subretinal space (39, 41). CCL2 is also capable of attracting effector T cells, regulatory T (T reg) cells, and MDSCs (42, 43).

CX3CL1 is a transmembrane protein with integrin-like ability to bind monocytes and T cells, which can also be cleaved into a soluble form with chemotactic capacity (44). Several ocular tissues, including the RPE, constantly expresses CX3CL1 to control the redistribution and activity of CX3CR1-expressing

microglia (40, 45). Dysfunctionality or loss of CX3CR1 results in the subretinal accumulation of microglia, which contributes to drusen-like lesions, retinal degeneration, and neovascularization (40). Also, prominent infiltration of inflammatory monocytes in the subretinal space has been associated with photoreceptor death through the P_2X_7R-dependent NLRP3 inflammasome activation and IL-1β production in *Cx3cr1*-deficient mice (37, 46, 47). Dysregulated microglia-mediated neurotoxicity upon CX3CR1 deficiency is also known in central nervous system (CNS)-related conditions, such as CNS response to systemic endotoxin-induced inflammation, Parkinson's disease, and amyotrophic lateral sclerosis (ALS) (48). On the other hand, subretinal accumulation of microglia and macrophages also increase during aging irrespective of CX3CR1 expression (49, 50). In a prospective case-control study, higher proportions of $CX3CR1^+$ and $CCR2^+$ non-classical monocytes were found from peripheral blood of patients suffering from wet AMD when compared to age-matched control subjects devoid of AMD (51). Together, the data suggest that mononuclear cells accumulated at the subretinal space contribute to the retinal degeneration and photoreceptor loss. The role of CX3CR1 in the cell infiltration remains elusive but its increased expression in the peripheral monocytes of wet AMD patients does not exclude disease-specific changes in chemokine receptors.

ADAPTIVE IMMUNITY IN AMD PATIENTS

In the case that acute inflammation cannot be resolved cannot be resolved, the adaptive immune system becomes activated (52). According to current knowledge, in AMD, this refers to T lymphocyte-dependent responses more than B lymphocytes. No differences in the levels of B cells between AMD patients and control subjects have been observed, but oxidative stress-induced neoepitopes and increased concentrations of retinal auto-antibodies in patients with either dry or wet AMD imply that B lymphocytes can be associated with the disease pathogenesis (53–55). In contrast to that, more findings point to the role of T lymphocytes in AMD. T cells can roughly be categorized as helper T (Th) cells, cytotoxic T (Tc) cells, γδ-T cells, and T reg cells (56).

Healthy RPE contributes to the formation of physical BRB and actively removes infiltrating T cells by killing them through Fas-mediated apoptosis or rendering them anergic (57, 58). There is evidence suggesting that in AMD, T lymphocytes can escape elimination or anergization or be functionally altered or impaired from being capable of responding to regulatory signals (52, 59). Also, disease-associated deviations in aging immune system have been reported. For example, increased levels of $CD28^-CD56^+$ T cells in AMD patients point toward an immunosenescent phenotype, as with similar association, found also in coronary artery disease, rheumatoid arthritis, and Behçet's uveitis (60, 61). Moreover, age-dependent reduction in the amounts of Th1 cells was observed in peripheral blood of healthy relatives but not in patients suffering either from dry or wet AMD (62). In a small study by Yu et al., higher levels of IFN-γ and IL-4 were measured from PHA-stimulated PBMC cultures of wet AMD patients in comparison to control subjects, suggesting reactivity of Th1 and Th2 cells in patients (63). The finding on Th1 cells is supported by Chen et al. who showed increased levels of IFN-γ and IL-17-expressing $CD4^+$ T cells in the circulation of wet AMD patients when compared to control subjects (64). Th1 and Th17 cells isolated from patients also shifted monocytes toward a pro-inflammatory M1 macrophage phenotype that has been associated with retinal damage (64). In addition to data implying systemic activation of adaptive immunity, in an experimental model of AMD, cytotoxic $CD8^+$ T cells directly facilitated RPE degeneration following the immunization of mice with carboxyethylpyrrole (CEP)-modified albumin in complete Freund's adjuvant (65). In another mouse model, laser-induced CNV resulted in the infiltration of IL-17-producing γδ-T cells into the eye, which subsequently promoted inflammation in RPE cells (56). Retinal infiltration of IL-17-producing γδ-T cells was also detected in mice deficient in anti-oxidant system-regulating nuclear erythroid 2-related factor 2 (Nrf2) exposed to a high-fat, cholesterol-rich diet (59). The findings of deleterious effects are contradictory to the role of γδ-T cells as intraepithelial lymphocyte (IEL)-like cells with protective functions upon inflammatory environment and RPE degeneration (66). The outcome is probably related to local conditions, since inflammasome-associated cytokine IL-1β and the alarmin protein high-mobility group box 1 (HMGB1) are capable of promoting IL-17 expression by γδ-T cells (67). Conversely, inhibition of IL-1β and HMGB1 or depletion of γδ-T cells prevented experimental CNV in laser-treated mice (67). Keeping in mind that inflammasome activity and autophagy are inversely dependent on each other, dysfunctional autophagy in aged RPE cells may promote infiltration of IL-17-producing γδ-T cells through inflammasome activation.

MYELOID-DERIVED SUPPRESSOR CELLS

Acute inflammation induces myelopoiesis, strongly expanding neutrophils and monocytes, the latter of which differentiate into macrophages or dendritic cells in tissues depending on local conditions (68, 69). Those cells are active in restoring tissue homeostasis by phagocytosis, respiratory bursts, and promotion of further immune responses by secreting cytokines and activating adaptive immunity (69). Upon persistent stress, myeloid cells remain partially differentiated and adopt immunosuppressive functions (69). MDSCs were initially characterized in mice on their expression of Gr-1 in addition to the classical myeloid marker CD11b (70). Gr-1 is comprised of Ly6C and Ly6G that represent monocytic and granulocytic MDSCs, respectively (71). Due to the lack of homolog for Gr-1, human MDSCs are generally called mononuclear/monocytic (M-MDSC) and polymorphonuclear/granuclocytic (PMN-MDSC) cells (72). M-MDSCs are defined as $CD11b^+CD14^+HLA\text{-}DR^{-/lo}CD15^-$ and PMN-MDSCs as $CD11b^+CD14^-CD15^+$ or $CD11b^+CD14^-CD66b^+$ (71). Also, the myeloid marker CD33 can be used to define MDSCs; it is expressed by M-MDSCs, whereas PMN-MDSCs display $DC33^{dim}$ staining (71). $Lin^-HLA\text{-}DR^-CD33^+$ are early stage MDSCs that can be found from human, but their equivalent in mice is not known yet (71). Physiologically, MDSCs are advantageous in semi-allogenic

situations, such as pregnancy or transplantation, but they are better known for their disadvantageous immunosuppressive functions in chronic pathologies, for example, in chronic infections or cancer (72, 73) (**Figure 2**). MDSCs can regulate both innate and adaptive immune responses, e.g., by modulating macrophages, inhibiting NK or T cell responses or by inducing regulatory T cells (2, 5, 74–79). Their non-immunological functions include promotion of angiogenesis and metastasis (2, 80). Factors by which MDSCs execute their effects include arginase 1 (Arg-1), indoleamine dioxygenase (IDO), IL-10, inducible nitric oxide synthase (iNOS), nitric oxide (NO), heme oxygenase 1 (HO-1), carbon monoxide (CO), prostaglandin E2 (PGE2), ROS, and cysteine depletion (2, 73). The anergization of NK cells is dependent on the membrane-bound TGF-β1 of MDSCs, and intracellular HO-1 of MDSCs regulates T cell proliferation by CO production (73, 75). HO-1, as a stress-responsive enzyme with immunoregulatory and cytoprotective properties, is capable of protecting against oxidative stress, regulating cell proliferation, modulating inflammatory responses, and facilitating angiogenesis (81). HO-1 has been observed as a central mediator in MDSC-associated suppression upon transplantation (82). Along with the expression of regulatory cytokine IL-10, HMOX-1 encoding for HO-1 was reduced in monocytic MDSCs of secondary progressive multiple sclerosis (MS) patients when compared to relapsing–remitting MS patients or healthy subjects (83). HO-1 also participates in the tumor microenvironment to protect tumor cells from apoptosis, to improve their growth and potentially also metastasis (81, 84). Collectively, MDSCs are beneficial in quenching acute inflammation, autoimmune diseases, and responses against (semi-)allografts but become detrimental upon chronic inflammatory and neoplastic conditions.

MDSCS IN THE MAINTENANCE OF RETINAL HOMEOSTASIS

Besides the contribution to physical BRB, RPE cells have also other means to maintain homeostasis at the retina (38). Secretion of TGF-β or thrombospondin-1 (TSP-1) and the expression of programmed death-ligand 1 (PD-L1/CD247/B7-H1) on the plasma membrane alleviate T and B cell responses, and the production of cathepsin L inhibitor CTLA-2α promotes the induction of $CD4^+CD25^+Foxp3^+$ T reg cells (85–90). RPE cells also produce soluble neuropeptides with immunomodulatory capacities. Kawanaka et al. showed that neuropeptides alpha-melanocyte stimulating factor (α-MSF) and neuropeptide Y (NPY) induced co-expression of Arg1 and NOS2 in resting macrophages, converting them into MDSC-resembling cells that showed significantly reduced secretion of pro-inflammatory cytokines upon exposure to lipopolysaccharide (LPS) (91). In contrast, cells expressing only Arg1 or NOS2 but not both were found from laser-wounded retina (91). Cells lacking co-expression were less efficient in inducing apoptosis in T cells and contributed to the development of pro-inflammatory milieu. As an additional mechanism, RPE cells have been shown capable of inducing MDSC differentiation from co-cultured bone

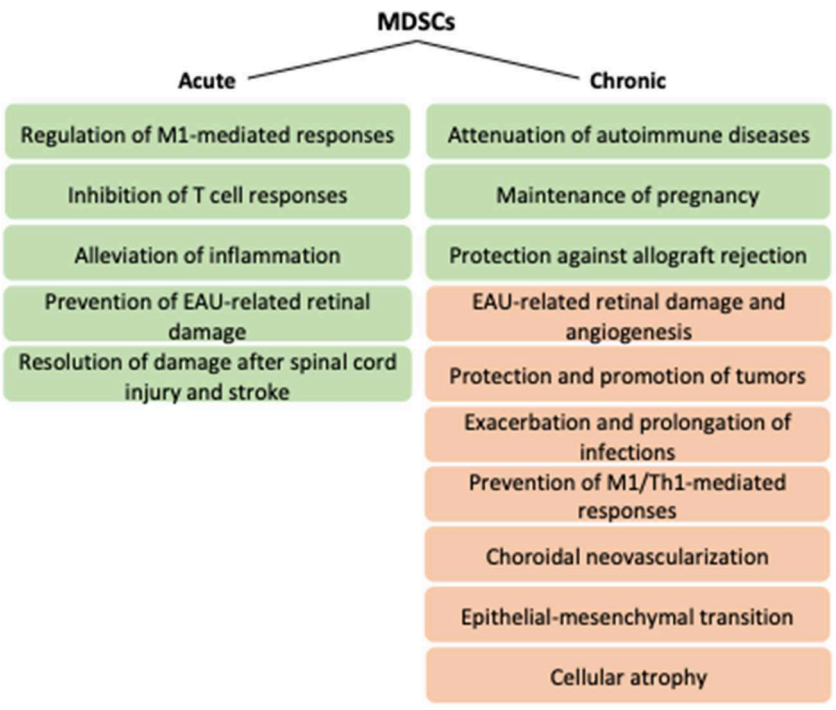

FIGURE 2 | Potential functions of MDSCs upon acute versus chronic conditions. Green and orange boxes refer to positive and negative effects, respectively. EAU, experimental autoimmune uveitis; M1, type 1 macrophage; MDSCs, myeloid-derived suppressor cells; Th1, type 1 helper T cell.

marrow (BM) progenitor cells upon exposure to granulocyte–macrophage colony-stimulating factor (GM-CSF) and IL-4 (7). In the absence of RPE cells, BM cells were differentiated into dendritic cells in the presence of given cytokines, as expected (7). $CD11b^+Gr\text{-}1^+$ MDSCs shared similar surface markers with tumor MDSCs, they efficiently inhibited T cell proliferation and inflammatory cytokine production, and their systemic delivery to mice immunized with the interphotoreceptor retinoid-binding protein $(IRBP)_{1--20}$ peptide in complete Freund's adjuvant (CFA) prevented EAU-related retinal injury (7). The pro-inflammatory cytokine IL-6 was needed for the process since its blockade reduced the RPE cell-induced MDSC differentiation. Instead, TGF-β did not participate in the differentiation process (7). Both IL-6 and TGF-β can be very harmful due to their capacity to induce inflammation and fibrosis, respectively, but probably concentrations and locations influence their effects (86).

POTENTIAL OF MDSCs IN PROVOKING ANGIOGENESIS IN DISEASED RETINA

Chronic inflammation is known as a promoter for MDSC differentiation and functionality. MDSCs have also been experimentally induced using different cytokine cocktails (92). Bunt et al. showed in murine cells that IL-1β-induced inflammation activated MDSCs through the TLR4/CD14 pathway making MDSCs to regulate macrophages by increasing their IL-10 and reducing IL-12 productions (93). That may refer to a homeostatic process where M2-type macrophages producing immunosuppressive IL-10 prevent the expansion of M1 population, which by releasing pro-inflammatory cytokines, such as IL-12 and TNF-α, is associated with tissue destruction and T helper 1 (Th1) cell activation (65). On the other hand, anti-inflammatory but pro-angiogenic M2 macrophages have been associated with choroidal neovascularization and the development of wet AMD (94, 95).

Drusen material accumulating between the RPE and the Bruch's membrane diminish the oxygen supply from the choroid to the retina (96). RPE cells suffering from hypoxia can result in the release of vascular endothelial growth factor (VEGF) already prior to the production of inflammatory markers (97). Upon laser-induced vessel formation, peak in the VEGF production coincided with the arrival of macrophages, supporting the link between RPE-associated promotion of neovascularization (98). Macrophages sense the need for oxygen by retinal cells and further potentiate the VEGF-mediated neovessel formation (10). In cancer, inflammation-induced MDSCs inhibit immunosurveillance to allow persistence and proliferation of premalignant and malignant cells (99). The capacity of MDSCs to induce angiogenesis has not been shown only in cancer studies but also in the neovascularization of an ischemic hind-limb of mice (80, 100).

It is intriguing to hypothesize that cyclooxygenase-2 (COX-2) in choroidal neovascular membranes could maintain elevated MDSC levels such that neovessel growth is promoted. COX-2 is the predominant cyclooxygenase in human RPE cells, and inflammatory cytokines further promote its expression (101). COX-2 activity is capable of recruiting MDSCs through CCL2 or PGE2. COX-2 converts arachidonic acid to PGE2 that plays a major role in the physiologic induction of MDSCs (102). Direct effects of PGE2 through the E-prostanoid (EP) receptor provide an alternative pathway for *Ccl-2*- or *Ccr-2*-deficient mice to develop atrophic (dry) and neovascular (wet) pathologies in the absence of the chemokine or its receptor (103). In an *in vitro* study with mouse primary RPE cells, the major lipofuscin component bis-retinoid N-retinylidene-N-retinylethanolamine (A2E) reduced PGE2 levels and promoted RPE cells to induce Th1 cell differentiation in IL-1β-dependent way, which might thereby contribute to further retinal degeneration (104, 105).

COX-2 inhibition by acetylsalisylic acid (aspirin, ASA) prevented the CCL2-mediated accumulation of $CD11b^+Ly6G^{hi}Ly6C^{lo}$ granulocytic MDSCs to the tumor microenviroment in mice with glioma (43). COX-2/CCL2 blockade also increased the expression of C-X-C Motif Chemokine 10 (CXCL10/Interferon γ-induced Protein 10/IP-10) that inhibits VEGF-mediated angiogenesis (43, 52). COX-2 is expressed by human choroidal neovascular membranes (106), and promotion of CXCL10 could result in its inhibition. CXCL10 is a ligand of C-X-C Motif Chemokine Receptor 3 (CXCR3 also known as GPR9 or CD183) that, along with C-C Chemokine Receptor Type 3 (CCR3), is associated with the development of wet AMD (52). Percentage of both $CD4^+$ Th and $CD8^+$ Tc cells expressing CXCR3 has been observed to be lower in the peripheral blood of patients with wet AMD in comparison to control subjects (62, 107), which may diminish the benefit of increased CXCL10 production following the COX-2 inhibition. Acetylsalisylic acid is a non-steroidal anti-inflammatory drug (NSAID) and COX-2 inhibitor that is commonly used at low doses for long periods due to its anti-thrombotic effects. A retrospective study on AREDS and AREDS2 data supports the inability of COX-2 inhibition to protect from neovascularization since the use of acetylsalisylic acid was not significantly associated with progression of either dry or wet AMD (108). Instead, a prospective double-blind randomized human study on the therapy of wet AMD with photodynamic therapy (PDT) supplemented with oral intake of the COX-2 inhibitor nabumetone resulted in the progression of macular atrophy (109). Collectively, the data on COX-2 inhibition suggest no beneficial effects on wet AMD but potential aggravation in the progression of dry AMD, thereby conflicting with the idea of COX-2-induced and MDSC-mediated neovascularization.

COMPLEMENT AND MDSCs

Due to facts concerning genetic predisposition and composition of drusen, it is evident that the complement pathway contributes to the pathogenesis of AMD. Excessive complement activation has also been observed in various studies to be harmful in pathologic retinal degenerative and angiogenic conditions (110).

Complement components produced by RPE cells contribute to the formation of sub-RPE deposits through complement-driven proteasome inhibition and release pro-inflammatory cytokines, such as IL-6 and IL-1β, that can amplify the response by further promoting expression of the C3a receptor (111, 112). Unstimulated RPE cells express significantly

higher levels of complement regulator genes in comparison to complement component genes but under inflammatory conditions, activated macrophages induce complement factor B (CFB) and C3 expression in RPE cells (113). Laser photocoagulation has also shown to induce the deposition of C3 and membrane attack complex (MAC) in the neovascular complex (114). Furthermore, MAC formation is capable of releasing angiogenesis-related growth factors, such as β-fibroblast growth factor (β-FGF), VEGF, and platelet-derived growth factor (PDGF) (114). The role of MDSCs has not been studied in relation to ocular complement activation but there is evidence on the MDSC contribution from other disease models. Complement inhibition reduces tumor growth with accompanying decrease in the both C3 and MDSC levels (115). Hsieh et al. also showed that C3 plays a major role in the conversion of bone marrow progenitor cells into MDSC by hepatic stellate cells (116, 117). Those MDSCs efficiently inhibited T cell responses *in vitro* and *in vivo*, and alleviated experimental autoimmune myasthenia gravis also by reducing anti-actylcholine receptor IgG levels and decreasing complement activation at the endplates of neuromuscular junctions (116–118).

Active pro-inflammatory complement components C3a and C5a (anaphylatoxins) are included in drusen material and efficiently promote choroidal neovascularization in mice by stimulating VEGF production in RPE and choroid cells (98). Conversely, normalized anaphylatoxin levels promoted recovery from CNV lesions and prevented fibrotic scar formation (119). A study on the ARPE-19 cell line originating from spontaneously transformed human RPE cells emphasized the role of C5a over C3a in the induction of VEGF production, but Nozaki et al. also found C3a to stimulate VEGF production in primary human RPE cells in addition to D407 RPE cell line (120, 121). Both C3a and C5a were found from the drusen, the proximity of RPE cells, and the Bruch's membrane of an AMD patient, whereas neither of them were present in the eye of a control subject without AMD (98). A study on $C3aR^{-/-}$ and $C5aR^{-/-}$ mice showed that complement components also play a role in the recruitment of neutrophils and macrophages that were observed to peak one and three days after the insult, respectively (98). Neutrophils further pave the way to other leukocytes by expressing MMP-9 that disrupts the integrity of BRB (122). In dry AMD, photoreceptor outer segments exposed to human serum following the BRB breakdown resulted in complement activation, C5a-mediated attraction of peripheral blood monocytes, and diminished survival of the RPE and neural retina (123). Complement activation in subretinal macrophages can potentially play a role in the pathogenesis of AMD (124). Also systemic complement activation in AMD patients has been shown (125, 126).

Substitution of histidine to tyrosine (Y402H) is one of the best-known polymorphic complement factor H (CFH) variants associated with AMD. By diminishing the functionality of the regulatory CFH, it results in overactive alternative complement pathway (10). Incomplete CFH activity has been shown to enhance C3 deposition and C5a release in non-small lung cancer cell lines (127–130). In addition to direct receptor binding, C5a can stimulate MDSCs also indirectly through IL-6, IL-1β, or VEGF (131). The role of C5a in cancer promotion is well known, and it is also considered as a key player in poor cancer prognosis on subjects suffering from an autoimmune disease with complement activation by immune complexes (the Arthus reaction) (132). According to a recent discovery, CFH(Y402H) also efficiently binds CD11b, preventing CD47-mediated elimination of mononuclear cells, such as macrophages and microglia, attracted to the subretinal space between the RPE and photoreceptor outer segments to restore homeostasis (133, 134). This may extend the presence of mononuclear cells at the retina beyond the need for homeostasis restoration, which predisposes to adverse effects, such as photoreceptor degeneration and choroidal neovascularization (41, 135, 136). CD11b is also expressed by both monocytic and granulocytic MDSCs (71) predisposing the retina to their prolonged impact in susceptible persons. Overall, complement and CFH(Y402H) are efficient in activating MDSC and may thereby prevent the removal of drusen material by immune cells.

MDSCs ENHANCE FIBROSIS

Choroidal neovascularization does not only cause rapid vision loss due to bleeding and swelling at the retina, but it also results in subretinal fibrosis that can develop despite the anti-VEGF therapy that prevents the neovessel formation (137). Conversely, epithelial-mesenchymal transition (EMT) can also cause resistance to anti-VEGF drugs, as suggested by studies on pancreatic cancer cells (138). Subretinal fibrosis is associated with the end stage pathogenesis of wet AMD (137). TGF-β signaling in myeloid cells promotes CCL2-dependent MDSC recruitment to the tumor microenvironment, and granulocytic MDSC-derived TGF-β promotes EMT upon metastasis, which is the advanced form of malignancy (139, 140). TGF-β is a multifunctional growth factor physiologically needed for the development and tissue repair, but excessive concentrations are associated with inflammation and tissue fibrosis, with detrimental consequences in the eye (141, 142).

CONCLUDING REMARKS

MDSCs have been found beneficial in various CNS disorders and autoimmune diseases (**Figure 2**). Both monocytic and granulocytic MDSCs have been shown to alleviate EAE (143–145). Monocytic MDSCs participated in resolving damage following experimental spinal cord injury in mice, alleviated inflammation after stroke in mice, and were found in increased numbers in the peripheral blood of ischemic stroke patients (146, 147). MDSCs induced by hepatic stellate cells efficiently inhibited T cell responses *in vitro* and *in vivo* and attenuated experimental autoimmune myasthenia gravis also by reducing anti-actylcholine receptor IgG levels and decreasing complement

activation at the endplates of neuromuscular junctions (116–118). MDSCs were observed beneficial also especially at the beginning of autoimmune uveoretinitis (6, 148–150). Adoptive transfer of RPE-induced MDSCs reduced EAU severity when detected 21 days after immunization when the acute phase peaks (7). However, upon combined deletion of CCL2 and CX3CR1, deficiency in macrophages and MDSCs during chronic EAU (90 days post-immunization) contributed to reduced retinal damage and angiogenesis (150). The data supports the overall idea of inflammation where the timing matters. In the acute phase, MDSCs probably participate in the restoration of homeostasis, but upon chronic inflammation, their capacity to promote atrophy and angiogenesis may overcome the benefits.

AUTHOR CONTRIBUTIONS

AK contributed to the planning of the content, writing of the manuscript, and preparing the figures. AS and KK contributed to the planning of the content and the critical evaluation of the text.

FUNDING

This study was financially supported by the grants from the Academy of Finland (AK297267, AK307341, KK296840, and AK328443), the Kuopio University Hospital VTR grant (KK5503743), the Emil Aaltonen Foundation, the Sigrid Juselius Foundation, the Päivikki and Sakari Sohlberg Foundation, the Finnish Cultural Foundation, and the Finnish Eye Foundation.

REFERENCES

1. Kondo M. Lymphoid and myeloid lineage commitment in multipotent hematopoietic progenitors. *Immunol Rev.* (2010) 238:37–46. doi: 10.1111/j.1600-065X.2010.00963.x
2. Gabrilovich DI, Nagaraj S. Myeloid-derived suppressor cells as regulators of the immune system. *Nat Rev Immunol.* (2009) 9:162–74. doi: 10.1038/nri2506
3. Kwak Y, Kim HE, Park SG. Insights into myeloid-derived suppressor cells in inflammatory diseases. *Arch Immunol Ther Exp*. (2015) 63:269–85. doi: 10.1007/s00005-015-0342-1
4. Ostrand-Rosenberg S, Beury DW, Parker KH, Horn LA. Survival of the fittest: how myeloid-derived suppressor cells survive in the inhospitable tumor microenvironment. *Cancer Immunol Immunother.* (2019) 69:215–21. doi: 10.1007/s00262-019-02388-8
5. Veglia F, Perego M, Gabrilovich D. Myeloid-derived suppressor cells coming of age. *Nat Immunol.* (2018) 19:108–19. doi: 10.1038/s41590-017-0022-x
6. Kerr EC, Raveney BJ, Copland DA, Dick AD, Nicholson LB. Analysis of retinal cellular infiltrate in experimental autoimmune uveoretinitis reveals multiple regulatory cell populations. *J Autoimmun.* (2008) 31:354–61. doi: 10.1016/j.jaut.2008.08.006
7. Tu Z, Li Y, Smith D, Doller C, Sugita S, Chan CC, et al. Myeloid suppressor cells induced by retinal pigment epithelial cells inhibit autoreactive T-cell responses that lead to experimental autoimmune uveitis. *Invest Ophthalmol Vis Sci.* (2012) 53:959–66. doi: 10.1167/iovs.11-8377
8. London A, Itskovich E, Benhar I, Kalchenko V, Mack M, Jung S, Schwartz M. Neuroprotection and progenitor cell renewal in the injured adult murine retina requires healing monocyte-derived macrophages. *J Exp Med.* (2011) 208:23–39. doi: 10.1084/jem.20101202
9. Wong WL, Su X, Li X, Cheung CM, Klein R, Cheng CY, Wong TY. Global prevalence of age-related macular degeneration disease burden projection for 2020 2040: a systematic review meta-analysis. *Lancet Glob Health.* (2014) 2:e106–16. doi: 10.1016/S2214-109X(13)70145-1
10. Ambati J, Atkinson JP, Gelfand BD. Immunology of age-related macular degeneration. *Nat Rev Immunol.* (2013) 13:438–51. doi: 10.1038/nri3459
11. Ardeljan D, Chan CC. Aging is not a disease: Distinguishing age-related macular degeneration from aging. *Prog Retin Eye Res.* (2013) 37:68–9. doi: 10.1016/j.preteyeres.2013.07.003
12. Ambati J, Fowler BJ. Mechanisms of age-related macular degeneration. *Neuron.* (2012) 75:26–39. doi: 10.1016/j.neuron.2012.06.018
13. Krogh Nielsen M, Subhi Y, Rue Molbech C, Nilsson LL, Nissen MH, Sorensen TL. Imbalances in tissue inhibitors of metalloproteinases differentiate choroidal neovascularization from geographic atrophy. *Acta Ophthalmol.* (2019) 97:84–90. doi: 10.1111/aos.13894
14. Lim LS, Mitchell P, Seddon JM, Holz FG, Wong TY. Age-related macular degeneration. *Lancet.* (2012) 379:1728–38. doi: 10.1016/S0140-6736(12)60282-7
15. Doyle SL, Campbell M, Ozaki E, Salomon RG, Mori A, Kenna PF, et al. NLRP3 has a protective role in age-related macular degeneration through the induction of IL-18 by drusen components. *Nat Med.* (2012) 18:791–8. doi: 10.1038/nm.2717
16. Gao J, Cui JZ, To E, Cao S, Matsubara JA. Evidence for the activation of pyroptotic and apoptotic pathways in RPE cells associated with NLRP3 inflammasome in the rodent eye. *J Neuroinflammation.* (2018) 15:15. doi: 10.1186/s12974-018-1062-3
17. Liu RT, Gao J, Cao S, Sandhu N, Cui JZ, Chou CL, et al. Inflammatory mediators induced by amyloid-beta in the retina and RPE *in vivo*: implications for inflammasome activation in age-related macular degeneration. *Invest Ophthalmol Vis Sci.* (2013) 54:2225–37. doi: 10.1167/iovs.12-10849
18. Zhao T, Gao J, Van J, To E, Wang A, Cao S, et al. Age-related increases in amyloid beta and membrane attack complex: evidence of inflammasome activation in the rodent eye. *J Neuroinflammation.* (2015) 12:121. doi: 10.1186/s12974-015-0337-1
19. Kaarniranta K, Sinha D, Blasiak J, Kauppinen A, Vereb Z, Salminen A, et al. Autophagy and heterophagy dysregulation leads to retinal pigment epithelium dysfunction and development of age-related macular degeneration. *Autophagy.* (2013) 9:973–84. doi: 10.4161/auto.24546
20. Kevany BM, Palczewski K. Phagocytosis of retinal rod and cone photoreceptors. *Physiology.* (2010) 25:8–15. doi: 10.1152/physiol.00038.2009
21. Kaarniranta K, Salminen A, Haapasalo A, Soininen H, Hiltunen M. Age-related macular degeneration (AMD): Alzheimer's disease in the eye? *J Alzheimers Dis.* (2011) 24:615–31. doi: 10.3233/JAD-2011-101908
22. Ao J, Wood JP, Chidlow G, Gillies MC, Casson RJ. Retinal pigment epithelium in the pathogenesis of age-related macular degeneration and photobiomodulation as a potential therapy? *Clin Exp Ophthalmol.* (2018) 46:670–86. doi: 10.1111/ceo.13121
23. Green DR, Galluzzi L, Kroemer G. Mitochondria and the autophagy-inflammation-cell death axis in organismal aging. *Science.* (2011) 333:1109–12. doi: 10.1126/science.1201940
24. Piippo N, Korkmaz A, Hytti M, Kinnunen K, Salminen A, Atalay M, et al. Decline in cellular clearance systems induces inflammasome signaling in human ARPE-19 cells. *Biochim Biophys Acta.* (2014) 1843:3038–46. doi: 10.1016/j.bbamcr.2014.09.015
25. Piippo N, Korhonen E, Hytti M, Kinnunen K, Kaarniranta K, Kauppinen A. Oxidative stress is the principal contributor to inflammasome activation in retinal pigment epithelium cells with defunct proteasomes and autophagy. *Cell Physiol Biochem.* (2018) 49:359–67. doi: 10.1159/000492886
26. Faber C, Jehs T, Juel HB, Singh A, Falk MK, Sorensen TL, Nissen MH. Early exudative age-related macular degeneration is associated with increased plasma levels of soluble TNF receptor II. *Acta Ophthalmol.* (2015) 93:242–7. doi: 10.1111/aos.12581
27. Krogh Nielsen M, Subhi Y, Molbech CR, Falk MK, Nissen MH, Sorensen TL. Systemic Levels of Interleukin-6 Correlate With Progression Rate

of Geographic Atrophy Secondary to Age-Related Macular Degeneration. *Invest Ophthalmol Vis Sci.* (2019) 60:202–8. doi: 10.1167/iovs.18-25878
28. Kauppinen A, Paterno JJ, Blasiak J, Salminen A, Kaarniranta K. Inflammation and its role in age-related macular degeneration. *Cell Mol Life Sci.* (2016) 73:1765–86. doi: 10.1007/s00018-016-2147-8
29. Forrester JV, Xu H. Good news-bad news: the Yin and Yang of immune privilege in the eye. *Front Immunol.* (2012) 3:338. doi: 10.3389/fimmu.2012.00338
30. Gupta N, Brown KE, Milam AH. Activated microglia in human retinitis pigmentosa, late-onset retinal degeneration, and age-related macular degeneration. *Exp Eye Res.* (2003) 76:463–71. doi: 10.1016/S0014-4835(02)00332-9
31. Ma W, Zhang Y, Gao C, Fariss RN, Tam J, Wong WT. Monocyte infiltration and proliferation reestablish myeloid cell homeostasis in the mouse retina following retinal pigment epithelial cell injury. *Sci Rep.* (2017) 7: 1538–43. doi: 10.1038/s41598-017-08702-7
32. Ghosh S, Padmanabhan A, Vaidya T, Watson AM, Bhutto IA, Hose S, et al. Neutrophils homing into the retina trigger pathology in early age-related macular degeneration. *Commun Biol.* (2019) 2:348. doi: 10.1038/s42003-019-0588-y
33. Ghosh S, Shang P, Yazdankhah M, Bhutto I, Hose S, Montezuma SR, et al. Activating the AKT2-nuclear factor-kappaB-lipocalin-2 axis elicits an inflammatory response in age-related macular degeneration. *J Pathol.* (2017) 241:583–8. doi: 10.1002/path.4870
34. Caicedo A, Espinosa-Heidmann DG, Pina Y, Hernandez EP, Cousins SW. Blood-derived macrophages infiltrate the retina and activate Muller glial cells under experimental choroidal neovascularization. *Exp Eye Res.* (2005) 81:38–47. doi: 10.1016/j.exer.2005.01.013
35. Chen M, Lechner J, Zhao J, Toth L, Hogg R, Silvestri G, et al. STAT3 activation in circulating monocytes contributes to neovascular age-related macular degeneration. *Curr Mol Med.* (2016) 16:412–23. doi: 10.2174/1566524016666160324130031
36. Saban DR. New concepts in macrophage ontogeny in the adult neural retina. *Cell Immunol.* (2018) 330:79–85. doi: 10.1016/j.cellimm.2018.04.008
37. Sennlaub F, Auvynet C, Calippe B, Lavalette S, Poupel L, Hu SJ, et al. CCR2 (+) monocytes infiltrate atrophic lesions in age-related macular disease and mediate photoreceptor degeneration in experimental subretinal inflammation in Cx3cr1 deficient mice. *EMBO Mol Med.* (2013) 5:1775–93. doi: 10.1002/emmm.201302692
38. Chen M, Luo C, Zhao J, Devarajan G, Xu H. Immune regulation in the aging retina. *Prog Retin Eye Res.* (2019) 69:159–72. doi: 10.1016/j.preteyeres.2018.10.003
39. Falk MK, Singh A, Faber C, Nissen MH, Hviid T, Sorensen TL. CX3CL1/CX3CR1 CCL2/CCR2 chemokine/chemokine receptor complex in patients with AMD. *PLoS ONE.* (2014) 9:e112473. doi: 10.1371/journal.pone.0112473
40. Combadiere C, Feumi C, Raoul W, Keller N, Rodero M, Pezard A, et al. CX3CR1-dependent subretinal microglia cell accumulation is associated with cardinal features of age-related macular degeneration. *J Clin Invest.* (2007) 117:2920–8. doi: 10.1172/JCI31692
41. Raoul W, Auvynet C, Camelo S, Guillonneau X, Feumi C, Combadiere C, Sennlaub F. CCL2/CCR2 and CX3CL1/CX3CR1 chemokine axes and their possible involvement in age-related macular degeneration. *J Neuroinflammation.* (2010) 7:87. doi: 10.1186/1742-2094-7-87
42. Deshmane SL, Kremlev S, Amini S, Sawaya BE. Monocyte chemoattractant protein-1 (MCP-1): an overview. *J Interferon Cytokine Res.* (2009) 29:313–26. doi: 10.1089/jir.2008.0027
43. Fujita M, Kohanbash G, Fellows-Mayle W, Hamilton RL, Komohara Y, Decker SA, et al. COX-2 blockade suppresses gliomagenesis by inhibiting myeloid-derived suppressor cells. *Cancer Res.* (2011) 71:2664–74. doi: 10.1158/0008-5472.CAN-10-3055
44. Bazan JF, Bacon KB, Hardiman G, Wang W, Soo K, Rossi D, et al. A new class of membrane-bound chemokine with a CX3C motif. *Nature.* (1997) 385:640–4. doi: 10.1038/385640a0
45. Silverman MD, Zamora DO, Pan Y, Texeira PV, Baek SH, Planck SR, Rosenbaum JT. Constitutive and inflammatory mediator-regulated fractalkine expression in human ocular tissues and cultured cells. *Invest Ophthalmol Vis Sci.* (2003) 44:1608–15. doi: 10.1167/iovs.02-0233
46. Eandi CM, Charles Messance H, Augustin S, Dominguez E, Lavalette S, Forster V, et al. Subretinal mononuclear phagocytes induce cone segment loss via IL-1beta. *Elife.* (2016) 5:16490. doi: 10.7554/eLife.16490
47. Hu SJ, Calippe B, Lavalette S, Roubeix C, Montassar F, Housset M, et al. Upregulation of P2RX7 in Cx3cr1-deficient mononuclear phagocytes leads to increased interleukin-1beta secretion and photoreceptor neurodegeneration. *J Neurosci.* (2015) 35:6987–96. doi: 10.1523/JNEUROSCI.3955-14.2015
48. Cardona AE, Pioro EP, Sasse ME, Kostenko V, Cardona SM, Dijkstra IM, et al. Control of microglial neurotoxicity by the fractalkine receptor. *Nat Neurosci.* (2006) 9:917–24. doi: 10.1038/nn1715
49. Chinnery HR, McLenachan S, Humphries T, Kezic JM, Chen X, Ruitenberg MJ, McMenamin PG. Accumulation of murine subretinal macrophages: effects of age, pigmentation and CX3CR1. *Neurobiol Aging.* (2012) 33:1769–76. doi: 10.1016/j.neurobiolaging.2011.03.010
50. Xu H, Chen M, Manivannan A, Lois N, Forrester JV. Age-dependent accumulation of lipofuscin in perivascular and subretinal microglia in experimental mice. *Aging Cell.* (2008) 7:58–68. doi: 10.1111/j.1474-9726.2007.00351.x
51. Subhi Y, Krogh Nielsen M, Molbech CR, Sorensen TL. Altered proportion of CCR2 (+) and CX3CR1 (+) circulating monocytes in neovascular age-related macular degeneration and polypoidal choroidal vasculopathy. *Clin Exp Ophthalmol.* (2018) 46:661–9. doi: 10.1111/ceo.13152
52. Niazi S, Krogh Nielsen M, Sorensen TL, Subhi Y. Neutrophil-to-lymphocyte ratio in age-related macular degeneration: a systematic review and meta-analysis. *Acta Ophthalmol.* (2019) 97:558–66. doi: 10.1111/aos.14072
53. Adamus G, Chew EY, Ferris FL, Klein ML. Prevalence of anti-retinal autoantibodies in different stages of Age-related macular degeneration. *BMC Ophthalmol.* (2014) 14:154. doi: 10.1186/1471-2415-14-154
54. Hector SM, Sorensen TL. Circulating monocytes and B-lymphocytes in neovascular age-related macular degeneration. *Clin Ophthalmol.* (2017) 11:179–84. doi: 10.2147/OPTH.S121332
55. Joseph K, Kulik L, Coughlin B, Kunchithapautham K, Bandyopadhyay M, Thiel S, et al. Oxidative stress sensitizes retinal pigmented epithelial (RPE) cells to complement-mediated injury in a natural antibody-, lectin pathway-, and phospholipid epitope-dependent manner. *J Biol Chem.* (2013) 288:12753–65. doi: 10.1074/jbc.M112.421891
56. Coughlin B, Schnabolk G, Joseph K, Raikwar H, Kunchithapautham K, Johnson K, et al. Connecting the innate and adaptive immune responses in mouse choroidal neovascularization via the anaphylatoxin C5a and gammadeltaT-cells. *Sci Rep.* (2016) 6:23794. doi: 10.1038/srep23794
57. Gregerson DS, Heuss ND, Lew KL, McPherson SW, Ferrington DA. Interaction of retinal pigmented epithelial cells and CD4 T cells leads to T-cell anergy. *Invest Ophthalmol Vis Sci.* (2007) 48:4654–63. doi: 10.1167/iovs.07-0286
58. Jorgensen A, Wiencke AK, la Cour M, Kaestel CG, Madsen HO, Hamann S, et al. Human retinal pigment epithelial cell-induced apoptosis in activated T cells. *Invest Ophthalmol Vis Sci.* (1998) 39:1590–9.
59. Zhao Z, Xu P, Jie Z, Zuo Y, Yu B, Soong L, et al. gammadelta T cells as a major source of IL-17 production during age-dependent RPE degeneration. *Invest Ophthalmol Vis Sci.* (2014) 55:6580–9. doi: 10.1167/iovs.14-15166
60. Faber C, Singh A, Kruger Falk M, Juel HB, Sorensen TL, Nissen MH. Age-related macular degeneration is associated with increased proportion of CD56 (+) T cells in peripheral blood. *Ophthalmology.* (2013) 120:2310–6. doi: 10.1016/j.ophtha.2013.04.014
61. Subhi Y, Nielsen MK, Molbech CR, Oishi A, Singh A, Nissen MH, Sorensen TL. T-cell differentiation and CD56+ levels in polypoidal choroidal vasculopathy and neovascular age-related macular degeneration. *Aging.* (2017) 9:2436–52. doi: 10.18632/aging.101329
62. Singh A, Subhi Y, Krogh Nielsen M, Falk MK, Matzen SMH, Sellebjerg F, Sorensen TL. Systemic frequencies of T helper 1 and T helper 17 cells in patients with age-related macular degeneration: a case-control study. *Sci Rep.* (2017) 7:605. doi: 10.1038/s41598-017-00741-4
63. Yu Y, Ren XR, Wen F, Chen H, Su SB. T-helper-associated cytokines expression by peripheral blood mononuclear cells in patients with polypoidal choroidal vasculopathy and age-related macular degeneration. *BMC Ophthalmol.* (2016) 16:80. doi: 10.1186/s12886-016-0251-z

64. Chen J, Wang W, Li Q. Increased Th1/Th17 responses contribute to low-grade inflammation in age-related macular degeneration. *Cell Physiol Biochem.* (2017) 44:357–67. doi: 10.1159/000484907
65. Cruz-Guilloty F, Saeed AM, Duffort S, Cano M, Ebrahimi KB, Ballmick A, et al. T cells and macrophages responding to oxidative damage cooperate in pathogenesis of a mouse model of age-related macular degeneration. *PLoS ONE.* (2014) 9:e88201. doi: 10.1371/journal.pone.0088201
66. Zhao Z, Liang Y, Liu Y, Xu P, Flamme-Wiese MJ, Sun D, et al. Choroidal gammadelta T cells in protection against retinal pigment epithelium and retinal injury. *FASEB J.* (2017) 31:4903–4916. doi: 10.1096/fj.201700533R
67. Hasegawa E, Sonoda KH, Shichita T, Morita R, Sekiya T, Kimura A, et al. IL-23-independent induction of IL-17 from gammadeltaT cells and innate lymphoid cells promotes experimental intraocular neovascularization. *J Immunol.* (2013) 190:1778–87. doi: 10.4049/jimmunol.1202495
68. Consonni FM, Porta C, Marino A, Pandolfo C, Mola S, Bleve A, Sica A. Myeloid-derived suppressor cells: ductile targets in disease. *Front Immunol.* (2019) 10:949. doi: 10.3389/fimmu.2019.00949
69. Gabrilovich DI. Myeloid-derived suppressor cells. *Cancer Immunol Res.* (2017) 5:3–8. doi: 10.1158/2326-6066.CIR-16-0297
70. Talmadge JE, Gabrilovich DI. History of myeloid-derived suppressor cells. *Nat Rev Cancer.* (2013) 13:739–52. doi: 10.1038/nrc3581
71. Bronte V, Brandau S, Chen SH, Colombo MP, Frey AB, Greten TF, et al. Recommendations for myeloid-derived suppressor cell nomenclature and characterization standards. *Nat Commun.* (2016) 7:12150. doi: 10.1038/ncomms12150
72. Pawelec G, Verschoor CP, Ostrand-Rosenberg S. Myeloid-derived suppressor cells: not only in tumor immunity. *Front Immunol.* (2019) 10:1099. doi: 10.3389/fimmu.2019.01099
73. Zhao Y, Wu T, Shao S, Shi B, Zhao Y. Phenotype, development, and biological function of myeloid-derived suppressor cells. *Oncoimmunology.* (2016) 5:e1004983. doi: 10.1080/2162402X.2015.1004983
74. Huang B, Pan PY, Li Q, Sato AI, Levy DE, Bromberg J, et al. Gr-1+CD115+ immature myeloid suppressor cells mediate the development of tumor-induced T regulatory cells and T-cell anergy in tumor-bearing host. *Cancer Res.* (2006) 66:1123–31. doi: 10.1158/0008-5472.CAN-05-1299
75. Li H, Han Y, Guo Q, Zhang M, Cao X. Cancer-expanded myeloid-derived suppressor cells induce anergy of NK cells through membrane-bound TGF-beta 1. *J Immunol.* (2009) 182:240–9. doi: 10.4049/jimmunol.182.1.240
76. Pan PY, Ma G, Weber KJ, Ozao-Choy J, Wang G, Yin B, et al. Immune stimulatory receptor CD40 is required for T-cell suppression and T regulatory cell activation mediated by myeloid-derived suppressor cells in cancer. *Cancer Res.* (2010) 70:99–108. doi: 10.1158/0008-5472.CAN-09-1882
77. Serafini P, Mgebroff S, Noonan K, Borrello I. Myeloid-derived suppressor cells promote cross-tolerance in B-cell lymphoma by expanding regulatory T cells. *Cancer Res.* (2008) 68:5439–49. doi: 10.1158/0008-5472.CAN-07-6621
78. Sinha P, Clements VK, Bunt SK, Albelda SM, Ostrand-Rosenberg S. Cross-talk between myeloid-derived suppressor cells and macrophages subverts tumor immunity toward a type 2 response. *J Immunol.* (2007) 179:977–83. doi: 10.4049/jimmunol.179.2.977
79. Suzuki E, Kapoor V, Jassar AS, Kaiser LR, Albelda SM. Gemcitabine selectively eliminates splenic Gr-1+/CD11b+ myeloid suppressor cells in tumor-bearing animals and enhances antitumor immune activity. *Clin Cancer Res.* (2005) 11:6713–21. doi: 10.1158/1078-0432.CCR-05-0883
80. Kim JA, March K, Chae HD, Johnstone B, Park SJ, Cook T, et al. Muscle-derived Gr1 (dim) CD11b (+) cells enhance neovascularization in an ischemic hind limb mouse model. *Blood.* (2010) 116:1623–6. doi: 10.1182/blood-2009-08-237040
81. Was H, Dulak J, Jozkowicz A. Heme oxygenase-1 in tumor biology and therapy. *Curr Drug Targets.* (2010) 11:1551–70. doi: 10.2174/1389450111009011551
82. De Wilde V, Van Rompaey N, Hill M, Lebrun JF, Lemaître P, Lhommé F, et al. Endotoxin-induced myeloid-derived suppressor cells inhibit alloimmune responses via heme oxygenase-1. *Am J Trans.* (2009) 9:2034–47. doi: 10.1111/j.1600-6143.2009.02757.x
83. Iacobaeus E, Douagi I, Jitschin R, Marcusson-Ståhl M, Andrén AT, Gavin C, et al. Phenotypic and functional alterations of myeloid-derived suppressor cells during the disease course of multiple sclerosis. *Immunol Cell Biol.* (2018) 96:820–30. doi: 10.1111/imcb.12042
84. Sunthamala N, Pientong C, Ohno T, Zhang C, Bhingare A, Kondo Y, et al. HPV16 E2 protein promotes innate immunity by modulating immunosuppressive status. *Biochem Biophys Res Commun.* (2014) 446:977–82. doi: 10.1016/j.bbrc.2014.03.042
85. Futagami Y, Sugita S, Vega J, Ishida K, Takase H, Maruyama K, et al. Role of thrombospondin-1 in T cell response to ocular pigment epithelial cells. *J Immunol.* (2007) 178:6994–7005. doi: 10.4049/jimmunol.178.11.6994
86. Holtkamp GM, Kijlstra A, Peek R de Vos AF. Retinal pigment epithelium-immune system interactions: cytokine production and cytokine-induced changes. *Prog Retin Eye Res.* (2001) 20:29–48. doi: 10.1016/S1350-9462(00)00017-3
87. Ke Y, Sun D, Jiang G, Kaplan HJ, Shao H. PD-L1 (hi) retinal pigment epithelium (RPE) cells elicited by inflammatory cytokines induce regulatory activity in uveitogenic T cells. *J Leukoc Biol.* (2010) 88:1241–9. doi: 10.1189/jlb.0610332
88. Mochizuki M, Sugita S, Kamoi K. Immunological homeostasis of the eye. *Prog Retin Eye Res.* (2013) 33:10–27. doi: 10.1016/j.preteyeres.2012.10.002
89. Sugita S, Horie S, Nakamura O, Futagami Y, Takase H, Keino H, et al. Retinal pigment epithelium-derived CTLA-2alpha induces TGFbeta-producing T regulatory cells. *J Immunol.* (2008) 181:7525–36. doi: 10.4049/jimmunol.181.11.7525
90. Sugita S, Horie S, Yamada Y, Mochizuki M. Inhibition of B-cell activation by retinal pigment epithelium. *Invest Ophthalmol Vis Sci.* (2010) 51:5783–8. doi: 10.1167/iovs.09-5098
91. Kawanaka N, Taylor AW. Localized retinal neuropeptide regulation of macrophage and microglial cell functionality. *J Neuroimmunol.* (2011) 232:17–25. doi: 10.1016/j.jneuroim.2010.09.025
92. Condamine T, Gabrilovich DI. Molecular mechanisms regulating myeloid-derived suppressor cell differentiation and function. *Trends Immunol.* (2011) 32:19–25. doi: 10.1016/j.it.2010.10.002
93. Bunt SK, Clements VK, Hanson EM, Sinha P, Ostrand-Rosenberg S. Inflammation enhances myeloid-derived suppressor cell cross-talk by signaling through Toll-like receptor 4. *J Leukoc Biol.* (2009) 85:996–1004. doi: 10.1189/jlb.0708446
94. Cao X, Shen D, Patel MM, Tuo J, Johnson TM, Olsen TW, Chan CC. Macrophage polarization in the maculae of age-related macular degeneration: a pilot study. *Pathol Int.* (2011) 61:528–35. doi: 10.1111/j.1440-1827.2011.02695.x
95. Yang Y, Liu F, Tang M, Yuan M, Hu A, Zhan Z, et al. Macrophage polarization in experimental and clinical choroidal neovascularization. *Sci Rep.* (2016) 6:30933. doi: 10.1038/srep30933
96. McHugh KJ, Li D, Wang JC, Kwark L, Loo J, Macha V, et al. Computational modeling of retinal hypoxia and photoreceptor degeneration in patients with age-related macular degeneration. *PLoS ONE.* (2019) 14:e0216215. doi: 10.1371/journal.pone.0216215
97. Arjamaa O, Aaltonen V, Piippo N, Csont T, Petrovski G, Kaarniranta K, Kauppinen A. Hypoxia and inflammation in the release of VEGF and interleukins from human retinal pigment epithelial cells. *Graefes Arch Clin Exp Ophthalmol.* (2017) 255:1757–62. doi: 10.1111/j.1755-3768.2016.0421
98. Nozaki M, Raisler BJ, Sakurai E, Sarma JV, Barnum SR, Lambris JD, et al. Drusen complement components C3a and C5a promote choroidal neovascularization. *Proc Natl Acad Sci U S A.* (2006) 103:2328–33. doi: 10.1073/pnas.0408835103
99. Sinha P, Clements VK, Fulton AM, Ostrand-Rosenberg S. Prostaglandin E2 promotes tumor progression by inducing myeloid-derived suppressor cells. *Cancer Res.* (2007) 67:4507–13. doi: 10.1158/0008-5472.CAN-06-4174
100. Yang L, DeBusk LM, Fukuda K, Fingleton B, Green-Jarvis B, Shyr Y, et al. Expansion of myeloid immune suppressor Gr+CD11b+ cells in tumor-bearing host directly promotes tumor angiogenesis. *Cancer Cell.* (2004) 6:409–21. doi: 10.1016/j.ccr.2004.08.031
101. Chin MS, Nagineni CN, Hooper LC, Detrick B, Hooks JJ. Cyclooxygenase-2 gene expression and regulation in human retinal pigment epithelial cells. *Invest Ophthalmol Vis Sci.* (2001) 42:2338–46.
102. Obermajer N, Muthuswamy R, Lesnock J, Edwards RP, Kalinski P. Positive feedback between PGE2 and COX2 redirects the differentiation of human dendritic cells toward stable myeloid-derived suppressor cells. *Blood.* (2011) 118:5498–505. doi: 10.1182/blood-2011-07-365825

103. Ambati J, Anand A, Fernandez S, Sakurai E, Lynn BC, Kuziel WA, et al. An animal model of age-related macular degeneration in senescent Ccl-2- or Ccr-2-deficient mice. *Nat Med.* (2003) 9:1390–7. doi: 10.1038/nm950
104. Ekkens MJ, Shedlock DJ, Jung E, Troy A, Pearce EL, Shen H, Pearce EJ. Th1 and Th2 cells help CD8 T-cell responses. *Infect Immun.* (2007) 75:2291–6. doi: 10.1128/IAI.01328-06
105. Shi Q, Wang Q, Li J, Zhou X, Fan H, Wang F, et al. A2E suppresses regulatory function of RPE cells in Th1 cell differentiation via production of IL-1beta and inhibition of PGE2. *Invest Ophthalmol Vis Sci.* (2015) 56:7728–38. doi: 10.1167/iovs.15-17677
106. Maloney SC, Fernandes BF, Castiglione E, Antecka E, Martins C, Marshall JC, et al. Expression of cyclooxygenase-2 in choroidal neovascular membranes from age-related macular degeneration patients. *Retina.* (2009) 29:176–80. doi: 10.1097/IAE.0b013e3181884fa6
107. Falk MK, Singh A, Faber C, Nissen MH, Hviid T, Sorensen TL. Dysregulation of CXCR3 expression on peripheral blood leukocytes in patients with neovascular age-related macular degeneration. *Invest Ophthalmol Vis Sci.* (2014) 55:4050–6. doi: 10.1167/iovs.14-14107
108. Keenan TD, Wiley HE, Agron E, Aronow ME, Christen WG, Clemons TE, et al. The association of aspirin use with age-related macular degeneration progression in the age-related eye disease studies: age-related eye disease study 2 report no. 20. *Ophthalmology.* (2019) 126:1647–56. doi: 10.1016/j.ophtha.2019.06.023
109. Sin M, Chrapek O, Karhanova M, Pracharova Z, Langova K, Rehak J. Progression of macular atrophy after PDT combined with the COX-2 inhibitor Nabumetone in the treatment of neovascular ARMD. *Biomed Pap Med Fac Univ Palacky Olomouc Czech Repub.* (2014) 158:138–43. doi: 10.5507/bp.2012.066
110. Xu H, Chen M. Targeting the complement system for the management of retinal inflammatory and degenerative diseases. *Eur J Pharmacol.* (2016) 787:94–104. doi: 10.1016/j.ejphar.2016.03.001
111. Fernandez-Godino R, Garland DL, Pierce EA. A local complement response by RPE causes early-stage macular degeneration. *Hum Mol Genet.* (2015) 24:5555–69. doi: 10.1093/hmg/ddv287
112. Fernandez-Godino R, Pierce EA. C3a triggers formation of sub-retinal pigment epithelium deposits via the ubiquitin proteasome pathway. *Sci Rep.* (2018) 8:9679. doi: 10.1038/s41598-018-28143-0
113. Luo C, Zhao J, Madden A, Chen M, Xu H. Complement expression in retinal pigment epithelial cells is modulated by activated macrophages. *Exp Eye Res.* (2013) 112:93–101. doi: 10.1016/j.exer.2013.04.016
114. Bora PS, Sohn JH, Cruz JM, Jha P, Nishihori H, Wang Y, et al. Role of complement and complement membrane attack complex in laser-induced choroidal neovascularization. *J Immunol.* (2005) 174:491–7. doi: 10.4049/jimmunol.174.1.491
115. Downs-Canner S, Magge D, Ravindranathan R, O'Malley ME, Francis L, Liu Z, et al. Complement inhibition: a novel form of immunotherapy for colon cancer. *Ann Surg Oncol.* (2016) 23:655–62. doi: 10.1245/s10434-015-4778-7
116. Chou HS, Hsieh CC, Yang HR, Wang L, Arakawa Y, Brown K, et al. Hepatic stellate cells regulate immune response by way of induction of myeloid suppressor cells in mice. *Hepatology.* (2011) 53:1007–19. doi: 10.1002/hep.24162
117. Hsieh CC, Chou HS, Yang HR, Lin F, Bhatt S, Qin J, et al. The role of complement component 3 (C3) in differentiation of myeloid-derived suppressor cells. *Blood.* (2013) 121:1760–8. doi: 10.1182/blood-2012-06-440214
118. Li Y, Tu Z, Qian S, Fung JJ, Markowitz SD, Kusner LL, et al. Myeloid-derived suppressor cells as a potential therapy for experimental autoimmune myasthenia gravis. *J Immunol.* (2014) 193:2127–34. doi: 10.4049/jimmunol.1400857
119. Parsons N, Annamalai B, Obert E, Schnabolk G, Tomlinson S, Rohrer B. Inhibition of the alternative complement pathway accelerates repair processes in the murine model of choroidal neovascularization. *Mol Immunol.* (2019) 108:8–12. doi: 10.1016/j.molimm.2019.02.001
120. Cortright DN, Meade R, Waters SM, Chenard BL, Krause JE. C5a, but not C3a, increases VEGF secretion in ARPE-19 human retinal pigment epithelial cells. *Curr Eye Res.* (2009) 34:57–61. doi: 10.1080/02713680802546658
121. Lee D, Son HG, Jung Y, Lee SV. The role of dietary carbohydrates in organismal aging. *Cell Mol Life Sci.* (2017) 74:1793–803. doi: 10.1007/s00018-016-2432-6
122. Zhou J, He S, Zhang N, Spee C, Zhou P, Ryan SJ, et al. Neutrophils compromise retinal pigment epithelial barrier integrity. *J Biomed Biotechnol.* (2010) 2010:289360. doi: 10.1155/2010/289360
123. Katschke KJ,Jr, Xi H, Cox C, Truong T, Malato Y, Lee WP, et al. Classical and alternative complement activation on photoreceptor outer segments drives monocyte-dependent retinal atrophy. *Sci Rep.* (2018) 8:7348. doi: 10.1038/s41598-018-30162-w
124. Jiao H, Rutar M, Fernando N, Yednock T, Sankaranarayanan S, Aggio-Bruce R, et al. Subretinal macrophages produce classical complement activator C1q leading to the progression of focal retinal degeneration. *Mol Neurodegener.* (2018) 13:45. doi: 10.1186/s13024-018-0278-0
125. Lynch AM, Mandava N, Patnaik JL, Frazer-Abel AA, Wagner BD, Palestine AG, et al. Systemic activation of the complement system in patients with advanced age-related macular degeneration. *Eur J Ophthalmol.* (2019) 1120672119857896. doi: 10.1177/1120672119857896. [Epub ahead of print].
126. Scholl HP, Charbel Issa P, Walier M, Janzer S, Pollok-Kopp B, Borncke F, et al. Systemic complement activation in age-related macular degeneration. *PLoS ONE.* (2008) 3:e2593. doi: 10.1371/journal.pone.0002593
127. Ajona D, Hsu YF, Corrales L, Montuenga LM, Pio R. Down-regulation of human complement factor H sensitizes non-small cell lung cancer cells to complement attack and reduces *in vivo* tumor growth. *J Immunol.* (2007) 178:5991–8. doi: 10.4049/jimmunol.178.9.5991
128. Corrales L, Ajona D, Rafail S, Lasarte JJ, Riezu-Boj JI, Lambris JD, et al. Anaphylatoxin C5a creates a favorable microenvironment for lung cancer progression. *J Immunol.* (2012) 189:4674–4683. doi: 10.4049/jimmunol.1201654
129. Markiewski MM, DeAngelis RA, Benencia F, Ricklin-Lichtsteiner SK, Koutoulaki A, Gerard C, et al. Modulation of the antitumor immune response by complement. *Nat Immunol.* (2008) 9:1225–1235. doi: 10.1038/ni.1655
130. Nitta H, Murakami Y, Wada Y, Eto M, Baba H, Imamura T. Cancer cells release anaphylatoxin C5a from C5 by serine protease to enhance invasiveness. *Oncol Rep.* (2014) 32:1715–9. doi: 10.3892/or.2014.3341
131. Darling VR, Hauke RJ, Tarantolo S, Agrawal DK. Immunological effects and therapeutic role of C5a in cancer. *Expert Rev Clin Immunol.* (2015) 11:255–63. doi: 10.1586/1744666X.2015.983081
132. Yoneda M, Imamura R, Nitta H, Taniguchi K, Saito F, Kikuchi K, et al. Enhancement of cancer invasion and growth via the C5a-C5a receptor system: Implications for cancer promotion by autoimmune diseases and association with cervical cancer invasion. *Oncol Lett.* (2019) 17:913–920. doi: 10.3892/ol.2018.9715
133. Calippe B, Augustin S, Beguier F, Charles-Messance H, Poupel L, Conart JB, et al. Complement factor H inhibits CD47-mediated resolution of inflammation. *Immunity.* (2017) 46:261–72. doi: 10.1016/j.immuni.2017.01.006
134. Toomey CB, Kelly U, Saban DR, Bowes Rickman C. Regulation of age-related macular degeneration-like pathology by complement factor H. *Proc Natl Acad Sci USA.* (2015) 112:E3040–9. doi: 10.1073/pnas.1424391112
135. Ma W, Zhao L, Fontainhas AM, Fariss RN, Wong WT. Microglia in the mouse retina alter the structure function of retinal pigmented epithelial cells: a potential cellular interaction relevant to AMD. *PLoS ONE.* (2009) 4:e7945. doi: 10.1371/journal.pone.0007945
136. Raoul W, Keller N, Rodero M, Behar-Cohen F, Sennlaub F, Combadiere C. Role of the chemokine receptor CX3CR1 in the mobilization of phagocytic retinal microglial cells. *J Neuroimmunol.* (2008) 198:56–61. doi: 10.1016/j.jneuroim.2008.04.014
137. Ishikawa K, Sreekumar PG, Spee C, Nazari H, Zhu D, Kannan R, Hinton DR. alphaB-crystallin regulates subretinal fibrosis by modulation of epithelial-mesenchymal transition. *Am J Pathol.* (2016) 186:859–73. doi: 10.1016/j.ajpath.2015.11.014
138. Carbone C, Moccia T, Zhu C, Paradiso G, Budillon A, Chiao PJ, et al. Anti-VEGF treatment-resistant pancreatic cancers secrete proinflammatory factors that contribute to malignant progression by inducing an EMT cell phenotype. *Clin Cancer Res.* (2011) 17:5822–32. doi: 10.1158/1078-0432.CCR-11-1185

139. Condamine T, Ramachandran I, Youn JI, Gabrilovich DI. Regulation of tumor metastasis by myeloid-derived suppressor cells. *Annu Rev Med.* (2015) 66:97–110. doi: 10.1146/annurev-med-051013-052304
140. Fan Q, Gu D, Liu H, Yang L, Zhang X, Yoder MC, et al. Defective TGF-beta signaling in bone marrow-derived cells prevents hedgehog-induced skin tumors. *Cancer Res.* (2014) 74:471–83. doi: 10.1158/0008-5472.CAN-13-2134-T
141. Dvashi Z, Goldberg M, Adir O, Shapira M, Pollack A. TGF-beta1 induced transdifferentiation of rpe cells is mediated by TAK1. *PLoS ONE.* (2015) 10:e0122229. doi: 10.1371/journal.pone.0122229
142. Saika S. TGFbeta pathobiology in the eye. *Lab Invest.* (2006) 86:106–15. doi: 10.1038/labinvest.3700375
143. Ioannou M, Alissafi T, Lazaridis I, Deraos G, Matsoukas J, Gravanis A, et al. Crucial role of granulocytic myeloid-derived suppressor cells in the regulation of central nervous system autoimmune disease. *J Immunol.* (2012) 188:1136–46. doi: 10.4049/jimmunol.1101816
144. Sendo S, Saegusa J, Morinobu A. Myeloid-derived suppressor cells in non-neoplastic inflamed organs. *Inflamm Regen.* (2018) 38:19. doi: 10.1186/s41232-018-0076-7
145. Zhu B, Kennedy JK, Wang Y, Sandoval-Garcia C, Cao L, Xiao S, et al. Plasticity of Ly-6C (hi) myeloid cells in T cell regulation. *J Immunol.* (2011) 187:2418–32. doi: 10.4049/jimmunol.1100403
146. Liesz A, Dalpke A, Mracsko E, Antoine DJ, Roth S, Zhou W, et al. DAMP signaling is a key pathway inducing immune modulation after brain injury. *J Neurosci.* (2015) 35:583–98. doi: 10.1523/JNEUROSCI.2439-14.2015
147. Saiwai H, Kumamaru H, Ohkawa Y, Kubota K, Kobayakawa K, Yamada H, et al. Ly6C+ Ly6G- Myeloid-derived suppressor cells play a critical role in the resolution of acute inflammation and the subsequent tissue repair process after spinal cord injury. *J Neurochem.* (2013) 125:74–88. doi: 10.1111/jnc.12135
148. Jeong HJ, Lee HJ, Ko JH, Cho BJ, Park SY, Park JW, et al. Myeloid-derived suppressor cells mediate inflammation resolution in humans and mice with autoimmune uveoretinitis. *J Immunol.* (2018) 200:1306–15. doi: 10.4049/jimmunol.1700617
149. Lee HJ, Ko JH, Jeong HJ, Ko AY, Kim MK, Wee WR, et al. Mesenchymal stem/stromal cells protect against autoimmunity via CCL2-dependent recruitment of myeloid-derived suppressor cells. *J Immunol.* (2015) 194:3634–45. doi: 10.4049/jimmunol.1402139
150. Zhao J, Chen M, Xu H. Experimental autoimmune uveoretinitis (EAU) -related tissue damage angiogenesis is reduced in CCL2 (-)/(-) CX(3) CR1gfp/gfp mice. *Invest Ophthalmol Vis Sci.* (2014) 55:7572–82. doi: 10.1167/iovs.14-15495

Conflict of Interest: The authors declare that the research was conducted in the absence of any commercial or financial relationships that could be construed as a potential conflict of interest.

frontiers in Immunology

ORIGINAL RESEARCH
published: 07 April 2020
doi: 10.3389/fimmu.2020.00574

Retinal Distribution and Extracellular Activity of Granzyme B: A Serine Protease That Degrades Retinal Pigment Epithelial Tight Junctions and Extracellular Matrix Proteins

Joanne A. Matsubara[1], Yuan Tian[1], Jing Z. Cui[1], Matthew R. Zeglinski[2,3], Sho Hiroyasu[2,3], Christopher T. Turner[2,3] and David J. Granville[2,3]*

[1] Department of Ophthalmology and Visual Sciences, University of British Columbia (UBC), Vancouver, BC, Canada,
[2] International Collaboration on Repair Discoveries (ICORD), University of British Columbia (UBC), Vancouver, BC, Canada,
[3] Department of Pathology and Laboratory Medicine, University of British Columbia (UBC), Vancouver, BC, Canada

OPEN ACCESS

Edited by:
Heping Xu,
Queen's University Belfast,
United Kingdom

Reviewed by:
Torben Lykke Sørensen,
University of Copenhagen, Denmark
Gerard Anthony Lutty,
John Hopkins Medicine, United States

***Correspondence:**
Joanne A. Matsubara
jms@mail.ubc.ca

Specialty section:
This article was submitted to Immunological Tolerance and Regulation, a section of the journal Frontiers in Immunology

Received: *31 October 2019*
Accepted: *12 March 2020*
Published: *07 April 2020*

Citation:
Matsubara JA, Tian Y, Cui JZ, Zeglinski MR, Hiroyasu S, Turner CT and Granville DJ (2020) Retinal Distribution and Extracellular Activity of Granzyme B: A Serine Protease That Degrades Retinal Pigment Epithelial Tight Junctions and Extracellular Matrix Proteins. Front. Immunol. 11:574. doi: 10.3389/fimmu.2020.00574

Granzymes are a family of serine proteases first shown to be intracellular initiators of immune-mediated cell death in target pathogenic cells. In addition to its intracellular role, Granzyme B (GzmB) has important extracellular functions in immune regulation and extracellular matrix (ECM) degradation. Verified substrates of extracellular GzmB activity include tight junctional and ECM proteins. Interestingly, little is known about the activity of GzmB in the outer human retina, a tissue in which the degradation of the tight junctional contacts of retinal pigment epithelial (RPE) cells and within the external limiting membrane, as well as remodeling of the ECM in Bruch's membrane, cause the breakdown of the blood-retinal barrier and slowing of metabolite transport between neuroretina and choroidal blood supply. Such pathological changes in outer retina signal early events in the development of age-related macular degeneration (AMD), a multifactorial, chronic inflammatory eye disease. This study is the first to focus on the distribution of GzmB in the outer retina of the healthy and diseased post-mortem human eye. Our results revealed that GzmB is present in RPE and choroidal mast cells. More immunoreactive cells are present in older (>65 years) compared to younger (<55 years) donor eyes, and choroidal immunoreactive cells are more numerous in eyes with choroidal neovascularization (CNV), while RPE immunoreactive cells are more numerous in eyes with soft drusen, an early AMD event. *In vitro* studies demonstrated that RPE-derived tight junctional and ECM proteins are cleaved by exogenous GzmB stimulation. These results suggest that the increased presence of GzmB immunoreactive cells in outer retina of older (healthy) eyes as well as in diseased eyes with CNV (from AMD) and eyes with soft drusen exacerbate ECM remodeling in the Bruch's membrane and degradation of the blood-retinal barrier. Currently there are no treatments that prevent remodeling of the Bruch's membrane and/or the loss of function of the outer blood-retinal barrier,

known to promote early AMD changes, such as drusen deposition, RPE dysfunction and pro-inflammation. Specific inhibitors of GzmB, already in preclinical studies for non-ocular diseases, may provide new strategies to stop these early events associated with the development of AMD.

Keywords: ZO-1, blood-eye barrier, Bruch's membrane, geographic atrophy, soft drusen, choroidal neovascularization, FITC-dextran permeability, ARPE-19

INTRODUCTION

Age-related macular degeneration (AMD) is a complex disease with many risk factors contributing to its pathogenesis (2–4). Despite the fact that clinical and genetic data support an association of a chronic, low-grade inflammatory response in the outer retina during the development of AMD, the exact underlying mechanisms and triggers of inflammation remain elusive (5). Genetic studies point to a central role of the innate immune response and particularly the complement cascade in the development and progression of AMD [for review see (6)]. However, we do not yet understand exactly what causes the earliest signs of inflammation in the retina.

We recently reported that the RPE and immune cells (primarily mast cells) in the choroid express Granzyme B (GzmB) (7), a serine protease that was once thought to function exclusively as intracellular initiators of immune-mediated cell death, capable of inducing apoptosis (a process requiring perforin, a pore-forming protein) in target cells. Earlier studies in non-ocular systems identified that GzmB is located on chromosome 14 in both human (14q.11.2) and mouse genomes. Several cytotoxic [natural killer (NK), CD8+, T], non-cytotoxic immune (mast, macrophages, basophils), and non-immune cells (spermatozoa, keratinocytes) express GzmB. In addition to its well-established intracellular role, GzmB also has important extracellular functions in immune regulation and the degradation of extracellular matrix (ECM) proteins (8–12). Experimental degranulation of choroidal mast cells in rodents resulted in RPE abnormalities and outer retinal barrier breakdown (13), however it is not yet known which of the many proteases, or other choroidal mast cell mediators, are involved (14).

Here we report the age-related changes and cellular distribution of GzmB in the healthy and diseased human outer retina, and *in vitro* evidence for GzmB's extracellular role in the disruption of the outer blood-retinal barrier (oBRB) function by cleavage of tight junctional proteins between retinal pigment epithelial (RPE) cells and ECM proteins in Bruch's Membrane (BM). BM is an important outer retinal ECM that regulates the exchange between the (1) metabolically active combination of photoreceptor and RPE and (2) the choriocapillaris blood supply. Several of the ECM proteins within BM are known substrates for extracellular GzmB activity, including fibronectin (FN), vitronectin (VN), and laminin (LAM) and a small subset of collagens (COL) (1, 15–18) (**Figure 1**). The remodeling of BM during aging and AMD is known to also affect RPE cell adhesion and function, which in turn, compromises oBRB function (18, 19). In addition to the breakdown of BM, outer retina is also compromised by the loss of function of the oBRB, which is maintained by the tight junctional contacts between RPE cells. Given that the breakdown of BM and loss of oBRB function are associated with the earliest events in the development of AMD (1, 19–21), we speculate that GzmB activity may promote early changes in outer retina that contribute to AMD development.

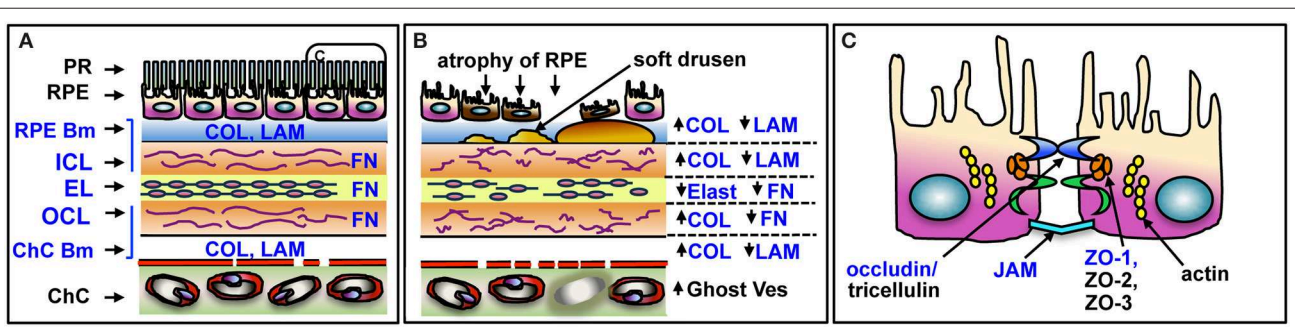

FIGURE 1 | Schematic of outer retina and substrates of GzmB in BM and RPE. **(A)** The five layers of BM and major ECM proteins are shown in blue text. The PR and RPE sit above the BM on the RPE basement membrane. The choriocapillaris sits below BM, on its basement membrane. **(B)** Changes in outer retina associated with AMD pathology. RPE undergo atrophy and cell death, soft drusen deposits accumulate below RPE. Laminin, elastin, and fibronectin undergo cleavage resulting in overall ECM fragility; altered forms of collagen increase, causing thickening of BM. Choriocapillaris undergoes atrophy, with closure of some vessels, identified as ghost vessels. **(C)** Enlargement of box in **(A)** depicting tight junctional and cell adhesion proteins on RPE cleaved by GzmB in blue text. PR, photoreceptors; RPE, retinal pigment epithelium; RPE Bm, basement membrane of RPE; ICL, inner collagenous layer; EL, elastin layer; OCL, outer collagenous layer; ChC Bm, basement membrane of the choriocapillaris; COL, collagen; LAM, laminin; FN, fibronectin; Ghost Ves, closed lumen of vessel with dead endothelial cells; JAM, junctional adhesion molecules; ZO, zonula occludins. Adapted from Nita et al. (1).

Our earlier work showed that GzmB cleaves ECM in non-ocular systems, implicating extracellular GzmB activity in pathological chronic inflammation, delayed wound healing, skin injuries, and cardiopulmonary disease (8–10, 12, 22). Here we address the evidence that age-related increases in extracellular GzmB in the outer retina promote pathological remodeling of the BM and alterations in RPE barrier function. Given that there are no treatment strategies that prevent pathological breakdown of BM or the oBRB, studies on the extracellular GzmB activity in ocular tissues may allow us further insights into novel immune-mediated mechanisms associated with degradation and remodeling of the outer retina during aging and AMD development.

MATERIALS AND METHODS

Sixteen pairs of non-diseased donor eyes, consented for research, were obtained from the Eye Bank of British Columbia (EBBC, Vancouver, British Columbia, Canada). Healthy eyes collected within 12 h following death were immersed in 10% buffered formalin after corneal tissues removed for corneal transplant purposes. Each normal donor eye had a medical/hospital history obtained by EBBC, and these eyes, to the best of our knowledge, were ocular disease free. These eyes were then embedded in paraffin and serial sections at 6 micra thickness were obtained. Every 20th section was stained for H & E and assessed by light microscopy. Tissue sections from the macular area were assessed to identify and screen for ocular pathologies. Healthy eyes had normal retinal organization, and did not display outer retinal fibrosis, RPE/PR degeneration, neovascularization, or hemorrhage. Healthy donor tissues with the following pathologies were excluded in this study: local or systemic infection, progressive brain pathologies, systemic diseases of unknown origin, lymphoproliferative, or myeloproliferative disorders or any intrinsic eye disease.

Diseased eyes with geographic atrophy (GA), choroidal neovascularisation (CNV), or soft drusen deposits were obtained from the Department of Pathology, UBC. Tissue sections from the macular area were stained by hematoxylin and eosin, and then assessed by ophthalmic pathologists to identify and screen for ocular pathologies. In total, 8 eyes with GA (from AMD), 6 eyes with CNV (from AMD), 9 eyes with numerous soft drusen (from non-AMD eyes) were included in this study. For cell culture studies, ARPE-19 (RPE cell line, ATCC) and primary fetal RPE cells were used. Primary RPE were isolated from human fetal donor eyes, with no known pathology, that were consented for research studies from the CARE program at BC Women's Hospital under Clinical Research Ethics Board (UBC) approval.

Immunohistochemistry

Human Outer Retina

The immunohistochemical procedures and analysis followed those previously described (23). Briefly, deparaffinized tissue sections (6 μm thickness) were probed with a primary antibody against GzmB (Abcam), followed by incubation in secondary antibody and developed in ABC–AEC system (Vector Labs). All sections were taken from central macular area of the retina and each cross section used in this analysis contained the optic nerve head to verify its retinal location. A list of primary and secondary antibodies, source, and dilutions is shown in **Table 1**. The immunoreactive RPE and immune cells in the choroidal layers were counted and normalized to 1,050 μm length units of BM. Approximately 4–6 sections per donor eye were analyzed. The immunoreactivity was compared among eyes from healthy older, healthy younger, GA, CNV, or soft drusen (an early marker of AMD) donors.

TABLE 1 | List of antibodies used.

Antigen	Antibody (Catalog No.)	Dilution	Source
GzmB	Rabbit polyclonal (ab4059)	1:100	Abcam, Burlingame, CA
ZO-1	Rabbit polyclonal (61-7300)	1:100	Thermo Fisher Scientific, Waltham, MA
JAM-A	Mouse monoclonal (14-3219-82)	1:100	Thermo Fisher Scientific, Waltham, MA
Occludin	Mouse monoclonal (E-5. SC-133256)	1:100	Santa Cruz Biotechnology, Dallas TX
Vinculin	Rabbit monoclonal (ab129002)	1:1,000	Abcam, Burlingame, CA
Fibronectin	Rabbit polyclonal (ab2413)	1:1,000	Abcam, Burlingame, CA
Laminin 5	Rabbit polyclonal (ab14509)	1:1,000	Abcam, Burlingame, CA
Collagen IV	Mouse monoclonal (G-2. SC-398655)	1:1,000	Santa Cruz Biotechnology, Dallas TX
Collagen I	Mouse monoclonal (E-6. SC-393573)	1:1,000	Santa Cruz Biotechnology, Dallas TX
CD68	Mouse monoclonal (M0876)	1:100	Dako Carpinteria, CA
Tryptase	Mouse monoclonal (ab2378)	1:100	Abcam, Burlingame, CA
Rabbit IgG Horseradish Peroxidase conjugated Antibody	Polyclonal Goat IgG (HAF008)	1:1,000	R&D Systems, Minneapolis, MN
Mouse IgG Horseradish Peroxidase conjugated Antibody	Polyclonal Donkey IgG (HAF018)	1:1,000	R&D Systems, Minneapolis, MN

ARPE-19 or Primary RPE Cells Grown in Chamber Slides or Transwell Inserts

Tight junctional proteins were visualized by immunofluorescence on both ARPE19 or primary RPE cells grown to confluence and stimulated in chamber slides. Tight junctional proteins were evident on ARPE19 (within 5–7 days) and on primary RPE (within 7–10 days) in culture. After GzmB stimulation, cells were fixed *in situ* with cold methanol, washed with PBS, and incubated in 2% normal goat serum (Vector Labs) for 30 min at room temperature (RT). Next, chamber slides were incubated with antibody against ZO-1 (Invitrogen), JAM-A (Invitrogen), or Occludin (Santa Cruz). All antibodies were

diluted at 1:100 in PBS with 0.1% TX-100 and chamber slides were incubated for 1 h at RT, then overnight at 4°C. Primary antibodies were omitted for negative controls. Next, slides were thoroughly washed with PBS, and then incubated with Alexa 488 conjugated goat anti-rabbit or anti-mouse secondary antibody (1:400) for 1 h at RT. Slides were washed with PBS, and then incubated with Hoechst 33258 (DAPI, Sigma, 1:500) for 20 min. A blade was used to remove chambers and silicon tapes, and marker pen was used to label the locations of different chambers on slides. Slides were mounted with glycerol (50:50 glycerol: PBS) and 1.5 mm coverslips. For transwell inserts, after GzmB stimulation and measurements of FITC-dextrans fluorescence, membranes at the bottom of inserts were cut out and adherent ARPE-19 cells underwent immunocytochemistry with ZO-1 primary antibody as above. An LSM 510 confocal laser-scanning microscope was used to image antibody labeling at 488 and 543 nm, DAPI (nuclei) was imaged at 405 nm and images stored as digital files. All settings on confocal were kept constant throughout the imaging sessions in order to compare intensity of fluorescent signals between groups.

Cell Culture

Primary RPE were grown as described previously (24). Briefly, passage 5–7 ARPE-19 cells (or passage 3–5 primary RPE cells) were seeded into 6 well plates in 1.0 mL Dulbecco's modified Eagle Medium/F12 medium (DMEM, Life Technologies) containing 10% fetal bovine serum (FBS), 100 U/mL penicillin and 100 μg/mL streptomycin and kept in a humidified chamber with 5% CO_2 at 37°C until confluent. Cells were washed with PBS and starved for 3 h in serum free DMEM before GzmB stimulation. GzmB was isolated YT cells, an autonomously proliferating human NK cell line devoid of GzmA and GzmK activity, and procedures were modified from Shi et al. (25). Next, DMEM medium with 0 nM (control) or 100 nM GzmB was added to wells and cells cultured at 37°C incubator for 5 h. After 5 h, supernatants were carefully removed and stored, and cells rinsed with PBS on ice. Total protein lysates were collected for western blot analysis. To determine effects of exogenous GzmB on the cleavage of RPE-derived ECM proteins WBs were undertaken using both supernatant and lysate samples.

In some studies, ARPE19, a human RPE cell line, were used at passage 5–7 (26). These cells were grown to confluence on chamber slides or transwell inserts. Briefly, $\sim 1.6 \times 10^5/cm^2$ cells were seeded in a laminin-coated Transwell insert (0.4 μm pore size, 12 mm diameter, Fisher Scientific) or on chamber slides (LabTek II) in 0.2 mL DMEM containing 10% FBS, 100 U/mL penicillin and 100 μg/mL streptomycin and kept in a humidified chamber with 5% CO_2 at 37°C. Next, the cells were washed with PBS, starved for 3 h in serum-free DMEM before GzmB stimulation. DMEM medium with GzmB (0, 1, 10, 50, 100) was added to culture slides for 5 h at 37°C. After 5 h, culture medium was removed and stored; cells were fixed *in situ* with 100% methanol on ice for 15 min.

MTT Cell Viability Assay

ARPE-19 cells were grown to 95% confluence in 96-well plates for MTT assays. Cells were then washed with PBS twice and then starved for 3 h in serum-free DMEM before GzmB stimulation at different concentrations (0, 10, 20, 50, 100 nM). Next, the 96-well plates were placed in 37°C incubator for 24 h. After 24 h, culture medium was removed, and 250 μl of 0.5 mg/ml MTT buffer (1:10 dilution in DMEM) was added to each well, incubated at 37°C for 2 h. MTT solution was removed, 250 μl DMSO added to each well and reincubated at 37°C for 15–20 min; next, absorbance at 570 nm wavelength was read using the Hybrid Multi-Mode Reader (BioTek Synergy H1).

Western Blot

To detect the cleaved products in primary RPE cultures after GzmB stimulation, confluent primary RPE cells were first starved (as above), then treated with GzmB (0 or 100 nM) in 37°C incubator for 5 h. After 5 h, culture supernatants were collected and aliquoted for later analysis, and RPE cells rinsed with PBS twice on ice. Next, the adherent cells were treated with 200 μl of lysis buffer [10 ml RIPA lysis buffer with proteinase inhibitor cocktail (Roche)] and cell lysates collected from each well, centrifuged for 10 min at 4°C, and aliquoted. Cell lysates were quantified with a BCA Assay (Pierce, Thermo Fisher) for total protein concentrations and run on gels under reducing conditions. Established blotting procedures were followed to visualize the proteins of interest. A list of primary and secondary antibodies, source and dilutions used in western blot is shown in **Table 1**. Targeted proteins on membranes were detected with Pierce™ ECL Western Blotting Substrate Kit (Thermo Fisher). Protein band intensity was measured using Image J (NIH). Vinculin, a high molecular weight (MW = 124 kDa) housekeeping gene, was used for quality control on supernatant samples.

FITC-Dextran Permeability Assay

Primary RPE cells were grown to confluence in transwell system inserts for 24-well plates for a functional assay of solute flux through the monolayer. For dextran permeability assay, the transwells were washed with PBS, and starved for 3 h in serum-free DMEM before GzmB stimulation. DMEM with 0 nM (controls) or 100 nM GzmB was placed in the upper insert of the transwell systems at 37°C for 5 h. After 5 h, the culture medium was removed without disturbing cells, and DMEM culture medium with 1 mg/ml FITC-dextran (70 kDa, Sigma) solution was added into all upper inserts for another 5 h. After 5 h, all inserts were removed and fluorescence intensity at 490 nm (excitation)/520 nm (emission) wavelengths was read using the Hybrid Multi-Mode Reader (BioTek Synergy H1). For trans-epithelial resistance measurements, transwells were placed in electric cell substrate impedance sensing apparatus, media changed to serum free and allowed to stabilize before addition of 0 nM (controls) or 50–100 nM GzmB in to lower or upper compartment. Averaged measurements of impedance, capacitance are graphed for 0–24 h.

Statistical Analysis

Data are presented as mean ± SEM. All experiments were repeated in triplicate or quadruplicate. Statistical analysis was performed using Prism Ver8 (GraphPad Software). To compare

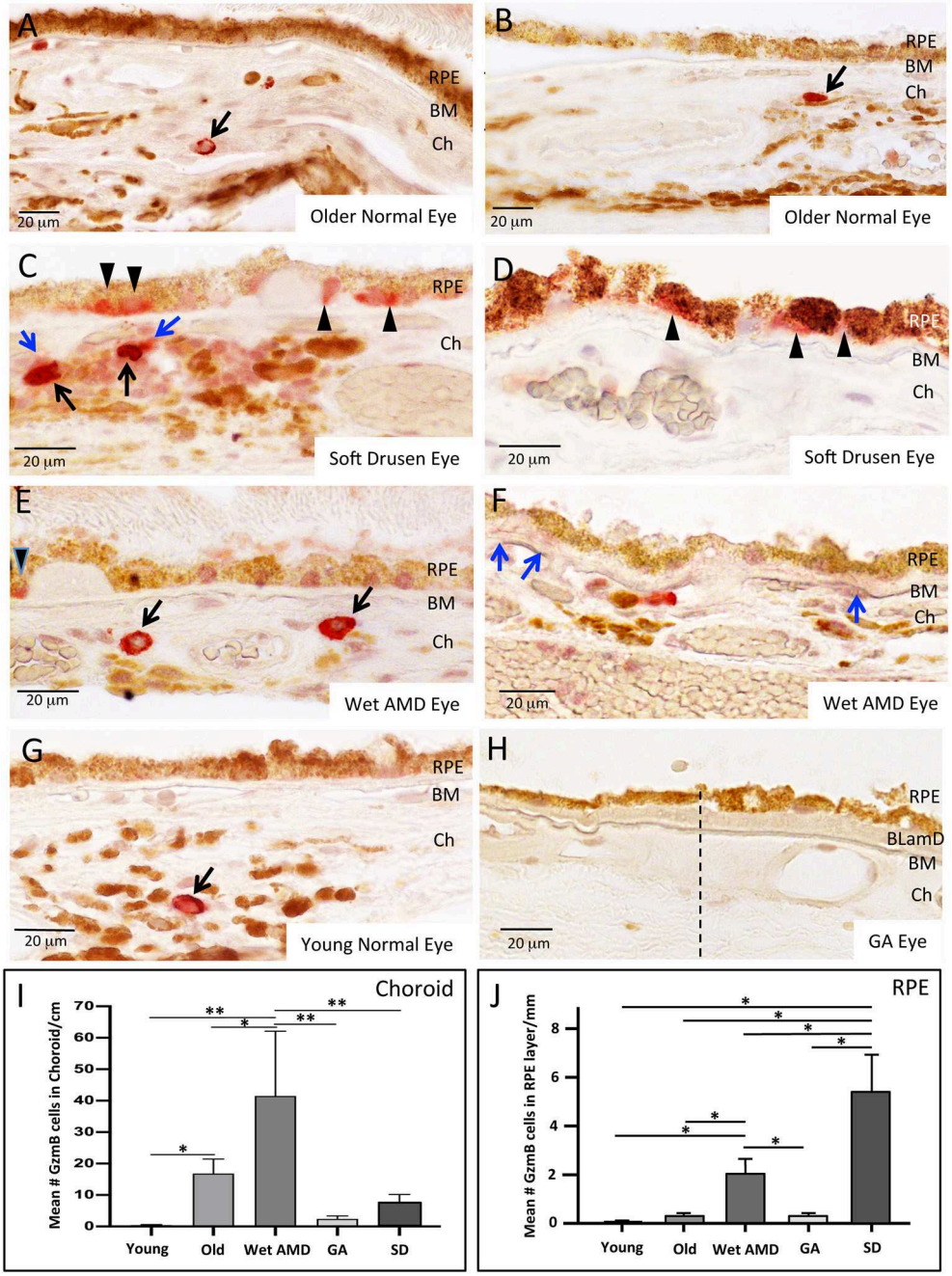

FIGURE 2 | GzmB Immunoreactivity in normal and diseased human outer retina. **(A,B)** Examples of GzmB immunoreactivity in an older normal eye. Strong labeling with amino-ethyl carbazole chromogen (red) indicates GzmB+ cells in the choroid (black arrows). RPE cells in older normal eyes rarely displayed GzmB immunoreactivity. **(C,D)** Examples of GzmB immunoreactivity in eyes with soft drusen, an early marker of AMD. Strong labeling with amino-ethyl carbazole chromogen (red) indicates GzmB+ cells in the choroid (black arrows), with a cloud of extracellular GzmB immunolabeling surrounding the choroidal mast cells (blue arrows). The basal compartment of the RPE cell near soft drusen sites also contains GzmB immunoreactivity (black arrowheads). Note GzmB+ RPE appear of the "non-uniform" phenotype (27). **(E,F)** Examples of GzmB immunoreactivity in a wet AMD eye. Strong labeling with amino-ethyl carbazole chromogen (red) indicates GzmB+ cells in the choroid (black arrows). Extracellular GzmB immunolabeling is evident in the basal laminar deposit (blue arrows) of a wet AMD eye. In wet AMD eyes, fewer RPE cells contained GzmB compared to eyes with soft drusen, however, one is shown in **(E)** near a drusen site (black arrowhead). **(G)** An example of GzmB immunoreactivity in a younger normal eye demonstrating a single choroidal mast cell (arrow). RPE cells in younger normal eyes rarely displayed GzmB immunoreactivity. **(H)** GzmB immunoreactivity in a GA eye. Note lack of red chromogen product in choroid and in RPE. Dash line indicates a change in the morphology of the RPE monolayer, with "non-uniform" and "dissociated" RPE phenotypes to the right of the dashed line (27). Note thickened basal laminar deposit (BLamD) and deterioration of the choriocapillaris. Additional images of a GA eye are shown in **Supplementary Figure 6**. **(I)** Analysis of GzmB immunoreactivity of

(Continued)

FIGURE 2 | choroidal cells in older (>65 years, $N = 8$) and younger (<55 years $N = 8$) normal donor eyes, wet AMD ($N = 6$), GA ($N = 8$), and soft drusen eyes ($N = 9$). The number of GzmB+ choroidal cells was significantly higher in wet AMD eyes compared to all other groups, while the number of GzmB+ choroidal cells in older eyes was significantly higher than younger eyes. One-way ANOVA Test and Tukey's multiple comparisons *post-hoc* test (*$p < 0.05$; **$p < 0.01$). **(J)** Analysis of GzmB immunoreactivity of RPE cells in older (>65 years, $N = 8$) and younger (<55 years $N = 8$) normal donor eyes, wet AMD ($N = 6$), GA ($N = 8$), and soft drusen ($N=9$). The number of GzmB+ RPE cells was significantly higher in soft drusen compared to all other groups, while the number of GzmB+ RPE cells in wet AMD eyes was significantly higher than younger, older and GA eyes, but significantly lower than soft drusen eyes. One-way ANOVA Test and Tukey's multiple comparisons *post-hoc* test. (*$p < 0.05$). Scale bar: 20 μm.

two groups, independent sample *T*-test was used for western blot and immunohistochemistry analysis of human tissue samples. To compare more than two groups, a one-way ANOVA test with Tukey's multiple comparisons *post-hoc* test was used. Statistical significance level was set at $p < 0.05$.

RESULTS

GzmB Immunohistochemistry in Human Outer Retina

Our earlier work showed that GzmB accumulates in cardiovascular, pulmonary and skin tissues with aging and/or chronic inflammation (10, 11, 28). Here, we assessed GzmB immunoreactivity in outer retina of postmortem eyes from older (>65 years) and younger (<55 years) donors. We assessed the GzmB+ cells in the choroidal stroma only and omitted blood cells that were clearly in vasculature. The older donor eyes had more GzmB+ labeling than younger eyes, consistent with our earlier findings in the retina of aged mouse models (7), (**Figures 2A,B,G,I**). The majority of GzmB+ cells were choroidal mast cells (identified by toluidine blue staining, **Supplementary Figure 1**) in the choriocapillaris and Sattler's layer, however within the choroidal stromal layers, a small number of macrophages (identified by CD68 immunoreactivity, **Supplementary Figure 4**) were also GzmB+. RPE were immunoreactive for GzmB, with slightly increased numbers in older donors. However, unlike the choroidal mast cells, the number of GzmB immunoreactive RPE in younger and older healthy donors did not reach significance (**Figures 2I,J**).

Next, we assessed the distribution of GzmB+ choroidal cells in donor eyes with geographic atrophy (GA from AMD), eyes with the exudative (wet) form of AMD and eyes with soft drusen (SD, an early precursor to AMD pathology). Wet AMD eyes contained greater numbers of GzmB+ choroidal cells compared to GA (**Figures 2E,H**, **Supplementary Figure 6**) or soft drusen eyes (**Figures 2C,D,I**). Extracellular GzmB labeling was also evident in the BM and basal laminar deposits in wet AMD eyes and in GA eyes (**Figure 2F**, **Supplementary Figures 5, 6**). In the CNV lesion of a wet AMD eye, extracellular GzmB immunoreactivity was present in the CNV lesion near hypertrophied RPE (**Supplementary Figure 5**).

The pattern of GzmB labeling in RPE cells amongst the donor eye groups was different from that observed for GzmB+ choroidal cells (**Figure 2J**). Eyes with soft drusen had higher numbers of RPE cells expressing GzmB than the CNV or GA eyes (**Figures 2C–F,H**). The RPE cells expressing GzmB were often spatially located near soft drusen deposits (**Figures 2C–E**). However, GzmB immunoreactivity was not located in RPE near hard drusen deposits (**Supplementary Figure 5**). Those RPE cells, which were immunoreactive for GzmB, usually had labeling in the basal cytoplasmic compartment of the RPE (**Figures 2C–E**) and appeared to belong to the categories of "non-uniform" RPE phenotypes (27).

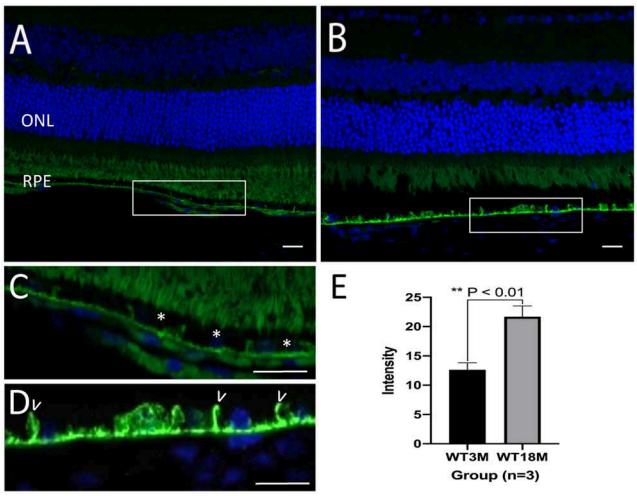

FIGURE 3 | Immunreactivity of GzmB in Bruch's Membrane and RPE layer of a young (3 month) and old (18 month) C57Bl/6J mouse retina. **(A)** GzmB immunoreactivity (green, 488 nm) is lower in mouse retina from 3 month old mouse compared to **(B)** an 18 month old mouse. Boxed areas are shown at higher power in **(C)** with GzmB punctate labeling (*) on Bruch's membrane of 3 month old, and in **(D)** which demonstrates stronger immunofluorescence intensity along BM and between RPE cell borders (some shown by white arrowheads) of the older mouse retina. **(E)** Independent-sample *T*-test ($n = 3$) between two groups shows the increased GzmB level in BM and RPE layers of 18M mice: mean ± SEM; *$p < 0.01$. DAPI (405 nm) labeling of nuclei is shown in blue. Scale bar = 20 μm.

In C57Bl/6J mice, GzmB immunoreactivity was present in outer retina, specifically in the extracellular matrix of BM and the intercellular spaces between RPE cells (**Figures 3A–D**). In the mouse models, there was an age-dependent increase in GzmB immunoreactivity (**Figure 3E**).

Extracellular GzmB Cleaves RPE Tight Junctional and Cell Adhesion Proteins

In vitro studies were undertaken to assess the impact of exogenous GzmB on RPE cell cultures. First we assessed the effect of GzmB on cell viability using an MTT assay. ARPE-19 cells stimulated with exogenous GzmB for 24 h, at concentrations from 10 to 100 nM, demonstrated no changes in cell viability

compared to controls (GzmB at 0 nM) (**Figure 4**). Next, ARPE-19 cells were grown and stimulated with GzmB at 1, 10, 50, and 100 nM for 6 h in chamber slides to assess the degradation in tight junctional protein ZO-1. Significant degradation of ZO-1 was observed at 50 and 100 nM GzmB as shown by loss of immunofluorescence (**Figures 5A–G**). Exogenous GzmB stimulation at 100 nM also cleaved and degraded JAM-A and Occludin, two additional tight junctional proteins on ARPE-19, as shown by loss of immunofluorescence (**Figures 6A–G**). These data extend earlier work by demonstrating that tight junctional proteins from an ocular source (e.g., RPE-derived) are substrates of GzmB.

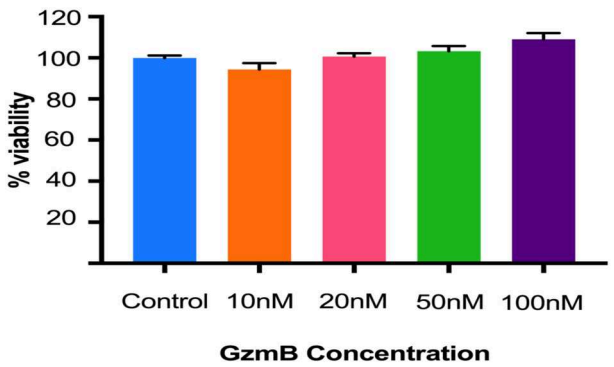

FIGURE 4 | GzmB does not affect the viability of ARPE-19 cells. Cells were treated with exogenous GzmB (10, 20, 50, 100 nM) for 24 h and compared to controls (GzmB = 0 nM). No significant changes were observed in viability at any of the GzmB concentrations. Data were analyzed using one-way ANOVA test and Tukey's multiple comparisons *post-hoc* test (mean ± SEM, $N = 5$ per group).

Extracellular GzmB Causes Increased Dextran Flux in Confluent ARPE-19 Cultures

It is hypothesized that the functional significance of GzmB cleavage of cell junctional proteins on RPE leads to the disruption of the blood-eye barrier, an early event in the pathogenesis of AMD (1, 17, 29–31). We tested the barrier function of primary RPE cells grown on transwell inserts by measuring fluorescence associated with movement of FITC-labeled dextrans (70 kDa) across the RPE monolayer, an established method and indicator of solute flux used routinely to test barrier function of RPE (32–34). Fluorescent dextrans were placed in the upper compartment and measured in the lower compartments after exogenous GzmB (100 nM) stimulation for 5 h (**Figures 7B–E**). After 5 h, fluorescent intensity was higher in lower wells of primary RPE cells stimulated with GzmB compared to controls ($p < 0.01$) (**Figure 7B**). Subsequent ZO-1 immunohistochemistry on primary RPE cells attached to the membrane of the transwell insert after GzmB stimulation demonstrated a loss of ZO-1 immunofluorescence intensity (**Figures 7C–E**), consistent with an increased permeability, as indicated by the observed increase in the FITC-dextran fluorescence in the lower compartment. We also tested the trans-epithelial resistance of the RPE monolayer grown on transwells for 10 h after exogenous GzmB (100 nM)

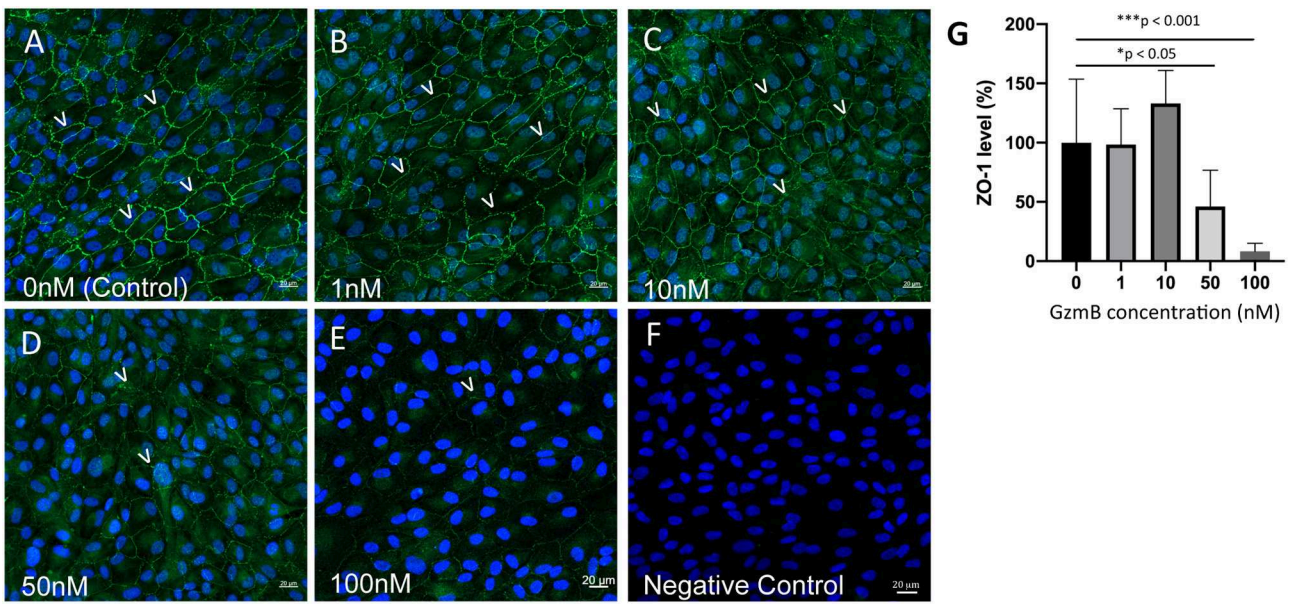

FIGURE 5 | Reduced immunoreactivity of ZO-1 in ARPE-19 cells stimulated by exogenous GzmB. **(A–E)** Note immunoreactivity of ZO-1 tight junctional contacts (green, 488 nm) between cells (some shown by white arrowheads) is reduced with increasing concentrations of GzmB (1, 10, 50, 100 nM) for 6 h. **(F)** Omission of primary antibody demonstrates lack of green ZO-1 immunolabeling. **(G)** Significant differences were observed between controls and 50 and 100 nM GzmB. A one-way ANOVA and Tukey's multiple comparisons *post-hoc* test ($N = 6$ per group) were used to compare control group with GzmB-treated groups: mean ± SEM; $^{*}p < 0.05$; $^{***}p < 0.001$. DAPI (405 nm) labeling of nuclei is shown in blue. Scale Bar = 20 µm.

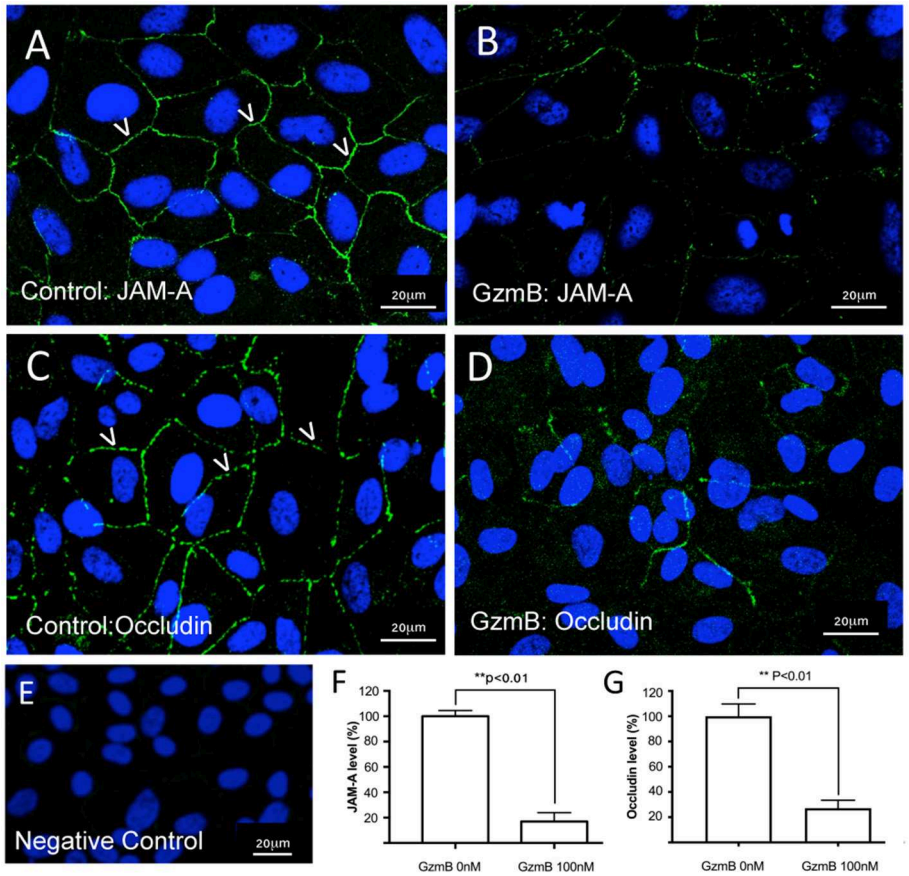

FIGURE 6 | Reduced immunoreactivity of JAM-A and Occludin in ARPE-19 cells stimulated by exogenous GzmB. **(A)** JAM-A immunoreactivity demonstrates tight junctional contacts (green 488 nm, some shown by white arrowheads) on RPE in controls wells (GzmB = 0 nM). **(B)** After 6 h with GzmB stimulation (100 nM), JAM-A immunoreactivity is reduced on ARPE-19. **(C)** Occludin immunoreactivity between cells (some shown by white arrowheads) in control wells (GzmB = 0 nM). **(D)** After 6 h with GzmB stimulation (100 nM), Occludin immunoreactivity is reduced on ARPE-19. **(E)** Omission of primary antibody demonstrates no immunoreactivity. Significant differences were observed for **(F)** JAM–A and **(G)** Occludin using an independent-sample *T*-Test ($N = 6$ per group) between control and GzmB-treated group: mean ± SEM; $^{**}p < 0.01$. Images were taken from ARPE-19 cells and are representative of primary RPE experiments undertaken at the same time. DAPI (405 nm) labeling of nuclei is shown in blue. Scale bar = 20 μm.

stimulation (**Figure 7A**). Note that the resistance is lowered by exogenous GzmB (gray and yellow traces), while control (unstimulated) RPE retained their resistance measurements at ∼160 ohms (blue and orange traces).

Extracellular GzmB Degrades Primary RPE-Derived ECM Proteins

Our earlier studies reported that GzmB cleaves ECM in non-ocular systems, implicating extracellular GzmB activity in pathological chronic inflammation, delayed wound healing, skin injuries, and cardiopulmonary disease (8–10, 12, 22). Age-related increases in GzmB (**Figure 2**), may promote the remodeling of Bruch's Membrane, an important ECM in outer retina. We studied the effect of exogenous GzmB on RPE-derived FN, LAM-5 (now known as LAM-332), COL-I and COL-IV. Primary RPE cultures were grown to confluence and stimulated with exogenous GzmB (0 nM controls vs. 100 nM GzmB) for 5 h. Supernatant samples containing secreted ECM proteins were probed with primary antibodies against FN, LAM-5 and COL-IV by western blot, and revealed several cleaved bands in those samples stimulated with 100 nM GzmB compared to controls (0 nM GzmB) (**Figures 8A–C**). Densitometric analysis revealed that the cleaved bands for FN and LAM-5 reached significance ($p < 0.05$), while that of COL-IV did not ($p > 0.05$) (**Figures 8D–F**). There were no cleaved bands observed for COL-I (**Supplementary Figure 2**), consistent with the earlier finding that COL-1 is not a substrate of GzmB (15, 16).

DISCUSSION

GzmB contributes to the pathology of autoimmune and/or chronic inflammatory conditions through the degradation of extracellular proteins and tissue matrices (8–10, 12, 22). Here we report GzmB expression in the healthy and diseased human retina and *in vitro* studies demonstrating the effects of exogenous

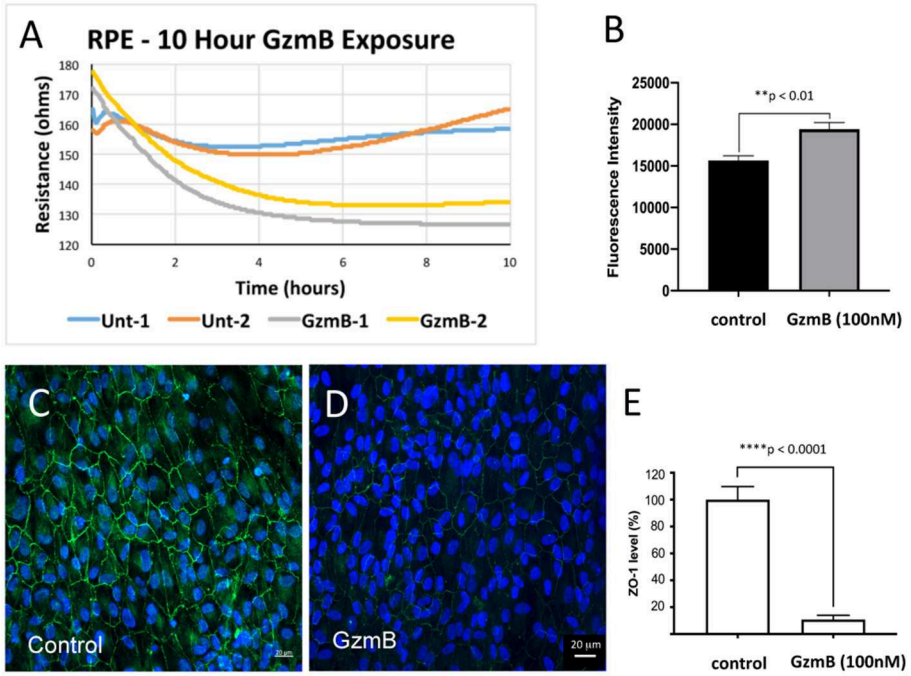

FIGURE 7 | Lowered trans-epithelial resistance and increased FITC-dextran flux after GzmB stimulation on primary RPE cells grown on transwell inserts. To test the primary RPE barrier function, cells were grown on transwell inserts and stimulated with GzmB at 100 nM. **(A)** Trans-epithelial resistance measurements on resting cells ranges from 160 to 180 ohms. After initiation of GzmB stimulation (time = 0), the resistance of RPE cultures decreases to 135–125 ohms (time = 10 h) as shown by yellow and gray traces. The control cells maintained resistance at 160–165 ohms (time = 10 h) as shown by the blue and orange traces. **(B)** FITC-dextran flux assay demonstrated increased FITC-dextran fluorescence intensity measured in the lower compartment of GzmB stimulated wells compared to control wells. **(C–E)** After the flux assay, the membranes on which cells were attached were cut out and subjected to immunocytochemistry. Strong ZO-1 immunolabeling on primary RPE cells on transwell insert membrane in control wells (0 nM GzmB) after 5 h shown in **(C,D)** in experimental wells (100 nM GzmB) after 5 h of GzmB stimulation. **(E)** The ZO-1 immunoreactivity was quantified in controls and GzmB stimulated wells and an independent-sample *T*-Test ($N = 6$) between control and GzmB-treated group was undertaken and graphed as mean ± SEM; $^{****}p < 0.0001$; $^{**}p < 0.01$. DAPI (405 nm) labeling of nuclei is shown in blue.

GzmB on RPE-derived tight junctional and ECM proteins. Our premise is that extracellular GzmB contributes to the onset and/or progression of AMD via the cleavage of key extracellular proteins in BM resulting in RPE dysregulation and barrier function abnormalities. Later stages of AMD including RPE atrophy and remodeling of BM with the release of sequestered angiogenic and pro-inflammatory factors, may develop gradually, in part due to the unchecked activity of extracellular GzmB.

GzmB Immunoreactivity in the Outer Retina

Aging is the major risk factor for AMD. The molecular inflammation (e.g., inflammaging, para-inflammation) hypothesis of aging suggests that by-products of low-grade inflammatory processes may accumulate in tissues, and serve as a bridge between normal aging and age-related pathological processes (35, 36). The human outer retina demonstrated a significant age-related increase in the number of GzmB+ cells, specifically in the choroid. This was consistent with our preliminary findings of an age-related increase in GzmB immunoreactivity in mouse outer retina, specifically the BM in mouse models (7) (**Figure 3**). In the mouse retina, GzmB immunoreactivity is evident in the extracellular matrix of BM and the intercellular spaces between RPE cells. This is in contrast to the findings in human tissues presented here, where the majority of immunoreactivity was intracellular, However, sparse extracellular GzmB immunoreactivity was evident in wet AMD eyes, in a CNV lesion in a wet AMD eye, and in the choroids of a soft drusen eye and a GA eye (**Figure 2C**, **Supplementary Figure 5**). Our human data allowed us to identify the cells that produce GzmB. Choroidal mast cells appear to be the major source of GzmB especially in CNV eyes. RPE cells appear to be an important source of GzmB in eyes with soft drusen and CNV. We hypothesize that GzmB's extracellular role in cleavage of the ECM causes the breakdown of the oBRB, an early event in the development of AMD. This is supported by our *in vitro* studies in which we demonstrated the cleavage of tight junctional and cell adhesion molecules as well as RPE-derived ECM proteins.

Interestingly, earlier reports of tryptase, another serine protease produced by mast cells in the choroid, has also been implicated in aging and the atrophic form of AMD leading to the GA in its late stage (29, 37). While tryptase is associated with GA, our work demonstrated that GzmB is rarely present in GA eyes, but more significantly in CNV and soft drusen eyes (**Figures 2G,H**, **Supplementary Figure 6**). Preliminary results

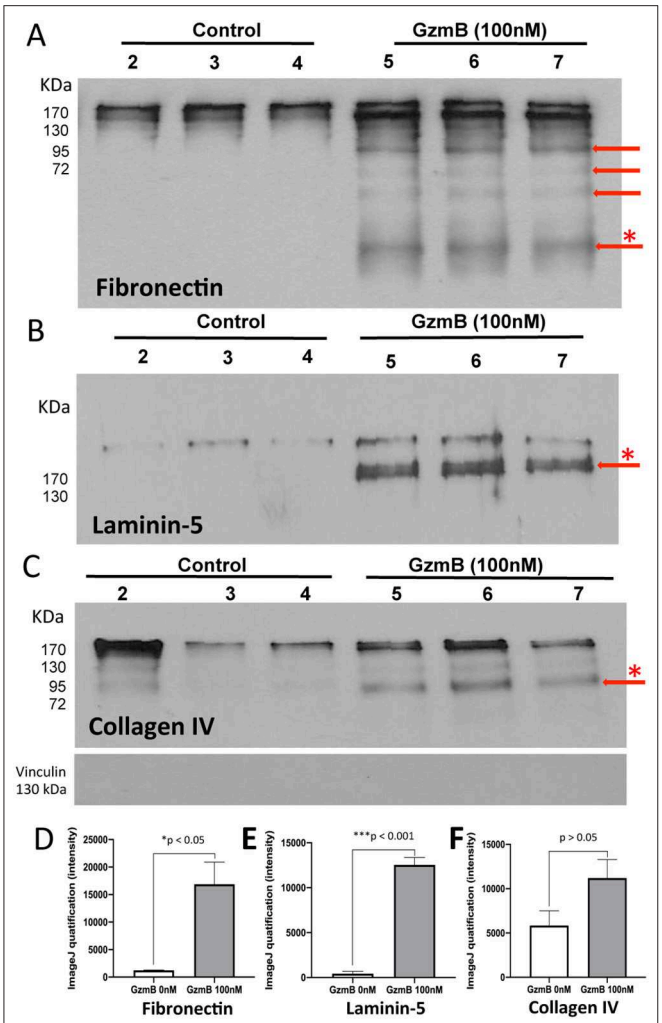

FIGURE 8 | Western blots reveal cleavage of primary RPE-derived extracellular matrix proteins by exogenous GzmB. Primary RPE cells were stimulated with GzmB (100 nM, 5 h), and both protein lysates and culture supernatant were collected. Western blot of supernatant samples were processed. **(A)** Western blot using antibody against fibronectin shows cleavage bands due to GzmB stimulation of primary RPE with 0 nM GzmB (controls, lanes 2–4) or 100 nM exogenous GzmB (lanes 5–7). Note cleavage bands at lower molecular weight, some identified by red arrows. The densiometric analysis of the band with asterisk (*) is graphed in **(D)** and demonstrates significant differences between control and 100 nM GzmB groups. **(B)** Western blot using antibody against Laminin-5 (now known as Laminin-332) shows supernatants from cultures of primary RPE with 0 nM (controls, lanes 2–4) or 100 nM exogenous GzmB (lanes 5–7). Note cleavage band, identified by red arrow, in samples from GzmB stimulation group (lanes 5–7), but not control lanes (2–4). The densiometric analysis of the band with asterisk (*) is graphed in **(E)** and demonstrates significant differences between control and 100 nM GzmB groups. **(C)** Western blot using antibody against Collagen IV shows supernatants from cultures of primary RPE with 0 nM (controls, lanes 2–4) or 100 nM exogenous GzmB (lanes 5–7). Note cleavage band, identified by red arrow, in samples from both GzmB stimulation group and controls. The densiometric analysis of the band with asterisk (*) is graphed in **(F)** and demonstrates no significance between control and 100 nM GzmB groups. Vinculin (124 kDa, housekeeping gene) antibody was used for quality control and demonstrates supernatant samples did not contain cell lysates.

suggest that different populations of mast cells are responsible for their secretion (**Supplementary Figure 3**). It is of note that GzmB is present in RPE cells (**Figure 2**), while tryptase is not produced by RPE, and importantly, tryptase does not cleave tight junctional proteins ZO-1 or JAM-A (38). Future studies will focus on the dual effects of these mast cell mediators toward understanding their separate or combined role in the development of AMD.

Next, we undertook *in vitro* cell studies to assess the role of exogenous GzmB on RPE-derived proteins, as immunoreactivity patterns can provide spatial localization within the outer retina, but does not allow for functional analysis. Of note, concentrations of exogenous GzmB, up to 100 nM, did not affect RPE cell viability. As such, we focused on the effects of GzmB cleavage on RPE cell-derived proteins.

GzmB Cleaves RPE Tight Junction and Cell Adhesion Proteins

RPE-derived tight junctional and cell adhesion proteins, ZO-1, JAM-A, and Occludin, were degraded by the application of exogenous GzmB *in vitro*. These tight junctional and adhesion proteins are essential components of the oBRB and ocular substrates GzmB. Thus, it is likely that during the aging process, tight junctional proteins may be subject to slow degradation due to increased age-related accumulation of extracellular GzmB (30, 31, 39). Earlier *in vivo* studies using lentiviral vector knockdown of ZO-1 in C57BL mice showed that loss of ZO-1 on RPE caused abnormal retinal barrier function, RPE proliferation and clumping, pyknosis, and eventual RPE death (30). In another study, ZO-1 and JAM-A were shown to deteriorate on RPE in a light-induced mouse model of AMD, which resulted in RPE atrophy (40). These rodent studies strongly suggest that disruption of the RPE cell-cell contacts leads to cytokine overexpression, macrophage recruitment and RPE atrophy *in vivo*. Future studies on GzmB-KO mouse models, as well as the apolipoprotein-E KO mouse, a model of accelerated aging (11, 28), may allow us to identify the detailed timeline and mechanism whereby the age-related increase in extracellular GzmB activity leads to cleavage of tight junctional proteins, subsequent RPE atrophy and loss of barrier function *in vivo*.

Consequences of GzmB Cleavage of ECM and Basement Membranes in BM

RPE cells control the synthesis of all the structural elements in BM (FN, COL I, III-IV, and LAM) (1, 41, 42). Our results showed that RPE-derived FN and LAM-5 were degraded by the application of exogenous GzmB *in vitro,* therefore validating that ocular FN and LAM-5 are substrates of GzmB. GzmB cleavage of COL-IV was present, but did not reach significance. It is possible that COL-IV is partially cleaved by GzmB; however, earlier studies suggest it may be a substrate of GzmA (39).

Preliminary work on human eye-cup preparations incubated in exogenous GzmB demonstrated reduced numbers of adherent RPE, suggesting that ECM degradation can also effect the

outer basement membrane potentially leading to RPE anoikis (data not shown) (1, 43). Similarly, extracellular GzmB may cause degradation of the choroidal basement membrane, which supports the endothelium and choriocapillaries, the principal blood supply to the outer retina. The loss of the endothelial cells can cause closure of capillaries and ghost vessels (44–46), which in turn stops the nutrient and gas exchange to the outer retina, altering RPE and photoreceptor function and, eventually, their cell death in GA. Future studies will use an *ex vivo* choroidal explant model to assess the role of exogenous GzmB (and inhibitors of GzmB) on endothelial cell viability, release of angiogenic factors such as VEGF from BM and subsequent choroidal sprouting (47–52).

GzmB's Putative Role in AMD

Our results demonstrating GzmB expression in both RPE and choroidal mast cells suggests that this serine protease may play multiple roles in the outer retina. Eyes with soft drusen (but without AMD) were more likely to have GzmB+ RPE cells than the other groups studied. These GzmB+ RPE cells appeared to have the RPE phenotype of "non-uniform" described earlier (53). Given that our sample of soft drusen eyes did not display AMD features, the "non-uniform" RPE may represent age-related changes in RPE. We do not yet know if soft drusen upregulates GzmB in nearby RPE cells or whether the degradation of tight junctional contacts between RPE (reported here in *in vitro* studies) may be caused by RPE or mast-cell derived GzmB. Future studies will identify whether soft drusen components upregulate GzmB in RPE cells *in vitro,* and mouse models will help us to clarify further the relationship between extracellular GzmB and the cleavage of ECM and tight junctions in outer retina.

Our results also show that CNV eyes had significantly more GzmB+ cells in the choroid than any other groups tested. Our group showed that GzmB cleaves FN and released VEGF from endothelial cell derived ECM *in vitro* and increased vascular permeability in skin *in vivo* using a Miles/Evan's Blue assay (54). These findings suggest that extracellular GzmB potentially promotes abnormal CNV by: (1) releasing sequestered VEGF from BM; and (2) promoting vascular leakage by disrupting choroidal endothelial cell function. However, future work is needed to understand GzmB's overall role in angiogenesis, as we also showed that GzmB cleavage of FN may also dysregulate angiogenesis by impairing endothelial cell adhesion, migration, and capillary formation resulting in vascular leakage *in vitro* (55).

VEGF plays a key role in CNV and is the target of FDA-approved anti-angiogenic drugs (e.g., Lucentis, Avastin, Eylea). While these drugs are effective, recent studies show a decline in long-term efficacy, which is believed to result from the emergence of VEGF-independent mechanisms involved in exacerbating the abnormal angiogenic milieu in the AMD eye. Moreover, some patients on anti-VEGF drugs do not benefit (e.g., non-responders) and their vision continues to diminish. Insights into a mechanism underlying resistance observed in some AMD non-responders come from a recent article by Wroblewski et al. that showed increased levels of GzmB from mast cells upon anti-VEGF treatment for cancer (tumor angiogenesis) (56). In Wroblewski et al., activity of extracellular GzmB was shown to liberate sequestered pro-angiogenic factors (from the tumor ECM) outside the VEGF-VEGFR2 axis. Increased GzmB also supported endothelial cell migration and vessel formation, and promoted tumor angiogenesis, despite anti-VEGF treatments. Inhibitors of mast cell degranulation increased the efficacy of anti-VEGF therapy in this model, providing supportive evidence that pharmacological inhibition of extracellular GzmB may ameliorate neovascularization in CNV.

Treating AMD is a multidimensional health care problem, with a global cost of vision impairment estimated to be nearly $343 billion worldwide. There is a need for early and prophylactic therapies for AMD. Here we present a novel concept to treat the earliest events in AMD, by targeting extracellular GzmB in outer retina, in order to suppress remodeling of BM and deterioration of the oBRB, two of the earliest events associated with AMD pathogenesis.

DATA AVAILABILITY STATEMENT

The datasets generated for this study are available on request to the corresponding author.

ETHICS STATEMENT

This study used primary human fetal RPE cells isolated from fetal donor eyes and adult post-mortem human eye tissues consented for research. The studies involving human participants were reviewed and approved by the Clinical Ethics Research Board of the University of British Columbia and strictly adhered to the Declaration of Helsinki. The patients/participants provided their written informed consent to participate in this study. This study used C57Bl6/J mice retina. The animal study was reviewed and approved by UBC Animal Care Committee.

AUTHOR CONTRIBUTIONS

JM and YT wrote the manuscript. JM and DG conceived and designed the study, obtained funding, analyzed and interpreted the data, and critically revised the manuscript. YT and JC performed the experiments, analyzed and interpreted the data and generated figures. MZ, SH, and CT provided expert opinion and technical advice on GzmB assays and assisted with study design and interpretation. MZ generated and purified endogenous GzmB from YT cells for use in this study. All authors read and approved the final manuscript.

FUNDING

This study was funded by Canadian Institutes of Health Research (CIHR) (to JM and DG), Natural Sciences and Engineering Research Council of Canada (NSERC) (JM), and Michael Smith Foundation for Health Research (DG). MZ and CT were funded through CIHR Fellowships. MZ was additionally

funded through a Michael Smith Foundation for Health Research Studentship. YT was funded through a Guangzhou Elite Project Overseas Scholarship.

ACKNOWLEDGMENTS

The authors thank Dr. Sijia Cao, Reed Huber and Eleanor To for preliminary work and technical assistance throughout the course of this study. Drs. Hua Ren and Chao Zhu provided bright-field photomicrographic assistance.

SUPPLEMENTARY MATERIAL

The Supplementary Material for this article can be found online at: https://www.frontiersin.org/articles/10.3389/fimmu.2020.00574/full#supplementary-material

REFERENCES

1. Nita M, Strzalka-Mrozik B, Grzybowski A, Mazurek U, Romaniuk W. Age-related macular degeneration and changes in the extracellular matrix. *Med Sci Monit*. (2014) 20:1003–16. doi: 10.12659/MSM.889887
2. Akhtar-Schafer I, Wang L, Krohne TU, Xu H, Langmann T. Modulation of three key innate immune pathways for the most common retinal degenerative diseases. *EMBO Mol Med*. (2018) 10:e8259. doi: 10.15252/emmm.201708259
3. Ambati J, Atkinson JP, Gelfand BD. Immunology of age-related macular degeneration. *Nat Rev Immunol*. (2013) 13:438–51. doi: 10.1038/nri3459
4. Jager RD, Mieler WF, Miller JW. Age-related macular degeneration. *N Engl J Med*. (2008) 358:2606–17. doi: 10.1056/NEJMra0801537
5. Nussenblatt RB, Lee RW, Chew E, Wei L, Liu B, Sen HN, et al. Immune responses in age related macular degeneration and a possible long term therapeutic strategy for prevention. *Am J Ophthalmol*. (2014) 158:5–11.e2. doi: 10.1016/j.ajo.2014.03.014
6. Copland DA, Theodoropoulou S, Liu J, Dick AD. A perspective of AMD through the eyes of immunology. *Invest Ophthalmol Vis Sci*. (2018) 59:AMD83–92. doi: 10.1167/iovs.18-23893
7. Matsubara JA, Granville D, Tian Y, Cui JZ. Potential role of extracellular granzyme b in the pathogenesis of age-related macular degeneration (AMD). In: *ARVO Annual Meeting*. Vancouver, BC. (2019)
8. Arias M, Martinez-Lostao L, Santiago L, Ferrandez A, Granville DJ, Pardo J. The untold story of granzymes in oncoimmunology: novel opportunities with old acquaintances. *Trends Cancer*. (2017) 3:407–22. doi: 10.1016/j.trecan.2017.04.001
9. Boivin WA, Cooper DM, Hiebert PR, Granville DJ. Intracellular versus extracellular granzyme B in immunity and disease: challenging the dogma. *Lab Invest*. (2009) 89:1195–220. doi: 10.1038/labinvest.2009.91
10. Hendel A, Hiebert PR, Boivin WA, Williams SJ, Granville DJ. Granzymes in age-related cardiovascular and pulmonary diseases. *Cell Death Differ*. (2010) 17:596–606. doi: 10.1038/cdd.2010.5
11. Hiebert PR, Wu D, Granville DJ. Granzyme B degrades extracellular matrix and contributes to delayed wound closure in apolipoprotein E knockout mice. *Cell Death Differ*. (2013) 20:1404–14. doi: 10.1038/cdd.2013.96
12. Turner CT, Lim D, Granville DJ. Granzyme B in skin inflammation and disease. *Matrix Biol*. (2019) 75–6:126–40. doi: 10.1016/j.matbio.2017.12.005
13. Bousquet E, Zhao M, Thillaye-Goldenberg B, Lorena V, Castaneda B, Naud MC, et al. Choroidal mast cells in retinal pathology: a potential target for intervention. *Am J Pathol*. (2015) 185:2083–95. doi: 10.1016/j.ajpath.2015.04.002
14. Dai H, Korthuis RJ. Mast cell proteases and inflammation. *Drug Discov Today Dis Models*. (2011) 8:47–55. doi: 10.1016/j.ddmod.2011.06.004
15. Parkinson LG, Toro A, Zhao H, Brown K, Tebbutt SJ, Granville DJ. Granzyme B mediates both direct and indirect cleavage of extracellular matrix in skin after chronic low-dose unltrviolet light irradiation. *Aging Cell*. (2015) 14:67–77. doi: 10.1111/acel.12298
16. Russo V, Klein T, Lim DJ, Solis N, Machado Y, Hiroyasu S, et al. Granzyme B is elevated in autoimmune blistering diseases and cleaves key anchoring proteins of the dermal-epidermal junction. *Sci Rep*. (2018) 8:9690. doi: 10.1038/s41598-018-28070-0
17. Buzza MS, Zamurs L, Sun J, Bird CH, Smith AI, Trapani JA, et al. Extracellular matrix remodeling by human granzyme B via cleavage of vitronectin, fibronectin, and laminin. *J Biol Chem*. (2005) 280:23549–58. doi: 10.1074/jbc.M412001200
18. Clark SJ, McHarg S, Tilakaratna V, Brace N, Bishop PN. Bruch's membrane compartmentalizes complement regulation in the eye with implications for therapeutic design in age-related macular degeneration. *Front Immunol*. (2017) 8:1778. doi: 10.3389/fimmu.2017.01778
19. Bhutto I, Lutty G. Understanding age-related macular degeneration (AMD): relationships between the photoreceptor/retinal pigment epithelium/Bruch's membrane/choriocapillaris complex. *Mol Aspects Med*. (2012) 33:295–317. doi: 10.1016/j.mam.2012.04.005
20. Chen M, Luo C, Zhao J, Devarajan G, Xu H. Immune regulation in the aging retina. *Prog Retin Eye Res*. (2019) 69:159–72. doi: 10.1016/j.preteyeres.2018.10.003
21. Mettu PS, Wielgus AR, Ong SS, Cousins SW. Retinal pigment epithelium response to oxidant injury in the pathogenesis of early age-related macular degeneration. *Mol Aspects Med*. (2012) 33:376–98. doi: 10.1016/j.mam.2012.04.006
22. Hiebert PR, Granville DJ. Granzyme B in injury, inflammation, and repair. *Trends Mol Med*. (2012) 18:732–41. doi: 10.1016/j.molmed.2012.09.009
23. Cao S, Wang JC, Gao J, Wong M, To E, White VA, et al. CFH Y402H polymorphism and the complement activation product C5a: effects on NF- κB activation and inflammasome gene regulation. *Br J Ophthalmol*. (2016) 100:713–8. doi: 10.1136/bjophthalmol-2015-307213
24. Kurji KH, Cui JZ, Lin T, Harriman D, Prasad SS, Kojic L, et al. Microarray analysis identifies changes in inflammatory gene expression in response to amyloid-beta stimulation of cultured human retinal pigment epithelial cells. *Invest Ophthalmol Vis Sci*. (2010) 51:1151–63. doi: 10.1167/iovs.09-3622
25. Shi L, Yang X, Froelich CJ, Greenberg AH. Purification and use of granzyme B. *Methods Enzymol*. (2000) 322:125–43. doi: 10.1016/S0076-6879(00)22013-2
26. Samuel W, Jaworski C, Postnikova OA, Kutty RK, Duncan T, Tan LX, et al. Appropriately differentiated ARPE-19 cells regain phenotype and gene expression profiles similar to those of native RPE cells. *Mol Vis*. (2017) 23:60–89. Available online at: http://www.molvis.org/molvis/v23/60
27. Curcio CA, Zanzottera EC, Ach T, Balaratnasingam C, Freund KB. Activated retinal pigment epithelium, an optical coherence tomography biomarker for progression in age-related macular degeneration. *Invest Ophthalmol Vis Sci*. (2017) 58:Bio211–26. doi: 10.1167/iovs.17-21872
28. Hiebert PR, Boivin WA, Abraham T, Pazooki S, Zhao H, Granville DJ. Granzyme B contributes to extracellular matrix remodeling and skin aging in apolipoprotein E knockout mice. *Exp Gerontol*. (2011) 46:489–99. doi: 10.1016/j.exger.2011.02.004
29. McLeod DS, Bhutto I, Edwards MM, Gedam M, Baldeosingh R, Lutty G. Mast cell-derived tryptase in geographic atrophy. *Invest Ophthalmol Vis Sci*. (2017) 58:5887–96. doi: 10.1167/iovs.17-22989
30. Georgiadis A, Tschernutter M, Bainbridge JW, Balaggan KS, Mowat F, West EL, et al. The tight junction associated signalling proteins ZO-1 and ZONAB regulate retinal pigment epithelium homeostasis in mice. *PLoS ONE*. (2010) 5:e15730. doi: 10.1371/journal.pone.0015730
31. Pardo J, Wallich R, Ebnet K, Iden S, Zentgraf H, Martin P, et al. Granzyme B is expressed in mouse mast cells *in vivo* and *in vitro* and causes delayed cell death independent of perforin. *Cell Death Differ*. (2007) 14:1768–79. doi: 10.1038/sj.cdd.4402183
32. Beasley S, El-Sherbiny M, Megyerdi S, El-Shafey S, Choksi K, Kaddour-Djebbar I, et al. Caspase-14 expression impairs retinal pigment epithelium

barrier function: potential role in diabetic macular edema. *Biomed Res Int*. (2014) 2014:417986. doi: 10.1155/2014/417986
33. Bailey TA, Kanuga N, Romero IA, Greenwood J, Luthert PJ, Cheetham ME. Oxidative stress affects the junctional integrity of retinal pigment epithelial cells. *Invest Ophthalmol Vis Sci*. (2004) 45:675–84. doi: 10.1167/iovs.03-0351
34. Miura Y, Roider J. Triamcinolone acetonide prevents oxidative stress-induced tight junction disruption of retinal pigment epithelial cells. *Graefes Arch Clin Exp Ophthalmol*. (2009) 247:641–9. doi: 10.1007/s00417-009-1041-6
35. Chung HY, Cesari M, Anton S, Marzetti E, Giovannini S, Seo AY, et al. Molecular inflammation: underpinnings of aging and age-related diseases. *Ageing Res Rev*. (2009) 8:18–30. doi: 10.1016/j.arr.2008.07.002
36. Xu H, Chen M, Forrester JV. Para-inflammation in the aging retina. *Prog Retin Eye Res*. (2009) 28:348–64. doi: 10.1016/j.preteyeres.2009.06.001
37. Bhutto IA, McLeod DS, Jing T, Sunness JS, Seddon JM, Lutty GA. Increased choroidal mast cells and their degranulation in age-related macular degeneration. *Br J Ophthalmol*. (2016) 100:720–6. doi: 10.1136/bjophthalmol-2015-308290
38. Arai R, Usui-Ouchi A, Ito Y, Mashimo K, Murakami A, Ebihara N. Effects of secreted mast cell mediators on retinal pigment epithelial cells: focus on mast cell tryptase. *Mediators Inflamm*. (2017) 2017:3124753. doi: 10.1155/2017/3124753
39. Santacruz MS. *Granzyme B Disrupts Cell-Cell Adhesion and Epithelial Barrier Function*. Vancouver, BC: University of British Columbia (2018).
40. Narimatsu T, Ozawa Y, Miyake S, Kubota S, Hirasawa M, Nagai N, et al. Disruption of cell-cell junctions and induction of pathological cytokines in the retinal pigment epithelium of light-exposed mice. *Invest Ophthalmol Vis Sci*. (2013) 54:4555–62. doi: 10.1167/iovs.12-11572
41. Aisenbrey S, Zhang M, Bacher D, Yee J, Brunken WJ, Hunter DD. Retinal pigment epithelial cells synthesize laminins, including laminin 5, and adhere to them through alpha3- and alpha6-containing integrins. *Invest Ophthalmol Vis Sci*. (2006) 47:5537–44. doi: 10.1167/iovs.05-1590
42. Fernandez-Godino R, Pierce EA, Garland DL. Extracellular matrix alterations and deposit formation in AMD. *Adv Exp Med Biol*. (2016) 854:53–8. doi: 10.1007/978-3-319-17121-0_8
43. Curcio CA, Johnson, M. Structure, function, and pathology of bruch's membrane. In: Ryan SJ, Sadda SR, Hinton DR, Schachat AP, Wilkinson CP, Wiedemann P, editors. *Retina,* 5th Ed. Los Angeles CA: Elsevier Inc (2012). p. 465–81. doi: 10.1016/B978-1-4557-0737-9.00020-5
44. Chirco KR, Sohn EH, Stone EM, Tucker BA, Mullins RF. Structural and molecular changes in the aging choroid: implications for age-related macular degeneration. *Eye*. (2017) 31:10–25. doi: 10.1038/eye.2016.216
45. Mullins RF, Johnson MN, Faidley EA, Skeie JM, Huang J. Choriocapillaris vascular dropout related to density of drusen in human eyes with early age-related macular degeneration. *Invest Ophthalmol Vis Sci*. (2011) 52:1606–12. doi: 10.1167/iovs.10-6476
46. Whitmore SS, Sohn EH, Chirco KR, Drack AV, Stone EM, Tucker BA, et al. Complement activation and choriocapillaris loss in early AMD: implications for pathophysiology and therapy. *Prog Retin Eye Res*. (2015) 45:1–29. doi: 10.1016/j.preteyeres.2014.11.005
47. Sack KD, Teran M, Nugent MA. Extracellular matrix stiffness controls VEGF signaling and processing in endothelial cells. *J Cell Physiol*. (2016) 231:2026–39. doi: 10.1002/jcp.25312
48. Wijelath ES, Murray J, Rahman S, Patel Y, Ishida A, Strand K, et al. Novel vascular endothelial growth factor binding domains of fibronectin enhance vascular endothelial growth factor biological activity. *Circ Res*. (2002) 91:25–31. doi: 10.1161/01.RES.0000026420.22406.79
49. Buczek-Thomas J, Rich CB, Nugent MA. Hypoxia induced heparan sulfate primes the extracellular matrix for endothelial cell recruitment by facilitating VEGF-fibronectin interactions. *Int J Mol Sci*. (2019) 20:E5065. doi: 10.3390/ijms20205065
50. Forsten-Williams K, Kurtagic E, Nugent MA. Complex receptor-ligand dynamics control the response of the VEGF system to protease injury. *BMC Syst Biol*. (2011) 5:170. doi: 10.1186/1752-0509-5-170
51. Goerges A, Nugent MA. pH regulates vascular endothelial growth factor binding to fibronectin: a mechanism for control of extracellular matrix storage and release. *J Biol Chem*. (2004) 279:2307–15. doi: 10.1074/jbc.M308482200
52. Ambesi A, McKeown-Longo P. Conformational remodeling of the fibronectin matrix selectively regulates VEGF signaling. *J Cell Sci*. (2014) 127(Pt 17):3805–16. doi: 10.1242/jcs.150458
53. Curcio CA. Soft drusen in age-related macular degeneration: biology and targeting via the oil spill strategies. *Invest Ophthalmol Vis Sci*. (2018) 59:Amd160–81. doi: 10.1167/iovs.18-24882
54. Hendel A, Hsu I, Granville DJ. Granzyme B releases vascular endothelial growth factor from extracellular matrix and induces vascular permeability. *Lab Invest*. (2014) 94:716–25. doi: 10.1038/labinvest.2014.62
55. Hendel A, Granville DJ. Granzyme B cleavage of fibronectin disrupts endothelial cell adhesion, migration and capillary tube formation. *Matrix Biol*. (2013) 32:14–22. doi: 10.1016/j.matbio.2012.11.013
56. Wroblewski M, Bauer R, Cubas Cordova M, Udonta F, Ben-Batalla I, Legler K, et al. Mast cells decrease efficacy of anti-angiogenic therapy by secreting matrix-degrading granzyme B. *Nat Commun*. (2017) 8:269. doi: 10.1038/s41467-017-00327-8

Conflict of Interest: DG is a co-Founder and serves as the Chief Scientific Officer of viDA Therapeutics. However, no viDA products were used in this manuscript.

The remaining authors declare that the research was conducted in the absence of any commercial or financial relationships that could be construed as a potential conflict of interest.

frontiers in Immunology

ORIGINAL RESEARCH
published: 21 May 2020
doi: 10.3389/fimmu.2020.00975

Kallistatin Attenuates Experimental Autoimmune Uveitis by Inhibiting Activation of T Cells

Fauziyya Muhammad[1], *Priscilla N. Avalos*[2], *M. H. Mursalin*[1], *Jian-Xing Ma*[3], *Michelle C. Callegan*[1,2,4] *and Darren J. Lee*[1,2,4]*

[1] Department of Microbiology and Immunology, University of Oklahoma Health Sciences Center, Oklahoma City, OK, United States, [2] Department of Ophthalmology/Dean McGee Eye Institute, University of Oklahoma Health Sciences Center, Oklahoma City, OK, United States, [3] Department of Physiology, University of Oklahoma Health Sciences Center, Oklahoma City, OK, United States, [4] Oklahoma Center for Neuroscience, University of Oklahoma Health Sciences Center, Oklahoma City, OK, United States

Experimental autoimmune uveoretinitis (EAU) is a mouse model of human autoimmune uveitis. EAU spontaneously resolves and is marked by ocular autoantigen-specific regulatory immunity in the spleen. Kallikrein binding protein (KBP) or kallistatin is a serine proteinase inhibitor that inhibits angiogenesis and inflammation, but its role in autoimmune uveitis has not been explored. We report that T cells activation is inhibited and EAU is attenuated in human KBP (HKBP) mice with no significant difference in the Treg population that we previously identified both before and after recovery from EAU. Moreover, following EAU immunization HKBP mice have potent ocular autoantigen specific regulatory immunity that is functionally suppressive.

Keywords: autoimmune disease, autoimmune uveitis, kallistatin, experimental autoimmune uveitis, T cells

OPEN ACCESS

Edited by:
Anne Fletcher,
Monash University, Australia

Reviewed by:
Igal Gery,
National Eye Institute (NEI), United States
Jarmila Heissigerova,
Charles University, Czechia

***Correspondence:**
Darren J. Lee
darren-lee@ouhsc.edu

Specialty section:
This article was submitted to Immunological Tolerance and Regulation, a section of the journal Frontiers in Immunology

Received: *29 January 2020*
Accepted: *24 April 2020*
Published: *21 May 2020*

Citation:
Muhammad F, Avalos PN, Mursalin MH, Ma J-X, Callegan MC and Lee DJ (2020) Kallistatin Attenuates Experimental Autoimmune Uveitis by Inhibiting Activation of T Cells. Front. Immunol. 11:975. doi: 10.3389/fimmu.2020.00975

INTRODUCTION

Uveitis is the third leading cause of blindness in Western countries, with an incidence between 25.6–122 cases per 100,000 a year, and a prevalence of 69–623 cases per 100,000 (1–4). While anterior uveitis is the most common form of uveitis, with 33% of these patients becoming chronic (5), posterior uveitis as the second most common form of uveitis is far more devastating. Approximately 17.6% of active uveitis patients experience transient or permanent vision loss (6), so a proper diagnosis and treatment are crucial for maintaining vision. Corticosteroids are the first line of treatment for uveitis patients, but due to the myriad of side-effects they are not a long-term treatment option (7–9). Therefore, immunosuppressive medications are used to control uveitis, with the goal of sustained remission (10–15). However, not all the immunosuppressive medications are effective and some chronic uveitis patients fail multiple treatment regimens. As such, additional immunosuppressive treatment options are necessary for the treatment of autoimmune uveitis.

Kallistatin (or kallikrein-binding protein) is a serine proteinase inhibitor that is encoded by *SERPINA4* (16, 17). Kallistatin was first identified as an inhibitor of tissue kallikrein (16, 18). Later, kallistatin has been investigated extensively for its role in diabetes (17, 19, 20). Type 1 diabetic patients have high serum levels of kallistatin (19), but the vitreous of diabetic retinopathy patients have low levels of kallistatin (19, 21). It has also been demonstrated that kallistatin has potent anti-inflammatory properties (22, 23). Therefore, it is of interest to determine if kallistatin could be a therapeutic alternative for autoimmune uveitis.

The most widely used model of human posterior autoimmune uveitis is the mouse model, experimental autoimmune uveitis (EAU). In the B10.RIII background, the disease is more severe and resolves more quickly compared to the more chronic C57BL/6J model. The onset of EAU is 12–14 days after immunization and resolution spontaneously occurs without relapse at 2–3 months after immunization (24–26). At resolution of EAU (post-EAU), regulatory immunity emerges in the spleen (27) and provides resistance to EAU during re-immunization and when adoptively transferred to mice that are immunized for EAU (27–30). Post-EAU regulatory immunity requires a regulatory T cell (Treg) that has been identified as $CD4^+CD25^+Nrp\text{-}1^-PD\text{-}1^+PD\text{-}L1^+Foxp3^+$ (29, 30).

A transgenic mouse that expresses human kallistatin under a chicken ß-actin promoter (TG-HKBP) has been studied with respect to angiogenesis related to diabetes (31). As such, in this report we asked if kallistatin over-expression affects T cell activation, provides resistance to EAU, and if regulatory immunity that provides resistance to EAU emerges in the spleen of post-EAU TG-HKBP mice. Our observations demonstrate that kallistatin over-expression provides resistance to EAU and does not affect the induction of regulatory immunity in the spleen of post-EAU TG-HKBP mice.

MATERIALS AND METHODS

Mice

All mouse procedures described in this study were approved by the University of Oklahoma Health Sciences Center Institutional Animal Care and Use Committee (OUHSC IACUC) and all mouse study methods were carried out in accordance with the relevant guidelines approved by the OUHSC IACUC. C57BL/6J mice were purchased from Jackson Laboratories. Transgenic mice expressing human kallikrein binding protein under the chicken β-actin promoter (TG-HKBP or HKBP) were generated in the Jian-Xing Ma Lab on a C57BL/6J background (31, 32). All TG-HKBP mice were genotyped to verify transmission of the transgene before inclusion in this study. Serum was previously collected from TG-HKBP mice to verify elevated expression (31). All mice were housed in the Dean McGee Eye Institute vivarium under specific-pathogen-free conditions in a 12-h light cycle with access to food and water *ad libitum*. When mice were purchased from Jackson Laboratories they were allowed 2 weeks to acclimate under conventional housing conditions before inclusion in experimental procedures. The methods of euthanasia of all mice were approved by OUHSC IACUC and are consistent with the IACUC policies and the 2013 AVMA Guidelines on Euthanasia. Euthanasia of all mice for this study was done with carbon dioxide or cervical dislocation followed by a secondary method such as decapitation, bilateral thoracotomy, exsanguination, or vital organ removal. Mice were randomly chosen for experimental groups.

Experimental Autoimmune Uveoretinitis (EAU)

EAU was induced in 6 to 10-week-old mice using the previously described immunization procedure (30). Complete Freund's adjuvant (CFA) with 5 mg/mL desiccated *M. tuberculosis* (Difco Laboratories, Detroit, MI) was emulsified with 2 mg/ml interphotoreceptor retinoid binding protein (peptides 1–20) (IRBP) (Genscript, Piscataway, NJ) to immunize mice for EAU. In order to minimize suffering mice were anesthetized with a ketamine/xylazine (100 mg/10 mg per kg) before immunization. The emulsion was injected subcutaneously at a volume of 200 μL total into two sites in the lower back followed by an intraperitoneal injection of 0.3 μg pertussis toxin. The course of EAU was evaluated every 3–4 days by fundus examination with a slit lamp microscope. Prior to examination of the retina, the iris was dilated with 1% tropicamide, and the cornea was flattened with a glass coverslip. We utilize a clinical scoring system that is validated by at least two members of the lab rather than histological examination because we have an interest in the resolution phase of EAU, so collecting mice over the course of disease for histological evaluation would significantly reduce the power of the study. As previously described, the clinical signs of observable infiltration and vasculitis in the retina were scored on a 5-point scale (33). Because the immunization procedure can elicit a score of 1, when the EAU score is 1 or lower, the disease is considered background or resolved. Both eyes were scored and the higher score was used to represent that mouse for that day, because the more severe score suggests that the systemic immune response is severe enough to elicit the greater score. The average score for the group of mice was then calculated. The highest score for each mouse over the entire course of disease was also determined and plotted for each group. Another masked member of the lab with experience evaluating EAU confirmed the clinical scores.

In vitro Stimulation

A single cell suspension that was depleted of red blood cells using RBC lysis buffer (Sigma, St Louis, MO) was made from the spleens collected into 5% FBS in RPMI supplemented with 10 μg/ml Gentamycin (Sigma), 10 mM HEPES (GE Healthcare), 1 mM Sodium Pyruvate (BioWhittaker), Nonessential Amino Acids 0.2% (BioWhittaker). Serum free media (SFM) consisting of RPMI-1640 with 1% ITS+1 solution (Sigma) and 0.1% BSA (Sigma) was used to resuspend the spleen cells with IRBP (50 μg/mL) or α-CD3 (clone 2C11, Biolegend). The spleen cells were then incubated for 48 h at 37°C and 5% CO_2 to reactivate antigen specific T cells. After the reactivation cells were collected for flow cytometry analysis or adoptive transfer (1×10^6) into recipient mice.

Intraocular Injection

Mice were anesthetized using isoflurane. $CD4^+$ splenocytes ($1 \times 10^6/\mu L$) were injected into the left and right eye of each mouse with a sterile borosilicate glass micropipette (Kimble Glass Inc., Vineland, NJ, USA) beveled to an approximate bore size of 10–20 μm (BV-10 KT Brown Type micropipette beveller, Sutter Instrument Co., Novato, CA, USA). The micropipettes were inserted just posterior to the superior limbus under stereomicroscopic visualization, and 1-μL volume was injected directly into the vitreous. Injection rates and volumes were

monitored using a programmable cell microinjector (Microdata Instruments, Plainfield, NJ, USA).

Flow Cytometry

Mouse spleen cells were washed with PBS with 1% BSA (staining buffer), blocked with mouse IgG in staining buffer, then stained with conjugated antibodies. Antibodies used were anti-CD4 (clone RM4-5, Biolegend, San Diego, CA), anti-CD25 (clone PC61, Biolegend), anti-PD-1 (clone 29F.1A12, Biolegend), anti-PD-L1 (clone 10F.9G2 Biolegend), anti-Nrp-1 (Cat FAB5994N, R&D Systems, Minneapolis, MN), anti-FoxP3 (clone FJK-16s, eBiosciences), anti-CD44 (clone IM7, Biolegend), anti-CD62L (clone MEL-14, Biolegend), anti-CD45.1 (clone A20, Biolegend), and anti-CD45.2 (clone 104, Biolegend).

Stained cells were analyzed in the Oklahoma Medical Research Facility (OMRF) Flow Cytometry Core Facility on a BD LSRII (BD Biosciences) data was analyzed using FlowJo Software (Tree Star, Inc., Ashland, OR).

Statistics

Statistical significance between maximum EAU scores and flow cytometry results was determined using non-parametric Mann-Whitney two-tailed test. Two-way ANOVA was also used to assess significant changes in the tempo of disease between the groups of treated EAU mice with post-test Bonferroni comparison analysis. Statistical significance was designated when $P \leq 0.05$ and analyzed using Prism 6 (GraphPad Software, Inc., La Jolla, CA).

RESULTS

Kallistatin Attenuates EAU

We first asked if there is a defect in the T cell response in TG-HKBP mice. Naïve and memory T cells were evaluated in splenic T cells that were non-specifically activated through CD3. As expected, wild-type T cells showed a significant elevation in memory T cells (CD44+) and significant reduction in naïve T cells (CD62L+) (**Figures 1A,B,E,F**). In contrast TG-HKBP T cells showed no significant change in memory or naïve T cell populations following CD3 activation (**Figures 1C–F**). This inhibition of T cell activation and the anti-inflammatory properties of kallistatin (kallikrein-binding protein) (23) prompted us to ask if it suppresses experimental autoimmune uveitis (EAU). TG-HKBP mice have been previously characterized in studies related to diabetic retinopathy, and serum kallistatin in these mice is over four-fold higher than the endogenous mouse kallistatin (31, 32). When TG-HKBP mice were immunized for EAU, a significant decrease in the severity and acceleration of resolution was observed in

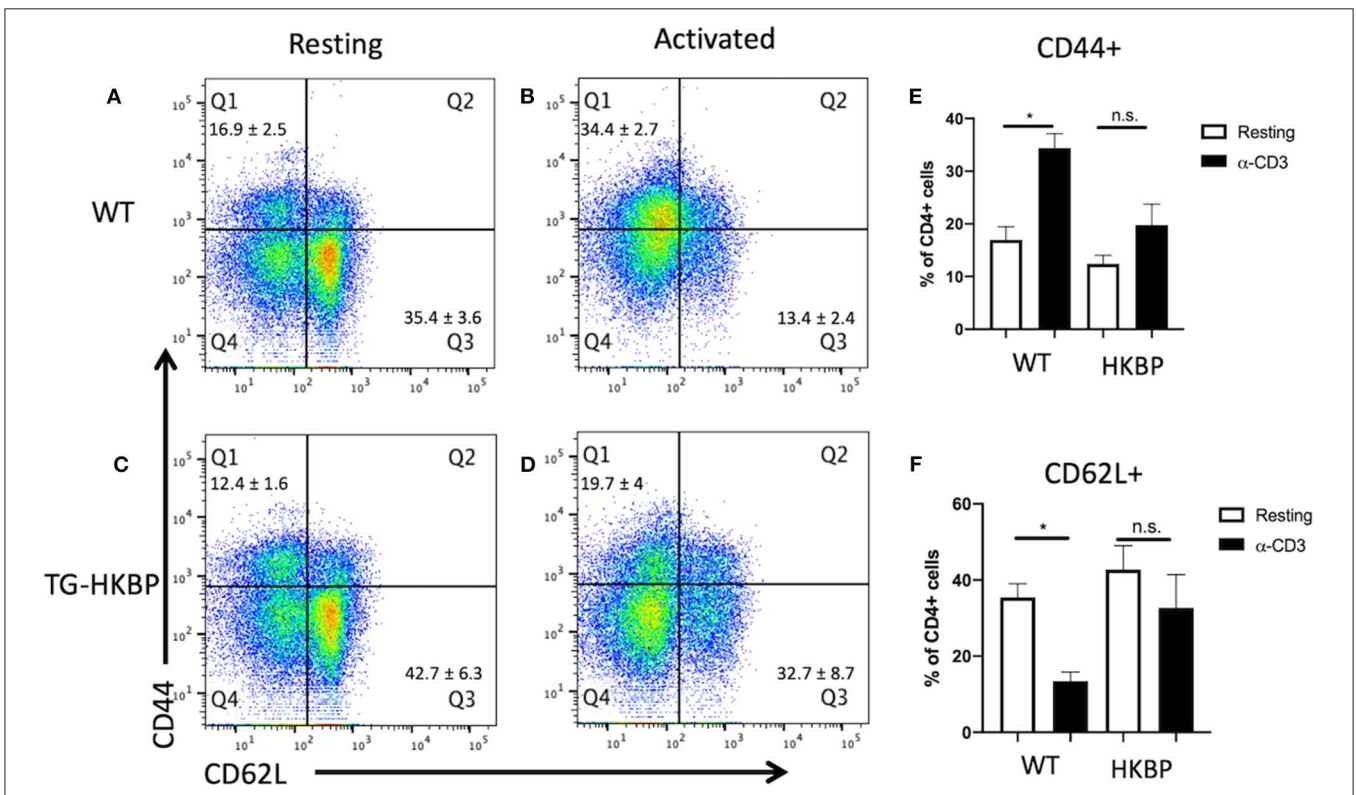

FIGURE 1 | T cell activation in T cells from TG-HKBP mice. Wild-type and TG-HKBP splenocytes were cultured ± α-CD3 for 2 days, stained for CD4, CD44, and CD62L, and analyzed by flow cytometry. Representative dot plots are shown for wild-type ($n = 5$) **(A,B)** and TG-HKBP ($n = 7$) **(C,D)**, and bar graphs show the mean ± SEM for the indicated group **(E,F)**. One to three mice were used for each experiment, and each experiment was repeated three times. Statistical significance ($P \leq 0.05$) is designated by *, n.s. indicates no significance.

TG-HKBP mice compared to wild-type mice immunized for EAU (**Figure 2A**). Because the tempo of disease can vary from mouse to mouse over the course of EAU, we also compared the maximum severity of each mouse over the entire course of disease by plotting the maximum score of each mouse (**Figure 2B**). The maximum EAU score also showed that TG-HKBP mice experienced significantly less severe EAU compared to wild-type mice (**Figure 2B**). Because the immunization procedure can elicit a score of 1, when the EAU score is 1 or lower, the disease is considered resolved. These observations demonstrate that kallistatin attenuates EAU and accelerates the resolution of EAU. Our clinical scores were also confirmed with fundus photos (**Figure 2C**). These observations demonstrate that kallistatin inhibits T cell activation resulting in the attenuation of EAU.

Kallistatin Does Not Significantly Change the Treg Compartment

We next sought to ask if the TG-HKBP mice have alterations in the Treg compartment. TG-HKBP mice have significantly less circulating B cells and a significantly greater percentage of circulating $CD4^+$ T cells (32). Regulatory T cells (Tregs) are necessary for the resolution of EAU (34) and for providing resistance to relapse (30, 35). Because we observed attenuated EAU in TG-HKBP mice, we asked if there is a change in the Treg compartment. Because the Tregs that provide resistance to relapse have been identified as $CD4^+CD25^+Nrp\text{-}1^-PD\text{-}1^+PD\text{-}L1^+Foxp3^+$ (30), we asked if TG-HKBP mice had an alteration in the number of these Tregs. The blood and bone marrow showed a trend toward an increase in $PD\text{-}1^+PD\text{-}L1^+Foxp3^+Nrp\text{-}1^-CD25^+CD4^+$ Tregs, but not a statistically significant increase (**Figures 3A–D**). These observations suggest suppression of EAU by TG-HKBP mice may be due to suppression of an inflammatory response but not necessarily an increase in the induction of Tregs.

Post-EAU Treg Cells Emerge in the Spleen of HKBP Mice

The post-EAU regulatory immunity that emerges in the spleen of mice at resolution of EAU provides resistance to relapse (29, 30, 34, 35), so that may be a mechanism to provide

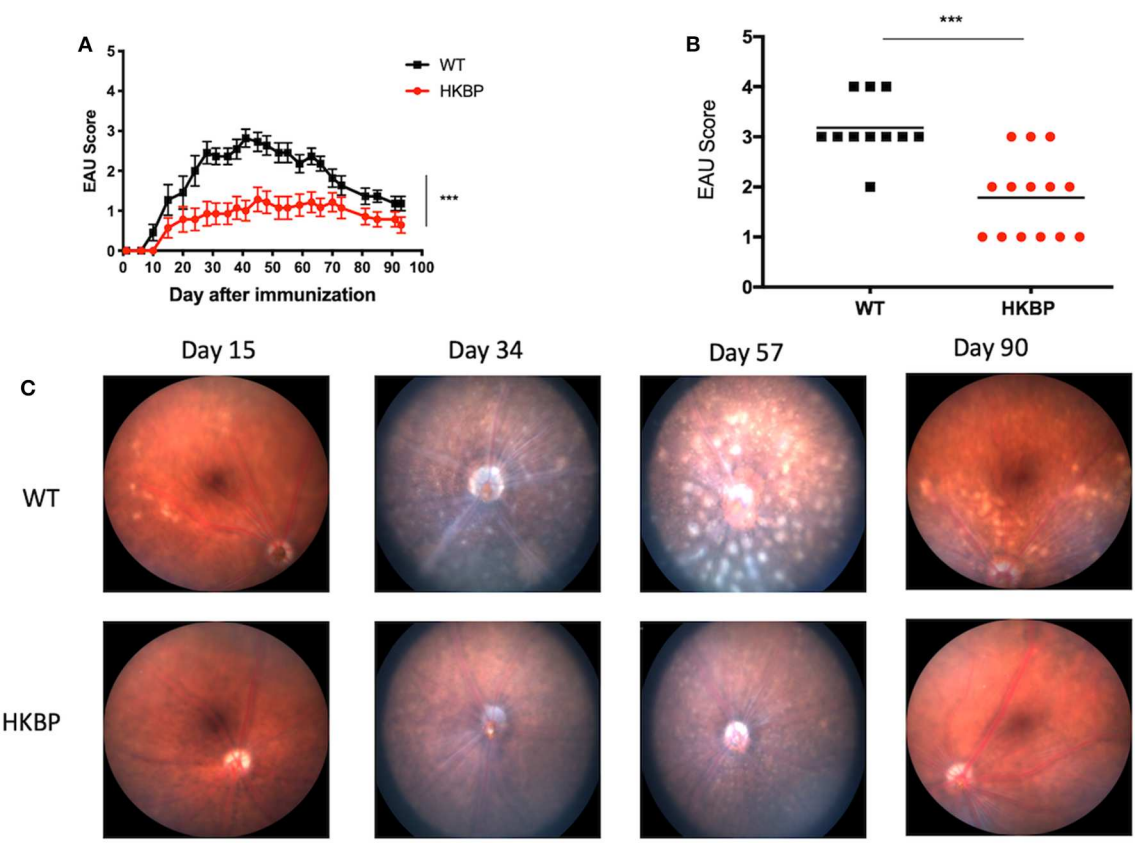

FIGURE 2 | EAU course of disease and maximum scores in TG-HKBP mice immunized for EAU. Wild-type and TG-HKBP mice were immunized for EAU and the clinical EAU score was assessed by slit lamp examination of the retina every 3–4 days. The highest score for each mouse on the indicated day was averaged with all the mice on that day and graphed with the SEM for WT (black squares, $n = 11$) and HKBP mice (red circle, $n = 14$) **(A)**. The highest EAU score for each mouse over the course of EAU was also determined (black squares, $n = 11$) and HKBP mice (red circle, $n = 14$) **(B)**. Representative images at the indicated time points are shown **(C)**. Statistical significance ($P \leq 0.05$) is designated by ***.

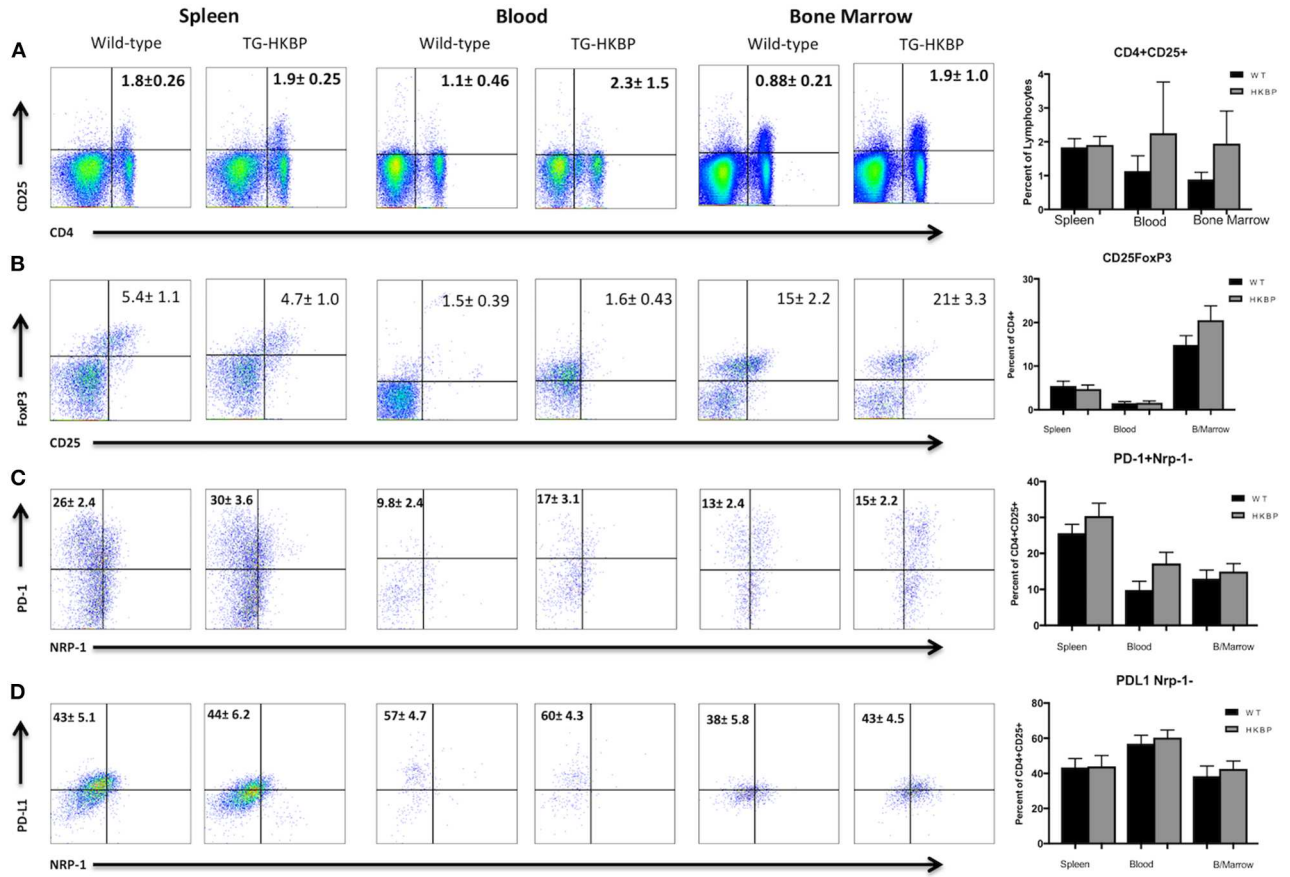

FIGURE 3 | Flow cytometry analysis of TG-HKBP mice for Treg cells. Spleen, blood, and bone marrow T cells from WT and TG-HKBP mice were stained for Treg cell markers. Representative flow plots with the mean and SEM of 3 independent experiments of 3–4 mice per experiment of WT mice ($n = 10$, black bars) and HKBP mice ($n = 11$, gray bars). CD4 and CD25 staining on T cells gated on the lymphocyte population based on FSC and SSC **(A)**, CD25 and FoxP3 staining of cells gated on CD4 **(B)**, NRP-1 and PD-1 staining of cells gated on CD4 and CD25 **(C)**, NRP-1 and PD-L1 staining of cells gated on CD4 and CD25 **(D)**.

sustained remission for uveitis patients in the clinical setting. A requirement of post-EAU regulatory immunity is resolution of EAU (27). Because the clinical EAU scores of TG-HKBP mice were significantly lower compared to wild-type mice, we therefore asked if the post-EAU TG-HKBP mice also had $CD4^+CD25^+Nrp\text{-}1^-PD\text{-}1^+PD\text{-}L1^+Foxp3^+$ Tregs in the spleen at resolution of EAU. The spleens from post-EAU TG-HKBP mice were collected and reactivated *in vitro* as has been done before (29, 30, 35). There was no significant difference between post-EAU wild-type and post-EAU TG-HKBP Treg cell populations in the spleen (**Figures 4A–D**). However, the percentage of PD-1 and PD-L1 expressing $CD4^+CD25^+$ T cells (**Figures 4C,D**) was increased compared to the unimmunized unstimulated T cells (**Figures 3C,D**). Because there is no significant difference between the post-EAU wild-type mice and TG-HKBP mice, these observations demonstrate that this post-EAU Treg population is present in the spleen of TG-HKBP mice.

Kallistatin Does Not Affect the Emergence of Post-EAU Regulatory Immunity

We next asked if the post-EAU regulatory immunity in TG-HKBP mice is functionally suppressive. The spleen of post-EAU TG-HKBP mice was collected and reactivated *in vitro* as has been done before (29, 30, 35). The reactivated splenocytes were then adoptively transferred to recipient mice immunized for EAU. As expected, mice that received splenocytes from post-EAU wild-type mice showed a significant suppression of EAU (29, 30, 33) compared to EAU mice that did not receive an adoptive transfer (**Figures 5A,B**). The mice that received post-EAU TG-HKPB splenocytes also showed a significant suppression of EAU (**Figure 5D**) and significantly lower maximum EAU scores compared to controls (**Figure 5E**). A representative fundus photo is shown at day 67 to confirm the clinical observations (**Figures 5C,F**). These observations demonstrate that kallistatin does not affect the emergence of post-EAU regulatory immunity in the spleen.

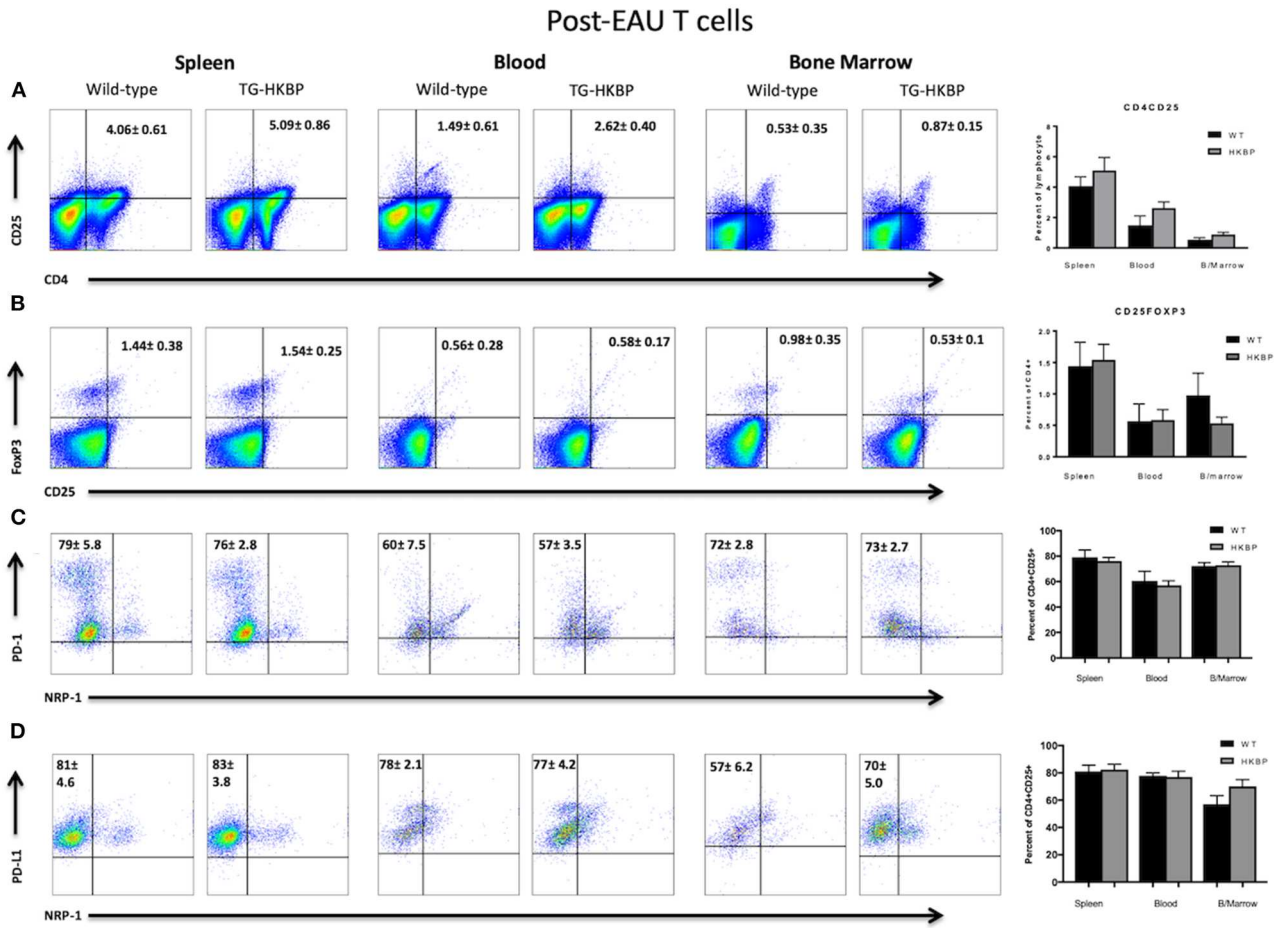

FIGURE 4 | Flow cytometry analysis of post-EAU TG-HKBP mice for Treg cells. Spleen, blood, and bone marrow T cells from WT and TG-HKBP mice were stained for Treg cell markers. Representative flow plots with the mean and SEM of 3 independent experiments of 3–7 mice per experiment of WT mice ($n = 6$, black bars) and HKBP mice ($n = 15$, gray bars). CD4 and CD25 staining on T cells gated on the lymphocyte population based on FSC and SSC **(A)**, CD25 and FoxP3 staining of cells gated on CD4 **(B)**, NRP-1 and PD-1 staining of cells gated on CD4 and CD25 **(C)**, NRP-1 and PD-L1 staining of cells gated on CD4 and CD25 **(D)**.

Kallistatin Promotes Tregs in an Intrinsic Manner

In order to determine if kallistatin mediated Treg induction is intrinsic or extrinsic, we transferred $CD4^+$ HKBP cells into wild-type mice to determine if FoxP3 expression is mediated through intrinsic T cell expression of kallistatin. Recipient mice were congenic (CD45.1) to identify the CD45.2 HKBP transferred cells. We found a significant elevation of FoxP3 expression in the transferred cells when HKBP cells were transferred to wild-type mice compared to wild-type cells transferred to the eyes of HKBP mice (**Figures 6A,C**). These observations show that kallistatin functions intrinsically in T cells. We next asked if this was an ocular specific effect by transferring congenic cells intravenously and assaying the spleen for FoxP3 expression in the transferred T cells. A similar pattern of expression with ocular injected cells was observed with a significant increase in FoxP3 expression in HKBP cells transferred to wild-type mice compared with wild-type cells transferred to HKBP mice (**Figures 6B,C**). These observations demonstrate that kallistatin functions intrinsically on T cells to maintain or induce Treg cells.

DISCUSSION

It has been previously demonstrated that a relationship between kallistatin and inflammation exists. This further illustrates a relationship between angiogenesis and inflammation. Previous reports demonstrate that TG-HKBP mice exhibit a reduction in B cells and a greater percentage of $CD4^+$ T cells (32). It has also been previously shown that TG-HKBP mice also have an impairment of wound healing due to defects in angiogenesis (17). In this report, we asked if kallistatin is capable of suppressing autoimmune uveitis. Our observations demonstrate that EAU is attenuated in TG-HKBP mice and display a reduction in severity and acceleration of resolution. This indicates the anti-inflammatory and anti-angiogenic properties of kallistatin are sufficient to suppress autoimmune uveitis and should be further investigated to

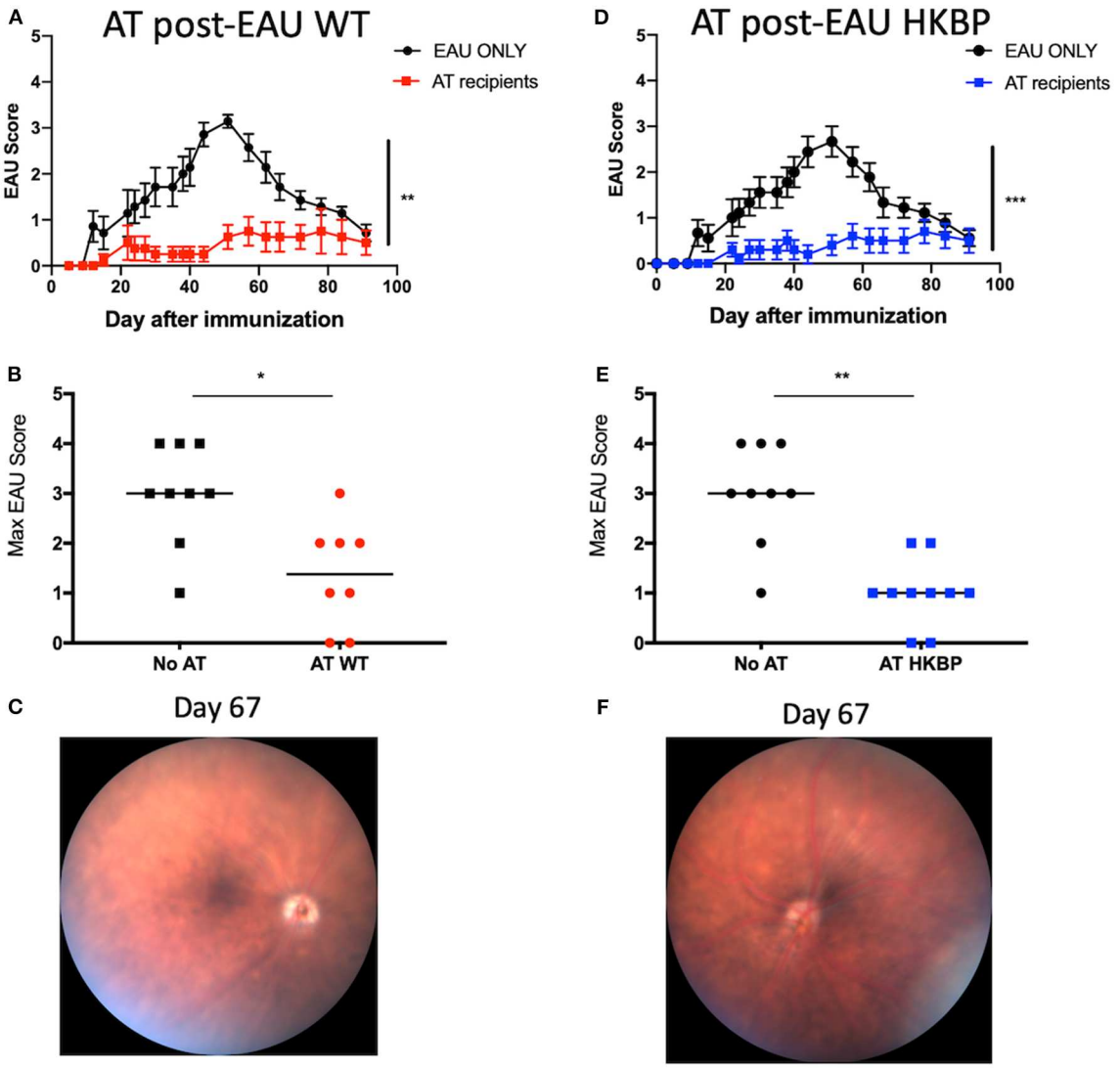

FIGURE 5 | EAU course of disease in recipient mice immunized for EAU that received splenocytes from post-EAU TG-HKBP mice. Post-EAU splenocytes from WT or TG-HKBP mice were reactivated *in vitro* and transferred to recipient mice that were immunized for EAU. Shown are clinical scores and representative retina images from recipient mice. Recipient scores are compared with EAU mice that did not receive cell transfer (black circles and squares). Mice that received WT post-EAU splenocytes (red squares and circles, $n = 8$) **(A,B)** and mice that received HKBP post-EAU splenocytes (blue squares $n = 10$) **(D,E)**. The same group of control EAU mice that did not receive a transfer are used for comparison **(A,B,D,E)**. A representative fundus image is shown for mice that received an adoptive transfer **(C,F)**. Statistical significance is designated by * ($P \leq 0.05$), ** ($P \leq 0.01$), and *** ($P \leq 0.005$).

develop novel treatments for autoimmune uveitis. However, the anti-angiogenic properties associated with elevated systemic kallistatin will need to be carefully considered if this is translated into a uveitis treatment. Another caveat to consider is that the overexpression of kallistatin is not equivalent to administration of the protein systemically because kallistatin likely has different properties in the eye compared to systemic kallistatin (17, 19, 21). Therefore, it may be the case that kallistatin given locally into the eye may be a suitable alternative to systemic administration.

It has been demonstrated that kallistatin is a Wnt/β-catenin inhibitor. This accounts for the reduction of lymphocytes because of the reduction of hematopoietic stem cells (32, 36–38). A reduction in T cells supports the hypothesis that EAU is suppressed because of a lack of effector T cells that can mediate inflammation. This may still be the case, but because we observe Treg cells that emerge at the resolution of EAU in TG-HKBP mice, it is likely that there are still pathogenic effector T cells being generated. However, given the anti-inflammatory properties and antagonism of TNF-α (23, 39) kallistatin has the capacity to limit the extent to which these effector T cells can mediate disease. Support for a kallistatin-mediated limitation of T cell activation is provided with the significant reduction of CD44+ TG-HKBP T cells following CD3 activation. As such,

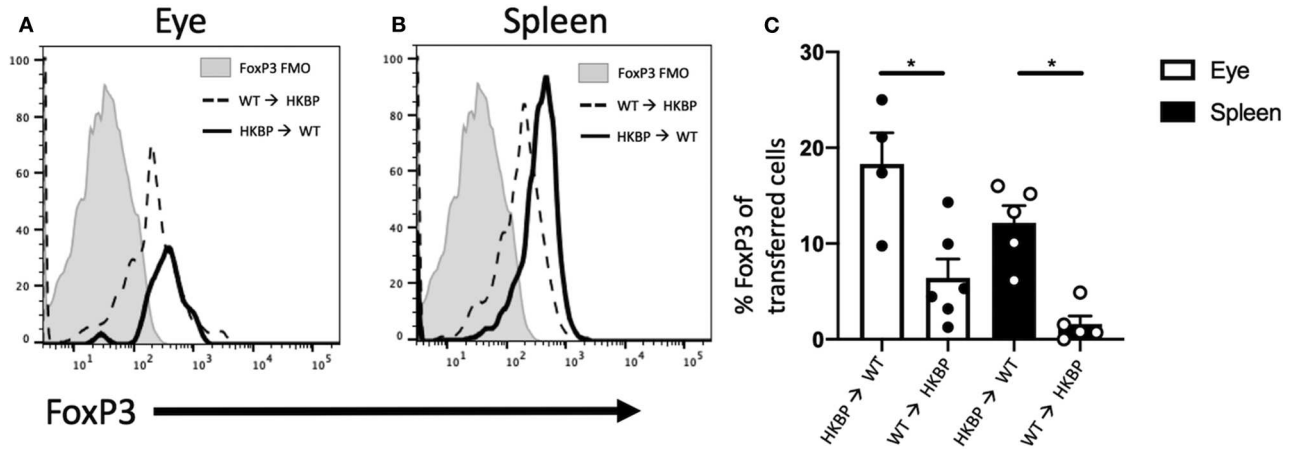

FIGURE 6 | FoxP3 expression in transferred HKBP or WT cells transferred to WT or HKBP mice. $CD4^+$ splenocytes were collected from donor HKBP or WT mice and transferred to recipient congenic mice. Donor cells were injected into the eyes (1×10^5 cells) or intravenously (1×10^6 cells). Forty eight-hours after the transfer the eyes were collected from mice that received an intraocular injection or the spleen was collected from mice that received an intravenous injection. Cells were then analyzed by flow cytometry for CD45.1, CD45.2, and FoxP3. Histograms shown are representative for all experiments, FoxP3 expression in the transferred cells collected from injected eyes **(A)**, or FoxP3 expression in the transferred cells collected from the spleen of intravenously injected mice **(B)**, the same fluorescence minus one (FMO) control is shown in both panels and is from the spleen. The mean ± SEM for all experiments are shown **(C)**. Each experiment included 1–3 mice and the experiment was repeated three times. Statistical significance ($P \leq 0.05$) is designated by *.

further studies are necessary to determine the exact mechanism whereby, kallistatin suppresses EAU.

Since mice that recover from EAU have regulatory immunity that provides resistance to EAU, it was of interest to determine if the post-EAU TG-HKBP mice also generate this regulatory immunity (29, 30, 35). Our observations demonstrate that not only is EAU attenuated in TG-HKBP mice, but they also generate regulatory immunity that is capable of providing resistance to relapse. The importance of this discovery is that if a uveitis patient is treated with kallistatin, there is still a generation of regulatory immunity that could provide sustained remission. However, overexpression of kallistatin is not equivalent to the administration of the protein as a therapeutic, but it has been demonstrated to confer greater survival in a sepsis model (40). Therefore, additional study assessing the efficacy of recombinant kallistatin is needed. We further show that the Tregs that emerge in the spleen of TG-HKBP mice share similar markers as the typical Tregs that normally emerge during EAU, so the Tregs likely emerge through similar mechanisms.

Because the TG-HKBP mice express serum levels similar to diabetic patients with vascular complications (17, 19), it may be the case that diabetic patients could be resistant to the development of autoimmune uveitis. However, because there are many mechanisms that promote autoimmune uveitis, this may only represent one such mechanism that provides resistance. As such, it has been observed that patients with diabetic retinopathy experience exacerbated uveitis (41, 42). This discrepancy is likely due to the status of ocular immune privilege, as is observed in diabetic retinopathy patients with lower kallistatin concentration in the vitreous (19, 21), and if systemic regulatory immunity has been established or not. In the case that ocular immune privilege has established regulatory immunity to protect against ocular inflammation, the patient would be protected against uveitis.

These observations demonstrate for the first time to our knowledge that kallistatin is effective in decreasing the severity of EAU and in accelerating the resolution of EAU. This suppression is likely due to multiple mechanisms that may include an inhibition of T cell activation and an intrinsic predisposition to regulatory activity in T cells. Importantly, in mice that overexpress kallistatin and have recovered from EAU, a functionally suppressive regulatory immunity is found in the spleen. This regulatory immunity in the spleen has a similar abundance of post-EAU Tregs that naturally emerge at resolution of EAU. Therefore, kallistatin suppresses autoimmune uveitis while also allowing for the emergence of systemic regulatory immunity that provides resistance to EAU.

DATA AVAILABILITY STATEMENT

The datasets generated for this study are available on request to the corresponding author.

ETHICS STATEMENT

This animal study was reviewed and approved by Institutional Animal Care and Use Committee, University of Oklahoma Health Science Center.

AUTHOR CONTRIBUTIONS

All experiments, analysis, and experimental design of this work were done by DL, PA, FM, MM, MC, and J-XM. The conceptual

design of this work and the writing of this manuscript was a collaborative effort between DL and J-XM.

FUNDING

This work was supported by National Institutes of Health (NIH) EY024951 (DL), EY029240 (DL), NIH Core Grant P30 EY021725, EY018659 (J-XM), EY019309 (J-XM), GM104934 (J-XM), EY028810 (MC), EY28066 (MC), Oklahoma Center for the Advancement of Science and Technology HR16-041 (J-XM), and in part by an unrestricted Research to Prevent Blindness grant (New York, NY, USA).

ACKNOWLEDGMENTS

We would like to thank the Oklahoma Medical Research Foundation Flow Cytometry Core facility and the Dean McGee Eye Institute Vivarium staff.

REFERENCES

1. Darrell RW, Wagener HP, Kurland LT. Epidemiology of uveitis. Incidence and prevalence in a small urban community. *Arch Ophthalmol*. (1962) 68:502–14. doi: 10.1001/archopht.1962.00960030506014
2. Reeves SW, Sloan FA, Lee PP, Jaffe GJ. Uveitis in the elderly: epidemiological data from the National Long-term Care Survey Medicare Cohort. *Ophthalmology*. (2006) 113:307.e1. doi: 10.1016/j.ophtha.2005.10.008
3. Suhler EB, Lloyd MJ, Choi D, Rosenbaum JT, Austin DF. Incidence and prevalence of uveitis in Veterans Affairs Medical Centers of the Pacific Northwest. *Am J Ophthalmol*. (2008) 146:890–896.e8. doi: 10.1016/j.ajo.2008.09.014
4. Hwang DK, Chou YJ, Pu CY, Chou P. Epidemiology of uveitis among the Chinese population in Taiwan: a population-based study. *Ophthalmology*. (2012) 119:2371–6. doi: 10.1016/j.ophtha.2012.05.026
5. Natkunarajah M, Kaptoge S, Edelsten C. Risks of relapse in patients with acute anterior uveitis. *Br J Ophthalmol*. (2007) 91:330–4. doi: 10.1136/bjo.2005.083725
6. Gritz DC, Wong IG. Incidence and prevalence of uveitis in Northern California; the Northern California Epidemiology of Uveitis Study. *Ophthalmology*. (2004) 111:491–500; discussion: 500. doi: 10.1016/j.ophtha.2003.06.014
7. Lee FF, Foster CS. Pharmacotherapy of uveitis. *Expert Opin Pharmacother*. (2010) 11:1135–46. doi: 10.1517/14656561003713534
8. Heiligenhaus A, Michels H, Schumacher C, Kopp I, Neudorf U, Niehues T, et al. Evidence-based, interdisciplinary guidelines for anti-inflammatory treatment of uveitis associated with juvenile idiopathic arthritis. *Rheumatol Int*. (2012) 32:1121–33. doi: 10.1007/s00296-011-2126-1
9. Lerman MA, Rabinovich CE. The future is now: biologics for non-infectious pediatric anterior uveitis. *Paediatr Drugs*. (2015) 17:283–301. doi: 10.1007/s40272-015-0128-2
10. Jabs DA, Rosenbaum JT, Foster CS, Holland GN, Jaffe GJ, Louie JS, et al. Guidelines for the use of immunosuppressive drugs in patients with ocular inflammatory disorders: recommendations of an expert panel. *Am J Ophthalmol*. (2000) 130:492–513. doi: 10.1016/S0002-9394(00)00659-0
11. Nguyen QD, Callanan D, Dugel P, Godfrey DG, Goldstein DA, Wilensky JT. Treating chronic noninfectious posterior segment uveitis: the impact of cumulative damage. Proceedings of an expert panel roundtable discussion. *Retina*. (2006) 26(Suppl.):1–16. doi: 10.1097/01.iae.0000250601.15893.5f
12. Siddique SS, Shah R, Suelves AM, Foster CS. Road to remission: a comprehensive review of therapy in uveitis. *Expert Opin Investig Drugs*. (2011) 20:1497–515. doi: 10.1517/13543784.2011.617741
13. Kruh J, Foster CS. The philosophy of treatment of uveitis: past, present and future. *Dev Ophthalmol*. (2012) 51:1–6. doi: 10.1159/000336183
14. Foster CS, Kothari S, Anesi SD, Vitale AT, Chu D, Metzinger JL, et al. The Ocular Immunology and Uveitis Foundation preferred practice patterns of uveitis management. *Surv Ophthalmol*. (2016) 61:1–17. doi: 10.1016/j.survophthal.2015.07.001
15. Maleki A, Meese H, Sahawneh H, Foster CS. Progress in the understanding and utilization of biologic response modifiers in the treatment of uveitis. *Expert Rev Clin Immunol*. (2016) 12:775–86. doi: 10.1586/1744666X.2016.1166052
16. Chao J, Chao L. Biochemistry, regulation and potential function of kallistatin. *Biol Chem Hoppe Seyler*. (1995) 376:705–13.
17. McBride JD, Jenkins AJ, Liu X, Zhang B, Lee K, Berry WL, et al. Elevated circulation levels of an antiangiogenic SERPIN in patients with diabetic microvascular complications impair wound healing through suppression of Wnt signaling. *J Invest Dermatol*. (2014) 134:1725–34. doi: 10.1038/jid.2014.40
18. Chao J, Li P, Chao L. Kallistatin suppresses cancer development by multi-factorial actions. *Crit Rev Oncol Hematol*. (2017) 113:71–8. doi: 10.1016/j.critrevonc.2017.03.011
19. Jenkins AJ, McBride JD, Januszewski AS, Karschimkus CS, Zhang B, O'Neal DN, et al. Increased serum kallistatin levels in type 1 diabetes patients with vascular complications. *J Angiogenes Res*. (2010) 2:19. doi: 10.1186/2040-2384-2-19
20. Yiu WH, Wong DW, Wu HJ, Li RX, Yam I, Chan LY, et al. Kallistatin protects against diabetic nephropathy in db/db mice by suppressing AGE-RAGE-induced oxidative stress. *Kidney Int*. (2016) 89:386–98. doi: 10.1038/ki.2015.331
21. Ma JX, King LP, Yang Z, Crouch RK, Chao L, Chao J. Kallistatin in human ocular tissues: reduced levels in vitreous fluids from patients with diabetic retinopathy. *Curr Eye Res*. (1996) 15:1117–23. doi: 10.3109/02713689608995143
22. Shen B, Smith RS Jr., Hsu YT, Chao L, Chao J. Kruppel-like factor 4 is a novel mediator of Kallistatin in inhibiting endothelial inflammation via increased endothelial nitric-oxide synthase expression. *J Biol Chem*. (2009) 284:35471–8. doi: 10.1074/jbc.M109.046813
23. Lu SL, Tsai CY, Luo YH, Kuo CF, Lin WC, Chang YT, et al. Kallistatin modulates immune cells and confers anti-inflammatory response to protect mice from group A streptococcal infection. *Antimicrob Agents Chemother*. (2013) 57:5366–72. doi: 10.1128/AAC.00322-13
24. Caspi RR, Roberge FG, Chan CC, Wiggert B, Chader GJ, Rozenszajn LA, et al. A new model of autoimmune disease. Experimental autoimmune uveoretinitis induced in mice with two different retinal antigens. *J Immunol*. (1988) 140:1490–5.
25. Caspi RR, Silver PB, Luger D, Tang J, Cortes LM, Pennesi G, et al. Mouse models of experimental autoimmune uveitis. *Ophthalmic Res*. (2008) 40:169–74. doi: 10.1159/000119871
26. Chen J, Qian H, Horai R, Chan CC, Caspi RR. Mouse models of experimental autoimmune uveitis: comparative analysis of adjuvant-induced vs spontaneous models of uveitis. *Curr Mol Med*. (2015) 15:550–7. doi: 10.2174/1566524015666150731100318
27. Kitaichi N, Namba K, Taylor AW. Inducible immune regulation following autoimmune disease in the immune-privileged eye. *J Leukoc Biol*. (2005) 77:496–502. doi: 10.1189/jlb.0204114
28. Lee DJ, Taylor AW. Following EAU recovery there is an associated MC5r-dependent APC induction of regulatory immunity in the spleen. *Invest Ophthalmol Vis Sci*. (2011) 52:8862–7. doi: 10.1167/iovs.11-8153
29. Lee DJ, Taylor AW. Both MC5r and A2Ar Are required for protective regulatory immunity in the spleen of post-experimental autoimmune uveitis in mice. *J Immunol*. (2013) 191:4103–11. doi: 10.4049/jimmunol.1300182
30. Lee DJ, Taylor AW. Recovery from experimental autoimmune uveitis promotes induction of antiuveitic inducible Tregs. *J Leukoc Biol*. (2015) 97:1101–9. doi: 10.1189/jlb.3A1014-466RR
31. Liu X, Zhang B, McBride JD, Zhou K, Lee K, Zhou Y, et al. Antiangiogenic and antineuroinflammatory effects of kallistatin through interactions with the canonical Wnt pathway. *Diabetes*. (2013) 62:4228–38. doi: 10.2337/db12-1710

32. McBride JD, Liu X, Berry WL, Janknecht R, Cheng R, Zhou K, et al. Transgenic expression of a canonical Wnt inhibitor, kallistatin, is associated with decreased circulating CD19+ B lymphocytes in the peripheral blood. *Int J Hematol*. (2017) 105:748–57. doi: 10.1007/s12185-017-2205-5
33. Namba K, Kitaichi N, Nishida T, Taylor AW. Induction of regulatory T cells by the immunomodulating cytokines alpha-melanocyte-stimulating hormone and transforming growth factor-beta2. *J Leukoc Biol*. (2002) 72:946–52. doi: 10.1189/jlb.72.5.946
34. Silver PB, Horai R, Chen J, Jittayasothorn Y, Chan CC, Villasmil R, et al. Retina-specific T regulatory cells bring about resolution and maintain remission of autoimmune uveitis. *J Immunol*. (2015) 194:3011–9. doi: 10.4049/jimmunol.1402650
35. Lee DJ, Preble J, Lee S, Foster CS, Taylor AW. MC5r and A2Ar deficiencies during experimental autoimmune uveitis identifies distinct T cell polarization programs and a biphasic regulatory response. *Sci Rep*. (2016) 6:37790. doi: 10.1038/srep37790
36. Malhotra S, Baba Y, Garrett KP, Staal FJ, Gerstein R, Kincade PW. Contrasting responses of lymphoid progenitors to canonical and noncanonical Wnt signals. *J Immunol*. (2008) 181:3955–64. doi: 10.4049/jimmunol.181.6.3955
37. Staal FJ, Langerak AW. Signaling pathways involved in the development of T-cell acute lymphoblastic leukemia. *Haematologica*. (2008) 93:493–7. doi: 10.3324/haematol.12917
38. Staal FJ, Sen JM. The canonical Wnt signaling pathway plays an important role in lymphopoiesis and hematopoiesis. *Eur J Immunol*. (2008) 38:1788–94. doi: 10.1002/eji.200738118
39. Yin H, Gao L, Shen B, Chao L, Chao J. Kallistatin inhibits vascular inflammation by antagonizing tumor necrosis factor-alpha-induced nuclear factor kappaB activation. *Hypertension*. (2010) 56:260–7. doi: 10.1161/HYPERTENSIONAHA.110.152330
40. Li P, Bledsoe G, Yang ZR, Fan H, Chao L, Chao J. Human kallistatin administration reduces organ injury and improves survival in a mouse model of polymicrobial sepsis. *Immunology*. (2014) 142:216–26. doi: 10.1111/imm.12242
41. Skarbez K, Priestley Y, Hoepf M, Koevary SB. Comprehensive review of the effects of diabetes on ocular health. *Expert Rev Ophthalmol*. (2010) 5:557–77. doi: 10.1586/eop.10.44
42. Oswal KS, Sivaraj RR, Murray PI, Stavrou P. Clinical course and visual outcome in patients with diabetes mellitus and uveitis. *BMC Res Notes*. (2013) 6:167. doi: 10.1186/1756-0500-6-167

Conflict of Interest: The authors declare that the research was conducted in the absence of any commercial or financial relationships that could be construed as a potential conflict of interest.

frontiers in Immunology

REVIEW
published: 03 July 2020
doi: 10.3389/fimmu.2020.01431

New Insights Into Immunological Therapy for Retinal Disorders

Atsunobu Takeda[1,2]*, *Ryoji Yanai*[3], *Yusuke Murakami*[1], *Mitsuru Arima*[1] and *Koh-Hei Sonoda*[1]

[1] Department of Ophthalmology, Graduate School of Medical Sciences, Kyushu University, Fukuoka, Japan, [2] Department of Ophthalmology, Clinical Research Institute, Kyushu Medical Center, National Hospital Organization, Fukuoka, Japan, [3] Department of Ophthalmology, Graduate School of Medicine, Yamaguchi University, Yamaguchi, Japan

In the twentieth century, a conspicuous lack of effective treatment strategies existed for managing several retinal disorders, including age-related macular degeneration; diabetic retinopathy (DR); retinopathy of prematurity (ROP); retinitis pigmentosa (RP); uveitis, including Behçet's disease; and vitreoretinal lymphoma (VRL). However, in the first decade of this century, advances in biomedicine have provided new treatment strategies in the field of ophthalmology, particularly biologics that target vascular endothelial growth factor or tumor necrosis factor (TNF)-α. Furthermore, clinical trials on gene therapy specifically for patients with autosomal recessive or X-linked RP have commenced. The overall survival rates of patients with VRL have improved, owing to earlier diagnoses and better treatment strategies. However, some unresolved problems remain such as primary or secondary non-response to biologics or chemotherapy, and the lack of adequate strategies for treating most RP patients. In this review, we provide an overview of the immunological mechanisms of the eye under normal conditions and in several retinal disorders, including uveitis, DR, ROP, RP, and VRL. In addition, we discuss recent studies that describe the inflammatory responses that occur during the course of these retinal disorders to provide new insights into their diagnosis and treatment.

Keywords: immune privilege, non-infectious uveitis, diabetic retinopathy, retinopathy of prematurity, retinitis pigmentosa, vitreoretinal lymphoma

OPEN ACCESS

Edited by:
Andrew W. Taylor, Boston University School of Medicine, United States

Reviewed by:
Seyed Mahmoud Hashemi, Shahid Beheshti University of Medical Sciences, Iran
Cristhian J. Ildefonso, University of Florida, United States

***Correspondence:**
Atsunobu Takeda
atakeda417@yahoo.co.jp

Specialty section:
This article was submitted to Autoimmune and Autoinflammatory Disorders, a section of the journal Frontiers in Immunology

Received: *11 March 2020*
Accepted: *03 June 2020*
Published: *03 July 2020*

Citation:
Takeda A, Yanai R, Murakami Y, Arima M and Sonoda K-H (2020) New Insights Into Immunological Therapy for Retinal Disorders. Front. Immunol. 11:1431. doi: 10.3389/fimmu.2020.01431

INTRODUCTION

In the last 2 decades, advances in the interdisciplinary collaboration of the fields of molecular biology, biochemistry, genetics, and biomedicine have resulted in tremendous breakthroughs in the treatment of refractory ocular disorders. Infliximab (IFX), a chimeric antibody of the tumor necrosis factor (TNF)-α, is a biologics that is used for treating ocular symptoms of Behçet's disease that have not been adequately controlled (1). Anti-vascular endothelial factor (VEGF) agents such as ranibizumab and aflibercept are used as the first-line therapy in the management of intractable retinal disorders such as neovascular age-related macular degeneration and diabetic macular edema (DME). These agents can also maintain remission in such cases (2, 3). For a long time, laser photocoagulation alone has been used for the primary treatment of etinopathy of prematurity (ROP). However, in 2018, ranibizumab was also validated for the treatment of ROP in Japan. Gene therapy clinical trials targeting the treatment of autosomal recessive or X-linked retinitis pigmentosa (RP), which is an incurable genetic retinal disorder, have been initiated (4). Furthermore, the overall survival of patients with vitreoretinal lymphoma (VRL), which is

a fetal retinal malignancy, has increased because of improved treatment strategies that involve intense systemic chemotherapy and/or radiotherapy (5–7). However, unmet needs remain in the management of these retinal disorders because of primary and secondary treatment failure or non-response to the biologics, or most cases of RP untargeted by gene therapy.

The eye, just like the brain and the testes, is an immune-privilege site (8). Ocular immune privilege is an active process in which the regulatory molecules and cells of the eye modulate the induction and the expression of inflammation (8–10). As long as the ocular immune-privilege system is working, a harmful immune response and degenerative eye diseases can be prevented. By limiting intraocular inflammation, immune privilege preserves the integrity of the visual axis and thereby prevents blindness (11). However, the mechanism of immune privilege can be compromised genetically and/or by environmental stimuli such as damage-associated molecular patterns, infection, and a chronic immune response, and thereby give rise to various retinal disorders (11).

Immunological responses to various environmental stimuli have been associated with the pathogenesis of uveitis and retinal vascular diseases such as diabetic retinopathy (DR) and ROP (11–13). Retinitis pigmentosa is a genetic disorder, although inflammatory responses to microenvironmental changes, such as rod cell death, which occur after the primary onset of the disease, may cause subsequent loss of cone cells (11). In VRL, oncogenic mutations of VRL cells and the evasion of immune surveillance because of the immunosuppressive ocular microenvironment may contribute to tumor growth.

In this review, we focus on the roles of immunological responses in a normal conditions and in several major retinal disorders including non-infectious uveitis (NIU), DR, ROP, RP, and VRL. In addition, we contemplate new approaches for the diagnosis and treatment of these intractable retinal disorders from an immunological point of view.

THE NORMAL IMMUNOLOGICAL CONDITION IN THE EYE

A properly elicited and regulated immune response by the human body is necessary for eliminating threats due to infectious microbes and tissue trauma to avoid irreversible tissue damage (11). Acute inflammation should be self-limiting and normally attenuated after the elimination of deleterious stimuli to enable physiological recovery. Chronic inflammation causes degenerative diseases with consequent loss of organ function.

Ocular immune privilege is believed to elicit self-limiting immune responses (14). Several soluble and cell-bound inhibitory factors are involved in the mechanism of ocular immune privilege to create an intraocular immunosuppressive microenvironment, which prevents excessive immune activation and subsequent tissue damage. These factors include transforming growth factor-beta (TGF-β)2 (15), retinoic acid (16), and multiple immunosuppressive factors in ocular fluids (17), and the constitutive expression of the Fas ligand (18), programmed death-ligand 1 (PD-L1) (19), galectins (20), membrane glycoprotein CD200 receptor 1 (21), cytotoxic T lymphocyte-associated protein (CTLA)-2a (22), B7 (23, 24) on the surface of ocular cells. For the maintenance of retinal homeostasis, these immunosuppressive molecules in the eye actively regulate the induction and the expression of inflammation to prevent excessive activation and subsequent tissue damage.

In addition to the abovementioned local immunosuppression, ocular immune privilege is associated with the development of a type of an antigen-specific systemic immune regulation, called "anterior chamber-associated immune deviation" ("ACAID") (8, 25). ACAID is induced by intrinsic intraocular bone marrow-derived antigen-presenting cells (APCs) that trap an antigen within the anterior chamber and migrates to the spleen via circulating blood (8, 26). Antigens from the anterior chamber can be transported to the regional lymph nodes (27). Tolerogenic $CD11c^+$ dendritic cells (DCs) also transport antigens to the thymus (27). APCs bearing the eye-derived antigen can elicit the development regulatory T (Treg) cells in these lymphoid organs. In the eye, innate immune cells such as microglial cells, neutrophils, monocyte-macrophages, natural killer (NK) cells, natural killer T (NKT) cells, and γδT cells can exhibit a broad range of antigen recognition and confer a widely distributed form of immunity, which constitutes the first line of defense against various invading pathogens (28).

The anterior chamber and the vitreous cavity or the posterior chamber of the eye have the capacity to induce systemic immune deviation (29). This phenomenon is called "vitreous cavity-associated systemic immune deviation" ("VCAID"). Research demonstrates that $F4/80^+$ hyalocytes are distributed over the retinal surface (30) and that murine hyalocytes are bone marrow-derived and turned over in 4 months (31). Hyalocytes have strong scavenger activity (30); therefore, we postulated that ocular hyalocytes capture an antigen on the retinal surface and carry it via the blood to the spleen, which induces antigen-specific Tregs (30).

NON-INFECTIOUS UVEITIS (NIU)

Human Non-infectious Uveitis

Non-infectious uveitis (NIU) is a sight-threatening disorder associated with systemic autoimmune diseases such as Behcet's disease, sarcoidosis, and Vogt–Koyanagi–Harada disease (32). NIU is often recurrent and causes tissue destruction and scarring, especially in the retina and uvea, which results in permanent loss of vision. Early studies showed that T-helper (Th) 1 and Th17 cells are the major effector cells and are crucial for development of uveitis (33). In many cases, the administration of several immunosuppressive drugs for an extended period is necessary to control inflammation in eyes with uveitis (34). These agents include corticosteroids, tacrolimus, and cyclosporine, which have a strong T cell-suppressive effect and have serious side effects, such as diabetes, hypertension, and nephrotoxicity (35, 36). A new generation of biological compounds that inhibit T cell activation such as monoclonal antibodies and recombinant forms of natural inhibitory molecules have emerged (36, 37). For example, IFX

is validated for the treatment of refractory ocular Behçet's disease (1, 38, 39). Adalimumab (ADA), which is a recombinant human immunoglobulin G1 monoclonal antibody to TNF-α, has also been validated for the treatment of patients with NIU in the United States and in Japan. ADA has been proven as an effective corticosteroid-sparing agent that reduces adverse effects associated with long-term usage of corticosteroids (34). Immunosuppressive therapeutic agents for treating non-infections uveitis (based on the guidelines of an international expert steering committee consisting of uveitis specialists are summarized in **Table 1**) (40). However, several studies report that IFX can cause the development of autoimmune diseases, primarily cutaneous vasculitis, lupus-like syndrome, and malignant lymphoma (41). In recent reports, some patients had a decreased response to IFX or ADA during the course of the treatment, owing to the development of antidrug antibodies against IFX or ADA (42–44). Therefore, new effective therapeutic targets for uveitis with less severe adverse effects need to be identified.

Experimental Autoimmune Uveitis

Experimental autoimmune uveitis (EAU) is an animal disease model of a T cell–mediated autoimmune disease that mimics many of the pathological features of human uveitis (45, 46). EAU is induced by injecting animals with purified retinal antigens such as S-Ag, a fragment (residues 1–20, GPTHLFQPSLVLDMAKVLLD) of the human interphotoreceptor retinoid-binding protein (hIRBP); rhodopsin (or opsin); phosducin, or recoverin. The disease is mediated by Th1 and Th17 cells (47, 48), which are generated from naive T cells in response to their exposure to proinflammatory cytokines and to the foreign antigens presented by APCs—including DCs, macrophages, NK cells, and B lymphocytes—in secondary lymphoid organs. Infiltration of inflammatory cells such as granulocytes and macrophages and other non-specific lymphocytes that can destroy ocular tissue also contributes to the development of EAU (48, 49). In the next section, we will discuss recent studies of EAU model mice and review studies on microglia, NK cells, NKT cells, DCs, the P2X7 receptor, Notch signaling, and the transcription factor Foxp3 (forkhead box P3), which have been identified as targets for translational medicine. Such research has provided insight into the mechanisms underlying disease pathogenesis and the basis for the development of new preventive or therapeutic approaches to human uveitis.

TABLE 1 | Systemic corticosteroid and immunomodulatory therapeutic agents for non-infectious uveitis.

Drugs	Drug administration route and dosage	Disease entities or cause	Evidence level (No. of publications)
Corticosteroid	Orally prednisolone, 20–60 mg/day Intravenously methylprednisolone, 1,000 mg/day Tapering to low-dose oral prednisone and addition of a corticosteroid sparing agent	NIU	
Mycophenolate preparations	Oral, 500–3,000 mg/day	NIU BCR VKH disease	2B¶ 2B/3 2B/3
Azathioprine§	Started at 1 mg/kg/day and increased to 2–3 mg/kg/day in steps of 50 mg every 2 weeks	NIU BD VKH disease	2B 2B 4
Methotrexate	Adult: oral, 6–25 mg/week Child: oral, 4–10 mg/week	NIU VKH disease	2B 2B/3
Cyclophosphamide	Oral, 20–100 mg/day Intravenos, 750–1,000 mg/m^2 of body surface area monthly infusions	NIU	4
Tacrolimus	Oral, 0.12–0.3 mg/kg	NIU	2B
Cyclosporine	Oral, 3–5 mg/kg	NIU	2B
Infliximab	Intravenous, 5 mg/kg at weeks 0, 2, and 6, and every 8 weeks thereafter	BD, BCR, sarcoidosis, idiopathic vasculitis, VKH disease Pediatric NIU (uveitis entities include JIA, BD, sarcoidosis, VKH disease)	2B (2), 3B (1), 4 (4) 2B (1), 4 (2), 5 (1)
Adalimumab	Initial dose of 80 mg, followed by 40 mg administered every other week starting 1 week after the initial dose	NIU (including different uveitis entities: BD, idiopathic uveitis, sarcoidosis, BRC, TINU, VKH disease, pars planitis; other: HLA-B27, JIA)	1B (4), 2B (4), 4 (5), 5 (2)

NIU, non-infectious uveitis; BCR, birdshot chorioretinopathy; VKH, Vogt–Koyanagi–Harada disease; BD, Behçet's disease; JIA, juvenile idiopathic arthritis; TINU, tubulointerstitial nephritis and uveitis.

¶*Evidence level 4 and grade C recommendation for mycophenolate sodium.*

§*Includes one study with methotrexate and mycophenolate mofetil as comparators.*

Advances in the Treatment of EAU

The important role of microglia in the regulation of inflammatory cell infiltration into the retina associated with the initiation of retinal autoimmune uveitis has recently been demonstrated (50). During the early phase of EAU (days 7–10), microglia have a direct effect on the increase in the number of various adherent vascular leukocytes, including T cells, major histocompatibility complex (MHC) class II^+ cells, and $CD11b^+$ cells. This effect was specific to microglia, given that it was not reproduced by other immune cell types such as monocytes-macrophages. Therefore, immunomodulatory therapies targeted at microglia are a primary focus in the development of new treatments for patients with uveitis.

We previously explained that NKT cells suppress the induction of Th17 cells and the ocular infiltration of hIRBP-specific T cells in EAU. However, in contrast to the ameliorating effects of NKT cell activation that is apparent during the initiation phase of EAU, the activation during the effector phase exacerbates disease pathology. This finding suggests that NKT cells have a dual role in EAU, depending on the phase of the disease (51).

$CD83^+CCR7^+$ NK cells induced by interleukin (IL)-18 released from DCs promote EAU (52). NK cells are negatively regulated by a soluble form of CD83 in EAU (53). In addition, DC–NK cell interactions that underlie the regulation of Th1 responses modulate the adaptive Th17 response and limit tissue-specific autoimmunity through the innate interferon (IFN)-γ-IL-27 axis in this model (54).

Treg cells are necessary for the resolution of EAU and the prevention of relapse (55, 56). A recent study demonstrated that $PD\text{-}1^+CD25^+CD4^+$ Treg cells require programmed cell death 1 (PD-1) stimulation through a melanocortin-adenosine pathway to suppress EAU. These Treg cells did not induce suppressor activity in APCs through the PD-1 pathway (57).

Many studies have demonstrated that monocytes-macrophages have a role in the development of EAU (58). Activated bone marrow–derived macrophages are required during the effector phase of EAU (45). However, in addition to their proinflammatory function, macrophages have suppressive effects on ocular inflammation, especially in the chronic phase. Suppressor of cytokine signaling 3 (SOCS3) in macrophages was recently found to be important in the suppressing the inflammation caused by these cells in EAU (59).

Extracellular adenosine triphosphate (ATP) is a key chemotactic signal for the recruitment of innate immune cells to sites of brain injury (60). ATP is actively released via exocytosis or transporters during the early phase of apoptotic cell death, whereas it is passively released from necrotic cells after the rupture of the plasma membrane. Extracellular ATP acts at P2X and P2Y purinergic receptors and induces the formation of inflammasomes, which are large intracellular multiprotein complexes that are key players in host defense during the innate immune response (61). The P2X receptor family consists of ligand-gated cation channels that open in response to the binding of extracellular ATP. Among the seven mammalian P2X receptors, P2RX7 shows the highest affinity for ATP and is highly expressed in immune cells such as monocytes and T lymphocytes (62, 63). Research has demonstrated that the genetic ablation of P2RX7 or the administration of the P2RX7 antagonist BBG in mice suppresses EAU clinically and histopathologically by attenuating hIRBP-dependent induction of interferon (IFN)-γ and IL-17 (64).

Dendritic Cells in the Eye

DCs are highly efficient APCs and have the unique ability to prime and activate naive T lymphocytes (65, 66). They are divided into three types, based on their function: immature DCs, mature DCs, and regulatory DCs. Under physiological conditions, DCs are widely distributed among tissues and organs (67) where they are in an immature state and contribute to immune surveillance. In the eyes of mice and rats, these cells are at the peripheral margin and in juxtapapillary areas of the retina (68, 69). The functions of DCs in the quiescent retina include promoting the generation of $Foxp3^+$ Treg cells and inhibiting the activation of naive T cells induced by splenic DCs and antigens (69).

Dendritic Cells in EAU

DCs have an essential role in innate immunity. They also link the innate and adaptive immune systems and are key for the induction of late immune responses. Cell-based therapy involving the *ex vivo* manipulation of mature or regulatory DCs has been adopted as a means to induce tolerance in autoimmune disease (70–72). Studies of the mechanisms of DC function in uveitis are thus warranted to identify new therapeutic targets for this condition. Mature DCs pulsed with uveitogenic antigens induce the development of EAU (69). Treatment with fixed immature DCs, but not with fixed mature DCs, has also been demonstrated to ameliorate the progression of EAU by inhibiting uveitogenic $CD4^+$ T cell activation and differentiation (73). In addition, impairment DC maturation with drugs prevents the generation of antigen-specific Th1 and Th17 cells and thereby attenuates EAU (74). Moreover, regulatory DCs induced *in vitro* suppress the development of EAU (75). These various data altogether indicate that the regulation of DC status is potentially beneficial for the treatment of uveitis.

In a previous study, conducted by the authors of the present review, we found that mouse spleen-derived DCs mediate the anti-inflammatory action of dietary ω-3 long-chain polyunsaturated fatty acids (LCPUFAs) in EAU (76). Histological analysis at 17 days after disease induction revealed retinal folds and immune cell infiltration in the eyes of EAU mice that received DCs from ω-6 LCPUFA–fed mice, and showed that such changes were markedly suppressed in EAU mice that received DCs from ω-3 LCPUFA–fed mice (**Figure 1A**) (77). Furthermore, DCs exposed to ω-3 LCPUFAs *in vivo* or *in vitro* suppressed T cell proliferation. This finding suggested that ω-3 LCPUFA–treated DCs attenuate inflammation mediated by T cells (**Figure 1B**). Cytokines released by activated DCs are essential for T cell differentiation, with IL-12 p70 promoting Th1 cell differentiation and with IL-6 and TGF–β promoting Th17 cell differentiation (78, 79). We also found that dietary ω-3 LCPUFAs acting via adoptively transferred DCs markedly inhibited IL-12 p70 and IL-6 production by T cells from EAU mice. This finding is consistent with the notion that ω-3 LCPUFAs suppress Th1 and Th17 cytokine production by $CD4^+$ T cells, through the

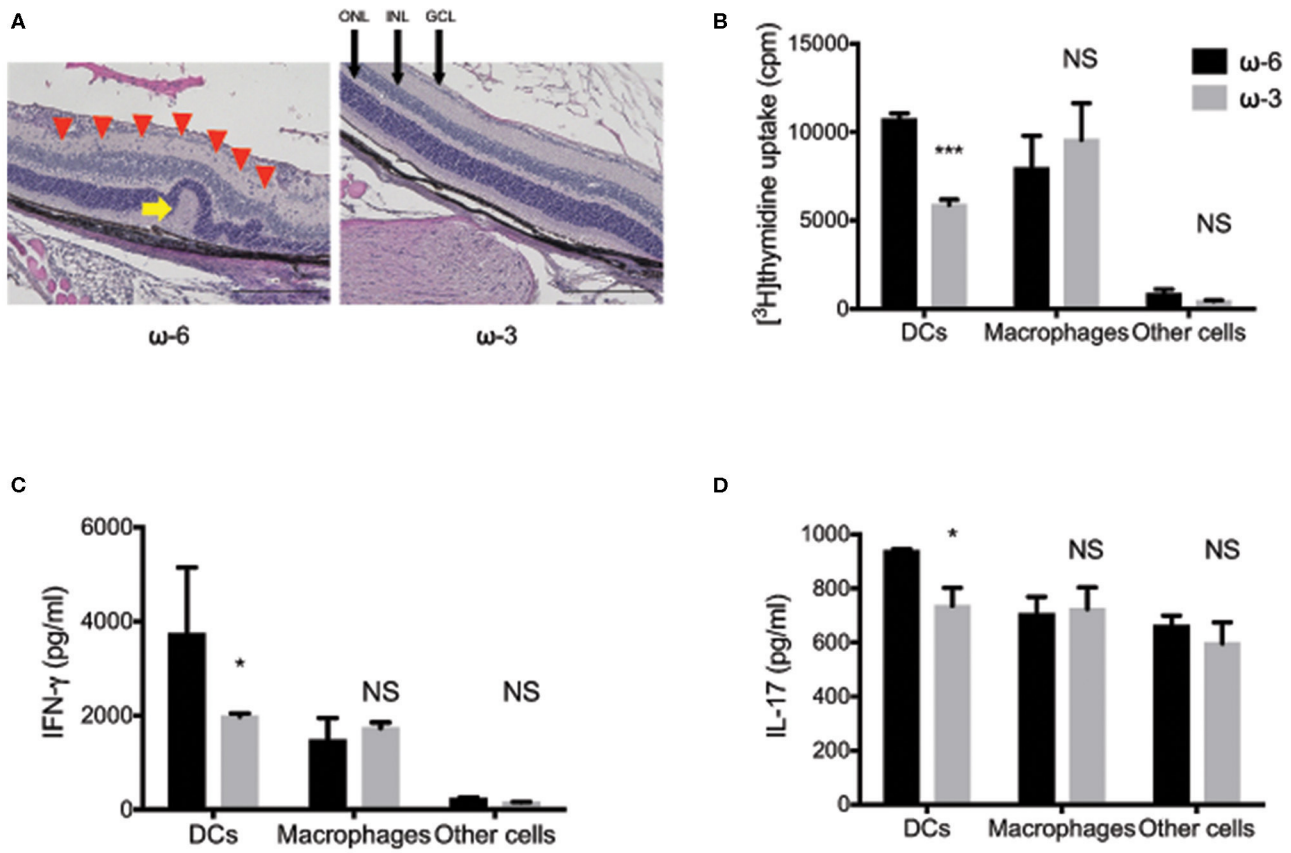

FIGURE 1 | The effects of ω-3 long chain polyunsaturated fatty acids in experimental autoimmune uveitis model mice. **(A)** Hematoxylin-eosin staining of retinal sections at 17 days after disease induction in experimental autoimmune uveitis (EAU) mice maintained on a diet enriched with ω-3 or ω-6 long-chain polyunsaturated fatty acids (LCPUFAs). A red arrowhead indicate inflammatory cells in the retina. A yellow arrow indicates a retinal fold. GCL, ganglion cell layer; INL, inner nuclear layer; ONL, outer nuclear layer. Scale bars, 200 μm. **(B–D)** The proliferation of T cells, as assessed by the measurement of [^{3}H]thymidine incorporation **(B)**, and by the production of interferon-γ **(C)**, and interleukin-17 **(D)** in co-cultures of CD4$^+$ T cells from EAU mice and the indicated antigen presenting cell fractions from mice fed with ω-3 or ω-6 LCPUFAs. Data are expressed as the means + the standard error of the mean (SEM). *$P < 0.05$, ***$P < 0.001$; NS, not significant vs. the corresponding value for the ω-6 LCPUFA diet (i.e., Sidak's multiple comparison test). The figure is reproduced from (77) with permission.

mediation of DCs (**Figures 1C,D**). Moreover, we also found that ω-3 LCPUFAs, acting via DCs, suppressed the production of proinflammatory cytokines and the anti-inflammatory cytokine IL-10. However, the DC-dependent anti-inflammatory effects of ω-3 LCPUFAs appear to outweigh their proinflammatory effects, at least in EAU.

DIABETIC RETINOPATHY

The global prevalence of diabetes mellitus (DM) tends to increase yearly, and the number of DM patients is estimated to reach 592 million within 20 years (80). Diabetic retinopathy (DR) is a representative microvascular complication of DM that causes visual impairment in working-age adults (81). Leasher et al. reported that blindness and moderate to severe visual impairment due to DR increased in 20 years (1990–2010) from 2.1 to 2.6% and from 1.3 to 1.9%, respectively (82). Vascular abnormalities such as hemorrhage, microaneurysm, capillary non-perfusion, and exudates are frequently observed in DR. Therefore, DR has been perceived as a disease that originates from vascular abnormalities. However, several lines of evidence indicate an association between inflammation and the pathophysiology of DR (12). The principal causes of visual impairment in DR are proliferative DR (PDR) and DME. In the next section, we will discuss the relationship between inflammation and PDR or DME formation.

Inflammation in PDR

PDR is characterized by the development of preretinal neovascularization and epiretinal fibrovascular membranes (FVMs) (81). Prolonged hyperglycemia, accumulation of advanced glycation end products, and oxidative stress under diabetic condition induce VEGF expression in the retina through protein kinase C activation. VEGF promotes leukostasis by increasing the expression of intercellular adhesion molecule-1 (ICAM-1) in retinal vascular endothelial cells (83). Low-grade inflammation initiated by leukocytes (e.g., monocytes and granulocytes) that adhere to endothelial cells via ICAM-1

induces vascular endothelial cell damage and cell death and promotes capillary loss and infiltration of leukocytes into the retina (84). Expanding inflammation and ischemia induces the further expression of VEGF and other angiogenic cytokines such as TNFα, IL-1β, IL-6, and IL-8. This negative cycle gradually advances DR (85). Van Hecke et al. showed that the prevalence of DR is positively associated with the serum levels of C-reactive protein (CRP) and soluble ICAM-1 (sICAM-1), which suggests that early vascular damage is actually caused by inflammation (86). Preventing the onset of DR is important to avoid DR-induced visual impairment. Therefore, the serum levels of CRP or sICAM-1 that indicate the level of the inflammatory activity may become useful biomarkers for predicting the onset of DR.

In a previous study with an experimental animal model, we previously reported that intravitreal injection of an anti-VEGF agent can attenuate the infiltration of leukocytes, especially macrophages, into the retina and can suppress preretinal neovascularization (87). Esser et al. demonstrated that inflammatory phase macrophages are localized in FVMs in PDR (88). This finding implied that macrophage-induced inflammation is associated with FVM formation. However, macrophages have diverse populations, and the role of each population differs (89). With regard to various populations of macrophages, Zhou et al. found that M2-like macrophages (i.e., CD163-positive macrophages) promote pre-retinal angiogenesis in DR (90). Kobayashi et al. also reported that some M2-like macrophages localized in the FVMs produce periostin (91). Periostin is a matricellular protein that is essential for FVM formation in PDR (92). Thus, we believe that M2-like macrophages may potentially become a new therapeutic target in treatment of PDR. The process from the onset of DR to the occurrence of PDR is summarized in **Figure 2**.

Inflammation in DME

Blood vessels in the central nervous system (CNS), including the retina have a vascular barrier function and maintain a proper neural microenvironment through strict control of vascular permeability (93). Retinal neural tissue is separated from the blood stream by the inner blood-retinal barrier (94). The collapse of the inner blood-retinal barrier under diabetic conditions results in DME, and persistent DME causes irreversible neural damage (94). Experimental investigations have proven that low-grade inflammation after leukostasis can disrupt the vascular barrier (83), and VEGF and some cytokines/chemokines that can increase vascular permeability are secreted from infiltrated leukocytes (94). Moreover, several clinical studies have demonstrated the upregulation of inflammatory cytokines/chemokines in the vitreous fluid of eyes with DME, which suggests a relationship between inflammation and the pathogenesis of DME (95).

VEGF is the most studied molecule that can increase vascular permeability (96). Regular intravitreal injections of anti-VEGF agents (i.e., anti-VEGF therapy) can improve vision and reduce the accumulation of macular fluid in DME. This therapy is the primary treatment modality for DME (3). However, clinical trials have demonstrated that ∼40% of patients are anti-VEGF resistant (97). Several studies were conducted to detect additional therapeutic targets for the treatment of DME. Sfikakis et al. demonstrated the therapeutic efficacy of the intravenous injection of IFX, an anti-TNFα antibody (98). Anti-inflammatory treatment for DME produces worthwhile results; however some concerns exist regarding the adverse effects of the therapy because of the need to administer high concentrations of IFX (5 mg/kg) multiple times to patients (98). Gale et al. conducted a clinical trial to evaluate the efficacy of an oral chemokine receptor (CCR) type 2 and type 5 (CCR2/CCR5) dual antagonist for treating DME because CCR2 and CCR5 signaling pathways are associated with vascular leakage, monocyte/macrophage infiltration, and increased VEGF expression in the retina of experimental DR models (99). However, its therapeutic efficacy is inferior to that of monthly intravitreal injections of an anti-VEGF agent (99). No molecule beyond VEGF has been found, although the development of a novel treatment for anti-VEGF–resistant DME is urgently needed.

To identify a new target molecule or a novel biomarker for predicting anti-VEGF resistance, many researchers have examined the relationship between the response to anti-VEGF treatment and the concentration of intraocular inflammatory cytokines/chemokines. Hillier et al. showed that an increase in baseline aqueous ICAM-1 is associated with a favorable anatomic response, whereas an increase in baseline aqueous VEGF is associated with an unfavorable anatomic response (100). Shimura et al. concluded that a favorable response was obtained in patients with increased baseline aqueous VEGF, soluble VEGF receptor-1, monocyte chemoattractant protein-1 (MCP-1), ICAM-1, IL-6, and IP-10 (101). Felfeli et al. compared aqueous cytokine concentrations at baseline and 2 months after anti-VEGF therapy; they reported that the aqueous levels of ICAM-1, MCP-1, placenta growth factor, and TGF-β2 decreased significantly in patients with a favorable response (102).

The results of animal experiments have revealed that VEGF induces endothelial ICAM-1 expression in the early stage of DR (83), and that ICAM-1 expression decreases in endothelial cells in the chronic stage of DR (103). Therefore, DME in the "early" stage with mild vascular injury (which does not indicate a short medical history of DR) may respond well to anti-VEGF therapy. Inflammatory cytokines and VEGF decreased in patients with a favorable response to the anti-VEGF therapy, which suggests that VEGF-dependent inflammation may have primarily contributed to DME formation in these patients. The detailed mechanisms of the association between inflammation and anti-VEGF resistance are not completely understood; however, the change in the quality of inflammation may cause treatment resistance. DME animal models such as Akimba mouse models (104), will provide new insights into the involvement of inflammation in the pathogenesis of DME in future research (**Figure 2**).

RETINOPATHY OF PREMATURITY

Retinopathy of prematurity (ROP) is a retinal vasoproliferative disorder that can lead to childhood blindness (105). Blencowe et al. reported that ROP occurs in 184,700 infants annually worldwide. Among these infants, ∼20,000 cases progress to

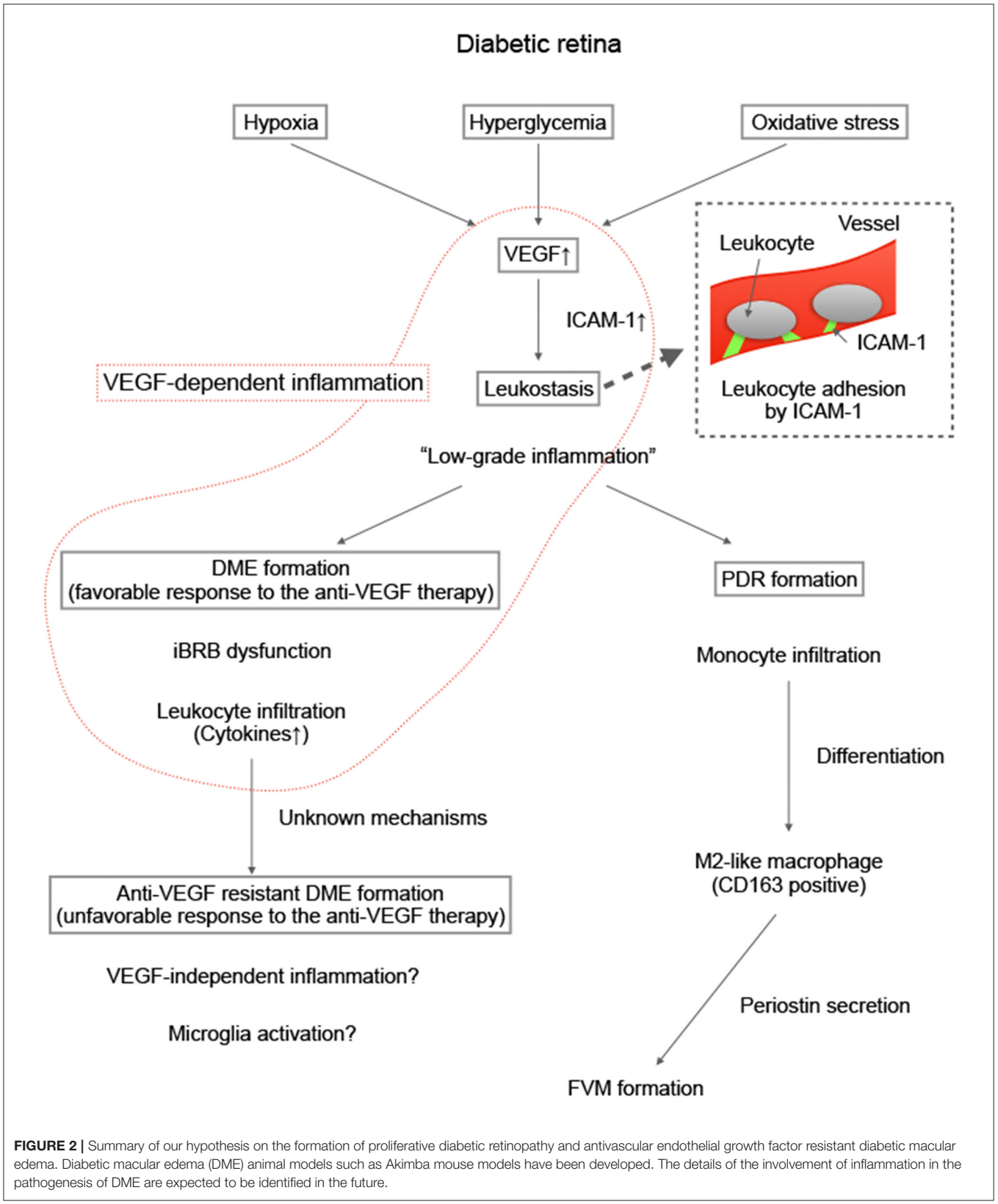

FIGURE 2 | Summary of our hypothesis on the formation of proliferative diabetic retinopathy and antivascular endothelial growth factor resistant diabetic macular edema. Diabetic macular edema (DME) animal models such as Akimba mouse models have been developed. The details of the involvement of inflammation in the pathogenesis of DME are expected to be identified in the future.

a stage that requires treatment (105). The incidence of ROP onset cases has been declining because neonatal management is improving every year (106) and because of a tendency toward a declining birthrate, especially in developed countries. However, a decrease in the number of cases does not necessarily mean a decrease in the number of treatments. Improved neonatal management indicates an increase in the survival rate of preterm infants. The gestational age (GA) and birth weight (BW) of infants enrolled in major large trials are steadily decreasing (107). Low GA and low BW are common risk factors for ROP progression (108). The risk of an increase in the relative proportion of severe ROP cases that require treatment may occur in the future.

Current primary treatments for ROP are retinal photocoagulation and anti-VEGF therapy. Large clinical trials such as the Early Treatment for Retinopathy Of Prematurity study and the Bevacizumab Eliminates the Angiogenic Threat of Retinopahty of Prematurity (BEAT-ROP) study have proven that both methods are effective (109, 110). However, severe ROP is sometimes accompanied by poor mydriasis and vitreous opacity. In such cases, performing laser photocoagulation in infants with ROP is difficult. Anti-VEGF therapy can be considered the first-line therapy for these patients. The BEAT-ROP study revealed that anti-VEGF therapy (i.e., the administration of bevacizumab) is associated with significantly less recurrence than laser photocoagulation in zone I ROP cases (110). To date, bevacizumab is generally used as an off-label drug in some limited facilities. The efficacy of intravitreal injection of ranibizumab (IVR) was recently proven (111). On account that ROP has been approved as one indication for ranibizumab, more infants with ROP are expected to benefit from anti-VEGF treatment in the future.

Inflammation in ROP

The recurrence rate of ROP after IVR monotherapy is ∼30% (111). The provision of optimal treatment at a proper time is essential to prevent the impairment of visual development in infants with ROP; therefore, the identification of a biomarker of ROP progression is very important. VEGF and many other molecules such as insulin-like growth factor-1, hypoxia-inducible factor-1, and reactive oxygen species, may be involved in the onset of ROP (108); however, Sato et al. reported that the vitreous concentrations of inflammatory cytokines/chemokines are increased in patients with ROP (13), which suggests an association between inflammation and ROP pathogenesis. Lyu et al. showed that high levels of aqueous VEGF and macrophage inflammatory protein (MIP)-1β at baseline were associated with the recurrence rate of ROP after IVR therapy (112). In a previous study, we reported that MIP-1β expression significantly increased in the retina of an ROP animal model (113). MIP-1β, also known as chemokine CC motif ligand 4, is a member of the CC chemokine family. Members of the CC chemokine family are characterized by their ability to direct the migration of leukocytes into the inflamed tissues. MIP-1β is upregulated very quickly after hypoxic stimulation in mouse retina (113). Therefore, its expression level may become a very sensitive sensor of retinal ischemia. The administration of a neutralizing antibody against MIP-1β inhibits physiological angiogenesis (113); therefore, we believe that MIP-1β has the potential to be a useful inflammatory biomarker of ROP progression or recurrence rather than a therapeutic target molecule. Moreover, Matsuda et al. reported that mast cell tryptase (MCT) released from mast cells is involved in angiogenesis in ROP (114). They demonstrated that MCT promotes angiogenesis by inducing the production of MCP-1 and other angiogenic factors from endothelial cells (114). On account that the serum MCT level is elevated in infants with ROP, MCT also has the potential to be a useful biomarker of ROP progression.

RETINITIS PIGMENTOSA

Gene Mutations and Microenvironment Alterations in Retinitis Pigmentosa

Retinitis pigmentosa refers to a subgroup of inherited retinal degenerations (IRDs) that cause progressive rod-cone degeneration (115). More than 90 causal genes have been identified for typical RP, and these genes are frequently related to the function, structure, and homeostasis of rod photoreceptor cells. Night blindness due to rod dysfunction and death is an early symptom of RP, followed by visual field constriction and loss of central vision due to secondary cone cell death. RP is a major cause of adult blindness in over one million patients globally; no effective treatment substantially delays the disease progression or restores the vision lost to RP (115).

Recent advances in gene therapy have shed light on the treatment of IRDs. Supplementation of the retinal pigment epithelium-specific 65 kDa protein (RPE65) gene in patients with Leber congenital amaurosis due to RPE65 mutations improves their light sensitivity and performance in the multi-luminance mobility test (116). This therapy has been approved in the United States and in Europe. Gene therapy for RP, which targets autosomal recessive or X-liked mutations (e.g., phosphodiesterase 6B, retinaldehyde-binding protein 1, retinitis pigmentosa GTPase regulator, MER proto-oncogene tyrosine kinase) has been assessed in clinical trials (4). However, a significant number of RP patients may not be indicated for gene therapy because of the following reasons: (1) adeno-associated viral vectors cannot accommodate large genes such as the eyes shut homolog, (2) gene correction or editing of autosomal dominant mutation *in vivo* is still challenging, and (3) many patients are first diagnosed in the mid- to late-stages of the disease when the rod cells are mostly lost. Therefore, the elucidation of the biological mechanisms that underlie retinal degeneration, especially in the secondary cone cell death phase, will be critical in developing novel treatments for RP, in addition to individualized gene therapy.

In RP, rods are expected to be injured because of gene mutations that are exclusively expressed or critically function in rod cells. However, why and how cones also die subsequent to rod cell death is puzzling. Accumulating evidence suggest that microenvironmental changes associated with rod cell death such as loss of trophic factors (117), metabolic alterations (118), oxidation (119), collapse of outer nuclear layer (120),

and inflammation (121), which are associated with rod cell death, may contribute to the secondary cone cell death. These factors mutually influence each other. For example, cytokines or chemokines released from a collapsed retina evoke inflammatory cell activation and migration, activated microglia or macrophages produce reactive oxygen species (ROS) to enhance oxidative stress, and, alternatively, oxidative stress triggers, or augments inflammatory response. The roles of oxidative stress and metabolic dysfunction in cone cell death in RP have been summarized in a previous review (119, 120). The present review focuses on inflammation and immunobiology as potential factors that mediate and modulate cone degeneration in RP. Assessing immune involvement in RP/IRDs from a broader perspective, including RP cases in the rod degeneration phase, is beyond the scope of this review and have been described in our previous recent review (11).

Clinical Findings of the Inflammatory Response and Its Relationship With Cone Degeneration in RP

Cell death and inflammation have a tight interaction with each other. Dying or dead cells stimulate phagocytes to mediate their clearance and maintain tissue homeostasis, whereas excessive activation of inflammatory cells can exert cytotoxicity and exacerbate the disease (122).

Without exception to this scenario, inflammatory cell infiltration is usually observed in the vitreous of RP patients. Using vitreous samples from post-mortem RP patients, Newsome et al. demonstrated that this cell infiltration consists of a mixed component of inflammatory cells including monocytes, NK cells, lymphocytes, and others cells (123). In a previous study, the authors of the present review graded the severity of inflammation in the anterior vitreous using *vivo* in slit-lamp biomicroscopy, and found that RP patients with a higher number of inflammatory cells had worse visual acuity and lower central retinal sensitivity (121). We also evaluated aqueous flare, a marker of blood-ocular barrier breakdown and inflammation. Our study data showed that aqueous flare values are increased in the eyes of RP patients, compared to these values in healthy individuals, and that aqueous flare values are negatively correlated with central visual function in RP patients (124). Consistent with our observation, independent groups have reported that aqueous flare values have a negative association with visual field area (125) and a positive correlation with inner retinal thickening, which occurs during retinal degeneration and remodeling, in RP patients (126). Daylight vision in the central and peripheral area is provided by cone cells; therefore, these findings suggest that inflammation may be implicated in retinal degeneration, especially in secondary cone cell death that occurs in RP. However, these studies were cross-sectional clinical studies and have the limitation that a cause-effect relationship could not be elucidated.

Cytokines and chemokines have critical roles in evoking the differentiation, activation, migration, and suppression of immune cells. A comprehensive measurement of inflammatory cytokines and chemokines in the aqueous humor and vitreous of the eyes of RP patients using multiplex enzyme-linked immunosorbent assay showed that IL-6, IL-8, and MCP-1 are elevated in the aqueous humor of RP patients, and that a greater variety of molecules (e.g., IL-1β, IL2, IL-4, IL-6, IL-8, IL-10, IFN-γ, MCP-1) are increased in the vitreous with more significant fold changes (121). Lu et al. also conducted multiple cytokine analyses and observed increased IL-6, IL-8, and MCP-1 levels and increased extracellular matrix-related proteins such as matrix metalloproteinases (127).

The inflammatory cytokines/chemokines elevated in RP are related to innate and acquired immunity. IL-1β, IL-8, and MCP-1 are pivotal molecules for activating and recruiting monocytes/macrophages and neutrophils to the inflammatory loci. IFN-γ, IL-2, IL-4, and IL-10 are produced primarily or partly by T lymphocytes, and they mediate the differentiation and polarization of Th cells and macrophages. These profiles of inflammatory cytokines/chemokines in RP are consistent with the infiltration of a variety of inflammatory cells into the vitreous, as described above (123). To develop an anti-inflammatory therapy for RP, further studies are needed to elucidate the key inflammatory cytokines/chemokines that critically contribute to the disease progression.

High sensitivity CRP (hs-CRP) is a serum inflammatory marker, and an increased hs-CRP is associated with age-related macular degeneration, DR, and uveitis (128, 129). The measurement of serum hs-CRP levels in RP patients without systemic disorders revealed that hs-CRP levels are ∼2 times higher in RP patients than in control subjects (130). In addition, a higher hs-CRP level is associated with a faster deterioration in central retinal sensitivity in RP patients (130). Taken together, these findings suggest that peripheral immune cells and ocular resident immune cells may be implicated in the disease progression of RP.

Functional Roles of Inflammatory Response in Cone Cell Death in RP

The findings outlined previously suggest that innate and acquired immunity are activated and involved in the pathology of RP. However, the function of each inflammatory cells (e.g., microglia, macrophages, and lymphocytes) and its regulatory mechanisms remains unclear and is a topic of interest.

Microglia, a resident macrophage in the CNS that derived from the embryonic yolk sac progenitors, are the most prominent immune cells in the retina (131). Microglia are long-lived cells that persist throughout the entire lifetime of mice, and can proliferate and repopulate after experimental depletion or during retinal degeneration (132). Monocytes in the peripheral blood do not invade the CNS in healthy conditions, although they can infiltrate and differentiate into macrophages in an aging or diseased retina with a dysfunctional blood-retinal barrier (133). These monocyte-derived macrophages resemble microglia in their morphology and their long life span, but have different functional features such as lower expression of colony-stimulating factor 1 receptor and higher expression of proinflammatory molecules such as MHC-II, IL-1β, and TNF-α (134). These two myeloid cells (i.e., tissue-resident microglia

and monocyte-derived macrophages) have been extensively investigated as pivotal innate immune cells that contribute to the health and disease of the retina.

Several reports have demonstrated the detrimental function of microglia/macrophages in retinal degeneration in experimental RP. In a previous study, suppression of activated microglia/macrophages with minocycline or toxin-induced depletion of CX3CR1-positive microglia/macrophages protected rod cells against cell death in retinal degeneration (rd) 10 mice (135, 136). However, attenuation of the homeostatic function of microglia by disrupting the CX3C chemokine ligand 1-CX3C chemokine receptor 1 axis or the complement component 3–complement receptor 3 axis accelerates rod degeneration, along with proinflammatory microenvironmental changes such as increased TNF-α and IL-6 levels (137, 138). Therefore, microglia/macrophages have a bidirectional function in RP, as expected from the basic understanding of the interaction between cell death and inflammation. Dissection of the protective and detrimental populations among microglia/macrophages and precise understanding of the differential function of microglia and macrophages in RP warrant further studies. In addition, clinical studies suggest a link between inflammatory markers and cone function; therefore, the effect of microglia/macrophages on cone cell death also requires further study.

Oxidative stress significantly contributes to cone cell death in RP. Campochiaro et al. postulated that rod cell loss in RP substantially reduces oxygen consumption in the retina, and the remaining cone cells are exposed to a high-level of oxygen and resultant ROS (119). They showed that oxidized proteins, lipids, and nucleic acids are accumulated in the outer retina (139), and that pharmacological or genetic suppression of oxidative stress leads to significant rescue of cone cells in animal models of RP (140).

Oxidative stress may have a direct harmful effect on cone cells, but it also affects microglial/macrophage activation in RP. In a previous study, we showed that treatment with anti-oxidant N-acetylcystein (NAC) substantially suppresses microglia/macrophage activation with reduced MCP-1, IL-1β, RANTES, and TNF-α expression (141). The anti-inflammatory effects of anti-oxidants are also observed in eyes with experimental retinal detachment that are treated with a free radical scavenger, edaravone (142). Our study further demonstrated that oxidative activation of microglia/macrophages is a key step in the augmentation of retinal inflammation and degeneration (including cone cell death) in rd10 mice. This activation is partly mediated by an oxidative DNA repair enzyme, MUTYH; an excessive activation of which leads to the formation of single strand breaks and increased expression of TNF-α in microglia/macrophages (143). The concept that oxidative stress alters homeostasis vs. neurotoxic balance of microglia and modulates cone cell survival and neuroinflammation in RP is shown in **Figure 3**.

Lymphocytes and lymphocyte-related cytokines are increased in the eyes of RP patients. In addition, several studies suggest the possible involvement of an autoimmune response and antiretinal autoantibodies in the progression of RP (144). However, the roles of acquired immunity in RP have been less investigated than the role of innate immunity.

Rohrer et al. crossed rd1 mice with *Scid* or *Rag1*$^{-/-}$ mice, both of which lack functional T and B lymphocytes, and showed that the deficiency of lymphocytes did not change rod cell death (145). In another study, Mishra et al. demonstrated that rod degeneration was mildly attenuated in rd1 *Nod.Scid* mice, which are deficient in T, B, and NK cells (146). These findings suggest that NK cells may play a minor role in rod cell death in RP, whereas lymphocytes may not have a significant function, at least solely by themselves. However, lymphocytes and their related molecules/factors are clinically observed in the mid- to late stage of RP. Thus, studying the roles of acquired immunity in cone cell death will be important in future research.

VITREORETINAL LYMPHOMA

Most primary vitreoretinal lymphomas (PVRL), which were previously termed as intraocular lymphomas, are related to high-grade non-Hodgkin's lymphoma, which is a subset of primary central nervous system lymphomas (PCNSL) (147). In Japan, 21 per 100,000 patients with ocular disorders have PVRL (148). PVRL comprises 1% of non-Hodgkin's lymphoma and <1% of intraocular tumors (149). Most cases of VRL are primary or secondary to CNS disease or may present simultaneously with it; however, it can also rarely be derived from systemic metastatic lymphoma (150). PVRL usually occurs in adults from the fifth to the sixth decades of life (151). No sex or racial predilection to the disease apparently exists, although some reports proposed that PVRL occurs more frequently in females than males (152).

Clinical Features of Vitreoretinal Lymphoma

The clinical ocular features of VRL, termed "masquerade syndrome," are often similar to those of chronic uveitis; therefore, a misdiagnosis of VRL sometimes leads to the administration of anti-inflammatory agents such as corticosteroids and thereby cause a delay in reaching a definitive diagnosis. The interval between the onset of the ocular or neurological findings and a definitive diagnosis is variable, and ranges from 4 to 40 months (152). The involvement of the CNS arises in 16–34% of patients with PVRL at presentation and develops in 42–92% of patients within a mean interval 8–29 months (151). Ocular involvement occurs in 15–20% of patients with PCNSL (151). Most patients with VRL have bilateral ocular involvement, but they often present with unilateral involvement at the initial visit owing to the uneven distribution of the disease. PVRL usually develops in the retina, the vitreous chamber, and/or the optic nerve, but can sometimes involve the anterior segment of the eye (153). Vitritis is the most common sign in VRL, and the findings has an "aurora borealis"-like appearance. In VRL, responses to corticosteroid therapy is initially observed but treatment resistance subsequently occurs. Multifocal whitish to yellow subretinal infiltrates are often observed. Coalescence of the lesions with "leopard skin"-like pigmentation, which is characteristic of VRL, is sometimes observed.

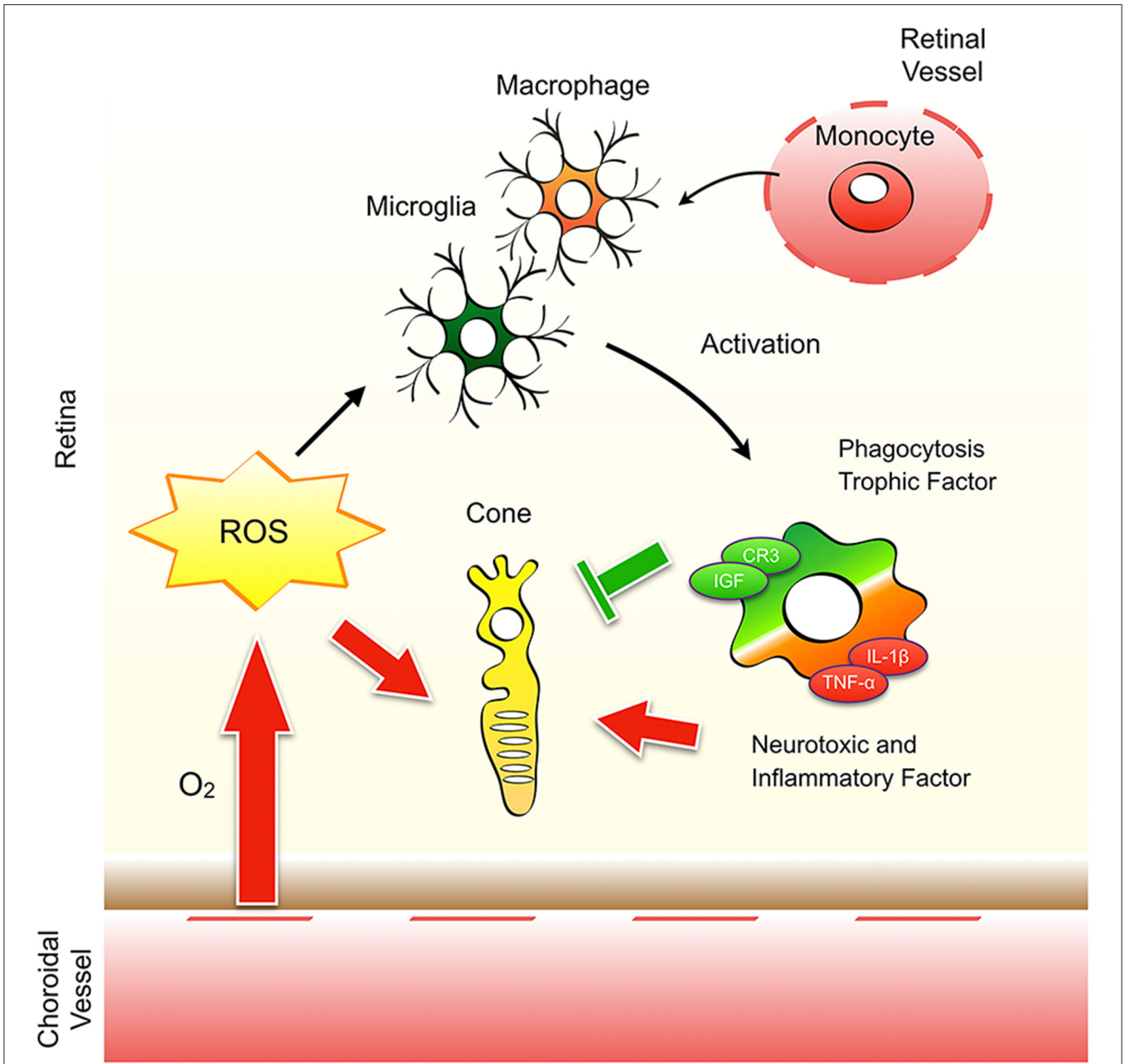

FIGURE 3 | Oxidative stress modulates cone cell survival and neuroinflammation in retinitis pigmentosa. The remaining cones in retinitis pigmentosa (RP) are exposed to a high level of oxygen and the resultant reactive oxygen species (ROS). ROS have a direct harmful effect on cone cells and affects the activation of microglia and monocyte-derived macrophages. Activated microglia/macrophage have a bidirectional function to protect or promote cone cell death. Which environmental factors (e.g., ROS, molecules released from dead cells) and cellular factors (e.g., microglia vs. macrophage) are critical to determine the homeostatic vs. neurotoxic function of microglia/macrophage in RP is unclear.

The overall survival of VRL patients has improved over the decades because of earlier diagnosis of the disease, which is a result of advances in molecular biological or genetic techniques. In addition, intense systemic chemotherapy and/or radiotherapy have also increased the overall survival rate. Several prospective studies have recently demonstrated that high-dose methotrexate (HD-MTX)-based chemotherapy with intravitreral MTX injections, subsequent whole brain radiotherapy (WBRT), and/or consolidation chemotherapy could improve overall survival and prevent CNS progression (5–7). Kaburaki et al. showed that a combination treatment protocol of intravitreral MTX injections, MTX-based systemic induction chemotherapy and consolidation high-dose cytarabine, and subsequent reduced-dose WBRT for the treatment of PVRL

accomplished a 4-year progression-free survival of 72.7% and a 4-year overall survival of 88.9% (7), which suggests that these intensive systemic therapeutic modalities should be introduced for CNS prophylaxis. Some cases are resistant to these regimens, although no standard regimens exist for the treatment of refractory and relapsed PCNSL. Retreatment with HD-MTX-based chemotherapy has been administered in some patients. WBRT or high-dose chemotherapy and autologous stem cell transplantation in younger patients who have not undergone these treatments as part of the first-line therapy are used as a salvage therapy instead (154). However, introducing these treatments to elderly patients and patients with a poor general condition is often difficult to prevent CNS progression and to treat PCNSL because of the possible occurrence of treatment-induced adverse events such as neurotoxicity and nephrotoxicity (155, 156). In the next section, we review the association of pathogenesis, especially the genetic or immunological aspects, with B-cell VRL to exhibit new diagnostic and/or therapeutic targets for the treatment of VRL.

Gene Mutations in Vitreoretinal Lymphoma

Most cases of PVRL can be classified as diffuse large B-cell lymphoma (DLBCL), whereas very few cases are classified as a T cell lymphoma or NK cell origin PVRL (152). Based on gene expression profiles, DLBCL is divided into three major subgroups: germinal center B-cell-like, activated B-cell-like (ABC)/non-germinal center, and primary mediastinal DLBCLs (157). The immunophenotype of most PCNSLs resembles ABC-DLBCLs, which are more aggressive and have poor prognostic outcomes, compared to the others (158).

High frequency of myeloid differentiation primary response gene 88 (MyD88) and CD79B mutations have been characterized in PCNSL (159). A single leucine-to-proline substitution at amino acid position 265 of Myd88 (*MYD88* L265P), is the most common mutation and accounts for more than 60% of VRLs (160). MYD88 is the adapter protein that mediates intracellular signaling pathways downstream of the toll-like receptor and the IL-1 receptor families. The CD79B mutation occurs in 35% of patients with PVRL, and is associated with the CNS progression of PVRL (161). The B-cell receptor (BCR) complex-associated protein β chain, CD79B, forms a complex with BCR and generates after recognition of an antigen to activate chronic BCR signaling. *MYD88* L265P and/or CD79B mutation contribute to the constitutive activation of NF-kB or BCR signaling, thereby promoting tumor growth.

Furthermore, in cases of PCNSL, because of the HLA locus mutation (chromosome 6q21.32), a shortage in HLA class I and II expression on tumor cells leads to escape from T or NK cell-mediated immune surveillance against tumor cells (162), which suggests that the lack of immune recognition of foreign antigens is one of the mechanisms that B-cell VRL cells preferentially retains in the eye.

PD-1, which is expressed on activated T-cells such as cytotoxic T lymphocytes (CTLs), interacts with its ligands (PD-L1 and PD-L2). These ligands are commonly expressed on tumor cells and upregulated in the tumor microenvironment (TME), thereby promoting inhibitory signaling of T cell receptors (TCRs) in CTL and subsequent tumor growth (163, 164). In PCNSL, investigations of copy number variations have revealed that frequent copy number gains at chromosome 9q24.1, which contains the PD-L1/PD-L2 locus (159). Chromosomal translocation involving the PD-L1/PD-L2 locus were also discovered in PCNSL, which indicates that immune evasion may be associated with the development of PCNSLs, including PVRL.

Diagnosis of Vitreoretinal Lymphoma

Cytological examination of the intraocular fluid or tissue is the gold standard for a definitive diagnosis of VRL. However, cytology alone can have a low diagnostic yield (40–60%) because of the limited amount of specimen that can be obtained, necrosis, and the fragility of VRL cells (165, 166). The vitrectomy cell block technique can improve diagnostic yield and can be utilized for immunohistochemistry of pan B-cell markers, including CD20 and CD79a, to establish a definitive diagnosis of lymphoma (167–169).

Several supplementary diagnostic methods can improve the definitive diagnosis of VRL. They include cytokine analysis to determine the ratio of IL-10 to IL-6 (i.e., the IL-10/ IL-6 ratio) (170), molecular analysis of the immunoglobulin heavy (IgH)/ TCR chain gene to confirm monoclonality, and flow cytometric identification of cell surface markers (171, 172). However, clonal expansions of lymphocytes have not been circumscribed in VRL. Therefore, molecular analysis with polymerase chain reaction and flow cytometric identification can sometimes yield false-positive results (173, 174).

Furthermore, *MYD88* L265P can be screened with new genetic techniques, including allele-specific polymerase chain reaction and next generation sequencing (NGS) using an oncogene gene panels, which allows for lower cellularity or a smaller volume of samples to confirm the definitive diagnosis of VRL (175, 176).

Etiopathogenesis in Vitreoretinal Lymphoma

As an exogenous factor, infection with the Epstein-Barr virus (EBV) is associated with PCNSL, specifically in immunocompromised patients such as individuals with acquired immune deficiency syndrome (AIDS) (177). EBV, which is a ubiquitous human herpes virus, affects most of the human population. EBV infects humans mostly in childhood and early adulthood, and subsequently spreads to B-lymphocytes and exists in a latent state. In patients with impaired cell-mediated immunity, such as patients with immune suppression and the elderly with immunosenescence, latent EBV may proliferate indiscriminately and drive neoplastic transformation to lymphoid malignancy (178). EBV, *Toxoplasma gondii*, and human herpes virus 8 are speculated as a cause of PVRL due to the detection of their gene expression in the intraocular fluids of some patients with PVRL (179).

On account that PVRL has selective tropism to CNS lesions, a theory has been proposed that chemokines and their receptors encourage the attraction and maintenance of VRL cells in intraocular tissues. In patients with B-cell chemokines, CXCL12, and CXCL13 are specifically expressed in retinal pigment epithelial cells and/or in the vitreous cavity

of patients with VRL. As a consequence, B-lymphoma cells [which express CXCR4 and CXCR5 (i.e., receptors for CXCL12 and CXCL13)] are recruited into intraocular tissues such as the retina, vitreous body, and subretina (180). CXCL13 levels are also increased in the vitreous humor of patients with VRL (181). CCL19 derived from astrocytes was recently reported to promote the retention of lymphoma cells, which express CCR7, and subsequent tumor growth in chronic gliosis lesions in mice (182).

Immune Evasion in Vitreoretinal Lymphoma

VRL cells can evade attacks by CTLs and NK cells because the eye is an immune-privileged site that possesses an immunosuppressive ocular microenvironment composed of soluble and cell surface inhibitory molecules. TGF-β is abundant in the vitreous humor to maintain an anti-inflammatory state in the eye (8). IL-10, which is widely regarded and has been analyzed as an immunosuppressive cytokine, has a pivotal role in the induction of immune tolerance in the eye (183). In cancer, regulatory cytokines in the TME such as IL-10 and TGF-β support tumor development by suppressing antitumor immunity in cancer (184, 185). Treg cells, which are a highly suppressive subset of T cells, increase regulatory cytokines secretion for the maintenance of self-tolerance and inhibition of autoimmunity, which result in tumor development (186, 187). In B-cell malignancies, including systemic DLBCL, the TME, which is formed with the reactive T-cells, macrophages, stromal cells, blood vessels, and extracellular matrix, regulates tumor cell survival or proliferation, and immune evasion for treatment resistance, associated with worse prognosis (188). Vitreous samples of B-cell VRL contain a large number of benign T cells and macrophages as well as tumor cells (174), which suggests that the infiltrating immune cells form the TME and support the suppression of anti-tumor immunity in the vitreous body.

Advances in the Treatment for Vitreoretinal Lymphoma

Based on the outcome of the genetic studies described previously, several new agents are currently being investigated as a salvage therapy in clinical trials assessing in patients with refractory or relapsed PCNSL and PVRL. In a prospective French multicenter phase II trial, monotherapy with ibrutinib, which targets Bruton's tyrosine kinase downstream of BCR, was effective and had objective response rates (ORRs) of up to 70% (189). Among 14 PVRL patients, the median progression-free survival (PFS) was 22.7 months. The median overall survival was not estimated because more than one-half of the PVRL patients were alive (**Table 2**). Immunomodulatory agent monotherapy with lenalidomide, which inhibits the NF-kB and PI3K/AKT pathways, achieved ORRs of up to 64% (192). However, in a prospective clinical study (191), lenalidomide in combination with intravenous rituximab for refractory or relapsed PCNSL and PVRL maintained an ORR of 35.6% owing to the short response to the therapy. Among 11 PVRL patients, the median PFS was 9.2 months. Nivolumab, an anti-PD-1 agent, has been reported to have responses and maintain complete remission in patients with relapsed/refractory PCNSL (193). In the future, the combination of these agents with MTX-based chemotherapy should be assessed as the first-line therapy for PVRL.

TABLE 2 | Salvage treatment regimen for PVRL in prospective clinical trials.

Agent	Number of patients	Median PFS (mo.)	Median OS (mo.)
CYVE + ASCT (190)	5	8	19.2
Ibrutinib (189)	14	22.7	Not estimated
Lenalidomide + rituximab (191)	11	9.2	Not reported

PVRL, primary vitreoretinal lymphoma; PFS, progression free survival; OS, overall survival; CYVE, high-dose cytarabine and etoposide; ASCT, autologous stem cell transplantation.

Furthermore, increased expression of proinflammatory cytokines related to CTLs, such as IFN-γ, granzyme A, and IP-10 occurs in the aqueous humor and/or vitreous of VRL patients (181), which suggests that CTLs are associated with the pathogenesis of VRL. In a previous study, we revealed that subretinal infiltration of VRL cells elicits the infiltration of T-cells into the vitreous cavity (194). However, we were unable to elucidate the association of the T cells with the prognosis of the VRL patients. Little data exist that elucidate the roles of reactive T cells in DLBCL-VRL. In the future, further detailed studies on the infiltration of T cells into the eyes of VRL patients may provide new insights into the pathogenesis of the disease and deliver new therapeutic targets such as augmentation of CTL and/or NK cells function.

CONCLUSION AND FUTURE DIRECTIONS

A profound understanding of the intricacies of immune responses will raise innovations for the management and treatment of these intractable retinal disorders. The generation of biologics, including IFX or ADA, has dramatically changed the treatment of NIU in the past few decades. However, during long-term treatment of NIU patients, a decreased response or adverse events to the biologics has emerged because of the development of antidrug antibodies or paradoxical effects. The development of selective small-molecule therapies is expected to resolve these problems. From the results of our analysis of EAU, the induction of regulatory DCs may be useful for the treatment of NIU.

In retinal vascular diseases, low-grade inflammation can destroy vascular integrity by the action of VEGF and some cytokines/chemokines from infiltrated leukocytes. Resistance to anti-VEGF therapy is sometimes observed in DR (including DME); therefore, developing a new therapy associated with low-grade inflammation as a "beyond VEGF" therapy for retinal vascular diseases, including DR and ROP, may be useful.

Immunological responses also affect the pathogenesis of RP, despite differences in genetic backgrounds. Targeting cytokines/chemokines associated with immunological responses

against RP may be an attractive target for the treatment of RP, in addition to gene therapy.

The recent introduction of molecular profiling technologies, including NGS, can exhibit the molecular characterization of several cancers to provide information on tumor diagnosis and specific targeted therapy. Several agents, which were selected on the basis of the molecular characterization, have been assessed in clinical trials of cases of refractory/relapsed PCNSL; however, the utility of these molecular profiling technologies has not been established. Considering the rarity of VRL, large-scale collaborative registries, tumor molecular profiling programs, and clinical trials in institutions across the world are necessary to enhance diagnosis, prognostication, and treatment outcomes in the future.

AUTHOR CONTRIBUTIONS

All authors listed have made a substantial, direct and intellectual contribution to the work, and approved it for publication.

FUNDING

This work were supported by grants from Japan Society for the Promotion of Science (JSPS) KAKENHI Grant no. 18K09471 to AT, 18K09449 to RY, 19K09952 to YM, and 18H02956 to K-HS from the Ministry of Education, Science, Sports and Culture, Japan, and grants from Novartis Pharma Research Grants (AT; Tokyo, Japan) and Alcon Pharma Research Grants (AT; Tokyo, Japan).

REFERENCES

1. Takeuchi M, Kezuka T, Sugita S, Keino H, Namba K, Kaburaki T, et al. Evaluation of the long-term efficacy and safety of infliximab treatment for uveitis in behcet's disease: a multicenter study. *Ophthalmology.* (2014) 121:1877–84. doi: 10.1016/j.ophtha.2014.04.042
2. Rosenfeld PJ, Brown DM, Heier JS, Boyer DS, Kaiser PK, Chung CY, et al. Ranibizumab for neovascular age-related macular degeneration. *N Engl J Med.* (2006) 355:1419–31. doi: 10.1056/NEJMoa054481
3. Heier JS, Korobelnik JF, Brown DM, Schmidt-Erfurth U, Do DV, Midena E, et al. Intravitreal aflibercept for diabetic macular edema: 148-week results from the VISTA and VIVID studies. *Ophthalmology.* (2016) 123:2376–85. doi: 10.1016/j.ophtha.2016.07.032
4. Garafalo AV, Cideciyan AV, Heon E, Sheplock R, Pearson A, WeiYang Yu C, et al. Progress in treating inherited retinal diseases: early subretinal gene therapy clinical trials and candidates for future initiatives. *Prog Retin Eye Res.* (2019) 30:100827. doi: 10.1016/j.preteyeres.2019.100827
5. Kreher S, Strehlow F, Martus P, Roth P, Hertenstein B, Roth A, et al. Prognostic impact of intraocular involvement in primary CNS lymphoma: experience from the G-PCNSL-SG1 trial. *Ann Hematol.* (2015) 94:409–14. doi: 10.1007/s00277-014-2212-z
6. Akiyama H, Takase H, Kubo F, Miki T, Yamamoto M, Tomita M, et al. High-dose methotrexate following intravitreal methotrexate administration in preventing central nervous system involvement of primary intraocular lymphoma. *Cancer Sci.* (2016) 107:1458–64. doi: 10.1111/cas.13012
7. Kaburaki T, Taoka K, Matsuda J, Yamashita H, Matsuda I, Tsuji H, et al. Combined intravitreal methotrexate and immunochemotherapy followed by reduced-dose whole-brain radiotherapy for newly diagnosed B-cell primary intraocular lymphoma. *Br J Haematol.* (2017) 179:246–55. doi: 10.1111/bjh.14848
8. Streilein JW. Ocular immune privilege: therapeutic opportunities from an experiment of nature. *Nat Rev Immunol.* (2003) 3:879–89. doi: 10.1038/nri1224
9. Taylor AW, Kaplan HJ. Ocular immune privilege in the year 2010: ocular immune privilege and uveitis. *Ocul Immunol Inflamm.* (2010) 18:488–92. doi: 10.3109/09273948.2010.525730
10. Benhar I, London A, Schwartz M. The privileged immunity of immune privileged organs: the case of the eye. *Front Immunol.* (2012) 3:296. doi: 10.3389/fimmu.2012.00296
11. Murakami Y, Ishikawa K, Nakao S, Sonoda KH. Innate immune response in retinal homeostasis and inflammatory disorders. *Prog Retin Eye Res.* (2019) 74:100778. doi: 10.1016/j.preteyeres.2019.100778
12. Antonetti DA, Barber AJ, Bronson SK, Freeman WM, Gardner TW, Jefferson LS, et al. Diabetic retinopathy: seeing beyond glucose-induced microvascular disease. *Diabetes.* (2006) 55:2401–11. doi: 10.2337/db05-1635
13. Sato T, Kusaka S, Shimojo H, Fujikado T. Simultaneous analyses of vitreous levels of 27 cytokines in eyes with retinopathy of prematurity. *Ophthalmology.* (2009) 116:2165–9. doi: 10.1016/j.ophtha.2009.04.026
14. Hori J, Yamaguchi T, Keino H, Hamrah P, Maruyama K. Immune privilege in corneal transplantation. *Prog Retin Eye Res.* (2019) 72:10075. doi: 10.1016/j.preteyeres.2019.04.002
15. Taylor AW, Ng TF. Negative regulators that mediate ocular immune privilege. *J Leukoc Biol.* (2018). 103, 1179–87. doi: 10.1002/JLB.3MIR0817-337R
16. Zhou R, Horai R, Mattapallil MJ, Caspi RR. A new look at immune privilege of the eye: dual role for the vision-related molecule retinoic acid. *J Immunol.* (2011) 187:4170–7. doi: 10.4049/jimmunol.1101634
17. Taylor AW. Ocular immune privilege and transplantation. *Front Immunol.* (2016) 7:37. doi: 10.3389/fimmu.2016.00037
18. Griffith TS, Brunner T, Fletcher SM, Green DR, Ferguson TA. Fas ligand-induced apoptosis as a mechanism of immune privilege. *Science.* (1995) 270:1189–92. doi: 10.1126/science.270.5239.1189
19. Sugita S, Usui Y, Horie S, Futagami Y, Yamada Y, Ma J, et al. Human corneal endothelial cells expressing programmed death-ligand 1 (PD-L1) suppress PD-1+ T helper 1 cells by a contact-dependent mechanism. *Invest Ophthalmol Vis Sci.* (2009) 50:263–72. doi: 10.1167/iovs.08-2536
20. Toscano MA, Commodaro AG, Ilarregui JM, Bianco GA, Liberman A, Serra HM, et al. Galectin-1 suppresses autoimmune retinal disease by promoting concomitant Th2- and T regulatory-mediated anti-inflammatory responses. *J Immunol.* (2006) 176:6323–32. doi: 10.4049/jimmunol.176.10.6323
21. Dick AD, Carter D, Robertson M, Broderick C, Hughes E, Forrester JV, et al. Control of myeloid activity during retinal inflammation. *J Leukoc Biol.* (2003) 74:161–6. doi: 10.1189/jlb.1102535
22. Sugita S, Horie S, Nakamura O, Maruyama K, Takase H, Usui Y, et al. Acquisition of T regulatory function in cathepsin L-inhibited T cells by eye-derived CTLA-2alpha during inflammatory conditions. *J Immunol.* (2009) 183:5013–22. doi: 10.4049/jimmunol.0901623
23. Sugita S, Streilein JW. Iris pigment epithelium expressing CD86 (B7-2) directly suppresses T cell activation *in vitro* via binding to cytotoxic T lymphocyte-associated antigen 4. *J Exp Med.* (2003) 198:161–71. doi: 10.1084/jem.20030097
24. Sugita S, Ng TF, Lucas PJ, Gress RE, Streilein JW. B7+ iris pigment epithelium induce CD8+ T regulatory cells; both suppress CTLA-4+ T cells. *J Immunol.* (2006) 176:118–27. doi: 10.4049/jimmunol.176.1.118
25. Vendomele J, Khebizi Q, Fisson S. Cellular and molecular mechanisms of anterior chamber-associated immune deviation (ACAID): what we have learned from knockout mice. *Front Immunol.* (2017) 8:1686. doi: 10.3389/fimmu.2017.01686
26. Stein-Streilein J, Streilein JW. Anterior chamber associated immune deviation (ACAID): regulation, biological relevance, and implications for therapy. *Int Rev Immunol.* (2002) 21:123–52. doi: 10.1080/08830180212066
27. Goldschneider I, Cone RE. A central role for peripheral dendritic cells in the induction of acquired thymic tolerance. *Trends Immunol.* (2003) 24:77–81. doi: 10.1016/S1471-4906(02)00038-8
28. Simon AK, Hollander GA, McMichael A. Evolution of the immune system in humans from infancy to old age. *Proc Biol Sci.* (2015) 282:20143085. doi: 10.1098/rspb.2014.3085

29. Sonoda KH, Sakamoto T, Qiao H, Hisatomi T, Oshima T, Tsutsumi-Miyahara C, et al. The analysis of systemic tolerance elicited by antigen inoculation into the vitreous cavity: vitreous cavity-associated immune deviation. *Immunology.* (2005) 116:390–9. doi: 10.1111/j.1365-2567.2005.02239.x
30. Sakamoto T, Ishibashi T. Hyalocytes: essential cells of the vitreous cavity in vitreoretinal pathophysiology? *Retina.* (2011) 31:222–8. doi: 10.1097/IAE.0b013e3181facfa9
31. Qiao H, Hisatomi T, Sonoda KH, Kura S, Sassa Y, Kinoshita S, et al. The characterisation of hyalocytes: the origin, phenotype, and turnover. *Br J Ophthalmol.* (2005) 89:513–7. doi: 10.1136/bjo.2004.050658
32. Barisani-Asenbauer T, Maca SM, Mejdoubi L, Emminger W, Machold K, Auer H. Uveitis- a rare disease often associated with systemic diseases and infections- a systematic review of 2619 patients. *Orphanet J Rare Dis.* (2012) 7:57. doi: 10.1186/1750-1172-7-57
33. Takeda A, Sonoda KH, Ishibashi T. The regulation of the differentiation of Th1 and Th17 cells in uveitis. *Inflam Regen.* (2013) 33:261–8. doi: 10.2492/inflammregen.33.261
34. Hasegawa E, Takeda A, Yawata N, Sonoda KH. The effectiveness of adalimumab treatment for non-infectious uveitis. *Immunol Med.* (2019) 42:79–83. doi: 10.1080/25785826.2019.1642080
35. Foster CS, Kothari S, Anesi SD, Vitale AT, Chu D, Metzinger JL, et al. The ocular immunology and uveitis foundation preferred practice patterns of uveitis management. *Surv Ophthalmol.* (2016) 61:1–17. doi: 10.1016/j.survophthal.2015.07.001
36. Mesquida M, Molins B, Llorenc V, Hernandez MV, Espinosa G, Dick AD, et al. Current and future treatments for behcet's uveitis: road to remission. *Int Ophthalmol.* (2014) 34:365–81. doi: 10.1007/s10792-013-9788-5
37. Arida A, Sfikakis PP. Anti-cytokine biologic treatment beyond anti-TNF in behcet's disease. *Clin Exp Rheumatol.* (2014) 32(4 Suppl 84):S149–55.
38. Okada AA, Goto H, Ohno S, Mochizuki M. Multicenter study of infliximab for refractory uveoretinitis in behcet disease. *Arch Ophthalmol.* (2012) 130:592–8. doi: 10.1001/archophthalmol.2011.2698
39. Kuroyanagi K, Sakai T, Kohno H, Okano K, Akiyama G, Aoyagi R, et al. Association between the major histocompatibility complex and clinical response to infliximab therapy in patients with Behcet uveitis. *Jpn J Ophthalmol.* (2015) 59:401–8. doi: 10.1007/s10384-015-0404-2
40. Dick AD, Rosenbaum JT, Al-Dhibi HA, Belfort R, Jr, Brezin AP, Chee SP, et al. Guidance on noncorticosteroid systemic immunomodulatory therapy in noninfectious uveitis: fundamentals of care for uveitiS (FOCUS) Initiative. *Ophthalmology.* (2018) 125:757–73. doi: 10.1016/j.ophtha.2017.11.017
41. Ramos-Casals M, Brito-Zeron P, Munoz S, Soria N, Galiana D, Bertolaccini L, et al. Autoimmune diseases induced by TNF-targeted therapies: analysis of 233 cases. *Medicine.* (2007) 86:242–51. doi: 10.1097/MD.0b013e3181441a68
42. Rutgeerts P, Feagan BG, Lichtenstein GR, Mayer LF, Schreiber S, Colombel JF, et al. Comparison of scheduled and episodic treatment strategies of infliximab in crohn's disease. *Gastroenterology.* (2004) 126:402–13. doi: 10.1053/j.gastro.2003.11.014
43. van der Laken CJ, Voskuyl AE, Roos JC, Stigter van Walsum M, de Groot ER, Wolbink G, et al. Imaging and serum analysis of immune complex formation of radiolabelled infliximab and anti-infliximab in responders and non-responders to therapy for rheumatoid arthritis. *Ann Rheum Dis.* (2007) 66:253–6. doi: 10.1136/ard.2006.057406
44. Bartelds GM, Krieckaert CL, Nurmohamed MT, van Schouwenburg PA, Lems WF, Twisk JW, et al. Development of antidrug antibodies against adalimumab and association with disease activity and treatment failure during long-term follow-up. *JAMA.* (2011) 305:1460–8. doi: 10.1001/jama.2011.406
45. Diedrichs-Mohring M, Kaufmann U, Wildner G. The immunopathogenesis of chronic and relapsing autoimmune uveitis - lessons from experimental rat models. *Prog Retin Eye Res.* (2018) 65:107–26. doi: 10.1016/j.preteyeres.2018.02.003
46. Mochizuki M, Sugita S, Kamoi K. Immunological homeostasis of the eye. *Prog Retin Eye Res.* (2013) 33:10–27. doi: 10.1016/j.preteyeres.2012.10.002
47. Yoshimura T, Sonoda KH, Miyazaki Y, Iwakura Y, Ishibashi T, Yoshimura A, et al. Differential roles for IFN-gamma and IL-17 in experimental autoimmune uveoretinitis. *Int Immunol.* (2008) 20:209–14. doi: 10.1093/intimm/dxm135
48. Luger D, Silver PB, Tang J, Cua D, Chen Z, Iwakura Y, et al. Either a Th17 or a Th1 effector response can drive autoimmunity: conditions of disease induction affect dominant effector category. *J Exp Med.* (2008) 205:799–810. doi: 10.1084/jem.20071258
49. Amadi-Obi A, Yu CR, Liu X, Mahdi RM, Clarke GL, Nussenblatt RB, et al. TH17 cells contribute to uveitis and scleritis and are expanded by IL-2 and inhibited by IL-27/STAT1. *Nat Med.* (2007) 13:711–8. doi: 10.1038/nm1585
50. Okunuki Y, Mukai R, Nakao T, Tabor SJ, Butovsky O, Dana R, et al. Retinal microglia initiate neuroinflammation in ocular autoimmunity. *Proc Natl Acad Sci USA.* (2019) 116:9989–98. doi: 10.1073/pnas.1820387116
51. Satoh M, Namba KI, Kitaichi N, Endo N, Kitamei H, Iwata D, et al. Invariant natural killer T cells play dual roles in the development of experimental autoimmune uveoretinitis. *Exp Eye Res.* (2016) 153:79–89. doi: 10.1016/j.exer.2016.10.003
52. Fu Q, Man X, Wang X, Song N, Li Y, Xue J, et al. CD83(+) CCR7(+) NK cells induced by interleukin 18 by dendritic cells promote experimental autoimmune uveitis. *J Cell Mol Med.* (2019) 23:1827–39. doi: 10.1111/jcmm.14081
53. Lin W, Man X, Li P, Song N, Yue Y, Li B, et al. NK cells are negatively regulated by sCD83 in experimental autoimmune uveitis. *Sci Rep.* (2017) 7:12895. doi: 10.1038/s41598-017-13412-1
54. Chong WP, van Panhuys N, Chen J, Silver PB, Jittayasothorn Y, Mattapallil MJ, et al. NK-DC crosstalk controls the autopathogenic Th17 response through an innate IFN-gamma-IL-27 axis. *J Exp Med.* (2015) 212:1739–52. doi: 10.1084/jem.20141678
55. Kitaichi N, Namba K, Taylor AW. Inducible immune regulation following autoimmune disease in the immune-privileged eye. *J Leukoc Biol.* (2005) 77:496–502. doi: 10.1189/jlb.0204114
56. Silver PB, Horai R, Chen J, Jittayasothorn Y, Chan CC, Villasmil R, et al. Retina-specific T regulatory cells bring about resolution and maintain remission of autoimmune uveitis. *J Immunol.* (2015) 194:3011–9. doi: 10.4049/jimmunol.1402650
57. Muhammad F, Wang D, Montieth A, Lee S, Preble J, Foster CS, et al. PD-1(+) melanocortin receptor dependent-Treg cells prevent autoimmune disease. *Sci Rep.* (2019) 9:16941. doi: 10.1038/s41598-019-53297-w
58. Merida S, Palacios E, Navea A, Bosch-Morell F. Macrophages and uveitis in experimental animal models. *Mediators Inflamm.* (2015) 2015:671417. doi: 10.1155/2015/671417
59. Chen M, Zhao J, Ali IHA, Marry S, Augustine J, Bhuckory M, et al. Cytokine signaling protein 3 deficiency in myeloid cells promotes retinal degeneration and angiogenesis through arginase-1 up-regulation in experimental autoimmune uveoretinitis. *Am J Pathol.* (2018) 188:1007–20. doi: 10.1016/j.ajpath.2017.12.021
60. Davalos D, Grutzendler J, Yang G, Kim JV, Zuo Y, Jung S, et al. ATP mediates rapid microglial response to local brain injury *in vivo*. *Nat Neurosci.* (2005) 8:752–8. doi: 10.1038/nn1472
61. Franchi L, Eigenbrod T, Munoz-Planillo R, Nunez G. The inflammasome: a caspase-1-activation platform that regulates immune responses and disease pathogenesis. *Nat Immunol.* (2009) 10:241–7. doi: 10.1038/ni.1703
62. Surprenant A, Rassendren F, Kawashima E, North RA, Buell G. The cytolytic P2Z receptor for extracellular ATP identified as a P2X receptor (P2X7). *Science.* (1996) 272:735–8. doi: 10.1126/science.272.5262.735
63. Di Virgilio F, Chiozzi P, Ferrari D, Falzoni S, Sanz JM, Morelli A, et al. Nucleotide receptors: an emerging family of regulatory molecules in blood cells. *Blood.* (2001) 97:587–600. doi: 10.1182/blood.V97.3.587
64. Takeda A, Yamada H, Hasegawa E, Arima M, Notomi S, Myojin S, et al. Crucial role of P2X7 receptor for effector T cell activation in experimental autoimmune uveitis. *Jpn J Ophthalmol.* (2018) 62:398–406. doi: 10.1007/s10384-018-0587-4
65. Steinman RM, Banchereau J. Taking dendritic cells into medicine. *Nature.* (2007) 449:419–26. doi: 10.1038/nature06175
66. Steinman RM. Lasker basic medical research award. Dendritic cells: versatile controllers of the immune system. *Nat Med.* (2007) 13:1155–9. doi: 10.1038/nm1643
67. Lin W, Liu T, Wang B, Bi H. The role of ocular dendritic cells in uveitis. *Immunol Lett.* (2019) 209:4–10. doi: 10.1016/j.imlet.2019.03.016

68. Xu H, Dawson R, Forrester JV, Liversidge J. Identification of novel dendritic cell populations in normal mouse retina. *Invest Ophthalmol Vis Sci.* (2007) 48:1701–10. doi: 10.1167/iovs.06-0697
69. Heuss ND, Lehmann U, Norbury CC, McPherson SW, Gregerson DS. Local activation of dendritic cells alters the pathogenesis of autoimmune disease in the retina. *J Immunol.* (2012) 188:1191–200. doi: 10.4049/jimmunol.1101621
70. Van Brussel I, Lee WP, Rombouts M, Nuyts AH, Heylen M, De Winter BY, et al. Tolerogenic dendritic cell vaccines to treat autoimmune diseases: can the unattainable dream turn into reality? *Autoimmun Rev.* (2014) 13:138–50. doi: 10.1016/j.autrev.2013.09.008
71. van Rhijn-Brouwer FC, Gremmels H, Fledderus JO, Radstake TR, Verhaar MC, van Laar JM. Cellular therapies in systemic sclerosis: recent progress. *Curr Rheumatol Rep.* (2016) 18:12. doi: 10.1007/s11926-015-0555-7
72. Mackern-Oberti JP, Llanos C, Vega F, Salazar-Onfray F, Riedel CA, Bueno SM, et al. Role of dendritic cells in the initiation, progress and modulation of systemic autoimmune diseases. *Autoimmun Rev.* (2015) 14:127–39. doi: 10.1016/j.autrev.2014.10.010
73. Oh K, Kim YS, Lee DS. Maturation-resistant dendritic cells ameliorate experimental autoimmune uveoretinitis. *Immune Netw.* (2011) 11:399–405. doi: 10.4110/in.2011.11.6.399
74. Suzuki J, Yoshimura T, Simeonova M, Takeuchi K, Murakami Y, Morizane Y, et al. Aminoimidazole carboxamide ribonucleotide ameliorates experimental autoimmune uveitis. *Invest Ophthalmol Vis Sci.* (2012) 53:4158–69. doi: 10.1167/iovs.11-9323
75. Usui Y, Takeuchi M, Hattori T, Okunuki Y, Nagasawa K, Kezuka T, et al. Suppression of experimental autoimmune uveoretinitis by regulatory dendritic cells in mice. *Arch Ophthalmol.* (2009) 127:514–9. doi: 10.1001/archophthalmol.2009.34
76. Shoda H, Yanai R, Yoshimura T, Nagai T, Kimura K, Sobrin L, et al. Dietary omega-3 fatty acids suppress experimental autoimmune uveitis in association with inhibition of Th1 and Th17 cell function. *PLoS ONE.* (2015) 10:e0138241. doi: 10.1371/journal.pone.0138241
77. Uchi SH, Yanai R, Kobayashi M, Hatano M, Kobayashi Y, Yamashiro C, et al. Dendritic cells mediate the anti-inflammatory action of omega-3 long-chain polyunsaturated fatty acids in experimental autoimmune uveitis. *PLoS ONE.* (2019) 14:e0219405. doi: 10.1371/journal.pone.0219405
78. Heink S, Yogev N, Garbers C, Herwerth M, Aly L, Gasperi C, et al. Trans-presentation of IL-6 by dendritic cells is required for the priming of pathogenic TH17 cells. *Nat Immunol.* (2017) 18:74–85. doi: 10.1038/ni.3632
79. Heufler C, Koch F, Stanzl U, Topar G, Wysocka M, Trinchieri G, et al. Interleukin-12 is produced by dendritic cells and mediates T helper 1 development as well as interferon-gamma production by T helper 1 cells. *Eur J Immunol.* (1996) 26:659–68. doi: 10.1002/eji.1830260323
80. Guariguata L, Whiting DR, Hambleton I, Beagley J, Linnenkamp U, Shaw JE. Global estimates of diabetes prevalence for 2013 and projections for 2035. *Diabetes Res Clin Pract.* (2014) 103:137–49. doi: 10.1016/j.diabres.2013.11.002
81. Cheung N, Mitchell P, Wong TY. Diabetic retinopathy. *Lancet.* (2010) 376:124–36. doi: 10.1016/S0140-6736(09)62124-3
82. Leasher JL, Bourne RR, Flaxman SR, Jonas JB, Keeffe J, Naidoo K, et al. Global estimates on the number of people blind or visually impaired by diabetic retinopathy: a meta-analysis from 1990 to 2010. *Diabetes Care.* (2016) 39:1643–9. doi: 10.2337/dc15-2171
83. Chibber R, Ben-Mahmud BM, Chibber S, Kohner EM. Leukocytes in diabetic retinopathy. *Curr Diabetes Rev.* (2007) 3:3–14. doi: 10.2174/157339907779802139
84. Capitao M, Soares R. Angiogenesis and inflammation crosstalk in diabetic retinopathy. *J Cell Biochem.* (2016) 117:2443–53. doi: 10.1002/jcb.25575
85. Roy S, Kern TS, Song B, Stuebe C. Mechanistic insights into pathological changes in the diabetic retina: implications for targeting diabetic retinopathy. *Am J Pathol.* (2017) 187:9–19. doi: 10.1016/j.ajpath.2016.08.022
86. van Hecke MV, Dekker JM, Nijpels G, Moll AC, Heine RJ, Bouter LM, et al. Inflammation and endothelial dysfunction are associated with retinopathy: the hoorn study. *Diabetologia.* (2005) 48:1300–6. doi: 10.1007/s00125-005-1799-y
87. Nakao S, Arima M, Ishikawa K, Kohno R, Kawahara S, Miyazaki M, et al. Intravitreal anti-VEGF therapy blocks inflammatory cell infiltration and re-entry into the circulation in retinal angiogenesis. *Invest Ophthalmol Vis Sci.* (2012) 53:4323–8. doi: 10.1167/iovs.11-9119
88. Esser P, Heimann K, Wiedemann P. Macrophages in proliferative vitreoretinopathy and proliferative diabetic retinopathy: differentiation of subpopulations. *Br J Ophthalmol.* (1993) 77:731–3. doi: 10.1136/bjo.77.11.731
89. Lawrence T, Natoli G. Transcriptional regulation of macrophage polarization: enabling diversity with identity. *Nat Rev Immunol.* (2011) 11:750–61. doi: 10.1038/nri3088
90. Zhou Y, Yoshida S, Nakao S, Yoshimura T, Kobayashi Y, Nakama T, et al. M2 macrophages enhance pathological neovascularization in the mouse model of oxygen-induced retinopathy. *Invest Ophthalmol Vis Sci.* (2015) 56:4767–77. doi: 10.1167/iovs.14-16012
91. Kobayashi Y, Yoshida S, Nakama T, Zhou Y, Ishikawa K, Arita R, et al. Overexpression of CD163 in vitreous and fibrovascular membranes of patients with proliferative diabetic retinopathy: possible involvement of periostin. *Br J Ophthalmol.* (2015) 99:451–6. doi: 10.1136/bjophthalmol-2014-305321
92. Ishikawa K, Yoshida S, Nakao S, Nakama T, Kita T, Asato R, et al. Periostin promotes the generation of fibrous membranes in proliferative vitreoretinopathy. *Faseb J.* (2014) 28:131–42. doi: 10.1096/fj.13-229740
93. Dejana E, Tournier-Lasserve E, Weinstein BM. The control of vascular integrity by endothelial cell junctions: molecular basis and pathological implications. *Dev Cell.* (2009) 16:209–21. doi: 10.1016/j.devcel.2009.01.004
94. Klaassen I, Van Noorden CJ, Schlingemann RO. Molecular basis of the inner blood-retinal barrier and its breakdown in diabetic macular edema and other pathological conditions. *Prog Retin Eye Res.* (2013) 34:19–48. doi: 10.1016/j.preteyeres.2013.02.001
95. Funatsu H, Noma H, Mimura T, Eguchi S, Hori S. Association of vitreous inflammatory factors with diabetic macular edema. *Ophthalmology.* (2009) 116:73–9. doi: 10.1016/j.ophtha.2008.09.037
96. Siemerink MJ, Augustin AJ, Schlingemann RO. Mechanisms of ocular angiogenesis and its molecular mediators. *Dev Ophthalmol.* (2010) 46:4–20. doi: 10.1159/000320006
97. Bressler SB, Ayala AR, Bressler NM, Melia M, Qin H, Ferris FL, et al. Persistent macular thickening after ranibizumab treatment for diabetic macular edema with vision impairment. *JAMA Ophthalmol.* (2016) 134:278–85. doi: 10.1001/jamaophthalmol.2015.5346
98. Sfikakis PP, Markomichelakis N, Theodossiadis GP, Grigoropoulos V, Katsilambros N, Theodossiadis PG. Regression of sight-threatening macular edema in type 2 diabetes following treatment with the anti-tumor necrosis factor monoclonal antibody infliximab. *Diabetes Care.* (2005) 28:445–7. doi: 10.2337/diacare.28.2.445
99. Gale JD, Berger B, Gilbert S, Popa S, Sultan MB, Schachar RA, et al. A CCR2/5 inhibitor, PF-04634817, is inferior to monthly ranibizumab in the treatment of diabetic macular edema. *Invest Ophthalmol Vis Sci.* (2018) 59:2659–69. doi: 10.1167/iovs.17-22731
100. Hillier RJ, Ojaimi E, Wong DT, Mak MYK, Berger AR, Kohly RP, et al. Aqueous humor cytokine levels and anatomic response to intravitreal ranibizumab in diabetic macular edema. *JAMA Ophthalmol.* (2018) 136:382–8. doi: 10.1001/jamaophthalmol.2018.0179
101. Shimura M, Yasuda K, Motohashi R, Kotake O, Noma H. Aqueous cytokine and growth factor levels indicate response to ranibizumab for diabetic macular oedema. *Br J Ophthalmol.* (2017) 101:1518–23. doi: 10.1136/bjophthalmol-2016-309953
102. Felfeli T, Juncal VR, Hillier RJ, Mak MYK, Wong DT, Berger AR, et al. Aqueous humor cytokines and long-term response to anti-vascular endothelial growth factor therapy in diabetic macular edema. *Am J Ophthalmol.* (2019) 206:176–83. doi: 10.1016/j.ajo.2019.04.002
103. Noda K, Nakao S, Zandi S, Sun D, Hayes KC, Hafezi-Moghadam A. Retinopathy in a novel model of metabolic syndrome and type 2 diabetes: new insight on the inflammatory paradigm. *Faseb J.* (2014) 28:2038–46. doi: 10.1096/fj.12-215715
104. Rakoczy EP, Ali Rahman IS, Binz N, Li CR, Vagaja NN, de Pinho M, et al. Characterization of a mouse model of hyperglycemia

and retinal neovascularization. *Am J Pathol.* (2010) 177:2659–70. doi: 10.2353/ajpath.2010.090883
105. Blencowe H, Lawn JE, Vazquez T, Fielder A, Gilbert C. Preterm-associated visual impairment and estimates of retinopathy of prematurity at regional and global levels for 2010. *Pediatr Res.* (2013) 74(Suppl 1):35–49. doi: 10.1038/pr.2013.205
106. Stoll BJ, Hansen NI, Bell EF, Walsh MC, Carlo WA, Shankaran S, et al. Trends in care practices, morbidity, and mortality of extremely preterm neonates, 1993-2012. *JAMA.* (2015) 314:1039–51. doi: 10.1001/jama.2015.10244
107. Quinn GE, Barr C, Bremer D, Fellows R, Gong A, Hoffman R, et al. Changes in course of retinopathy of prematurity from 1986 to 2013: comparison of three studies in the united states. *Ophthalmology.* (2016) 123:1595–600. doi: 10.1016/j.ophtha.2016.03.026
108. Hellstrom A, Smith LE, Dammann O. Retinopathy of prematurity. *Lancet.* (2013) 382:1445–57. doi: 10.1016/S0140-6736(13)60178-6
109. Good WV, Early Treatment for Retinopathy of Prematurity Cooperative G. Final results of the early treatment for retinopathy of prematurity (ETROP) randomized trial. *Trans Am Ophthalmol Soc.* (2004) 102:233–48; discussion 48–50.
110. Mintz-Hittner HA, Kennedy KA, Chuang AZ, Group B-RC. Efficacy of intravitreal bevacizumab for stage 3+ retinopathy of prematurity. *N Engl J Med.* (2011) 364:603–15. doi: 10.1056/NEJMoa1007374
111. Stahl A, Lepore D, Fielder A, Fleck B, Reynolds JD, Chiang MF, et al. Ranibizumab versus laser therapy for the treatment of very low birthweight infants with retinopathy of prematurity (RAINBOW): an open-label randomised controlled trial. *Lancet.* (2019) 394:1551–9. doi: 10.1016/S0140-6736(19)31344-3
112. Lyu J, Zhang Q, Jin H, Xu Y, Chen C, Ji X, et al. Aqueous cytokine levels associated with severity of type 1 retinopathy of prematurity and treatment response to ranibizumab. *Graefes Arch Clin Exp Ophthalmol.* (2018) 256:1469–77. doi: 10.1007/s00417-018-4034-5
113. Ishikawa K, Yoshida S, Nakao S, Sassa Y, Asato R, Kohno R, et al. Bone marrow-derived monocyte lineage cells recruited by MIP-1beta promote physiological revascularization in mouse model of oxygen-induced retinopathy. *Lab Invest.* (2012) 92:91–101. doi: 10.1038/labinvest.2011.141
114. Matsuda K, Okamoto N, Kondo M, Arkwright PD, Karasawa K, Ishizaka S, et al. Mast cell hyperactivity underpins the development of oxygen-induced retinopathy. *J Clin Invest.* (2017) 127:3987–4000. doi: 10.1172/JCI89893
115. Hartong DT, Berson EL, Dryja TP. Retinitis pigmentosa. *Lancet.* (2006) 368:1795–809. doi: 10.1016/S0140-6736(06)69740-7
116. Maguire AM, Russell S, Wellman JA, Chung DC, Yu ZF, Tillman A, et al. Efficacy, safety, and durability of voretigene neparvovec-rzyl in RPE65 mutation-associated inherited retinal dystrophy: results of phase 1 and 3 trials. *Ophthalmology.* (2019) 126:1273–85. doi: 10.1016/j.ophtha.2019.06.017
117. Ait-Ali N, Fridlich R, Millet-Puel G, Clerin E, Delalande F, Jaillard C, et al. Rod-derived cone viability factor promotes cone survival by stimulating aerobic glycolysis. *Cell.* (2015) 161:817–32. doi: 10.1016/j.cell.2015.03.023
118. Petit L, Ma S, Cipi J, Cheng SY, Zieger M, Hay N, et al. Aerobic glycolysis is essential for normal rod function and controls secondary cone death in retinitis pigmentosa. *Cell Rep.* (2018) 23:2629–42. doi: 10.1016/j.celrep.2018.04.111
119. Campochiaro PA, Mir TA. The mechanism of cone cell death in retinitis pigmentosa. *Prog Retin Eye Res.* (2018) 62:24–37. doi: 10.1016/j.preteyeres.2017.08.004
120. Punzo C, Xiong W, Cepko CL. Loss of daylight vision in retinal degeneration: are oxidative stress and metabolic dysregulation to blame? *J Biol Chem.* (2012) 287:1642–8. doi: 10.1074/jbc.R111.304428
121. Yoshida N, Ikeda Y, Notomi S, Ishikawa K, Murakami Y, Hisatomi T, et al. Clinical evidence of sustained chronic inflammatory reaction in retinitis pigmentosa. *Ophthalmology.* (2013) 120:100–5. doi: 10.1016/j.ophtha.2012.07.006
122. Gadani SP, Walsh JT, Lukens JR, Kipnis J. Dealing with danger in the CNS: the response of the immune system to injury. *Neuron.* (2015) 87:47–62. doi: 10.1016/j.neuron.2015.05.019
123. Newsome DA, Michels RG. Detection of lymphocytes in the vitreous gel of patients with retinitis pigmentosa. *Am J Ophthalmol.* (1988) 105:596–602. doi: 10.1016/0002-9394(88)90050-5
124. Murakami Y, Yoshida N, Ikeda Y, Nakatake S, Fujiwara K, Notomi S, et al. Relationship between aqueous flare and visual function in retinitis pigmentosa. *Am J Ophthalmol.* (2015) 159:958–63 e1. doi: 10.1016/j.ajo.2015.02.001
125. Nishiguchi KM, Yokoyama Y, Kunikata H, Abe T, Nakazawa T. Correlation between aqueous flare and residual visual field area in retinitis pigmentosa. *Br J Ophthalmol.* (2019) 103:475–80. doi: 10.1136/bjophthalmol-2018-312225
126. Nagasaka Y, Ito Y, Ueno S, Terasaki H. Increased aqueous flare is associated with thickening of inner retinal layers in eyes with retinitis pigmentosa. *Sci Rep.* (2016) 6:33921. doi: 10.1038/srep33921
127. Lu B, Yin H, Tang Q, Wang W, Luo C, Chen X, et al. Multiple cytokine analyses of aqueous humor from the patients with retinitis pigmentosa. *Cytokine.* (2020) 127:154943. doi: 10.1016/j.cyto.2019.154943
128. Seddon JM, Gensler G, Milton RC, Klein ML, Rifai N. Association between C-reactive protein and age-related macular degeneration. *JAMA.* (2004) 291:704–10. doi: 10.1001/jama.291.6.704
129. Laursen JV, Hoffmann SS, Green A, Nybo M, Sjolie AK, Grauslund J. Associations between diabetic retinopathy and plasma levels of high-sensitive C-reactive protein or von Willebrand factor in long-term type 1 diabetic patients. *Curr Eye Res.* (2013) 38:174–9. doi: 10.3109/02713683.2012.713153
130. Murakami Y, Ikeda Y, Nakatake S, Fujiwara K, Tachibana T, Yoshida N, et al. C-Reactive protein and progression of vision loss in retinitis pigmentosa. *Acta Ophthalmol.* (2018) 96:e174–e9. doi: 10.1111/aos.13502
131. Ginhoux F, Greter M, Leboeuf M, Nandi S, See P, Gokhan S, et al. Fate mapping analysis reveals that adult microglia derive from primitive macrophages. *Science.* (2010) 330:841–5. doi: 10.1126/science.1194637
132. Zhang Y, Zhao L, Wang X, Ma W, Lazere A, Qian HH, et al. Repopulating retinal microglia restore endogenous organization and function under CX3CL1-CX3CR1 regulation. *Sci Adv.* (2018) 4:eaap8492. doi: 10.1126/sciadv.aap8492
133. Ginhoux F, Lim S, Hoeffel G, Low D, Huber T. Origin and differentiation of microglia. *Front Cell Neurosci.* (2013) 7:45. doi: 10.3389/fncel.2013.00045
134. Paschalis EI, Lei F, Zhou C, Kapoulea V, Dana R, Chodosh J, et al. Permanent neuroglial remodeling of the retina following infiltration of CSF1R inhibition-resistant peripheral monocytes. *Proc Natl Acad Sci USA.* (2018) 115:E11359–E68. doi: 10.1073/pnas.1807123115
135. Peng Y, Zhang Y, Huang B, Luo Y, Zhang M, Li K, et al. Survival and migration of pre-induced adult human peripheral blood mononuclear cells in retinal degeneration slow (rds) mice three months after subretinal transplantation. *Curr Stem Cell Res Ther.* (2014) 9:124–33. doi: 10.2174/1574888X09666131219115125
136. Zhao L, Zabel MK, Wang X, Ma W, Shah P, Fariss RN, et al. Microglial phagocytosis of living photoreceptors contributes to inherited retinal degeneration. *EMBO Mol Med.* (2015) 7:1179–97. doi: 10.15252/emmm.201505298
137. Zabel MK, Zhao L, Zhang Y, Gonzalez SR, Ma W, Wang X, et al. Microglial phagocytosis and activation underlying photoreceptor degeneration is regulated by CX3CL1-CX3CR1 signaling in a mouse model of retinitis pigmentosa. *Glia.* (2016) 64:1479–91. doi: 10.1002/glia.23016
138. Silverman LI, Dulatova G, Tandeski T, Erickson IE, Lundell B, Toplon D, et al. *In vitro* and *in vivo* evaluation of discogenic cells, an investigational cell therapy for disc degeneration. *Spine J.* (2020) 20:138–49. doi: 10.1016/j.spinee.2019.08.006
139. Shen J, Yang X, Dong A, Petters RM, Peng YW, Wong F, et al. Oxidative damage is a potential cause of cone cell death in retinitis pigmentosa. *J Cell Physiol.* (2005) 203:457–64. doi: 10.1002/jcp.20346
140. Komeima K, Rogers BS, Lu L, Campochiaro PA. Antioxidants reduce cone cell death in a model of retinitis pigmentosa. *Proc Natl Acad Sci USA.* (2006) 103:11300–5. doi: 10.1073/pnas.0604056103
141. Yoshida N, Ikeda Y, Notomi S, Ishikawa K, Murakami Y, Hisatomi T, et al. Laboratory evidence of sustained chronic inflammatory reaction in retinitis pigmentosa. *Ophthalmology.* (2013) 120:e5–12. doi: 10.1016/j.ophtha.2012.07.008
142. Roh MI, Murakami Y, Thanos A, Vavvas DG, Miller JW. Edaravone, an ROS scavenger, ameliorates photoreceptor cell death after experimental

retinal detachment. *Invest Ophthalmol Vis Sci.* (2011) 52:3825–31. doi: 10.1167/iovs.10-6797
143. Nakatake S, Murakami Y, Ikeda Y, Morioka N, Tachibana T, Fujiwara K, et al. MUTYH promotes oxidative microglial activation and inherited retinal degeneration. *JCI Insight.* (2016) 1:e87781. doi: 10.1172/jci.insight.87781
144. McMurtrey JJ, Tso MOM. A review of the immunologic findings observed in retinitis pigmentosa. *Surv Ophthalmol.* (2018) 63:769–81. doi: 10.1016/j.survophthal.2018.03.002
145. Rohrer B, Demos C, Frigg R, Grimm C. Classical complement activation and acquired immune response pathways are not essential for retinal degeneration in the rd1 mouse. *Exp Eye Res.* (2007) 84:82–91. doi: 10.1016/j.exer.2006.08.017
146. Mishra A, Das B, Nath M, Iyer S, Kesarwani A, Bhattacharjee J, et al. A novel immunodeficient NOD.SCID-rd1 mouse model of retinitis pigmentosa to investigate potential therapeutics and pathogenesis of retinal degeneration. *Biol Open.* (2017) 6:449–62. doi: 10.1242/bio.021618
147. Chan CC, Sen HN. Current concepts in diagnosing' and managing primary vitreoretinal (intraocular) lymphoma. *Discov Med.* (2013) 15:93–100.
148. Mochizuki M, Singh AD. Epidemiology and clinical features of intraocular lymphoma. *Ocul Immunol Inflamm.* (2009) 17:69–72. doi: 10.1080/09273940902957305
149. Bardenstein DS. Intraocular lymphoma. *Cancer Control.* (1998) 5:317–25. doi: 10.1177/107327489800500403
150. Cao X, Shen D, Callanan DG, Mochizuki M, Chan CC. Diagnosis of systemic metastatic retinal lymphoma. *Acta Ophthalmol.* (2011) 89:e149–54. doi: 10.1111/j.1755-3768.2009.01797.x
151. Sagoo MS, Mehta H, Swampillai AJ, Cohen VM, Amin SZ, Plowman PN, et al. Primary intraocular lymphoma. *Surv Ophthalmol.* (2014) 59:503–16. doi: 10.1016/j.survophthal.2013.12.001
152. Venkatesh R, Bavaharan B, Mahendradas P, Yadav NK. Primary vitreoretinal lymphoma: prevalence, impact, and management challenges. *Clin Ophthalmol.* (2019) 13:353–64. doi: 10.2147/OPTH.S159014
153. Fend F, Ferreri AJ, Coupland SE. How we diagnose and treat vitreoretinal lymphoma. *Br J Haematol.* (2016) 173:680–92. doi: 10.1111/bjh.14025
154. Grommes C, Nayak L, Tun HW, Batchelor TT. Introduction of novel agents in the treatment of primary CNS lymphoma. *Neuro Oncol.* (2019) 21:306–13. doi: 10.1093/neuonc/noy193
155. Correa DD, Shi W, Abrey LE, Deangelis LM, Omuro AM, Deutsch MB, et al. Cognitive functions in primary CNS lymphoma after single or combined modality regimens. *Neuro Oncol.* (2012) 14:101–8. doi: 10.1093/neuonc/nor186
156. Kasenda B, Loeffler J, Illerhaus G, Ferreri AJ, Rubenstein J, Batchelor TT. The role of whole brain radiation in primary CNS lymphoma. *Blood.* (2016) 128:32–6. doi: 10.1182/blood-2016-01-650101
157. Alizadeh AA, Eisen MB, Davis RE, Ma C, Lossos IS, Rosenwald A, et al. Distinct types of diffuse large B-cell lymphoma identified by gene expression profiling. *Nature.* (2000) 403:503–11. doi: 10.1038/35000501
158. Pasqualucci L, Dalla-Favera R. The genetic landscape of diffuse large B-cell lymphoma. *Semin Hematol.* (2015) 52:67–76. doi: 10.1053/j.seminhematol.2015.01.005
159. Chapuy B, Roemer MG, Stewart C, Tan Y, Abo RP, Zhang L, et al. Targetable genetic features of primary testicular and primary central nervous system lymphomas. *Blood.* (2016) 127:869–81. doi: 10.1182/blood-2015-10-673236
160. Bonzheim I, Giese S, Deuter C, Susskind D, Zierhut M, Waizel M, et al. High frequency of MYD88 mutations in vitreoretinal B-cell lymphoma: a valuable tool to improve diagnostic yield of vitreous aspirates. *Blood.* (2015) 126:76–9. doi: 10.1182/blood-2015-01-620518
161. Yonese I, Takase H, Yoshimori M, Onozawa E, Tsuzura A, Miki T, et al. CD79B mutations in primary vitreoretinal lymphoma: Diagnostic and prognostic potential. *Eur J Haematol.* (2019) 102:191–6. doi: 10.1111/ejh.13191
162. Riemersma SA, Jordanova ES, Schop RF, Philippo K, Looijenga LH, Schuuring E, et al. Extensive genetic alterations of the HLA region, including homozygous deletions of HLA class II genes in B-cell lymphomas arising in immune-privileged sites. *Blood.* (2000) 96:3569–77. doi: 10.1182/blood.V96.10.3569
163. Francisco LM, Salinas VH, Brown KE, Vanguri VK, Freeman GJ, Kuchroo VK, et al. PD-L1 regulates the development, maintenance, and function of induced regulatory T cells. *J Exp Med.* (2009) 206:3015–29. doi: 10.1084/jem.20090847
164. Liu Y, Yu Y, Yang S, Zeng B, Zhang Z, Jiao G, et al. Regulation of arginase I activity and expression by both PD-1 and CTLA-4 on the myeloid-derived suppressor cells. *Cancer Immunol Immunother.* (2009) 58:687–97. doi: 10.1007/s00262-008-0591-5
165. Davis JL, Miller DM, Ruiz P. Diagnostic testing of vitrectomy specimens. *Am J Ophthalmol.* (2005) 140:822–9. doi: 10.1016/j.ajo.2005.05.032
166. Kimura K, Usui Y, Goto H. Clinical features and diagnostic significance of the intraocular fluid of 217 patients with intraocular lymphoma. *Jpn J Ophthalmol.* (2012) 56:383–9. doi: 10.1007/s10384-012-0150-7
167. Ito T, Takeda A, Fujiwara K, Hasegawa E, Nakao S, Ohishi Y, et al. Risk factors for failure of vitrectomy cell block technique in cytological diagnosis of vitreoretinal lymphoma. *Graefes Arch Clin Exp Ophthalmol.* (2019) 257:1029–36. doi: 10.1007/s00417-019-04266-6
168. Intzedy L, Teoh SC, Hogan A, Mangwana S, Mayer EJ, Dick AD, et al. Cytopathological analysis of vitreous in intraocular lymphoma. *Eye.* (2008) 22:289–93. doi: 10.1038/sj.eye.6702965
169. Kase S, Namba K, Iwata D, Mizuuchi K, Kitaichi N, Tagawa Y, et al. Diagnostic efficacy of cell block method for vitreoretinal lymphoma. *Diagn Pathol.* (2016) 11:29. doi: 10.1186/s13000-016-0479-1
170. Whitcup SM, Stark-Vancs V, Wittes RE, Solomon D, Podgor MJ, Nussenblatt RB, et al. Association of interleukin 10 in the vitreous and cerebrospinal fluid and primary central nervous system lymphoma. *Arch Ophthalmol.* (1997) 115:1157–60. doi: 10.1001/archopht.1997.01100160327010
171. Baehring JM, Androudi S, Longtine JJ, Betensky RA, Sklar J, Foster CS, et al. Analysis of clonal immunoglobulin heavy chain rearrangements in ocular lymphoma. *Cancer.* (2005) 104:591–7. doi: 10.1002/cncr.21191
172. Davis JL, Viciana AL, Ruiz P. Diagnosis of intraocular lymphoma by flow cytometry. *Am J Ophthalmol.* (1997) 124:362–72. doi: 10.1016/S0002-9394(14)70828-1
173. Sugita S, Takase H, Sugamoto Y, Arai A, Miura O, Mochizuki M. Diagnosis of intraocular lymphoma by polymerase chain reaction analysis and cytokine profiling of the vitreous fluid. *Jpn J Ophthalmol.* (2009) 53:209–14. doi: 10.1007/s10384-009-0662-y
174. Davis JL, Ruiz P, Jr, Shah M, Mandelcorn ED. Evaluation of the reactive T-cell infiltrate in uveitis and intraocular lymphoma with flow cytometry of vitreous fluid (an American Ophthalmological Society thesis). *Trans Am Ophthalmol Soc.* (2012) 110:117–29.
175. Tan WJ, Wang MM, Ricciardi-Castagnoli P, Tang T, Chee SP, Lim TS, et al. Single-cell MYD88 sequencing of isolated B cells from vitreous biopsies aids vitreoretinal lymphoma diagnosis. *Blood.* (2019) 134:709–12. doi: 10.1182/blood.2019000022
176. Cani AK, Hovelson DH, Demirci H, Johnson MW, Tomlins SA, Rao RC. Next generation sequencing of vitreoretinal lymphomas from small-volume intraocular liquid biopsies: new routes to targeted therapies. *Oncotarget.* (2017) 8:7989–98. doi: 10.18632/oncotarget.14008
177. MacMahon EM, Glass JD, Hayward SD, Mann RB, Becker PS, Charache P, et al. Epstein-Barr virus in AIDS-related primary central nervous system lymphoma. *Lancet.* (1991) 338:969–73. doi: 10.1016/0140-6736(91)91837-K
178. Crombie JL, LaCasce AS. Epstein barr virus associated B-cell lymphomas and iatrogenic lymphoproliferative disorders. *Front Oncol.* (2019) 9:109. doi: 10.3389/fonc.2019.00109
179. Chan CC. Molecular pathology of primary intraocular lymphoma. *Trans Am Ophthalmol Soc.* (2003) 101:275–92.
180. Chan CC, Shen D, Hackett JJ, Buggage RR, Tuaillon N. Expression of chemokine receptors, CXCR4 and CXCR5, and chemokines, BLC and SDF-1, in the eyes of patients with primary intraocular lymphoma. *Ophthalmology.* (2003) 110:421–6. doi: 10.1016/S0161-6420(02)01737-2
181. Usui Y, Wakabayashi Y, Okunuki Y, Kimura K, Tajima K, Matsuda R, et al. Immune mediators in vitreous fluids from patients with vitreoretinal B-cell lymphoma. *Invest Ophthalmol Vis Sci.* (2012) 53:5395–402. doi: 10.1167/iovs.11-8719
182. O'Connor T, Zhou X, Kosla J, Adili A, Garcia Beccaria M, Kotsiliti E, et al. Age-related gliosis promotes central nervous system lymphoma through CCL19-mediated tumor cell retention. *Cancer Cell.* (2019) 36:250–67 e9. doi: 10.1016/j.ccell.2019.08.001

183. Sonoda KH, Faunce DE, Taniguchi M, Exley M, Balk S, Stein-Streilein J. NK T cell-derived IL-10 is essential for the differentiation of antigen-specific T regulatory cells in systemic tolerance. *J Immunol.* (2001) 166:42–50. doi: 10.4049/jimmunol.166.1.42
184. Czarneski J, Lin YC, Chong S, McCarthy B, Fernandes H, Parker G, et al. Studies in NZB IL-10 knockout mice of the requirement of IL-10 for progression of B-cell lymphoma. *Leukemia.* (2004) 18:597–606. doi: 10.1038/sj.leu.2403244
185. Douglas RS, Capocasale RJ, Lamb RJ, Nowell PC, Moore JS. Chronic lymphocytic leukemia B cells are resistant to the apoptotic effects of transforming growth factor-beta. *Blood.* (1997) 89:941–7. doi: 10.1182/blood.V89.3.941
186. Vignali DA, Collison LW, Workman CJ. How regulatory T cells work. *Nat Rev Immunol.* (2008) 8:523–32. doi: 10.1038/nri2343
187. Nishikawa H, Sakaguchi S. Regulatory T cells in cancer immunotherapy. *Curr Opin Immunol.* (2014) 27:1–7. doi: 10.1016/j.coi.2013.12.005
188. Fowler NH, Cheah CY, Gascoyne RD, Gribben J, Neelapu SS, Ghia P, et al. Role of the tumor microenvironment in mature B-cell lymphoid malignancies. *Haematologica.* (2016) 101:531–40. doi: 10.3324/haematol.2015.139493
189. Soussain C, Choquet S, Blonski M, Leclercq D, Houillier C, Rezai K, et al. Ibrutinib monotherapy for relapse or refractory primary CNS lymphoma and primary vitreoretinal lymphoma: final analysis of the phase II 'proof-of-concept' iLOC study by the Lymphoma study association (LYSA) and the French oculo-cerebral lymphoma (LOC) network. *Eur J Cancer.* (2019) 117:121–30. doi: 10.1016/j.ejca.2019.05.024
190. Soussain C, Hoang-Xuan K, Taillandier L, Fourme E, Choquet S, Witz F, et al. Intensive chemotherapy followed by hematopoietic stem-cell rescue for refractory and recurrent primary CNS and intraocular lymphoma: societe francaise de greffe de moelle osseuse-therapie cellulaire. *J Clin Oncol.* (2008) 26:2512–8. doi: 10.1200/JCO.2007.13.5533
191. Ghesquieres H, Chevrier M, Laadhari M, Chinot O, Choquet S, Molucon-Chabrot C, et al. Lenalidomide in combination with intravenous rituximab (REVRI) in relapsed/refractory primary CNS lymphoma or primary intraocular lymphoma: a multicenter prospective 'proof of concept' phase II study of the French oculo-cerebral lymphoma (LOC) network and the lymphoma study association (LYSA)dagger. *Ann Oncol.* (2019) 30:621–8. doi: 10.1093/annonc/mdz032
192. Houillier C, Choquet S, Touitou V, Martin-Duverneuil N, Navarro S, Mokhtari K, et al. Lenalidomide monotherapy as salvage treatment for recurrent primary CNS lymphoma. *Neurology.* (2015) 84:325–6. doi: 10.1212/WNL.0000000000001158
193. Nayak L, Iwamoto FM, LaCasce A, Mukundan S, Roemer MGM, Chapuy B, et al. PD-1 blockade with nivolumab in relapsed/refractory primary central nervous system and testicular lymphoma. *Blood.* (2017) 129:3071–3. doi: 10.1182/blood-2017-01-764209
194. Takeda A, Yoshikawa H, Fukuhara T, Hikita S, Hijioka K, Otomo T, et al. Distinct profiles of soluble cytokine receptors between B-cell vitreoretinal lymphoma and uveitis. *Invest Ophthalmol Vis Sci.* (2015) 56:7516–23. doi: 10.1167/iovs.15-17465

Conflict of Interest: The authors declare that the research was conducted in the absence of any commercial or financial relationships that could be construed as a potential conflict of interest.

Advantages of publishing in Frontiers

OPEN ACCESS
Articles are free to read for greatest visibility and readership

FAST PUBLICATION
Around 90 days from submission to decision

HIGH QUALITY PEER-REVIEW
Rigorous, collaborative, and constructive peer-review

TRANSPARENT PEER-REVIEW
Editors and reviewers acknowledged by name on published articles

Frontiers
Avenue du Tribunal-Fédéral 34
1005 Lausanne | Switzerland

Visit us: www.frontiersin.org
Contact us: frontiersin.org/about/contact

REPRODUCIBILITY OF RESEARCH
Support open data and methods to enhance research reproducibility

DIGITAL PUBLISHING
Articles designed for optimal readership across devices

FOLLOW US
@frontiersin

IMPACT METRICS
Advanced article metrics track visibility across digital media

EXTENSIVE PROMOTION
Marketing and promotion of impactful research

LOOP RESEARCH NETWORK
Our network increases your article's readership